

# **The role of wild-type SOD1 in SOD1 mouse models of ALS**

**A thesis presented in partial fulfilment of the requirements for the  
degree of Doctor of Philosophy to the University of London**

**Rosie Kate Anna Bunton-Stasyshyn**

**Department of Neurodegenerative Disease**

**UCL Institute of Neurology**

**University College London**

**Declaration**

I, Rosie Kate Anna Bunton-Stasyshyn, confirm that the work presented in this thesis is my own.  
Where information has been derived from other sources, I confirm that this has been indicated  
in the thesis

## Abstract

Amyotrophic lateral sclerosis (ALS) is the most common form of adult onset motor neuron disease. It is primarily sporadic, however a proportion of cases are inherited and of these ~10% are caused by mutations in the gene *SOD1*. Recent research points to a possible role for wild-type (WT) SOD1 in ALS. This thesis addresses questions about the role of WT-SOD1 in ALS in the context of mouse models of ALS.

The first set of experiments address whether pathogenically misfolded SOD1 can act in a “prion-like” way, recruiting WT-SOD1 into a pathogenic conformation *in vivo*. *SOD1* transgenic mice were intracerebrally inoculated with homogenates prepared from central nervous system tissue from mouse or human which contains pathogenic SOD1. Pathology was assessed at a number of post-inoculation time-points to determine whether misfolding of transgenically expressed SOD1<sup>G93A</sup> was increased, or misfolding of transgenically expressed WT-SOD1 was induced.

The project described above used transgenic mice bred onto an endogenous *Sod1* null background because evidence from the prion field suggests that the endogenous protein could interfere with transmission of human misfolded SOD1. The effect of endogenous SOD1 on the disease phenotype of *SOD1*<sup>G93A</sup> transgenic mice was not known, therefore mice of 4 genotypes were examined: WT, *Sod1*<sup>-/-</sup>, Tg *SOD1*<sup>G93A</sup> and *Sod1*<sup>-/-</sup>;Tg *SOD1*<sup>G93A</sup>. Grip-strength and survival was measured. Muscle and spinal cord pathology were also examined at two time-points.

Finally, a project to create a new mouse model of SOD1-fALS is described; a genomically humanised mouse with an inducible *LoxP*-Cre mutant/WT allele. Cloning of the targeting constructs was carried out using a combination of traditional restriction endonuclease cloning and recombineering. Finalising the constructs and embryonic stem cell targeting is underway.

This work aims to increase our understanding of how WT-SOD1 may be involved in both familial and sporadic ALS and provide more accurate models SOD1-fALS.

## **Acknowledgements**

I owe a great deal of thanks to Professor Elizabeth Fisher for her keen supervision, guidance and support throughout my PhD and especially during the writing of this Thesis. Many thanks also to Professor Linda Greensmith for always being available with her expert eye.

Thank you to all the members of the Fisher, Greensmith and Isaacs labs, past and present, all of who have played their part in making my PhD an incredible learning experience and an awful lot of fun along the way. I would also like to thank all the members of staff from the UCL Department of Neurodegenerative Disease and the MRC Prion unit who were essential for the work I have presented in this Thesis. There are too many to mention individually, but in particular I would like to thank Julian Pietrzyk, Beverly Burke, Heesoon Park, Hubert Slawinski and at the Prion Unit BSF, Mike Brown, Tom Horan, Robin Labesse-Garbal, Leila Zakka, Juliette Ajok-Omona, Jackie Swann, Lucy Cooper, Craig Fitzhugh, Emma Trice and Charlotte Bailey.

I am eternally grateful to Dr Anny Devoy for seeing potential in me and opening the door for me to get my foot in. Thanks also to Anny, for having a brain so jam packed full of academic and technical skill and knowledge, being happy to share and always being up for a scientific adventure.

Another particularly whole hearted thanks must go to Dr Phil McGoldrick. Phil has taught and helped me a huge amount and has done so with patience and generosity with his time and brain power. I owe him a great deal.

To Dr Rabia Begum, Dr Chris McKinnon, Dr Barney Bryson, Dr Sarah Mizielinska, Rachele Saccon and Jayne Holby – Thank you all for the absolutely indispensable support each one of you has provided me both in and out of the lab. I am very lucky indeed to have had you guys with me for my PhD and I hope I get to keep you for life!

Finally, thank you to my mum, my dad and my brother for being the best. And my heartfelt thanks to Foxy and Liz for putting up with me and looking after me, especially during the writing of this Thesis and all that came with it.



## Table of Contents

<b>Declaration.....</b>	<b>2</b>
<b>Abstract.....</b>	<b>3</b>
<b>Acknowledgements .....</b>	<b>4</b>
<b>Table of Contents .....</b>	<b>5</b>
<b>List of Figures .....</b>	<b>13</b>
<b>List of Tables.....</b>	<b>16</b>
<b>Abbreviations .....</b>	<b>18</b>
 <b>CHAPTER 1. INTRODUCTION.....</b>	 <b>20</b>
<b>1.1 Amyotrophic Lateral Sclerosis.....</b>	<b>20</b>
1.1.1 Clinical Disease Course.....	20
1.1.2 Pathophysiological Disease Course.....	22
1.1.3 Genetics .....	24
<b>1.2 SOD1-fALS.....</b>	<b>28</b>
1.2.1 SOD1.....	30
<b>1.3 Modelling Genetic Diseases in Mice .....</b>	<b>31</b>
1.3.1 Why Mice? .....	31
1.3.2 Tool Box for Manipulating the Mouse Genome .....	32
1.3.2.1 Random Mutagenesis and Transgene Insertions.....	32
1.3.2.2 The Advent of Gene Targeting.....	33
1.3.2.1 Site Specific Recombinases .....	34
1.3.2.2 Conditional and Inducible Cassettes.....	37
1.3.2.1 Enhancing Targeting with Engineered Nucleases .....	40
1.3.2.2 Refinements in In Vitro DNA Engineering.....	40
<b>1.4 SOD1 Mouse Models.....</b>	<b>48</b>
1.4.1 SOD1 Transgenic Mice .....	48
1.4.1.1 SOD1 <sup>G93A</sup> Transgenic Mouse.....	48
1.4.1.2 SOD1 <sup>WT</sup> Transgenic Mouse.....	53
1.4.2 Sod1 KO Models.....	55
1.4.3 Effects of Background Strain on Phenotypes.....	56
<b>1.5 How Do Mutations in SOD1 Cause ALS? .....</b>	<b>62</b>
1.5.1 The Effect of Mutations on SOD1 Function .....	62
1.5.2 The Effect of Mutations on Biochemical Characteristics of SOD1 .....	62

1.5.3 Proposed Pathogenic Mechanisms in SOD1-fALS .....	63
1.5.3.1 Oxidative Stress.....	63
1.5.3.2 Mitochondrial Dysfunction .....	64
1.5.3.3 Endoplasmic Reticulum-Stress and the Unfolded Protein Response (UPR) .....	64
1.5.3.4 Axonal Transport Deficits.....	65
1.5.3.5 SOD1 and RNA.....	65
1.5.3.6 Non-Cell Autonomous Mechanisms .....	66
1.5.4 Protein Misfolding and Aggregation .....	67
1.5.4.1 SOD1 Aggregates .....	67
1.5.4.2 Pre-aggregate Species.....	68
1.5.4.3 Prion-Like Protein Misfolding Mechanism.....	69
1.5.5 Wild-type SOD1 Pathogenicity.....	75
<b>1.6 Current Questions In Mouse Models of SOD1-fALS and Research Project Aims .....</b>	<b>76</b>
1.6.1 Does SOD1 Have Prion-Like Properties Within the CNS? .....	76
1.6.1.1 Aim: Propagation of SOD1 Misfolding In Vivo .....	76
1.6.2 Does Endogenous Mouse <i>Sod1</i> Affect the Disease Phenotype of the <i>SOD1<sup>G93A</sup></i> -fALS Transgenic Mouse? .....	76
1.6.2.1 Aim: Endogenous <i>Sod1</i> in SOD1G93A Transgenic Mice .....	78
1.6.3 Can We Improve on Current Mouse Models of SOD1-fALS? .....	78
1.6.3.1 Aim: A New Mouse Model of SOD1-fALS.....	78
<b>CHAPTER 2. MATERIALS AND METHODS.....</b>	<b>79</b>
<b>2.1 General Molecular Biology Protocols .....</b>	<b>79</b>
2.1.1 Extraction/Purification of Nucleic Acids .....	79
2.1.1.1 Ear/Tail Biopsy DNA Preparation .....	79
2.1.1.2 Pure Plasmid Preparations.....	79
2.1.1.3 Rapid Plasmid Preparation.....	79
2.1.1.4 Fast DNA Preparations for Plasmid Screening PCR.....	79
2.1.1.5 Purification of DNAs From Agarose Gel and Molecular Biology Buffers .....	80
2.1.2 Polymerase Chain Reaction .....	81
2.1.2.1 Touchdown PCR .....	81
2.1.2.2 Standard Plasmid Screening PCR .....	82
2.1.2.3 Gradient PCR.....	82
2.1.2.4 SOD1 Transgene Genotyping PCR.....	82
2.1.2.5 <i>Sod1</i> Knockout Genotyping PCR .....	83

2.1.3 Quantitative Real Time PCR (qPCR) <i>SOD1</i> Transgene Copy Number Assay.....	84
2.1.4 Restriction Endonuclease Digestion.....	86
2.1.5 Restriction Endonuclease Cloning.....	87
2.1.6 Sanger Sequencing.....	87
2.1.7 Agarose Gel Electrophoresis .....	89
<b>2.2 Bacterial Culture .....</b>	<b>90</b>
2.2.1 Culture Conditions for <i>Escherichia coli</i> Strains Used .....	90
2.2.2 Overnight Culture .....	90
2.2.3 Measurement of <i>E.coli</i> Suspension Concentration.....	90
2.2.4 Transformation of Chemically Competent <i>E.coli</i> .....	90
2.2.5 Preparation and Transformation of Electrocompetent <i>E.coli</i> .....	91
2.2.5.1 Making <i>E.coli</i> Electrocompetent.....	91
2.2.5.2 Electroporation Transformation .....	91
2.2.6 Glycerol Stocks.....	91
<b>2.3 Plasmids, BACs and Cassettes .....</b>	<b>92</b>
2.3.1 BAC Selection .....	92
2.3.2 Antibiotic Resistance Cassettes .....	92
2.3.2.1 FRT Flanked Neo Cassette.....	92
2.3.2.2 rpsL_Gen Positive/Negative Selection .....	93
2.3.3 Custom Plasmids.....	94
2.3.3.1 <i>SOD1_hSUBarms_pMS</i> .....	94
2.3.3.2 <i>SOD1_Exon4+5_pMA</i> .....	95
<b>2.4 BAC Recombineering.....</b>	<b>96</b>
2.4.1 Red/ET Recombineering System .....	96
2.4.1.1 Transformation of pRed/ET Plasmid.....	96
2.4.1.2 Induction of Red/ET Recombinase Expression .....	97
2.4.2 SW102 Recombineering System .....	97
2.4.2.1 Induction of SW102 Recombinase Expression.....	98
2.4.3 General Recombineering Protocol.....	98
2.4.4 Preparation of Inserts and Subcloning Vectors for Recombineering .....	98
2.4.4.1 PCR Amplification.....	99
2.4.4.2 Addition of Homology Arms by PCR Amplification .....	99
2.4.4.3 Linearization by Restriction Endonuclease Digestion .....	99
2.4.4.4 Oligonucleotides .....	99
2.4.5 Sibling Selection .....	99

<b>2.5 Mice .....</b>	<b>100</b>
2.5.1 Housing and General Husbandry .....	100
2.5.1.1 Humane Endpoints.....	101
2.5.2 Human <i>SOD1</i> <sup>G93A</sup> Transgenic Mice .....	101
2.5.3 Human Wild-Type <i>SOD1</i> Transgenic Mice .....	101
2.5.4 <i>Sod1</i> Knockout Mice .....	102
2.5.5 TgG93A, Sod1ko Cross .....	102
2.5.6 TgWT, Sod1ko Cross.....	104
<b>2.6 Mouse Experimental Procedures .....</b>	<b>105</b>
2.6.1 Mouse Experimental Procedures Specific to the Transmission Project .....	105
2.6.1.1 Neurological Checks.....	105
2.6.2 Inoculation of Mice .....	105
2.6.2.1 Inoculant Preparation .....	105
2.6.2.2 Inoculation Protocol.....	106
2.6.2.3 TgG93A Transmission Inoculation Schedule .....	107
2.6.2.4 TgWT Transmission Inoculation Schedule .....	107
2.6.3 Mouse Experimental Procedures Specific to the Characterisation Project.....	108
2.6.3.1 Weekly Weights .....	108
2.6.3.2 Grip Strength.....	108
2.6.3.3 Survival.....	109
2.6.4 Perfusion with Paraformaldehyde .....	109
<b>2.7 Histology of Paraffin Embedded Tissues.....</b>	<b>109</b>
2.7.1 Harvesting of Tissues .....	110
2.7.2 Paraffin Embedding Samples and Sectioning .....	110
2.7.3 Immunostaining .....	110
2.7.4 Immunostaining .....	110
2.7.5 Analysis .....	110
2.7.5.1 Spinal Cord Pathology .....	111
2.7.5.2 Brain Pathology.....	111
<b>2.8 Histology of Frozen Tissues.....</b>	<b>112</b>
2.8.1 Neuromuscular Junction (NMJ) Staining.....	112
2.8.1.1 Sampling and Embedding .....	112
2.8.1.2 Cutting and Staining.....	113
2.8.1.3 Analysis .....	114
2.8.2 Muscle Fibre Typing .....	114

2.8.2.1 Sampling and Embedding .....	114
2.8.2.2 Cutting and Staining.....	114
2.8.2.3 Analysis .....	115
2.8.3 Motor Neuron Counts.....	116
2.8.3.1 Sampling and Embedding .....	116
2.8.3.2 Cutting and Staining.....	116
2.8.3.3 Analysis .....	116
<b>2.9 Statistical Analyses.....</b>	<b>116</b>
 <b>CHAPTER 3. SOD1 TRANSMISSION PROJECT .....</b>	 <b>117</b>
<b>3.1 Aims .....</b>	<b>117</b>
<b>3.2 Introduction.....</b>	<b>117</b>
<b>3.3 Results.....</b>	<b>120</b>
3.3.1 Inheritance Patterns of <i>SOD1</i> Tg and KO Allele .....	120
3.3.1.1 Inheritance Patterns in Male TgWT;Sod1het X Female NTg;Sod1het Matings ....	121
3.3.1.2 Inheritance Patterns in Male TgWT;Sod1hom X Female NTg;Sod1het Matings ..	122
3.3.1.3 Inheritance Patterns in Male TgG93A;Sod1het X Female NTg;Sod1het Matings .	124
3.3.1.4 Inheritance Patterns in Male TgG93A;Sod1hom X Female NTg;Sod1het Matings	125
3.3.2 Transmission in <i>SOD1</i> <sup>G93A</sup> Transgenic Mice.....	128
3.3.2.1 Premature Death and Exclusions .....	128
3.3.2.2 Age Differences Between Groups .....	128
3.3.2.3 SEDI Brain Pathology.....	129
3.3.3 Transmission in Wild-Type SOD1 Transgenic Mice .....	138
3.3.3.1 Premature Death and Exclusion .....	139
3.3.3.2 Age Differences Between Groups .....	142
3.3.3.3 Misfolded SOD1 Pathology .....	147
<b>3.4 Conclusions.....</b>	<b>153</b>
3.4.1 Inheritance Patterns of Human WT and G93A Transgenes and a <i>Sod1</i> KO Allele .....	153
3.4.2 Does Mutant SOD1 Display Prion-Like Properties <i>In Vivo</i> ? .....	155
3.4.2.1 No Evidence for Self-Seeded Aggregation in TgG93A;Sod1ko Mice.....	155
3.4.2.2 Cross-Seeded Aggregation of SOD1 in TgWT;Sod1ko Mice .....	156
3.4.3 Future Work .....	159
 <b>CHAPTER 4. THE EFFECT OF WILD-TYPE ENDOGENOUS <i>SOD1</i> IN THE G93A MUTANT <i>SOD1</i> MOUSE.....</b>	 <b>160</b>

<b>4.1 Introduction.....</b>	<b>160</b>
<b>4.2 Aims .....</b>	<b>161</b>
<b>4.3 Results.....</b>	<b>161</b>
4.3.1 Transgene Copy Number .....	163
4.3.2 Behavioural Characterisation.....	164
4.3.2.1 Starting Weight .....	164
4.3.2.2 Disease Onset.....	166
4.3.2.3 Survival.....	167
4.3.2.4 Grip-Strength .....	168
4.3.3 Histological Characterisation .....	169
4.3.3.1 Motor Neuron Counts.....	169
4.3.3.2 Neuromuscular Junctions .....	171
4.3.3.3 Muscle Fibre Typing.....	175
4.3.4 Can Transgenically Expressed Human SOD1 Compensate for Sod1ko Female Subfertility?.....	183
<b>4.4 Discussion.....</b>	<b>185</b>
4.4.1 Does Endogenous Mouse SOD1 Effect the Disease Phenotype of the TgG93A Mouse? .....	185
4.4.2 Can Transgenic Human SOD1 Compensate for <i>Sod1</i> KO Phenotypes? .....	188
4.4.2.1 Transgenically Expressed WT Human SOD1 Rescues MN Axonopathy in Sod1 KO Animals.....	190
4.4.3 Future Work .....	191
 <b>CHAPTER 5. TOWARDS MAKING A HUMANISED <i>SOD1</i> MOUSE .....</b>	 <b>193</b>
<b>5.1 Aims .....</b>	<b>193</b>
<b>5.2 Results.....</b>	<b>193</b>
5.2.1 Construct Design.....	193
5.2.2 Selection of Mutations.....	196
5.2.2.1 SOD1 <sup>E100G</sup> .....	197
5.2.2.2 SOD1 <sup>L126delTT</sup> .....	204
5.2.3 BACs Sequence Confirmation .....	212
5.2.3.1 Human SOD1 BAC .....	212
5.2.3.2 Mouse Sod1 BACs .....	213
5.2.4 Cloning .....	215
5.2.4.1 Subcloning SOD1 into SOD1_hSUBarms_pMS.....	215

5.2.4.2 Subcloning SOD1 Using SOD1_hSUBarms_pMS+rpsL as Vector Template .....	221
5.2.4.3 Cloning the Neomycin Cassette into hSOD1_SC_pMS.....	229
5.2.4.4 Intron 3 LoxP Insertion Using Oligonucleotide Recombineering .....	231
<b>5.3 Gene Bridges Construct Completion.....</b>	<b>239</b>
<b>5.4 Future Work .....</b>	<b>242</b>
5.4.1 Confirmation of Gene Bridges Finalised Construct.....	242
5.4.2 Using the Targeting Construct to Derive Humanised <i>SOD1</i> Mice.....	243
<b>CHAPTER 6. DISCUSSION .....</b>	<b>245</b>
<b>6.1 Misfolding of SOD1 Within the Prion Paradigm .....</b>	<b>245</b>
6.1.1 SEDI/USOD Outcome Measures.....	246
6.1.2 SOD1 Aggregation and Pathogenicity .....	248
6.1.3 Alternative Outcome Measures.....	250
6.1.4 Wild-type SOD1 Toxicity Outside the Prion Paradigm .....	250
<b>6.2 Human:Mouse SOD1 Interaction in SOD1-fALS mice.....</b>	<b>252</b>
<b>6.3 Mechanisms of WT SOD1 Pathogenicity.....</b>	<b>255</b>
<b>6.4 The <i>SOD1</i> Humanised Mouse.....</b>	<b>256</b>
<b>6.5 Conclusions.....</b>	<b>257</b>
<b>CHAPTER 7. APPENDICES .....</b>	<b>259</b>
<b>7.1 Appendix 1 - Full Table of Mutant <i>SOD1</i> Transgenic Mice .....</b>	<b>259</b>
<b>7.2 Appendix 2 - Detailed Materials and Equipment .....</b>	<b>269</b>
7.2.1 Molecular Biology .....	269
7.2.1.1 Reagents.....	269
7.2.1.2 Kits.....	269
7.2.1.3 Enzymes .....	269
7.2.2 Bacterial Artificial Chromosomes.....	270
7.2.2.1 Human SOD1 BAC .....	270
7.2.2.2 C57BL/6J Mouse Sod1 BACs.....	271
7.2.2.3 C57BL/6N Mouse Sod1 BAC.....	272
7.2.3 Bacterial Culture .....	273
7.2.3.1 Reagents.....	273
7.2.3.2 Antibiotics .....	273

7.2.4 Histology .....	274
7.2.4.1 Reagents and Kits.....	274
7.2.4.2 Antibodies .....	274
7.2.5 Protein Biochemistry Reagents.....	274
7.2.6 Equipment.....	275
7.2.7 Prepared Solutions and Materials.....	275
7.2.7.1 LB Media .....	275
7.2.7.2 LB Agar Plates.....	275
7.2.7.3 Bacterial Freezing Media 2X .....	275
7.2.7.4 Tris-EDTA-Citrate Buffer pH 7.8 10X .....	276
7.2.7.5 TRIS (0.5M) Buffered Saline (9%) 10X.....	276
7.2.7.6 4% Paraformaldehyde in Dulbecco's Phosphate Buffered Saline.....	276
7.2.7.7 Gallocyanine Stain.....	276
7.2.7.8 Laemmli Sample Buffer - 20 ml.....	276
7.2.7.9 1.5 M Tris-Cl pH 6.8 – 50ml.....	277
<b>7.3 Appendix 3 - Premature Deaths for the Cross-Seeded SOD1 Transmission Experiment</b>	<b>278</b>
<b>7.4 Appendix 4 - Kaplan-Meier Survival Graphs of TgWT;Sod1ko Mice Split Between Mouse and Human Inocula .....</b>	<b>281</b>
<b>7.5 Appendix 5 - Relative Transgene Copy Number and Other exclusion for Individual Animals .....</b>	<b>282</b>
<b>7.6 Appendix 6 - Fibre Typing Montages .....</b>	<b>284</b>
7.6.1 EDL Fibre Typing: Myosin Heavy Chain type 2A and 2B .....	285
7.6.2 EDL Fibre Typing: Myosin Heavy Chain Type 1 and 2B .....	290
7.6.3 TA Fibre Typing: Myosin Heavy Chain Type 2A and 2B.....	295
7.6.4 TA Fibre Typing: Myosin Heavy Chain Type 1 and 2B .....	300
<b>References .....</b>	<b>305</b>



## List of Figures

Figure 1.1 Neuromuscular system and neuromuscular junctions .....	23
Figure 1.2 ALS SOD1 mutations .....	29
Figure 1.3 <i>SOD1</i> chromosomal location, genomic, mRNA and protein structure .....	31
Figure 1.4 Homologous recombination gene targeting.....	35
Figure 1.5 Site-specific recombinase systems .....	36
Figure 1.6 Knock-Out Mouse Project (KOMP) conditional knock-out first allele .....	38
Figure 1.7 Allele switching .....	39
Figure 1.8 Recombineering strategies .....	41
Figure 1.9 Red/ET recombineering .....	43
Figure 1.10 pRed/ET.....	44
Figure 1.11 Methods for removing antibiotic selection cassettes.....	46
Figure 1.12 <i>SOD1</i> transgene .....	52
Figure 1.13 Genetic heterogeneity of F2 hybrids .....	57
Figure 1.14 Background strain effects on survival of TgG93A mice .....	58
Figure 1.15 Prion-like mechanisms .....	70
Figure 2.1 HyperLadder.....	89
Figure 2.2 FRT-PGK-gb2-neo-FRT cassette.....	93
Figure 2.3 rpsL_Gen plasmid.....	94
Figure 2.4 <i>SOD1_hSUBarms_pMS</i> .....	95
Figure 2.5 <i>SOD1_Exon4+5_pMA</i> .....	96
Figure 2.6 RedET plasmid.....	97
Figure 2.7 Breeding scheme for producing transgenic KO cross colonies .....	103
Figure 2.8 Location of intra-cerebral injection .....	107
Figure 2.9 Definition of spinal cord regions.....	111
Figure 2.10 Definition of brain regions .....	112
Figure 3.1 SEDI and USOD epitopes .....	118
Figure 3.2 Breeding scheme.....	121
Figure 3.3 Brain region division .....	129
Figure 3.4 SEDI stained TgG93A;Sod1ko sagittal brain sections 24 hours post-inoculation ....	131
Figure 3.5 Quantification of SEDI stained TgG93A;Sod1ko brains at 24 hours post-inoculation .....	133
Figure 3.6 SEDI stained TgG93A;Sod1ko sagittal brain sections 40 days post-inoculation .....	136
Figure 3.7 Quantification of SEDI stained TgG93A;Sod1ko brains at 40 days post-inoculation	138
Figure 3.8 Kaplan-Meier survival graph of TgWT;Sod1ko mice .....	141

Figure 3.9 Average age at cull- 7 day time-point.....	143
Figure 3.10 Average age at cull- 90 day time-point.....	144
Figure 3.11 Average age at cull- 180 day time-point.....	145
Figure 3.12 Average age at cull- 365 day time-point.....	146
Figure 3.13 Average age at cull- 660 day time-point.....	147
Figure 3.14 SEDI staining of TgWT;Sod1ko cords at 90 days post-inoculation.....	148
Figure 3.15 Division of spinal cord regions .....	149
Figure 3.16 USOD stained TgWT;Sod1ko spinal cord sections 90 days post-inoculation.....	151
Figure 3.17 Quantification of USOD stained TgWT;Sod1ko spinal cords at 90 days post-inoculation .....	152
Figure 4.1 Average relative transgene copy number for Sod1wt and Sod1ko mice .....	163
Figure 4.2 Body weight at 57-70 days of age.....	165
Figure 4.3 Onset.....	166
Figure 4.4 Survival.....	167
Figure 4.5 Grip-strength.....	168
Figure 4.6 Spinal cord motor neuron counts .....	169
Figure 4.7 Lumbar spinal cord motor neurons .....	170
Figure 4.8 Neuromuscular junctions in the EDL hind limb muscle .....	172
Figure 4.9 Neuromuscular junction quantification.....	173
Figure 4.10 Neuromuscular junction quantification for non-transgenic mice .....	174
Figure 4.11 Indistinct fibre boundaries and freezing artefacts.....	176
Figure 4.12 EDL fibre typing quantification .....	177
Figure 4.13 EDL fibre typing: Myosin heavy chain type 2A and 2B.....	178
Figure 4.14 EDL fibre typing: Myosin heavy chain type 1 and 2B.....	179
Figure 4.15 TA fibre typing quantification .....	180
Figure 4.16 TA fibre typing: Myosin heavy chain type 2A and 2B .....	181
Figure 4.17 TA fibre typing. Myosin heavy chain type 1and 2B.....	182
Figure 4.18 Fertility of human WT SOD1 transgenic and Sod1 KO mice .....	184
Figure 4.19 Neurophysiological assessment of TA functional innervation.....	191
Figure 5.1 <i>SOD1</i> humanising construct.....	194
Figure 5.2 Schematic representations of selected <i>SOD1</i> humanisation mutations .....	198
Figure 5.3 Humanisation mutation pedigrees .....	201
Figure 5.4 Subcloning SOD1 into SOD1_hSUBarms_pMS.....	216
Figure 5.5 PCR screen D of <i>E.coli</i> transformed with SOD1_hSUBarms PCR.....	218
Figure 5.6 Nested PCR.....	219
Figure 5.7 Screening PCR D and E of hSOD1_SC_pMS with nested PCR strategy .....	220

Figure 5.8 Subcloning <i>SOD1</i> into SOD1_hSUBarms_pMS+rpsL .....	222
Figure 5.9 PCR screen of SOD1_hSUBarms_pMS+rpsL.....	224
Figure 5.10 Screening PCRs for <i>SOD1</i> subcloning recombineering experiment using SOD1_hSUBarms_pMS+rpsL as vector template.....	225
Figure 5.11 Screening PCRs of retransformation of <i>SOD1</i> subcloning recombineering experiment using SOD1_hSUBarms_pMS+rpsL as vector template.....	227
Figure 5.12 Deletion within the spectinomycin resistance cassette of an hSOD1_SC_pMS clone .....	228
Figure 5.13 Insertion of neomycin resistance cassette into hSOD1_SC_pMS.....	229
Figure 5.14 PCR screen of hSOD1_SC+Neo_pMS recombineering experiment .....	230
Figure 5.15 PCR Screen of retransformation of hSOD1_SC+Neo_pMS recombineering experiment.....	231
Figure 5.16 Screening PCR sibling pools of <i>LoxP</i> site insertion into SOD1_SC+neo_pMS .....	234
Figure 5.17 Optimisation of <i>LoxP</i> insertion screening PCR.....	234
Figure 5.18 PCR screen of 5 mL cultures of second <i>LoxP</i> insertion recombineering experiment .....	235
Figure 5.19 Screening PCR of 1/1k dilution and full concentration of second <i>LoxP</i> insertion recombineering experiment .....	236
Figure 5.20 PCR screen of 5 mL cultures of the third <i>LoxP</i> insertion recombineering experiment .....	238
Figure 5.21 PCR screen of ~1 mL full concentration of the third <i>LoxP</i> insertion recombineering experiment.....	239
Figure 5.22 Remaining steps for construction of the humanising <i>SOD1</i> targeting construct ..	241

## List of Tables

Table 1.1 Clinical criteria for El Escorial diagnostic categories .....	22
Table 1.2 Genes causative of ALS.....	26
Table 1.3 Mutant SOD1 transgenic mice .....	49
Table 1.4 Comparison of disease related phenotype seen in TgWT and TgG93A mice .....	54
Table 1.5 Variation in spinal vertebrae in different inbred lines of mice .....	60
Table 1.6 Prion-like proteins in neurodegenerative diseases.....	73
Table 2.1 Touchdown PCR master mix .....	81
Table 2.2 Standard plasmid screening PCR master mix.....	82
Table 2.3 Transgene genotyping primers .....	83
Table 2.4 Genotyping PCR master mix.....	83
Table 2.5 KO genotyping primers.....	84
Table 2.6 Primers and probes for <i>SOD1</i> transgene copy number qPCR assay .....	85
Table 2.7 Prime and probe stock for <i>SOD1</i> transgene copy number qPCR assay .....	85
Table 2.8 <i>SOD1</i> transgene copy number qPCR master mix .....	86
Table 2.9 Template quantities used for Sanger sequencing of PCR products .....	88
Table 2.10 Sanger sequencing reaction master mix .....	88
Table 2.11 Primers for amplification of FRT-PGK-gb2-neo-FRT .....	93
Table 2.12 Primers for amplification of rpsL_Gen cassette .....	93
Table 2.13 Short form nomenclature of mouse genotypes.....	101
Table 2.14 Details of inocula .....	106
Table 2.15 G93A inoculation schedule.....	107
Table 2.16 WT inoculation schedule .....	108
Table 3.1 Mutant mouse nomenclature used within text .....	120
Table 3.2 Observed genotype ratios of offspring from TgWT;Sod1het X NTg;Sod1het matings .....	121
Table 3.3 Observed genotype ratios of offspring from TgWT;Sod1hom X NTg;Sod1het matings .....	122
Table 3.4 Pair-wise comparisons for TgWT;Sod1hom X NTg;Sod1het matings.....	123
Table 3.5 Observed genotype ratios of offspring from TgG93A;Sod1het X NTg;Sod1het matings .....	124
Table 3.6 Pair-wise comparisons for TgG93A;Sod1het X NTg;Sod1het matings .....	125
Table 3.7 Observed genotype ratios of offspring from TgG93A;Sod1hom X NTg;Sod1het matings.....	126
Table 3.8 Pair-wise comparisons for TgG93A;Sod1hom X NTg;Sod1het matings .....	127

Table 3.9 Inoculum used for TgG93A transmission experiment.....	128
Table 3.10 Average age at scheduled cull.....	129
Table 3.11 Inoculum used for TgWT transmission experiment .....	138
Table 3.12 Causes of premature death.....	140
Table 3.13 Number of animals surviving to scheduled cull date .....	142
Table 4.1 Motor unit characteristics.....	161
Table 4.2 Experimental genotypes.....	162
Table 4.3 Genotype ratios.....	162
Table 4.4 Relative transgene copy number for excluded animals.....	163
Table 4.5 Fibre type antibody summary .....	175
Table 4.6 Fertility of <i>Sod1</i> KO and WT SOD1 transgenic mice .....	183
Table 4.7 Age at start of mating.....	183
Table 5.1 Summary of clinical data for E100G individuals.....	199
Table 5.2 Summary of averaged clinical data for E100G cases.....	199
Table 5.3 Summary of clinical data for L126delTT individuals.....	208
Table 5.4 Summary of L126delTT mutant <i>SOD1</i> transgenic mice phenotypes.....	211
Table 5.5 Mismatches between E10 BAC and reference sequence (GRCh37.p6) .....	212
Table 5.6 Mismatches between L18 and N21 BACs and reference sequence (NCBIM37) .....	214
Table 5.7 Primers for amplification of SOD1_hSUBarms subcloning vector .....	217
Table 5.8 Primer pairs for <i>SOD1</i> subcloning screening PCRs .....	218
Table 5.9 Primers pair for amplification step 1 of SOD1_hSUBarms nested PCR.....	220
Table 5.10 Primer pair for amplification of rpsL_gen+BamHI .....	221
Table 5.11 Primers for SOD1_hSUBarms_pMS+rpsL screening PCR .....	223
Table 5.12 Results of SOD1 subcloning screening PCRs A, B and C .....	226
Table 5.13 Results of SOD1_SC screening for retransformations PCRs A, B, C and SOD1_hSUBarms_pMS+rpsL.....	228
Table 5.14 Primers for amplification of FRT_Neo_SC_targ .....	229
Table 5.15 Primers for screening PCR for hSOD1_SC+Neo_pMS .....	230
Table 5.16 <i>LoxP</i> targeting oligonucleotide.....	232
Table 5.17 Screening primers for <i>LoxP</i> insertion .....	232
Table 5.18 Growth profiles .....	237

## Abbreviations

aa	Amino acid
ALS	Amyotrophic lateral sclerosis
BAC	Bacterial artificial chromosome
bp	Base pair
BSA	Bovine serum albumin
CCS	Copper chaperone for SOD1
cDNA	Coding DNA
CmR	Chloramphenicol resistance cassette
CypD	Cyclophilin D
DBR	Derlin binding region
DPBS	Dulbecco's phosphate buffered saline (Minus CaCl <sub>2</sub> and MgCl <sub>2</sub> )
DSB	Double stranded DNA breaks
dsDNA	Double stranded DNA
EDL	Extensor digitorum longus
ENU	<i>N</i> -ethyl- <i>N</i> -nitrosourea
ER	Endoplasmic reticulum
ESC	Embryonic stem cells
fALS	Familial amyotrophic lateral sclerosis
fE	Fusion exon
gDNA	Genomic DNA
hE	Human exon
HLI	HyperLadder I
HLIV	HyperLadder IV
HR	Homologous recombination
hrs	Hours
huSOD1	Human SOD1
IMS	Inter-membrane space
indels	Small insertions/deletions
iPSC	Induced pluripotent stem cell
IVF	In vito fertilisation
kb	Kilobase
KD	Knock-down
KI	Knock-in
KO	Knock-out
KOMP	Knock-out mouse project
LB-Cm	Luria broth with chloramphenicol selection
LB-Gent	Luria broth with gentamycin selection
LBHI	Lewy body hyaline inclusions
LB-Kana	Luria broth with kanamycin selection
LB-Spc	Luria broth with spectinomycin selection
LB-Spc+Strep	Luria broth with spectinomycin and streptomycin selection
LB-Strep	Luria broth with streptomycin selection
LMN	Lower motor neuron
MBD	Maltose binding domain
MBM	Metal binding mutant
MCS	Multiple cloning site

mE	Mouse exon
mESC	Mouse embryonic stem cell
MHC	Myosin heavy chain
mins	Minutes
MN	Motor neuron
moSOD1	Mouse SOD1
MU	Motor unit
NCAM	Neural cell adhesion molecule
NFh	Neurofilament heavy chain
NGS	Normal goat serum
NHEJ	Non-homologous end joining
NMJ	Neuromuscular junction
ntc	No template PCR control
o/n	Over night
OCT	Optimum cutting temperature freezing medium
PBS	Phosphate buffered saline
PBS+tr	PBS plus 0.2% triton X-100
PBS+tw	PBS plus 0.1% tween
PFA	Paraformaldehyde
PNF	Phosphorylated neurofilament
r/t	Room temperature
ROS	Reactive oxygen species
sALS	Sporadic amyotrophic lateral sclerosis
SEDI	SOD1 exposed dimer interface
Sod1het	Heterozygous KO of mouse <i>Sod1</i>
Sod1ko	Homozygous KO of mouse <i>Sod1</i>
Sod1wt	Wild-type mouse <i>Sod1</i>
SpcR	Spectinomycin resistance cassette
ssDNA	Single stranded DNA
SSR	Site specific recombinase
SSR-RM	Site specific recombinase recognition motif
TA	Tibialis anterior
TgG93A	Tg(SOD1*G93A)1Gur
TgWT	Tg(SOD1)2Gur
TS	Triceps surae
UMN	Upper motor neuron
UPR	Unfolded protein response
USOD	Unfolded SOD1
UTR	Untranslated region
v/v	Volume/volume
w/v	Weight/volume
WTL	Wild-type like
YAC	Yeast artificial chromosome

# Chapter 1. Introduction

## 1.1 AMYOTROPHIC LATERAL SCLEROSIS

### 1.1.1 Clinical Disease Course

Amyotrophic lateral sclerosis (ALS) is the most common adult onset motor neuron disease, with an average onset at 62 and diagnosis at 64 (Chiò et al., 2013). It is a devastating and fatal disease, with patients surviving on average only 3-5-years after diagnosis with the majority of patients dying from respiratory failure or related complications (Valdmanis et al., 2008).

Initial symptoms of disease include a progressive weakness of the voluntary muscles. This can be accompanied by, or later develop to include, upper motor neuron (UMN) signs, such as spasticity and increased reflex reactions, and lower motor neuron (LMN) signs, such as muscle wasting, reduced tone and fasciculations. In the majority of cases, ~ 70%, the first signs of the disease occur in the limbs, often asymmetrically. In ~25% of cases bulbar muscles are the first affected, causing difficulty with speech and swallowing. In a minority of cases, ~5%, the first symptoms are in the muscles of the trunk, often affecting breathing (Kiernan et al., 2011). In almost all cases (with the occasional exception of those with a very short disease course) symptoms of the disease progress both in terms of their severity, developing from initial weakness to paralysis, and also their location, spreading out from an initial focal site of onset through contiguous regions of the body (Fujimura-Kiyono et al., 2011). Muscles controlling voluntary movement are primarily affected, with those involved in functions such as eye movement and bladder and bowel control typically being spared (Kiernan et al., 2011).

The hallmark of ALS is a progressive motor weakness that involves symptoms of both UMN and LMN dysfunction with the sparing of sensory function. There can, however, be heterogeneity in clinical presentation, with some cases predominating with UMN or LMN signs (Burrell et al., 2011). Age at onset can range from mid-teens to over 90-years of age (Andersen et al., 1996; Gouveia et al., 2007) and although 50% of patients die within 2.5-years of onset, 15-20% will survive past 5-years (Talbot, 2009) and in rare cases survival has exceeded 40-years (Grohme et al., 2001). On the other hand, shorter disease course has been found to correlate with older age and body mass at onset, bulbar onset, and faster progression from the initial site of onset or to respiratory dysfunction (Traxinger et al., 2013; Fujimura-Kiyono et al., 2011; Chiò et al., 2002; Magnus et al., 2002).

While once considered a pure motor system disorder (Strong et al., 1996), it is increasingly apparent that ALS often includes a component of cognitive dysfunction. Recent investigation suggests that 51% of ALS cases also have some component of cognitive impairment, with 15%



reaching the diagnostic criteria for frontotemporal dementia (FTD) (Ringholz et al., 2005). There are several forms of FTD, but broadly it is a dementia affecting the frontal lobe function producing changes to personality and behaviour including disinhibition, and problems with fluency of speech or language comprehension (Talbot et al., 2006; Giordana et al., 2011). It is now clear that the ALS and FTD are often comorbid, and, as shall be discussed further in Section 1.1.3, they also share both genetic and neuropathological characteristics (Orr, 2011; Giordana et al., 2011).

Population statistics vary, but meta-analysis of global data provides a median incidence (per 100,000) of 1.90 and prevalence of 4.48, with incidence peaking at between 60 and 75-years of age (Chiò et al., 2013). Men are 1.2-1.5 times more likely to be diagnosed with ALS than women, although this difference decreases with age (Manjaly et al., 2010). Many attempts have been made to identify possible environmental risk factors for ALS; exercise, smoking, certain occupations, and exposure to a range of chemical have all been associated with increased risk of developing ALS, although definitive replicable evidence for such associations is currently lacking (Al Chalabi et al., 2013).

There is no diagnostic laboratory test for ALS, nor a definitive clinical test. The Revised El Escorial Criteria is the standard diagnostic protocol. It involves both positive inclusion and negative exclusion criteria resulting in a range of diagnostic categories as summarised in Table 1.1 (Brooks et al., 2000).

Despite a large number of clinical trials examining the effect of over 50 compounds (Turner et al., 2001) there is currently only one drug treatment available for ALS, Riluzole, which can increase survival by only 2-3 months on average (Miller et al., 2012). Symptomatic treatment and palliative care are the main methods for managing the disease, with a multidisciplinary approach covering nutrition, physiotherapy, respiratory and pain management all being important to help improve and maintain quality of life (Kiernan et al., 2011; Miller et al., 2009a; Miller et al., 2009b).

**Table 1.1 Clinical criteria for El Escorial diagnostic categories**

<b>Clinically definite</b>	UMN signs with LMN signs in the bulbar region plus at least two other regions OR UMN and LMN signs in at least 3 spinal regions
<b>Clinically probable</b>	UMN and LMN signs in 2 spinal cord regions with some UMN signs rostral to LMN signs
<b>Clinically probable. Laboratory-supported</b>	UMN and LMN signs in 1 region, OR UMN signs alone with EMG defined LMN signs in 2 regions
<b>Clinically Possible</b>	UMN and LMN signs in 1 region OR UMN signs in 2 or more regions, OR LMN signs rostral to UMN signs
<b>UMN signs used for diagnosis include:</b>	spasticity, increased muscle tone and clonus (rhythmic tremor like reflex in response to forced extension or flexion of muscle), bilateral facial weakness affecting the lower portion of the face, and spastic dysarthria (difficulty with speech).
<b>LMN signs used for diagnosis include:</b>	muscle weakness, atrophy, fasciculations (uncontrollable twitching in a single muscle group) and flaccid dysarthria

(Brooks et al., 2000; Economides et al., 2013; Kiernan et al., 2011; Ravits et al., 2007b; Wijesekera et al., 2009)

### **1.1.2 Pathophysiological Disease Course**

Underlying the progressive weakness and paralysis seen in ALS is the degeneration and death of both UMNs and LMNs causing denervation of skeletal muscles (Figure 1.1) (Ota et al., 2005; Mendonça et al., 2005; Miki et al., 2010).

Examination of the spinal cord (SC) and brain of ALS patients using scanning technologies such as magnetic resonance imaging (MRI) and diffusion tensor tomography (DTI) have revealed *in vivo* correlations between the severity of atrophy and the severity of clinical disease with the regional distribution of atrophy also mirroring the clinical presentation disease (Branco et al., 2013; Valsasina et al., 2007; Cohen-Adad et al., 2012; Thorns et al., 2013; Schuster et al., 2013).

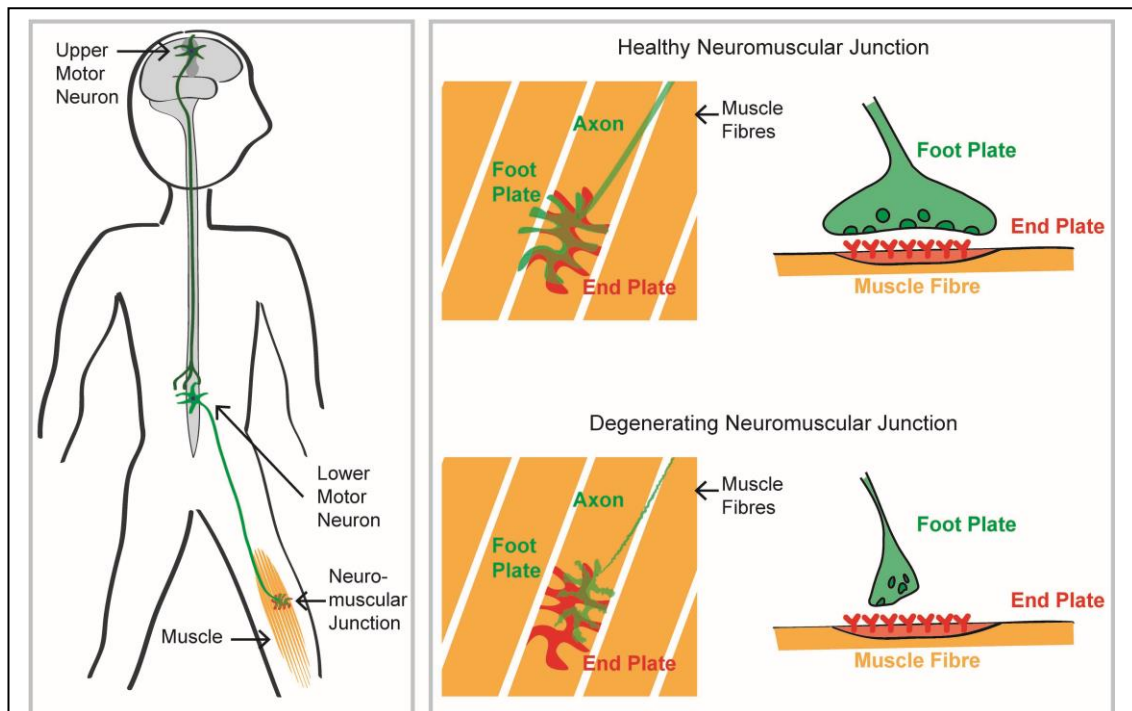


**Figure 1.1 Neuromuscular system and neuromuscular junctions**

Left panel: Upper motor neurons (UMNs), whose cell bodies reside in the motor cortex, synapse in the spinal cord with lower motor neurons (LMN). The axons of LMNs project out of the spinal cord to synapse with the muscle at the neuromuscular junction (NMJ). Degeneration or loss of either UMNs or LMNs results in the loss of connection between the motor cortex and the muscle.

Right panel: Once inside the muscle, the LMN axon branches and each branch innervates a single muscle fibre. The foot plate of the axon is the pre-synaptic terminal from which acetylcholine is released. The end plate of the muscle fibre is the post-synaptic terminal and is populated with nicotinic acetylcholine receptors.

In a healthy NMJ, the foot plate and end plate are closely aligned to ensure efficient signal transduction. In a degenerating NMJ the foot plate and the axon degenerate and retract, reducing the efficiency of signal transduction and eventually losing contact altogether.

UMN= upper motor neuron. LMN= lower motor neuron. NMJ= Neuromuscular junction

Post mortem examination of the LMNs also reveals a gradation of MN loss along the axis of the SC mirroring the spread of disease symptoms, with an average of 55% loss ranging from 8-90% at different levels of the LMN tract (Ravits et al., 2007a).

Gliosis is a widespread in ALS, being reported in both dorsal and ventral horns of the SC (O'Reilly et al., 1995; Ota et al., 2005; Schiffer et al., 1996; McGeer et al., 2002) and in both motor and non-motor regions of the cortical grey and white matter (Sugiyama et al., 2013;

Nagy et al., 1994; Kushner et al., 1991). Astrocytosis has also been detected *in vivo* using positron emission tomography (PET) techniques (Johansson et al., 2007).

Inclusions containing TDP43 are very consistently reported in MNs and astrocytes in the ventral horns (Nishihira et al., 2008) and have been reported in oligodendrocytes in the SC (Mackenzie et al., 2007) as well as both motor and non-motor regions of the brain stem (Miki et al., 2010). Ubiquitin and TDP43 often co-localise in LMN inclusions (Mackenzie et al., 2007). Ubiquitin positive cytoplasmic, intra-neuronal inclusions are commonly reported in the MNs of the brain stem and SC and can take the form of compact, round inclusions or filamentous “skein like” inclusions (Ota et al., 2005; Mackenzie et al., 2007; Leigh et al., 1991). p62 immunoreactivity is also present in many ubiquitinated inclusions (Mizuno et al., 2006).

Other neuropathological inclusions of note include: neurofilament heavy chain (NFh) accumulations in spinal MN cell bodies and axons (Mendonça et al., 2005); phosphorylated neurofilament (PNF) inclusions, often co-localising with ubiquitin (Troost et al., 1992; Takahashi et al., 1997); Lewy body-like hyaline inclusions (LBHI), which are round eosinophilic inclusions, often ubiquitin positive and found in the LMNs (Sasaki et al., 2010); astrocytic hyaline-inclusions, of a similar nature to LBHI but present in astrocytes particularly in long surviving ALS patients (Kato et al., 1997); Bunina bodies, which are small (1-5 µm) eosinophilic granules occasionally co-localising with TDP43 (Mori et al., 2010; Ota et al., 2005).

### 1.1.3 Genetics

When Charcot first described ALS in 1873, he stated that it was never an inherited disease and even used this as a way of differentiating between ALS and spinal muscular atrophy (cited in (Andersen et al., 2011)). It is now, however, firmly established that although the majority of cases of ALS are sporadic (sALS) a significant percentage is heritable or familial (fALS). This percentage has been reported from as low as 0.8% up to 23%, with suggestion that even this may be an underestimate (Andersen et al., 2011). The disease phenotype of fALS and sALS are often reported as being indistinguishable (e.g. (Lattante et al., 2012)).

*SOD1* was the first gene in which ALS causing mutations were identified, in 1993 (Rosen et al., 1993). Mutations in *SOD1* cause 12-24% of fALS, typically showing an autosomal dominant pattern of inheritance, and are also present in up to 7% of sALS (Valdmanis et al., 2008; Pasinelli et al., 2006). Many other genes have subsequently been identified as causative of ALS when mutated, with varying levels of prevalence, and are summarised in Table 1.2. Several risk loci have also been identified and it was calculated that genetic determinants are responsible for 60% of the risk of developing ALS with the remaining 40% being environmental (Al Chalabi et al., 2010).

In many cases mutation specific neuropathologies are seen in fALS patients. For example in mutant *SOD1* cases, proteinaceous SOD1 aggregates are often present (Kato et al., 2000) or when *TARDBP* or *FUS* are mutated their protein products are found to mislocalise away from the nucleus and into the cytoplasm (as reviewed by (Blokhuys et al., 2013)). In the case of repeat expansions in *C9orf72*, RNA aggregates and proteinaceous aggregates containing atypical transcription/translation products occur (Mackenzie et al., 2014).

The previously mentioned link between ALS and FTD is further cemented when considering the genetics behind these disorders. As is summarised in Table 1.2, many of the genes mutated in ALS are also mutated in FTD. In some families mutation carriers may be diagnosed with ALS, FTD or comorbid ALS-FTD, and although the diseases affect different areas of the nervous system, the pathologies are similar (Fecto et al., 2011; Ferrari et al., 2011).

**Table 1.2 Genes causative of ALS**

The table is arranged by date of publication. AD= autosomal dominant. AR= autosomal recessive. \* Year gene (or linkage) was published

Gene symbol	Protein name	Year *	Chromosomal locus	Inheritance	Links to FTD?	Frequency	Main pathway implicated	Ref
<i>SOD1</i>	Superoxide dismutase 1 / Cu,Zn superoxide dismutase	1993	21q22	AD	no	20% FALS	Oxidative stress	1
<i>ALS2</i>	Alsin	2001	2q33	AR	no	Rare- juvenile	Endosomal trafficking and cell signalling	2
	Unknown	2003	20ptel-p13	AD	no	Rare	Unknown gene	3
<i>SETX</i>	Senataxin	2004	9q34	AD	no	Rare- juvenile	RNA processing	4
<i>VAPB</i>	Vesicle-associated membrane protein-associated protein B	2004	20q13.3	AD	no	Rare	Endosomal trafficking and cell signalling	5
<i>TARDBP</i>	TAR DNA-binding protein 43 (TDP43)	2008	1p36.2	AD	yes	5% FALS, more in some groups	RNA processing	6
<i>FUS</i>	Fused in sarcoma	2009	16p11.2	AD	yes	4–5% FALS-juvenile	RNA processing	7, 8
<i>DAO</i>	D-amino acid oxidase	2010	12q24	AD	no	Rare	Glutamate excitotoxicity	9
<i>OPTN</i>	Optineurin	2010	10p13	AD and AR	no	Rare	Endosomal trafficking and cell signalling	10
<i>VCP</i>	Valosin-containing protein	2010	9p13-p12	AD	yes	1% of FALS	Ubiquitin/protein degradation	11

Gene symbol	Protein name	Year *	Chromosomal locus	Inheritance	Links to FTD?	Frequency	Main pathway implicated	Ref
<i>SIGMAR1</i>	$\sigma$ Non-opioid receptor 1	2010	9p13.3	AD and AR	yes	Rare- adult and juvenile		12, 13
<i>SPG11</i>	Spatacin	2010	15q15–q21	AR	no	Rare- juvenile		14
<i>UBQLN2</i>	Ubiquilin 2	2011	Xp11	X-linked	yes		Ubiquitin/protein degradation	15
<i>C9orf72</i>	Chromosome 9 open reading frame 72	2011	9q21–q22	AD	yes	22.5-46% FALS, 21% of SALS		16, 17
<i>PFN1</i>	Profilin 1	2012	17p13.2	AD	no	Rare	Cytoskeleton/ transport	18
<i>hnRNPA1</i>	Heterogenous nuclear ribonucleoprotein A1	2013	12q13.3	AD	no	Rare	RNA processing	19

1- (Rosen et al., 1993); 2- (Yang et al., 2001); 3-(Sapp et al., 2003); 4- (Chen et al., 2004); 5- (Nishimura et al., 2004); 6- (Sreedharan et al., 2008); 7- (Kwiatkowski et al., 2009); 8- (Vance et al., 2009); 9- (Mitchell et al., 2010); 10- (Maruyama et al., 2010); 11- (Johnson et al., 2010a); 12- (Luty et al., 2010); 13- (Al-Saif et al., 2011); 14- (Orlacchio et al., 2010); 15- (Deng et al., 2011); 16- (Renton et al., 2011); 17- (DeJesus-Hernandez et al., 2011); 18- (Wu et al., 2012); 19- (Kim et al., 2013)

## 1.2 SOD1-fALS

Over 150 mutations in *SOD1* have now been identified in ALS cases (ALS Online Database, ALSOD. <http://alsod.iop.kcl.ac.uk/>). As illustrated in Figure 1.2, mutations are distributed throughout the protein sequence. The majority of the mutations are missense point mutations (Turner et al., 2008), however silent point mutations, deletions, insertions and mutations in non-coding sequence have all been identified (e.g. (Hu et al., 2011; Zinman et al., 2009; Valdmanis et al., 2009; Birve et al., 2010; Zu et al., 1997)).

Mutations in *SOD1* are thought to cause disease via an as yet undefined dominant gain of function rather than a loss of function; although some mutations reduce the function of SOD1, many have little or no effect and some have even been found to increase the activity of the enzyme (reviewed by (Saccon et al., 2013)) and mice expressing the mutant human protein develop an ALS like disease phenotype, while *Sod1* null mice do not recapitulate the disease (Shefner et al., 1999).

SOD1-fALS has been described as very similar to sALS in terms of site of onset, progression, duration and cause of death (Synofzik et al., 2010). It has been suggested that SOD1-fALS cases are less likely to develop the cognitive deficits sometimes seen in sALS (Wicks et al., 2009) however cases of SOD1-fALS concurrent with both cognitive decline and diagnosis with ALS-FTD have been reported in the literature (e.g. (Masè et al., 2001; Battistini et al., 2005; Katz et al., 2012)).

The neuropathology seen in SOD1-fALS is also similar to that of sALS (Nakamura et al., 2014; Kato, 2008; Hineno et al., 2012; Hineno et al., 2012; Kato et al., 1996; Tan et al., 2007), although some distinctions have been made; neuronal and astrocytic SOD1 pathology is ubiquitously reported in SOD1-fALS but often reported as absent in non-SOD1-fALS and sALS (Kato et al., 1996; Kato, 1999; Bruijn et al., 1998; Hineno et al., 2012; Kato et al., 2000; Kato et al., 2001b; Shibata et al., 1996b; Shibata et al., 1996a). Bunina bodies are also reported as absent in SOD1-fALS (e.g. (Nakamura et al., 2014; Shibata et al., 1996a; Tan et al., 2007)). The absence of TDP43 pathology in SOD1-fALS has been described as a defining difference between SOD1-fALS and non-SOD1-fALS/sALS (Mackenzie et al., 2007; Tan et al., 2007), although cases of TDP43 pathology in SOD1-fALS cases have been reported (Okamoto et al., 2011; Maekawa et al., 2009; Sumi et al., 2009).



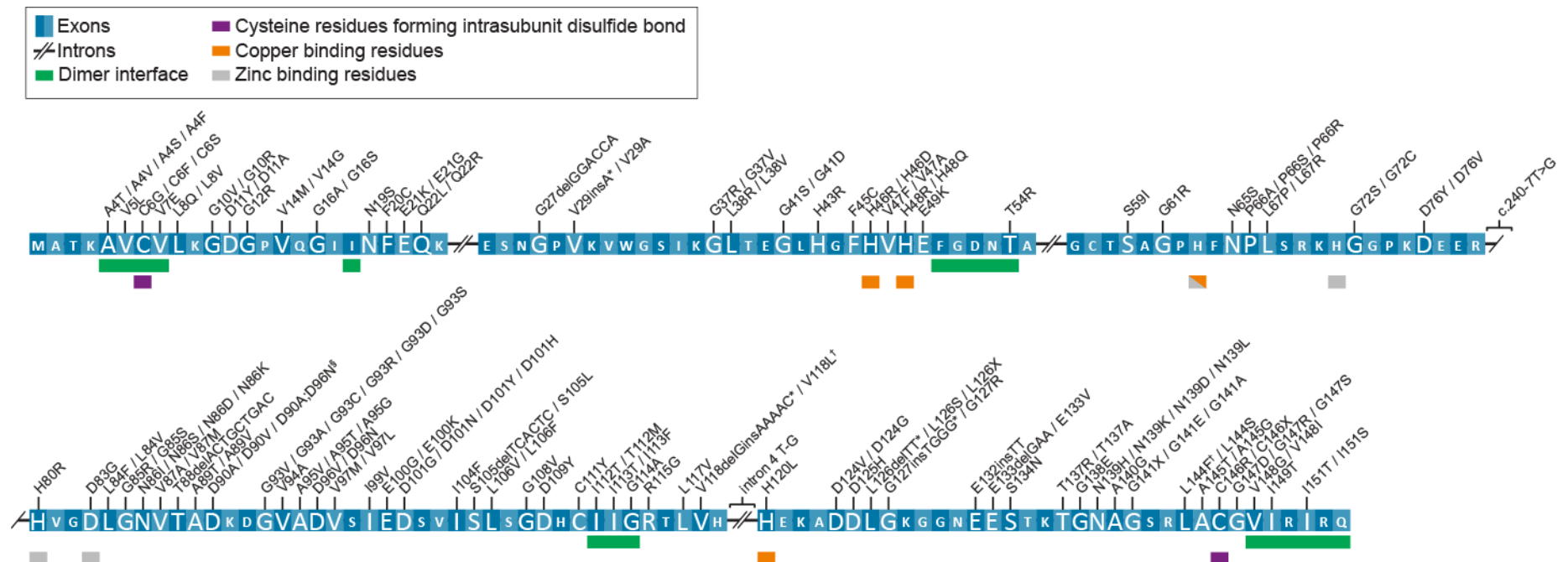


**Figure 1.2 ALS SOD1 mutations**

The amino acid sequence of SOD1 is shown, with exons and introns of the corresponding gDNA sequence indicated. ALS causing disease mutations are annotated. Only variations that are predicted to affect the amino acid sequence of the protein are included and pathogenicity has not been shown for all. ALSOD mutations, InsAexon2 and E133del are the same as mutations V29insA and E133delGAA, respectively, and so have not been annotated separately. Similarly, we believe D125TT to be L126delTT and E133insTT to be E132insTT. Information about highlighted structural elements is from (Wang et al., 2006a). Mutations were collected from ALS online database (ALSOD, <http://alsod.iop.kcl.ac.uk>), and additional references (Pramatarova et al., 1994) and (Kobayashi et al., 2012).

†= Locations where two nucleotide changes results in the same amino acid substitution; \*= Frame shift mutations which result in a premature stop codon; §= compound heterozygotes. Modified from Saccon et al., (2013).

### 1.2.1 SOD1

The human *SOD1* gene is 9,310 base pairs (bp) long and resides on human chromosome 21, q22.11. The gene has 5 exons and is transcribed into a 966 bp mRNA transcript which is translated into a 154 amino acid (aa) protein (Figure 1.3). The protein is highly conserved sharing 73% aa sequence across mammals (Wang et al., 2006a).

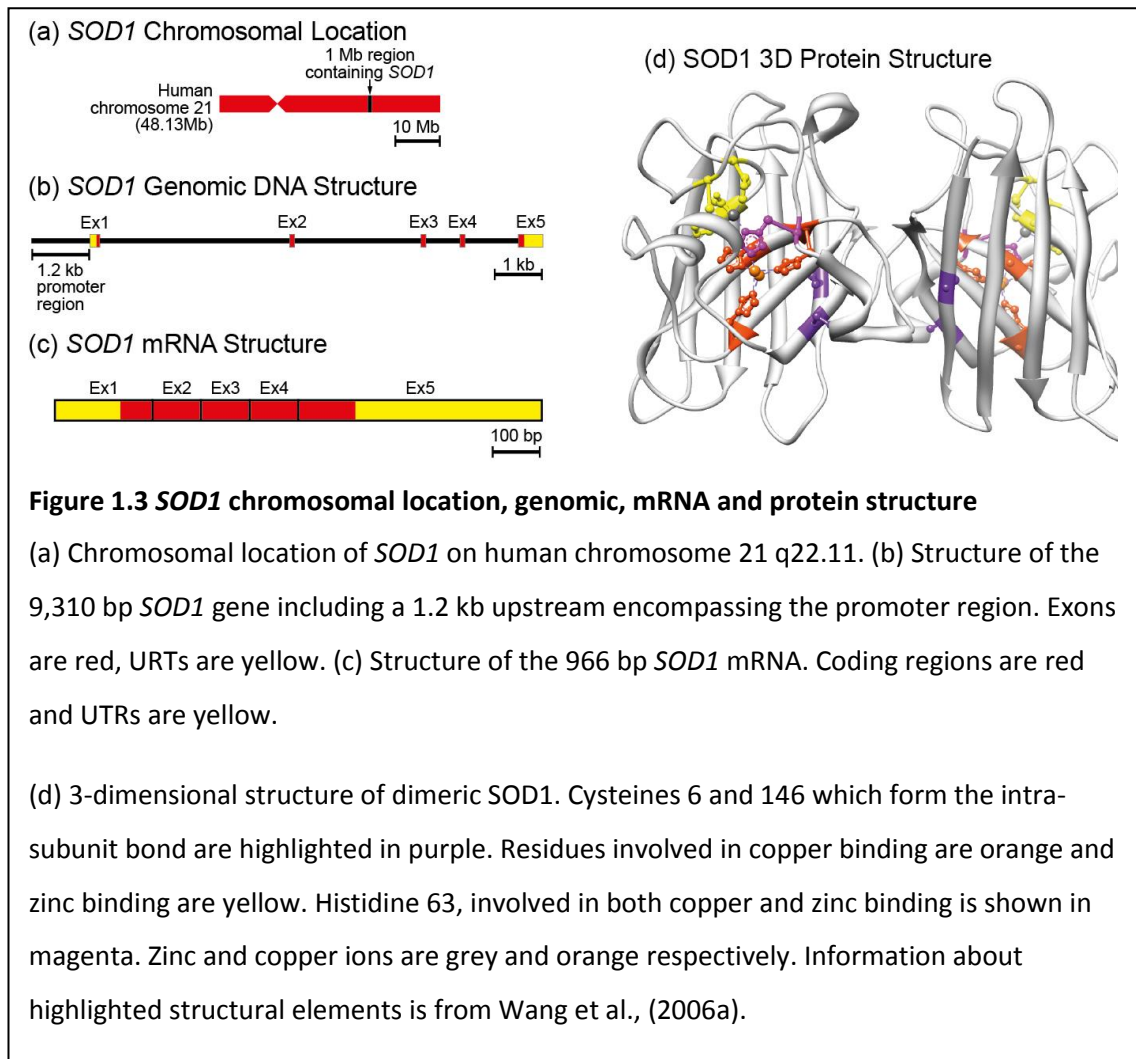
A broad range of transcription factor binding sites have been mapped to between -1,200 and +1 bp from the transcriptional start site of the *SOD1* gene (Miao et al., 2009; Park et al., 2002; Yoo et al., 1999a; Romanuik et al., 2009; Yoo et al., 1999b). There are also 2 functional transcripts differing in their 3' untranslated regions (UTR), with the longer transcript directing higher expression levels (Sherman et al., 1983; Kilk et al., 1995). Protein expression levels *in vivo*, however, appear remarkably stable within tissues across time and in response to environmental insult (Miao et al., 2009; Radyuk et al., 2004).

SOD1 is ubiquitously expressed in all cell types (Leitch et al., 2009; Bordo et al., 1994) and within the central nervous system (CNS) it is particularly abundant in the MNs of the SC (Lindenau et al., 2000). Within the cell SOD1 is primarily located in the cytosol (Crapo et al., 1992) but is also found on the outer membrane and inter-membrane space (IMS) of the mitochondria (Sturtz et al., 2001; Kawamata et al., 2010).

Its canonical role in the cell, where it functions as a 32 kilodalton (kDa) homodimer, is as an anti-oxidant enzyme, catalysing the conversion of toxic reactive oxygen species (ROS) to hydrogen peroxide and oxygen, guarding the cell against oxidative stress (Zelko et al., 2002). Several post-translational modifications (highlighted in Figure 1.3d) are needed for SOD1 to become functional; the nascent protein must bind a structurally important zinc ion and then, interacting with copper chaperon for SOD1 (CCS), bind an enzymatically important copper ion and form an intra-subunit disulphide bond before dimerising (Banci et al., 2012). Once in its fully mature dimeric state, SOD1 is a remarkably stable protein with a half-life of unfolding of approximately 200-years (Rumfeldt et al., 2009).

Additional functions of SOD1 have also been proposed; Reddi and Culotta (2013) have suggested that SOD1 may act as an O<sub>2</sub>/glucose dependent regulator of respiration via hydrogen peroxide (H<sub>2</sub>O<sub>2</sub>) dependent stabilisation of casein kinase 1 gamma (CK1γ). Homma et al., (2013) have suggested that SOD1 may act as a zinc sensitive endoplasmic reticulum (ER) stress activator, by binding to Derlin-1 when zinc levels are reduced. Zhu et al., (2008) have also proposed that SOD1 may have a role in nitrotyrosine production in the liver.

The effects of ALS mutations on the biological function and biophysical properties of SOD1 along with posited pathogenic mechanisms will be discussed in more detail later in Section 1.5.



## 1.3 MODELLING GENETIC DISEASES IN MICE

### 1.3.1 Why Mice?

Mice are currently the most genetically pliable organism available to researchers and have often been the species in which techniques to manipulate the genome have been pioneered. They were the first mammalian species into which researchers introduced exogenous genetic sequence (Jaenisch et al., 1974), and the first species with embryonic stem cells (ESC) successfully cultured *in vitro*, in 1981 (Martin, 1981; Evans et al., 1981). It would not be until 2008 that another species of ESCs, that of the rat, would be successfully cultured (Buehr et al., 2008; Li et al., 2008). As shall be discussed, the availability of mouse ESCs (mESCs) was essential in the development of targeted genetic engineering technologies.

While it is now possible to genetically manipulate other mammalian model organisms, such as rats, pigs and even non-human primates (e.g. (Niu et al., 2014; Prather et al., 2008; Huang et al., 2011)), the mouse is still the most genetically tractable of mammalian models and is relatively cheap and fast to work with. Compared to some even cheaper and faster model organisms, such as the fruit fly or zebra fish, the genetic and physiological similarities between

humans and mice make the mouse a more attractive model for many diseases, particularly those effecting complex systems such as the nervous system.

The genetic mouse resources now available to researchers is vast: over 1,200 human diseases have at least 1 mouse model available for them and there are over 35,500 searchable mutant alleles listed on the Jackson Laboratories Mouse Genome Informatics website

([www.informatics.jax.org](http://www.informatics.jax.org) Feb 2014).

The following section will describe some of the main techniques in the ever expanding tool box for manipulating the mouse genome.

### **1.3.2 Tool Box for Manipulating the Mouse Genome**

#### *1.3.2.1 RANDOM MUTAGENESIS AND TRANSGENE INSERTIONS*

One of the earlier techniques for manipulating the mouse genome was the use of random mutagenic agents, such as *N*-ethyl-*N*-nitrosourea (ENU), to mutagenize a male mouse resulting in point mutations at a near random distribution every 1-1.5 kb within the sperm produced by the male (Acevedo-Arozena et al., 2008). The offspring of such mutagenized males can then either be screened phenotypically or sperm banks can be made from the male offspring which can then be screened for mutations in a particular gene of interest and the sperm used for *in vitro* fertilisation. Although these techniques have been highly useful in analysing gene function and producing novel disease models there is no control over the site or sequence of the mutations.

Insertional transgenesis allows a specific genetic sequence of interest to be introduced into the mouse genome. In 1980, Gordon et al., created the first transgenic mice using pronuclear injection of purified DNA into oocytes, which were then re-implanted into pseudo-pregnant females. The exogenous DNA was stably integrated into the genomes of a number of the resultant pups. Although previously transgenic mice had been produced by injecting viruses into mouse blastocysts (Jaenisch et al., 1974; Jaenisch, 1976) this was the first example of confirmed integration of purified DNA. The following year a number of papers revealed that the techniques could produce transgenic mice not only capable of germ-line transmission of the transgenic DNA to their offspring (Gordon et al., 1981; Costantini et al., 1981) but also that transgenes constructed from exogenous mammalian genes were expressed, producing functional proteins, and could be carried through successive generations (Wagner et al., 1981a; Wagner et al., 1981b).

Theoretically, any DNA sequence that can be cloned can be used as a transgene vector, the main limiting factor being the amount of DNA that can be maintained in a plasmid. Because of

the size limit of traditional plasmid backbones transgenes have often been constructed using a promoter sequence followed by the coding DNA (cDNA) sequence of the gene of interest, into which desired mutations can be added using *in vitro* mutagenesis .

Using this technique the injected DNA is integrated into the genome of a number of the pups at a random genomic locus. If the injection is carried out at the ideal developmental stage, the single cell oocyte, every cell in the resultant pups should contain the insertion, including the germ-cells, however in practice, not every pup may be capable of germ-line transmission. Concatemerisation of the transgene often occurs, resulting in transgene arrays of up to 1000 copies (Lo, 1986), which can effect expression levels, although a direct correlation between transgene copy number and expression level is not always apparent (Epstein et al., 1987). Bacterial artificial chromosome (BAC) and yeast artificial chromosome (YAC) transgenes go some way to alleviate this potential problem as BAC/YACs are more likely to integrate as a relatively low copy transgene array (Chandler et al., 2007). The integration site of random insertional transgenics will also differ between different lines and this can affect the resultant phenotype due to the chromatin environment of the transgene and the potential of disrupting genes around the site of insertion (e.g. (Epstein et al., 1987; Nishioka et al., 2005)).

#### 1.3.2.2 THE ADVENT OF GENE TARGETING

The convergence of *in vitro* mESC culture and two further discoveries opened the gateway to new techniques for targeted manipulation of the mouse genome (Martin, 1981; Evans et al., 1981). The first discovery was that homologous recombination (HR) between exogenous DNAs happens at a relatively high frequency in mammalian cells (e.g. (Folger et al., 1982; Kucherlapati et al., 1984; Lin et al., 1984; Miller et al., 1983; de Saint Vincent et al., 1983; Subramani et al., 1983)) and that this property can be harnessed to recombine exogenous plasmid DNA with an endogenous chromosomal locus in a targeted fashion, called “gene targeting” (e.g. (Folger et al., 1984; Lin et al., 1985; Smith et al., 1984; Smithies et al., 1984; Thomas et al., 1986)). The second was that cultured mESCs could be introduced into blastocysts to produce chimeric pups composed of a mixture of host and injected donor cells (Bradley et al., 1984) and crucially, mESCs that have undergone genetic manipulation could retain their pluripotency and participate in the formation of chimeric pups (Robertson et al., 1986; Gossler et al., 1986). In 1989 these technological advances were brought together and the first gene targeted mice were born (Thompson et al., 1989; Zijlstra et al., 1989; Schwartzberg et al., 1989).

Using *in vitro* recombinant DNA engineering, a targeting construct can be made with homology arms (regions of homology to the targeted chromosomal loci) flanking a cassette containing the desired modification, as shown in Figure 1.4. The targeting construct is introduced into the

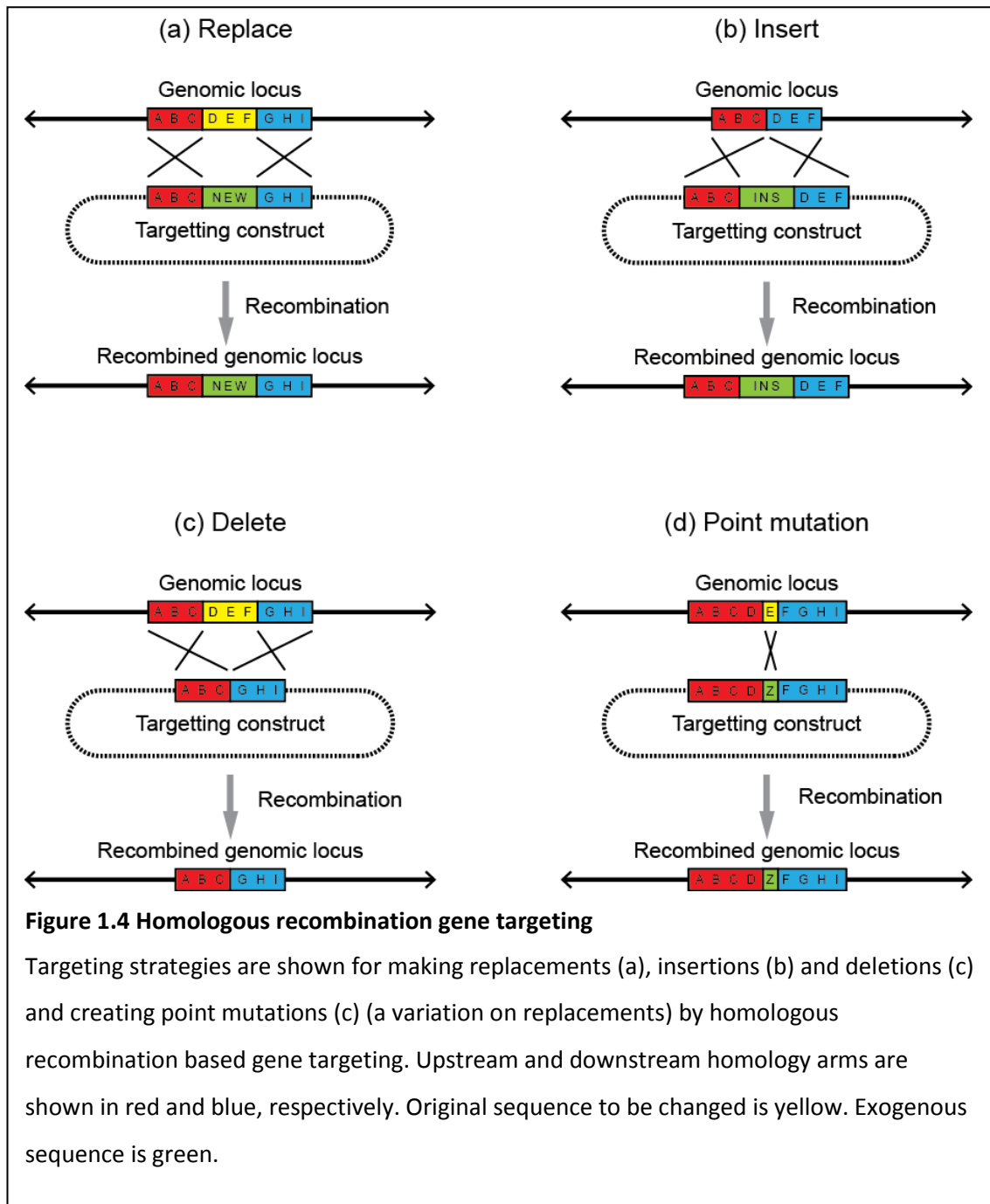
mESCs, typically by electroporation, and cells are selected by antibiotic resistance conferred by a cassette included in the construct. In the majority of cases the targeting construct will be integrated randomly, as in random integration transgenesis, however in some cells the innate HR machinery facilitates the targeted integration of the construct. Once correctly targeted mESC clones have been identified they can be used for blastocysts injection. The chimeric offspring then need to be mated to check for integration of the donor mESCs into the germ-cells, thus producing a new line of germ-line gene targeted mice.

This method of gene targeting can be used to create replacements (Figure 1.4a), insertions (Figure 1.4b), deletions (Figure 1.4c) and point mutations (Figure 1.4d). Depending on the design of the targeting construct, such mutations are classed as knock-outs (KO) or knock-ins (KI); KOs disrupt a gene's function either by disrupting its transcription or by changing the sequence such that the mRNA is not transcribed into a functional protein. This can be done by deleting a portion of the gene, or by inserting sequence to disrupt it. KIs change the gene product and can range from single point mutations to entire gene replacements (e.g. (Rathinam et al., 2011)). These strategies have an advantage over traditional random integration transgenesis as the inserted/edited sequence will reside in the endogenous locus within the natural chromatin environment of the gene and under the influence of the endogenous promoters and other *cis* factors.

HR targeting has also been used for the targeted insertion of transgenes into surrogate genomic loci. Loci with an open chromatin structure where disruption is known to cause minimal unwanted secondary effects are used as surrogates, helping to overcome some of the potential pitfalls of traditional transgenesis. The *Rosa26* and *Hprt* (hypoxanthineguanine phosphoribosyltransferase) loci are two common examples (e.g. (Freyer et al., 2013; D'Acunzo et al., 2014; Heaney et al., 2004)).

### 1.3.2.1 SITE SPECIFIC RECOMBINASES

Site specific recombinases (SSR) encompass a number of enzymes that facilitate the recombination of DNA at specific SSR recognition motifs (SSR-RM). There are several classes of SSRs, and the most commonly used in mouse genetic engineering, both *in vitro* and *in vivo*, are the tyrosine simple/bidirectional recombinases (for brevity, simply referred to as SSRs in the following text) (Hirano et al., 2011). The 2 most widely used SSRs are Cre (causes recombination), which recognises *LoxP* (locus for crossing over (x), P1) sites (Austin et al., 1981; Sternberg et al., 1981), and FLP (flippase), which recognises *FRT* (FLP recombination target) sites (McLeod et al., 1986).



As illustrated in Figure 1.5, SSRs facilitate directional recombination between SSR-RMs. Excision/insertion and inversion reactions (Figure 1.5 a and b) are achieved by the recombination of 2 SSR-RMs. For cassette exchange (Figure 1.5c), 4 SSR-RMs are used; 2 flanking the target locus and 2 flanking the donor cassette. Two cross-over events, one at either side of the target and donor are required for successful cassette exchange (Bouhassira et al., 1997; Economides et al., 2013; Oberdoerffer et al., 2003; Seibler et al., 1997; Wallace et al., 2007).

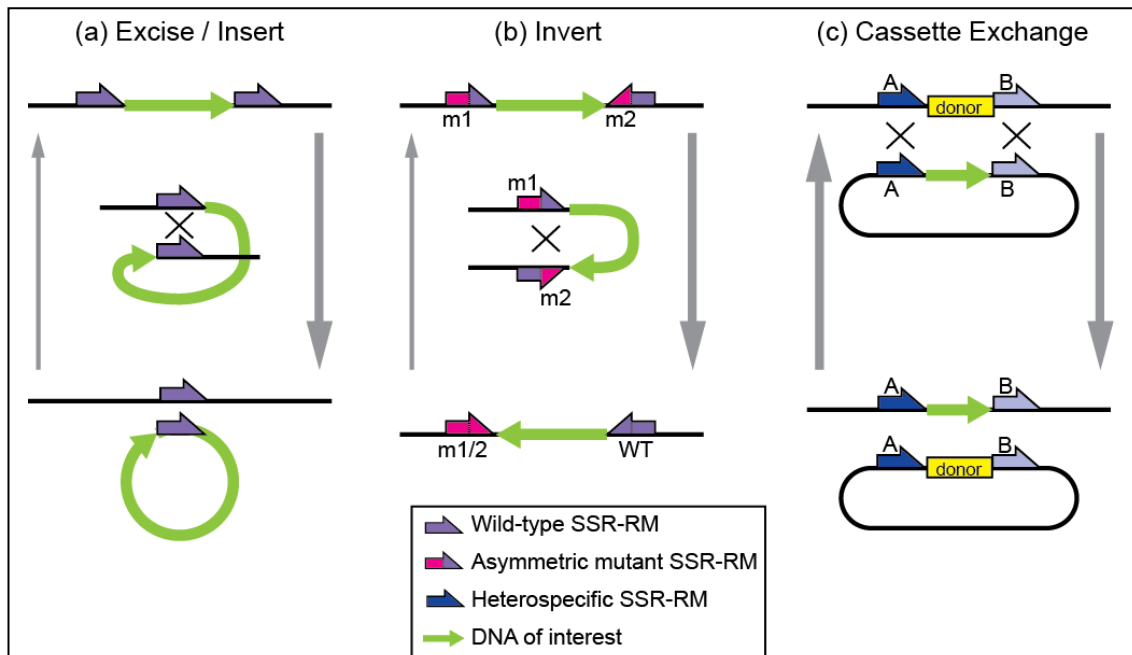


**Figure 1.5 Site-specific recombinase systems**

Site specific recombinases (SSR) recognise a specific SSR-recognition motif (SSR-RM) facilitating recombination between SSR-RMs.

(a) For excision (downward reaction) 2 SSR-RMs arranged in the same orientation flanking the cassette. Recombination between SSRs excises the cassette, leaving a single SSR-RM in its place and a circularisation of the excised cassette with a single SSR-RM. In the reverse (upward) reaction, insertion results from the recombination of a single SSR-RM at the target location and the SSR-RM present on the circular donor. In this case an excess of the donor vector is required to push the balance of the reaction towards integration and away from excision (Seibler et al., 1997).

(b) For inversion 2 SSR-RMs are arranged in opposing orientation, directing the inversion of the flanked cassette within the original locus. Using normal SSR-RMs this reaction is reciprocal, however, asymmetrical mutant SSR-RMs have been designed which strongly favour unidirectional recombination. Two mutant SSR-RMs, m1 and m2, will recombine to produce one wild-type (purple) and one double mutant (pink m1/2) SSR-RM, which have reduced recombination efficiency, reducing the likelihood of a reciprocal, upward, recombination (Oberdoerffer et al., 2003; Turan et al., 2011; Economides et al., 2013).

(c) For cassette exchange the genomic locus to be replaced is flanked by 2 SSR-RMs, as is a donor cassette and 2 cross-over events, one on either side, are required for successful exchange.

(Continued.... )



Using normal SSR-RMs, the likelihood of recombination between any pair of SSR-RMs would be equally likely, potentially resulting in excisions as shown in *a*. The use of heterospecific SSR-RMs, which have been mutated such that they will only recombine with a matching mutant (labelled A (dark blue) and B (light blue)) allows recombination to be directed specifically to exchange of the cassettes (Wallace et al., 2007).

In order to use SSR systems for targeting in mESCs it is first necessary to introduce the SSR-RMs into the genome of the mESC using HR gene-targeting. Once in place however, SSR systems are more efficient than HR in mESC targeting, particularly when large stretches of DNA (>100 kb) are manipulated (Wallace et al., 2007) and mESC lines with *LoxP* or *FRT* sites at the *Rosa26* locus are also available for streamlined targeted insertional transgenesis (Tchorz et al., 2012; Sandhu et al., 2011). The construction of targeting vectors is also easier for SSR targeting as rather than long homology arms, the short (~34 bp) SSR-RMs are all that is needed for targeting. One drawback of this system is that SSR-RMs are left within the mouse genome, either at the site of excision, or flanking the region which has been inserted/inverted/exchanged. For this reason care needs to be taken with their positioning to ensure that off target effects are not caused by their presence within coding/regulatory sequence.

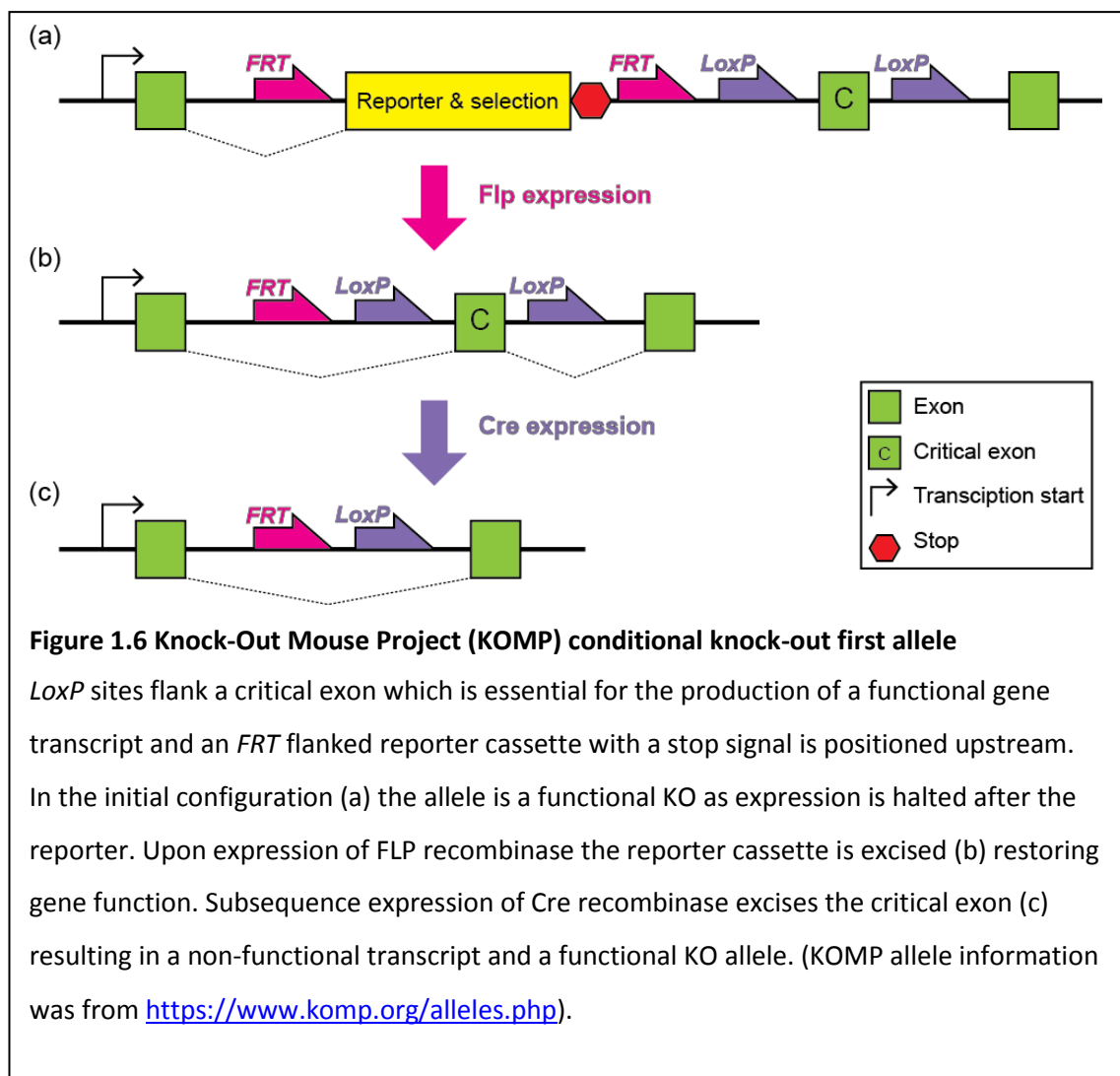
### 1.3.2.2 *CONDITIONAL AND INDUCIBLE CASSETTES*

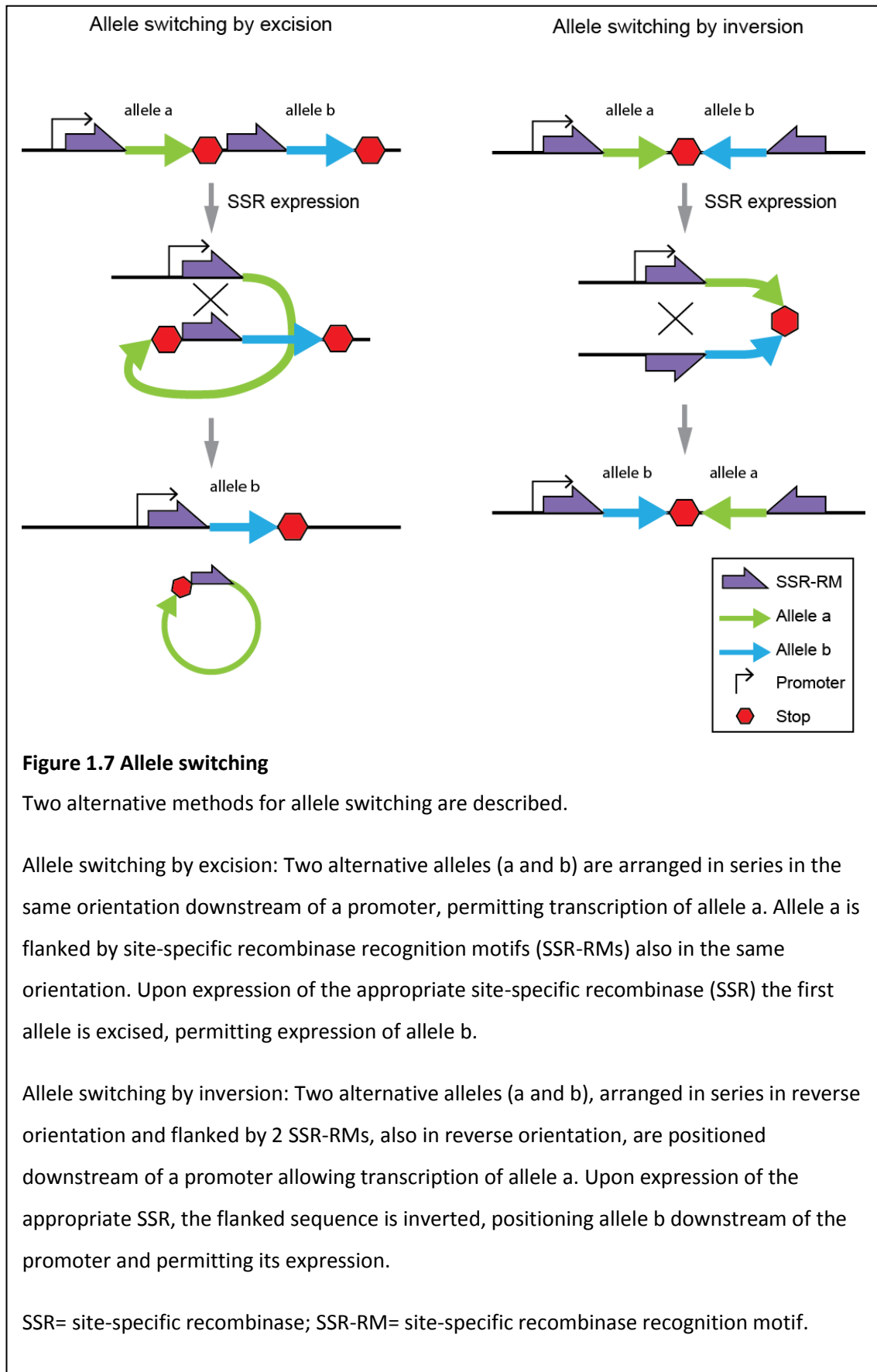
Conditional expression of a transgene can be achieved by engineering the transgene vector to contain the coding sequence of a gene under the control of a tissue specific promoter. Using this technique mutant *SOD1* transgenic mice have been made with expression directed specifically to muscle, using the myosin light chain or the chicken skeletal muscle  $\alpha$ -actin promoter (Dobrowolny et al., 2008; Wong et al., 2010), or specifically to neurons, using the Thy1.2 promoter (Jaarsma et al., 2008).

Inducible transgene expression is also possible. For example, promoter systems have been designed which require a small molecule, such as tetracycline, to dimerise with the transcription factor elements to allow transcription, or the reverse, where small molecules block transcription (Pollock et al., 2002; Rivera, 1998). Animals can be dosed with these molecules in their drinking water and thus expression can be induced or halted at any time.

Conditional or inducible transgenes directing the expression of SSRs can be combined with mice with engineered genomes containing SSR-RM driven “DNA machinery” to allow conditional/inducible editing of the mouse genome *in vivo*. As an illustrative example of how such machinery works, a Knock-Out Mouse Project (KOMP) KO-first strategy as illustrated in

Figure 1.6. KOMP is currently attempting to produce KO alleles for all known mouse genes, and a number of these are being produced using this strategy. Homologous recombination gene targeting is used to insert *LoxP* sites flanking a “critical exon” without which the gene product will become non-functional. Upstream of the 5’ *LoxP* site is an *FRT* flanked cassette containing a reporter and antibiotic selection, for use when targeting the mESCs, with a strong stop signal to halt further transcription. In its initial state, Figure 1.6a, the allele is a functional KO as the normal coding sequence of the gene is disrupted by the reporter/selection cassette. Upon expression of FLP, the reporter/selection cassette is excised, restoring normal transcription of the gene as shown in Figure 1.6b. Upon subsequent expression of Cre, the “critical exon” is excised disrupting the normal coding sequence of the gene and resulting in a function KO as illustrated in Figure 1.6c. Other examples of how SSR-RMs can be used for *in vivo* excision or inversion to switch alleles are shown in Figure 1.7.





### 1.3.2.1 ENHANCING TARGETING WITH ENGINEERED NUCLEASES

Engineered nucleases are a new class of tool for genome editing and include zinc finger nucleases (ZFN) (Hauschild-Quintern et al., 2013), transcription activator-like effector nucleases (TALENs) (Feng et al., 2013), and the clustered regularly interspaced short palindromic repeats (CRISPR) –Cas9 systems (Ran et al., 2013).

There are differences between the various engineered nucleases, however the basic methodology and their application is the same; the nucleases are engineered to target a specific genomic locus where they produce a double stranded DNA break (DSB). DSBs are repaired via 2 major pathways; non-homologous end joining (NHEJ) or HR. Repair via NHEJ frequently results in small insertions or deletions (Bogdanove et al., 2011) at the cut site, which can result in a functional KO by causing a frame shift in the coding sequence (Jones et al., 2014). Alternatively, combining targeted DSBs with HR gene targeting can increase the efficiency of targeted integration, for example when used in conjunction with ZFNs, HR targeting has been reported at 100,000 times increased efficiency (Gaj et al., 2013; Hauschild-Quintern et al., 2013).

### 1.3.2.2 REFINEMENTS IN IN VITRO DNA ENGINEERING

The bedrock of molecular cloning is the use of restriction endonucleases (RE) and DNA ligases to “cut and paste” fragments of DNA between plasmids and these techniques are now standard in labs the world over. A major problem with these techniques is that they depend upon the presence of unique RE sites and manipulations are limited by their locations. Because of this, it is often necessary to include extraneous sequence when designing a vector and this could have unintended/uncontrolled functional repercussions.

Recombineering (recombination-mediated genetic engineering) harnesses the HR pathway of DNA repair, in a similar way to HR gene-targeting, to recombine DNA elements *in vivo* in *Escherichia coli* (*E.coli*) allowing precision manipulation of DNA free from the constraints of RE site location.

Recombineering uses short (from ~50 bp) regions of homology between a linear vector and a resident plasmid to recombine the two and can be used to mutagenize a plasmid recipient, or subclone sequence from a plasmid donor, as shown in Figure 1.8. Recombineering is independent of the endogenous HR pathway and instead depends on a set of proteins which can be expressed either from a transiently transformed plasmid or a cassette stably integrated into the *E.coli* genome. For illustrative purposes the *E. coli*  $\lambda$  phage Red/ET system (Gene Bridges) will be described and is illustrated in Figure 1.9. Several phage or prophage derived

systems have been developed which rely on orthologous sets of proteins, although not all are expressed in all systems.

The protein Red $\alpha$  (also called *exo*, and equivalent to RecE in prophage systems) is a 5'-3' exonuclease. It digests blunt ended linear double stranded DNA (dsDNA) leaving 3' single stranded DNA (ssDNA) overhangs, as shown in Figure 1.9b, and is required for recombineering with dsDNA donors (Hill et al., 1997).

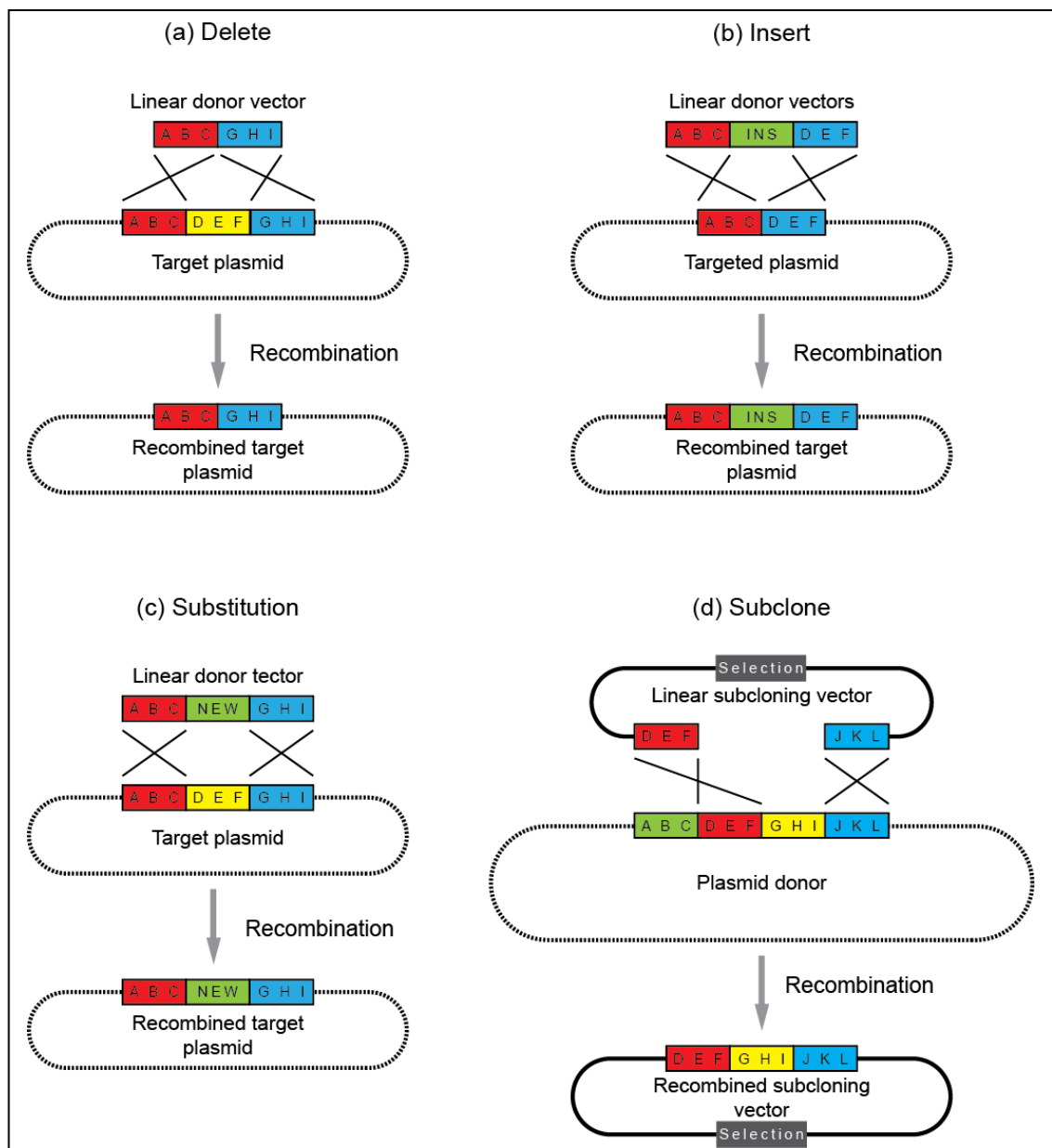


**Figure 1.8 Recombineering strategies**

Strategies are illustrated for engineering deletions (a), insertions (b) or substitutions (c) in a resident target plasmid, or for subcloning out of a resident plasmid (d) by recombineering in *E. coli*. Upstream and downstream homology arms are shown in red and blue, respectively.

Red $\beta$  (also called bet, and is equivalent to RecT in prophage systems) is a ssDNA binding protein which binds to these ssDNA overhangs, protecting them from degradation, as shown in Figure 1.9c. Red $\beta$  also promotes annealing to complementary ssDNA (Karakousis et al., 1998; Muniyappa et al., 1986), and in some situations may promote strand exchange between a dsDNA target and bound ssDNA (Muniyappa et al., 1986; Karakousis et al., 1998). Thus Red $\beta$  promotes the recombination between a linear donor vector and its plasmid target.

A third protein, Gam, blocks the dsDNA exonuclease activity of the endogenous RecBCD protein which, if not blocked, would degrade the linear DNA donor. The use of *recBCD* null *E.coli* is undesirable as these mutants have reduced viability (Friedman et al., 1986).

The RecA protein is also expressed in the Red/ET system. RecA is an endogenous *E.coli* protein, but *RecA* null mutants are usually used for propagation of BACs due the high level of unwanted background recombination that constitutive expression can cause (Hill et al., 2000; Swaminathan et al., 2001). RecA binds ssDNA overhangs, in conjunction with Red $\beta$ , and facilitates strand invasion into homologous dsDNA increasing the HR efficiency, as shown in Figure 1.9d. Targeted HR can also occur in the absence of *RecA*, however efficiency is reduced and thought to depend on plasmid replication for exposing ssDNA on the target plasmid (Court et al., 2002; Wang et al., 2006b; Maresca et al., 2010). The exact mechanisms of  $\lambda$  Red recombination have not yet been elucidated, but it has been suggested that Red $\alpha$  may completely digest dsDNA donors to ssDNA intermediates either before or during the complementation to homologous sequence (Mosberg et al., 2010; Maresca et al., 2010).

The expression of the recombineering proteins must be strictly controlled to reduce unwanted recombination events during plasmid/BAC propagation and the Red/ET plasmid (Figure 1.10) contains several safeguards against unwanted transcription; the pBAD promoter which controls expression of the Red/ET proteins and requires L-arabinose to be added to the culture medium to induce expression (Guzman et al., 1995). Secondly, the plasmid replication of origin, oriR101, is dependent on the temperature sensitive RepA protein (also expressed from pRed/ET) for replication. Temporarily raising the temperature from 30 °C to 37-43 °C makes RepA dysfunctional and the plasmid is quickly lost during cell replication (Miller et al., 1995), further closing the window of potential expression.

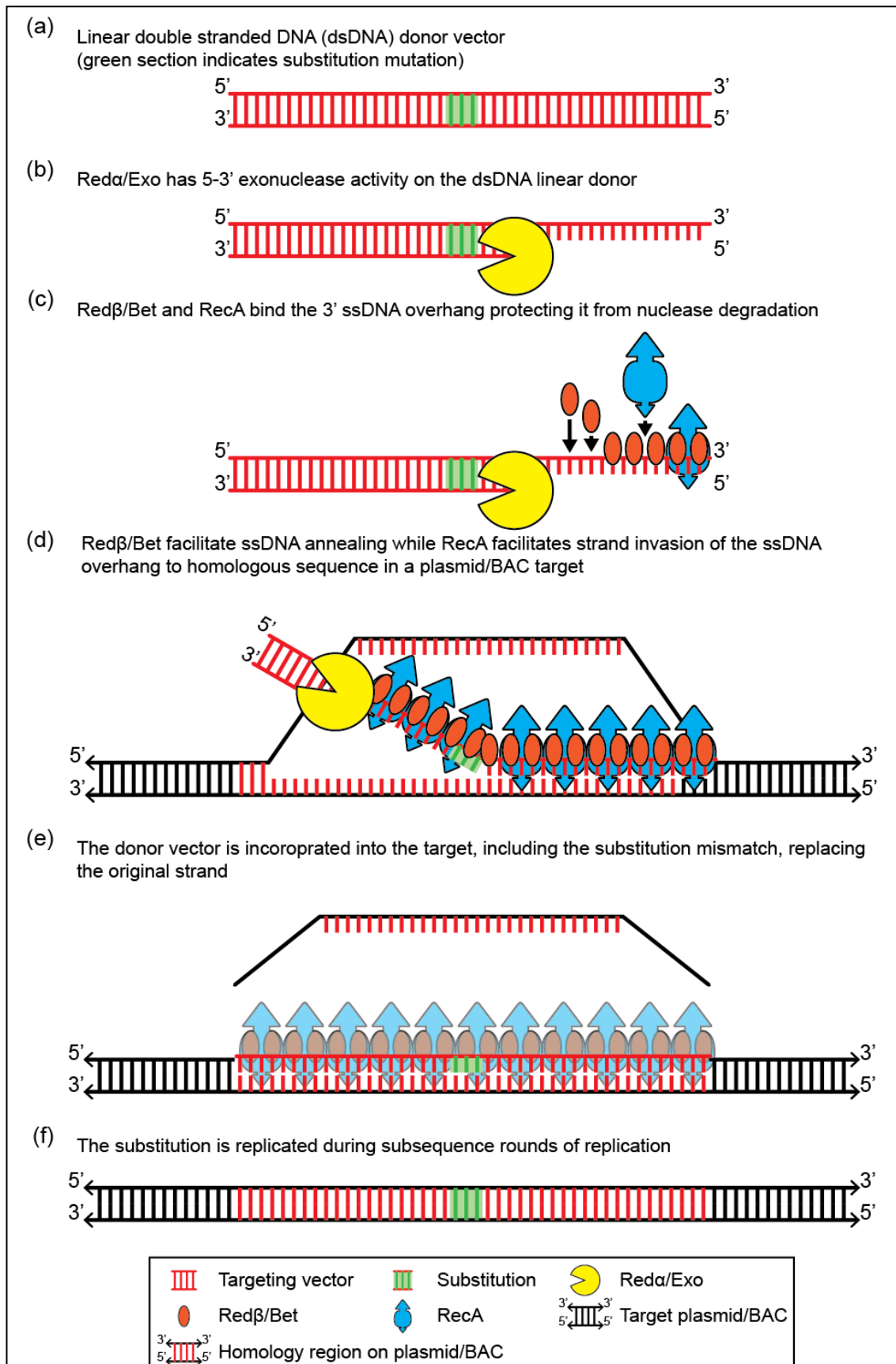


**Figure 1.9 Red/ET recombineering**

(a) a linear double stranded DNA (dsDNA) donor vector comprised on homology arms (red) flanking a desired substitution (green) is introduced into *E.coli* containing a target plasmid.

- (b) Red $\alpha$  creates single stranded DNA (ssDNA) overhangs via its 5-3' exonuclease activity.
- (c) Red $\beta$  binds to the ssDNA overhangs, protecting it from degradation. RecA also binds the ssDNA overhangs.
- (d) Red $\beta$  promotes annealing if the bound ssDNA to complementary ssDNA during replication or when homologous ssDNA is exposed by partial denaturation of dsDNA. RecA facilitates strand invasion of its bound ssDNA into homologous dsDNA.
- (e) facilitated by both Red $\beta$  and RecA, the donor vector is incorporated into the target plasmid.
- (f) upon subsequent replication of the plasmid within the host *E.coli*, the modified DNA is propagated.

ssDNA= single stranded DNA; dsDNA= double stranded DNA

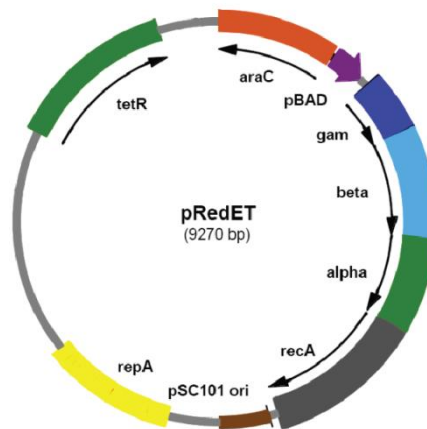


**Figure 1.10 pRed/ET**

The pRed/ET (Gene Bridges) plasmid contains two safeguards against ectopic expression of the Red/ET proteins. *gam*, *red $\beta$* , *red $\alpha$* , and *recA* are all under transcriptional control of the L-arabinose inducible pBAD promoter. The plasmid origin of replication, oriR101, is dependent on expression of the temperature sensitive RepA; by raising the temperature to 37-43°C, RepA becomes dysfunctional and the plasmid can no longer replicate and propagate during cell division.

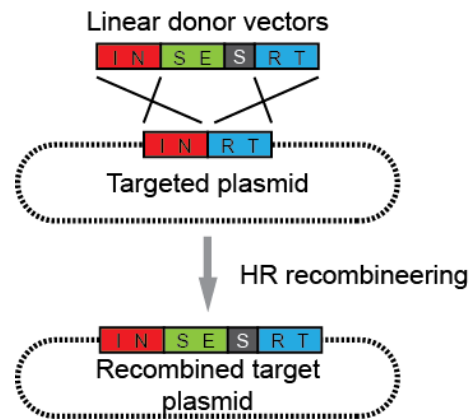
(Plasmid diagram taken from <http://www.genebridges.com/>)



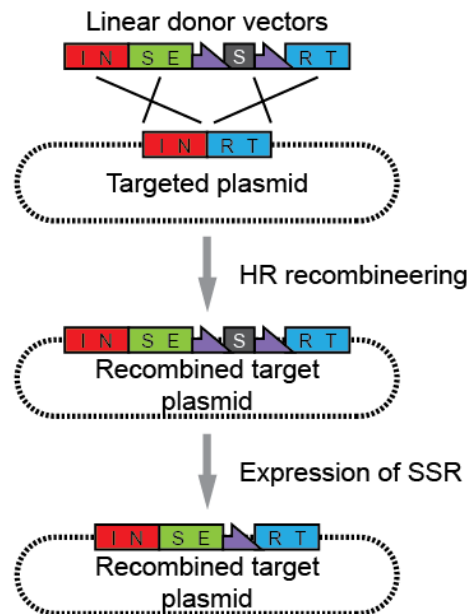
Oligo recombineering, which uses ssDNA oligonucleotide (oligo) donors, appears to be affected primarily by the annealing of the oligo to the lagging strand of the replication fork, with the oligo acting as an Okazaki fragment during DNA extension. This process only requires the Red $\beta$  protein and can occur independent of RecA (Ellis et al., 2001; Maresca et al., 2010; Li et al., 2003). Oligo recombineering is particularly efficient when the oligo is complementary to the lagging strand of the replication fork with reports of point mutations being correctly inserted in over 1% of unselected surviving cells and 24 bp insertions having a success rate of over 0.7% (Swaminathan et al., 2001).

For larger modifications or increased efficiency it is desirable to include a selectable marker with the modifications in order to reduce the number of clones it is necessary to screen. When subcloning, this can be done by selection for the antibiotic resistance present on the backbone of the subcloning vector, as shown in Figure 1.8d. When a resident plasmid/BAC is modified, an antibiotic resistance cassette may be inserted for selection at the same time as the modification is made, however, as shown in Figure 1.11a, this can cause a disruption in the desired sequence. Figure 1.11b shows a method using SSRs to remove the selection cassette leaving a single SSR-RM in its place and Figure 1.11c shows a 2-step recombineering method using a positive/negative selection cassette to produce seamless modifications.

(a) Insertion with selection



(b) Excising selection using SSRs



(c) Seamless insertions using positive/negative selection

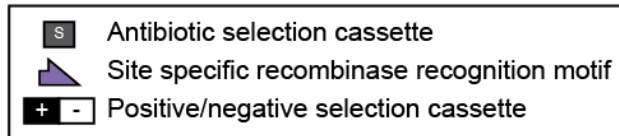
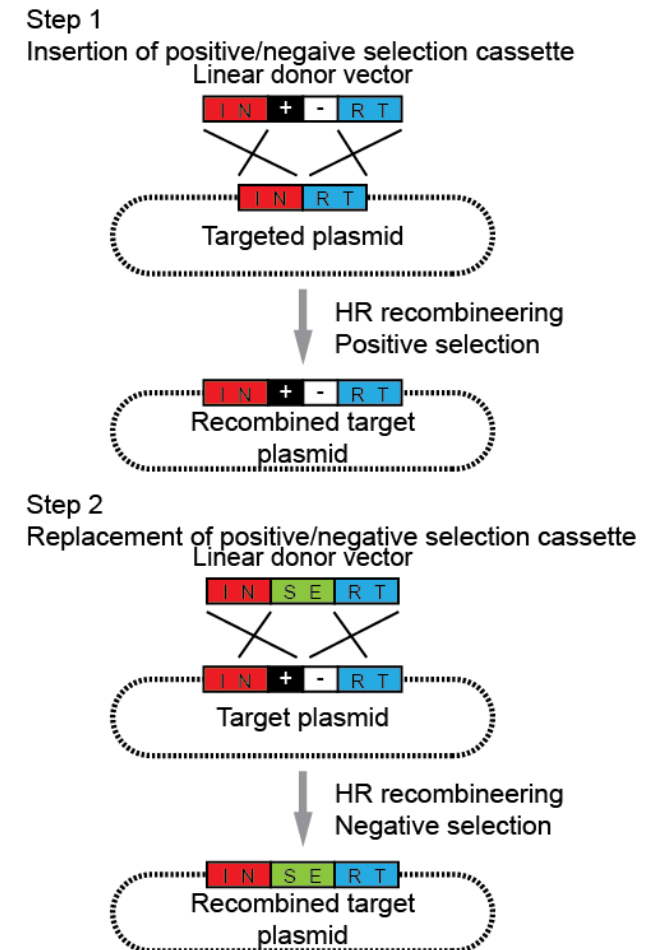


Figure 1.11 Methods for removing antibiotic selection cassettes

(a) Inclusion of an antibiotic selection cassette for reducing background of un-recombined plasmid during recombineering can potentially disrupt the sequence.

(b) By flanking the inserted selection cassette with SSR-RMs the cassette can be deleted, once a correctly recombined clone has been identified, by expression of an appropriate SSR via either a transformed plasmid (Tuntufye et al., 2011) or a stably incorporated, inducible cassette (Warming et al., 2005). This method leaves in place a single SSR-RM which could cause disruption to the desired sequence and precludes further use of this SSR.

(c) Seamless modifications are possible by using positive/negative antibiotic selection cassettes (+/- cassette). The +/- cassette is first inserted into the target location by recombineering and selected for. It is then replaced, again by recombineering, with the desired modification and selected against. In this way it is possible to create seamless modifications to the resident target plasmid (Wang et al., 2009d; Warming et al., 2005; Westenberg et al., 2010).

SSR-RM= with site-specific recombinase recognition motifs; SSR= site-specific recombinase; +/- cassette= positive/negative antibiotic selection cassette

## 1.4 SOD1 MOUSE MODELS

### 1.4.1 SOD1 Transgenic Mice

Just one year after Rosen et al., (1993) discovered the first *SOD1* mutations in ALS, Gurney et al., (1994) presented the first mutant *SOD1* transgenic mice. Table 1.3 summarises a selection of the great number of *SOD1* transgenic mice which have been subsequently produced (a more comprehensive list is presented in Section 7.1, Appendix 1) which includes mice expressing tagged proteins (Watanabe et al., 2005), experimental mutations (Wang et al., 2003; Deng et al., 2008), mutant mouse *Sod1* (Ripps et al., 1995) and conditional/inducible lines (e.g. (Pramatarova et al., 2001; Jaarsma et al., 2008; Wang et al., 2008; Wang et al., 2009b)).

The majority of these mice have been created using an 11.58 kb EcoRI-BamHI fragment of human *SOD1* genomic DNA (gDNA) which includes sufficient promoter sequence (~500 bp) to direct expression of the human SOD1 (huSOD1) in a pattern similar to the endogenous mouse SOD1 (moSOD1) (Epstein et al., 1987). Not all of the mutant SOD1 transgenic mice display ALS like phenotypes (as summarised in Table 1.3 and Section 7.1, Appendix 1). Those that do have varying ages of onset and survival which often correlate with the level of transgene expression and/or the number of copies in the transgene array (e.g. (Wong et al., 1995; Watanabe et al., 2005; Gurney et al., 1994; Tu et al., 1996; Zhang et al., 1997)).

Two of the SOD1 transgenic lines which are used in the work presented in this thesis will be described in more detail in the following subsections.

#### 1.4.1.1 *SOD1*<sup>G93A</sup> TRANSGENIC MOUSE

One of the first SOD1 mutations to be transgenically expressed in mice was the G93A mutation in exon 4 of the *SOD1* gene. Four founder lines were originally established (Gurney et al., 1994). The line used in the work described here, designated as G1H by the original authors (current strain definition: Tg(*SOD1*\*G93A)1Gur, referred to as TgG93A in the following text), is derived from one of these original lines but has a 40% expansion, resulting in 25 copies in the transgene array (Chiu et al., 1995). The transgene, shown in Figure 1.12, was constructed by isolating a 0.54 kb HindIII-NsiI fragment of patient genomic DNA (gDNA), which encompassed the G93A mutant exon 4. This was then cloned into the matching RE sites of a plasmid containing an 11.58 kb EcoRI-BamHI gDNA fragment encompassing the *SOD1* locus (9.31 kb) and flanking sequence (0.48 kb 5' & 1.79 kb 3'), including promoter sequence as described above. The transgene integration site has been mapped to band E of mouse chromosome 12 (Achilli et al., 2005).

**Table 1.3 Mutant SOD1 transgenic mice**

Rows are arranged by the location of the mutation used. Lines used in the work presented in this Thesis are highlighted in yellow. Lines which failed to develop ALS like phenotypes are highlighted in pink.

All figures are for hemizygous mice unless specified. Protein expression and dismutase activity were assayed from spinal cord, unless specified.

(\*1) Protein expression is expressed as fold increase relative to endogenous Sod1 level

(\*2) SOD1 activity is expressed as fold difference compared to NTg

Tg= transgene; Hom= homozygous; nr= not reported; nq= measured but not quantified; yrs= years; (\$) = symptoms and survival shown for homozygotes; (#)= introduces a stop codon at position 133; ¥ = promoter region 483 bp 3' of exon 1; ¼ = EcoRI-BamHI human gDNA fragment is 11.58 kb and included SOD1 gene plus 0.5 kb 5' & 1.8 kb 3'

Mutation	Promoter	Tg fragment	Tg copy	Protein (*1)	Activity (*2)	Symptom onset (weeks)	Survival (weeks)	notes	Ref
WT	Human SOD1 (¥)	gDNA E-B (¼)	7	50 (24 fold in ref 19)	8.6	36 (hom)	367d (hom)		1, 2, 3, 19
A4V	Human SOD1 (¥)	gDNA E-B (¼)	~5	nr	~1.4	none			2
G37R (line 106)	Human SOD1 (¥)	gDNA E-B (¼)	nr	5.3	7.2	22-30	25–29		4
G37R	NFL (see notes)	cDNA		4.3 and 2.8	nr	none (up to 1.5 yrs)	none (up to 1.5 yrs)	Neurofilament light chain (NFL) promoter Neuron specific expression. Two lines reported	5
G37R (see notes)	Mouse prion promoter	cDNA	nr	nq	nq	28-36 (hom)	onset +1-3 weeks	Co-integration of SOD1 transgene with construct encoding wild-type human presenilin 1 (hPS1) with PrP promoter	6

Mutation	Promoter	Tg fragment	Tg copy	Protein (*1)	Activity (*2)	Symptom onset (weeks)	Survival (weeks)	notes	Ref
H46R/H48Q/H63G/H120G (line 125)	Human SOD1 (¥)	gDNA E-B (α)	nr	nq	1	nr	39-52	H46R/H48Q ALS mutations with H63G/H120G experimental mutations to disrupt copper binding	7
E77X (stop)	Human SOD1 (¥)	gDNA E-B (α)	nq	nr	nr	none	normal	RNA "barely detected" Experimental, non-ALS, mutation	8
G85R (line 148)	Human SOD1 (¥)	gDNA E-B (α)	nr	1	1	33	35		9
G85R (line 74)	Human SOD1 (¥)	gDNA E-B (α)	nr	0.2	nr	51-61	onset +2 weeks		9
G85R	Thy1.2	cDNA		nq	nq	none (up to 87)		Bicistronic expression of SOD1 and EGFP in postnatal motor neurons	10
G85R (floxed)	nr	gDNA un-specified fragment	nr	1.5	1	44	50	LoxP flanked transgene	11
G86R (mouse)	nr	gDNA mouse	nr	nr	1	13-17	13-17	Tg made from gDNA mouse SalI fragment, however SalI cuts within intron 3	12
G93A (line G1)	Human SOD1 (¥)	gDNA E-B (α)	18	nr	~4	12-16	20		2
G93A (line G1H)	Human SOD1 (¥)	gDNA E-B (α)	25	17	>4 (8.9 fold in ref 14)	13	19.4	Protein expression described as equal to the N1029 line in ref 16. High transgene copy number derived from G1 line	13, 14, 16
G93A (line G1del)	Human SOD1 (¥)	gDNA E-B (α)	8	nr	nr	28	36	Low transgene copy number derived from G1 line	15, 16
G93A (line T1 crossed to line T3)	Thy1.2	cDNA	nr			77-104	84-104	Postnatal motor neurons specific expression. Double transgenic line produced by crossing 2 independent Thy1.2 transgenic lines	17
L126delTT (#) (line D1)	Human SOD1 (¥)	gDNA E-B (α)	1	nr	nr	none			18
L126delTT (#) (line D2)	Human SOD1 (¥)	gDNA E-B (α)	5	See notes	1	63 (34 in hom)	68 (36 in hom)	Protein: below western detection threshold	18

Mutation	Promoter	Tg fragment	Tg copy	Protein (*1)	Activity (*2)	Symptom onset (weeks)	Survival (weeks)	notes	Ref
L126delTT-FLAG (#) (line DF2)	Human SOD1 (¥)	gDNA E-B (ㄨ)	3	nr	nr	none		FLAG tagged SOD1	18
L126delTT-FLAG (#) (line DF7)	Human SOD1 (¥)	gDNA E-B (ㄨ)	4	nq	1	49 (17 for hom)	53 (18 for hom)	FLAG tagged SOD1	18

1- (Graffmo et al., 2012); 2- (Gurney et al., 1994); 3- (Jaarsma et al., 2000); 4- (Wong et al., 1995); 5- (Pramatarova et al., 2001); 6- (Wang et al., 2005b); 7- (Wang et al., 2003); 8- (Deng et al., 2008); 9- (Bruijn et al., 1997); 10- (Lino et al., 2002); 11- (Wang et al., 2009b); 12- (Ripps et al., 1995); 13- (Chiu et al., 1995); 14- (Tu et al., 1996); 15- (Zhang et al., 1997); 16- (Gurney, 1997); 17- (Jaarsma et al., 2008); 18- (Watanabe et al., 2005); 19- (Jonsson et al., 2006b).

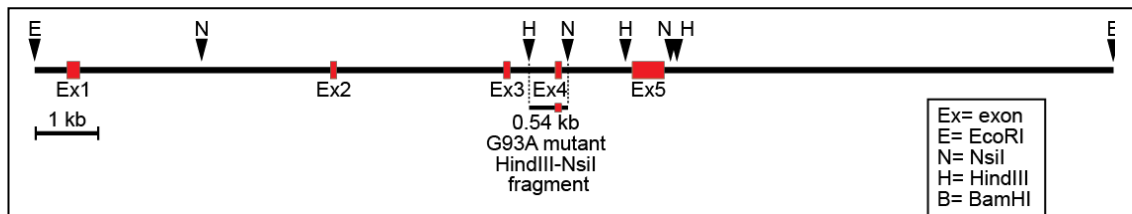


**Figure 1.12 SOD1 transgene**

The 11.58 kb EcoRI-BamHI human gDNA fragment used for transgene construction by Gurney et al., (1994) is shown. The 0.54 kb HindIII-NsI fragment was isolated patient gDNA containing exon 4 in which the G93A mutation is located. This was then cloned into the matching HindIII-NsI sites in the full length fragment. The transgene encompasses the *SOD1* locus (9.31 kb) and is flanked by 0.48 kb 5' and 1.79 kb 3'.

These mice were described in detail by Chiu et al., (1995) who maintained them on a BL6/SJL background. The first sign of disease is a plateau, and then gradual loss, of body weight starting at around 75-days of age. A fine tremor in one or more of the limbs is the typical first sign of motor disturbance seen in these mice at around 13-weeks of age and spreading to all limbs with increasing age. Spasticity (increased resistance of limbs), limb-grasping (crossing of limbs in toward the body when held by the tail, rather than the usual splaying of limbs) and clonus (a rhythmic tremor in response to forced flexion) develop along with weakness and atrophy of the muscles especially evident in the hind limbs. Gait disturbance, in the form of a dropped pelvis, becomes apparent and as strength in the hind limbs deteriorates the mouse appears to drag the body using the forelimbs. As degeneration proceeds, tremor and spasticity are reduced presumably due to decreasing muscle force. The animals reach the end stage, defined by Chiu et al., (1995) as an inability to right themselves within 30 seconds when placed on their sides, at an average of 136-days when the mice had also lost 10% of their body weight and had coarsened fur due to a lack of grooming. Loss of muscle strength can be detected at 40-days of age using electrophysiological techniques and the pattern of loss is suggestive of a preferential loss, or decline in functionality, of larger MNs innervating faster muscle fibres (Hegedus et al., 2007; Hegedus et al., 2008), similar to the pattern seen in ALS patients (Dengler et al., 1990).

This mouse line has a progressive loss of spinal MNs apparent from 100-days of age resulting in a 50% loss of MNs within the cervical and lumbar SC by end stage (Gould et al., 2006; Fischer et al., 2004; Chiu et al., 1995). Vacuolated SC MNs are apparent from ~80-days, later spreading to the brain stem (Fischer et al., 2004; Dal Canto et al., 1994). Vacuoles are also present in the mitochondria, which are morphologically abnormal, with signs of “unravelling” of the membranes (Dal Canto et al., 1994). Denervation and reinnervation of skeletal muscles can be



detected from 47-days of age and by 80-days axonal degeneration can be detected in the ventral roots, with preferential loss of large calibre axons (Chiu et al., 1995; Fischer et al., 2004). Astrocytosis is also apparent in the SC from 82-days of age (Tu et al., 1996) and swollen axons containing spheroid neurofilament inclusions are present in the ventral SC from 82-days of age, worsening with age (Tu et al., 1996; Gurney et al., 1994). Inclusions containing SOD1 are prevalent, especially in the ventral horn MNs (Gurney et al., 1994). p62 staining becomes apparent from 35-days of age and ubiquitin aggregation from 60-days, and by 120-days p62, ubiquitin and SOD1 are co-localised (Gal et al., 2007). TDP43 pathology is typically reported as absent in this and other mutant SOD1 transgenic mice (Robertson et al., 2007), although TDP43 mislocalisation has been reported once, at end stage in this mouse line (Shan et al., 2009).

#### *1.4.1.2 SOD1<sup>WT</sup> TRANSGENIC MOUSE*

When the first G93A mutant *SOD1* transgenic line was made, 3 wild-type (WT) *SOD1* transgenic lines were also established (Gurney et al., 1994) one of which (referred to as N1029/N29 in the original papers, current strain definition Tg(SOD1)2Gur) is used in the work presented in this thesis and referred to as TgWT. This mouse was made using the same EcoRI-BamHI gDNA fragment as described above and is thought to carry 7 copies in the transgene array. They are reported to have comparable huSOD1 protein expression to the TgG93A line (3.2 vs. 4.3 ng/μg total brain protein, G93A vs. WT) and both have 4 times the normal level of huSOD1 activity (Tu et al., 1996), although not all reports agree (e.g. (Graffmo et al., 2012; Jaarsma et al., 2000)). This line is commonly used as a control for the TgG93A mouse. This TgWT line was originally reported as free from motor deficits up to 1 year of age (Chiu et al., 1995; Dal Canto et al., 1995; Tu et al., 1996) however, elsewhere mild motor deficits have been reported from 58-weeks of age (Jaarsma et al., 2000).

Strong SOD1 staining is seen in the lateral ventral horn (Gurney et al., 1994) and throughout the SC grey matter in the TgWT mouse. Staining is homogeneously distributed at an early age but becomes stronger and less homogeneous from 30-weeks of age when it appears focussed within the axons of the MNs (Jaarsma et al., 2000). SOD1 inclusions are present in the ventral horn MNs and ventral root by 86-weeks (1.7-years) (Jonsson et al., 2006b). Mild axonal degeneration and vacuolisation is seen from 30-35-weeks of age (Jaarsma et al., 2000; Chiu et al., 1995; Dal Canto et al., 1995), however no indication of denervation/reinnervation of the skeletal muscles was noted when examined at a similar age (Chiu et al., 1995).

Neurofilament and mitochondrial pathology which is qualitatively similar to that seen in the TgG93A line has also been noted, although it is less severe and occurs at a later age, for example the neurofilament pathology appears at 18.6-weeks rather than 11.7 (Tu et al., 1996;

Dal Canto et al., 1995; Jaarsma et al., 2000). Similarly, MN vacuolisation (Tu et al., 1996), gliosis (Jaarsma et al., 2000), MN degeneration and death (Jaarsma et al., 2000) have all been reported but to a milder extent and with a later occurrence than in the TgG93A line, as summarised in Table 1.4.

**Table 1.4 Comparison of disease related phenotype seen in TgWT and TgG93A mice**

	<b>WT</b>	<b>G93A</b>
<b>Motor deficits</b>	58-weeks mild (1)	Onset:13-weeks (91-days) Paralysis: 19.4-weeks (136-days) (2)
<b>Muscle denervation/reinnervation</b>	not seen upto 38-weeks (2)	6.7-weeks (47-days) (5, 6)
<b>Axonal degeneration</b>	30-35 weeks(1, 2, 3)	11.4-weeks (80-days) (5, 6)
<b>Neurofilament pathology</b>	18.6- weeks (130-days) (4)	11.7-weeks (82-days) (4)
<b>Mitochondrial vacuolisation</b>	30-40-weeks (1)	5.3-weeks (37-days) (2)
<b>MN vacuolisation</b>	28.5-weeks (4)	11.4-weeks (80-days) (5, 6)
<b>Astrocytosis</b>	50-60-weeks (1)	14.3-weeks (100-days) (7)
<b>Microgliosis</b>	30-weeks white matter 75-weeks to 2-years grey matter (1)	14.3-weeks (100-days) (7)
<b>Ubiquitin pathology</b>	2-years (in neurites) (1)	8.6-weeks (60-days) (8)
<b>Motor neuron loss</b>	20-30% at 2 years (1)	From 100-days (14.3 weeks). 50% loss by end stage (5)

1- (Jaarsma et al., 2000); 2- (Chiu et al., 1995); 3- (Dal Canto et al., 1995); 4- (Tu et al., 1996); 5- (Fischer et al., 2004); 6- (Gould et al., 2006); 7- (Hall et al., 1998); 8- (Gal et al.,

Of note, Graffmo et al., (2012) recently examined homozygous TgWT mice and reported the same phenotype as TgG93A mice but with a longer time-scale; hind limb weakness occurring around 36-weeks (253-days) and end-stage by 52-weeks (367-days). Misfolded SOD1 and astrocytosis was detected in the SC from 100-days and 40% loss of MNs in the thoracic SC was

reported at end stage. These homozygous mice were described as expressing huSOD1 at an equal level to hemizygous TgG93A mice, contrary to other comparisons (e.g. (Tu et al., 1996)) and had been bred onto a different background due to a failure to produce homozygotes on the original C57BL/6J background. Effects of background strain will be discussed in Section 1.4.3.

### 1.4.2 *Sod1* KO Models

A third mouse used in the work described in this thesis is a *Sod1* KO mouse created by Matzuk et al., (1998), designated *Sod1*<sup>tm1Leb</sup>. This mouse was created by targeting a PGK-*Hprt* cassette to delete exons 1 and 2 of the endogenous *Sod1* gene resulting in a complete absence of the protein product in homozygous KO mice (Matzuk et al., 1998). These mice do not develop an ALS like phenotype, helping to delineate the gain of function mechanism of mutant *SOD1* toxicity. All of the following phenotypes refer to the homozygous null mice.

*Sod1*<sup>tm1Leb</sup> mice suffer from a range of phenotypes, many related to premature ageing, including impaired fertility (Ishii et al., 2005; Matzuk et al., 1998; Noda et al., 2012; Tsunoda et al., 2012), vascular dysfunction (Groleau et al., 2011; Didion et al., 2002), impaired endothelium vasodilation (Cooke et al., 2003; Morikawa et al., 2003), age related hearing loss (Keithley et al., 2005; Johnson et al., 2010b), age-related macular degeneration (Imamura et al., 2006; Hashizume et al., 2008), and premature aging of the skin (Murakami et al., 2009).

These mice also display some phenotypes relevant to MN degeneration, such as accelerated denervation of the skeletal muscles appearing to a mild extent at 1.5-months and prominently by 10-months (Kostrominova, 2010). This phenotype has been more extensively examined in another *Sod1* null mouse (*Sod1*<sup>tm1Cje</sup>) but findings related from either line are expected to be comparable as they are both targeted mutations with a complete absence of moSOD1 protein (Huang et al., 1997). *Sod1*<sup>tm1Leb</sup> mice have been reported as suffering a more profound muscle denervation than the *Sod1*<sup>tm1Cje</sup> mice, however the 2 lines were compared on different genetic backgrounds which could account for this (Kostrominova, 2009). Effects of background strain will be discussed further in Section 1.4.3. *Sod1*<sup>tm1Cje</sup> mice show reduced motor coordination at 13-months of age along with tremor and gait abnormalities. An age related loss of muscle mass is detectable from 3-4-months developing to ~50% loss in the hind limbs by 20-months, with the decrease in muscle size apparently being due to a preferential loss of fast muscle fibres (Muller et al., 2006; Jang et al., 2010). Muscle denervation is also accelerated with 78% of neuromuscular junctions (NMJs. See Figure 1.1) denervated by 18-months, whereas no denervated NMJs were detected in wild-type mice of the same age (Jang et al., 2010). Similar results have also been obtained in another *Sod1* KO line (e.g. *Sod1*<sup>tm1Cep</sup>)(Shefner et al., 1999; Flood et al., 1999). Histological abnormality of the muscle mitochondria is reported from 22-

months and mitochondria isolated from *Sod1* KO muscles are dysfunctional, with 75% decrease in ATP production and 3-fold increase in hydrogen peroxide production at 20-months of age (Jang et al., 2010). Although some of the phenotypes of *Sod1* null mice have been described as premature aging, evidence suggests that the reduction in muscle strength is qualitatively different to that seen in old age (Larkin et al., 2011; Larkin et al., 2013).

### 1.4.3 Effects of Background Strain on Phenotypes

Inbred mouse strains are used in order to minimise background genetic heterogeneity in order to isolate the effects of a particular mutation or genetic manipulation. Many strains of inbred mice exist and phenotypes related to a particular mutation can differ depending on the background strain onto which it is bred. This must be taken into consideration when comparing results obtained on different backgrounds.

The original *SOD1*<sup>G93A</sup> transgenic mouse line (Gurney et al., 1994) was produced using F1 BL6SJL oocytes and bred by crossing to B6SJL F1 mice. This involves mating a C57BL/6 female to an SJL male to produce BL6SJL F1 mice which are heterozygous at every genomic locus (e.g. one allele is from C57BL/6 and the other is from SJL as illustrated in Figure 1.13). A female BL6SJL F1 is then crossed to a male from the transgenic colony, producing BL6SJL F2 offspring. As illustrated in Figure 1.13, at this point genetic heterogeneity is introduced. At each genomic locus, offspring from this cross will have a 50% chance of being heterozygous and 25% chance of being homozygous for either of the original alleles. As genetic variability can result in phenotypic variability it is often desirable to use a pure inbred line to produce a congenic to this strain. This is achieved by backcrossing the donor line to a recipient inbred line for 10 generations, resulting in ~99.8% of all genomic loci being homozygous for the recipient allele (Silver, 1995).

In TgG93A mice, Mead et al., (2011) found that the time to reach end stage was significantly less variable when mice are congenic to C57BL/6J compared to a B6SJL background. Figure 1.14 illustrates the variance of survival times measured for TgG93A mice on different background strains. Heterogeneity between publications may be due to different humane end points or genetic drift (including changes in the transgene copy number), so data are grouped by publication. Differences in disease onset, electrophysiological measures of disease progression, drug response and both quantitative and qualitative difference in MN transcriptome profiles are also seen between TgG93A on different background strains (Wooley et al., 2005; Mancuso et al., 2012; Nardo et al., 2013; Pizzasegola et al., 2009; Pan et al., 2012).

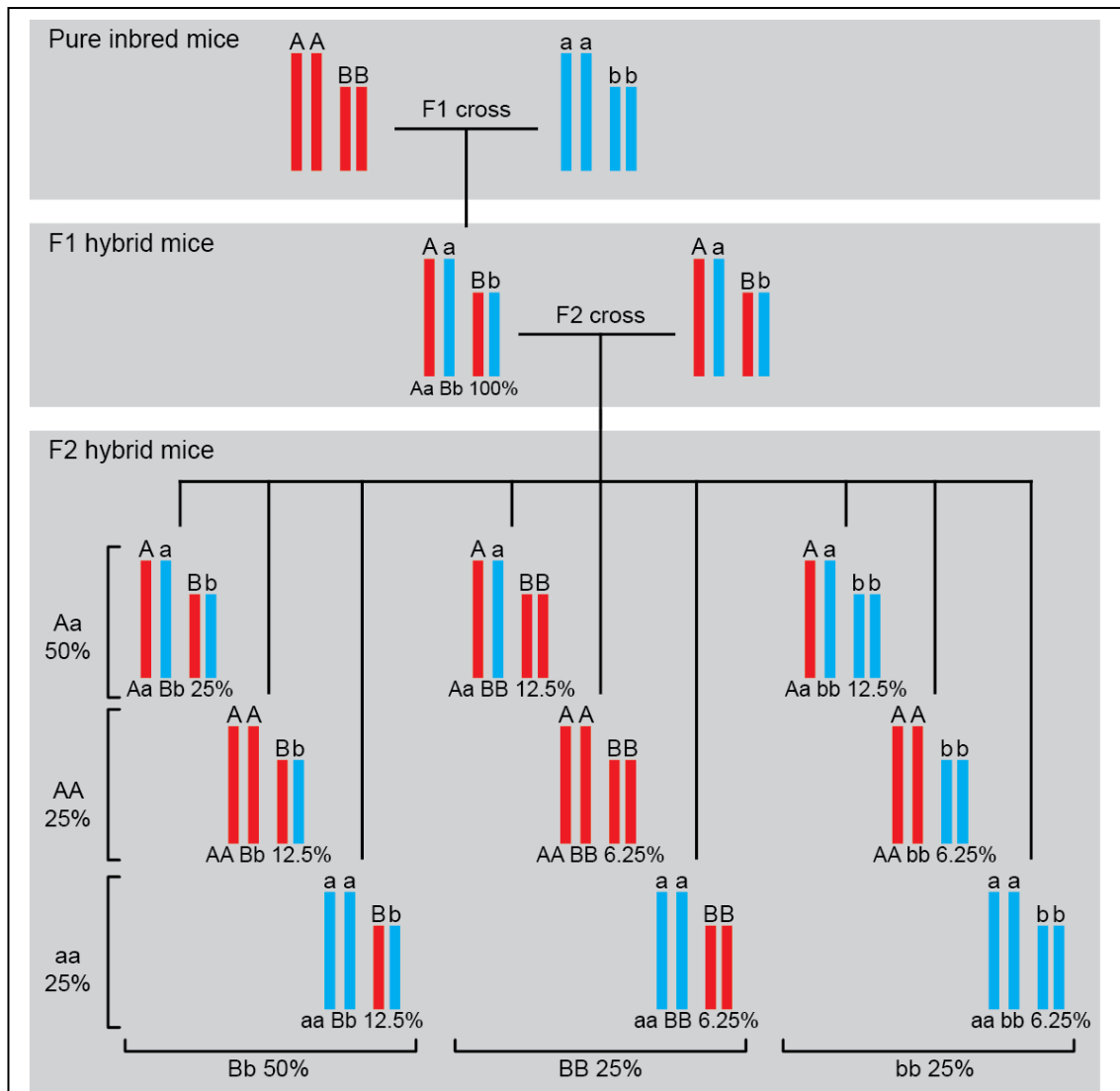


**Figure 1.13 Genetic heterogeneity of F2 hybrids**

The figure illustrates the level of genetic heterogeneity introduced at an F2 cross. The proportion of offspring with the genonotype illustrated is labelled. As can be seen, in an F1 hybrid every animal is heterozygous at every genetic locus (Aa and Bb). In an F2 hybrid there is a 50% chance of each locus being heterozygous (Aa or Bb), and a 25% chance of each locus being homozygous for either of the original parental strain alleles (AA or aa and BB or bb). This example uses just 2 loci, and without recombination, to illustrate the considerable heterogeneity present in an F2 hybrid.

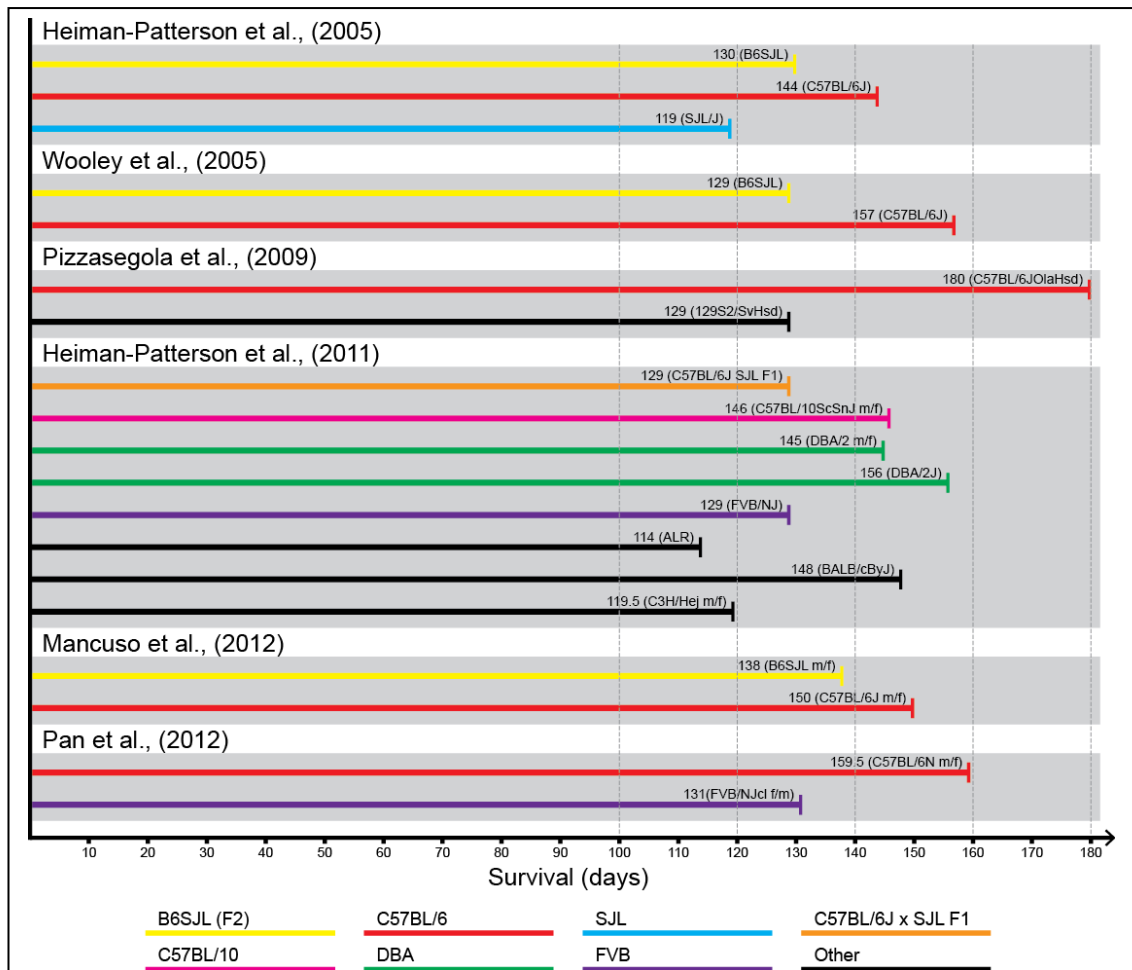


**Figure 1.14 Background strain effects on survival of TgG93A mice**

The figure shows survival time for TgG93A transgenic mice congenic on various inbred strains or maintained by mating to an F1 hybrid taken from papers which present data for 2 or more background strains. Where male and female survival was given separately, the average is plotted. Data are colour coded according background strain and grouped by publication as variation can arise from differences between end-point definition and due variation in the transgene copy number between labs. The paper by Heiman-Patterson et.al. (2011) includes data collected in different labs. The full strain ID is given above each line along with survival in days.

Sexual dimorphism in the onset and survival of TgG93A mice is also reported, and this is itself further augmented by background strain (Heiman-Patterson et al., 2005; Mancuso et al., 2012; Pan et al., 2012). These background and gender differences are not due to changes in expression levels of the transgene (Heiman-Patterson et al., 2011; Mancuso et al., 2012; Nardo et al., 2013; Pan et al., 2012) and similar effects have also been reported with other *SOD1* transgenes (e.g. (Kunst et al., 2000; Graffmo et al., 2012; Acevedo-Arozena et al., 2011; Pan et al., 2012)).

As summarised in Table 1.5, there is also significant variation between inbred lines in spinal column vertebrae composition and some lines show greater within strain variation than others (Green, 1941; Green, 1951; McLaren et al., 1955; Rigaud et al., 2008). Strain differences in the underlying SC neuroanatomy are also apparent, for example although the sciatic nerve of both DBA/2J and C57BL/6J mice is composed primarily of L3 and L4 nerves, in DBA/2J mice the contribution of L3 and L4 is equal, whereas in C57BL/6J mice it is predominantly composed of L4 nerves (Rigaud et al., 2008).

**Table 1.5 Variation in spinal vertebrae in different inbred lines of mice**

The number shown is the percentage of mice identified with the combinations of thoracic and lumbar spinal vertebrae number indicated at the top of the table.

The table is arranged by strain. Where a single configuration is present more than 75% of the time, these are highlighted in bright green. Where a single configuration is present between 74-25% it is highlighted in blue.

Asym= asymmetrical; na= not analysed

Thoracic	Number of vertebrae												ref
	13	14	na	13	14	na	12	13	14	na	12	13	
Lumbar	5	5	5	5 (asym 6th)	5 (asym 6th)	5 (asym 6th)	6	6	6	6	7	7	
C57BL	2.1			2.5				95.4					1
C57BL	0.4			1.7				97.8					1
C57BL/How			0.5			0.5				98.9			2
C57BL/6J			6			8				86			3
C3H	96.5			2.5				1					1
C3H/Bi (Craigie)			78.7			16				5.3			2
C3H/Bi (Green)			95.3			2.3				2.3			2
C3H/St			98.9			1.1							2
DBA	95.3			2.9				1.8					1
DBA/2J			97			3							3
BalbC		54			16.5			11	18.1				4
C	58.2			7.2				34.6					1
Bagg albino		56			13.5			17.8	12.5			0.2	1



	Number of vertebrae												
Thoracic	13	14	na	13	14	na	12	13	14	na	12	13	
Lumbar	5	5	5	5 (asym 6th)	5 (asym 6th)	5 (asym 6th)	6	6	6	6	7	7	ref
L		59			11.7			11.3	18				1
P				8.4			88.1				3.6		1
A	2.1			4.2				93.7					1
Leaden	1.1	0.3		2.9				95.7					1
N	0.6			2.6				96.8					1
Gates				1.9			2.5	15.3			80.3		1

1- (Green, 1941); 2- (McLaren et al., 1955); 3- (Rigaud et al., 2008); 4- (Green, 1951).

## **1.5 HOW DO MUTATIONS IN *SOD1* CAUSE ALS?**

### **1.5.1 The Effect of Mutations on *SOD1* Function**

When mutations in *SOD1* were first identified it was suggested that a loss or reduction of dismutase activity might be the cause of disease (e.g. (Rosen et al., 1993; Bowling et al., 1993; Deng et al., 1993)) and consistent with this idea, reduced activity was identified in red blood cells (RBCs) of *SOD1*-fALS cases (Deng et al., 1993; Bowling et al., 1993; Robberecht et al., 1994). This theory was quickly dismissed; in mouse models, rather than reduced *SOD1* activity producing ALS like symptoms (Reaume et al., 1996), expression of mutant hu*SOD1* in conjunction with endogenous mo*SOD1* resulted in ALS like symptoms despite often increased activity levels (e.g. (Dal Canto et al., 1994; Wong et al., 1995; Ripps et al., 1995; Bruijn et al., 1998)). Direct assay of a variety of ALS mutants also revealed that many retained full activity (Borchelt et al., 1994).

Derlin-1 binding has been demonstrated as increased in 124 ALS *SOD1* mutants, suggesting that *SOD1*'s putative function in ER-stress activation may be pathologically perturbed in *SOD1*-fALS (Fujisawa et al., 2012; Homma et al., 2013). Indeed blocking mutant *SOD1* – Derlin-1 interaction attenuated toxicity in primary spinal MN culture lending further credence to this proposed mechanism of toxicity (Nishitoh et al., 2008). However, although a CNS specific interaction of Derlin-1 and mutant *SOD1* has been shown in a transgenic *SOD1*-fALS mouse (Nishitoh et al., 2008), the functional consequence of this interaction have not yet been demonstrated outside of cell culture. Also of note, Derlin-1 has not been identified in unbiased screens for mutant *SOD1* interactors in *SOD1*-fALS mice (e.g. (Watanabe et al., 2008; Zetterström et al., 2011)).

The effect of ALS mutations on the recently proposed role of *SOD1* in glucose/oxygen dependent respiration repression have not yet been evaluated, however mutation of copper binding residues (resulting in dismutase inactive *SOD1*) does block this activity (Reddi et al., 2013).

### **1.5.2 The Effect of Mutations on Biochemical Characteristics of *SOD1***

ALS causing mutations in *SOD1* are found throughout the aa sequence, affecting all domains of the protein and are sometimes categorised as “wild-type like” (WTL) or “metal binding mutants” (MBM) according to their abilities to bind metal ions and form an enzymatically active dimer (e.g. (Rodriguez et al., 2002)).

Decreased thermal stability, increased aggregation propensity and increased dimer dissociation have all been associated with ALS mutation of *SOD1* (Rodriguez et al., 2002;

Vassall et al., 2011; Khare et al., 2004; Khare et al., 2006; Lindberg et al., 2002). Attempts to correlate disease severity with enzymatic activity, half-life, proteolysis resistance, mutation position, protein charge and aggregation propensity both *in vivo* and *in vitro* have generally failed to produce convincing associations (e.g. (Prudencio et al., 2009b; Vassall et al., 2011; Lindberg et al., 2002; Ratovitski et al., 1999)).

A correlation between decreased thermal stability of apo (metal free) SOD1 mutants with decreased disease duration was proposed but at present, is based on a limited number of mutations (Lindberg et al., 2002; Kitamura et al., 2011). A link has also been suggested between the propensity of the mutant SOD1 dimer to dissociate into monomers and the severity of the disease; specifically, when glutathionylation of SOD1 is taken into consideration a correlation is apparent (McAlary et al., 2013).

### **1.5.3 Proposed Pathogenic Mechanisms in SOD1-fALS**

Although many ALS disease mechanisms have been proposed, often as a result of investigation of SOD1-fALS mice, at present it is unknown which are the primary causes of degeneration and which are secondary or downstream consequences of disease. Here a brief description is given of some of the main proposed mechanisms with a focus on those directly relevant to SOD1-fALS and those elucidated using SOD1-fALS mouse models.

#### ***1.5.3.1 OXIDATIVE STRESS***

There is a trend towards a ~50% reduction in SOD1 activity assayed from SOD1-fALS patient tissue, independent of the effect of the same mutation on recombinant SOD1 (Saccon et al., 2013). Several other lines of evidence also suggest that oxidative stress may be involved in ALS, even if it is not caused by loss of SOD1 function as a direct consequence of mutation.

Oxidative damage of proteins, lipids, DNA and mRNA along with other markers of increased oxidative stress are present in the SC of SOD1-fALS, and some sALS cases, post mortem and have been detected in peripheral bodily fluids (urine, blood, cerebrospinal fluid) of ALS patients (Bowling et al., 1993; Abe et al., 1995; Shaw et al., 1995; Beal et al., 1997; Ferrante et al., 1997a; Smith et al., 1998; Tohgi et al., 1999; Bogdanov et al., 2000; Sasaki et al., 2000; Shibata et al., 2001; Shibata et al., 2004; Simpson et al., 2004; Babu et al., 2008; Chang et al., 2008; Murata et al., 2008; Cova et al., 2010) with levels reportedly correlating with disease measures in some cases (Bogdanov et al., 2000; Murata et al., 2008; Cova et al., 2010).

These findings are mirrored in SOD1-fALS mouse models (e.g. (Ferrante et al., 1997b; Andrus et al., 1998; Poon et al., 2005; Liu et al., 1998; Liu et al., 1999; Casoni et al., 2005; Liu et al., 2007; Cha et al., 2000; Lee et al., 2009)), where SOD1 is itself identified as heavily oxidised (Andrus et al., 1998). This is of interest as oxidation is implicated in the monomerisation, misfolding and

aggregation of both WT and mutant SOD1 (Rakhit et al., 2002; Ezzi et al., 2007; Wilcox et al., 2009). Also of note, oxidised mRNA species identified in the SC of SOD1-fALS mice are enriched for transcripts involved in mitochondrial function, cytoskeleton and protein synthesis, folding and degradation, all of which are implicated in ALS (Chang et al., 2008).

Increased pro-oxidant activity has actually been demonstrated for some ALS SOD1 mutants (Yim et al., 1996; Yim et al., 1997; Wiedau-Pazos et al., 1996; Roe et al., 2002; Elliott, 2001), however, this is unlikely to be a primary cause of disease as, just like its anti-oxidant activity, this is dependent on copper binding and SOD1 with reduced or ablated copper binding is still capable of affecting disease (Subramaniam et al., 2002; Wang et al., 2003).

### *1.5.3.2 MITOCHONDRIAL DYSFUNCTION*

Structural abnormalities of the mitochondria are reported in sALS MNs (Sasaki et al., 1996b; Siklós et al., 1996) and are highly cited in SOD1-fALS mouse models (e.g. (Dal Canto et al., 1994; Dal Canto et al., 1995; Wong et al., 1995; Kong et al., 1998; Martin et al., 2007)).

Furthermore, mitochondrial function is severely impaired in MNs of SOD1-fALS mouse models, and in post mortem CNS, blood and muscle biopsy of ALS patients (Mattiuzzi et al., 2002; Jung et al., 2002; Martin et al., 2007; Fujita et al., 1996; Swerdlow et al., 1998; Wiedemann et al., 1998; Vielhaber et al., 1999; Crugnola et al., 2010), although muscle abnormalities may not be specific to ALS (Krasnianski et al., 2005).

It has been proposed that an increased propensity to localise to the mitochondrial IMS of mutant, compared to WT, SOD1 may result in impaired mitochondrial respiratory capacity (Ferri et al., 2006). Mutant SOD1 targeted specifically to the IMS in mice impairs mitochondrial respiratory capacity and reproduces some key ALS like symptoms including MN loss and muscular weakness and wasting, although muscle denervation is not observed (Igoudjil et al., 2011). This suggests that mutant SOD1 can affect toxicity at the mitochondria, however localisation to other cellular compartments may be required to recapitulate the full ALS phenotype.

### *1.5.3.3 ENDOPLASMIC RETICULUM-STRESS AND THE UNFOLDED PROTEIN RESPONSE (UPR)*

Newly synthesised proteins are guided in their correct folding by chaperones within the ER. Overloading of the ER results in ER-stress, eliciting the unfolded protein response (UPR), the suppression of protein translation and eventually apoptosis (Schröder, 2008). As described above, SOD1 is implicated in the activation of ER-stress with mutations potentially increasing its activity in this pathway (Homma et al., 2013; Nishitoh et al., 2008; Fujisawa et al., 2012).

Markers of increased ER-stress are present in ALS patient tissue (Atkin et al., 2008; Ito et al., 2009) and in SOD1-fALS mice (Kikuchi et al., 2006; Saxena et al., 2009; Ito et al., 2009).

Manipulation of the UPR, by genetic or pharmacological means, has been shown to affect the degenerative process of SOD1-fALS mice (Wang et al., 2011b; Kalmar et al., 2008; Kiernan et al., 2004). However, distinguishing a specific effect of mutant SOD1 from a non-specific overload of the ER potentially caused by the transgenic overexpression of a mutant protein makes interpretation challenging.

#### *1.5.3.4 AXONAL TRANSPORT DEFICITS*

Slow anterograde and fast retrograde axonal transport deficits are apparent in most SOD1-fALS mice ((Zhang et al., 1997; Williamson et al., 1999; Bilsland et al., 2010; Warita et al., 1999), cf (Marinkovic et al., 2012)) and fast anterograde and retrograde transport is disturbed in primary MNs expressing mutant SOD1, resulting in a depletion of mitochondria in the axon (De Vos et al., 2007). There is also evidence of anterograde transport deficits in post mortem ALS SC, including mislocalised mitochondria (Sasaki et al., 1996a).

A direct physical interaction between mutant SOD1 and the dynein complex (a driver of retrograde transport) has been identified in cell, mouse and rat models of SOD1-fALS (Zhang et al., 2007), and in a cell model, blocking this interaction can reduce aggregation and, in some cases, mutant SOD1 toxicity (Ström et al., 2008). A further link between SOD1, retrograde transport and ALS is that a fast retrograde axonal transport deficit caused by a mutation in the *cytoplasmic dynein heavy chain 1 (Dnchc1)* gene in mice results in SOD1 aggregation in conjunction with a progressive motor phenotype (Hafezparast et al., 2003). Kinesin based fast anterograde transport is also inhibited by mutant and oxidised WT SOD1 (Bosco et al., 2010). Deficits in axonal transport can cause multiple toxic effects including cytoskeletal abnormality and mitochondrial disturbance, deficits which it has been proposed that spinal MNs may be particularly sensitive to given their morphology (Chevalier-Larsen et al., 2006).

#### *1.5.3.5 SOD1 AND RNA*

The role of RNA metabolism in ALS was brought into focus when mutations in genes encoding 2 RNA binding proteins, TDP43 and FUS, were identified as relatively common causes of fALS (as reviewed (Lattante et al., 2013)), but SOD1 has also been implicated in RNA metabolism.

Mutant SOD1 may down regulate vascular endothelial growth factor (VEGF) expression by directly binding its mRNA transcript, competing with RNA stabilising proteins (Lu et al., 2007; Lu et al., 2009; Li et al., 2009). There are several lines of evidence that a reduction in VEGF may have pathogenic consequence for example a polymorphism in the *VEGF* promoter is associated with increased risk of ALS and lower age of onset (Su et al., 2014) and a similar deletion in the

promoter of the mouse gene results in a late-onset MN degenerative phenotype reminiscent of ALS (Oosthuysen et al., 2001). Furthermore, in SOD1-fALS mice increasing VEGF expression attenuates the disease phenotype (Keifer et al., 2014).

Mutant SOD1 also reduces the stability of low molecular weight neurofilament (*NFL*) mRNA, by binding its 3' UTR (Ge et al., 2005; Volkening et al., 2009; Chen et al., 2014). Reduced *NFL* mRNA is reported in sALS and in SOD1-fALS mouse models (Menzies et al., 2002) and disturbance of the balance between different neurofilament subunits can result in accumulation of neurofilament in MNs and axonal hypotrophy (Julien, 1999). A similar pattern of reduced *NFL* mRNA and mutant SOD1 binding the 3' UTR were reported in MNs differentiated from SOD1-fALS induced pluripotent stem cells (iPSC) (Chen et al., 2014). Down regulation of *NFL* is however unlikely to be a primary cause of SOD1-fALS however, as knocking-out *Nfl* in a SOD1-fALS mouse attenuated, rather than exacerbated, the disease phenotype (Williamson et al., 1998).

#### *1.5.3.6 NON-CELL AUTONOMOUS MECHANISMS*

Although the degeneration and death of MNs is a defining feature of ALS, other cell types are also implicated in disease pathogenesis. The fact that astrocytes expressing mutant SOD1 are toxic to neurons has been firmly established in multiple co-culture experiments (Nagai et al., 2007; Marchetto et al., 2008; Di Giorgio et al., 2008; Fritz et al., 2013; Kunze et al., 2013) and mutant SOD1 microglial toxicity also seems likely although the effect may be indirect (Thonhoff et al., 2012; Zhao et al., 2010). Mouse models with transgenic expression of mutant SOD1 directed to specific cell types have helped to elucidate cell-specific roles in disease progression.

Mice with transgenes directing expression of mutant SOD1 to the MNs have produced greatly varying results from a complete absence of behavioural or pathological phenotype (Pramatarova et al., 2001; Lino et al., 2002), MN loss with no behavioural motor phenotype (Wang et al., 2008) to full pathological and behavioural phenotype similar to the constituent transgenic mice (Jaarsma et al., 2008).

Mice in which *LoxP* flanked transgenes are excised from particular cell types have provided more consistent results. Evidence from mice in which the transgene is excised from neuronal lineages suggests that neuronal mutant SOD1 is a key determinant of disease onset and influences disease progression (Boill  e et al., 2006; Yamanaka et al., 2008a; Wang et al., 2009c). Experiments using chimeric mice in which all MNs and oligodendrocytes were derived from mutant SOD1 progenitors while all other tissues are chimeric gave similar results (Yamanaka et al., 2008b).

Similar models have been used to examine the role of mutant SOD1 in glial cells and reveal that both astrocytic and microglial mutant SOD1 is primarily responsible for determining the progression of degeneration with minimal impact on onset (Boillée et al., 2006; Wang et al., 2009c; Beers et al., 2006; Wang et al., 2011a; Yamanaka et al., 2008a; Gong et al., 2000).

Transgenic mice with mutant SOD1 expression directed to skeletal muscle reveal a directly toxic effect of muscular atrophy and reduced strength (Wong et al., 2010; Dobrowolny et al., 2008). Whether such expression can affect the innervating MNs however is still unclear, as in one line there was no evidence for either proximal or distal MN degeneration (Dobrowolny et al., 2008), whereas another line developed motor symptoms, and MN degeneration including 50% loss of MNs (Wong et al., 2010).

## **1.5.4 Protein Misfolding and Aggregation**

### ***1.5.4.1 SOD1 AGGREGATES***

The pathological hallmark of many neurodegenerative diseases is the aggregation of the disease specific protein. In SOD1-fALS, non-amyloid SOD1 inclusions are found in the MNs (e.g. (Wang et al., 2002b; Kerman et al., 2010; Kato et al., 2000; Kato et al., 1996; Kato et al., 1997; Okamoto et al., 1991)). Whether such aggregates are themselves pathogenic or are secondary consequences is contentious (Mulligan et al., 2013).

Correlations between disease phenotype and aggregation pathology in SOD1-fALS mice have been cited as supporting a causal link between the two. For example the tissues in which aggregates occur are those affected in ALS (Wang et al., 2002b) and aggregate level correlates with disease progression (Wang et al., 2002a; Wang et al., 2005b; Cheroni et al., 2005; Turner et al., 2003). It has also been suggested that expression level must reach a level sufficient to cause aggregation in order for ALS like symptoms to arise (Wang et al., 2005b).

Double transgenic mice expressing both mutant and WT SOD1 generally develop disease earlier with reduced survival times. When examined, an increase in mutant protein and a co-localisation of WT with mutant SOD1 in aggregates is reported, increasing the total aggregate burden (Deng et al., 2006; Prudencio et al., 2010; Wang et al., 2009b; Jaarsma et al., 2000; Fukada et al., 2001; Jaarsma et al., 2008). Again this correlates increased aggregation with a more aggressive phenotype, however, there are exceptions; when an L126Z mutant SOD1-fALS mouse was crossed to 2 different WT SOD1 transgenics with different expression levels, the cross to the higher expresser produced a more aggressive phenotype in conjunction with aggregated WT SOD1 but with no increase in mutant SOD1 aggregation. With the lower WT SOD1 expressing line, no change to the phenotype was detected, although a higher level of both WT and mutant SOD1 aggregation was observed (Prudencio et al., 2010). Furthermore,

SOD1 aggregate inclusions are not typically reported until after denervation of the muscles has commenced and the mouse is symptomatic (Gould et al., 2006; Bruijn et al., 1997; Wang et al., 2002b; Johnston et al., 2000; Koyama et al., 2006).

Investigation of aggregate toxicity in cell culture models has yielded evidence suggesting that increasing the level of soluble SOD1 increases toxicity, while increasing recruitment of mutant SOD1 into insoluble inclusions decreased toxicity (Weisberg et al., 2012; Brotherton et al., 2013). Similarly, co-expression of WT and mutant SOD1 in cell and *Caenorhabditis elegans* (*C.elegans*) models slows aggregation concurrent with increasing toxicity when measured (Prudencio et al., 2009a; Prudencio et al., 2010; Witan et al., 2008; Witan et al., 2009).

Misfolded SOD1 can overload the ubiquitin proteasome system (UPS) causing it to become dysfunctional (Urushitani et al., 2002) which can cause increased SOD1 aggregation (Bendotti et al., 2012). UPS dysfunction is observed in SOD1-fALS mice, but not until after onset (Cheroni et al., 2009) and SOD1 aggregation elicited by UPS inhibition isn't necessarily toxic (Lee et al., 2002), suggesting that this is not a primary cause of mutant SOD1 toxicity.

Aggregated SOD1 is therefore unlikely a primary cause of disease. Secondary toxicity may be caused for example, by perturbing axonal transport (Sau et al., 2011) or by sequestration of essential cellular proteins (Pasinelli et al., 2004; Weisberg et al., 2012; Ligon et al., 2005; Zhang et al., 2007; Bergemalm et al., 2010) but a direct causal role for any of these has not been demonstrated.

#### *1.5.4.2 PRE-AGGREGATE SPECIES*

A pre-aggregated soluble form of SOD1, present before phenotypic onset may be the toxic form of SOD1 (Karch et al., 2009). Biochemical analysis of symptomatic SOD1-fALS mouse SC reveals a huge range of SOD1 species ranging from fully soluble monomers and dimers to insoluble and detergent resistant monomers, dimers, oligomers and high-molecular weight species. In contrast, in reducing conditions, the SC of TgWT mice at 38-weeks old contains only fully soluble or membrane bound monomers (Koyama et al., 2006).

A common feature of SOD1 mutants is an increased propensity for dimers to monomerise (Khare et al., 2006; Rakhit et al., 2004) and impaired folding and dimerisation (Bruns et al., 2007), suggesting that mutation could result in a shift in the population from dimer towards monomer. However, monomerisation is also an essential step towards the formation of higher molecular weight species and aggregates (Rakhit et al., 2004; Ray et al., 2004) so this propensity towards monomerisation could also hasten the path to aggregation. Zetterström et al., (2007; 2013) identified a soluble hydrophobic SOD1 fraction, composed of disordered monomers, as enriched in the SC of 4 different mutant SOD1-fALS mice as compared to TgWT



mice. Unlike total SOD1, the level of this fraction correlated with survival in the 4 mutant lines implicating monomeric SOD1 in disease.

Other oligomeric species, both soluble and insoluble, have been identified in SOD1-fALS mice and are present pre-onset and correlate with phenotypic progression (Johnston et al., 2000; Wang et al., 2009a). The SEDI antibody recognises the SOD1 exposed dimer interface, and so cannot react with natively dimeric SOD1. In SOD1-fALS mice, MNs are labelled diffusely at pre-symptomatic age and with inclusion morphology at disease onset (Rakhit et al., 2007) and when used for immunotherapy onset is delayed (Liu et al., 2012), implicating a non-native-dimeric species in pathogenesis.

How such monomeric or oligomeric species might cause toxicity has not been established. Exposure of SOD1's Derlin-1 binding region and activation of ER-stress could result from monomerisation or some non-native oligomeric conformations (Nishitoh et al., 2008; Fujisawa et al., 2012). Johnston et al., (2000) suggest that misfolded oligomeric SOD1 could disrupt retrograde axonal transport by competing with other transport targets and overwhelm the system. Aberrant copper binding of mutant monomeric SOD1 resulting in oxidative stress has also been proposed as a potential mode of mutant SOD1 toxicity (Kishigami et al., 2010).

#### *1.5.4.3 PRION-LIKE PROTEIN MISFOLDING MECHANISM*

The prion diseases are a group of neurodegenerative diseases caused by misfolding of the prion protein (PrP). Similar to other neurodegenerative diseases, prion diseases can be sporadic or caused by mutation of the *PRNP* gene. However it can also be caused by infection with a misfolded PrP (PrP<sup>Sc</sup>) which can induce the correctly folded "cellular" PrP (PrP<sup>C</sup>) to misfold and take on the characteristics of PrP<sup>Sc</sup>. The disease is transmitted within and between cells via conversion of PrP<sup>C</sup> to PrP<sup>Sc</sup> (Acquatella-Tran Van Ba et al., 2013).

The misfolded/aggregated proteins which are present in most neurodegenerative diseases were thought to arise from a failure to correctly fold, or a *de novo* misfolding, with misfolding events occurring somewhat independently but in response to a shared stressor. A prion-like model of misfolding is becoming increasingly prevalent, in which misfolding at a discrete focus can act as a seed or template, to recruit and propagate misfolding between cells (Guest et al., 2011). The term "prion-like" is used here to describe two main concepts, which are illustrated in Figure 1.15. Firstly, the ability of a misfolded protein "X" to recruit a correctly folded protein "X" to become misfolded, either by a process of templated misfolding or seeded aggregation. Secondly, the capacity for such a process to propagate between cells. This model is particularly appealing in the case of ALS where the disease is clinically characterised by a focal onset spreading to regions innervated by contiguous segments of the SC (e.g. (Fujimura-Kiyono et al.,

2011)), or, as has also been demonstrated in some cases, several focal sites of onset with regional spread (Sekiguchi et al., 2014).

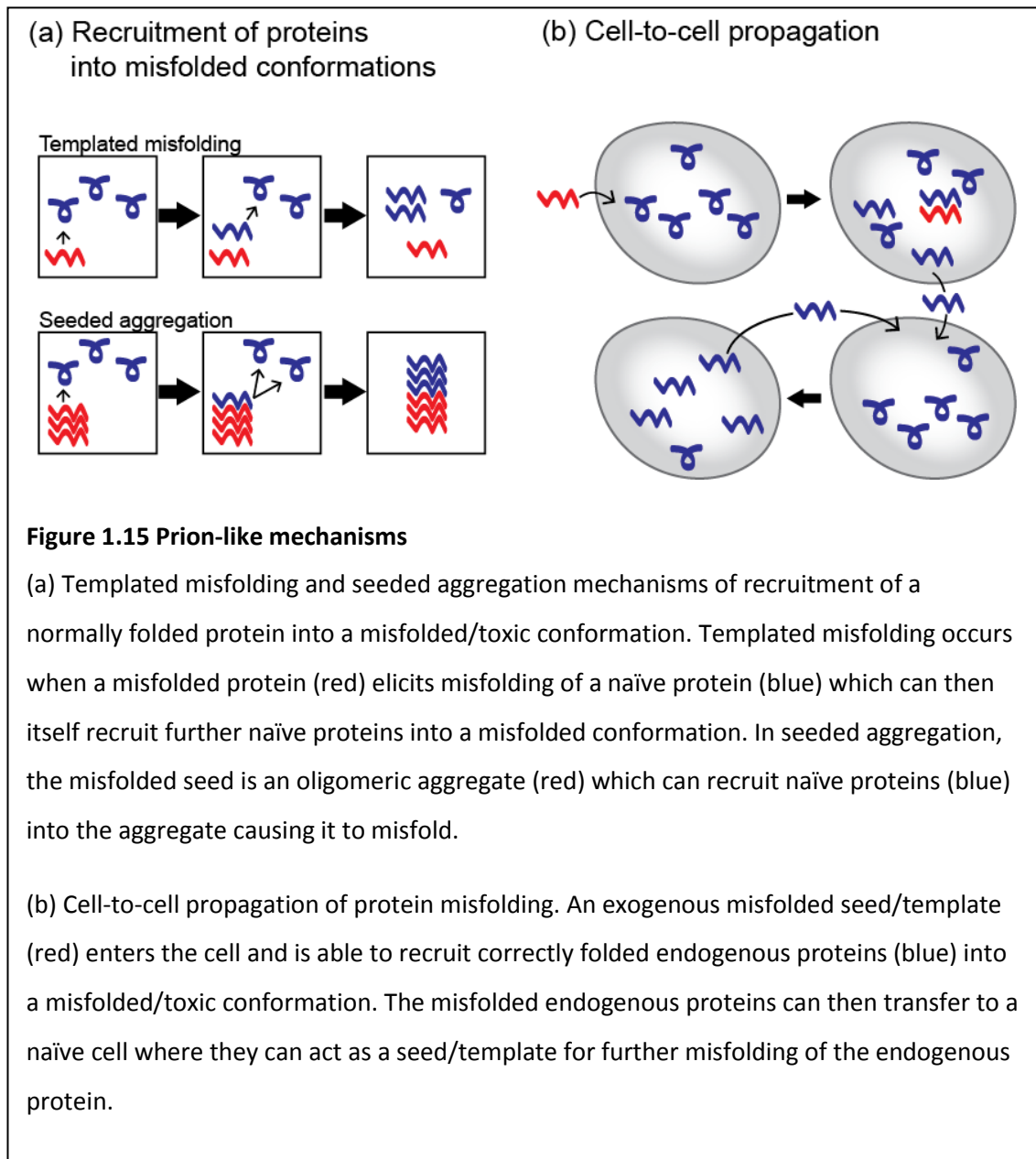


**Figure 1.15 Prion-like mechanisms**

(a) Templated misfolding and seeded aggregation mechanisms of recruitment of a normally folded protein into a misfolded/toxic conformation. Templated misfolding occurs when a misfolded protein (red) elicits misfolding of a naïve protein (blue) which can then itself recruit further naïve proteins into a misfolded conformation. In seeded aggregation, the misfolded seed is an oligomeric aggregate (red) which can recruit naïve proteins (blue) into the aggregate causing it to misfold.

(b) Cell-to-cell propagation of protein misfolding. An exogenous misfolded seed/template (red) enters the cell and is able to recruit correctly folded endogenous proteins (blue) into a misfolded/toxic conformation. The misfolded endogenous proteins can then transfer to a naïve cell where they can act as a seed/template for further misfolding of the endogenous protein.

Whether SOD1 displays prion-like properties has been examined *in vitro*, for example by Chia et al., (2010) who used an amyloid fibrillisation assay to measure the aggregation propensity of recombinant proteins. Self-seeding was demonstrated by a reduction in the time it took for G93A mutant SOD1 to form amyloid fibrils by the addition of either G93A pre-formed fibrils, or TgG93A SC lysate. Cross-seeding of WT SOD1 by mutant SOD1 was similarly demonstrated. Hwang et al., (2010) also demonstrated both self-seeding and cross-seeding with recombinant proteins (but not tissue lysates) using an *in vitro* assay which produced aggregate species with structural properties similar to aggregates seen in SOD1-fALS, such as being non-amyloid and recognised by the SEDI antibody. Some SOD1-fALS mice develop amyloid pathology with

thioflavin fluorescence (e.g. mutants G37R, G85R, and G93A (Wang et al., 2002b; Furukawa et al., 2008)) however, when assessed, amyloid features are reported as absent in SOD1-fALS and sALS patients (e.g. (Wang et al., 2002b; Kerman et al., 2010; Kato et al., 2000; Kato et al., 1996; Kato et al., 1997; Okamoto et al., 1991)). Further examination of the *in vitro* non-amyloid seeding potential of SOD1-fALS mice and patient tissue is needed.

Cellular models have also illuminated prion-like properties of SOD1. In an early example, Urushitani et al., (2006) found that transgenic SOD1 primary MNs secreted SOD1 into the culture medium and that recombinant mutant SOD1 and high concentrations of apo WT SOD1 were both highly toxic to non-transgenic primary MNs when applied to the culture medium. One year later, Ezzi et al., (2007) confirmed that recombinant extracellular mutant SOD1 was toxic to primary MNs and extended this finding to oxidised WT SOD1.

Extracellular mutant SOD1 aggregates were shown to be efficiently internalised by a mouse neuronal like cell line, where they induced the aggregation of stably expressed mutant (but not WT) SOD1. These seeded aggregates persisted for up to 1 month and were themselves transmitted between cells (Munch et al., 2011) demonstrating aggregated SOD1 self-seeding and cell-to-cell propagation. Similar self-seeding was observed by recombinant mutant amyloid fibrils in the same cell line expressing a tagged human mutant SOD1 (Furukawa et al., 2013).

Transient expression of mutant SOD1 can also induce the sustained misfolding of the endogenously expressed WT SOD1 in human cell lines. Furthermore, this misfolded WT SOD1 can transmit between cells via conditioned media, eliciting further misfolding in naïve cells and even in primary neurons from WT SOD1 transgenic mice (Grad et al., 2011; Grad et al., 2014). These experiments exemplify cross-seeded templated misfolding and sustained cell-to-cell propagation of self-seeded templated misfolding. In another human cell line, exogenously applied recombinant mutant SOD1 (both aggregated and non-aggregated) and aggregated WT SOD1 not only elicits aggregation of endogenous SOD1, but also activate ER stress and apoptotic cell death (Sundaramoorthy et al., 2013), demonstrating ALS relevant toxicity related to self-seeded and cross-seeded reactions.

Also of note is the finding that astrocytes derived from SOD1-fALS mice have increased secretion of SOD1 in exosomes, as compared to TgWT mice, and that these mutant SOD1 containing exosomes are toxic to primary cultures (Basso et al., 2013).

Together this evidence demonstrates that in cell models, both self-seeded and cross-seeded misfolding can be transmitted cell-to-cell and that this process can be self-propagating with

previously naïve SOD1 itself acting as a template/seed. Furthermore, some evidence also suggests that these processes may have toxic consequences.

Similar work has been carried out exploring the prion-like properties of other “hallmark” neurodegenerative proteins and, as summarised in Table 1.6, has been extended to include *in vivo* examination of prion-like mechanisms in transgenic mouse models of several neurodegenerative diseases. The ability of intracerebral inoculation of misfolded proteins to induce misfolding and spread of pathology, and even in some cases to induce a disease phenotype has been demonstrated, as summarised in Table 1.6. Although *in vivo* prion-like mechanisms of SOD1 have not yet been explicitly examined in animal models, experiments using non-human primates commencing in the 1950s to examine a possible viral aetiology of ALS are relevant; in 1963, Zil’ber et al., reported the successful induction of ALS in monkeys by intracerebral inoculation with CNS homogenates of ALS patients. 2-5-years after the inoculation, weight loss, muscle atrophy and paralysis developed, and MN loss was demonstrated most mortem. Furthermore, the disease was successfully passaged to 2 subsequent generations. Subsequent attempts to replicate these results by inoculation into non-human primates, small laboratory mammals and birds all failed (Gajdusek et al., 1964; Gibbs et al., 1972).

**Table 1.6 Prion-like proteins in neurodegenerative diseases**

The table summarises evidence available for prion-like properties of several neurodegenerative disease “hallmark” proteins. Positive cases are highlighted in green and negative cases are highlighted in pink.

			<b>Tau</b>	<b>α-synuclein</b>	<b>Aβ</b>	<b>SOD1</b>	<b>TDP43</b>
<b>Seeded-aggregation</b>	<i>in vitro</i>		Yes (1)	Yes (6)	Yes (11)	Yes (14, 15, 16)	Yes (21)
<b>Seeded-aggregation</b>	<b>in cell culture</b>		Yes (1, 2, 3)	Yes (7)		Yes (16, 17, 18, 19, 20)	Yes (22) and using a protein transduction reagent (21)
<b>Cell-to-cell spread</b>	<b>in cell culture</b>		Yes (1, 2)	Yes (7, 8)		Yes (17, 20)	Yes (22)
<b>Cell-to-cell spread</b>	<b>in mice</b>	<b>recombinant</b>	Yes, earlier presence in mutant tau mouse (23)	Yes, earlier presence in mutant α-Syn mouse (9)	Yes, earlier presence in mutant APP mice (12)		
<b>Cell-to-cell spread</b>	<b>in mice</b>	<b>lysate</b>	Yes, in WT Tau mice (4, 5)	Yes, earlier presence in mutant α-Syn mouse (9)	Yes, earlier presence in mutant APP mice (12, 13)		
<b>Clinical disease</b>	<b>in mice</b>	<b>recombinant</b>		Yes earlier than in mutant α-Syn mouse (9)	No (13)		

			Tau	$\alpha$ -synuclein	A $\beta$	SOD1	TDP43
Clinical disease	in mice	lysate	Cell death but no symptomatic disease in WT Tau mice (4)	Yes earlier than in mutant $\alpha$ -Syn mouse (9, 10)	cell death but no symptomatic disease (13)		

1- (Frost et al., 2009); 2- (Kfoury et al., 2012); 3- (Santa-Maria et al., 2012); 4- (Clavaguera et al., 2009); 5- (Clavaguera et al., 2013); 6- (Yonetani et al., 2009) 7- (Desplats et al., 2009); 8- (Hansen et al., 2011); 9- (Luk et al., 2012); 10- (Mougenot et al., 2012); 11- (Petkova et al., 2005); 12- (Stöhr et al., 2012); 13- (Meyer-Luehmann et al., 2006); 14- (Chia et al., 2010); 15- (Hwang et al., 2010); 16- (Grad et al., 2011); 17- (Munch et al., 2011); 18- (Sundaramoorthy et al., 2013); 19- (Furukawa et al., 2013); 20- (Grad et al., 2014); 21- (Furukawa et al., 2011); 22- (Nonaka et al., 2013); 23- (Iba et al., 2013)

### 1.5.5 Wild-type SOD1 Pathogenicity

That WT SOD1 can be found in aggregates in SOD1-fALS patients has been known for some time (e.g. (Bruijn et al., 1998)) and SOD1 aggregates have been reported in some, but not all, sALS cases (Shibata et al., 1994; Shibata et al., 1996a; Matsumoto et al., 1996; Watanabe et al., 2001a). More recently, misfolded SOD1 antibodies are increasingly revealing misfolded SOD1 in sALS and non-SOD1 fALS (Bosco et al., 2010; Forsberg et al., 2010; Forsberg et al., 2011; Pokrishevsky et al., 2012; Gruzman et al., 2007), although there are exceptions (Furukawa, 2012; Ling et al., 2013).

As has been touched upon above, in models of prion-like misfolding, WT SOD1 can take on mutant-like properties. Other, non-prion, mechanisms such as oxidative damage, demetalation or loss or gain of post-translational modifications can also cause WT SOD1 to misfold and become toxic to MNs (e.g. (Ezzi et al., 2007; Redler et al., 2011; Proctor et al., 2011; Rakhit et al., 2004; Lindberg et al., 2004; Urushitani et al., 2006; Estévez et al., 1999)). Misfolding and oxidisation of WT SOD1 has also been reported to result from expression of either mutant or WT TDP43 or WT FUS expression in cellular models (Pokrishevsky et al., 2012).

In transgenic mice expressing WT SOD1, ALS related pathology is present at a late stage (Dal Canto et al., 1995). With higher level of WT SOD1 expression, motor dysfunction and MN loss occur in conjunction with misfolded SOD1 detectable by pathology and biochemistry (Graffmo et al., 2012; Jaarsma et al., 2000). In cellular and *in vitro* models, misfolded-oxidised WT SOD1 can mimic mutant SOD1, disturbing anterograde axonal transport, activating ER-stress and interacting with Bcl-2 to cause mitochondrial damage (Bosco et al., 2010; Sundaramoorthy et al., 2013; Pasinelli et al., 2004; Guareschi et al., 2012).

Evidence from SOD1 transgenic mice suggests that the presence of WT SOD1 exacerbates the mutant SOD1 toxicity (Deng et al., 2006; Prudencio et al., 2010; Wang et al., 2009b; Jaarsma et al., 2000; Jaarsma et al., 2008), possibly by increasing solubility (Fukada et al., 2001). Correctly folded and metalated WT SOD1 has also been found to exacerbate the toxicity of zinc deficient misfolded WT SOD1 in primary MN (Sahawneh et al., 2010).

WT SOD1 could potentially increase the toxicity of mutant/misfolded SOD1 by stabilising a pre-aggregated toxic species which would result in the slowed aggregation reported with co-expression in cellular models (Weisberg et al., 2012; Brotherton et al., 2012; Prudencio et al., 2009a; Prudencio et al., 2010; Witan et al., 2008; Witan et al., 2009). Heterodimerisation between mutant/misfolded and WT SOD1 monomers has been posited as a possible mechanism by which WT SOD1 could affect this (Witan et al., 2009; Witan et al., 2008;

Weichert et al., 2014). Thus WT SOD1 has potential to cause toxicity via both prion-like and non-prion like pathways.

## **1.6 CURRENT QUESTIONS IN MOUSE MODELS OF SOD1-fALS AND RESEARCH PROJECT AIMS**

### **1.6.1 Does SOD1 Have Prion-Like Properties Within the CNS?**

Misfolded SOD1 can act as a seed to promote both amyloid and non-amyloid aggregation *in vitro* and in cell culture misfolded SOD1 is able to transfer between cells and act as a template or seed to elicit misfolding via both self-seeding and cross-seeding reactions. In mouse models of other neurodegenerative diseases exogenous sources of misfolded hallmark proteins can elicit misfolding and pathological changes and in some cases can even produce symptomatic disease. It is not yet known whether the prion-like properties of SOD1 revealed by *in vitro* and cellular models can translate *in vivo* in an animal.

#### ***1.6.1.1 AIM: PROPAGATION OF SOD1 MISFOLDING IN VIVO***

Does SOD1 have prion-like properties in an *in vivo* model? This work aimed to investigate whether exogenous mutant human SOD1 can elicit the aggregation of transgenically expressed human SOD1 in mice.

To assess cross-seeded-aggregation *in vivo*, SC homogenate of TgG93A mice at a symptomatic age were intracerebrally inoculated into young TgG93A mice and the consequences on the misfolded SOD1 aggregate pathology were measured to see if an increase resulted, as has been reported in similar experiments with mutant  $\alpha$ -Synuclein and APP mice (Luk et al., 2012; Mougenot et al., 2012; Stöhr et al., 2012; Meyer-Luehmann et al., 2006). A second set of experiments was carried out to assess cross-seeded-aggregation of WT SOD1 by mutant SOD1 *in vivo*, as has been demonstrated in transgenic Tau mice (Clavaguera et al., 2009; Clavaguera et al., 2013). In these experiments, TgWT mice were intracerebrally inoculated with SC homogenate from symptomatic TgG93A mice and SOD1-fALS motor cortex.

The aim of this work was to assess whether some of the prion-like properties of SOD1 which have been established *in vitro* and in cellular models are relevant to SOD1 within the CNS. In particular we have aimed to evaluate whether seeded-aggregation of transgenically expressed SOD1 can occur and spread through the CNS.

### **1.6.2 Does Endogenous Mouse *Sod1* Affect the Disease Phenotype of the *SOD1*<sup>G93A</sup>-fALS Transgenic Mouse?**

The phenotype of transgenic mouse models of some neurodegenerative diseases have been found to be affected by the endogenous mouse homologue of the human protein being



expressed. In mouse models of infectious human prion disease, for example, the presence of the mouse PrP in conjunction with human PrP significantly lengthens the incubation period between inoculation and disease onset and produces more variable phenotypes than when the mouse gene is knocked-out (Telling et al., 1995; Collinge et al., 1995). Mice expressing WT human tau from a genomic transgene remained healthy with no disease pathology when the endogenous mouse *Mapt* gene was functional (Duff et al., 2000), however, when mouse *Mapt* was knocked-out, hyperphosphorylated tau accumulated and a pattern of pathology similar to that seen in AD, including neuronal death, developed (Andorfer et al., 2003; Andorfer et al., 2005). Similarly, in a mutant  $\alpha$ -synuclein model which developed only mild late onset motor disturbance and rarely any pathology, ablation of the endogenous counterpart resulted in reduced survival, progressive motor disturbance and characteristic pathology (Cabin et al., 2005).

Two previous publications have touched upon the role of endogenous moSOD1 in SOD1-fALS mice; in 1998, Bruijn et al., compared G85R mutant SOD1 transgenic mice, with or without an endogenous *Sod1* KO. Comparing 5 animals of each genotype revealed no difference in survival. Motor axon number was also not significantly different between genotypes, but only three *Sod1*<sup>+/+</sup> and two *Sod1*<sup>-/-</sup> animals were examined and variance between animals was high. In 2006, Deng et al., carried out a similar cross with a G93A mutant SOD1 transgenic and found a modest delay in disease onset and longer survival in the *Sod1*<sup>-/-</sup> mice.

WT and mutant huSOD1 appear to interact to exacerbate the disease process, as described above, but differences in these interactions are apparent when one of these elements is derived from human and one from mouse; while double transgenic mice expressing both mutant and WT huSOD1 have a more severe phenotype than single mutant transgenics, the addition of WT huSOD1 does not affect the phenotype of the G86R mutant moSOD1 transgenic mouse (Audet et al., 2010). Both WT huSOD1 and moSOD1 slow the aggregation of mutant huSOD1 in a cell culture model (Prudencio et al., 2009a), but when aggregates develop, only WT huSOD1, but not WT moSOD1, co-aggregates with mutant huSOD1 (Prudencio et al., 2009a; Grad et al., 2011). When aggregation of mutant moSOD1 was examined in the presence of WT huSOD1, co-aggregation was not detected; whether WT moSOD1 affected the speed of aggregation was not assessed (Qualls et al., 2013).

WT huSOD1 and moSOD1 have a similar aggregation propensity when transiently expressed in cells, however the ALS mutation, G85R, produces significantly less aggregation in the context of moSOD1 than huSOD1 (Karch et al., 2010). In line with this the moSOD1 dimer is significantly more stable than the huSOD1 dimer in terms of resistance to thermal and

chemical denaturants (Jonsson et al., 2006a). The functional consequences of these similarities and differences in a disease model are not clear.

#### ***1.6.2.1 Aim: ENDOGENOUS SOD1 IN SOD1G93A TRANSGENIC MICE***

The aim of this section of work was to look again at the potential effects of WT moSOD1 in the TgG93A mouse model of SOD1-fALS by examining TgG93A mice with and without the endogenous protein. Behavioural and histological techniques were used to assess whether endogenous WT moSOD1 effects the progression of disease, MN survival and aspects of neuromuscular atrophy.

### **1.6.3 Can We Improve on Current Mouse Models of SOD1-fALS?**

All currently available mouse models of SOD1-fALS are traditional random integration transgenics. A huge amount of information about the disease processes and pathogenic mechanisms of mutant SOD1 have been gleaned using these models, however there are drawbacks to this type of mouse model such as artificially high expression and fast disease progression making examination of early disease processes more difficult.

New tools for genetically engineering mice open the possibility for more refined alterations of the mouse genome, allowing us to more precisely mimic the genomic context of human disease. Could creating a mouse which more closely reflects the genetic architecture of mutant *SOD1* in SOD1-fALS patients provide a more accurately model the disease?

#### ***1.6.3.1 Aim: A NEW MOUSE MODEL OF SOD1-FALS***

Using a combination of traditional restriction endonuclease cloning and recombineering, targeting constructs were produced to genomically humanise the mouse *Sod1* locus. The construct was designed to replace the mouse locus with the full *SOD1* gDNA sequence, including an ALS mutation. The construct design also includes engineered DNA sequence to facilitate a Cre dependent switch from expression of mutant to WT SOD1.

## Chapter 2. Materials and Methods

### 2.1 GENERAL MOLECULAR BIOLOGY PROTOCOLS

#### 2.1.1 Extraction/Purification of Nucleic Acids

##### *2.1.1.1 EAR/TAIL BIOPSY DNA PREPARATION*

For each ear biopsy/0.5 mm piece of tail tissue 50  $\mu$ L Extraction Solution (Sigma) and 12.5  $\mu$ L Tissue Prep Solution (Sigma) were added. Samples were incubated at room temperature (r/t) for 20 mins and then at 95 °C for 4 mins. Samples were centrifuged at maximum speed in a bench top microfuge (see Section 7.2, Appendix 2) for 30 secs and 50  $\mu$ L Neutralisation Solution B (Sigma) added and mixed by vortexing. Samples were then centrifuged at maximum speed for 7 mins. For PCR, 1  $\mu$ L of a 1/10 dilution in ddH<sub>2</sub>O was used as template.

##### *2.1.1.2 PURE PLASMID PREPARATIONS*

Qiagen kits were used for preparation of plasmid DNA when removal of bacterial genomic DNA was necessary. QIAprep Spin Miniprep Kit, QIAGEN Plasmid Maxi Kit or QIAGEN Large-Construct Kit was used according to the manufacturer's instructions.

##### *2.1.1.3 RAPID PLASMID PREPARATION*

5 mL overnight culture was centrifuged 7000 rcf for 5 mins and supernatant discarded. The pellet was resuspended in 250  $\mu$ L Qiagen buffer P1 by pipetting and transferred to a 1.5 mL microfuge tube. 300  $\mu$ L Qiagen buffer P2 was added and mixed thoroughly but gently by inversion, for no longer than 5 mins. 350  $\mu$ L Qiagen buffer P3 was added and mixed thoroughly but gently by inversion. The tube was then centrifuged at full speed for 10 mins in a bench top microfuge and the supernatant transferred to a fresh tube. 0.6 volumes isopropanol (roughly 540  $\mu$ L) was added to the supernatant and mixed thoroughly but gently by inversion. The tube was then centrifuged at full speed for 20 mins and the supernatant aspirated and discarded. The pellet was then washed in 500  $\mu$ L 70% (v/v) ethanol, centrifuged at full power for 5 mins and the supernatant aspirated and discarded. The pellet was allowed to air dry for 10 mins before resuspension. Typically resuspension was in 20  $\mu$ L ddH<sub>2</sub>O.

##### *2.1.1.4 FAST DNA PREPARATIONS FOR PLASMID SCREENING PCR*

###### *2.1.1.4.1 Individual Colonies*

Using a sterile 20/200  $\mu$ L pipette tip, an individual colony was picked from a Luria Broth (LB) agar base plate. The tip was swirled in 50  $\mu$ L ddH<sub>2</sub>O in a 96 well plate or PCR tube strip, and then the tip used to streak onto a small area of a fresh LB agar plate.

#### 2.1.1.4.2 Liquid Cultures

100 µL culture was transferred to a 96 well PCR plate, sealed with plastic film and centrifuged at full power for 15 mins. The sealing film was then removed and the plate was inverted over tissue paper and tapped sharply to remove media. 100 µL ddH<sub>2</sub>O was added to each well and the plate sealed with individual cap strips. Using a PCR thermo-cycler the following programme was run: Lid heated to 100 °C. 105 °C for 10 mins, 4 °C for 5 mins. The plate was then centrifuged at full power for 15 mins to pellet debris and 1 µL supernatant used as template in a 10 µL PCR.

#### *2.1.1.5 PURIFICATION OF DNAs FROM AGAROSE GEL AND MOLECULAR BIOLOGY BUFFERS*

##### 2.1.1.5.1 Gel Extraction

For extraction of DNA from agarose gel after electrophoresis, bands were visualised using ethidium bromide stained gels (see Section 2.1.7) on an ultra violet gel illuminator and excised using a clean scalpel blade. Qiagen kits, QIAquick Gel Extraction Kit and QIAEX II Gel Extraction Kit were used for purification according to the manufacturer's guidelines for size of the DNA fragment to be purified following the manufacturer's instructions.

##### 2.1.1.5.2 DNA Purification from Molecular Biology Buffers

For purification of PCR products Qiagen QIAquick PCR Purification Kit was used following manufacturer's instructions.

For purification of DNA fragments from restriction endonuclease (RE) digestions and for sequencing reactions, microCLEAN (Microzone) was used following the manufacturer's instructions.

##### 2.1.1.5.3 Phenol:Chloroform Purification of DNA

Two volumes phenol:chloroform was added to the DNA sample and mixed thoroughly by inversion. The sample was centrifuged at full speed for 5-10 mins in a bench top microfuge. The top, aqueous phase was transferred to a fresh tube. Two volumes of chloroform was then added and inverted to mix, before repeating the centrifuge and removing the aqueous phase to a fresh tube. 2-3 volumes 100% ethanol was added, mixed thoroughly by inversion, and incubated at room temperature for 10 mins. The sample was then centrifuged at full speed for 20 mins and the supernatant aspirated. If not pellet was visible a further incubation at 4 °C or at -20 °C was carried out. The sample was washed in 1 volume 70% ethanol before a further centrifuge and aspiration step. Pellets were air dried before resuspension in H<sub>2</sub>O or Tris-EDTA buffer pH 8 (TE. Sigma).

## 2.1.2 Polymerase Chain Reaction

All primers were purchased from Sigma Aldrich as desalted lyophilised pellets. Stocks were reconstituted in ddH<sub>2</sub>O to 100 µM and stored at -20 °C. Working dilutions were made to 5 µM with ddH<sub>2</sub>O and stored at -20 °C.

For screening and genotyping PCRs where 100% faithful amplification of the target sequence was not required, Sigma-Aldrich REDTaq ReadyMix (REDTaq), a 2X mega mix was used. Extension was carried out at 72 °C and extension time was calculated based on 1 min per 2 kb to be amplified. This mega mix contains gel loading dye and buffer so PCR products were loaded directly onto agarose gels.

For PCR amplification for recombineering products or other applications where faithful amplification of the target sequence was required Invitrogen AccuPrime *Pfx* SuperMix (AccuPrime) a 1.1X mega mix was used. Extension was carried out at 68 °C and extension time was calculated based on 1 min per 1 kb to be amplified. For gel electrophoresis, an appropriate volume of Bioline Crystal 5X DNA Loading Buffer Blue was mixed with the product before loading onto the gel.

### 2.1.2.1 TOUCHDOWN PCR

Touchdown PCR was used for amplification of products for sequencing and recombineering using AccuPrime *Pfx* SuperMix. The touchdown PCR master mix is given in Table 2.1.

**Table 2.1 Touchdown PCR master mix**

	n=1	Final concentration
<b>AccuPrime 1.1X</b>	22 µL	
<b>Template (usually 10 ng/µL)</b>	1 µL	0.4 ng/µL
<b>Forward primer (5 µM)</b>	1 µL	0.2 µM
<b>Reverse primer (5 µM)</b>	1 µL	0.2 µM
	25 µL	

Cycling conditions for touchdown PCR (unless otherwise specified):

1	95 °C	5 mins	
2	95 °C	15 secs	Denature
3	68 °C	30 secs	Anneal
Decrease by 1 °C each cycle			
4	68 °C	1 min per kb	Extend
5	Cycle from step 2, 12 times		
6	95 °C	15 secs	Denature
7	55 °C	30 secs	Anneal
8	68 °C	1 min per kb	Extend
9	Cycle from step 6, 21 times		

10	68 °C	1 min per kb	Final extension
11	4 °C	Forever	

### 2.1.2.2 STANDARD PLASMID SCREENING PCR

Template was 1  $\mu$ L plasmid DNA prepared by either the “rough” or “rapid” protocol described above.

Two to four primers were used in combination depending upon the particular screening PCR. Where possible, multiplex primer combinations were used to include both internal controls and test primers in the same PCR. 1  $\mu$ L each primer (5  $\mu$ M) was added and an appropriate volume of ddH<sub>2</sub>O added to give a final volume of 10  $\mu$ L. The screening PCR master mix is given in Table 2.2.

**Table 2.2 Standard plasmid screening PCR master mix**

	n=1	Final concentration
ddH <sub>2</sub> O	X $\mu$ L	To make up to 10 $\mu$ L total volume
REDTaq (2X)	5 $\mu$ L	1X
Template	1 $\mu$ L	
Primer (5 $\mu$ M)	X $\mu$ L	0.5 $\mu$ M for each primer
	10 $\mu$ L	

Cycling conditions for standard plasmid screening PCR (unless otherwise specified):

1	95 °C	5 mins	
2	95 °C	30 secs	Denature
3	55 °C	30 secs	Anneal
4	72 °C	30 secs per kb	Extension
Cycle from step 2, 35 times			
5	72 °C	5 mins	Final extension
6	4 °C	Forever	

### 2.1.2.3 GRADIENT PCR

The gradient PCR used the same master mix as is given in Table 2.2.

Cycling conditions were as follows:

1	95 °C	5 mins	
2	95 °C	30 secs	Denature
3	45-55°C	30 secs	Anneal
4	72°C	30 secs	Extend
5	Cycle from step 2, 35 times		

### 2.1.2.4 SOD1 TRANSGENE GENOTYPING PCR

The same PCR protocol was used to genotype both the wild-type (WT) and G93A SOD1 transgenic mice.

Primers details are given in Table 2.3. A working stock mix of primer was prepared by adding 20  $\mu\text{L}$  each of the 4 stock primers (100  $\mu\text{M}$ ) to 120  $\mu\text{L}$  ddH<sub>2</sub>O to produce a working stock mix of 5  $\mu\text{M}$  per primer.

Template was 1  $\mu\text{L}$  of a 1/10 dilution in ddH<sub>2</sub>O of genomic DNA prepared as described in Section 2.1.1.1. The genotyping master mix is given in Table 2.4.

**Table 2.3 Transgene genotyping primers**

	Forward	Reverse
<b>Control</b>	CTAGGCCACAGAATTGAAAGATCT	GTAGGTGGAAATTCTAGCATCATC
<b>Transgene</b>	CATCAGCCCTAATCCATCTGA	CGCGACTAACAATCAAAGTGA

**Table 2.4 Genotyping PCR master mix**

	n=1	Final concentration
<b>ddH<sub>2</sub>O</b>	3 $\mu\text{L}$	
<b>REDTaq (2X)</b>	5 $\mu\text{L}$	1X
<b>Template</b>	1 $\mu\text{L}$	
<b>Primer mix (5 <math>\mu\text{M}</math>)</b>	1 $\mu\text{L}$	0.5 $\mu\text{M}$ per primer
	10 $\mu\text{L}$	

Cycling conditions for *SOD1* transgene genotyping PCR:

1	95 °C	3 mins	
2	95 °C	30 secs	Denature
3	60 °C	30 secs	Anneal
4	72 °C	45 secs	Extend
Cycle from step 2 35 times			
5	72 °C	2 mins	Final extension
6	4 °C	Forever	

PCR products were resolved on a 2% agarose 45 mM Tris-borate, 1 mM EDTA (ethylenediaminetetraacetic acid) (TBE) gel (see Section 2.1.7 below for details) running at 100 V (~7 V/cm) for 30 mins.

A control band of 324 bp amplifies across an intron/exon boundary (exon 3/intron 3) from the gene *Interleukin 2 (Il2)* on chromosome 3. This control fragment should be present in all samples and acts as a control to check that the PCR has been successful. A band of 236 bp amplifies across exon 4 of the *SOD1* transgene, from intron 3 to intron 4.

#### 2.1.2.5 *SOD1* KNOCKOUT GENOTYPING PCR

Primers details are given in Table 2.5 and were taken from the Jackson Laboratory (Jax) website (<http://jaxmice.jax.org/>). A working stock mix of primer was prepared by adding 20  $\mu\text{L}$

each of the 4 stock primers (100  $\mu$ M) to 120  $\mu$ L ddH<sub>2</sub>O to produce a working stock mix of 5  $\mu$ M per primer.

Template was 1  $\mu$ L of a 1/10 dilution in ddH<sub>2</sub>O of genomic DNA prepared as described above in Section 2.1.1.1. The genotyping PCR master mix is given in Table 2.4, above.

**Table 2.5 KO genotyping primers**

	Forward	Reverse
<b>Control</b>	TGAACCAGTTGTGTTGTCAGG	TCCATCACTGGTCACTAGCC
<b>KO</b>	TGTTCTCCTCTTCCTCATCTCC	ACCCTTTCCAAATCCTCAGC

Cycling conditions for the *Sod1* knockout genotyping PCR:

1	95 °C	3 mins	
2	95 °C	20 secs	Denature
3	61 °C	1 min	Anneal
4	72 °C	1 min	Extend
Cycle from step 2 35 times			
5	72 °C	5 mins	Final extension
6	4 °C	Forever	

PCR products were resolved on a 2% agarose TBE gel (see Section 2.1.7 below) running at 100 V (~7 V/cm) for 30 mins.

In the presence of the wild-type allele a 123 bp band is amplified from exon 2 to intron 2 of *Sod1* on chromosome 16. In the presence of the knockout (KO) allele a band of 240 bp is amplified. This larger band presumably amplifies from the selection cassette which was used to replace exon 1 and exon 2, however the sequence of this cassette was not published by Matzuk et al., (1998) and details are not given on the Jax website where these primers were taken from, so this could not be confirmed.

### 2.1.3 Quantitative Real Time PCR (qPCR) *SOD1* Transgene Copy Number Assay

The qPCR copy number assay of transgene copy number was developed from the protocol published on the Jackson Laboratory website (<http://jaxmice.jax.org>). The assay used TaqMan (Applied Biosystems) reagents and used relative standard curve quantitation of multiplex reactions, containing one measure of the transgene (Tg) and one internal endogenous control (EC).

The oligos detailed in Table 2.6 were ordered from Sigma as lyophilised pellets and resuspended to 100  $\mu$ M according to the manufacturer's instructions.



**Table 2.6 Primers and probes for *SOD1* transgene copy number qPCR assay**

Name	5' label	Sequence	3' label
Endogenous control (EC) forward primer	-	CACGTGGGCTCCAGCATT	-
Endogenous control (EC) reverse primer	-	TCACCAGTCATTTCTGCCTTTG	-
Transgene (Tg) forward primer	-	GGGAAGCTGTTGTCCCAAG	-
Transgene (Tg) reverse primer	-	CAAGGGGAGGTAAAAGAGAGC	-
EC probe	Cy5	CCAATGGTCGGGCACTGCTCAA	Black Hole Quencher 2
Tg probe	6-FAM	CTGCATCTGGTCTTGCAAAACA CCA	Black Hole Quencher 1

The endogenous control primers amplified 74 bp from exon 24 of the *Apob* gene on mouse chromosome 12. The transgene primers amplified 88 bp from intron 4 of the human *SOD1* transgene.

A 50X master mix of primer and probe (all stocks at 100  $\mu$ M) was made to reduce variability between assays as detailed in Table 2.7.

**Table 2.7 Prime and probe stock for *SOD1* transgene copy number qPCR assay**

	Volume for 100 $\mu$ L of 50X stock	Conc. in 50X stock	Final conc. (0.2 $\mu$ L in 10 $\mu$ L reaction)
EC forward primer	40 $\mu$ L	40 $\mu$ M	0.8 $\mu$ M
EC reverse primer	40 $\mu$ L	40 $\mu$ M	0.8 $\mu$ M
Tg forward primer	5 $\mu$ L	5 $\mu$ M	0.1 $\mu$ M
Tg reverse primer	5 $\mu$ L	5 $\mu$ M	0.1 $\mu$ M
EC probe	5 $\mu$ L	5 $\mu$ M	0.1 $\mu$ M
Tg probe	5 $\mu$ L	5 $\mu$ M	0.1 $\mu$ M

Experimental templates were extracted as described in Section 2.1.1.1 and a 1/20 dilution in ddH<sub>2</sub>O was used. TaqMan Universal PCR Master Mix with passive internal reference, and AmpErase UNG (Applied Biosystems), was used in the master mix detailed in Table 2.8.

**Table 2.8 *SOD1* transgene copy number qPCR master mix**

	<b>n=1</b>
<b>ddH<sub>2</sub>O</b>	3.8 µL
<b>TaqMan Universal PCR Master Mix (2X)</b>	5 µL
<b>Primer &amp; probe mix (50X)</b>	0.2 µL
<b>DNA</b>	1 µL
	10 µL

A 5 point standard curve was created for each assay plate using a known copy number DNA supplied by Jackson Laboratories (JAXref). The 5 DNA concentrations used to create the standard curve were 100, 20, 4, 0.8 and 0.16 ng/µL. For each point on the standard curve, 6 replicate reactions were set up. Three of these replicates were measured for the *SOD1* Tg standard curve and three were measured for the EC standard curve.

Each experimental DNA sample was assayed over 4 replicate reactions. Two control DNAs, also in 4 replicates, were included in each assay plate; JAXref was used as one reference and a second was a known reduced copy number DNA.

Applied Biosystems 7500 Software v2.0.1 was used to set up a standard (2 hr) run, using default baseline and threshold settings and the following cycling conditions:

1	50 °C	2 mins
2	95 °C	10 mins
3	95 °C	15 secs
4	60 °C	1 min
Cycle from 3 another 39 times		

At the end of the run, the standard curve was first checked for amplification outliers and to ensure that the experimental values fell within the standard curve. Next, experimental outliers as identified by the software were excluded and the analysis re-run.

The delta Ct was calculated by subtracting the mean *SOD1* Tg Ct from the mean EC Ct for each replicate group. The delta-delta Ct was then calculated by subtracting the replicate group delta Ct from the JAXref delta Ct. Relative quantity was then calculated as 2 to the power of the negative delta-delta Ct.

### **2.1.4 Restriction Endonuclease Digestion**

Restriction endonucleases (RE) were purchased from New England BioLabs (NEB) and digests carried out using the supplied buffer and bovine serum albumin (BSA) according to the manufacturer's guidelines. Reaction volumes were between 40 and 100 µL depending on the

concentration of the DNA to be digested and to ensure that the concentration of glycerol was not above that recommended by the manufacturer. Concentration of glycerol in the final reaction should be kept below 10% as levels higher than this can result in the inhibition of enzymatic activity or star activity resulting aberrant cutting activity.

Where possible, enzymes were heat inactivated according to the manufacturer's instructions. RE digests were analysed by agarose gel electrophoresis to check for expected band sizes. Digested DNA was purified using MicroCLEAN or QIAquick PCR Purification Kit or bands separated by agarose gel electrophoresis and the appropriate band excised and gel extracted as described in Section 2.1.1.5.1.

### **2.1.5 Restriction Endonuclease Cloning**

1 µg plasmid DNA (vector) or PCR (insert) was digested using 20 U *Bam*HI-HF (NEB) for 4 hrs at 37 °C in a volume of 10 µL. 1 µL was analysed by agarose gel electrophoresis to check success of the digest. The digested vector was de-phosphorylated to stop it re-ligating back on itself. 10 U alkaline phosphatase calf intestinal (CIP) (NEB) was added to the remaining digest reaction and incubated at 37 °C for 2 hrs. QIAquick PCR Purification Kit was used to purify both insert and vector.

Ligations were carried out using roughly a 3:1 ratio of insert:vector, by copy number. ~500 ng total DNA was incubated with 400 U T4 DNA ligase (NEB) and 1X ligase buffer in a 20 µL volume at 16 °C overnight. The enzyme was then heat deactivated at 65 °C for 15 mins and 1 µL of the reaction was transformed into chemically competent DH10B *E.coli* as described in Section 2.2.4.

### **2.1.6 Sanger Sequencing**

For sequencing directly from BACs or plasmids, 50-100 ng template DNA was used. When sequencing template was a PCR product Table 2.9 was referred to for template quantities: Sequencing reactions were set up on ice and out of direct light due to the photosensitivity of BigDye Terminator v1.1, in a 96 well plate as detailed in Table 2.10. BetterBuffer was used as standard as it was found to be more reliable. When longer reads were required, BetterBase was used.

**Table 2.9 Template quantities used for Sanger sequencing of PCR products**

Template size	Quantity
100-200 bp	1-3 ng
200-500 bp	3-10 ng
500-1000 bp	5-20 ng
1000-2000 bp	10-40 ng
>2000 bp	20-50 ng

**Table 2.10 Sanger sequencing reaction master mix**

	n=1
ddH <sub>2</sub> O	X µL
BetterBase/Buffer (MicroZone)	5 µL
BigDye v1.1 (Applied Biosystems)	1 µL
Betaine (5M) (Sigma Aldrich)	1 µL
Template	X µL
Primer (5 µM)	1 µL
	15 µL

For sequencing from PCR products the following amplification protocol was followed:

1	96 °C	1 min	
2	96 °C	30 secs	Denature
3	50 °C	15 secs	Anneal
4	60 °C	3 mins	Extension
Cycle from step 2, 29 more times			
5	15 °C	5 mins	Final extension
6	4 °C	forever	

For sequencing directly from BACs and plasmids, the following amplification protocol was followed:

1	96 °C	5 mins	
2	96 °C	30 secs	Denature
3	55 °C	15 secs	Anneal
4	60 °C	6 mins	Extension
Cycle from step 2, 34 more times			
5	5 °C	Forever	

After amplification each reaction was precipitated by addition of 37.5 µL (2.5 X volumes) 100% ethanol, 1.5 µL (0.1 X volumes) 125 mM EDTA and 1.5 µL (0.1 X volumes) 3M sodium acetate and mixed. The plate was incubated at r/t for 15 mins and then centrifuged for 30 mins at 2500 x g. The plate was then inverted over tissue and centrifuged for ~10 secs to remove the supernatant. 70 µL 70% ethanol was then added, and the plate centrifuged for 15 mins at 2000 x g. Again, the plate was inverted over tissue and centrifuged for 1 min at 100 x g. Sample were allowed to air dry for 10 mins away from direct light and stored at -20 °C if not to be

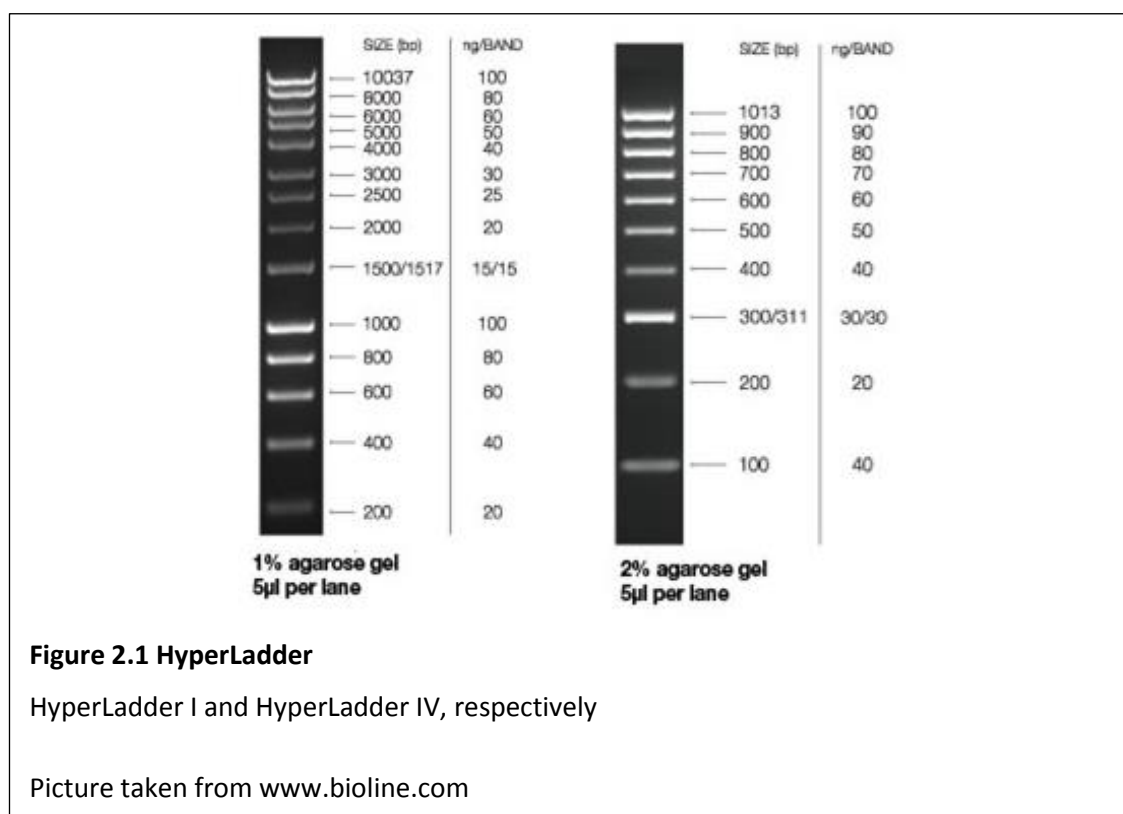
processed immediately. 20  $\mu\text{L}$  of formamide was added to each well of the plate and the reactions denatured by incubation at 95  $^{\circ}\text{C}$  for 5-10 mins before chilling briefly either on ice or on a 4  $^{\circ}\text{C}$  thermal cycler. Reactions were analysed by capillary electrophoresis on an ABI 3730XI DNA analyser.

## 2.1.7 Agarose Gel Electrophoresis

Agarose gel electrophoresis was carried out using a horizontal submarine gel tank (Mupid). A voltage of  $\sim 7\text{V}/\text{cm}$  was used for most applications, unless otherwise specified. 10X concentrate 45 mM Tris-borate, 1 mM EDTA (TBE) was purchased from commercial suppliers and a 1X dilution in  $\text{ddH}_2\text{O}$  was used as running buffer and for preparation of gels.

Gels were typically made using 100 mL TBE to produce a gel of approximately 6 mm thickness. Invitrogen UltraPure Agarose was dissolved in the TBE by heating in a microwave, taking care not to over boil. Ethidium bromide was then added to a concentration of 0.05  $\mu\text{g}/\text{mL}$  before pouring the gel.

Once run, gels were visualised, and a digital photograph was taken, using a UV illuminator. Quantitative DNA ladders were used to approximate the size of the DNA bands on the gel. For expected bands of less than 1 kb, Bioline HyperLadder IV was used and for bands of over 1 kb Bioline HyperLadder I was used. 2.5  $\mu\text{L}$  ladder was used for sizing of bands. When the ladder was also to be used for quantitation 5  $\mu\text{L}$  of ladder was loaded (see Figure 2.1).



## 2.2 BACTERIAL CULTURE

All bacterial work was carried out aseptically, under a Bunsen flame.

Liquid bacterial culture was in Miller's Modification Luria Broth (LB) unless otherwise stated. Miller's Modification LB is lower in salts than regular LB and so reduces the chance of arcing when electroporating *E.coli* that have been cultured using it.

Volumes of up to 1 mL were contained in 1.5 mL microfuge tubes and incubated in an thermomixer (Eppendorf), shaking at 300 rpm. For volumes over 1 mL appropriate size plastic-ware was used and incubation was in a bench top incubator (see Section 7.2, Appendix 2), shaking at 200 rpm.

Bacteria grown on Luria Agar Base plates (LB plates) were incubated in a stationary bench top incubator.

For details on preparation of plates and media and antibiotic concentrations, see Section 7.2, Appendix 2.

### 2.2.1 Culture Conditions for *Escherichia coli* Strains Used

SW102 *E.coli* were always cultured at 30 °C unless otherwise specified.

DH10B *E.coli* containing high copy plasmids, or no plasmid, were cultured at 37 °C unless otherwise stated. DH10B *E.coli* containing low copy plasmids or BACs were cultured at 30 °C unless otherwise stated.

### 2.2.2 Overnight Culture

A 15 mL falcon tube containing 5 mL LB with appropriate antibiotics was inoculated with a single colony from an LB agar plate and cultured overnight for ~16 hrs.

### 2.2.3 Measurement of *E.coli* Suspension Concentration

Concentration of *E.coli* grown in liquid culture was estimated by spectrophotometry.

Briefly, 1 mL LB or liquid culture was aliquoted into a disposable cuvette. The LB only aliquot was used to blank the equipment after which the OD<sub>600</sub> of the culture was measured.

Concentration was estimated as OD<sub>600</sub> of 1 being roughly equal to 1x10<sup>9</sup> cells/mL.

### 2.2.4 Transformation of Chemically Competent *E.coli*

Chemically competent *E.coli* were purchased from Invitrogen. MAXefficiency DH10B Competent cells and One Shot TOP10 Competent *E.coli* were used according to the manufacturer's instructions.

## 2.2.5 Preparation and Transformation of Electrocompetent *E.coli*

Note- “§” indicates points of deviation from this protocol referenced in Section 2.4 BAC Recombineering.

### 2.2.5.1 MAKING *E.COLI* ELECTROCOMPETENT

500 µL overnight culture was used to inoculate 10 mL LB plus appropriate antibiotics in a 50 mL Falcon tube and grown for ~3 hrs until OD<sub>600</sub> reached 0.5-0.6. At this point 1.5 mL aliquots were taken for each planned transformation.

(§1) Aliquots were transferred to an ice water slurry and chilled for ~5 mins before being centrifuged in a pre-chilled, 4 °C bench top microfuge for 15 secs. Supernatant was tipped out and the inverted tube tapped sharply on the side of the waste pot to remove as much media as possible. 1 mL sterile, ice-cold, 10% glycerol (v/v in ddH<sub>2</sub>O) was then added to wash the cells and the tube inverted to mix. The centrifuge and wash step was repeated once. Samples were centrifuged a third time and supernatant tipped out leaving between 50-100 µL. The tubes were placed on ice and processed one at a time.

### 2.2.5.2 ELECTROPORATION TRANSFORMATION

(§2) 1 µL of plasmid DNA suspended in ddH<sub>2</sub>O at 10 ng/µL was added to the tube containing the electrocompetent *E.coli* and the tube was tapped gently to mix. The cell suspension was then transferred to a pre-chilled 1 mm gap electroporation cuvette and immediately electroporated in a Biorad *E.coli* Pulser at 1.35 kV, with the time constant set to 5 msec. The actual time constant was noted with readings from 5.3 to 4.8 msec being acceptable. If shorter readings were achieved, DNA was diluted 1:1 in ddH<sub>2</sub>O to reduce salt content before repeating the electroporation on a spare aliquot of electrocompetent *E.coli* was washed for a third time to reduce residual salts from the growing media.

Immediately after electroporating, 1 mL LB (no antibiotics) was added to the cuvette to resuspend the *E.coli* and the cells were transferred to a fresh 1.5 mL tube. Bacteria were cultured for 90 mins without antibiotics to allow time for expression of antibiotic resistance. (§3) After this time, an appropriate dilution of the cell suspension was plated onto LB agar plates with appropriate antibiotics. Plates were incubated overnight at 30 °C to obtain individual colonies.

## 2.2.6 Glycerol Stocks

750 µL overnight culture was added to 750 µL bacterial freezing media (Section 7.2, Appendix 2) in a 2 mL cryotube and inverted to mix. These were placed in a polystyrene rack in a plastic box to slow freeze time and transferred to a -70 °C freezer. Once frozen, tubes were transferred into a regular freezer box.

When removing glycerol stocks from the freezer to streak LB agar plates, tubes were kept on dry ice.

## 2.3 PLASMIDS, BACs AND CASSETTES

### 2.3.1 BAC Selection

Human and C57BL/6J (BL/6J) BACs were selected using National Center for Biotechnology Information's (NCBI) CloneDB (<http://www.ncbi.nlm.nih.gov/clone/>) searching by species and gene. BACs were selected based on the position of the *SOD1* sequence being central to the insert. One human BAC was selected: RP11-535E10 (E10) which resides in the pBACe3.6 (Frengen et al., 1999) backbone. Two BL/6J BACS were selected: RP24-363N21 (N21) and RP24-238L18 (L18) both of which reside in the pTARBAC1 (Zeng et al., 2001) backbone. BACs were ordered from Children's Hospital Oakland Research Institute (CHORI) BACPAC Resource Center (<http://bacpac.chori.org/home.htm>).

The National Institute of Genetics (Japan) (NIG) mouse genome database was used to search for an appropriate C57BL/6N (BL/6N) BAC (<http://molossinus.lab.nig.ac.jp/msmdb/BacDetail>). One *Sod1* containing BAC was selected: B6Ng01-068O19 (O19) which resides in the pBACe3.6 (Frengen et al., 1999) backbone. BACs were ordered from Riken Bioresource Center (<http://dna.brc.riken.jp/en/NBRPB6Nbacen.html>).

Full details of each BAC can be found in Section 7.2.2, Appendix 2.

### 2.3.2 Antibiotic Resistance Cassettes

#### 2.3.2.1 *FRT FLANKED NEO CASSETTE*

FRT-PGK-gb2-neo-FRT cassette plasmid was purchased from Gene Bridges. In eukaryotic cells the mouse Phosphoglucokinase (PGK) promoter allows for selection with G418/neomycin. In Prokaryotic cells, such as *E.coli* the gb2 promoter, a modified Em7 promoter, allows for selection by kanamycin. The cassette is flanked by *FRT* sites allowing use of FLP recombinase to excise the sequence. See Figure 2.2. Primers detailed in Table 2.11 were used for amplification of the 1,601 bp cassette.



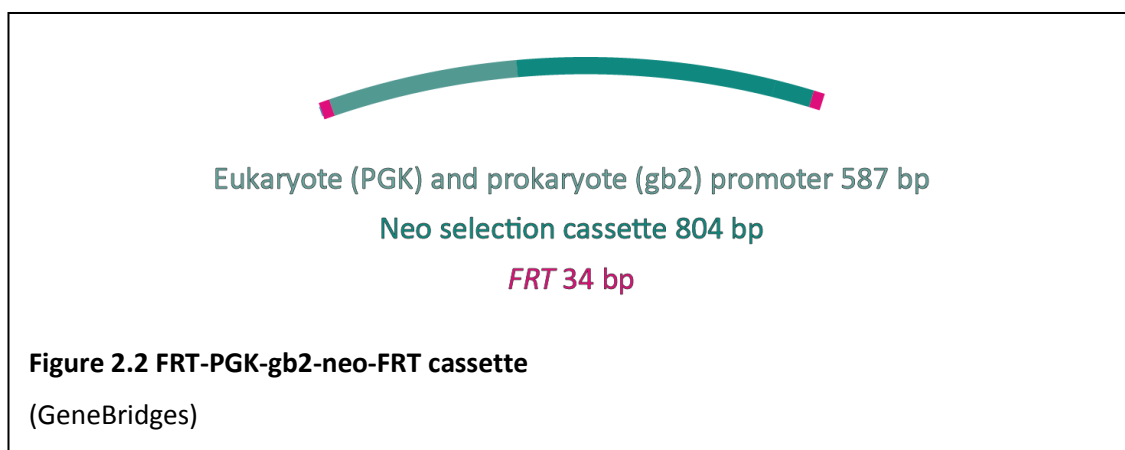


**Table 2.11 Primers for amplification of FRT-PGK-gb2-neo-FRT**

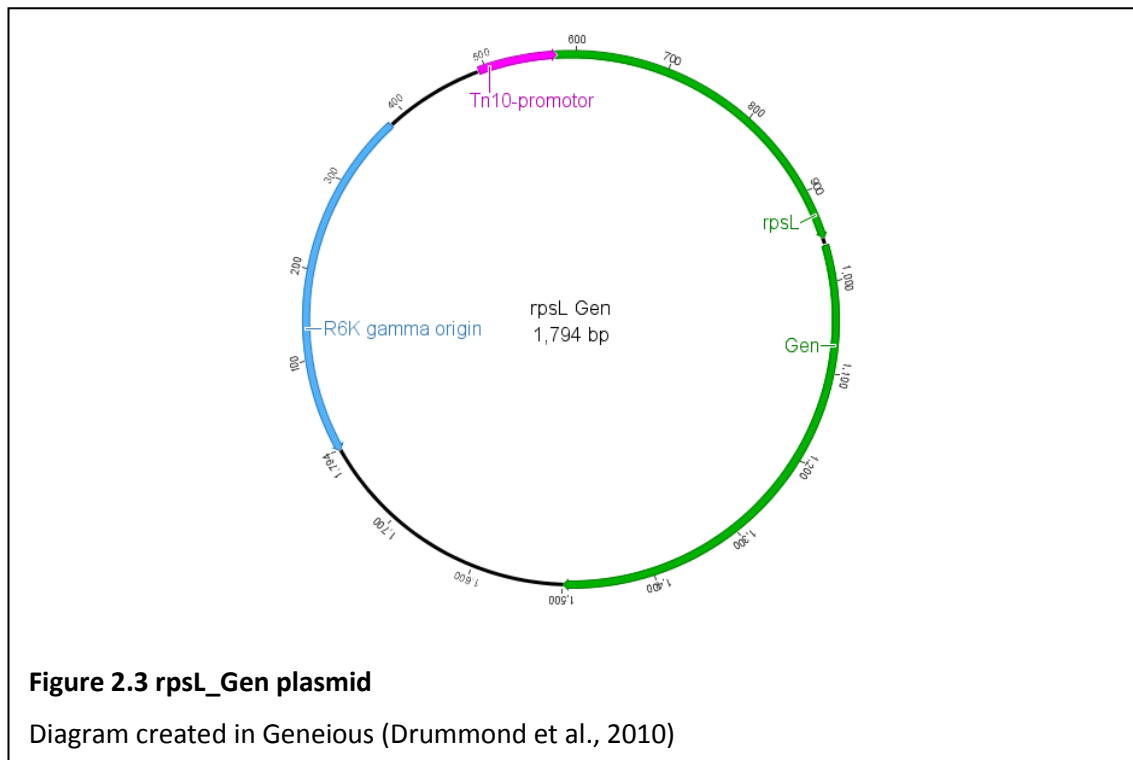
Primer name	Primer sequence
<b>FRT_FOR</b>	CGCGAAGTTCCTATTCTCTAGAAAG
<b>FRT_REV</b>	CTATAGGGCTCGAGGAAGTTC

### 2.3.2.2 *rpsL\_Gen* POSITIVE/NEGATIVE SELECTION

The *rpsL\_Gen* positive/negative selection cassette was a kind gift from Dr Andrew Smith, and is shown in Figure 2.3. The plasmid has a polycistronic operon encoding a gentamicin resistance gene (*Gen*) and an *rpsL* gene which confers sensitivity to streptomycin. Primer details in Table 2.12 were used for amplification of the 1,077 bp cassette.

**Table 2.12 Primers for amplification of *rpsL\_Gen* cassette**

Primer name	Primer sequence
<b><i>rpsL_ge_F</i></b>	GAGCATGTTTCTGCGTAGTGTCAGC
<b><i>rpsL_ge_R</i></b>	CATCCTGTAGGTGTAGACGACGACG



### 2.3.3 Custom Plasmids

In order to speed up the construction process of our BAC targeting vector custom plasmids were purchased from GeneArt.

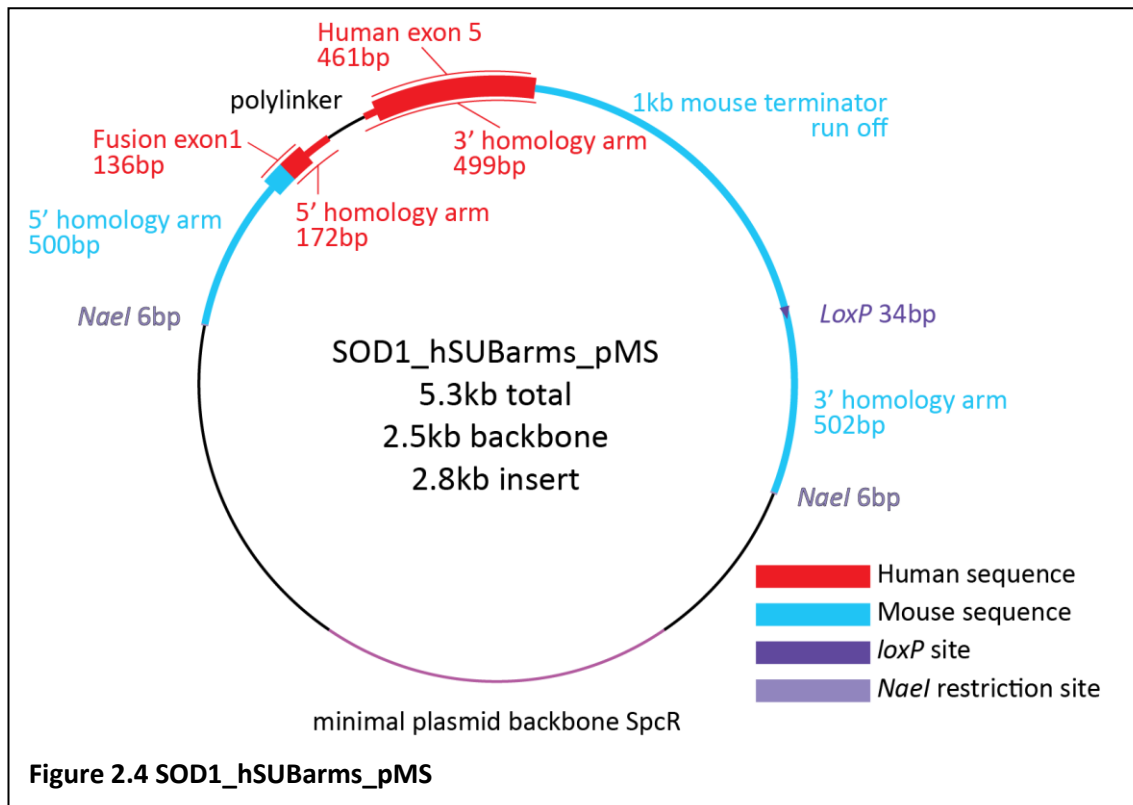
Plasmids were supplied as 5 µg lyophilised DNA and resuspended in 50 µL ddH<sub>2</sub>O to give a concentration of 100 ng/µL. Long terms stocks were stored at -70 °C, working stocks were stored at -20 °C.

#### 2.3.3.1 *SOD1\_hSUBARMS\_PMS*

The *SOD1\_hSUBarms\_pMS* plasmid was designed for subcloning the human *SOD1* sequence out of a BAC, and cloning this subclone into a *Sod1* containing mouse BAC. It is illustrated in Figure 2.4.

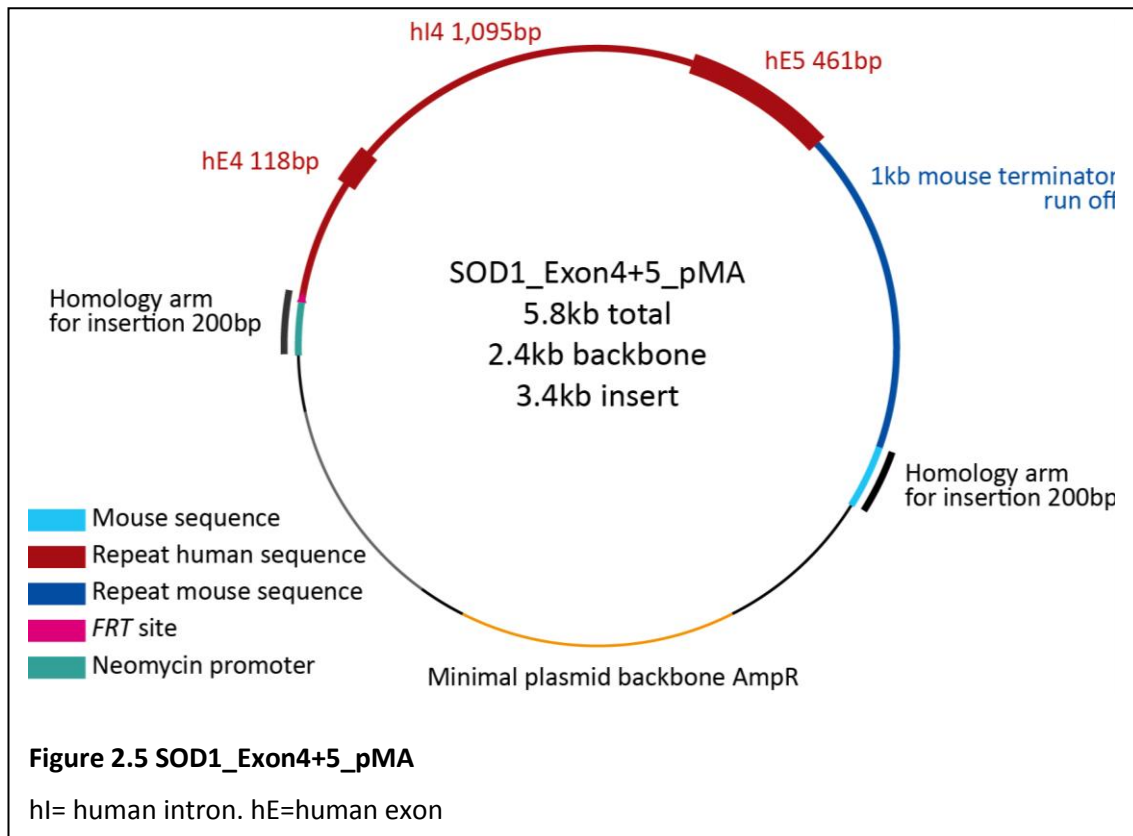
For the purpose of subcloning human *SOD1* into the plasmid, the construct contains a 172 bp region of homology to the 5' sequence of *SOD1* from the start codon in exon 1, through to 100 bp of intron 1. After a 98 bp polylinker there is a 499 bp homology region to the 3' human *SOD1* sequence including all of exon 5 and 36 bp of intron 4.

For the purpose of cloning the *SOD1* sequence into a *Sod1* containing mouse BAC the construct contains 500 bp of mouse sequence 5' to the mouse *Sod1* sequence including exon 1 up to the start codon (at which point the sequence becomes that of human) and 436 bp of 5' sequence. There are also 502 bp of sequence matching sequence 3' of the mouse *Sod1* sequence.



### 2.3.3.2 SOD1\_Exon4+5\_pMA

The purpose of the SOD1\_Exon4-5\_pMA was for introduction of a repeat section of human exons 4-5 as part of the selectable mutation machinery. It contains a 3,046 bp cassette with human genomic sequence running from 356 bp of intron 3 to the end of exon 5, continuing with 1 kb of mouse genomic sequence 3' of exon 5'. Flanking this 3,046 bp repeat cassette is 200 bp of mouse and engineered sequence to target the cassette to the desired location in the humanising construct (Figure 2.5).



## 2.4 BAC RECOMBINEERING

### 2.4.1 Red/ET Recombineering System

Red/ET recombineering was carried out using Gene Bridges Quick & Easy BAC Modification Kit.

Using the Red/ET system, *Red $\alpha$* , *Red $\beta$*  and *Red $\gamma$*  recombinase proteins are expressed in *E.coli* via a transiently transformed plasmid, pRed/ET (illustrated in Figure 2.6). A polycistronic operon encodes the recombinase proteins under a temperature sensitive and L-arabinose inducible promoter. *Red $\alpha$* , *Red $\beta$*  and *Red $\gamma$*  are equivalent to *exo*, *bet* and *gam* (as described above in Section 1.3.2). The plasmid is lost after each heat induction and must be re-transformed for each round of recombineering.

#### 2.4.1.1 TRANSFORMATION OF PRED/ET PLASMID

20 ng pRed/ET plasmid was transformed by electroporation into DH10B *E.coli*, already containing the target BAC or plasmid as described in Section 2.2.5 Preparation and Transformation of Electrocompetent *E.coli*. After electroporation, *E.coli* were cultured at 30 °C for 1 hr in LB (no antibiotics). 100  $\mu$ L cell suspension was then spread onto an LB agar plate containing tetracycline (tet) and appropriate antibiotics to maintain the target BAC or plasmid, protected from light in a cardboard box because tet is light sensitive, and incubated at 30 °C overnight (~16 hrs). The following day, plates should be populated with individual colonies. Plates were stored at 4 °C for up to 1 week.

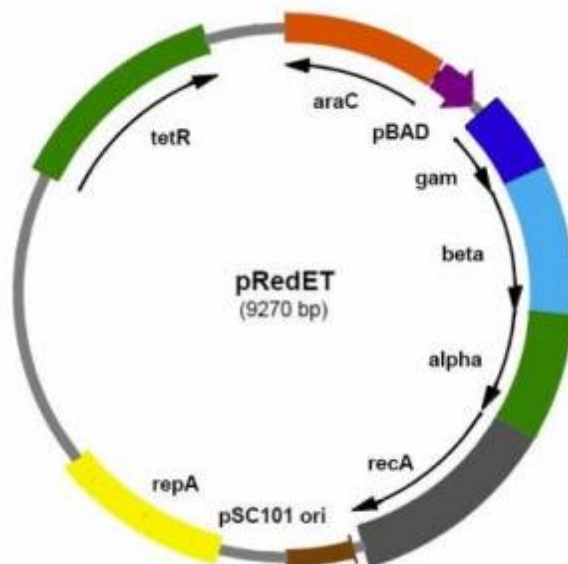


**Figure 2.6 RedET plasmid**

Picture taken from [www.GeneBridges.com](http://www.GeneBridges.com)

#### 2.4.1.2 INDUCTION OF RED/ET RECOMBINASE EXPRESSION

1 mL LB with tet and appropriate antibiotics to maintain the target BAC or plasmid was inoculated with a single colony and cultured overnight at 30 °C, protected from light.

For each recombineering experiment, one induced and one un-induced control was prepared as follows. 1.4 mL LB with the same antibiotics was inoculated with 40 µL overnight culture and cultured at 30 °C for around 2 hrs until OD<sub>600</sub> reached ~0.3.

The experimental culture was induced by adding 50 µL 10% (w/v) L-arabinose. The control culture was left un-induced by not adding L-arabinose. Both I and UI cultures were then incubated at 37 °C for 45 mins to 1 hr. Cultures were then transferred to an ice water slurry.

The protocol described in Section 2.4.3 General Recombineering Protocol, was then followed.

#### 2.4.2 SW102 Recombineering System

SW102 *E.coli* are derived from DH10B *E.coli*. They have been modified to express *exo*, *bet* and *gam* from a stably integrated defective λ prophage which is under control of a temperature sensitive repressor. Thus SW102 *E.coli* can be used directly for recombineering following induction at 42 °C, rather than re-transforming the expression plasmid for each round of recombineering (Warming et al., 2005).

#### **2.4.2.1 INDUCTION OF SW102 RECOMBINASE EXPRESSION**

500  $\mu$ L overnight culture of SW102 *E.coli* harbouring the target BAC or plasmid was used to inoculate 10 mL LB (plus appropriate antibiotics) and grown for ~3 hrs until OD<sub>600</sub> reached 0.5-0.6.

For each recombineering experiment, once the initial culture has reached OD<sub>600</sub> ~0.5-0.6, two 1.5 mL aliquots of the cell suspension were taken, one to be induced (I) and one to act as an un-induced control (UI). Both I and UI were incubated at 30 °C for 5 mins to ensure that both aliquots were at temperature. I was then transferred to 42 °C to induce recombinase expression and both I and UI were incubated for a further 15 mins. Both aliquots are then transferred to an ice-water slurry.

The protocol described in Section 2.4.3 General Recombineering Protocol was then followed.

### **2.4.3 General Recombineering Protocol**

*E.coli* bacteria were induced as described for the specific system used (see Section 2.4.1 for Red/ET and 2.4.2 for SW102). The protocol in Section 2.2.5 Preparation and Transformation of Electrocompetent *E.coli*, was then followed from (§1), but with the following modifications:

§2- 1  $\mu$ L linear DNA suspended in ddH<sub>2</sub>O at 100 ng/ $\mu$ L, or, in the case of synthetic oligonucleotides, 200 ng/ $\mu$ L in TE, was transformed into the electrocompetent *E.coli*.

§3- After the 90 min recovery period, samples were centrifuged in a room temperature bench top microfuge for 15 secs and supernatant tipped off. Cells were resuspended in the medium remaining in the tube and the entire suspension spread onto LB agar plates with antibiotics selective for the desired modification. Plates were incubated overnight at 30 °C.

The number of colonies grown on each plate was counted, with the number on the un-induced control plate used as a guide for how many clones from the induced plate to screen. PCR screening was then carried out as described in Section 2.1.2.2.

### **2.4.4 Preparation of Inserts and Subcloning Vectors for Recombineering**

Except in the case of synthetic oligonucleotides (where concentration is calculated based on details supplied by the manufacturers), concentration of inserts/vectors was calculated by nanodrop spectrophotometer and diluted to 100 ng/ $\mu$ L in ddH<sub>2</sub>O. Concentration was then checked by agarose gel electrophoresis using an appropriate quantitative DNA ladder (see Section 2.1.7).

#### *2.4.4.1 PCR AMPLIFICATION*

A nested PCR strategy was used to amplify the insert or subcloning vectors used for recombineering.

Touchdown PCR (see Section 2.1.2.1) was used to amplify the target fragment from plasmid DNA template. The first set of primers was designed to amplify the insert/subcloning vector, plus 10-20 bp flanking either side.

Plasmid DNA template was then separated from the PCR product by RE digestion (where available) followed by agarose gel electrophoresis and gel extraction. The retrieved PCR product was then used as template for a further touchdown PCR with primers designed to amplify just the section required for recombineering. PCR products were purified using microCLEAN and resuspended in ddH<sub>2</sub>O.

#### *2.4.4.2 ADDITION OF HOMOLOGY ARMS BY PCR AMPLIFICATION*

The protocol described in Section 2.4.4.1, was used with the following modifications:

- 1- The first set of primers is designed to amplify the target with no additional flanking sequence.
- 2- The second pair of primers is identical to the first, but with 40-50 bp added to the 5' end of the primer designed to act as homology arms for targeting during recombineering.

#### *2.4.4.3 LINEARIZATION BY RESTRICTION ENDONUCLEASE DIGESTION*

In some cases where it was not possible or desirable to amplify the insert or subcloning vector by PCR, RE digestion was used to extract the desired sequence from its resident plasmid.

RE digestion was carried out as described in Section 2.1.4. The desired fragment was then separated from the unwanted portion by gel electrophoresis and gel extraction as described (see Section 2.1.7 and 2.1.1.5.1).

#### *2.4.4.4 OLIGONUCLEOTIDES*

For small insertions, deletions and base pair changes synthetic oligonucleotides (oligos) were used for recombineering.

Synthetic oligos are designed with 50-60 bp of homology either side of the desired change. Lyophilised oligos were resuspended to a concentration of 200 ng/μL in TE.

### **2.4.5 Sibling Selection**

For unselected recombineering modifications (without an addition of a new antibiotic selection cassette) or modifications with a low probability and/or high background, sibling-

selection (sib-selection) was used to increase the likelihood of identifying a correctly modified clone by initially screening ~10 clones per screening PCR.

A 96 well cell-culture plate was prepared with 200  $\mu$ L LB plus antibiotics per well (leaving some empty wells to allow for controls when screening). Appropriate antibiotics are used for either maintenance of the plasmid or selection of the modified plasmid.

At point (§3) in the recombineering protocol, rather than plating the recombineering experiment onto selective LB agar plates, the cell suspension was diluted to ~ 10 cells/ $\mu$ L and 1  $\mu$ L added to each well of the prepared 96-well cell-culture plate. The plate was grown overnight in a shaking incubator before screening.

DNA was prepared as described in Section 2.1.1.4 Fast DNA Preparations for Plasmid Screening PCR and PCR screened for the desired recombination. For wells in which the correct recombination was detected, 1  $\mu$ L culture was diluted and used to inoculate another 96 well cell-culture plate and re-screened. After the second screening, 10  $\mu$ L from those wells screened positive was spread onto selective LB agar plates and individual colonies screened.

## **2.5 MICE**

All animals were maintained and all animal experiments were carried out in accordance with the Animals (Scientific Procedures) Act 1986 and Home Office Project licence No. 30/2290.

Within the text of this thesis, a shortened form of nomenclature will be used to describe the various genotypes of mice used. The nomenclature is explained below in Sections 2.5.2 - 2.5.6 and for clarity presented here in Table 2.13 and repeated at the beginning of each relevant Results chapter.

### **2.5.1 Housing and General Husbandry**

Animals were housed in Tecniplast individually ventilated cages (IVCs) with grade 5 dust-free autoclaved wood bedding and had constant access to food and water, if mice appeared to start losing their ability to move freely around the cage or when weight loss started to become apparent, hydrogel was placed at ground level in the cage and paper bedding was removed to reduce possible impedance to their movement. The animal house was maintained at a constant temperature of 19-23 °C with 55 $\pm$ 10% humidity in a 12 hr light:dark cycle.

When animals were allocated to experimental groups (usually between 35-60-days of age) they were moved into standardised group housing (5 mice per cage) which in addition to equal quantities of wood bedding, all had paper bedding and a translucent red “mouse house” for nesting.



All weighing and behavioural assessments were carried out in class 2 animal handling cabinet.

**Table 2.13 Short form nomenclature of mouse genotypes**

Transgene (Tg) allele	Knockout (KO) allele	Short form (used in text)
Non-transgenic	<i>Sod1</i> <sup>+/+</sup> (WT)	NTg;Sod1wt
Non-transgenic	<i>Sod1</i> <sup>+/-</sup> (heterozygous KO)	NTg;Sod1het
Non-transgenic	<i>Sod1</i> <sup>-/-</sup> (homozygous KO)	NTg;Sod1ko
<i>SOD1</i> <sup>G93A</sup> Tg hemizygous	<i>Sod1</i> <sup>+/+</sup> (WT)	TgG93A;Sod1wt
<i>SOD1</i> <sup>G93A</sup> Tg hemizygous	<i>Sod1</i> <sup>+/-</sup> (heterozygous KO)	TgG93A;Sod1het
<i>SOD1</i> <sup>G93A</sup> Tg hemizygous	<i>Sod1</i> <sup>-/-</sup> (homozygous KO)	TgG93A;Sod1ko
<i>SOD1</i> <sup>WT</sup> Tg hemizygous	<i>Sod1</i> <sup>+/+</sup> (WT)	TgWT;Sod1wt
<i>SOD1</i> <sup>WT</sup> Tg hemizygous	<i>Sod1</i> <sup>+/-</sup> (heterozygous KO)	TgWT;Sod1het
<i>SOD1</i> <sup>WT</sup> Tg hemizygous	<i>Sod1</i> <sup>-/-</sup> (homozygous KO)	TgWT;Sod1ko

### 2.5.1.1 HUMANE ENDPOINTS

Humane endpoints were defined as: 15% body weight loss, a loss of the righting reflex (ability to right itself when placed on its side), or paralysis which prevented the animal from moving about the cage. Other welfare issues were assessed on a case by case basis.

## 2.5.2 Human *SOD1*<sup>G93A</sup> Transgenic Mice

B6.Cg-Tg(SOD1\*G93A)1Gur/J mice (Gurney et al., 1994; Chiu et al., 1995) (Jax stock code 004435) were purchased from Jackson Laboratories. These mice were purchased already congenic on a C57CL/6J background. For general maintenance, the line was bred by backcrossing hemizygous transgenic males in trios with C57BL/6J females. Within the text of this thesis these animals will be referred to as TgG93A and non-transgenic littermates as NTg.

Genotyping was carried out using the protocol as described in Section 2.1.2.4.

For breeding stock, animals were killed at 120-days of age in order to avoid development of symptoms and unnecessary suffering.

## 2.5.3 Human Wild-Type *SOD1* Transgenic Mice

B6SJL-Tg(SOD1)2Gur/J mice (Gurney et al., 1994) (Jax stock code 002297) were purchased from Jackson Laboratories. These mice were purchased on a C57BL/6J x SJL/J hybrid background. The F1 animals were backcrossed to C57BL/6J for at least 4 generations before being used in experimental crosses. Including the original F1 cross to C57BL/6J, 5 generations of crosses should theoretically result in offspring homozygous for BL/6J at ~96.9% of the genome, with ~3.1% in a BL/6J, SJL heterozygous state.

For general maintenance, the line was bred by backcrossing hemizygous transgenic males in trios with C57BL/6J females. Within the text of this thesis these animals will be referred to as TgWT and non-transgenic littermates as NTg.

Genotyping was carried out using the protocol as described in Section 2.1.2.4.

#### **2.5.4 *Sod1* Knockout Mice**

B6;129S-*Sod1*<sup>tm1Leb</sup>/J mice (Matzuk et al., 1998) (Jax stock number 002972) were purchased from Jackson laboratory. These mice were purchased on a C57BL/6J x 129S hybrid background. The F1 animals were backcrossed to C57BL/6J for at least 4 generations before being used in experimental crosses. Including the original F1 cross to C57BL/6J, 5 generations of crosses should theoretically result in offspring homozygous for BL/6J at ~96.9% of the genome, with ~3.1% in a BL/6J, 129S heterozygous state.

Within the text of this thesis these animals will be referred to as Sod1wt (homozygous for the wild-type *Sod1* allele), Sod1het (heterozygous for the *Sod1* KO allele) and Sod1ko (homozygous for the *Sod1* KO allele).

Genotyping was carried out using the protocol described in Section 2.1.2.5.

Sod1het males were mated in trios with two Sod1het females in order to produce Sod1ko males for further breeding. Sod1ko males were bred in trios with two C57BL/6J females in order to produce Sod1het females needed for breeding of the transgene x KO crossed colonies.

#### **2.5.5 TgG93A, Sod1ko Cross**

This line of mice was produced by crossing TgG93A with Sod1ko mice. A two-step cross was used to initiate the line as illustrated in

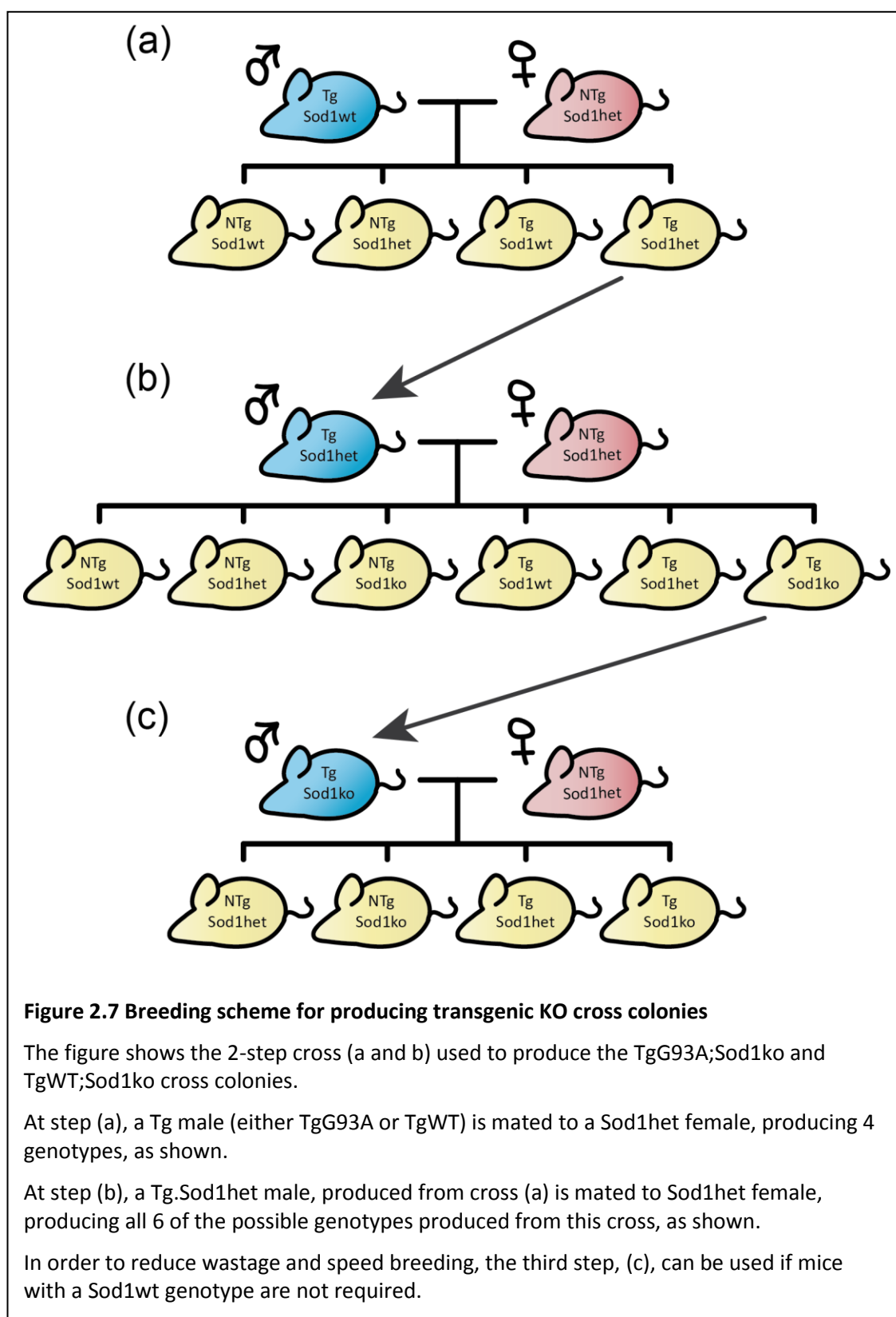
Figure 2.7. TgG93A males (from the *SOD1*<sup>G93A</sup> transgenic colony) were mated to Sod1het females (from the *Sod1* KO colony), producing both NTg and TgG93A offspring with either Sod1het or Sod1wt genotypes, as illustrated in

Figure 2.7a, resulting in 4 possible genotype combinations: NTg;Sod1wt, NTg;Sod1het, TgG93A;Sod1wt and TgG93A;Sod1het.

For the second step, shown in

Figure 2.7b, male TgG93A;Sod1het offspring were mated to Sod1het females (from the *Sod1* KO colony), producing 6 genotype combinations: NTg;Sod1wt, NTg;Sod1het, NTg;Sod1ko, TgG93A;Sod1wt, TgG93A;Sod1het, TgG93A;Sod1ko). For on-going maintenance of the colony,

and production of mice for use in the cross characterisation project (described in Chapter 4)  
this is the breeding scheme that was used.



For the Transmission project (described in Chapter 3), a third level of the crossing scheme was used, as illustrated in

Figure 2.7 c. TgG93A;Sod1ko males were mated to Sod1het females (from the *Sod1* KO colony) producing 4 possible genotype combinations: NTg;Sod1het, NTg;Sod1ko, TgG93A;Sod1het and TgG93A;Sod1ko. Female offspring with a TgG93A;Sod1ko genotype were used in the experiment.

Genotyping was carried out using the protocols described in Sections 2.1.2.4 and 2.1.2.5. For animals with TgG93A;Sod1ko genotype result, the PCRs were repeated to confirm the genotype.

### **2.5.6 TgWT, Sod1ko Cross**

This line of mice was produced by crossing TgWT with the Sod1ko mice. The same 2-step cross was used to produce the line, as described for the TgG93A Sod1ko cross. As is shown in

Figure 2.7 a, in the first step, TgWT males (from the WT *SOD1* transgenic colony) were mated to Sod1het females (from the *Sod1* KO colony), producing 4 possible genotype combinations: NTg;Sod1wt, NTg;Sod1het, TgWT;Sod1wt, TgWT;Sod1het.

For the second step, illustrated in

Figure 2.7 b, male TgWT;Sod1het offspring from the first step were mated to Sod1het females (from the *Sod1* KO colony), producing 6 possible genotype combinations: NTg;Sod1wt, NTg;Sod1het, NTg;Sod1ko, TgWT;Sod1wt, TgWT;Sod1het, TgWT;Sod1ko. This is the mating scheme that was used for on-going colony maintenance.

In order to produce animals for use in the Transmission project (described in Chapter 3) a third level of the crossing scheme was used, as is shown in

Figure 2.7c. TgWT;Sod1ko males were mated to Sod1het females (from the *Sod1* KO colony) producing 4 possible genotype combinations: NTg;Sod1het, NTg;Sod1ko, TgWT;Sod1het and TgWT;Sod1ko. Female offspring with a TgWT;Sod1ko genotype were used in the experiment.

Genotyping was carried out using the protocols described in Sections 2.1.2.4 and 2.1.2.5. For animals with TgWT;Sod1ko genotype result, the PCRs were repeated to confirm the genotype.

## **2.6 MOUSE EXPERIMENTAL PROCEDURES**

### **2.6.1 Mouse Experimental Procedures Specific to the Transmission Project**

All experiments were carried out using female mice. Animals were allocated to experimental groups sequentially with longer incubation periods allocated first and each inoculation group being filled one at a time.

#### *2.6.1.1 NEUROLOGICAL CHECKS*

Weekly neurological checks were carried out by technical staff at the MRC Prion Unit Biological Services Facility. Once a week, each animal was lifted out of its cage by its tail and observed for signs of onset defined as: tremor in the rear limbs when suspended up the tail, rear limbs moving toward the midline of the body rather than being held out in a splayed position as is normal. Observations were carried out by an animal technician and whenever possible, the same technician carried out all observations.

### **2.6.2 Inoculation of Mice**

#### *2.6.2.1 INOCULANT PREPARATION*

Details of the tissues used are given in Table 2.14. Tissues were stored at -70 °C until being defrosted on ice for preparation of inocula. Inocula were prepared in a class 1 microbiological safety cabinet by Dr Graham Jackson.

A stock 10% (w/v) homogenate of tissue was prepared in Dulbecco's Phosphate Buffered Saline, minus  $\text{CaCl}_2$  and  $\text{MgCl}_2$  (DPBS, Gibco). Tissue and DPBS were measured into a sterile bijoux tube. A sterile 19G needle was then attached to a syringe and used to disrupt the tissue. Once the tissue was disrupted, the sample was aspirated at least 5 times through the needle. Aspiration was then repeated using a 21G needle and then a 23G needle. The 10% homogenate was then transferred to a cryotube for storage at -70 °C.

For preparation of 1% homogenates to be used as inocula, the 10% homogenate was thoroughly defrosted on ice and mixed by shaking. An appropriate volume of DPBS was dispensed into a sterile bijoux tube followed by an appropriate volume of the 10% homogenate. A syringe fitted with a 26G needle was then used to aspirate the sample at least 5 times. Aliquots were then dispensed into cryotubes for storage at -70 °C.

**Table 2.14 Details of inocula**

Name	ID	Species	Genotype	Age at death	Sex	Tissue used
<b>m-TgG93A</b>	I12250	mouse	TgG93A;Sod1ko	100 days	female	spinal cord
<b>m-TgWT</b>	I12251	mouse	TgWT;Sod1ko	100 days	female	spinal cord
<b>m-NTg</b>	I12252	mouse	NTg;Sod1ko	100 days	female	spinal cord
<b>h-D101G</b>	I13029	human	SOD1 <sup>+D101G</sup>	46 years	female	motor cortex
<b>h-I113T</b>	I13031	human	SOD1 <sup>+I113T</sup>	47 years	male	motor cortex
<b>h-cntrl1</b>	I13033	human	SOD1 <sup>+/+</sup>	52 years	female	motor cortex
<b>h-cntrl2</b>	I13035	human	SOD1 <sup>+/+</sup>	40 years	male	motor cortex
<b>DPBS</b>	I56	n/a	DPBS only control			

### 2.6.2.2 INOCULATION PROTOCOL

Inoculations were carried out by technical staff at the MRC Prion Unit Biological Services Facility.

Inocula were removed from the -70 °C freezer and allowed to thaw completely and return to room temperature.

Animals were anaesthetised by inhalation of a mixture of oxygen and isoflurane within an induction chamber. Oxygen flow was set to 2-4 L/min and the isoflurane vaporiser was set to 5% for anaesthetic induction. Five animals were placed in the induction chamber at a time and were monitored by the anaesthetist.

Once anaesthetised, one animal at a time was removed from the chamber and depth of anaesthesia was checked by pedal reflex and blink reflex. The mouse's head was held stable using a pair of forceps. A 25G needle fitted to a 1 mL syringe was used for intra-cerebral inoculations. The needle was positioned in the right front quadrant of the head (see Figure 2.8) and inserted through the skull into the cerebrum and 30 µL inoculum dispensed. The animal was then taken by the anaesthetist back to the home cage which was rested on a heat mat. The animal was placed on a tissue at the front of the cage and observed until fully recovered and mobile.

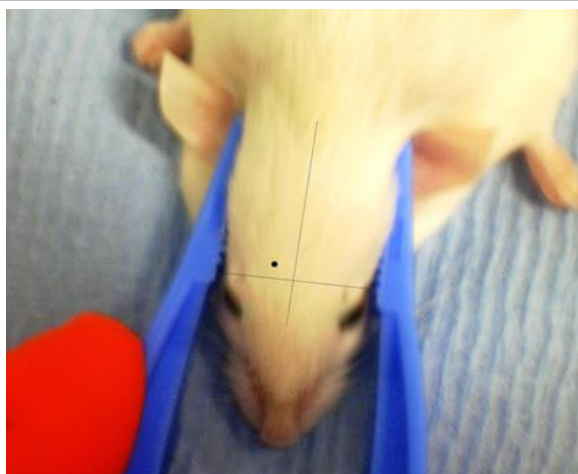


**Figure 2.8 Location of intra-cerebral injection**

Marked with black dot. Image kindly provided by Gavin Graham

### *2.6.2.3 TgG93A TRANSMISSION INOCULATION SCHEDULE*

TgG93A;Sod1ko mice, were inoculated at 50-days of age  $\pm 1$  day. Four different inocula were used and there were two post-inoculation time-points for harvesting of tissues for histological analysis. There was also one group of non-inoculated controls. Table 2.15 details inoculum used and the number of animals per group.

**Table 2.15 G93A inoculation schedule**

Table shows number of animals allocated to each group

Inoculum	Post-inoculation cull time-point (days)	
	40	1
m-TgG93A	11	3
m-TgWT	10	3
m-NTg	10	3
DPBS	10	3
non-inoculated	10	0

### *2.6.2.4 TgWT TRANSMISSION INOCULATION SCHEDULE*

TgWT;Sod1ko mice, were inoculated at 70-days of age  $\pm 15$  days. Eight different inocula were used. There were 5 time-points for harvesting of tissues for histological analysis. Non-inoculated controls were also taken at each of the time-points. Table 2.16 details inoculum used and the number of animals per group.

**Table 2.16 WT inoculation schedule**

Table shows number of animals in each group

	Post-inoculation cull time-point (days)				
	660	295	180	90	7
Inoculum	660	295	180	90	7
m-TgG93A	20	10	10	10	10
m-TgWT	20	10	10	10	10
m-NTg	20	10	10	10	10
h-D101G	20	10	10	10	10
h-I113T	20	10	10	10	10
h-cntrl1	20	10	10	10	10
h-cntrl2	20	10	10	10	10
DPBS	20	10	10	10	10
non-inoculated	20	10	10	10	10

### 2.6.3 Mouse Experimental Procedures Specific to the Characterisation Project

All experiments were carried out using female mice. One allocated to the experiment, animals were group house according to birth order and their genotypes blinded to both technical staff and the experimenter by censoring cage cards.

#### 2.6.3.1 WEEKLY WEIGHTS

Mice were weighed by technical staff at the MRC Prion Unit Biological Services Facility.

Once a week on a set day and at approximately the same time of day (between 8 and 21 am) all experimental animals were weighed using digital scales. When a mouse reached 10% weight loss as calculated from its maximum body weight, they were weighed on a daily basis and hydrogel was placed at ground level in the cages.

#### 2.6.3.2 GRIP STRENGTH

Grip strength was measured twice a week (Monday and Thursday or Tuesday and Friday) between 1 pm and 4 pm using a Grip-strength meter bio-GS3 (Bioseb).

The mouse was moved from its home cage into an empty tecniplast cage. The mouse was then lifted by the base of the tail and place with all 4 feet on the mesh of the grip strength meter and held for a moment to allow the mouse to settle on the grip. It was then drawn horizontally back away from the mesh in one smooth movement and replaced into the empty cage. Four measures were taken during each session. Grip-strength was measured in grams with 2 decimal places. The empty cage was cleaned with 70% ethanol and allowed to dry between cages of animals.



The 4 individual measurements were averaged and divided by the weight of the animal for that week. If the experimenter was not available to take the measurements none were taken as it was decided that missed measurements were more desirable than the inter-operator variability in measurements.

Animals were measured from 50-52-days of age, with the first two measurements being taken as training. Measurements were then averaged into 2-week bins starting from the 57-59 day time-point, resulting in 6 bins: 57-70, 71-84, 85-98, 99-112, and 113-126-days of age. As the data were to be analysed by ANOVA, no higher age brackets were used to avoid excluding animals which died earlier.

### **2.6.3.3 SURVIVAL**

The humane end points are defined in Section 2.5.1.1. All animals reached 15% weight loss before either losing righting reflex or severe paralysis. Animals which died or were culled for “non-ALS” causes, for example as a result of malocclusion or tumours, were not used for survival or any subsequent experimental measures.

On reaching the humane end point, the animal was culled by exposure to a rising concentration of CO<sub>2</sub> and both brain and spinal cord (SC) were harvested and snap frozen.

### **2.6.4 Perfusion with Paraformaldehyde**

Animals were anaesthetised with 200 µL sodium pentobarbital (Euthatal) by intraperitoneal injection. Depth of anaesthesia was checked by blink reflex and paw pinch.

When the animal was sufficiently anaesthetised it was pinned on its back by all 4 feet and the abdominal cavity opened exposing the sternum. The diaphragm was punctured and the sternum cut from the lower, outer edge of the ribs to the top, mid-sternum avoiding the blood vessels in the centre of the rib cage. The rib cage was inflected back to expose the heart and the pericardium removed. With the perfusion pump set to 0.3 mL/min pumping ice cold sterile 0.9% NaCl, a 27G needle was inserted into the left ventricle and the right atrium cut to allow flow through. The pump was then switched to 3 mL/min and the limbs unpinned.

Blood was first cleared by perfusing for 4 mins with 0.9% NaCl (~12 mL) before switching to ice cold 4% paraformaldehyde (PFA) in PBS Dulbecco A (PBS-DA. Oxoid) for 8 mins (~24 mL).

## **2.7 HISTOLOGY OF PARAFFIN EMBEDDED TISSUES**

Sections were stained with haematoxylin and eosin to assess morphological characteristics.

Immunostaining with SEDI and USOD was used to assess misfolded SOD1 load.

### **2.7.1 Harvesting of Tissues**

Tissues were harvested by technical staff at the MRC Prion Unit Biological Services Facility. At the predetermined time-points, mice were culled by CO<sub>2</sub> inhalation in batches of 5. Brains and spinal columns were dissected out fresh and post-fixed in 10% buffered formal saline (BFS) (Pioneer Research).

### **2.7.2 Paraffin Embedding Samples and Sectioning**

Paraffin embedded histological samples were processed by the MRC Prion Unit Histology Group. Brains and SCs were fixed in 10% Buffered Formal Saline (BFS. Pioneer Research Chemicals). Brains were cut into two sagittal sections and SCs were cut into three sections: cervical, thoracic and sacral. These sections were processed and embedded into paraffin wax blocks on a tissue embedding machine using standard procedures. Serial sagittal sections from the central plane of the brain were cut at a thickness of 3 µm, placed on to Super-frost slides (VWR) and allowed to dry at 37 °C for a minimum of 2 hrs, before being transferred to a 60 °C oven overnight.

### **2.7.3 Immunostaining**

All pre- and post-staining treatments and staining were carried out on a Ventana automated immunohistochemical staining machine using proprietary reagents. All sections were de-waxed and rehydrated before staining and dehydrated after staining according to manufacturer's instructions and using Ventana's proprietary reagents. Antibodies were diluted in Antibody Diluent (Ventana). Colour development was carried out using a 3,3'-diaminobenzidine tetrahydrochloride (DAB) detection system and counterstaining was carried out using Haematoxylin and Bluing Reagent (Ventana) according to the manufacturer's instructions. After staining and dehydration, sections were mounted using Pertex, a xylene based mounting medium, and cover-slipped on a DIAPATH cover-slipping machine. All steps were carried out at room temperature unless specified.

### **2.7.4 Immunostaining**

Section slides were incubated as follows: Pre-treatment in Discovery MCC1 (a proprietary antigen retrieval solution containing Tris/EDTA pH 8.0 Ventana), incubated in a proprietary citrate buffer (Ventana) at 96 °C for 30 mins. Blocking for 10 mins. SEDI rabbit antibody (Rakhit et al., 2007) at a 1:100 dilution for 5 hrs. Swine anti-rabbit biotinylated antibody at a 1:200 dilution for 30 mins.

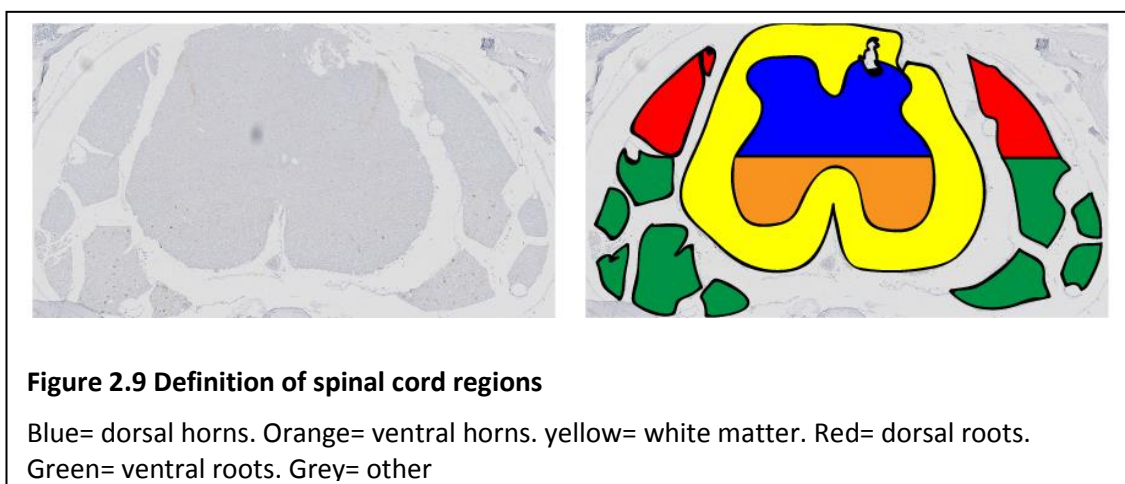
### **2.7.5 Analysis**

Slides were scanned at 40X using a Leica SCN400F slide scanner. Definiens tissue Studio software was used to define regions of interest as described below. Within each region and

areas positive for brown DAB chromogen were highlighted by the software and manually curated to remove artefacts. The total area and stained area were then computed and the ratio of the two used as the output. All analysis of images was done blind to experimental group. Statistical analysis was by ANOVA.

#### *2.7.5.1 SPINAL CORD PATHOLOGY*

Five slides, averaging ~4 sections per slide, were analysed per animal and results from multiple sections averaged for analysis. Cord sections were categorised into the following regions: anterior horn, dorsal horn, white matter, ventral roots and dorsal roots and “other”, as shown in Figure 2.9. Regions were analysed as above.



#### *2.7.5.2 BRAIN PATHOLOGY*

One sagittal section was analysed per animal. Brain sections were categorised into the following regions: Cortex, olfactory bulb, corpus callosum, hippocampus, cerebellum, brain stem and “other”, as shown in Figure 2.10. Regions were analysed as above.

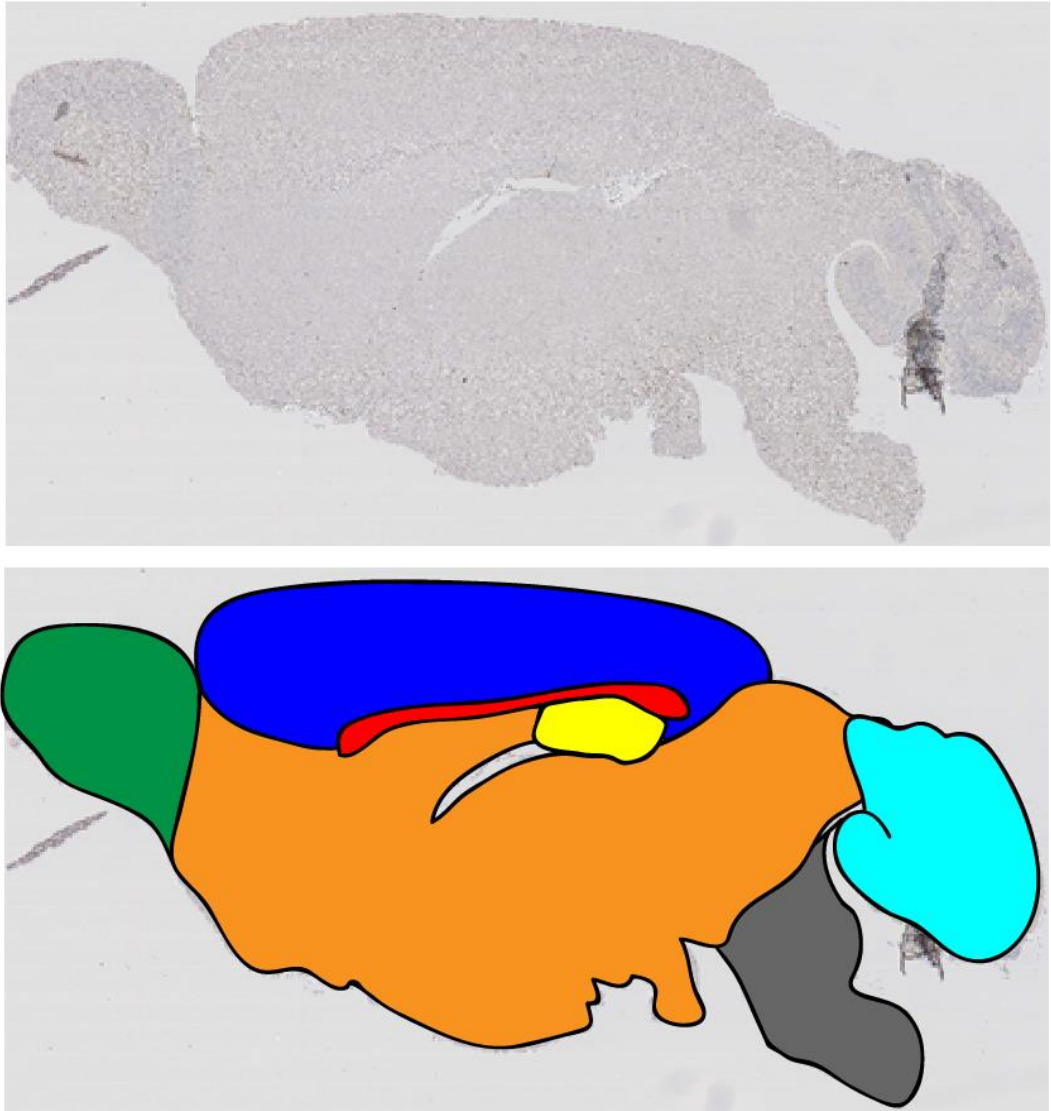


**Figure 2.10 Definition of brain regions**

Blue= cortex. Dark green= olfactory bulb. Red= corpus callosum. yellow= hippocampus. Pale blue= cerebellum. Grey= brain stem. Orange= other

## **2.8 HISTOLOGY OF FROZEN TISSUES**

### **2.8.1 Neuromuscular Junction (NMJ) Staining**

#### *2.8.1.1 SAMPLING AND EMBEDDING*

The extensor digitorum longus (EDL) of the left leg was dissected immediately after perfusing, pinned out in a gentle stretch and post fixed for 1-4 hrs in 4% PFA at 4 °C. Muscles were then transferred to 40% sucrose, 0.001% sodium azide in PBS to cryoprotect overnight at 4 °C.

The following day muscles were frozen in OCT freezing medium (Sakura) in foil moulds on a sheet of aluminium pre-chilled in dry-ice. Muscles were stored at -20 °C.

### *2.8.1.2 CUTTING AND STAINING*

20 µm longitudinal sections were cut in 2 series, using a Bright™ cryostat and collected onto poly-lysine coated slides (VWR) and air-dried for ~1 hr at room temp. One of the 2 series was stained for counting. As NMJs are ~40 µm in size, all NMJs should be captured, but repeated counting of the same NMJ avoided.

Sections were circled with a PAP pen (Invitrogen) and allowed to dry for 30 mins. All subsequent steps were carried out in a humidified chamber. Staining was carried out using reagents from the Vector M.O.M. Immunodetection Kit BASIC (Vector Laboratories).

Sections were washed 3 x 5 mins with PBS to remove OCT.

Sections were blocked for 1 hr with 3.5% M.O.M. blocking reagent (Vector Labs) diluted in PBS with 0.2% Triton X-100 (PBS+tr).

Sections were washed 2 x 2 mins with PBS+tr.

Sections were incubated for 5 mins with M.O.M. diluent (7.5% M.O.M protein concentrate (Vector Labs) diluted in PBS+tr).

Sections were incubated with primary antibodies for 30 mins at a 1:10 dilution in M.O.M. diluent. Antibodies used were Mouse monoclonal anti-synaptic vesicle (SV2, Developmental Studies Hybridoma Bank) and Mouse monoclonal anti-neurofilament (165 kDa) (2H3, Developmental Studies Hybridoma Bank)

Sections were washed 2 x 2 mins PBS+tr.

Sections were incubated with M.O.M. biotinylated anti-mouse secondary antibody diluted 1:250 in M.O.M. diluent for 10 mins.

Sections were washed 2 x 2 mins with PBS+tr.

Fluorescent labelling was performed using Streptavidin-Alexafluor 488 (1:200 Invitrogen), α-Bungarotoxin-Rhodamine (1:500 Sigma) and DAPI (1:500 Sigma ) diluted in PBS+tr and incubated for 30 mins in darkened, humidified chamber.

Sections were washed 3 x 5 mins with PBS (no Triton X-100). Slides were cover slipped using fluorescence mounting media (Dako), dried at room temperature for 24 hrs (light excluded) and stored at -20 °C.

### *2.8.1.3 ANALYSIS*

NMJs were visualised using a Leica DMR epifluorescent microscope. The total number of NMJs on each muscle were counted by methodically scanning the red fluorescence channel to identify end plates, the region on the muscle fibre which is populated by nicotinic acetylcholine receptors (AChR) and receives inputs from the MNs.  $\alpha$ -Bungarotoxin (in the red channel) binds the AChR of the neuromuscular end plate. Once identified, the innervation status of the end plate was assessed by switching between the red and green channels to establish the level of co-localisation between the muscle fibre end plate (red), and the foot plate of the MN (green), the pre-synaptic region of the MN which synapses with the end plate. Anti-neurofilament (in the green channel) binds within the axons of the incoming MNs and anti-synaptic vesicle (also in the green channel) binds to the synaptic vesicles populating the pre-synaptic nerve terminals of the incoming MNs. In a normal, healthy, NMJ, the whole of the end plate (red) will co-localise with the foot plate (green), and are classified as “fully innervated”. When the red and the green channel were not aligned, or the alignment was very minimal, the NMJ was classified as “denervated”. When an intermediate level of co-localisation was present, whereby it was clear that the two were not fully aligned, but a significant alignment was still present, the NMJ was classified as “partially innervated”. All analysis was carried out blind to genotype.

## **2.8.2 Muscle Fibre Typing**

### *2.8.2.1 SAMPLING AND EMBEDDING*

Muscles harvested for fibre type analysis needed to be harvested fresh and unfixed. For this reason, the leg was removed at the beginning of the perfusion protocol while perfusing with 0.9% NaCl; the right leg was partially skinned to aid visualisation and cut off close to the hip while avoiding damage to the surrounding structures. The remaining skin was then removed and the leg stored on ice in PBS for 1-3 hrs. The tibialis anterior (TA) and EDL and triceps surae (TS, a muscle group containing the medial and lateral gastrocnemius, soleus and plantaris muscles) dissected. The belly of the muscle was trimmed out and the muscles arranged vertically on a small cork board in OCT. The mount was then submerged in isopentane chilled in liquid nitrogen for ~1 min to freeze and then transferred to liquid nitrogen for 10 mins-1 hr before being stored at -80 °C.

### *2.8.2.2 CUTTING AND STAINING*

Transverse sections of 12  $\mu$ m were cut using a Bright™ cryostat. Six serial sections were collected per poly-lysine coated slides (VWR) and air-dried for ~1 hr at room temperature. Sections were circled with PAP pen as shown in and allowed to dry for 30 mins. All subsequent steps were carried out in a humidified chamber.

Sections were stained as follows:

Wash 5 mins in PBS.

Block 30 mins in 5% normal goat serum (NGS) diluted in PBS+tr.

Sections were washed 3X 2 mins PBS+tr.

Sections were incubated with primary antibodies (detailed below) diluted in PBS+tr 2% NGS for 1 hr.

Sections were then washed 3X 2 mins in PBS+tr.

Secondary antibodies, Alexa Fluor 488 goat anti-mouse IgM ( $\mu$  chain) (Invitrogen) and Alexa Fluor 568 goat anti-mouse IgG (H+L) (Invitrogen) and DAPI, were diluted in PBS+tr with 2% normal goat serum at 1:500 dilution and incubated for 2 hrs with light excluded.

Sections were washed 3X 2 mins in PBS (no Triton X-100). Slides were cover slipped using fluorescence mounting media (Dako), dried at room temperature for 24 hrs (light excluded) and stored at -20 °C.

To differentiate different fibre types, three primary antibody combinations (all from Developmental Studies Hybridoma Bank) were used to stain serial sections as follows:

Protocol A: BF-F3 (IgM, anti-myosin heavy chain 2B) 1:5 dilution and SC-71 (IgG1, anti-myosin heavy chain 2A) 1:10 dilution.

Protocol B: BF-F3 (IgM, anti-myosin heavy chain 2B) 1:5 dilution and BF-35 (IgG1, anti-myosin heavy chain all but 2X) 1:5 dilution.

Protocol C: BF-F3 (IgM, anti-myosin heavy chain 2B) 1:5 dilution and BA-D5 (IgM, anti-myosin heavy chain, slow, alpha- and beta-) 1:10 dilution.

### *2.8.2.3 ANALYSIS*

Type 2A fibres were quantified using staining protocol A. Type 1 fibres were quantified using staining protocol C.

The entire muscle was imaged by sequential imaging at 10X magnification on a Zeiss 710 confocal microscope using the same settings. Captured images were montaged in Adobe Photoshop. Volocity Image Analysis Software was used for semi-automated quantitation of the area containing myosin heavy chain 2B and 2A or 1, and the proportion of staining (2A/2B or 1/2B) was calculated for the TA and EDL. A qualitative assessment of the TS was also carried out with the help of Dr Barney Bryson. All analysis was carried out blind to genotype.

## 2.8.3 Motor Neuron Counts

### 2.8.3.1 SAMPLING AND EMBEDDING

After perfusion, the spinal column was dissected and post fixed in 4% PFA overnight. The following day, the SC was dissected from the column and submerged in 40% sucrose, 0.001% sodium azide in PBS to cryoprotect and stored at 4 °C for a minimum of 24 hrs.

The SC ventral roots were pinned out in order to identify the lumbar SC region from L2-L5 roots, inclusive, and this region (referred to hereafter as the lumbar cord) was excised. The lumbar cord was mounted directly onto the cryostat chuck by cooling the chuck in liquid nitrogen and embedding the cord *in situ* in OCT medium. The mount was then left to equilibrate in the cryostat for a minimum of 30 mins before cutting.

### 2.8.3.2 CUTTING AND STAINING

20 µm serial sections were cut in 3 series, using a Bright™ cryostat. 24 sections were collected onto each poly-lysine coated slides (VWR), air-dried for ~1 hr at room temperature and stored at -20 °C. One of the 3 series was stained for counting per animal to avoid re-counting the same MN twice.

The nissl stain, gallocyanine, was used. Sections were air dried for 15 mins before staining and were stained by submerging the slides as follows:

Gallocyanine stain (see Section 7.2.7, Appendix 2) 20 mins. 2X ddH<sub>2</sub>O 10 secs. 70% ethanol 1 min. 90% ethanol 1 min. 2X 100% ethanol 1 min. 2X Histo-clear (National Diagnostics) 2 mins. Slides were then cover slipped with DPX mounting medium.

### 2.8.3.3 ANALYSIS

A minimum of 40 sections were counted per SC, and where more than 40 sections were counted, numbers were standardised to 40 sections.

Motor neurons were identified as greater than 20 µm, polygonal cells with a visible nucleus and nucleolus. Cells within the sciatic pool in every third section were counted. All analysis was carried out blind to genotype.

## 2.9 STATISTICAL ANALYSES

Statistics were carried out using IBM SPSS, except Chi Square test for inheritance ratios which was carried out using GraphPad online tool (<http://graphpad.com/quickcalcs/chisquared1/>).



## Chapter 3. SOD1 Transmission Project

The work described in this Chapter was carried out in conjunction with Dr Anny Devoy, Dr Pietro Fratta and Mr Luc Masset (UCL Department of Neurodegenerative Disease) and with the assistance of technical staff of the MRC Prion Unit.

### 3.1 AIMS

SOD1 displays prion-like properties *in vitro* and in cellular models. The main aim of the work described in this chapter was to examine whether SOD1 can act in a prion-like way, seeding aggregation in a mouse model.

Transgenic mice expressing huSOD1 were intracerebrally inoculated with tissue homogenates containing mutant huSOD1 species, or with control homogenates or a vehicle only control. After a period of incubation, misfolded SOD1 aggregate pathology was assessed.

For experiments investigating self-seeded aggregation potential, mice transgenically expressing G93A mutant huSOD1 were inoculated with spinal cord (SC) homogenates from the same mouse line; seeding mutant huSOD1 with mutant huSOD1. To assess cross-seeded aggregation potential, mice transgenically expressing WT huSOD1 were inoculated with either mutant SOD1 transgenic mouse SC homogenate, or human SOD1-fALS motor cortex homogenates; seeding WT huSOD1 with mutant huSOD1. Premature deaths, potentially caused by toxicity of the mutant huSOD1 species in the inocula, were also monitored.

All of the mice used in these experiments were bred on to an endogenous *Sod1* null background. This is common practice in the Prion field, where the endogenous *Prnp* can perturb the transmission of non-mouse PrP<sup>Sc</sup> species (Telling et al., 1995; Collinge et al., 1995). Breeding the mice for use in these experiments also allowed us to examine whether the inheritance patterns of the WT and G93A mutant transgenes, and the *Sod1* null allele followed Mendelian ratios.

### 3.2 INTRODUCTION

Misfolded SOD1 histopathology is used in this Chapter to assess differences between experimental conditions. Both WT and mutant SOD1 transgenic mice have high levels of SOD1 detectable by histopathology (Jaarsma et al., 2000). Our aim was to specifically measure the misfolded portion of the transgenic protein, therefore misfolded SOD1 antibodies were used.

Several conformation specific SOD1 antibodies have been produced that can detect misfolded SOD1 species present in SOD1-fALS and mutant SOD1 transgenic mice (e.g. (Rakhit et al., 2007;

Kerman et al., 2010; Prudencio et al., 2011; Jonsson et al., 2004)). In this Chapter two of these antibodies are used: SEDI and USOD.

The SEDI (SOD1 exposed dimer interface) antibody recognises aa 143-151 of the SOD1 protein which, in the correctly folded SOD1 dimer, are hidden within the dimer interface (Figure 3.1) (Rakhit et al., 2007). The SEDI antibody was shown to specifically detect monomeric misfolded SOD1 species by immunoprecipitation (IP) and immunohistochemistry of spinal cords of 3 mutant huSOD1 transgenic mouse lines (G37R, G85R and G93A). In G37R transgenic mice, the area of SEDI staining was further defined as being within the MNs and astrocytes of the ventral horn with particularly high abundance in the axons and white matter tracts. Lower level staining of spinal cords from mice transgenically expressing WT huSOD1 was detected, with staining particularly prevalent in the white matter tracts. Neuronal SEDI staining was also reported in the spinal cord of an A4V SOD1-fALS case (Rakhit et al., 2007).

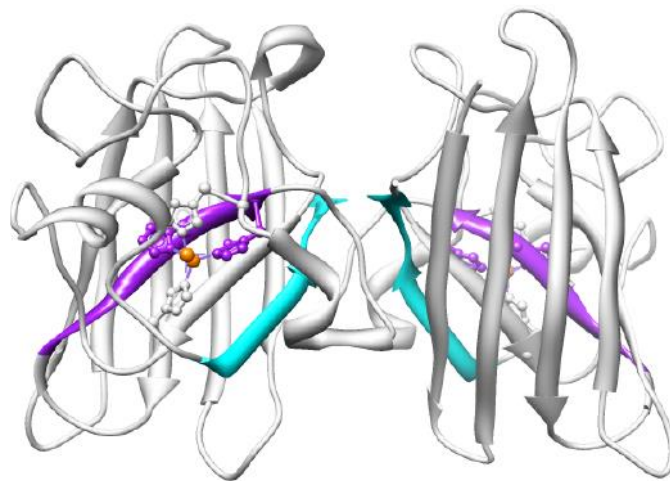


**Figure 3.1 SEDI and USOD epitopes**

The 3D structure of SOD1 is shown. SEDI epitope (aa 143-153) is highlighted in cyan. The USOD epitope (aa 42-48) is highlighted in purple. Copper atoms are shown in orange.

SEDI has subsequently identified, via immunohistochemistry, monomeric misfolded SOD1 in the periphery of vacuoles and in intraneuronal inclusions in the SC of SOD1-fALS patients with a number of different mutations (A4T, A4V, V14M,  $\Delta$ G27/P28, I113T) (Zinman et al., 2009; Liu et al., 2009; Kerman et al., 2010). However, in non-SOD1-fALS and sALS similar SEDI pathology is reported as absent (Liu et al., 2009).

SEDI has also shown specificity for recombinant non-amyloid aggregated WT huSOD1, but not non-aggregated WT huSOD1 by competition enzyme-linked immunosorbent assay (ELISA) (Hwang et al., 2010) and a higher affinity to A4V mutant huSOD1, as compared to WT huSOD1, by immunocytochemistry in a cell culture model (Prudencio et al., 2011). Monomer misfolded

huSOD1 was also detected in the cerebrospinal fluid of G93A and G37R transgenic mice by SEDI IP, and immunisation with the SEDI peptide delayed onset of disease in both of these models, suggesting that the epitope targeted by SEDI is disease relevant (Liu et al., 2012).

USOD (unfolded SOD1) detects a region of the SOD1 protein, involved in copper binding, which is buried within the correctly folded dimer and monomer (Figure 3.1) (Kerman et al., 2010). USOD also reacts with recombinant misfolded WT huSOD1 which had been destabilised by various chemical compounds, but not correctly folded holo (metalated) SOD1. This antibody detected misfolded huSOD1, by immunohistochemistry and IP, in SOD1-fALS SC (A4V and  $\Delta$ G27/P28 mutations) but not sALS, and labelled similar structures to SEDI when used in immunohistochemistry on an A4V SOD1-fALS SC. In a G93A mutant SOD1 transgenic mouse, USOD immunohistochemistry revealed vacuolated structures in the ventral horns and roots; a similar pattern to that described by Rakhit et al., (2007) with SEDI. To our knowledge no other groups have reported the use of USOD in other patient or mouse tissues, although Linares et al., (2013) used USOD IP to detect a reduction in misfolded SOD1 in the spinal cords of G93A SOD1 transgenic rats in response to pharmacological treatment.

Weichert et al., (2014) used IP with both SEDI and USOD to assess misfolding of a recombinant huSOD1 which had polypeptide linkers to produce homo and hetero WT and/or mutant dimers. Both SEDI and USOD showed a similar pattern, with high affinity to recombinant mutant (A4V, G37R, G41D, G41S, G85R and G93C) homodimers, reduced affinity for mutant:WT heterodimers and low affinity for WT homodimers. The fact that SEDI was able to precipitate these forms of SOD1 suggests that although described as “obligate dimers” the polypeptide linker actually allowed the dimer to dissociate, but presumably limited the dimerisation of the protein to the subunit that it was linked to.

In this Chapter SEDI and USOD were used in immunohistochemistry to assess misfolded huSOD1 pathology in WT and G93A mutant transgenic huSOD1 mice. Both of these antibodies have been validated as identifying misfolded huSOD1 in SOD1-fALS and mutant huSOD1 transgenic mice, while reactivity to WT huSOD1 is more limited in transgenic mice and absent in non-SOD1 patient tissue.

### 3.3 RESULTS

The nomenclature used to refer to different mouse lines within the text of this chapter is summarised in Table 3.1.

**Table 3.1 Mutant mouse nomenclature used within text**

Both the WT and G93A mutant *SOD1* transgenes are human

Tg allele	KO allele	Short form (used in text)
Non-transgenic	<i>Sod1</i> <sup>+/+</sup> (WT)	NTg;Sod1wt
Non-transgenic	<i>Sod1</i> <sup>+/-</sup> (heterozygous KO)	NTg;Sod1het
Non-transgenic	<i>Sod1</i> <sup>-/-</sup> (homozygous KO)	NTg;Sod1ko
<i>SOD1</i> <sup>WT</sup> Tg hemizygous	<i>Sod1</i> <sup>+/+</sup> (WT)	TgWT;Sod1wt
<i>SOD1</i> <sup>WT</sup> Tg hemizygous	<i>Sod1</i> <sup>+/-</sup> (heterozygous KO)	TgWT;Sod1het
<i>SOD1</i> <sup>WT</sup> Tg hemizygous	<i>Sod1</i> <sup>-/-</sup> (homozygous KO)	TgWT;Sod1ko
<i>SOD1</i> <sup>G93A</sup> Tg hemizygous	<i>Sod1</i> <sup>+/+</sup> (WT)	TgG93A;Sod1wt
<i>SOD1</i> <sup>G93A</sup> Tg hemizygous	<i>Sod1</i> <sup>+/-</sup> (heterozygous KO)	TgG93A;Sod1het
<i>SOD1</i> <sup>G93A</sup> Tg hemizygous	<i>Sod1</i> <sup>-/-</sup> (homozygous KO)	TgG93A;Sod1ko

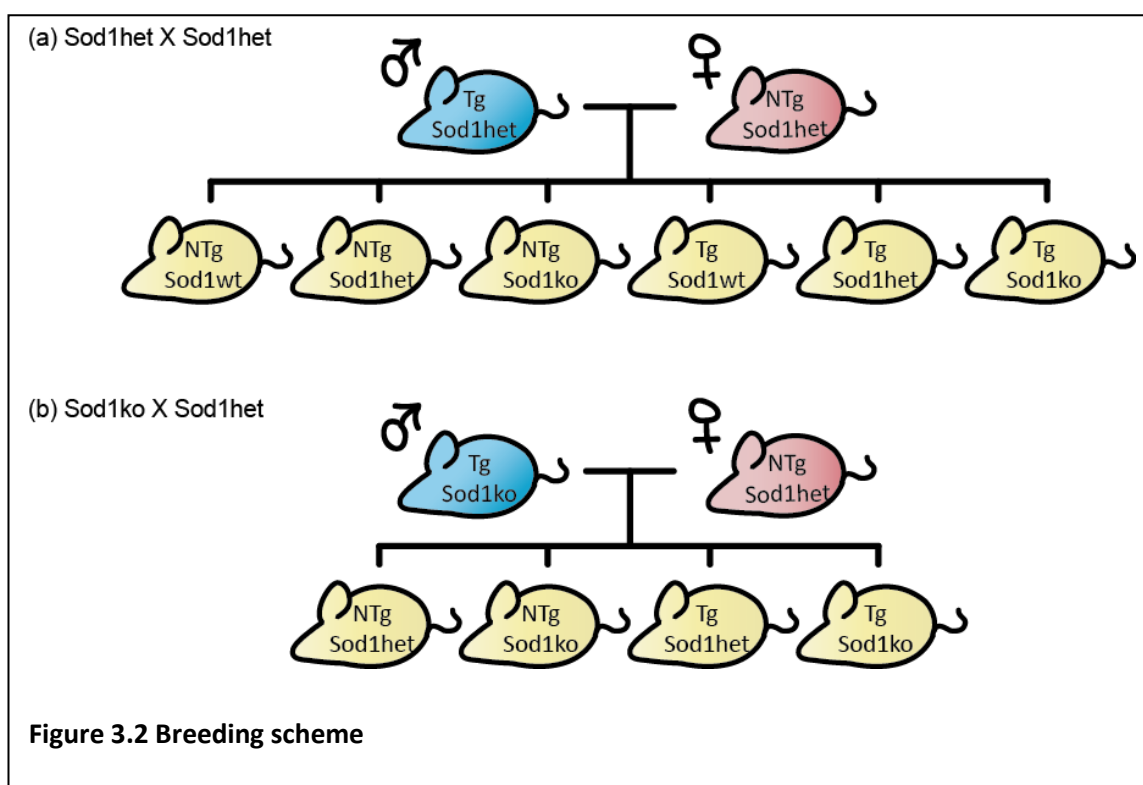
#### 3.3.1 Inheritance Patterns of *SOD1* Tg and KO Allele

To produce mice with the genotypes needed for the projects presented in this Thesis and other work in our laboratory, we used two breeding strategies (Figure 3.2).

The first is a cross between male Tg (WT or G93A);Sod1het mice and female NTg;Sod1het mice which can give rise to offspring of 6 possible genotypes as summarised in Figure 3.2a. This scheme was used when transgenic mice with both Sod1wt and Sod1ko genotypes were required.

The second is a cross between male Tg (WT or G93A);Sod1ko mice and females NTg;Sod1het mice, which can give rise to offspring of 4 potential genotypes as summarised in Figure 3.2b. This breeding scheme was used when only transgenic mice with a Sod1ko genotype were needed.

The number of offspring with different genotypes was monitored for each breeding scheme for both WT and G93A transgenic mice, using trio matings of 1 male mated to 2 female mice.



### 3.3.1.1 INHERITANCE PATTERNS IN MALE *TgWT;SOD1HET* X FEMALE *NTG;SOD1HET* MATINGS

The number of offspring of the 6 potential genotypes was monitored from 17 trios. Results are summarised in Table 3.2. The observed ratios did not differ significantly from the expected ratios.  $\chi^2(5) = 4.599$ ,  $p > 0.05$ .

**Table 3.2 Observed genotype ratios of offspring from *TgWT;Sod1het* X *NTg;Sod1het* matings**

The omnibus  $\chi^2$  showed that observed ratios did not differ from the expected Mendelian ratios.

Genotype	Number of animals born	Observed ratio	Expected Mendelian ratio
NTg;Sod1wt	62	0.1480	0.125
NTg;Sod1het	91	0.2172	0.25
NTg;Sod1ko	48	0.1146	0.125
TgWT;Sod1wt	52	0.1241	0.125
TgWT;Sod1het	113	0.2697	0.25
TgWT;Sod1ko	53	0.1265	0.125
<b>TOTAL</b>	<b>419</b>	<b>1</b>	<b>1</b>

### 3.3.1.2 INHERITANCE PATTERNS IN MALE *TgWT;Sod1<sup>HOM</sup>* X FEMALE *NTg;Sod1<sup>HET</sup>* MATINGS

The number of offspring of the 4 potential genotypes was monitored from 81 trios. Results are summarised in Table 3.3. The observed ratios differed significantly from the expected ratios.  $\chi^2(3) = 12.402$ ,  $p < 0.01$ .

**Table 3.3 Observed genotype ratios of offspring from *TgWT;Sod1<sup>hom</sup>* X *NTg;Sod1<sup>het</sup>* matings**

The omnibus  $\chi^2$  showed that observed ratios were significantly different from the expected Mendelian ratios.

Genotype	Number of animals born	Observed ratio	Expected Mendelian ratio
<b>NTg;Sod1het</b>	535	0.2761	0.25
<b>NTg;Sod1ko</b>	426	0.2198	0.25
<b>TgWT;Sod1het</b>	487	0.2513	0.25
<b>TgWT;Sod1ko</b>	490	0.2528	0.25
<b>TOTAL</b>	<b>1938</b>	<b>1</b>	<b>1</b>

Eight post-hoc  $\chi^2$  comparisons were carried out using a Bonferroni adjusted significance threshold of  $p = 0.00625$ . The results, including  $\chi^2$  statistics are summarised in Table 3.4

The ratio of NTg;Sod1het offspring compared to NTg;Sod1ko offspring was significantly higher than the expected ratio. All other observed ratios did not differ significantly from the expected ratios.

**Table 3.4 Pair-wise comparisons for TgWT;Sod1hom X NTg;Sod1het matings**

Significant comparisons are highlighted in green. Significance relative to non-adjusted levels : \*\* p<0.01.

Genotype	Mice born	Observed Ratio	Expected Mendelian Ratio
<b>Comparison 1- <math>\chi^2(1)=0.132</math>, p&gt;0.00625</b>			
NTg	961	0.4959	0.5
TgWT	977	0.5041	0.5
TOTAL	<b>1938</b>	<b>1</b>	
<b>Comparison 2- <math>\chi^2(1)=5.798</math>, p&gt;0.00625</b>			
Sod1het	1022	0.5273	0.5
Sod1ko	916	0.4727	0.5
TOTAL	<b>1938</b>	<b>1</b>	<b>1</b>
<b>Comparison 3- <math>\chi^2(1)=12.363</math>, p&lt;0.00125 **</b>			
NTg;Sod1het	535	0.5567	0.5
NTg;Sod1ko	426	0.4433	0.5
TOTAL	961		
<b>Comparison 4- <math>\chi^2(1)=2.254</math>, p&gt;0.00625</b>			
NTg;Sod1het	535	0.5235	0.5
TgWT;Sod1het	487	0.4765	0.5
TOTAL	1022	1	1
<b>Comparison 5- <math>\chi^2(1)=1.976</math>, p&gt;0.00625</b>			
NTg;Sod1het	535	0.5220	0.5
TgWT;Sod1ko	490	0.4780	0.5
TOTAL	1025	1	1
<b>Comparison 6- <math>\chi^2(1)=4.076</math>, p&gt;0.00625</b>			
NTg;Sod1ko	426	0.4666	0.5
TgWT;Sod1het	487	0.5334	0.5
TOTAL	913	1	1
<b>Comparison 7- <math>\chi^2(1)=4.472</math>, p&gt;0.00625</b>			
NTg;Sod1ko	426	0.4651	0.5
TgWT;Sod1ko	490	0.5349	0.5
TOTAL	916	1	1
<b>Comparison 8- <math>\chi^2(1)=0.009</math>, p&gt;0.00625</b>			
TgWT;Sod1het	487	0.4985	0.5
TgWT;Sod1ko	490	0.5015	0.5
TOTAL	977	1	1

### 3.3.1.3 INHERITANCE PATTERNS IN MALE *TgG93A;Sod1<sup>HET</sup>* X FEMALE *NTg;Sod1<sup>HET</sup>* MATINGS

The number of offspring of the 6 potential genotypes was measured from 106 trios. Results are summarised in Table 3.5. The observed ratios differed significantly from the expected ratios.  $\chi^2(5) = 47.858$ ,  $p < 0.001$ .

**Table 3.5 Observed genotype ratios of offspring from *TgG93A;Sod1<sup>het</sup>* X *NTg;Sod1<sup>het</sup>* matings**

The omnibus  $\chi^2$  showed that observed ratios differed significantly from the expected Mendelian ratios.

	Number of animals born	Observed ratio	Expected Mendelian ratio
<b>NTg;Sod1wt</b>	<b>225</b>	<b>0.1530</b>	<b>0.125</b>
<b>NTg;Sod1het</b>	453	0.3080	0.25
<b>NTg;Sod1ko</b>	148	0.1006	0.125
<b>TgG93A;Sod1wt</b>	161	0.1094	0.125
<b>TgG93A;Sod1het</b>	313	0.2128	0.25
<b>TgG93A;Sod1ko</b>	171	0.1162	0.125
<b>TOTAL</b>	<b>1471</b>	<b>1</b>	<b>1</b>

Eighteen post-hoc  $\chi^2$  comparisons were carried out using a Bonferroni adjusted significance level of  $p = 0.002778$ . The comparisons and their  $\chi^2$  statistics are summarised in Table 3.6.

The observed ratio of NTg offspring compared to TgG93A offspring was significantly higher than the expected ratio.

The observed ratio of NTg;Sod1wt offspring compared to NTg;Sod1ko, TgG93A;Sod1wt and TgG93A;Sod1het offspring was significantly higher than the expected ratio.

The observed ratio of NTg;Sod1het offspring compared to NTg;Sod1ko, TgG93A;Sod1wt, TgG93A;Sod1het and TgG93A;Sod1ko was significantly higher than the expected ratio. None of the other comparisons were significantly different.



**Table 3.6 Pair-wise comparisons for TgG93A;Sod1het X NTg;Sod1het matings**

Significant comparisons are highlighted in green. Significance relative to non-adjusted levels: \*  $p < 0.05$ . \*\*  $p < 0.01$ . \*\*\*  $p < 0.001$ .

Genotype	Mice born	Observed Ratio	Expected Ratio
<b>Comparison 1- <math>\chi^2(1)=22.271</math>, <math>p &lt; 0.000056</math> ***</b>			
NTg	826	0.5615	0.5
Tg	645	0.4385	0.5
TOTAL	1471	1	1
<b>Comparison 2- <math>\chi^2(1)=0.016</math>, <math>p &gt; 0.002778</math></b>			
Sod1wt	386	0.3351	0.3333
Sod1het	766	0.6649	0.6667
TOTAL	1152	1	1
<b>Comparison 3- <math>\chi^2(1)=6.367</math>, <math>p &gt; 0.002778</math></b>			
Sod1wt	386	0.5475	0.5
Sod1ko	319	0.4525	0.5
TOTAL	705	1	1
<b>Comparison 4- <math>\chi^2(1)=0.007</math>, <math>p &gt; 0.002778</math></b>			
NTg;Sod1wt	225	0.3319	0.3333
NTg;Sod1het	453	0.6681	0.6667
TOTAL	678	1	1
<b>Comparison 5- <math>\chi^2(1)=15.895</math>, <math>p &lt; 0.000556</math> **</b>			
NTg;Sod1wt	225	0.6032	0.5
NTg;Sod1ko	148	0.3968	0.5
TOTAL	373	1	1
<b>Comparison 6- <math>\chi^2(1)=10.611</math>, <math>p &lt; 0.002778</math> *</b>			
NTg;Sod1wt	225	0.5829	0.5
TgG93A;Sod1wt	161	0.4171	0.5
TOTAL	386	1	1
<b>Comparison 7- <math>\chi^2(1)=17.444</math>, <math>p &lt; 0.000056</math> ***</b>			
NTg;Sod1wt	225	0.4182	0.3333
TgG93A;Sod1het	313	0.5818	0.6667
TOTAL	538	1	1
<b>Comparison 8- <math>\chi^2(1)=7.364</math>, <math>p &gt; 0.002778</math></b>			
NTg;Sod1wt	225	0.5682	0.5
TgG93A;Sod1ko	171	0.4318	0.5
TOTAL	396	1	1
<b>Comparison 9- <math>\chi^2(1)=20.506</math>, <math>p &lt; 0.000056</math> ***</b>			
NTg;Sod1het	453	0.7537	0.6667
NTg;Sod1ko	148	0.2463	0.3333
TOTAL	601	1	1
<b>Comparison 10- <math>\chi^2(1)=13.975</math>, <math>p &lt; 0.000556</math> **</b>			
NTg;Sod1het	453	0.7378	0.6667
TgG93A;Sod1wt	161	0.2622	0.3333
TOTAL	614	1	1
<b>Comparison 11- <math>\chi^2(1)=25.587</math>, <math>p &lt; 0.000056</math> ***</b>			
NTg;Sod1het	453	0.5914	0.5
TgG93A;Sod1het	313	0.4086	0.5
TOTAL	766	1	1
<b>Comparison 12- <math>\chi^2(1)=9.873</math>, <math>p &lt; 0.002778</math> *</b>			
NTg;Sod1het	453	0.7260	0.6667
TgG93A;Sod1ko	171	0.2740	0.3333
TOTAL	624	1	1
<b>Comparison 13- <math>\chi^2(1)=0.547</math>, <math>p &gt; 0.002778</math></b>			
NTg;Sod1ko	148	0.4790	0.5
TgG93A;Sod1wt	161	0.5210	0.5
TOTAL	309	1	1
<b>Comparison 14- <math>\chi^2(1)=0.313</math>, <math>p &gt; 0.002778</math></b>			
NTg;Sod1ko	148	0.3210	0.3333
TgG93A;Sod1het	313	0.6790	0.6667
TOTAL	461	1	1
<b>Comparison 15- <math>\chi^2(1)=1.658</math>, <math>p &gt; 0.002778</math></b>			
NTg;Sod1ko	148	0.4639	0.5
TgG93A;Sod1ko	171	0.5361	0.5
TOTAL	319	1	1
<b>Comparison 16- <math>\chi^2(1)=0.085</math>, <math>p &gt; 0.002778</math></b>			
TgG93A;Sod1wt	161	0.3397	0.3333
TgG93A;Sod1het	313	0.6603	0.6667
TOTAL	474	1	1
<b>Comparison 17- <math>\chi^2(1)=0.301</math>, <math>p &gt; 0.002778</math></b>			
TgG93A;Sod1wt	161	0.4849	0.5
TgG93A;Sod1ko	171	0.5151	0.5
TOTAL	332	1	1
<b>Comparison 18- <math>\chi^2(1)=0.869</math>, <math>p &gt; 0.002778</math></b>			
TgG93A;Sod1het	313	0.6467	0.6667
TgG93A;Sod1ko	171	0.3533	0.3333
TOTAL	484	1	1

### 3.3.1.4 INHERITANCE PATTERNS IN MALE TgG93A;SOD1HOM X FEMALE NTG;SOD1HET MATINGS

The number of offspring of the 4 potential genotypes was measured from 77 trios. Results are summarised in Table 3.7. The observed ratios differed significantly from the expected ratios.  $\chi^2(3) = 17.453$ ,  $p < 0.001$ .

Eight post-hoc  $\chi^2$  comparisons were carried out using a Bonferroni corrected significance level of  $p = 0.00625$ . These comparisons and the  $\chi^2$  statistics are summarised in Table 3.8.

**Table 3.7 Observed genotype ratios of offspring from TgG93A;Sod1<sup>hom</sup> X NTg;Sod1<sup>het</sup> matings**

The omnibus  $\chi^2$  showed that observed ratios were significantly different to the expected Mendelian ratios.

<b>Genotype</b>	<b>Number of animals born</b>	<b>Observed ratio</b>	<b>Expected Mendelian ratio</b>
<b>NTg;Sod1<sup>het</sup></b>	330	0.2992	0.25
<b>NTg;Sod1<sup>ko</sup></b>	252	0.2285	0.25
<b>TgG93A;Sod1<sup>het</sup></b>	240	0.2176	0.25
<b>TgG93A;Sod1<sup>ko</sup></b>	281	0.2548	0.25
<b>TOTAL</b>	<b>1103</b>	<b>1</b>	<b>1</b>

The observed ratio of NTg;Sod1<sup>het</sup> offspring compared to NTg;Sod1<sup>ko</sup> and TgG93A;Sod1<sup>het</sup> offspring was significantly higher than the expected ratio. No of the other comparisons was significant.

These results will be discussed in Section 3.4.1.

**Table 3.8 Pair-wise comparisons for TgG93A;Sod1hom X NTg;Sod1het matings**

Significant comparisons are highlighted in green. Significance relative to non-adjusted levels: \*  $p < 0.05$ . \*\*  $p < 0.01$ .

Genotype	Mice born	Observed ratio	Expected Mendelian ratio
<b>Comparison 1- <math>\chi^2(1)=</math>, <math>p &gt; 0.00625</math></b>			
NTg	582	0.5277	0.5
Tg	521	0.4723	0.5
<b>TOTAL</b>	<b>1103</b>	<b>1.0000</b>	<b>1.0000</b>
<b>Comparison 2- <math>\chi^2(1)=</math>, <math>p &gt; 0.00625</math></b>			
Sod1het	570	0.5168	0.5
Sod1ko	533	0.4832	0.5
<b>TOTAL</b>	<b>1103</b>	<b>1</b>	<b>1</b>
<b>Comparison 3- <math>\chi^2(1)=10.454</math>, <math>p &lt; 0.00625</math> *</b>			
NTg;Sod1het	330	0.5670	0.5
NTg;Sod1ko	252	0.4330	0.5
<b>TOTAL</b>	<b>582</b>	<b>1</b>	<b>1</b>
<b>Comparison 4- <math>\chi^2(1)=14.211</math>, <math>p &lt; 0.00125</math> **</b>			
NTg;Sod1het	330	0.5789	0.5
TgG93A;Sod1het	240	0.4211	0.5
<b>TOTAL</b>	<b>570</b>	<b>1</b>	<b>1</b>
<b>Comparison 5- <math>\chi^2(1)=3.930</math>, <math>p &gt; 0.00625</math></b>			
NTg;Sod1het	330	0.5401	0.5
TgG93A;Sod1ko	281	0.4599	0.5
<b>TOTAL</b>	<b>611</b>	<b>1</b>	<b>1</b>
<b>Comparison 6- <math>\chi^2(1)=0.293</math>, <math>p &gt; 0.00625</math></b>			
NTg;Sod1ko	252	0.5122	0.5
TgG93A;Sod1het	240	0.4878	0.5
<b>TOTAL</b>	<b>492</b>	<b>1</b>	<b>1</b>
<b>Comparison 7- <math>\chi^2(1)=1.578</math>, <math>p &gt; 0.00625</math></b>			
NTg;Sod1ko	252	0.4728	0.5
TgG93A;Sod1ko	281	0.5272	0.5
<b>TOTAL</b>	<b>533</b>	<b>1</b>	<b>1</b>
<b>Comparison 8- <math>\chi^2(1)=3.226</math>, <math>p &gt; 0.00625</math></b>			
TgG93A;Sod1het	240	0.4607	0.5
TgG93A;Sod1ko	281	0.5393	0.5
<b>TOTAL</b>	<b>521</b>	<b>1</b>	<b>1</b>

### 3.3.2 Transmission in *SOD1*<sup>G93A</sup> Transgenic Mice

In cellular models of prion-like seeded aggregation, self-seeding is consistently reported (Munch et al., 2011; Furukawa et al., 2013; Grad et al., 2011; Grad et al., 2014; Sundaramoorthy et al., 2013). Cross-seeded aggregation of WT SOD1 by mutant SOD1 is also reported in some cellular models (Grad et al., 2011; Grad et al., 2014; Sundaramoorthy et al., 2013), however, this is not consistent (Munch et al., 2011). We therefore first tested whether self-seeded aggregation could be detected in a mutant huSOD1 transgenic mouse.

Fifty day old TgG93A;Sod1ko mice were inoculated with SC homogenate from 100-days old TgG93A;Sod1ko mice (as described in Section 2.6.2). Several control inocula were also used as summarised in Table 3.9. Animals were culled at either 24 hours or 40-days post-inoculation and the misfolded SOD1 burden in the brain was assayed.

Where pair-wise comparisons are carried out between inoculum groups, comparison is to the m-NTg inoculated animals; because this inoculum has no human or mouse SOD1, if an effect is due to prion-like properties of SOD1 they should be absent in this group, however non-specific effects due to inoculation with CNS homogenate will be controlled for.

**Table 3.9 Inoculum used for TgG93A transmission experiment**

The experimental inoculum is highlighted in blue, control inocula are in white

Name	Species	Genotype	Age at death	Sex	Tissue used
m-TgG93A	mouse	TgG93A;Sod1ko	100 days	female	spinal cord
m-TgWT	mouse	TgWT;Sod1ko	100 days	female	spinal cord
m-NTg	mouse	NTg;Sod1ko	100 days	female	spinal cord
PBS	n/a	PBS only controls			

#### 3.3.2.1 PREMATURE DEATH AND EXCLUSIONS

Only 1 animal was culled before its pre-defined cull date and this was due to malocclusion and not related to any experimental procedure. One animal, from the m-TgG93A 40 day time-point was found dead after the inoculation procedure. Both of these animals were excluded from the data set.

#### 3.3.2.2 AGE DIFFERENCES BETWEEN GROUPS

The average age of mice at their scheduled cull date, split by inoculum group, is shown in Table 3.10. Two one-way ANOVAS were carried out, one for each time-point, to check for variance in age between inoculum groups. There was no difference in the age at cull between inoculum groups in either the 24 hour ( $F(3,11)=0.40$ ,  $p>0.05$ ) or 40 day ( $F(4,50)=1.503$ ,  $p>0.05$ ) time-points.

**Table 3.10 Average age at scheduled cull**

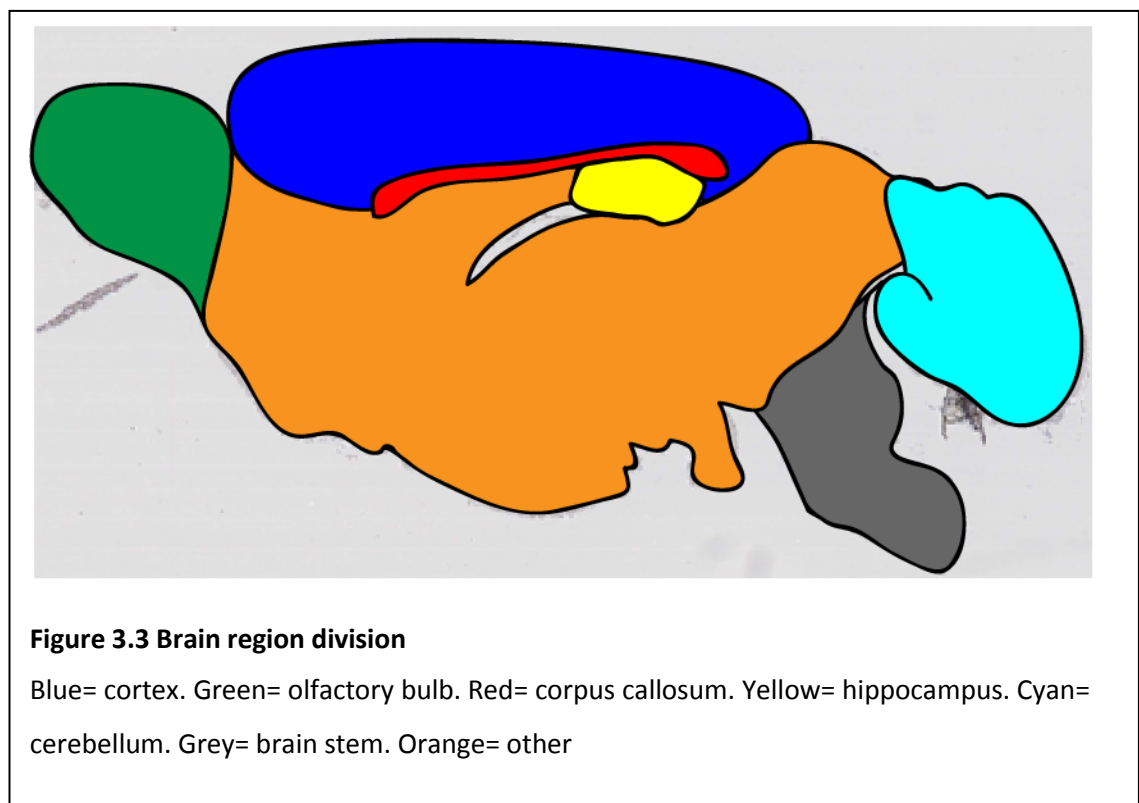
Table shows number of animals inoculated per group and their mean (and SEM) age in days

Inoculum	24 hour time-point			40 day time-point		
	n=	mean	SEM	n=	mean	SEM
NI	0	-	-	10	89.900	0.100
PBS	3	52.333	0.667	10	89.700	0.335
m-NTg	3	51.000	1.000	10	89.200	0.389
m-TgWT	3	51.333	0.333	10	89.900	0.180
m-TgG93A	3	51.333	1.333	11	90.636	0.730

### 3.3.2.3 SEDI BRAIN PATHOLOGY

The brain was divided into regions as shown in Figure 3.3 and analysed using Definiens tissue Studio software, as described in Section 2.7.5, to give the proportion of each region stained. Because the proportions were very small, the numbers presented have been multiplied by 1000.

Analyses for this project are on-going and at present, data are available for inoculated TgG93A;Sod1ko mice, but not for non-inoculated controls or for NTg;Sod1ko mice inoculated with m-TgG93A.

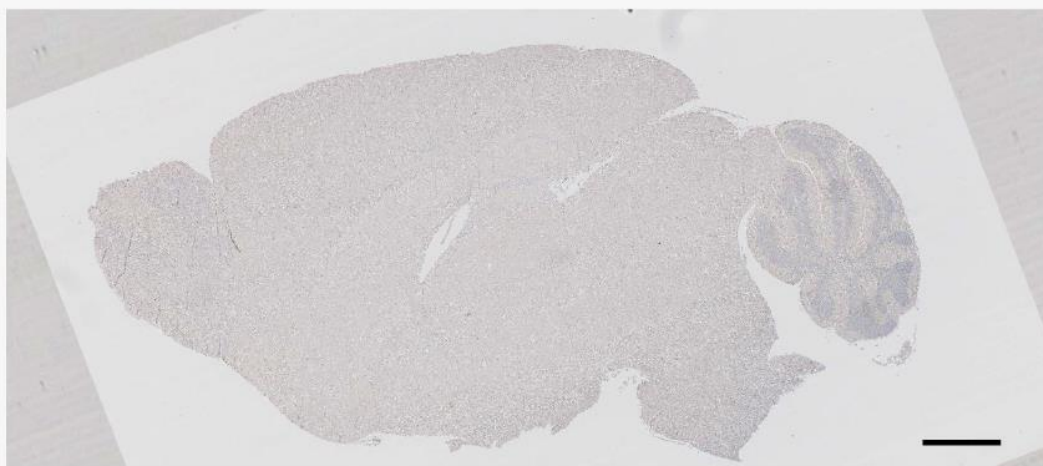


### 3.3.2.3.1 Twenty-four Hours Post-Inoculation

Figure 3.4 shows examples of SEDI staining of sagittal brain sections 24 hours post-inoculation.

Data were analysed by one-way ANOVA with planned comparisons to the m-NTg control inoculated group. The results for each region analysed are summarised in Figure 3.5

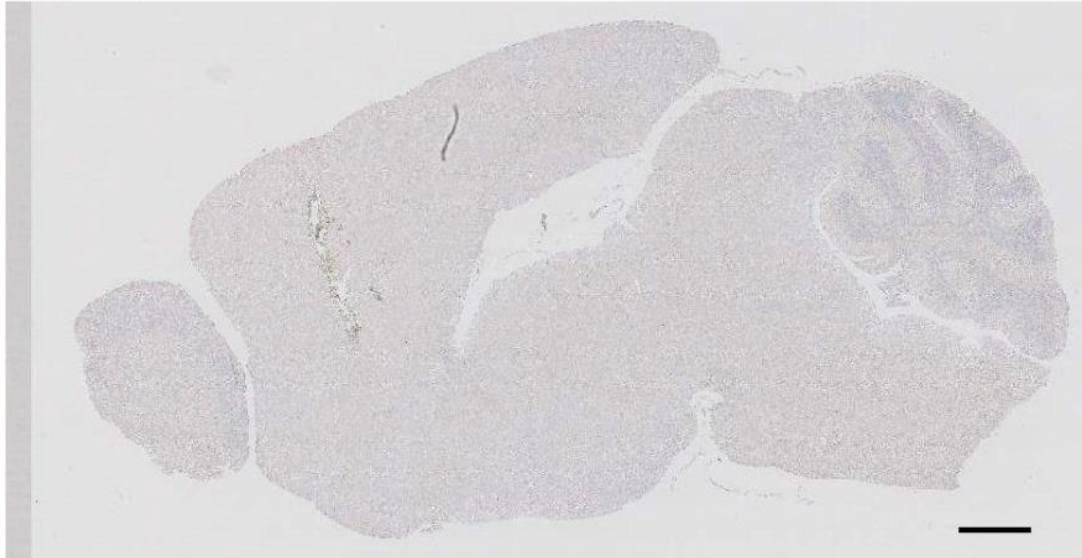
(a) PBS



(b) m-NTg



(c) m-TgWT



(d) m-TgG93A

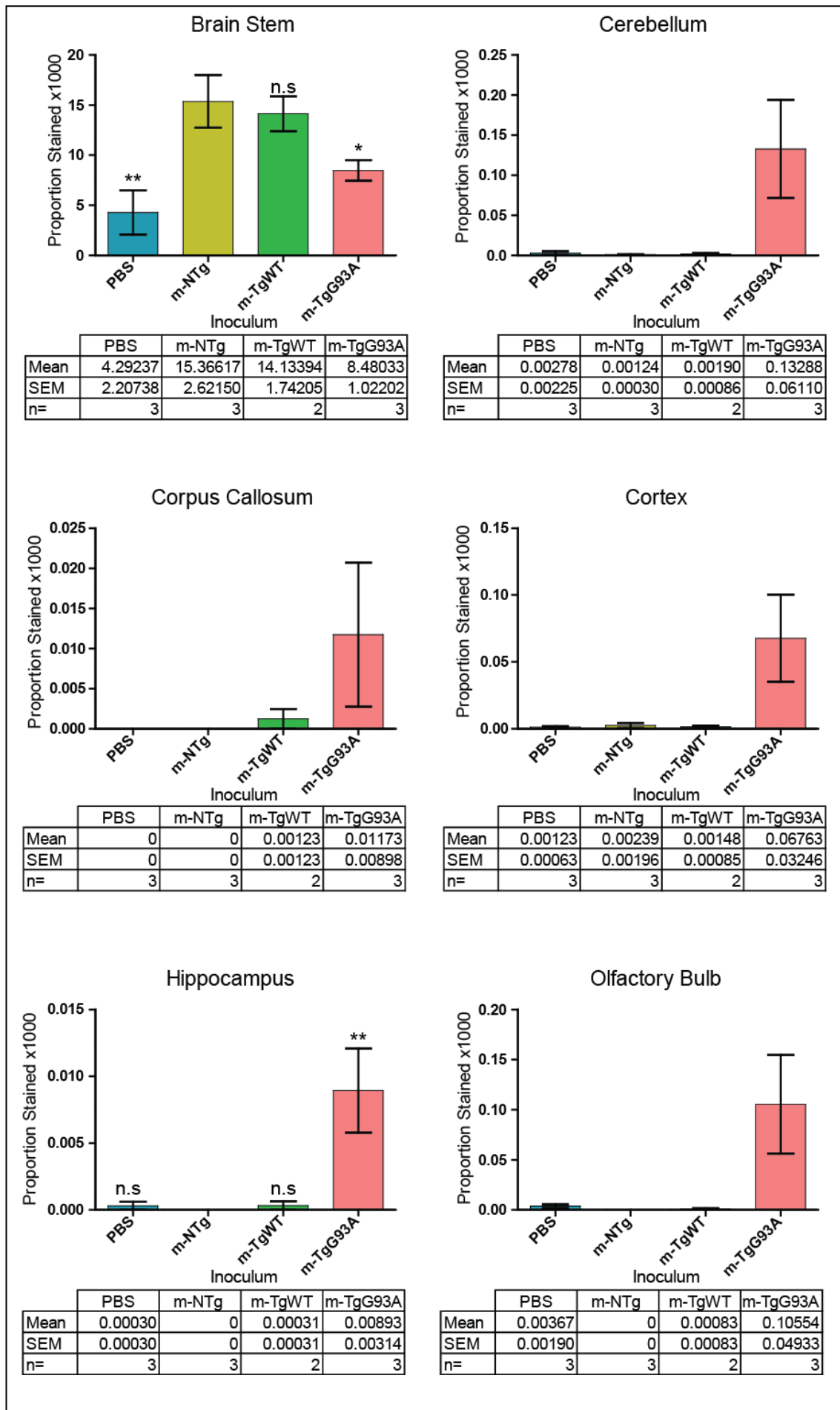


**Figure 3.4 SEDI stained TgG93A;Sod1ko sagittal brain sections 24 hours post-inoculation**

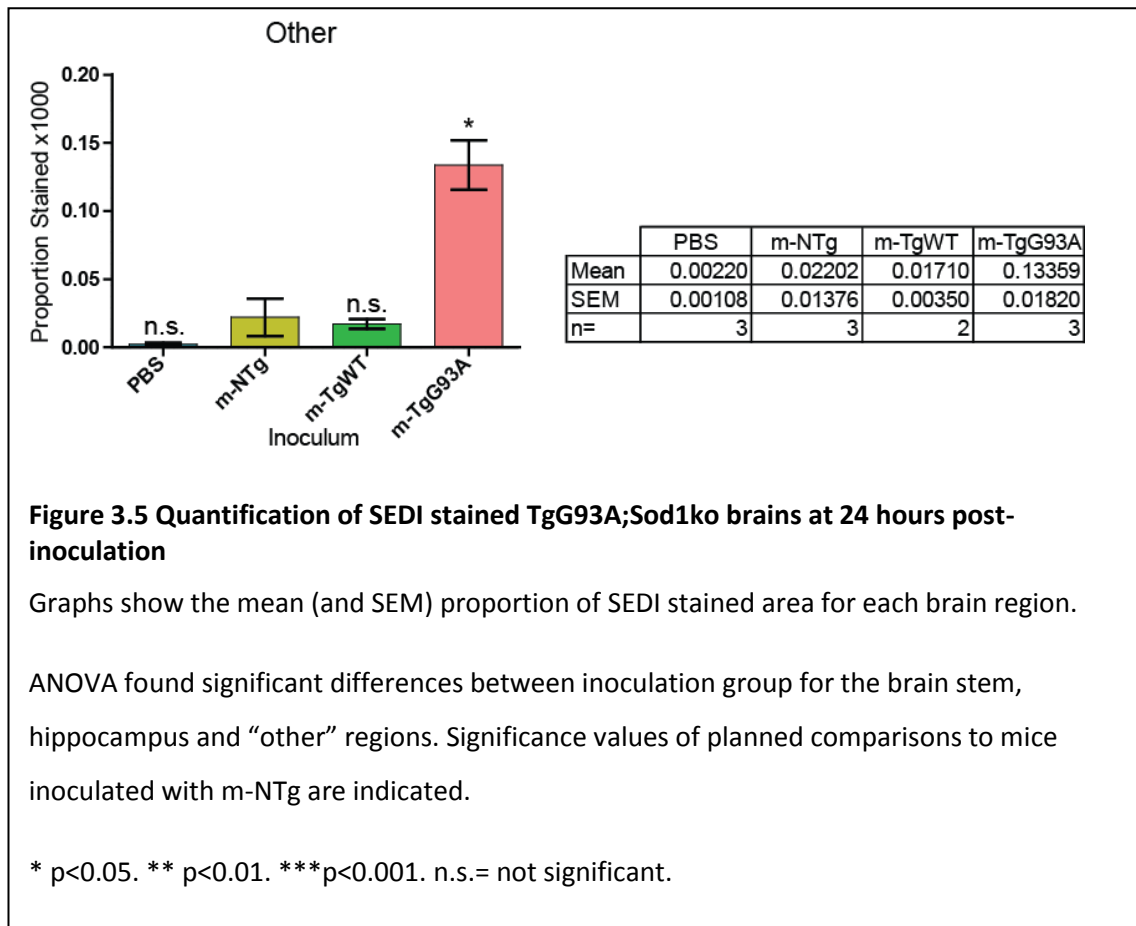
Representative examples of sagittal brain sections of TgG93A;Sod1ko mice 24 hours after inoculation (51-days of age) inoculated with (a) PBS only, (b) m-NTg, (c) m-TgWT, or (d) m-TgG93A.

Scale bar= 1mm. SEDI staining is brown, and sections were counterstained with haematoxylin









In the brain stem there was a significant difference in the area of SEDI staining between inoculum groups:  $F(3,7)=6.328$ ,  $p < 0.05$ . A larger proportion of the brain stem stained positive for SEDI in mice inoculated with m-NTg than mice inoculated with either PBS ( $t(7)=3.943$ ,  $p < 0.01$ ), or m-TgG93A ( $t(7)=2.452$ ,  $p < 0.05$ ), but did not differ from mice inoculated with m-TgWT ( $t(7)=0.392$ ,  $p > 0.05$ )

In the hippocampus there was a significant difference in the area of SEDI staining between inoculum groups:  $F(3,7)=6.497$ ,  $p < 0.05$ . Mice inoculated with m-NTg had a significantly smaller proportion of the hippocampus stained with SEDI than did mice inoculated with m-TgG93A ( $t(7)=-3.738$ ,  $p < 0.01$ ), but did not differ from either mice inoculated with PBS ( $t(7)=-0.124$ ,  $p > 0.05$ ) or m-TgWT ( $t(7)=-0.118$ ,  $p > 0.05$ ).

In the “other” region there was a significant difference in the area of SEDI staining between inoculum groups:  $F(3,7)=23.784$ ,  $p < 0.001$ . Mice inoculated with m-NTg had a significantly smaller proportion of the “other” region stained positive for SEDI than mice inoculated with m-TgG93A ( $t(7)=-6.436$ ,  $p < 0.001$ ), but did not differ from mice inoculated with PBS ( $t(7)=1.143$ ,  $p > 0.05$ ) or m-TgWT ( $t(7)=0.254$ ,  $p > 0.05$ ).

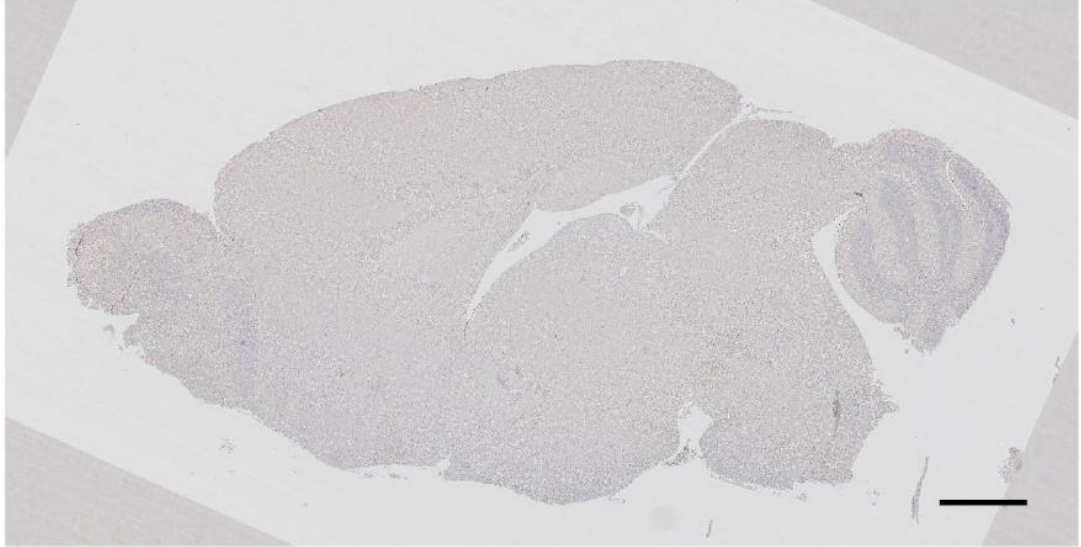
There was no significant difference in the area of SEDI staining between inoculum groups in the cerebellum ( $F(3,7)=3.889$ ,  $p>0.05$ ), corpus callosum ( $F(3,7)=1.373$ ,  $p>0.05$ ), cortex ( $F(3,7)=3.483$ ,  $p>0.05$ ) or olfactory bulb ( $F(3,7)=3.765$ ,  $p>0.05$ ). Although the differences in these regions did not reach statistical significance, a non-significant trend of mice inoculated with m-TgG93A having increased SEDI staining can be seen (Figure 3.5).

#### 3.3.2.3.2 Forty-Days Post-Inoculation

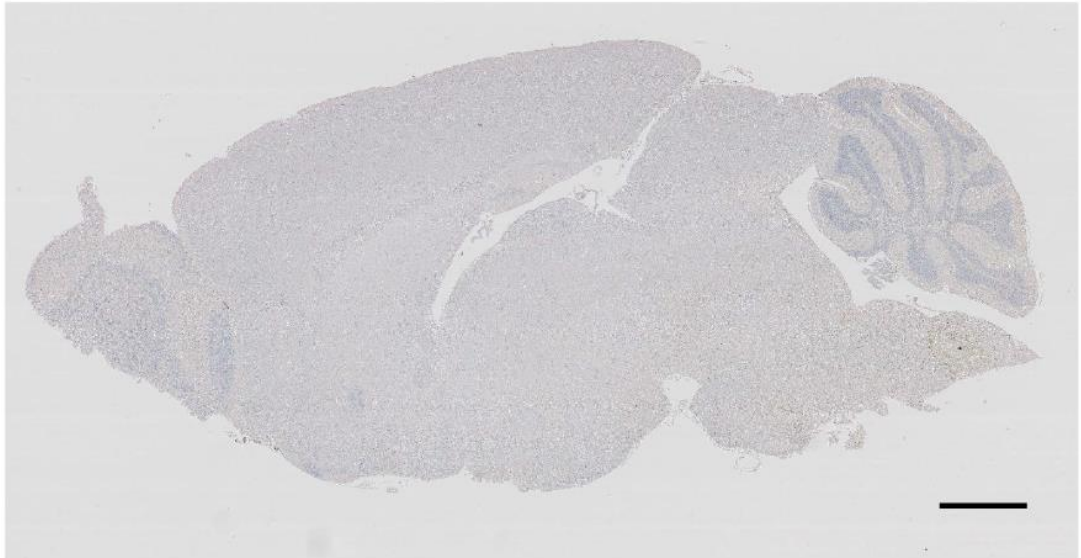
Figure 3.6 shows examples of SEDI staining in sagittal brain sections 40-days post-inoculation. Data were analysed by one-way ANOVA with planned comparisons to the m-NTg control inoculated group. Results for each region analysed as summarised in Figure 3.7.

There was no significant difference in the area of SEDI staining between inoculum groups for any of the brain regions (brain stem:  $F(3,34)=0.973$ ,  $p>0.05$ , cerebellum:  $F(3,33)=0.333$ ,  $p>0.05$ , corpus callosum:  $F(3,34)=1.078$ ,  $p>0.05$ , cortex:  $F(3,34)=1.432$ ,  $p>0.05$ , hippocampus:  $F(3,34)=0.756$ ,  $p>0.05$ , olfactory bulb:  $F(3,33)=0.063$ ,  $p>0.05$ , "other"  $F(3,34)=1.558$ ,  $p>0.05$ ).

(a) PBS



(b) m-NTg



(continued...)

(c) m-TgWT



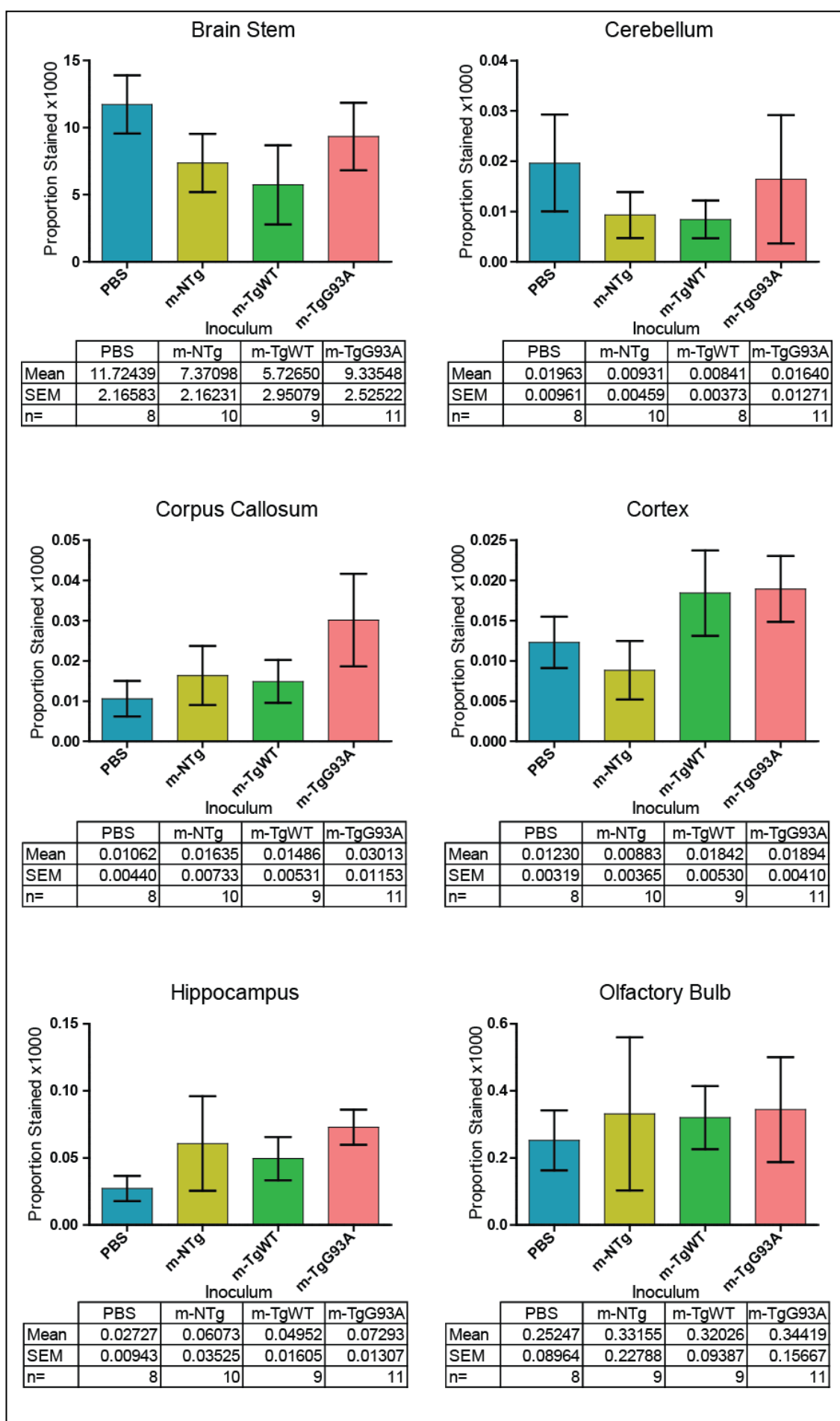
(d) m-TgG93A

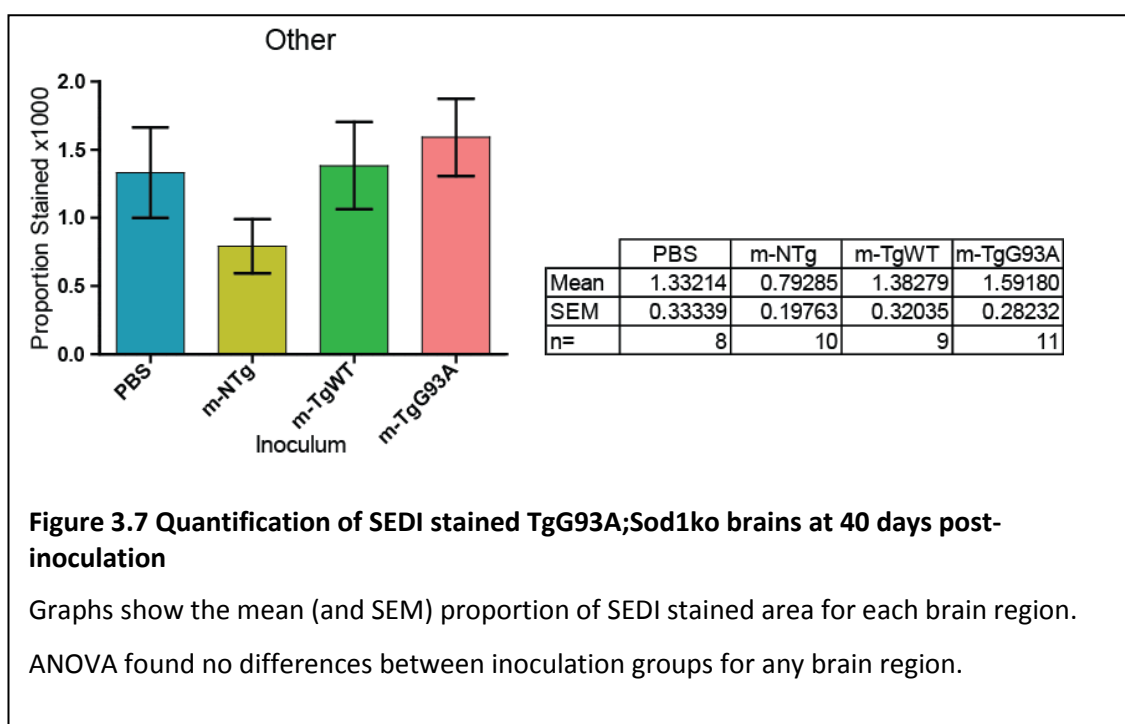


**Figure 3.6 SEDI stained TgG93A;Sod1ko sagittal brain sections 40 days post-inoculation**

Representative examples of sagittal brain sections of TgG93A;Sod1ko mice 40-days after inoculation (91-days of age) inoculated with (a) PBS only, (b) m-NTg, (c) m-TgWT or (d) m-TgG93A.

Scale bar= 1mm. SEDI staining is brown, and sections were counterstained with haematoxylin





### 3.3.3 Transmission in Wild-Type SOD1 Transgenic Mice

Cross-seeded misfolding of WT SOD1, by mutant misfolded SOD1, has been reported in some (Grad et al., 2011; Sundaramoorthy et al., 2013) but not all (Munch et al., 2011) cellular models of prion-like SOD1. We next tested whether cross-seeded aggregation could be detected in a WT huSOD1 transgenic mouse.

Seventy day old TgWT;Sod1ko mice were intracerebrally inoculated with SC homogenate from 100-days old TgG93A;Sod1ko mice, or motor cortex homogenate from SOD1-fALS patients (as described in Section 2.6.2). Several control inocula were also used as summarised in Table 3.11.

**Table 3.11 Inoculum used for TgWT transmission experiment**

Experimental inocula, containing mutant SOD1, are highlighted in blue, control inocula are white.

Name	Species	Genotype	Age at death	Sex	Tissue used
m-TgG93A	mouse	TgG93A,Sod1ko	100 days	female	spinal cord
m-TgWT	mouse	TgWT,Sod1ko	100 days	female	spinal cord
m-NTg	mouse	NTg,Sod1ko	100 days	female	spinal cord
h-D101G	human	SOD1 <sup>+/-D101G</sup>	46 years	female	motor cortex
h-I113T	human	SOD1 <sup>+/-I113T</sup>	47 years	male	motor cortex
h-cntrl1	human	SOD1 <sup>+/+</sup>	52 years	female	motor cortex
h-cntrl2	human	SOD1 <sup>+/+</sup>	40 years	male	motor cortex
PBS	n/a	PBS only control			

Where pair-wise comparisons are carried out between inoculum groups, comparison is to the m-NTg inoculated animals; as this inoculum is devoid of either human or mouse SOD1, if an effect is due to prion-like properties of SOD1 they should be absent in this group, however non-specific effects due to the inoculation with CNS material will be controlled for.

### *3.3.3.1 PREMATURE DEATH AND EXCLUSION*

During the experiment a number of animals died or were culled before their scheduled cull date. Table 3.12 shows causes of premature death split between inoculum groups. A full list of all animals that died prematurely, broken down by inoculum and time-point group, can be found in Section 7.3, Appendix 3.

In total 211 animals, or 37.7% of all animals entering the experiment, were excluded from the final data set due to premature death. Table 3.13 shows the number of animals in each inocula and time-point group to survive to its scheduled cull date.

The most common causes of premature death/cull were weight loss and self-inflicted injury due to over-grooming and scratching which accounted for 34.6% and 30.8% of the 211 premature deaths, respectively. The next most common cause of death was intolerance to the inoculation/anaesthetic procedure, which accounted for 20.9% of premature deaths. Other individual causes were responsible for the death/cull of very small numbers of animals (all less than 4% of premature deaths).

Of the 211 cases that were culled prior to their scheduled cull date, 184 were from the 2 longest time-points of 365 and 660-days post-inoculation. Kaplan-Meier survival analysis was used to compare the survival of animals in the 2 longest time-points for the most common causes of premature death (weight loss and scratching) and other disease relevant causes (hind limb paralysis and impaired righting reflex). Figure 3.8 shows the Kaplan-Meier survival graph (for increased clarity, the same data is displayed in Section 7.4, Appendix 4 with data split onto 2 graphs, one showing data for mice inoculated with mouse tissues, and another showing data from mice inoculated with human tissues). There was a significant effect of inoculum group on survival ( $\chi^2(8)=40.246$ ,  $p<0.001$ ).

**Table 3.12 Causes of premature death**

Inoculum	Inoculation / anaesthetic	Scratch-ing	Weight loss	Found dead	Abdominal swelling	Abnormal breathing	Hind limb paralysis	Righting reflex	Missing presumed dead	Culled in error	Pro-lapsed rectum	Tumour	TOTAL (pre-mature / total)
<b>Non-inoculated</b>	0	2	7	1	0	0	0	0	3	1	0	2	<b>16/61</b>
<b>PBS</b>	4	7	3	1	1	0	0	0	1	1	1	0	<b>19/65</b>
<b>m-NTg</b>	5	6	9	0	1	0	1	0	0	1	0	0	<b>23/63</b>
<b>m-TgWT</b>	2	11	8	2	0	0	0	1	0	0	0	0	<b>24/60</b>
<b>m-TgG93A</b>	1	9	10	0	0	0	0	0	0	1	0	0	<b>21/62</b>
<b>h-cntrl1</b>	8	3	14	0	1	1	0	0	1	0	0	0	<b>28/63</b>
<b>h-cntrl2</b>	9	7	6	1	0	0	0	0	0	0	0	0	<b>23/60</b>
<b>h-D101G</b>	6	11	6	1	0	0	0	1	0	0	0	0	<b>25/62</b>
<b>h-I113T</b>	9	9	10	2	1	0	0	1	0	0	0	0	<b>32/64</b>
<b>TOTAL</b>	<b>44</b>	<b>65</b>	<b>73</b>	<b>8</b>	<b>4</b>	<b>1</b>	<b>1</b>	<b>3</b>	<b>5</b>	<b>4</b>	<b>1</b>	<b>2</b>	<b>211/560</b>



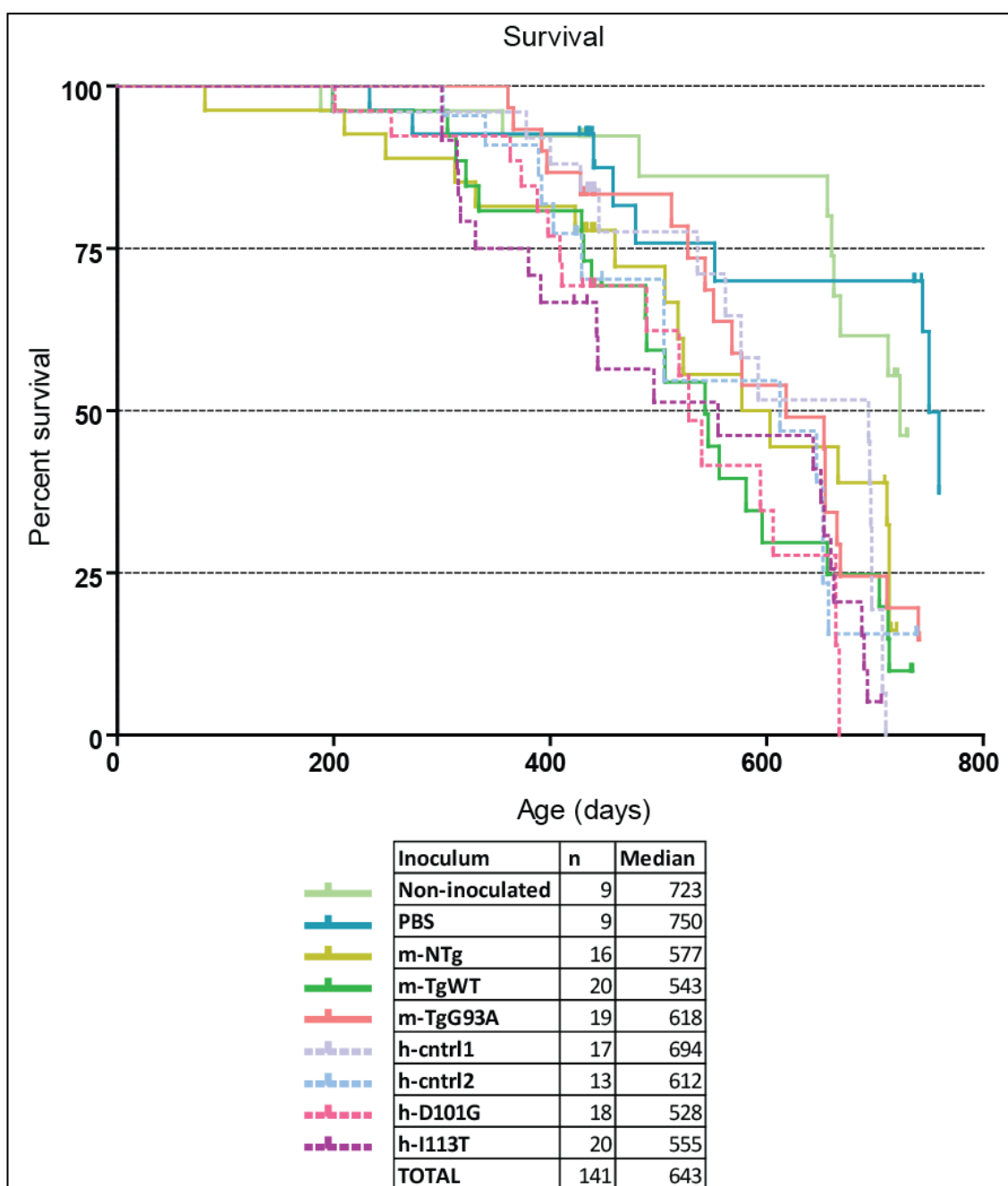


**Figure 3.8 Kaplan-Meier survival graph of TgWT;Sod1ko mice**

Mice from the 2 longest time-points (365 and 660-days post-inoculation) that were culled before their scheduled cull date due to weight loss, self-inflicted scratching wounds, hind limb paralysis and impaired righting reflex were included in the analysis. There was a significant effect of inoculation group on likelihood of survival  $\chi^2(8)=40.246$ ,  $p<0.001$ . Pair-wise comparisons to m-NTg inoculated mice did not reveal any significant differences.

This data is also presented in 2 graphs in Section 7.4, Appendix 4, split between mouse and human inocula.

**Table 3.13 Number of animals surviving to scheduled cull date**

Table shows the number of animals surviving to the scheduled cull date / the number of animals allocated to the group

	Time-point (days post-inoculation)				
Inoculum	7	90	180	365	660
Non-inoculated	8/11	10/10	10/10	9/10	8/20
PBS	10/10	9/10	9/10	9/15	9/20
m-NTg	10/10	10/10	9/13	7/10	4/20
m-TgWT	10/10	10/10	10/10	4/10	2/20
m-TgG93A	10/10	10/10	10/10	8/10	3/22
h-cntrl1	9/10	9/13	9/10	8/10	0/20
h-cntrl2	9/10	9/10	10/15	7/10	2/15
h-D101G	9/10	10/10	10/12	8/10	0/20
h-I113T	10/10	9/10	9/10	3/10	1/24

Eight further pair-wise comparisons were carried out to compare the survival of each inoculum group to mice inoculated with m-NTg. A Bonferroni adjusted significance level of 0.00625 was used. There was no significant difference between survival of the m-NTg inoculated mice compared to the survival of non-inoculated mice ( $\chi^2(1)=5.654$ ,  $p>0.00625$ ) or mice inoculated with PBS ( $\chi^2(1)=7.292$ ,  $p>0.00625$ ), m-TgWT ( $\chi^2(1)=0.952$ ,  $p>0.00625$ ), m-TgG93A ( $\chi^2(1)=0.02$ ,  $p>0.00625$ ), h-cntrl1 ( $\chi^2(1)=1.233$ ,  $p>0.00625$ ), h-cntrl2 ( $\chi^2(1)=0.263$ ,  $p>0.00625$ ), h-D101G ( $\chi^2(1)=3.232$ ,  $p>0.00625$ ) or h-I113T ( $\chi^2(1)=3.437$ ,  $p>0.00625$ ). Comparisons of m-NTg inoculated to both non-inoculated and PBS inoculated animals had p values below the uncorrected cut-off of  $p=0.05$  ( $p=0.017$  and  $p=0.007$ , respectively), suggesting that the significant omnibus  $\chi^2$  could be due to differences between animals inoculated with tissue homogenates and those non-inoculated or inoculated with PBS.

### 3.3.3.2 AGE DIFFERENCES BETWEEN GROUPS

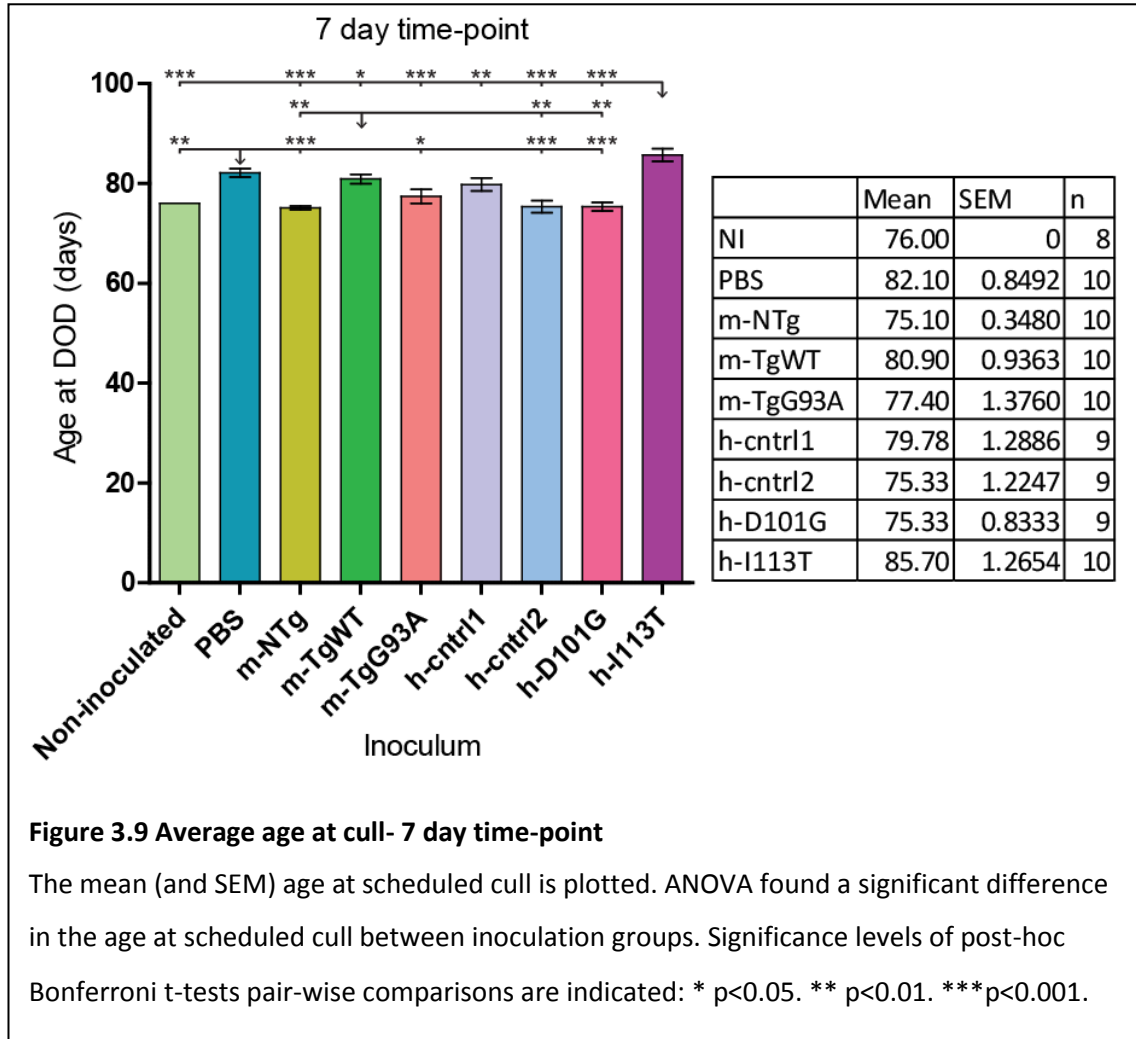
#### 3.3.3.2.1 Age at Cull - 7 Day Time-Point

Figure 3.9 shows the average age at cull date for animals in the 7 day post-inoculation time-point. A one-way ANOVA revealed significant differences in the age at cull date between inoculation groups:  $F(8,84)=13.621$ ,  $p<0.001$ . Bonferroni post-hoc comparisons were carried out to identify pair-wise differences.

PBS inoculated animals had a significantly higher age at cull than animals inoculated with m-NTg ( $p<0.001$ ), m-TgG93A ( $p<0.05$ ), h-cntrl2 ( $p<0.001$ ) and h-D101G ( $p<0.001$ ) and non-inoculated animals ( $p<0.01$ ).

Mice inoculated with m-TgWT were significantly older at cull than mice inoculated with m-NTg ( $p<0.01$ ) h-cntrl2 ( $p<0.01$ ) and h-D101G ( $p<0.01$ ).

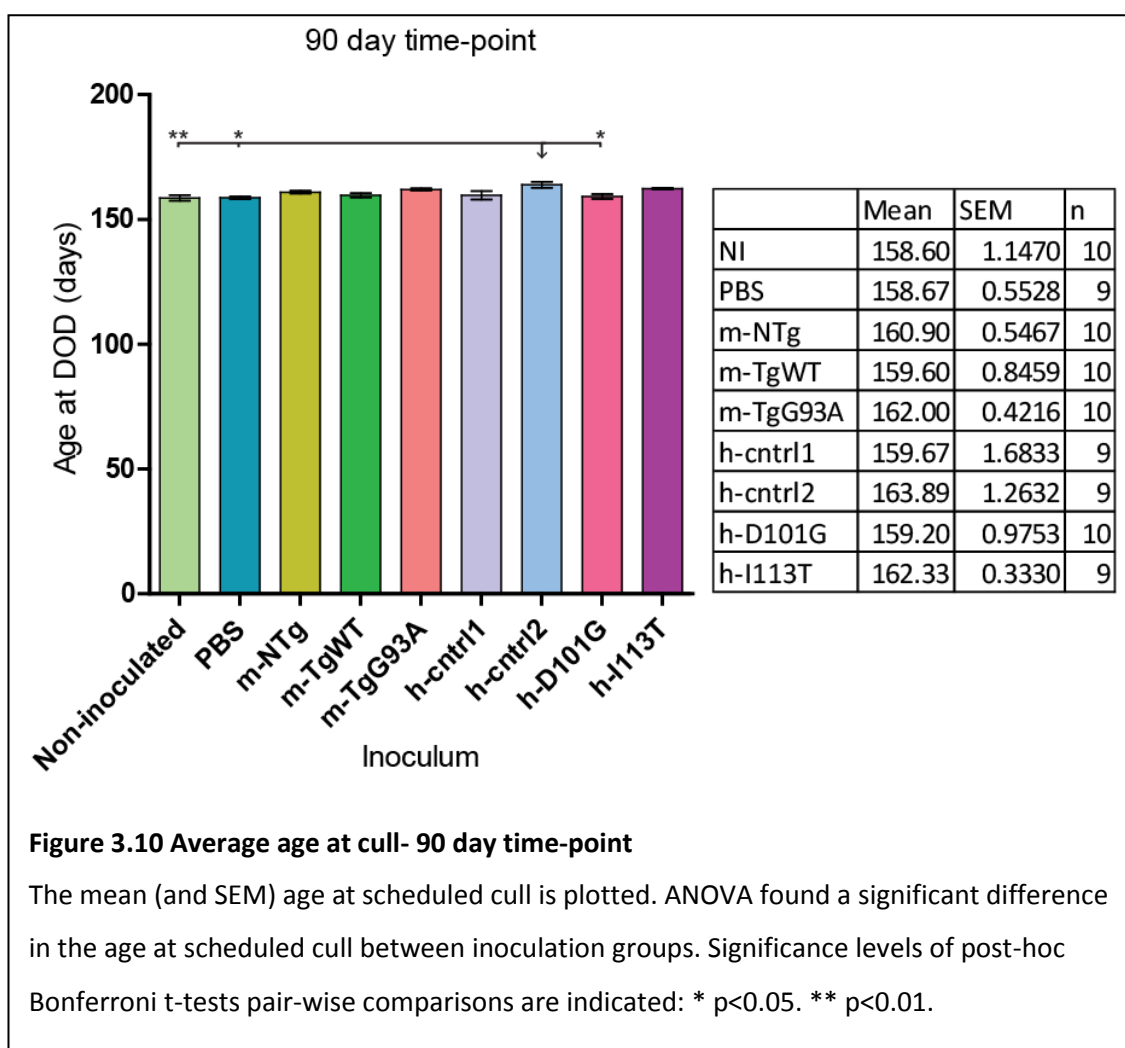
Mice inoculated with h-I113T were significantly older at cull than mice inoculated with m-NTg ( $p<0.001$ ), m-TgWT ( $p<0.05$ ), m-TgG93A ( $p<0.001$ ), h-cntrl1 ( $p<0.01$ ) h-cntrl2 ( $p<0.001$ ) and h-D101G ( $p<0.001$ ) and non-inoculated mice ( $p<0.001$ ).



### 3.3.3.2.2 Age at Cull - 90 Day Time-Point

Figure 3.10 shows the average age at cull date for animals in the 90 day post-inoculation time-point. A one-way ANOVA revealed significant differences in the age at cull date between inoculation groups at the 90 day time-point:  $F(8,85)=3.722$ ,  $P<0.01$ . Bonferroni post-hoc comparisons were carried out to identify pair-wise differences.

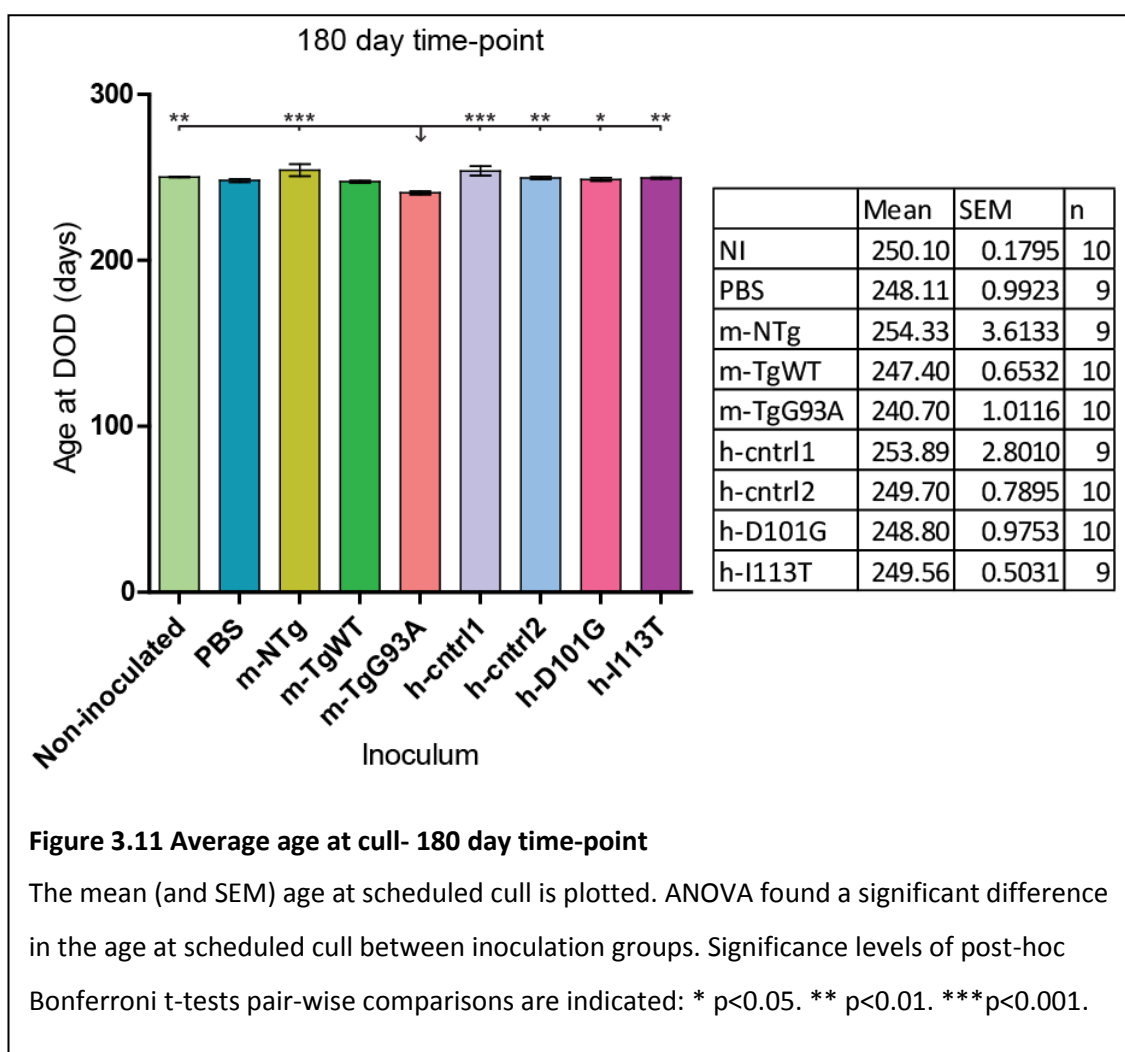
Mice inoculated with h-cntrl2 had significantly higher age at cull than mice inoculated with PBS ( $p<0.01$ ) or h-D101G ( $p<0.05$ ) or non-inoculated animals ( $p<0.01$ ).



### 3.3.3.2.3 Age at Cull - 180 Day Time-Point

Figure 3.11 shows the average age at cull date for animals in the 180 day post-inoculation time-point. A one-way ANOVA revealed significant differences in the age at cull date between inoculation groups at the 180 day time-point:  $F(8,85)=6.244$ ,  $p < 0.001$ . Bonferroni post-hoc comparisons were carried out to identify pair-wise differences.

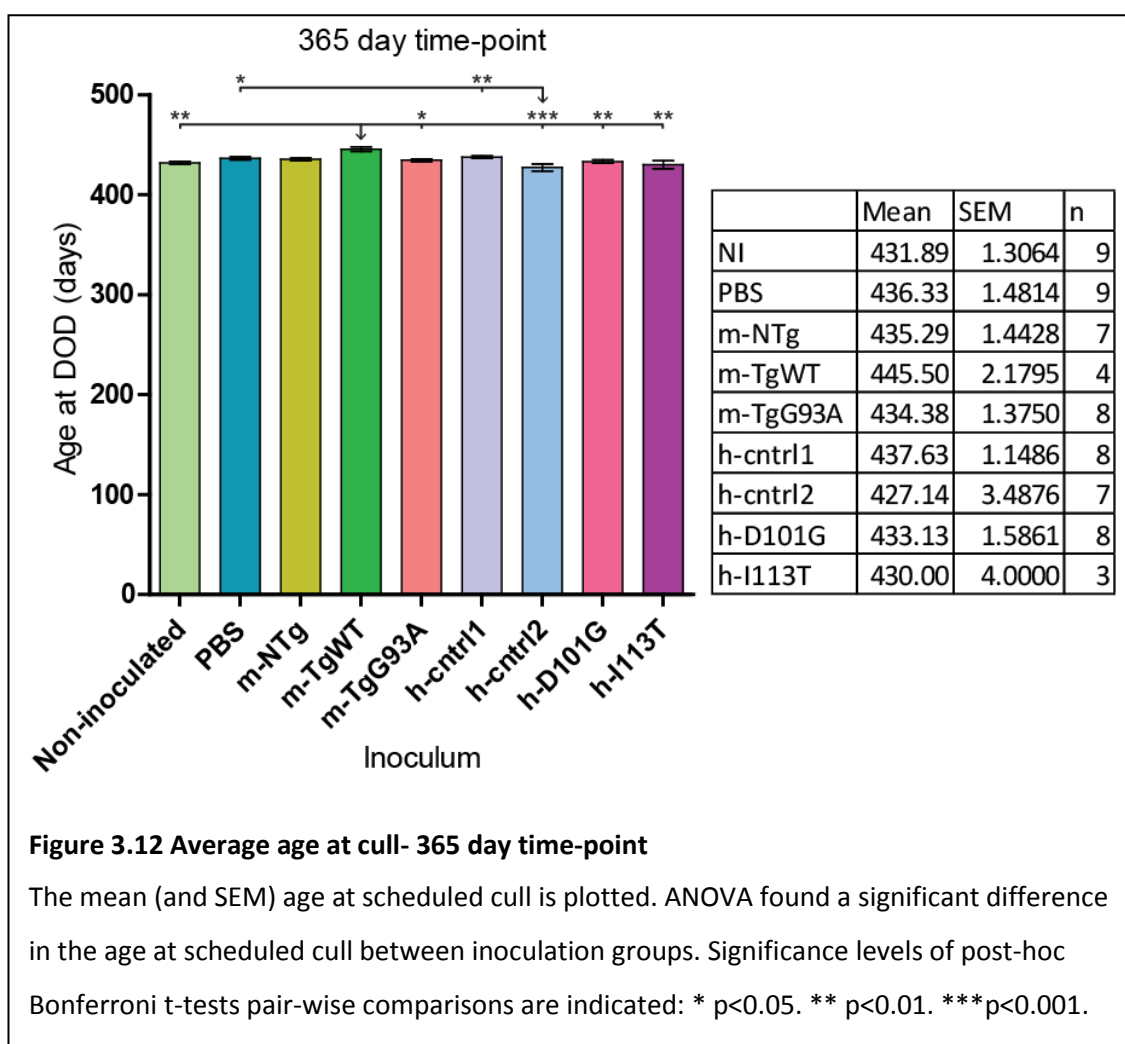
Mice inoculated with m-TgG93A had significantly lower age at cull date than mice inoculated with m-NTg ( $p < 0.001$ ), h-cntrl1 ( $p < 0.001$ ), h-cntrl2 ( $p < 0.01$ ), h-D101G ( $p < 0.05$ ) or h-I113T ( $p < 0.01$ ) or non-inoculated animals ( $p < 0.001$ ).



### 3.3.3.2.4 Age at Cull - 365 Day Time-Point

Figure 3.12 shows the average age at cull date for animals in the 365 day post-inoculation time-point. A one-way ANOVA revealed significant differences in the age at cull date between inoculation groups at the 365 day time-point:  $F(8,62)=5.546$ ,  $p < 0.001$ . Bonferroni post-hoc comparisons were carried out to identify pair-wise differences.

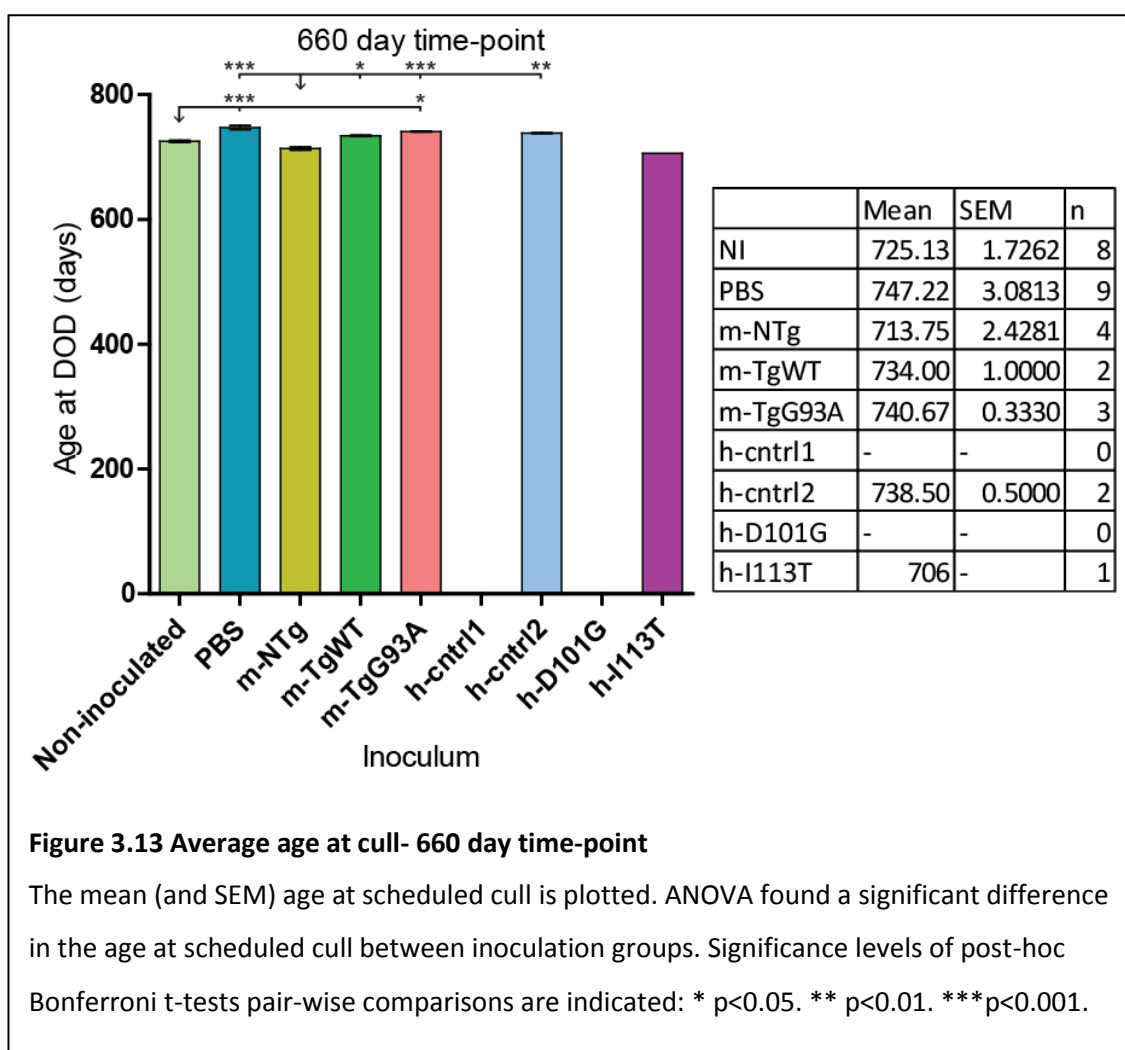
Mice inoculated with m-TgWT were significantly older at their cull date than mice inoculated with m-TgG93A ( $p < 0.05$ ), h-cntrl2 ( $p < 0.001$ ), h-D101G ( $p < 0.01$ ) or h-I113T ( $p < 0.01$ ) or non-inoculated animals ( $p < 0.01$ ). Mice inoculated with h-cntrl2 were significantly younger at their cull date than mice inoculated with PBS ( $p < 0.05$ ) or h-cntrl1 ( $p < 0.01$ ).



### 3.3.3.2.5 Age at Cull - 660 Day Time-Point

Figure 3.13 shows the average age at cull date for animals in the 660 day post-inoculation time-point. Because only one mouse in the h-I113T inoculum group survived until its allocated cull date, and no mice from either the h-cntrl1 or h-D101G inoculum groups survived, these groups were excluded from the analyses. A one-way ANOVA revealed significant differences in the age at cull date between inoculation groups at the 660 day time-point:  $F(5,27)=18.877$ ,  $p < 0.001$ . Bonferroni post-hoc comparisons were carried out to identify pair-wise differences.

Non-inoculated mice had significantly lower ages at their cull date than did mice inoculated with PBS ( $p < 0.001$ ) and m-TgG93A ( $p < 0.05$ ). Mice inoculated with m-NTg had significantly lower ages at their cull date than did mice inoculated with PBS ( $p < 0.001$ ), m-TgWT ( $p < 0.05$ ), m-TgG93A ( $p < 0.001$ ) or h-cntrl2 ( $p < 0.01$ ).

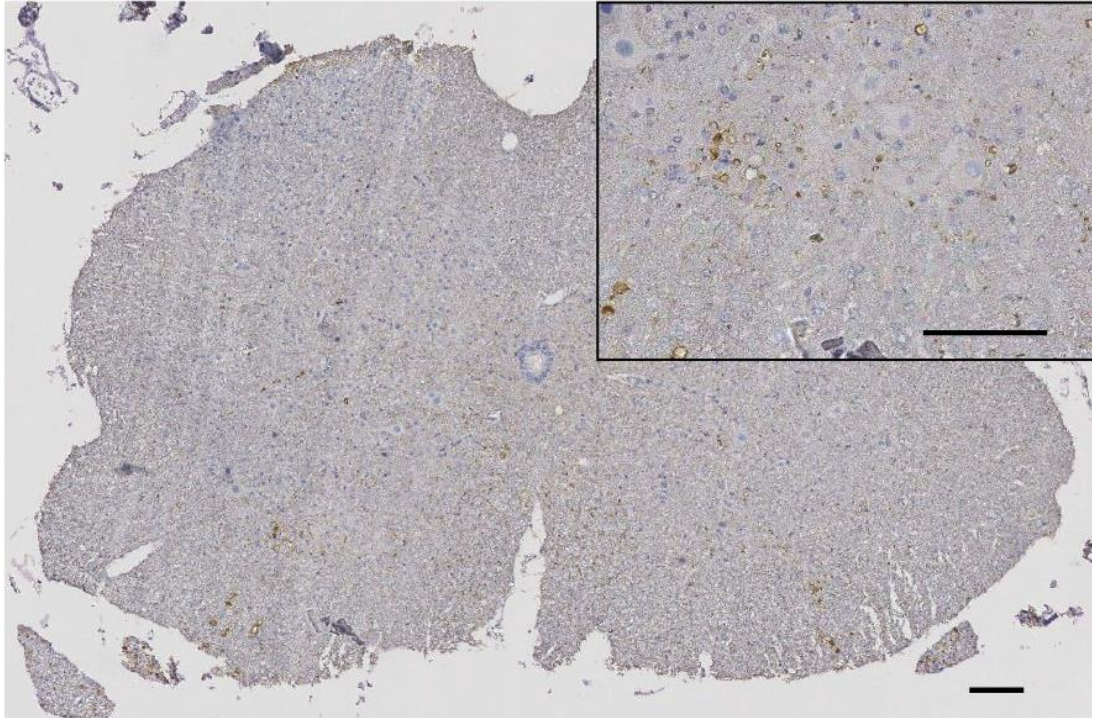


### 3.3.3.3 MISFOLDED SOD1 PATHOLOGY

Initial testing of SEDI staining of spinal cords of mice culled at 180-days post-inoculation revealed very high levels of staining even in mice inoculated with PBS and m-NTg as shown in Figure 3.14. For this reason, the USOD antibody was tested for analysis at an earlier time-point of 90-days post-inoculation. Data collection and analysis is on-going for this project. At this time data are available for USOD stained spinal cords of mice in the 90 day time-point, inoculated with PBS, m-NTg, m-TgWT and m-TgG93A. Five animals have been analysed per inoculum group except for the m-NTg group where only 4 animals have been analysed.



(a) PBS



(b) m-NTg

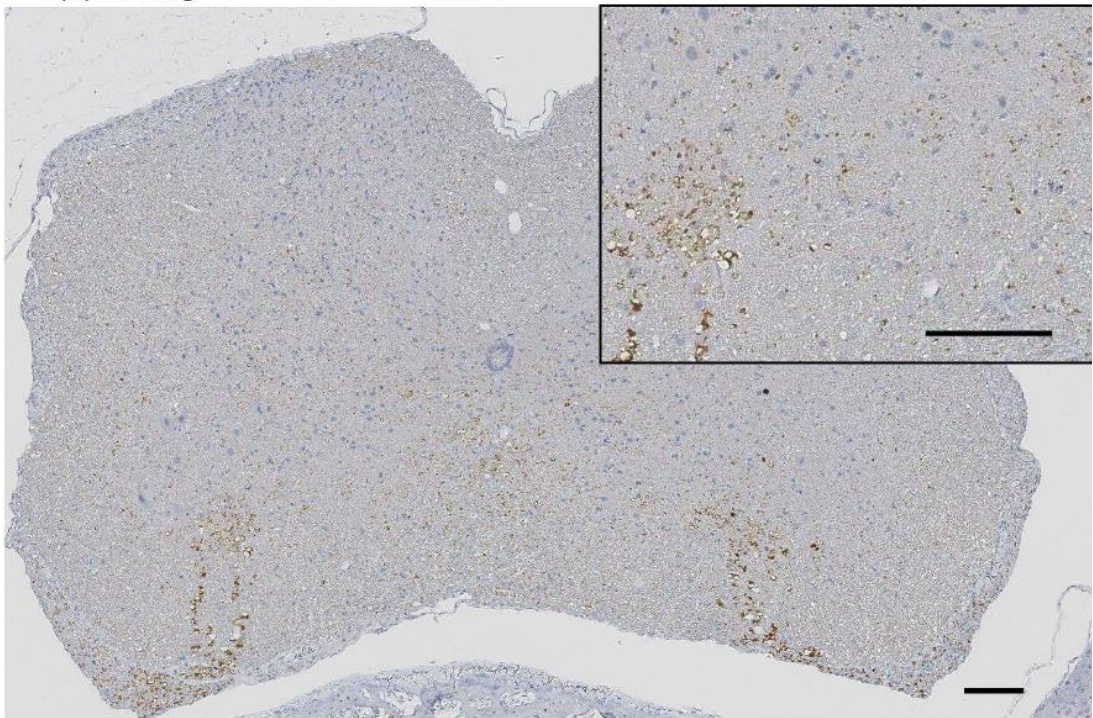


**Figure 3.14 SEDI staining of TgWT;Sod1ko cords at 90 days post-inoculation**

Examples of SEDI stained spinal cords of TgG93A;Sod1ko mice inoculated with (a) PBS or (b) m-NTg. High staining can be seen in both cases, particularly in the ventral horns and white matter tracts. Inset shown higher magnification of ventral horn.

Scale bar= 100µm. SEDI staining is brown, and sections were counterstained with haematoxylin



### 3.3.3.3.1 USOD Spinal Cord Pathology

The cords were divided into regions as shown in Figure 3.15 and analysed using Definiens tissue Studio software, as described in Section 2.7.5, to give the proportion of each region stained. Because the proportions were very small the numbers presented in Figures and Tables have been multiplied by 1000.

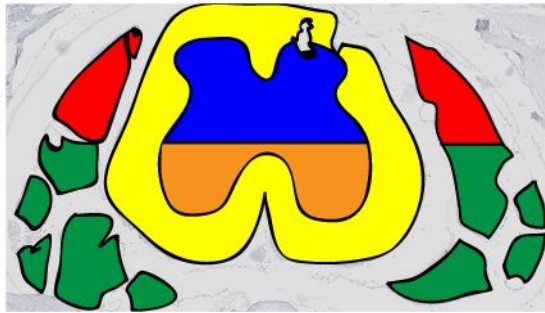


**Figure 3.15 Division of spinal cord regions**

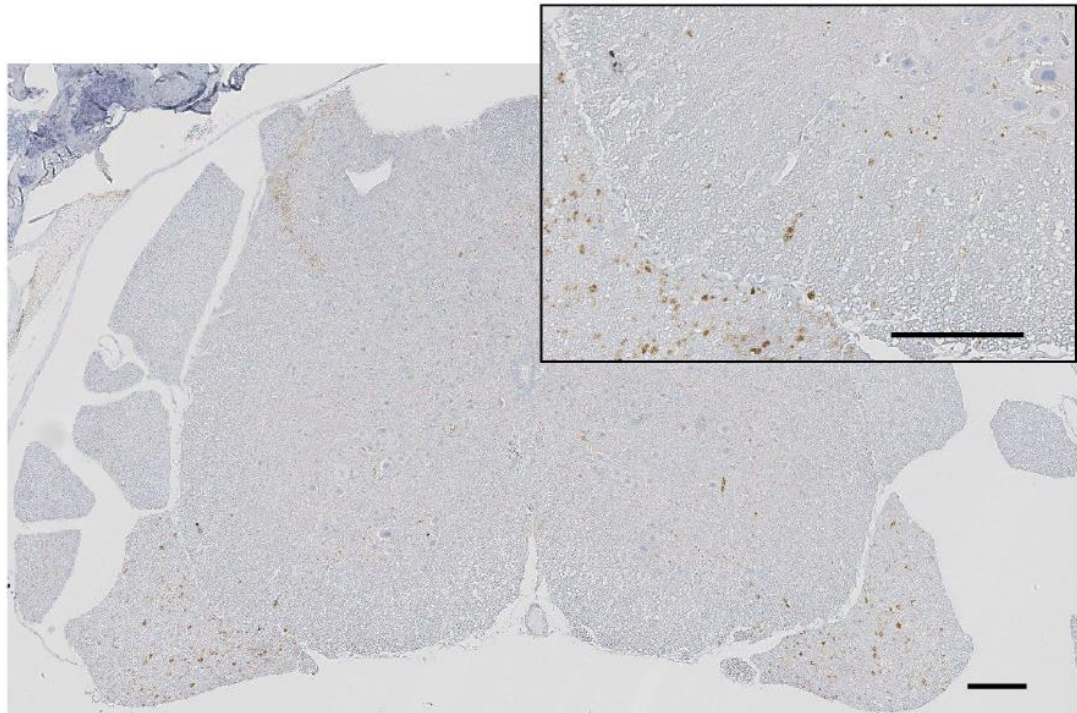
Blue= dorsal horns. Orange= ventral horns. Yellow= white matter. Red= dorsal roots. Green= ventral roots.

Figure 3.16 shows examples of USOD stained spinal cord sections at 90-days post-inoculation. Data were analysed by one-way ANOVA with planned comparisons to the m-NTg control inoculated group. Results for each region analysed as summarised in Figure 3.17.

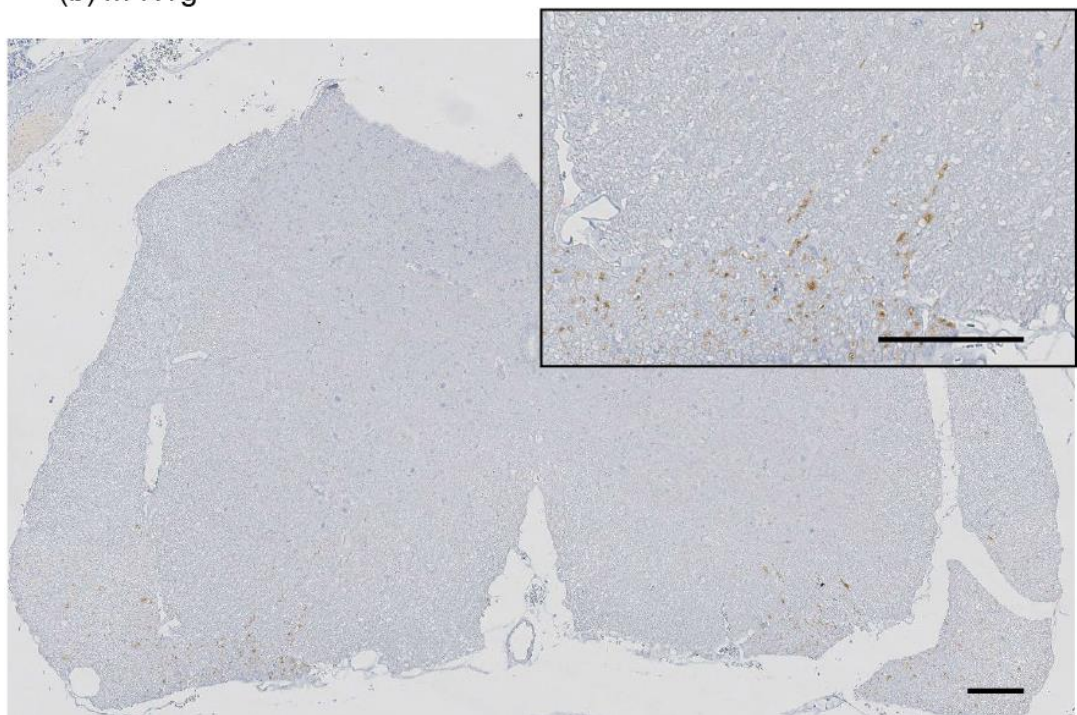
There was no difference in the area of USOD staining between inoculum groups for the ventral horns ( $F(3,18)=1.761$ ,  $p>0.05$ ), dorsal horns ( $F(3,16)=0.585$ ,  $p>0.05$ ), white matter ( $F(3,16)=0.675$ ,  $p>0.05$ ) or the dorsal roots ( $F(3,16)=1.068$ ,  $p>0.05$ ).

There was a significant difference in the proportion of USOD staining between inoculum groups in the ventral roots ( $F(3,16)=3.735$ ,  $p<0.05$ ). As shown in Figure 3.17, mice inoculated with m-NTg had a significantly smaller proportion of USOD staining within the ventral roots compared to mice inoculated with m-TgG93A ( $t(13)=-2.311$ ,  $p<0.05$ ) but did not differ to animals inoculated with PBS ( $t(13)=0.002$ ,  $p>0.05$ ) or m-TgWT ( $t(13)=-0.620$ ,  $p>0.05$ ).

(a) PBS



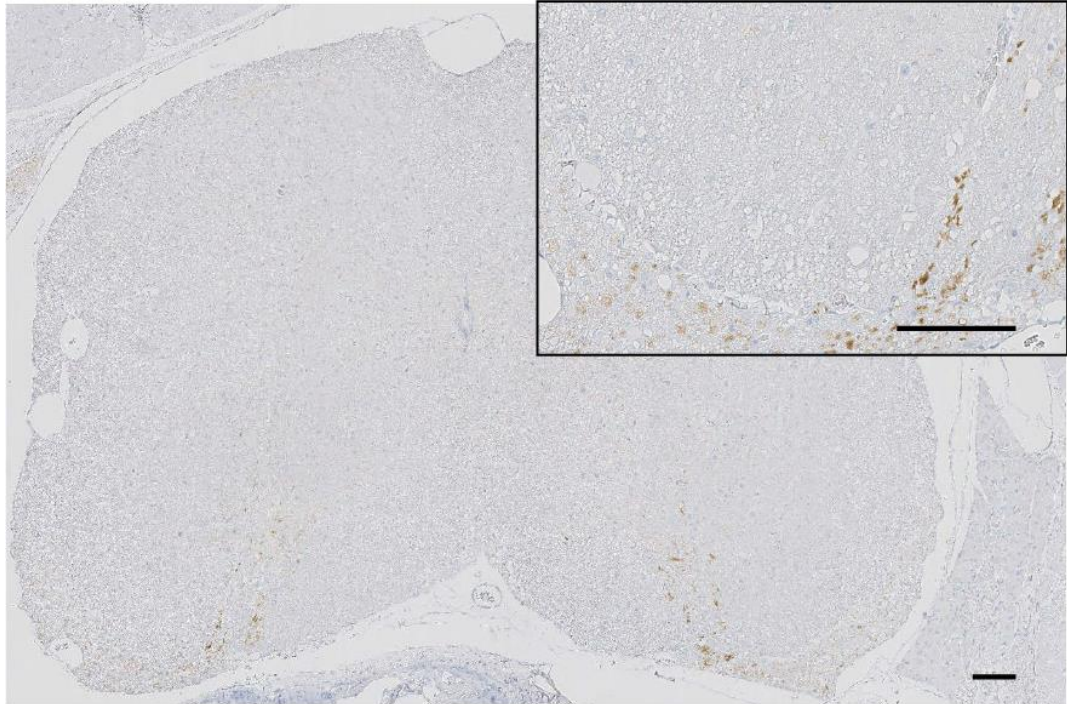
(b) m-NTg



(continued...)



(c) m-TgWT



(d) m-TgG93A

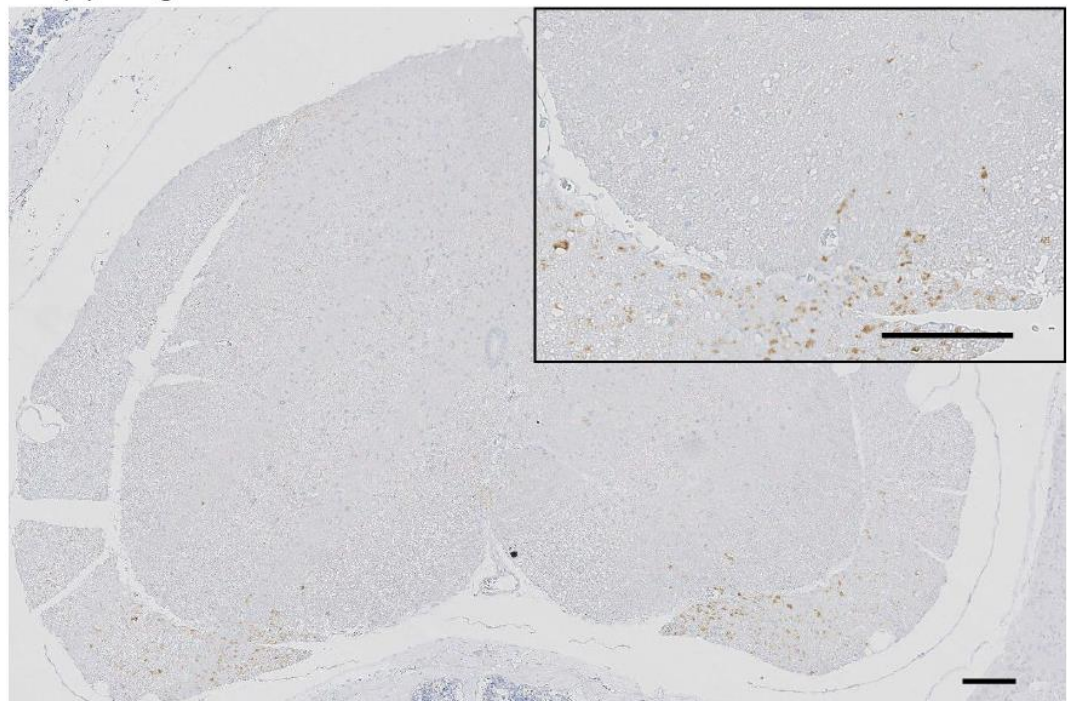


**Figure 3.16 USOD stained TgWT;Sod1ko spinal cord sections 90 days post-inoculation**

Representative examples of USOD stained spinal cords of TgWT;Sod1ko mice ninety-days post-inoculation (160-days of age), inoculated with (a) PBS only, (b) m-NTg, (c) m-TgWT or (d) m-TgG93A. Inset shows higher magnification of ventral horn white matter and roots.

Scale bar= 100µm. USOD staining is brown, and sections were counterstained with haematoxylin

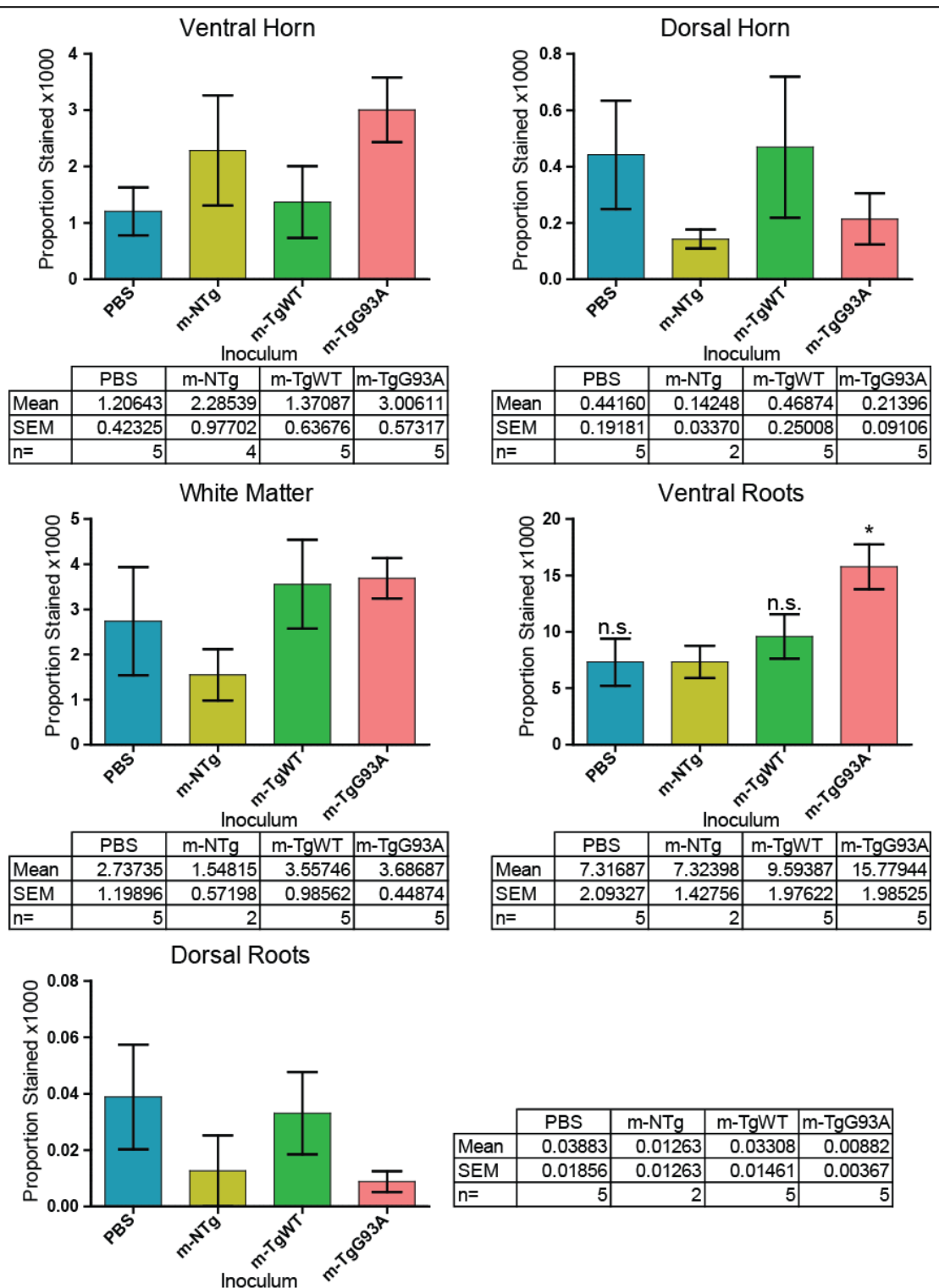


**Figure 3.17 Quantification of USOD stained TgWT;Sod1ko spinal cords at 90 days post-inoculation**

Graphs show the mean (and SEM) proportion of USOD stained area for each spinal cord region. ANOVA found a significant difference in the proportion of USOD stained area between inoculation groups in the ventral roots only. Significance values of planned comparisons to mice inoculated with m-NTg are indicated. n.s.= not significant; \*  $p < 0.05$

### 3.4 CONCLUSIONS

#### 3.4.1 Inheritance Patterns of Human WT and G93A Transgenes and a *Sod1* KO Allele

The inheritance of the WT SOD1 transgene appears to follow Mendelian ratios as its inheritance did not differ from the expected ratio in either of the breeding schemes examined.

In our breeding scheme crossing TgG93A;Sod1het males to NTg;Sod1het females, the ratio of NTg to TgG93A offspring was significantly higher than the expected ratio, with a p value of less than 0.0001. Pair-wise comparisons also identified significantly fewer TgG93A;Sod1wt and TgG93A;Sod1het offspring compared to NTg;Sod1wt offspring. There were also fewer TgG93A;Sod1ko compared to NTg;Sod1wt offspring, however this was not significantly different from the Mendelian ratio; the p value was 0.0067, which although low, was above the corrected significance cut off for multiple comparisons. The ratio of the number of offspring with any of the 3 TgG93A genotypes compared to NTg;Sod1het offspring was also significantly lower than the expected ratio. These results show that in matings between TgG93A;Sod1het males and NTg;Sod1het females, the G93A mutant SOD1 transgene is inherited at a lower frequency than would be expected according to Mendelian inheritance. The overall inheritance of the *Sod1* KO allele was not significantly different from the expected Mendelian ratio. Within the NTg offspring there were significantly fewer NTg;Sod1ko offspring compared to NTg;Sod1wt offspring, but within the TgG93A offspring, neither the number of TgG93A;Sod1het nor TgG93A;Sod1ko offspring was different from the expected number as compared to TgG93A;Sod1wt offspring. This suggests that in NTg animals, Sod1ko pups are less common than expected, but in TgG93A animals, inheritance is Mendelian.

In our mating scheme crossing TgG93A;Sod1ko males to NTg;Sod1het females, the ratio of NTg to TgG93A offspring did not differ from the expected ratio, even at an uncorrected significance threshold. However the ratio of NTg;Sod1het mice compared to TgG93A;Sod1het mice was higher than expected, although this did not hold true in those animals with a Sod1ko genotype. The inheritance of the *Sod1* null allele showed a similar pattern as in offspring of matings with TgG93A;Sod1het males, the overall ratio was not different from the Mendelian ratio, but within NTg offspring more Sod1het animals were born than Sod1ko.

Inheritance of the *Sod1* null allele showed the same pattern in offspring of TgWT;Sod1ko males. Because the omnibus  $\chi^2$  for matings using TgWT;Sod1het males was not significant, no pairwise comparisons were carried out.

The fact that the omnibus  $\chi^2$  for matings using TgWT;Sod1het males was not significant and that for matings using TgWT;Sod1ko males was, is most likely due to the sample size. Over 4

times more animals were born from matings using TgWT;Sod1ko males as compared to those using TgWT;Sod1het males. All matings for which full data were available were used in the analysis and the discrepancy is because animals of the TgWT;Sod1ko genotype were most commonly required for experiments and so more matings were set up using TgWT;Sod1ko males as these were least wasteful for their production. If the n number is artificially increased for inheritance from TgWT;Sod1het matings to match that of TgWT;Sod1ko matings, then a highly significant omnibus  $\chi^2$  results. This suggests that an error has been made either due to under-powering the analysis of matings using TgWT;Sod1het males, or over-powering for matings using TgWT;Sod1ko males. Under-powering analysis is commonly caused by having a smaller sample size than is appropriate and can result in a type 2 error, where the null hypothesis is accepted, even though the experimental hypothesis is actually correct. Similarly, over-powering analysis can occur when an inappropriately large sample size is used; as the sample size increases, relative error decreases, making a type 1 error, where the experimental hypothesis is accepted erroneously, more likely (Coolican, 1999).

The consistent finding across the 3 mating schemes for which pairwise comparisons were carried out is that overall there is no difference between expected and observed ratio when comparing Sod1ko offspring to either Sod1het (in the case of matings using Sod1ko males) or Sod1wt (in the case of matings using Sod1het males). However, when only NTg offspring are considered, the ratios are significantly different, with fewer NTg;Sod1ko offspring than expected.

In summary, these results suggest a tendency towards less TgG93A offspring being born than Mendelian inheritance would predict, but for normal Mendelian inheritance of the WT huSOD1 transgene.

The Sod1ko genotype appears to be less common than expected within a NTg population, however this does not hold true within either WT or G93A huSOD1 transgenic populations. *Sod1* null sperm are known to have reduced fertilising ability (Tsunoda et al., 2012; Garratt et al., 2013) which could be responsible for a lower number of Sod1ko pups born to Sod1het males as *Sod1*<sup>-</sup> sperm would be less viable than *Sod1*<sup>+</sup> sperm. In the case of Sod1ko males, all sperm would be *Sod1*<sup>-</sup> and so any difference would likely be maternal; either reduced inheritance of the *Sod1* null allele from the mother, or reduced viability of the zygote/embryo. *Sod1* null females are known to have reduced fertility (Matzuk et al., 1998) with increased levels of oxidative stress in the uterus (Noda et al., 2012). However *Sod1* null oocytes are just as viable for *in vitro* fertilisation as WT oocytes and transplanted Sod1ko embryos survive normally within WT surrogate mothers (Noda et al., 2012). To our knowledge, similar examination has not been made of Sod1het female fertility, although we may speculate that

Sod1het females also have increased levels of oxidative stress in the uterus due to reduced SOD1 activity. The reduced number of Sod1ko offspring could therefore, be as a result of *Sod1* null oocytes/zygotes being more sensitive than WT oocytes/zygotes to the increased oxidative stress of the Sod1ko or Sod1het uterus. The lack of a difference in frequency of the *Sod1* null allele in SOD1 transgenic mice could be due to the restoration of SOD1 activity by the huSOD1 transgene, thus reducing in utero oxidative stress.

### **3.4.2 Does Mutant SOD1 Display Prion-Like Properties *In Vivo*?**

**3.4.2.1 NO EVIDENCE FOR SELF-SEEDED AGGREGATION IN TgG93A;SOD1KO MICE**  
TgG93A mice have a limited lifespan surviving to around 152-days (average on C57BL/6J background. See Figure 1.14) limiting the incubation time available in this line of mice. It is currently unknown whether self-seeded transmission of misfolded SOD1 species occurs *in vivo* and if it does, what timescale is required for misfolded SOD1 pathology to spread through the CNS. For these reasons we decided to examine the misfolded SOD1 pathology in the brains of our animals in the first instance rather than the spinal cords, as the inoculations were intracerebral.

An examination of the brains from animals 24 hours post-inoculation was carried out to assess the penetration of the inoculum into different brain regions. At this time-point significantly higher levels of misfolded SOD1, as detected using the SEDI antibody, were apparent in the hippocampus and the region defined as “other” in mice inoculated with m-TgG93A compared to mice inoculated with m-NTg. A similar, but non-significant, trend was also seen in the cerebellum, corpus callosum, cortex and olfactory bulb (Figure 3.5). Levels of misfolded SOD1 in the brain stem were lower in animals inoculated with both PBS and m-TgG93A, compared to mice inoculated with m-NTg, but there was no difference between m-NTg and m-TgWT inoculated animals. Because we do not have data for non-inoculated control mice at this time-point, it is not clear whether these lower levels are due to a decrease from baseline, or a smaller relative increase in response to inoculation. The meaning of this result is not clear at this time; as the m-NTg inoculum does not contain any SOD1 species, misfolded or otherwise, it is unlikely that an increase in SEDI staining would have occurred in animals inoculated with m-NTg as compared to those inoculated with m-TgG93A, which contains mutant SOD1. Neither does it seem likely that intracerebral inoculation with PBS and m-TgG93A could cause a decrease in the area of misfolded SOD1, particularly over such a short timescale. The differences in SEDI staining in the brain stem at this time-point could be indicative of baseline differences between the groups as the brain stem is the structure furthest from the site of inoculation, and so the inocula may not have penetrated to this region.

Data from all other brain regions suggest that at 24 hours post-inoculation the inoculum is present throughout the brain (with the exception of the brain stem) and that the mutant misfolded SOD1 present in the m-TgG93A inoculum is detectable using the SEDI antibody. Tissues from NTg;Sod1ko mice, inoculated with m-TgG93A have also been collected at 40-days post-inoculation to determine whether the inoculum is still detectable at this time-point however these tissues have not yet been processed.

We examined the accumulation of misfolded SOD1 at 40-days post-inoculation when mice were 90-days old. SEDI staining has been shown to increase in TgG93A mice between 20 and 63-days of age; however a decrease is seen between 100 and 120-days, presumed to be due to MN death (Rakhit et al., 2007). Ninety-days of age was therefore chosen as an appropriate age to maximise the length of incubation time while minimising the chances of missing an increase in the accumulation of misfolded SOD1 due to MN loss.

At 40-days post-inoculation there was no detectable difference in the area of SEDI staining between inocula in any brain region, suggesting that self-seeded propagation of misfolded SOD1 does not occur in this model, at least over the time scale of this experiment. This also suggests that if any of the original inoculum is still present by this time, it is not present at a detectable level. The TgG93A mouse has one of the most aggressive degenerative processes of the published mutant SOD1 mice (see Table 1.3). Although it has not been possible to detect self-seeded transmission of misfolded SOD1 in this model, it is still possible that in an alternative model, with a less aggressive phenotype, a longer incubation time could reveal the presence of such a phenomenon. Alternatively a line such as the A4V mutant SOD1 transgenic mouse, which expresses an ALS mutant SOD1 but does not display clinical characteristics could have been used to examine whether conversion to a disease phenotype and pathology could be caused by intra-cerebral inoculation with misfolded species, as it is when this line is crossed to a WT SOD1 transgenic line.

#### *3.4.2.2 CROSS-SEEDED AGGREGATION OF SOD1 IN TgWT;SOD1ko MICE*

Many of the animals in this experiment died before their scheduled cull dates, particularly those in the longer time-point groups. We examined whether these premature deaths were related to the inoculation group of the animal. The omnibus Kaplan-Meier analysis showed a highly significant effect of inocula group on survival, however pair-wise comparisons did not reveal any differences between mice inoculated with m-NTg and any of the other inoculated or the non-inoculated mice. This suggests that the effect of inoculum group was not due to the presence of misfolded SOD1 species in some of the inocula. A more likely explanation is that non-inoculated or PBS inoculated mice survive longer than those inoculated with CNS homogenates; the pair-wise comparison between m-NTg inoculated and both PBS and non-



inoculated mice were below the non-adjusted significance threshold and visual inspection of the Kaplan-Meier graph is also suggestive of this trend.

The area of misfolded SOD1 in the brain of TgG93A;Sod1ko mice was not affected by inoculation with m-TgG93A, however the potential incubation period was limited by the lifespan of these mice and the baseline burden of misfolded SOD1 may make detection of potentially small increases within this timescale problematic. TgWT mice can live to at least 2-years of age (Jaarsma et al., 2000) and so allow a much larger timescale for incubation. As a longer incubation time was possible in this line of mice, we decided to first look at the spinal cord to see if we could identify transmission of misfolded SOD1 and spread from the initial site of inoculation in the brain down into the spinal cord in response to inoculation with m-TgG93A homogenate. Our initial qualitative assessment of spinal cords of mice inoculated with PBS or m-NTg in the 180 day time-point was that the SEDI staining was already high at this time and was particularly abundant in the ventral white matter tracts as described by Rakhit et al., (2007). As an alternative, we decided to use the USOD antibody to stain sections from mice at the earlier, 90 day time-point. This antibody at the earlier time-point produced a lower baseline level of staining in both PBS and m-NTg inoculated animals and so we chose this method to continue our analysis. Significant differences in the ages between the different inoculum groups within this time-point were identified, however these differences were all in relation to mice inoculated with h-cntrl2, and so should not have a bearing on these results. For future analyses however, in which this other inoculum group is included, it may be appropriate to include age at death as a potential covariate.

Five spinal cord regions were examined. Significant differences were found between inoculum groups for USOD staining area in the ventral roots; mice inoculated with m-TgG93A were found to have a significantly larger area of USOD staining than mice inoculated with m-NTg. This result suggests that a cross-seeded increase in misfolding of WT SOD1 may occur in mice inoculated with m-TgG93A. It is possibly relevant that this difference is seen in the ventral roots, as the ventral roots contain the axons of the LMNs. This suggests that the effect may be MN specific making it particularly relevant to ALS, or that the passage of cell-to-cell transmission favours descending tracts away from the site of initial misfolding, or in this case inoculation. It is however important to note that the ventral roots of only 2 mice inoculated with m-NTg were used for the comparisons. The 2 mice inoculated with m-NTg that are missing from the ventral root analysis had much higher USOD staining in the ventral horns than did the 2 animals that were included in the analysis (4.909 and 2.765 compared to 0.625 and 0.982 proportion stained (x1000) respectively). Re-sectioning and analysis of the spinal

cords from these animals and completion of the analysis for rest of the animals in these cohorts will be required to have confidence in this finding.

Experiments using monkeys have provided evidence that a pathogenic species (thought then to be viral and now postulated to be proteinaceous) might be present within CNS tissue of ALS patients which is able to “infect” WT monkeys (Zil'ber et al., 1963). The genotype of the patients whose tissues were used is unknown and histopathological evidence for the presence of inclusions composed of SOD1 or other ALS proteins such as TDP43 are also not available. For these reasons it is only possible to speculate as to whether misfolded ALS proteins could have been responsible for this apparent transmission of disease. Despite the multiple passages of disease described by Zil'ber et al., (1963) attempts by subsequent groups to replicate these findings, in monkeys and other laboratory species, failed (Gajdusek et al., 1964; Gibbs et al., 1972).

More recent experiments have used transgenic mice which express mutant and WT forms of the respective proteins to examine prion-like properties of at least 3 hallmark neurodegenerative disease proteins (see Table 1.6). Such experiments have successfully demonstrated prion-like transmission of misfolded protein pathology and even phenotypic neurological degeneration in mice expressing mutant proteins. These have often used stereotactic injections allowing targeting of specific disease relevant brain regions and tight control over the amount of inoculum introduced. Luk et al., (2012), for example, inoculated a mutant  $\alpha$ -synuclein transgenic mouse model of Parkinson's Disease with amyloid misfolded  $\alpha$ -synuclein in the form of tissue homogenates or recombinant proteins. Inoculations were stereotactic and specifically targeted the neocortex and striatum, allowing them to map the spread of pathology from the site of inoculation along connective neuronal pathways.

One potential criticism of the work presented here is that we have little control over the specific brain region or regions which are targeted by the inoculation protocol used. However, results from our 24 hour time-point in TgG93A;Sod1ko mice suggest that in fact the inocula penetrated throughout the brain and thus should contact relevant structures such as the motor cortex with its descending tracts to the spinal cord. This project was carried out in collaboration with the MRC Prion Unit and the methodology borrows from that commonly used in the prion field. Prion-like transmission of  $\alpha$ -synuclein has also been demonstrated using a similar methodology to that used here, for example by Watts et al., (2013) who successfully induced both misfolded  $\alpha$ -synuclein pathology and symptomatic “disease” in inoculated mutant  $\alpha$ -synuclein transgenic mice. In this paper self-seeding was demonstrated by inoculating mice with homogenates prepared from “sick” mutant mouse tissue, and cross-seeding by inoculation with patient tissue that had been neuropathologically confirmed as

containing misfolded/aggregated  $\alpha$ -synuclein but was not from patients with known  $\alpha$ -synuclein mutations. Both types of inocula induced a similar pattern of pathology and disease phenotype, however, mice inoculated with human tissues had a shorter incubation period, despite containing WT and not mutant  $\alpha$ -synuclein and at a much lower concentration than in the transgenic mouse tissue. This lends increased impetus to the analysis of our mice inoculated with SOD1-fALS patient tissue homogenates to compare the levels of SOD1 misfolding between human and mouse inocula.

### **3.4.3 Future Work**

The primary goal at present is to complete the analysis of the USOD stained spinal cords at the 90 day time-point for our cross-seeding transmission experiment in all inoculated and non-inoculated control groups. This work is underway. Once completed, and depending on the results an appropriate second time-point and set of inocula can be chosen on for the next step of the analysis.

A question that we have not yet addressed is whether our chosen outcome measures of SEDI and USOD can reliably detect increasing misfolded SOD1 pathology. As previously described, in TgG93A mice, Rakhit et al., (2007) found that SEDI staining increased between 20 and 63-days of age, but then a decline from 100 to 120-days. The fact that SEDI staining decreases during the later stages of degeneration makes the task of choosing an appropriate time-point in our self-seeding transmission experiment particularly difficult; it is important that our outcome measure is able to pick up potentially small differences at earlier time-points in order to avoid the drop in staining area due to loss of MNs. The USOD antibody was shown to be immunoreactive in G93A mutant SOD1 transgenic mice by Kerman et al., (2010) however only 1 time-point was assessed and, to our knowledge, no other examples of USOD pathology in the G93A SOD1, or similar, transgenic mice have been published. In addition to our 90 day old non-inoculated mice, we have now collected tissue from TgG93A;Sod1ko mice at 70 and 120-days of age in order to assess whether we can indeed detect changes in SEDI and USOD staining in this line over time. Potential alternative outcome measures will be discussed briefly in Section 6.1.

## Chapter 4. The Effect of Wild-Type Endogenous *Sod1* in the G93A Mutant *SOD1* Mouse

### 4.1 INTRODUCTION


It is well established that the presence of WT huSOD1 has an exacerbating effect on the degenerative process seen in SOD1-fALS transgenic mice (Deng et al., 2006; Prudencio et al., 2010; Wang et al., 2009b; Jaarsma et al., 2000; Jaarsma et al., 2008), however a similar effect is not apparent when the mutant SOD1 being expressed is mouse rather than human (Audet et al., 2010). Previous attempts to address the question of whether the endogenous WT moSOD1 protein affects the phenotype of SOD1-fALS mouse models have provided limited and mixed results suggesting that its presence may worsen disease (Bruijn et al., 1998; Deng et al., 2006). In this Chapter I aim to more thoroughly characterise differences between G93A mutant huSOD1 transgenic mice with and without endogenous moSOD1 expression.

Although the ultimate result of mutant SOD1 toxicity in SOD1-fALS mouse models, and in ALS, is MN loss (e.g. (Chiu et al., 1995; Mendonça et al., 2005)) the earliest evidence of neuronal degeneration is detected at the distal axon, for example by examining NMJs, and this has led to the suggestion that the process is one of die-back rather than forward (Fischer et al., 2004).

Evidence of axonal degeneration can also be detected within muscle; the motor unit (MU) is the functional unit of a single MN and the group of muscle fibres it innervates. Each MU can be categorised according to the type of MN and muscle fibres it is composed of, as summarised in Table 4.1 (Gordon et al., 2004; Augusto et al., 2004). Remodelling of the MU occurs in response to both mechanical and degenerative nerve damage, with surviving MN axons reinnervating the NMJ end-plates of muscle fibres which have lost their neuronal connection. This compensatory reinnervation results in an increased size of the MU as extra muscle fibres are recruited. Reinnervation of a muscle fibre by a MN of a type distinct to that which originally innervated it can cause conversion of the fibre to match that of the incoming MU (as reviewed by (Gordon et al., 2004).

In ALS and SOD1-fALS mice the fastest, type 2B, MUs are affected earlier in the degenerative process with slower MUs affected later (Schmied et al., 1999; Frey et al., 2000; Pun et al., 2006). Thus, it is possible to monitor the progression of MN degeneration by examining changes in muscle fibre type composition indicative of reinnervation by slower type MNs.

**Table 4.1 Motor unit characteristics**

Motor neuron properties	Muscle fibre properties				
Motor neuron size	Muscle fibre type	Myosin heavy chain isoform	Histochemical classification	Fibre diameter	Fatigue index
Small  	Type 1	Type 1	slow-oxidative (SO)	small	slow (S)
	Type 2a	Type 2A	fast-oxidative/glycolic (FOG)	intermediate	fast- fatigue-resistant (FR)
	Type 2x (also referred to as 2d)	Type 2X		intermediate	fast- fatigue-intermediate (FI)
	Type 2b	Type 2B	fast-glycolic (FG)	large	fastest-fatigable (FF)
Large					

## 4.2 AIMS

The aim of the work described in this Chapter was to examine the effect of endogenous moSOD1 protein on ALS disease related phenotypes in a SOD1-fALS mouse model. Behavioural measures of disease progression were:

- Survival
- Body weight
- Grip-strength

Histological examination also evaluated:

- Motor neuron survival in the sciatic pool of the spinal cord (SC)
- NMJ integrity in the extensor digitorum longus (EDL), as a measure of MN axonal/muscle health
- Muscle fibre type changes as a measure of denervation and re-innervation by motor neurons

## 4.3 RESULTS

Only female mice were used in this study in order to minimise the variability within and between groups due to gender differences. Females were chosen because, 1) female transgenic mice were not used for breeding and so were more freely available and 2) reduced variability in disease related measures has been reported in female mice as compared to males (Mead et al., 2011).

Four genotypes were used in the experiments described. These are listed in Table 4.2 including the short form nomenclature used within the text.

**Table 4.2 Experimental genotypes**

Tg allele	KO allele	Short form (used in text)
Non-transgenic	<i>Sod1</i> <sup>+/+</sup> (WT)	NTg;Sod1wt
Non-transgenic	<i>Sod1</i> <sup>-/-</sup> (homozygous KO)	NTg;Sod1ko
<i>SOD1</i> <sup>G93A</sup> Tg hemizygous	<i>Sod1</i> <sup>+/+</sup> (WT)	TgG93A;Sod1wt
<i>SOD1</i> <sup>G93A</sup> Tg hemizygous	<i>Sod1</i> <sup>-/-</sup> (homozygous KO)	TgG93A;Sod1ko

Ideally littermate matching would have been carried out, particularly between TgG93A;Sod1wt and TgG93A;Sod1ko mice, however this was not feasible due to the inheritance ratios; the mice used in this experiment were bred as described in Figure 2.7 in Section 2.5.5, by crossing TgG93A;Sod1het males to NTg;Sod1het females, producing 6 possible genotypes. The inheritance ratios of these genotypes (which were described in more detail in Section 3.3.1) are presented in Table 4.3. Over 50% of all pups born were Sod1het and so not required for experiments. Furthermore, as only female mice were used, another ~50% from each litter would be discounted due to gender. This left ~25% of animals per litter of the correct sex and of one of the required genotypes. As an average C57BL/6J litter is ~7 pups (Brady et al., 2012) litter matching was not feasible.

**Table 4.3 Genotype ratios**

Ratio of each genotype according to Mendelian inheritance ratios

Genotype	Expected	Observed
NTg;Sod1wt	0.125	0.1530
NTg;Sod1het	0.25	0.3080
NTg;Sod1ko	0.125	0.1006
TgG93A;Sod1wt	0.125	0.1094
TgG93A;Sod1het	0.25	0.2128
TgG93A;Sod1ko	0.125	0.1162

### 4.3.1 Transgene Copy Number

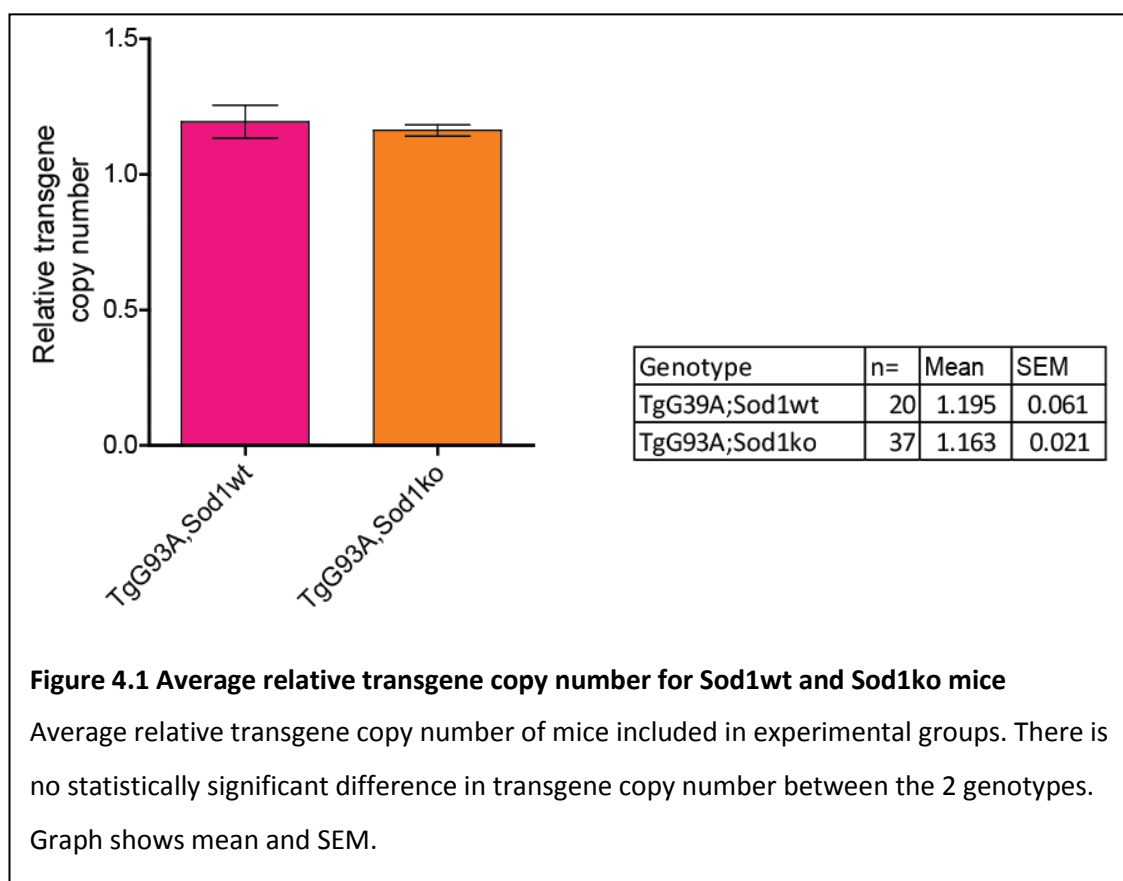
Because there is a correlation between the copy number of the G93A transgene array and the phenotypes displayed by the mice (Alexander et al., 2004) it was important to control for differences in copy number between experimental genotypes.

Quantitative real time PCR (qPCR) was used to obtain the relative copy number of the transgene array as described in Section 2.1.3. Mice with a relative copy number of 0.8 or below (20% below the reference sample obtained from Jackson Laboratories) were excluded from the experiment. Twelve TgG93A;Sod1wt and 7 TgG93A;Sod1ko animals were excluded, as summarised in Table 4.4. Data for individuals is presented in Section 7.5, Appendix 5.

Figure 4.1 shows the average relative copy number for TgG93A;Sod1wt and TgG93A;Sod1ko animals included in the experimental groups. There is no difference in transgene copy number between the 2 genotypes;  $t(23,688)=0.508$ ,  $p>0.05$ .

**Table 4.4 Relative transgene copy number for excluded animals**

Genotype	n=	Mean	SEM
TgG39A;Sod1wt	12	0.65986	0.01567
TgG93A;Sod1ko	7	0.57513	0.78955



## 4.3.2 Behavioural Characterisation

### 4.3.2.1 STARTING WEIGHT

*Sod1* null mice have decreased body weight from an early age, as compared to WT mice (Kostrominova et al., 2007; Muller et al., 2006; Noda et al., 2012) however, evidence of early body weight deficits in TgG93A mice is mixed (e.g. (Chiu et al., 1995; Smittkamp et al., 2008) c.f. (Teuchert et al., 2006)). I sought to examine whether early body weight deficits were apparent in our TgG93A colony and whether the mutant human *SOD1* transgene was able to attenuate the decreased body weight reported in *Sod1* KO mice. Results are summarised in Figure 4.2. A one-way analysis of variance (ANOVA) with planned pair-wise comparisons was used to analyse differences in body weight at 57-70-days of age between the 4 genotypes. The overall ANOVA was significant ( $F(3)=12.942$ ,  $p<0.001$ ).

The first two planned pair-wise comparisons sought to answer the question of whether, in our colony, the G93A *SOD1* transgene and/or the *Sod1*ko genotype reduced the body weight of mice.

The first planned comparison (marked (1) in Figure 4.2) found that in our colony the body weight of TgG93A;*Sod1*wt mice was significantly lower than NTg;*Sod1*wt mice ( $t(39.302)=3.479$ ,  $p<0.01$ ). The second planned pair-wise comparison (marked (2) in Figure 4.2) confirmed previous findings that *Sod1* null mice have significantly reduced body weight as compared to WT mice at this age ( $t(60.784)=5.296$ ,  $p<0.001$ ).

To evaluate whether the G93A *SOD1* transgene was able to attenuate the early reduced body weight of NTg;*Sod1*ko mice, a set of pair-wise comparisons were required; the first comparison (marked (3a) in Figure 4.2) found that, unlike in NTg mice, in those mice with the G93A *SOD1* transgene, there was no difference in body weight between mice with either the *Sod1*wt or *Sod1*ko genotypes ( $t(29.987)=0.086$ ,  $p>0.05$ ). The second comparison (marked (3b) in Figure 4.2) found that, similar to TgG93A;*Sod1*wt mice, TgG93A;*Sod1*ko mice have significantly lower body weight than NTg;*Sod1*wt mice ( $t(64.705)=4.134$ ,  $p<0.001$ ). The final comparison (marked (3c) in Figure 4.2) found that TgG93A;*Sod1*ko mice had significantly higher body weight than NTg;*Sod1*ko mice ( $t(49.086)=-2.16$ ,  $p<0.05$ ). Together, these comparisons suggest that mutant huSOD1 can compensate for the reduction in body weight seen in NTg;*Sod1*ko, but only insofar as to increase the body weight to the level of TgG93A;*Sod1*wt mice.



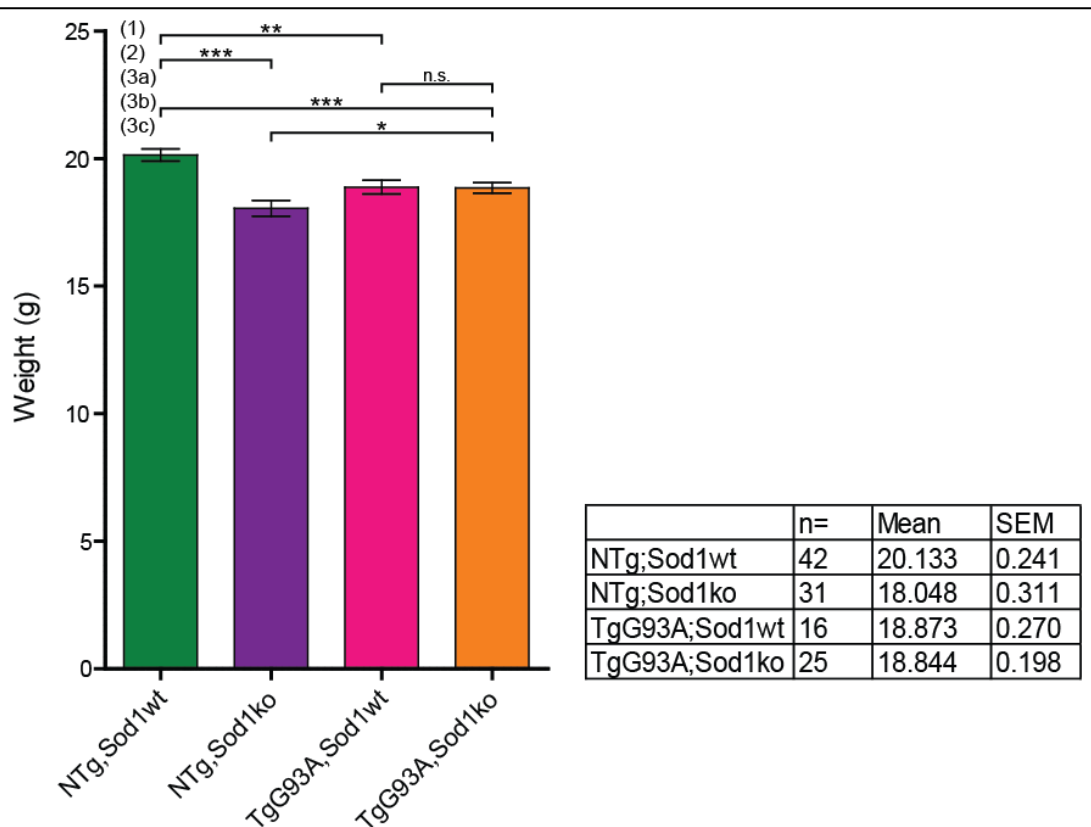
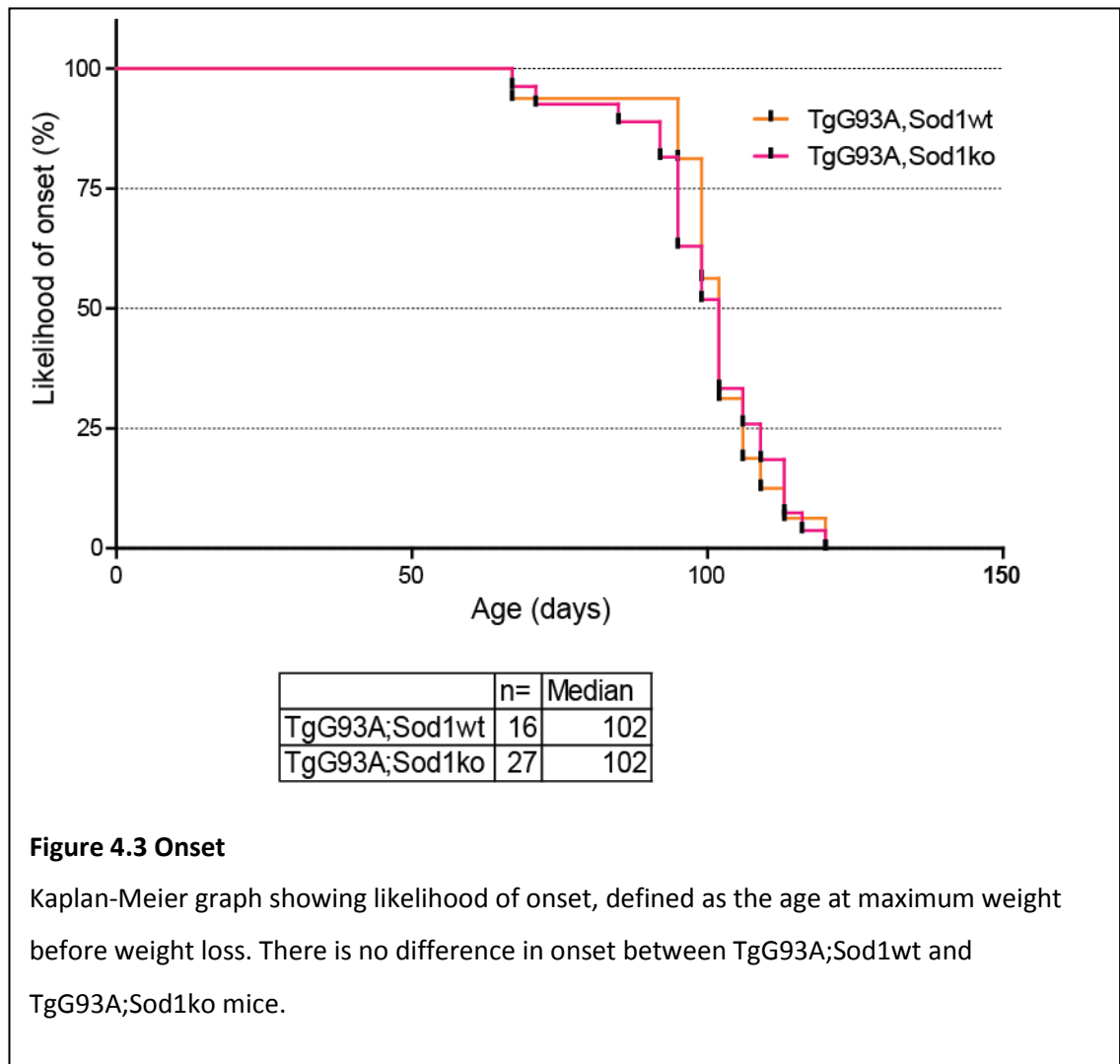


**Figure 4.2 Body weight at 57-70 days of age**

Average (mean and SEM) body weight of mice at 57-70 days of age. Transgenic expression of G93A mutant human SOD1 rescues the reduced body weight of NTg;Sod1ko mice to levels of the TgG93A;Sod1wt mouse. \*  $p < 0.05$ . \*\*  $p < 0.01$ . \*\*\*  $p < 0.001$ .

#### 4.3.2.2 DISEASE ONSET

Age at peak body weight before weight loss was used as a marker for disease onset. There was no significant difference in disease onset between TgG93A;Sod1wt and TgG93A;Sod1ko mice (Log-rank  $\chi^2(1)=0.0278$ ,  $p>0.05$ ) as shown in Figure 4.3.



### 4.3.2.3 SURVIVAL

Survival was measured using the humane end points defined in Section 2.5.1. All mice reached 15% weight loss first before any of the other end points. Twenty nine TgG93A;Sod1wt animals and 16 TgG93A;Sod1ko were assessed. Two animals of each genotype were excluded because they were not weighed daily from the time they reached 10% weight loss and so accurate time to death could not be assessed. Another 8 from each genotype were excluded due to loss of transgene copy number.

Figure 4.4 shows the Kaplan-Meier survival curves for the 2 genotypes. There was no significant difference in survival time between the 2 genotypes: Log-rank  $\chi^2(1)=1.769$ ,  $p>0.05$

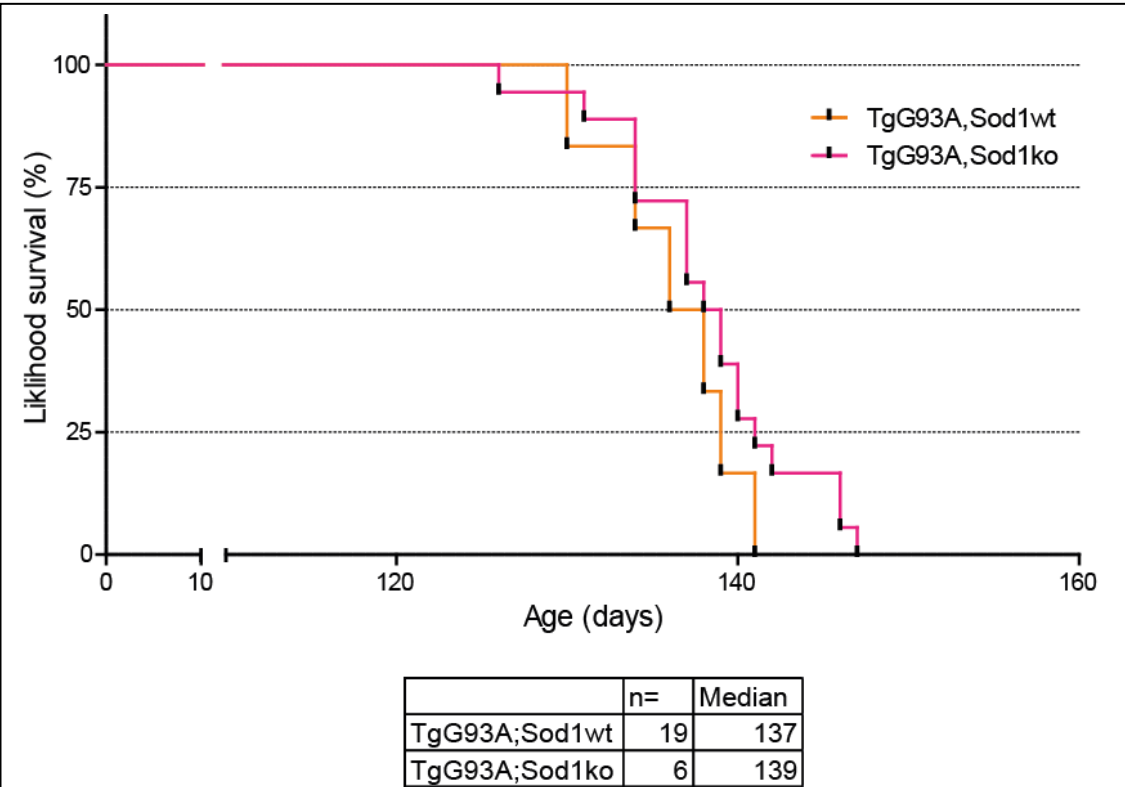


**Figure 4.4 Survival**

Kaplan-Meier survival graph. The humane end-point used to delineate survival was 15% body weight loss. There was no difference in survival between TgG93A;Sod1wt and TgG93A;Sod1ko mice.

#### 4.3.2.4 GRIP-STRENGTH

Grip-strength was measured in order to monitor potential differences in disease progression between TgG93A;Sod1wt and TgG93A;Sod1ko mice. Grip-strength was measured twice a week, and corrected for body weight as described in Section 2.6.3. Data were grouped into bins: 57-70 days; 71-84 days; 85-98 days; 99-112 days; 113-124 days. Five cases were excluded due to missing data (2 TgG93A;Sod1wt and 3 TgG93A;Sod1ko) and 43 due to loss of transgene copy number (16 TgG93A;Sod1wt and 27 TgG93A;Sod1ko). Data are summarised in Figure 4.5.

Bonferroni corrected independent t-tests were used to compare grip-strength of the 2 genotypes at each time-point. The grip-strength of the 2 genotypes was found to significantly differ at the 71-84 day time-point only, with TgG93A;Sod1wt mice having significantly lower grip-strength than the TgG93A;Sod1ko mice ( $t(36)=-3.146$ ,  $p<0.05$ ). There was no difference at the other 4 time-points. This suggests that TgG93A;Sod1ko mice maintain muscle strength for longer than the TgG93A;Sod1wt mice during the initial stages of degeneration, but that this difference is not sustained.

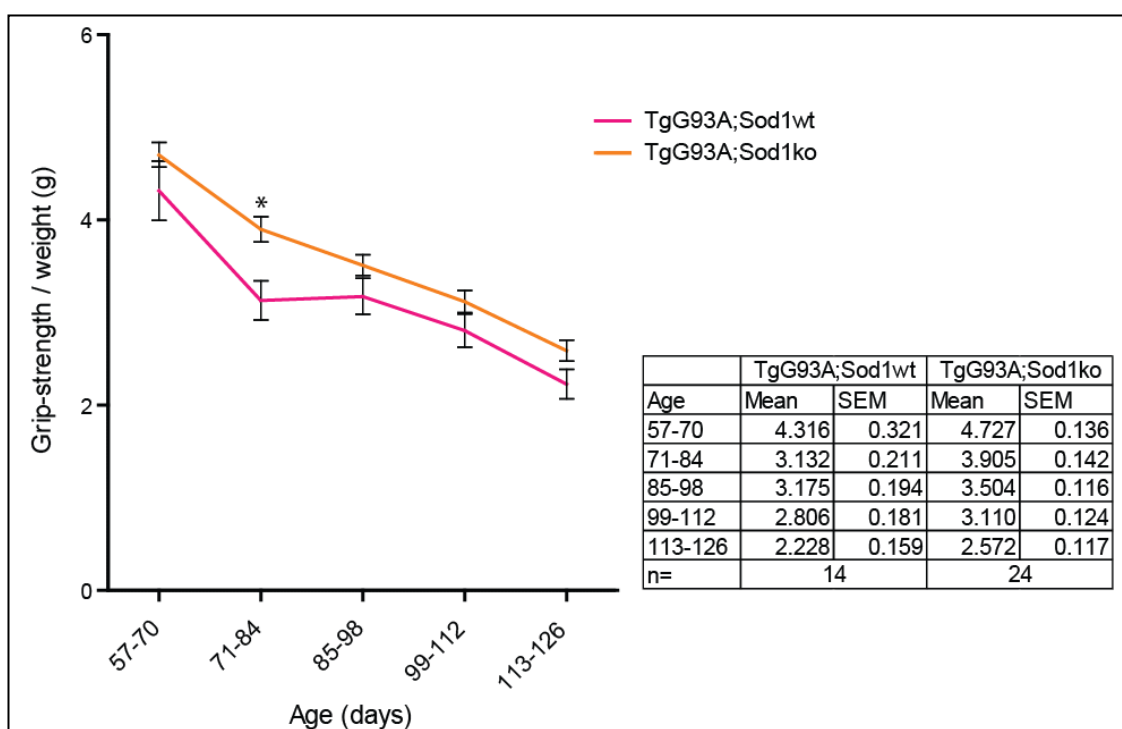


**Figure 4.5 Grip-strength**

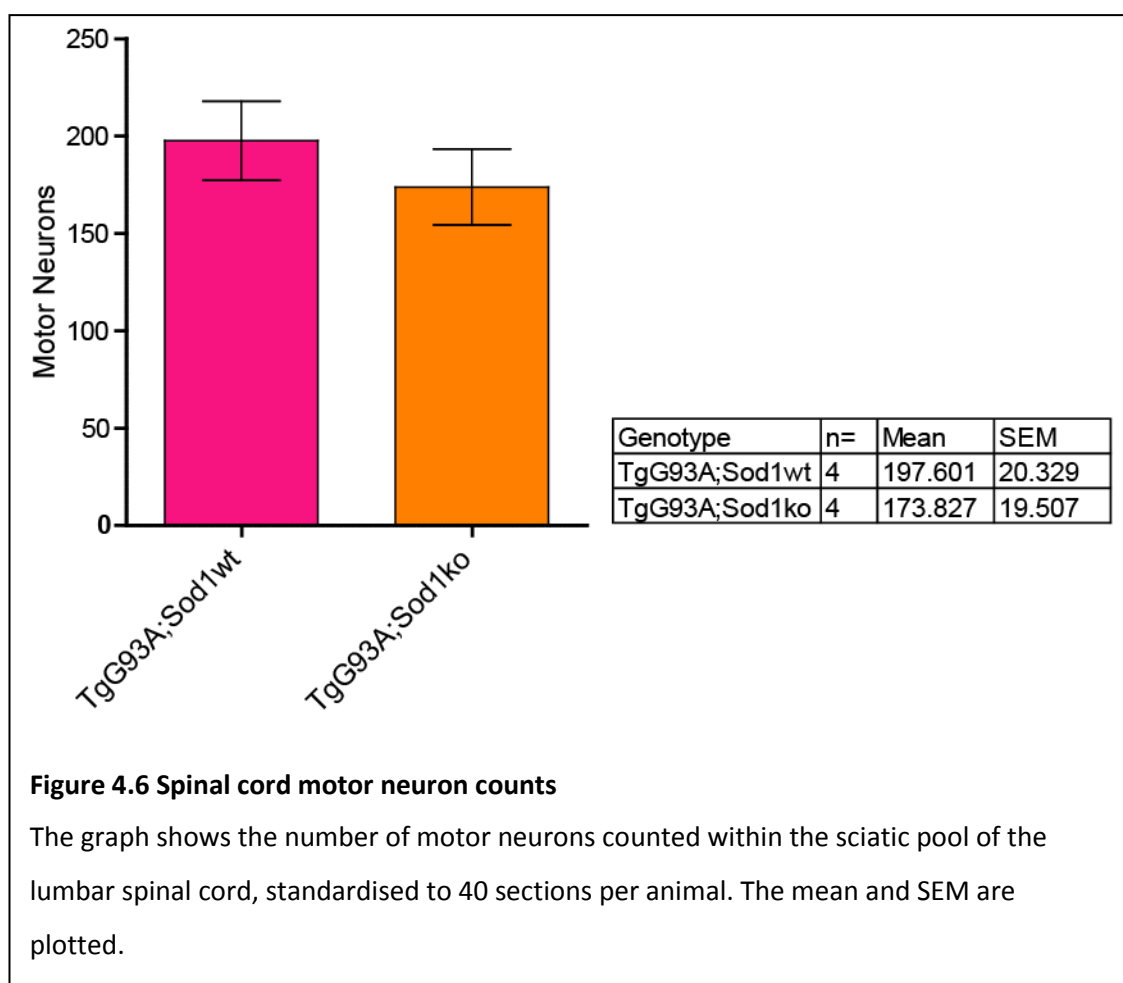
Grip-strength was measured twice weekly, corrected for body weight and averaged into 2-week bins. Although TgG93A;Sod1ko had consistently higher grip-strength than TgG93A;Sod1wt, they only differed significantly at the 71-84 day time-point. \*  $p<0.05$ . Graph shows mean and SEM are plotted.

### 4.3.3 Histological Characterisation

#### 4.3.3.1 MOTOR NEURON COUNTS

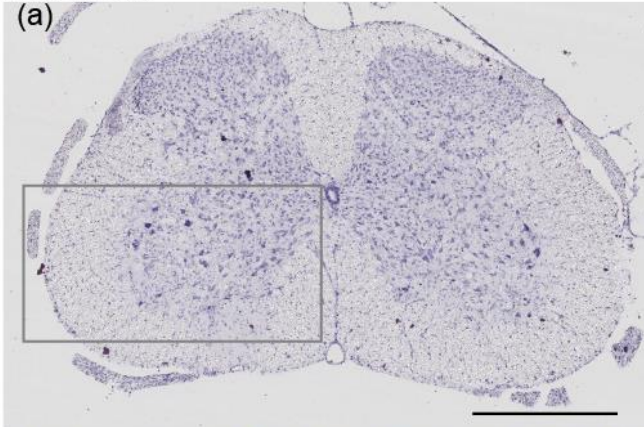
The number of MNs within the sciatic pool was counted for TgG93A;Sod1wt and TgG93A;Sod1ko mice at 120-days of age as described in Section 2.8.3. Data are summarised in Figure 4.6 and representative examples from each genotype are shown in Figure 4.7. There was no significant difference in the number of MNs between the 2 genotypes.  $t(6)=0.844$ ,  $p>0.05$ .

MNs from the earlier 75 day time-point were not counted as loss at this age was not anticipated (Gould et al., 2006; Fischer et al., 2004; Chiu et al., 1995; Kong et al., 1998).



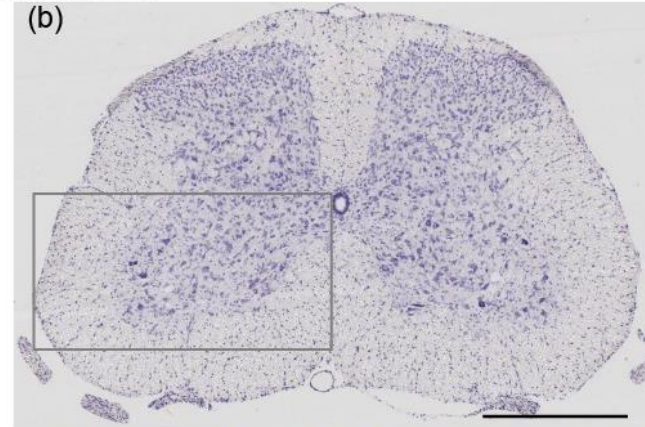
TgG93A;Sod1wt

(a)

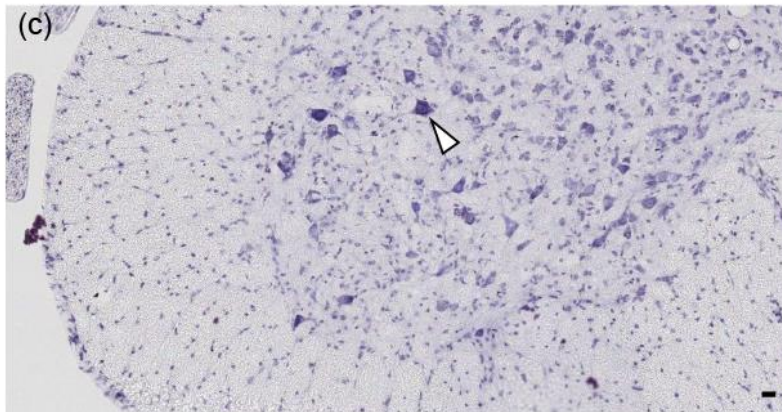


TgG93A;Sod1ko

(b)



(c)



(d)

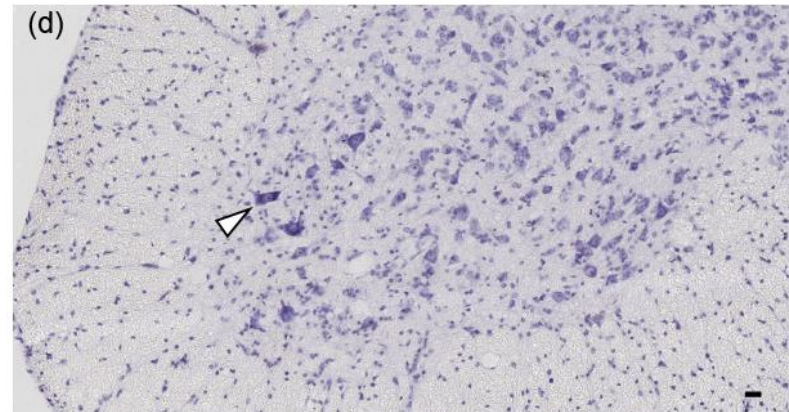


**Figure 4.7 Lumbar spinal cord motor neurons**

Representative lumbar spinal cord sections of TgG93A;Sod1wt (a and c) and TgG93A;Sod1ko (b and d) mice at 120-days old, stained with nissl stain, gallocyanine. In (c) and (d) arrow heads indicate motor neurons displaying the defining features: dense staining, polygonal shape and greater than 20 $\mu$ m.

Scale bars: (a) and (c) 500 $\mu$ m. (b) and (d) 20 $\mu$ m

#### 4.3.3.2 NEUROMUSCULAR JUNCTIONS

Next I examined neuromuscular junction (NMJ) innervation in the EDL hind limb muscle, comparing TgG93A animals of either Sod1wt or Sod1ko genotype. As shown in Figure 1.1, when the axons of the LMNs degenerate they retract away from muscle fibre. This can be detected histologically by examining co-localisation between the axonal foot-plate and the post-synaptic motor end-plate on the muscle fibre. NMJs on the EDL were counted and classified as fully innervated, partially innervated, or fully denervated, as shown in Figure 4.8.

Two time-points were examined for each genotype, an early disease time-point of 75 ( $\pm 1$ ) days of age and a late disease time-point of 120 ( $\pm 1$ ) days. The two genotypes were compared by t-test at each time-point for four measures: 1) total number of NMJs, 2) proportion of fully innervated NMJs, 3) proportion of intermediately innervated NMJs and 4) proportion of fully denervated NMJs. Results are summarised in Figure 4.9. The only significant difference was in the total number of NMJs at 75-days of age; TgG93A;Sod1ko animals had significantly more NMJs than TgG93A;Sod1wt animals ( $t(7)=-3.056$   $p<0.05$ ).

To explore this difference further I next examine NMJs of NTg;Sod1wt mice compared to NTg;Sod1ko mice at 120 ( $\pm 1$ ) days of age. Results are summarised in Figure 4.10. Again, the total number of NMJs was significantly different between the 2 groups, however the direction was different; NTg;Sod1wt animals had significantly more NMJs than did NTg;Sod1ko animals genotypes ( $t(5)=2.897$ ,  $p<0.05$ ). The proportions of fully innervated, intermediately innervated and fully denervated were not statistically different between the 2 genotypes.

These data suggests that although TgG93A;Sod1ko animals start off with more NMJs compared to TgG93A;Sod1wt mice, they show the same pattern of NMJ degeneration as the TgG93A;Sod1wt mice, and any advantage is not maintained. These results mirror the results of the grip-strength analysis, where TgG93A;Sod1ko mice were found to maintain muscle strength, as compared to TgG93A;Sod1wt mice at 71-84-days, but lose this advantage at later ages.

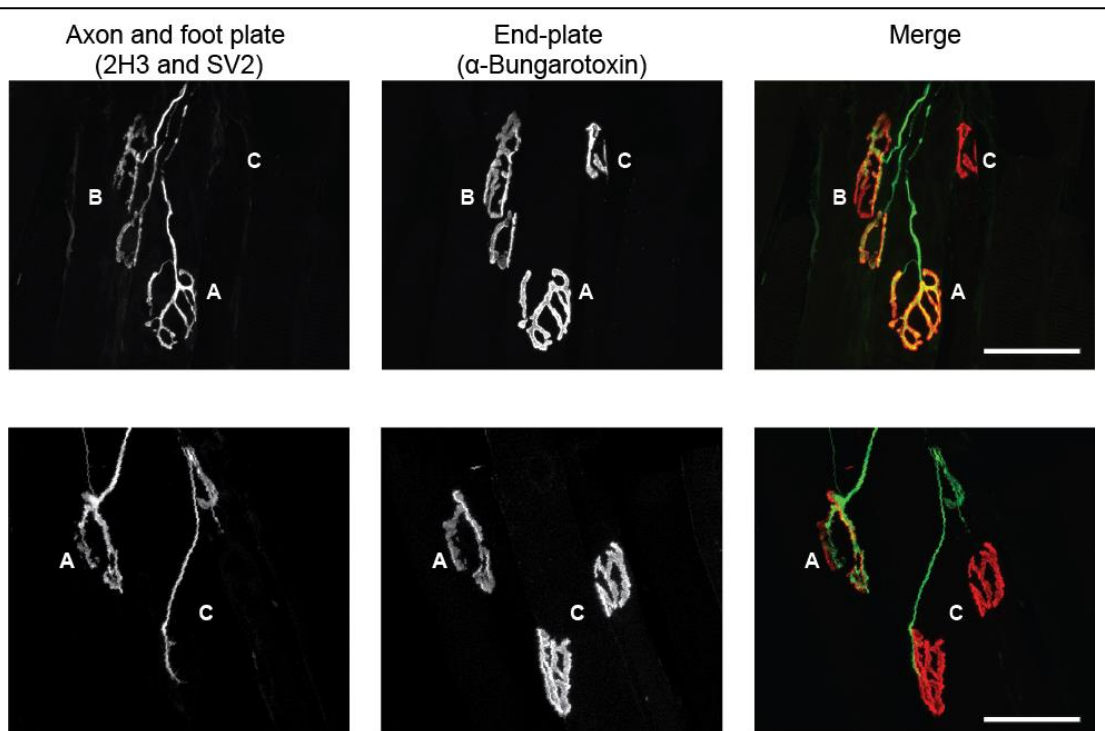


**Figure 4.8 Neuromuscular junctions in the EDL hind limb muscle**

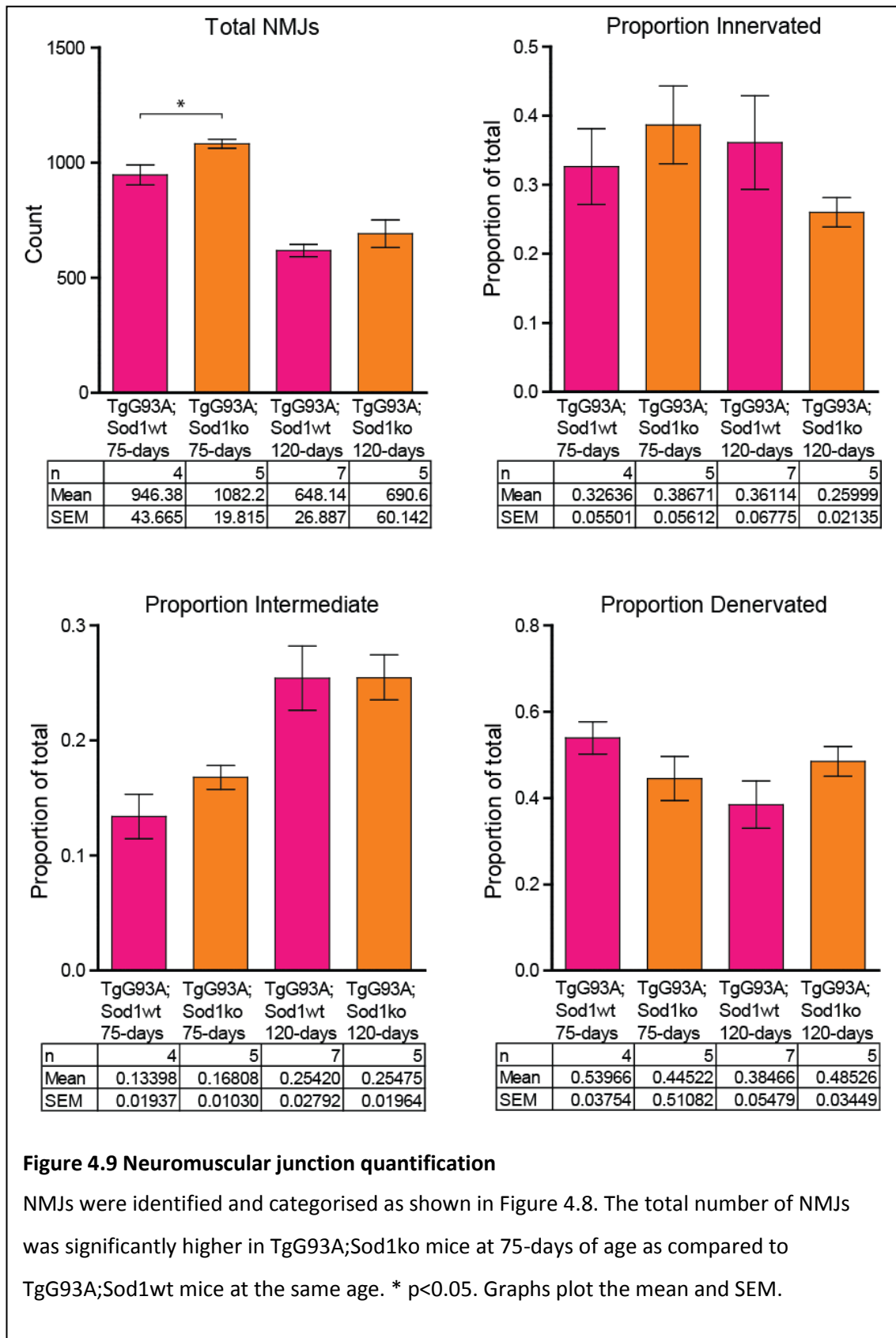
Examples of neuromuscular junctions (NMJs) exhibiting different levels of innervation.

Extensor digitorum longus (EDL) muscles were longitudinally sectioned into 2 series and 1 whole series was quantified. NMJs were identified by  $\alpha$ -bungarotoxin labelled post-synaptic end-plates. Once identified, NMJs were categorised according to co-localisation with the pre-synaptic foot-plate labelled with anti-synaptic vesicle 2, and anti-neurofilament, as shown:

A= Fully innervated. Complete overlap between end-plate and foot-plate; B= Intermediate innervation. Partial overlap between end-plate and foot-plate; C= Fully denervated. No, or very limited, co-localisation between end-plate and foot-plate.

Scale bar shows 50 $\mu$ m





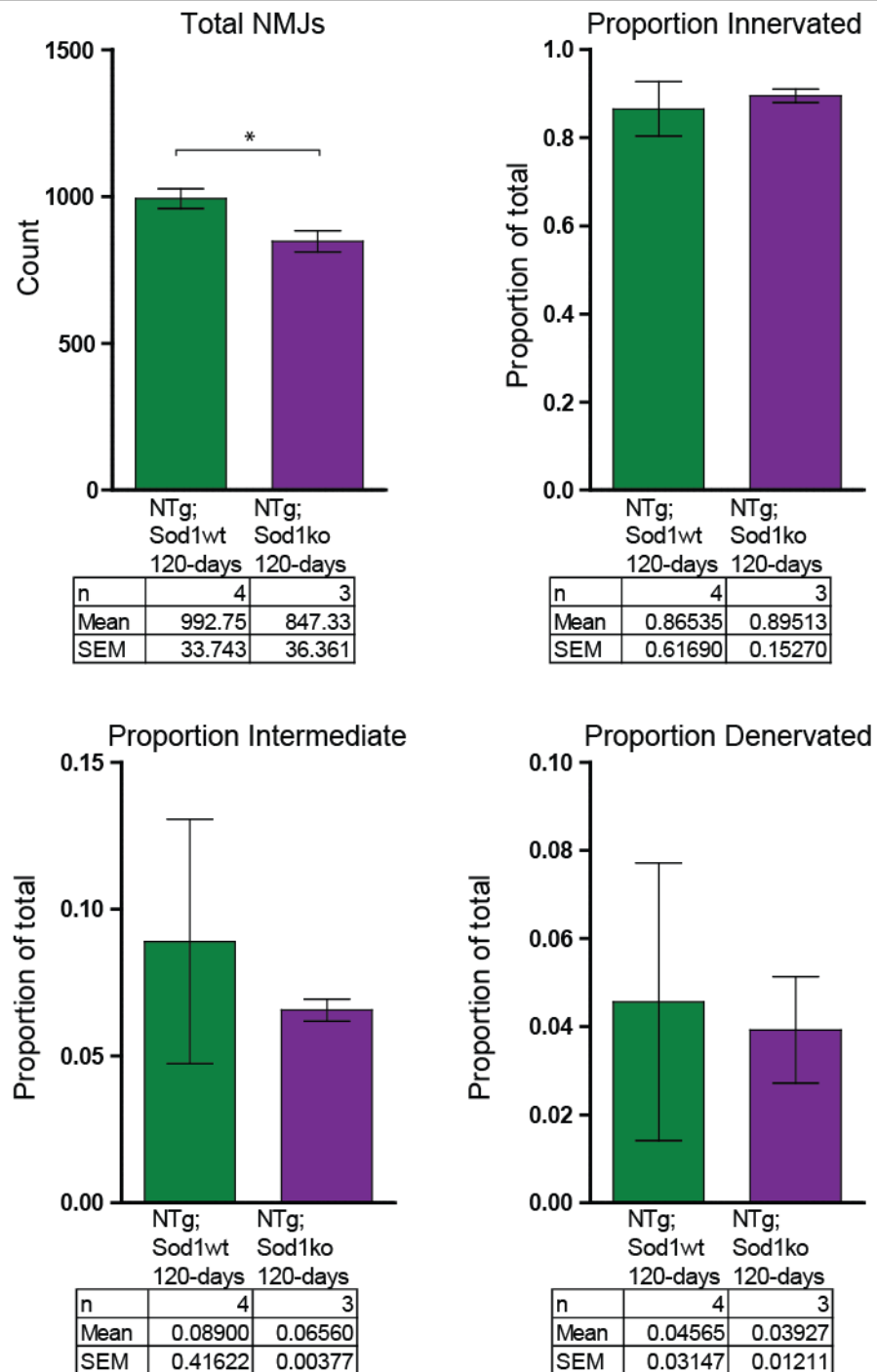


**Figure 4.10 Neuromuscular junction quantification for non-transgenic mice**

NMJs were identified and categorised as shown in Figure 4.8. The total number of NMJs was significantly higher in NTg;Sod1wt mice than in NTg;Sod1ko mice. \*  $p < 0.05$ . Graphs plot the mean and SEM.

#### 4.3.3.3 MUSCLE FIBRE TYPING

Although the total number of MNs did not differ between TgG93A;Sod1wt and TgG93A;Sod1ko mice at 75-days of age, the TgG93A;Sod1wt mice had fewer NMJs in total.

Next I examined the pattern of expression of different myosin heavy chain (MHC) proteins in the skeletal muscles of TgG93A;Sod1wt and TgG93A;Sod1ko mice.

Large fast-firing MNs are preferentially affected in SOD1-fALS mouse models, with reinnervation of the skeletal muscle by the slower-firing surviving MNs (Frey et al., 2000; Pun et al., 2006). To address whether this pattern of denervation/reinnervation differed between the TgG93A;Sod1wt and TgG93A;Sod1ko mice by examining the expression of different MHC proteins in skeletal muscle fibres. Muscle sections were prepared and analysed as described in Section 2.8.2. Antibody combinations (summarised in Table 4.5) labelled type 2B (fastest-glycolic) fibres on all sections in combination with either type 1 (slow-oxidative) or type 2A (fast-oxidative/glycolic) fibres.

The originally planned method of analysis was to categorise and count individual muscle fibres. However, due to difficulty in identifying individual fibres (example shown in Figure 4.11a) this method was not possible. An alternative was to use image analysis software to quantify the area of staining. However, calculation of the area stained as a proportion of the total area of the section was not possible due to freezing artefacts in many of the tissue sections (as shown in Figure 4.11b). For these reasons, analysis was carried out by quantifying the area stained in each channel and calculating the ratio of slower fibre type MHC area (type 1 or 2A) divided by the fastest fibre type MHC area (type 2B). The higher the ratio, the higher the proportion of slower fibre MHC area as compared to fastest fibre MHC area, indicating a conversion from fast to slow fibres as degeneration progresses.

**Table 4.5 Fibre type antibody summary**

Antibody	Antigen	Fibre type	Fatigue index	Type 2A /2B	Type 1 /2B
BA-D5	myosin heavy chain slow (type 1)	Type 1	slow (S)	unstained	red
SC-71	myosin heavy chain type 2A	Type 2a	fast- fatigue-resistant (FR)	red	unstained
		Type 2x	fast- fatigue-intermediate (FI)	unstained	unstained
BF-F3	myosin heavy chain type 2B	Type 2b	fastest- fatigable (FF)	green	green

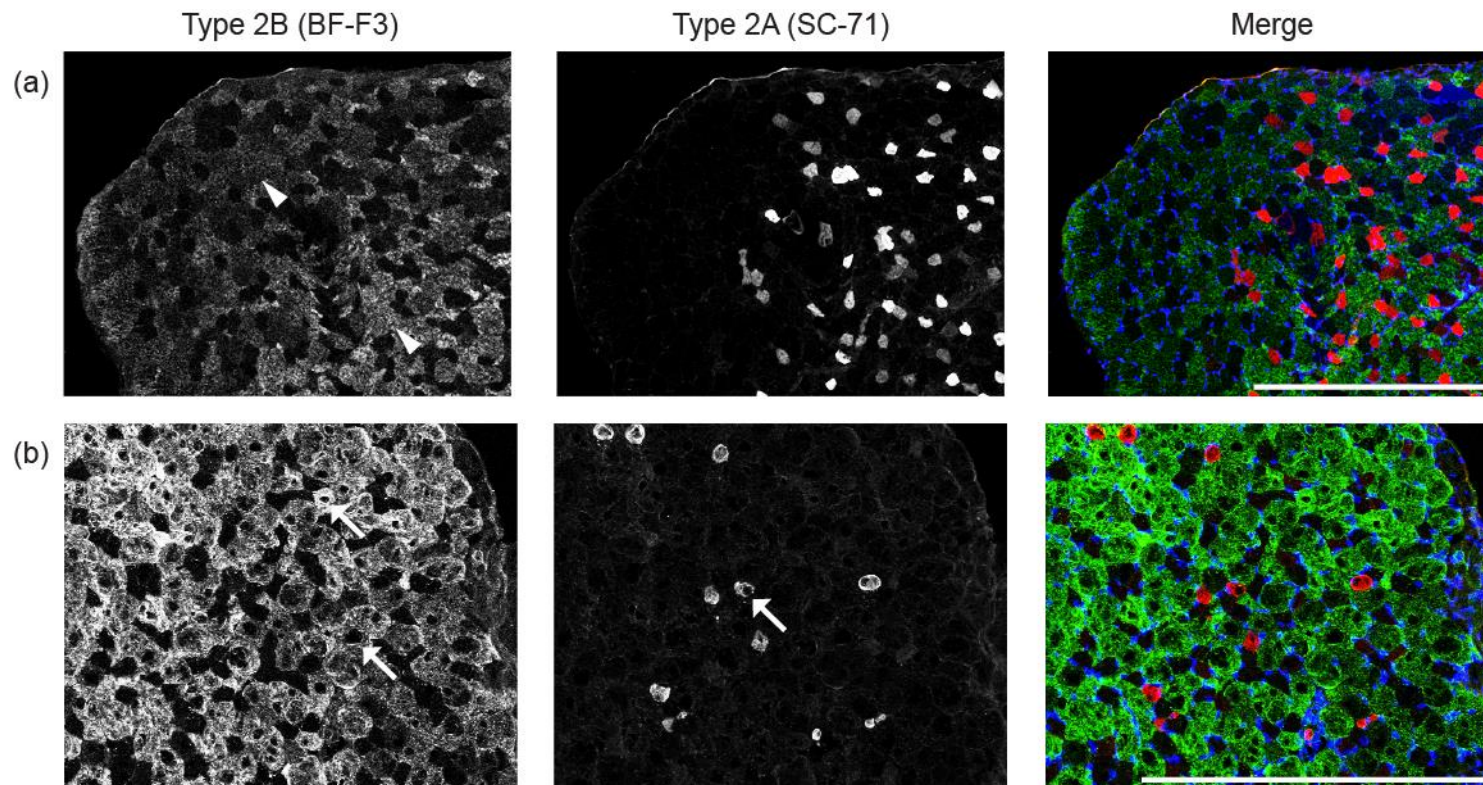
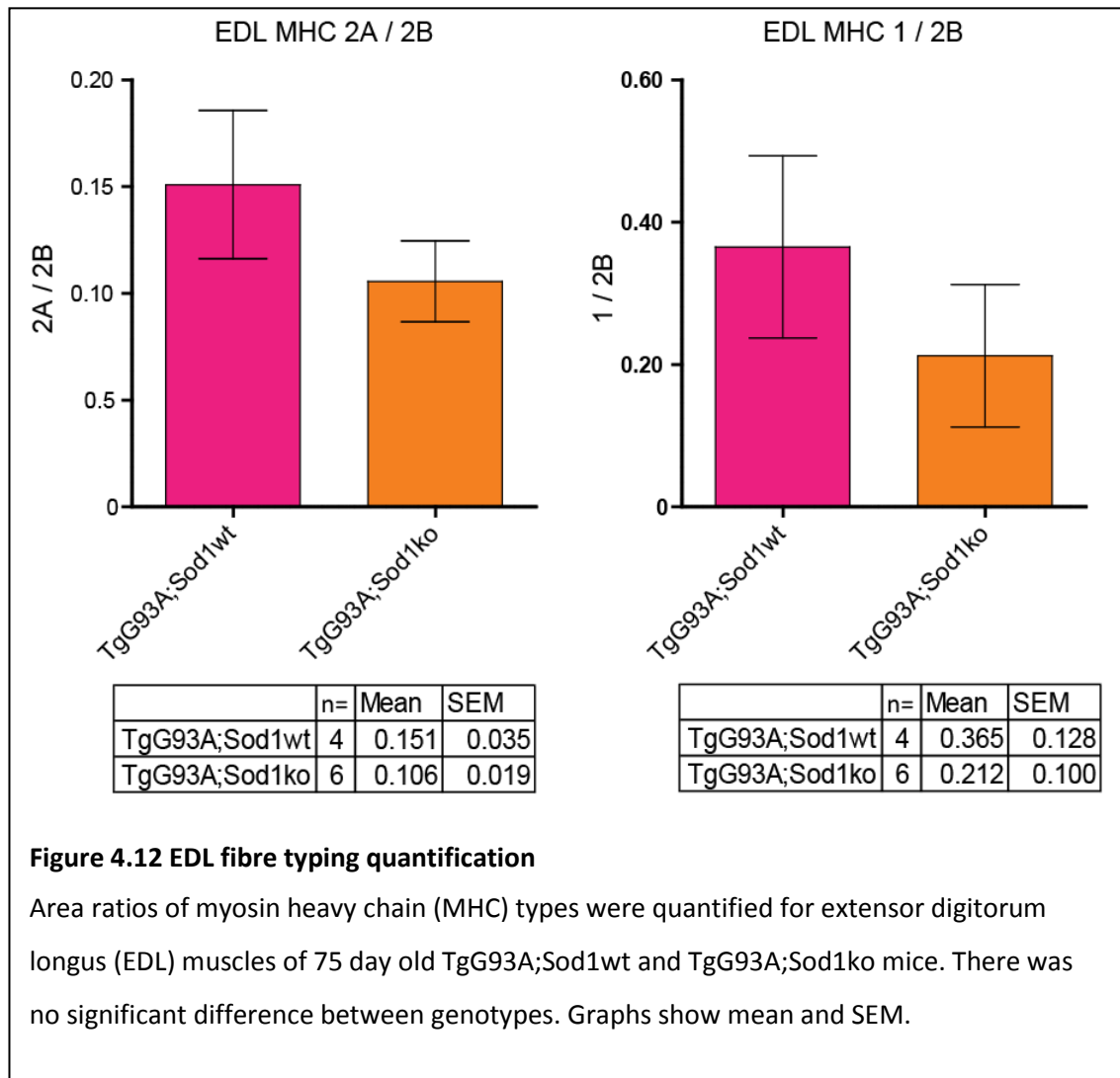


**Figure 4.11 Indistinct fibre boundaries and freezing artefacts**

Transverse muscle sections were immunostained for different myosin heavy chain isoforms in order to identify muscle fibre type composition. a- arrow head indicates area in which discrimination of individual muscle fibre boundaries was not possible. b- arrows indicate freezing artefacts that cause wholes within the muscle fibres precluding accurate calculation of area stained as a proportion of the total area of the muscle section.

#### 4.3.3.3.1 Fibre Types in the Extensor Digitorum Longus

Data are summarised in Figure 4.12 and representative images of EDL muscles from the 2 genotypes, stained for MHC 2A / 2B and for MHC 1 / 2B are shown in Figure 4.13 and Figure 4.14, respectively (see Section 7.6, Appendix 6 for images from all animals). There was no significant difference between TgG93A;Sod1wt and TgG93A;Sod1ko for either the proportion of MHC 2A / 2B area ( $t(8)=1.1254$ ,  $p>0.05$ ) or MHC 1 / 2B area ( $t(8)=0.950$ ,  $p>0.05$ ).





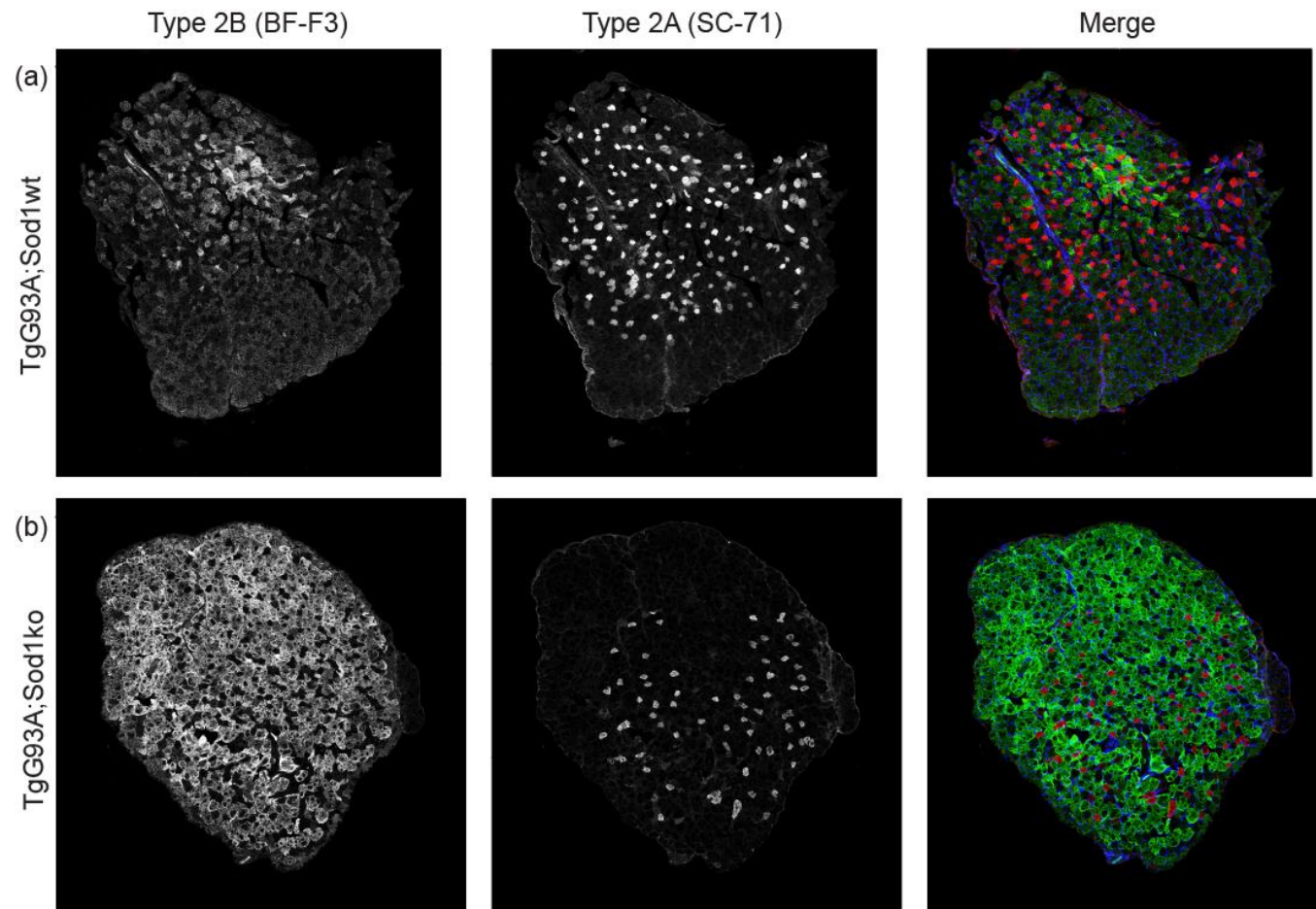


**Figure 4.13 EDL fibre typing: Myosin heavy chain type 2A and 2B**

Representative transverse sections of extensor digitorum longus (EDL) muscles of TgG93A;Sod1wt and TgG93A;Sod1ko immunostained for myosin heavy chain type 2B and type 2A. Scale bar 500µm.

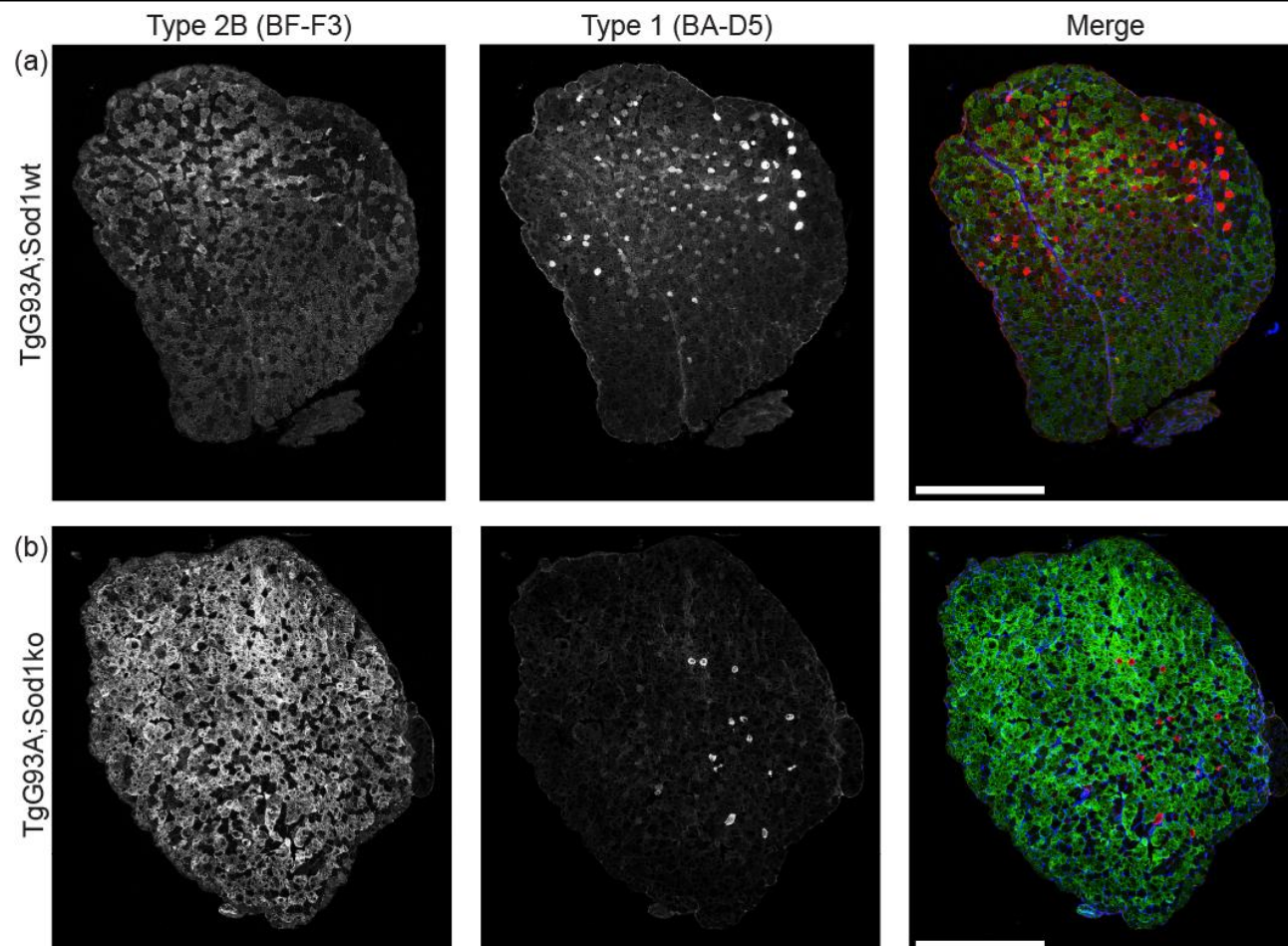
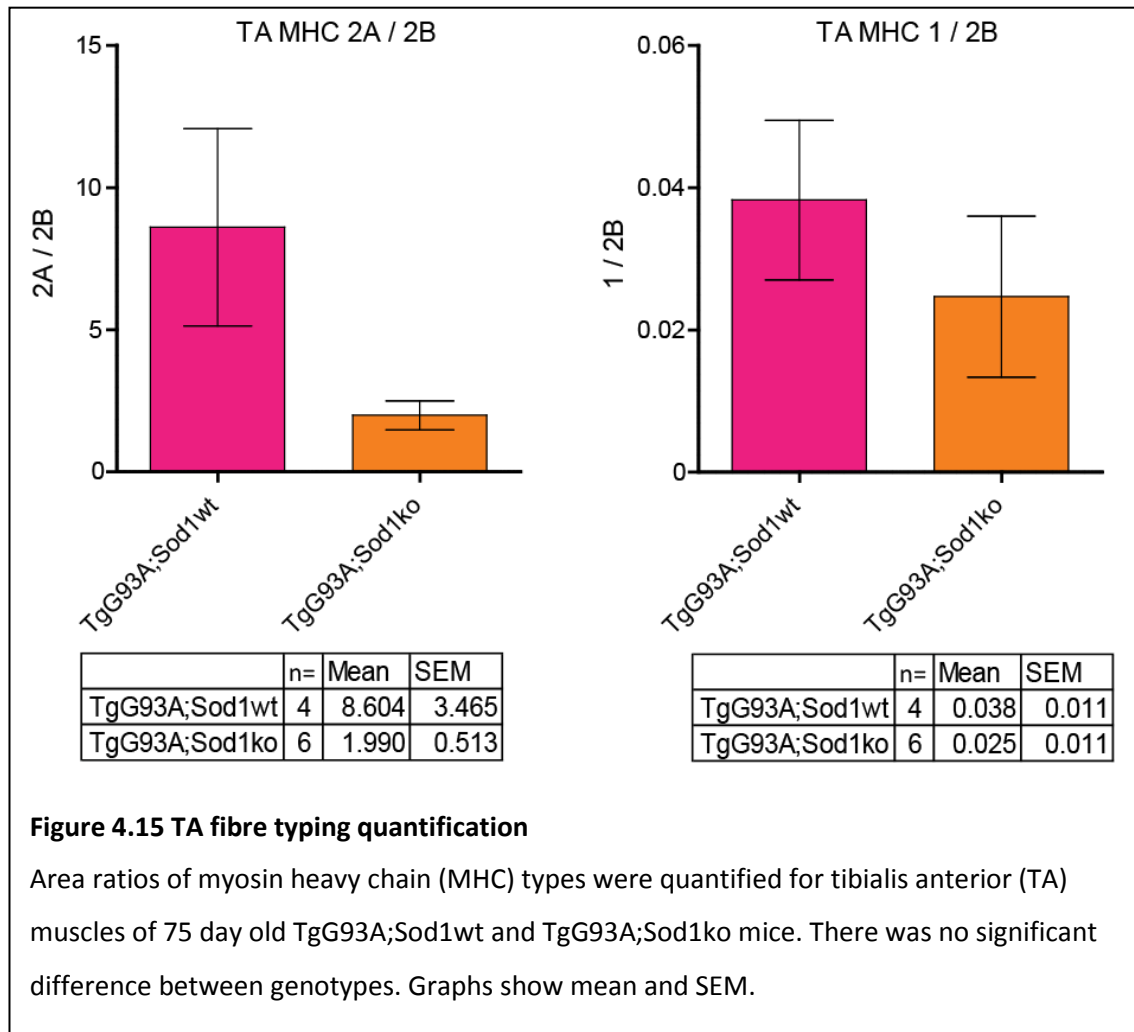


**Figure 4.14 EDL fibre typing: Myosin heavy chain type 1 and 2B**

Representative transverse sections of extensor digitorum longus (EDL) muscles of TgG93A;Sod1wt and TgG93A;Sod1ko immunostained for myosin heavy chain type 2B and type 1. Scale bar 500µm.

#### 4.3.3.3.2 Fibre Types in the Tibialis Anterior

Data are summarised in Figure 4.15 and representative images of tibialis anterior (TA) muscles from the 2 genotypes, stained for MHC 2A / 2B and for MHC 1 / 2B are shown in Figure 4.16 and Figure 4.17, respectively (see Section 7.6, Appendix 6 for images from all animals). No significant difference was found between TgG93A;Sod1wt and TgG93A;Sod1ko for either the proportion of MHC 2A / 2B area ( $t(3.132)=1.888$ ,  $p>0.05$ ) or MHC 1 / 2B area ( $t(8)=0.814$ ,  $p>0.05$ ).





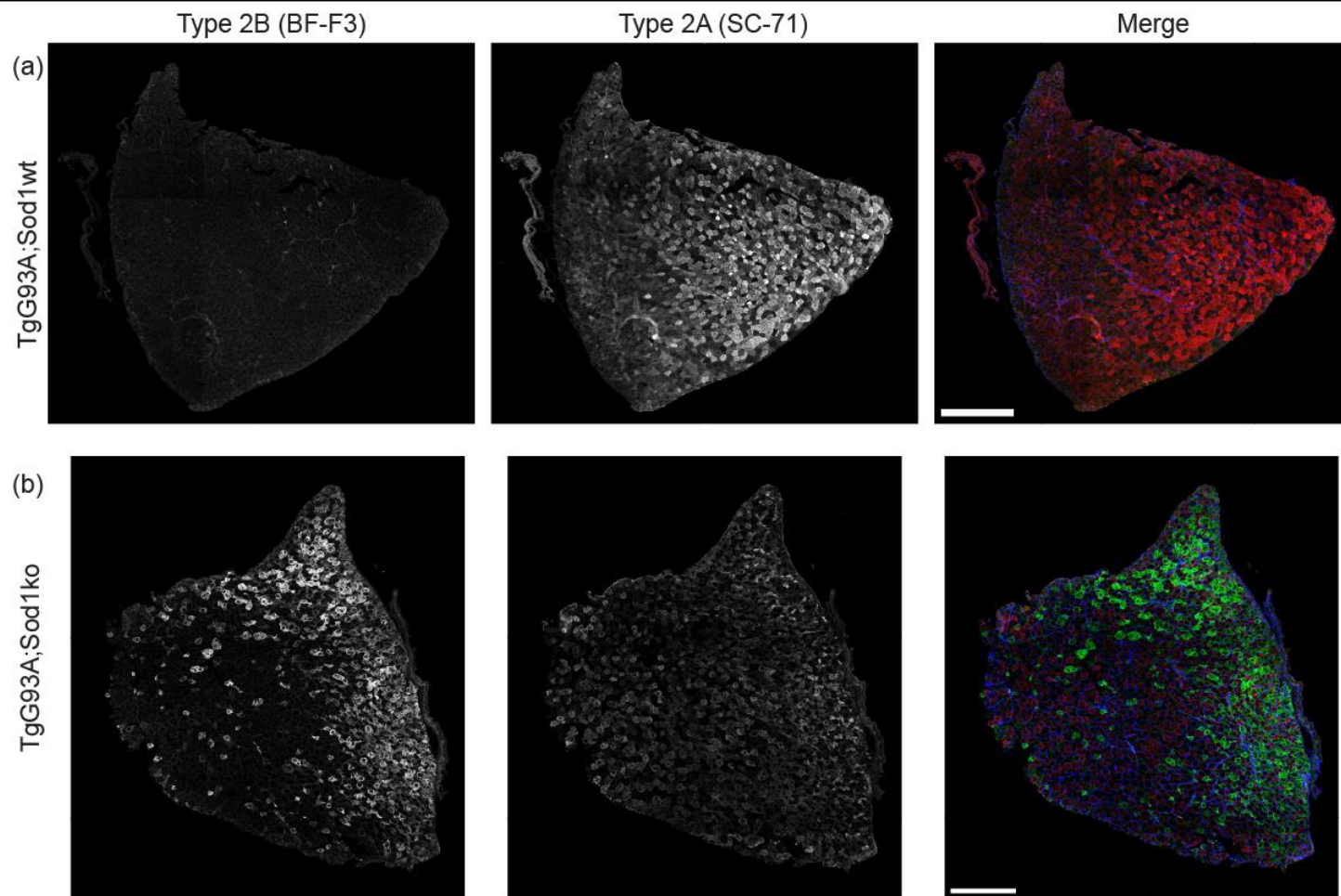


**Figure 4.16 TA fibre typing: Myosin heavy chain type 2A and 2B**

Representative transverse sections of tibialis anterior (TA) muscles of TgG93A;Sod1wt and TgG93A;Sod1ko immunostained for myosin heavy chain type 2B and type 2A. Scale bar 500µm.

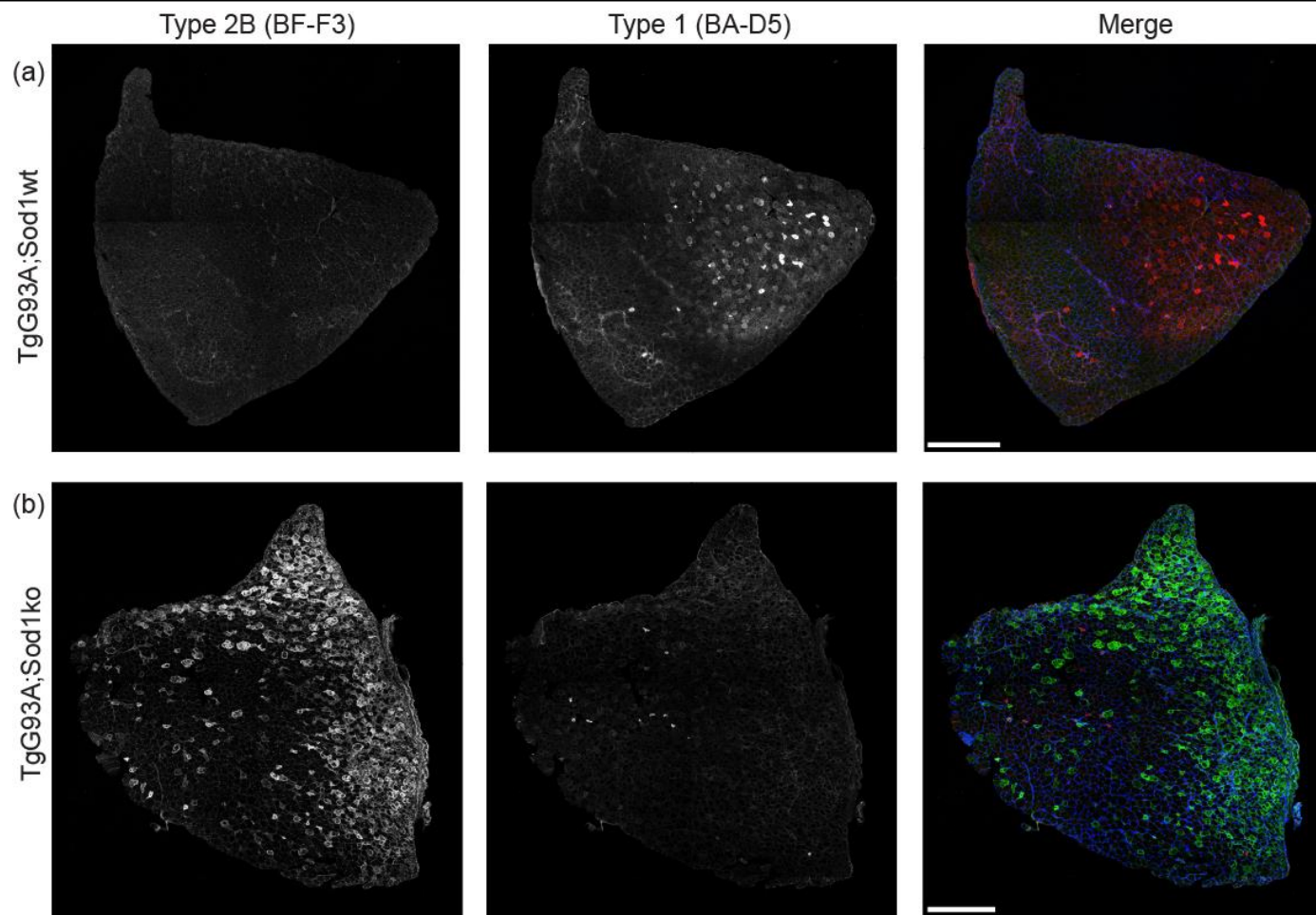


**Figure 4.17 TA fibre typing. Myosin heavy chain type 1 and 2B**

Representative transverse sections of tibialis anterior (TA) muscles of TgG93A;Sod1wt and TgG93A;Sod1ko immunostained for myosin heavy chain type 2B and type 1. Scale bar 500µm.

### 4.3.4 Can Transgenically Expressed Human SOD1 Compensate for Sod1ko Female Subfertility?

To examine whether transgenically expressed WT huSOD1 could save the subfertility reported in female Sod1ko mice (Ishii et al., 2005; Matzuk et al., 1998; Noda et al., 2012; Tsunoda et al., 2012), female mice of 4 genotypes (NTg;Sod1wt, NTg;Sod1ko, TgWT;Sod1wt and TgWT;Sod1ko) were mated to WT males, with proven fertility, for 6-months and the number of litters, total number of pups and the number of pups surviving to weaning (~40-days of age) were counted. Data were analysed by multivariate ANCOVA with Bonferroni post-hoc comparisons, with the age of male and female mice at the start of the matings as co-variants. The results are summarised in Table 4.6 and Figure 4.18 and the co-variants are summarised in Table 4.7.

Both TgWT;Sod1wt and TgWT;Sod1ko mice were severely subfertile; only 3/12 TgWT;Sod1wt and 2/12 TgWT;Sod1ko females produced any litters, with a maximum litter size of 2 pups and no pups survived to weaning for either maternal genotype.

The maternal age covariate did not significantly co-vary with the number of litters, total pups born or pups surviving to weaning ( $p>0.05$ ). The paternal age covariate was found significantly co-vary with the number of litters ( $F(1)=4.307$ ,  $p<0.05$ ), total pups born ( $F(1)=7.339$ ,  $p<0.05$ ) and for pups surviving to weaning ( $F(1)=8.148$ ,  $p<0.01$ ). Therefore paternal age must be considered as a potential affecter of differences in these measures.

**Table 4.6 Fertility of Sod1 KO and WT SOD1 transgenic mice**

Maternal genotype	n=	Litters		Pups born		Pups survived to weaning		Pups/litter	
		Mean	SEM	Mean	SEM	Mean	SEM	Mean	SEM
NTg;Sod1wt	12	4.583	0.267	28.833	1.551	22.917	0.480	6.437	0.359
NTg;Sod1ko	14	3.714	0.255	14.500	0.822	10.571	0.581	3.987	0.17
TgWT;Sod1wt	12	0.250	0.115	0.167	0.112	0	0		
TgWT;Sod1ko	12	0.167	0.112	0.333	0.225	0	0		

**Table 4.7 Age at start of mating**

Maternal genotype	Female age			Male age		
	Mean	SEM	n=	Mean	SEM	n=
NTg;Sod1wt	49.167	2.011	12	52.000	2.791	6
NTg;Sod1ko	58.286	2.971	14	94.571	7.885	7
TgWT;Sod1wt	39.833	2.332	12	81.667	1.504	6
TgWT;Sod1ko	53.750	3.429	12	83.333	4.249	6

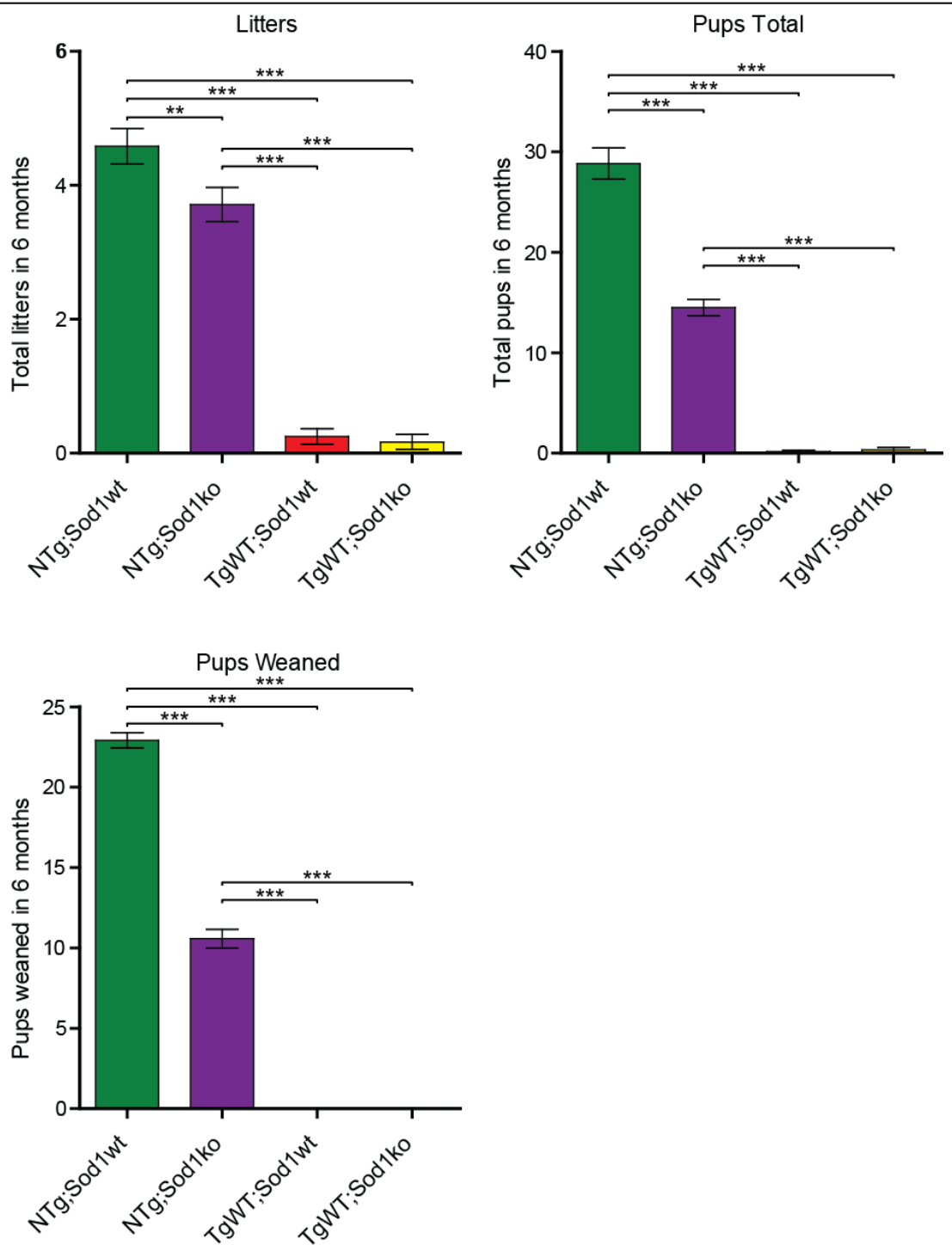


**Figure 4.18 Fertility of human WT SOD1 transgenic and Sod1 KO mice**

Female mice of 4 genotypes (NTg;Sod1wt, NTg;Sod1ko, TgWT;Sod1wt and TgWT;Sod1ko) were mated to WT males, of proven fertility, for 6-months and the number of litters and pups were counted. \*  $p < 0.05$ . \*\*  $p < 0.01$ . \*\*\*  $p < 0.001$ . Graphs shown mean and SEM.

The main effect of maternal genotype had a significant effect on the number of litters ( $F(3)=119.832$ ,  $p<0.001$ ). Post-hoc Bonferroni comparisons found no significant difference between TgWT;Sod1wt and TgWT;Sod1ko females for the number of litters. Both NTg;Sod1wt and NTg;Sod1ko females produced significantly more litters than both TgWT;Sod1wt and TgWT;Sod1ko females ( $p<0.001$ ). Compared to NTg;Sod1wt females, NTg;Sod1ko females produced significantly fewer litters ( $p<0.001$ ), with NTg;Sod1ko producing 0.81 times as many.

The main effect of maternal genotype had a significant effect on the total number of pups born ( $F(3)=220.192$ ,  $p<0.001$ ). Post-hoc Bonferroni comparisons identified no significant difference between TgWT;Sod1wt and TgWT;Sod1ko females ( $p>0.05$ ) for the total number of pups born. Both NTg;Sod1wt and NTg;Sod1ko females produced significantly more pups than both TgWT;Sod1wt and TgWT;Sod1ko females ( $p<0.001$ ). Compared to NTg;Sod1wt females, NTg;Sod1ko females produced significantly fewer pups ( $p<0.001$ ), with NTg;Sod1ko producing 0.5 times as many.

The main effect of maternal genotype had a significant effect of the number of pups surviving to weaning ( $F(3)=669.184$ ,  $p<0.001$ ). Post-hoc Bonferroni comparisons identified no significant difference between TgWT;Sod1wt and TgWT;Sod1ko females for the number of pups surviving to weaning. Both NTg;Sod1wt and NTg;Sod1ko females produced significantly more pups which survived to weaning than both TgWT;Sod1wt and TgWT;Sod1ko females ( $p<0.001$ ). Compared to NTg;Sod1wt females, NTg;Sod1ko mice produced significantly fewer pups that survived to weaning ( $p<0.001$ ), with NTg;Sod1ko producing 0.46 times as many.

Because so few litters were produced by females of both TgWT genotypes, a separate ANCOVA was carried out to examine whether the number of pups produced per litter differed between females of the two NTg genotypes, data are summarised in Table 4.6. Neither maternal nor paternal age was a significant covariate with the number of pups produced per litter ( $p>0.05$ ). The main effect of maternal genotype had a significant effect on the number of pups produced per litter ( $F(1)=26.391$ ,  $p>0.001$ ). Compared to NTg;Sod1wt females, NTg;Sod1ko females produced significantly fewer pups per litter, 0.62 as many.

## **4.4 DISCUSSION**

### **4.4.1 Does Endogenous Mouse SOD1 Effect the Disease Phenotype of the TgG93A Mouse?**

The data presented here suggest that endogenous moSOD1 does not affect the onset or survival of the TgG93A mouse. Grip-strength was similar for TgG93A;Sod1wt and TgG93A;Sod1ko mice at our earliest time-point (57-70-days) but differed at 71-84-days with TgG93A;Sod1ko mice having higher grip-strength than TgG93A;Sod1wt mice. This early

advantage of the Sod1ko genotype in maintaining muscle strength in TgG93A mice is lost at later time-points; although the average grip-strength of TgG93A;Sod1ko mice is higher than the TgG93A;Sod1wt mice at all time-points the difference is only statistically significant at 71-84-days of age.

Neither MN number nor NMJ number or innervation status differed between TgG93A;Sod1wt and TgG93A;Sod1ko mice at the later time-point (120-days). The earlier histological time-point of 75-days of age was chosen based on the difference in grip-strength seen at this age. At 75-days of age TgG93A;Sod1ko mice have on significantly more (~14% on average) NMJs on the EDL than TgG93A;Sod1wt mice (1082.2 vs 946.38 respectively) however the pattern of innervation/denervation does not differ significantly between genotypes. Loss of the acetylcholine receptors (AChR) that form the post-synaptic end-plate of the NMJ can result from prolonged denervation (Rich et al., 1989) and a progressive loss of NMJs is reported in SOD1-fALS mice (Seijffers et al., 2014) so one possible explanation of a lower total number of NMJs in the TgG93A;Sod1wt mice is that an early pre-symptomatic degeneration of the MN axons, which is absent or less profound in the TgG93A;Sod1ko mice, leads to their loss. A reduction in the number of functional motor units (MU) can be detected from as early as 45-days of age in G93A-SOD1-fALS mice compared to WT mice (Hegedus et al., 2007), along with reductions in end-plate size (Kalmar et al., 2012). This is before denervation of NMJs is usually reported by histological examination, and is unlikely due to a reduced number of MNs as TgG93A;Sod1wt mice have a normal compliment of MNs until at least 100-days of age (Gould et al., 2006; Fischer et al., 2004; Chiu et al., 1995; Kong et al., 1998). Together this is suggestive of an early, pre-symptomatic denervation of the skeletal muscles in the TgG93A mouse. Differences in this process between TgG93A;Sod1wt and TgG93A;Sod1ko mice, could therefore be the cause of the distinction in number of NMJs reported here. However, because earlier time-points were not investigated here it is also possible that the lower number of NMJs seen in the TgG93A;Sod1wt compared to the TgG93A;Sod1ko mice, rather than being due to a degenerative process, could be due to a developmental difference; the formation of the neuromuscular network could be less robust in the TgG93A;Sod1wt mice resulting in fewer NMJs. Alternatively, the muscles of the TgG93A;Sod1wt mice could contain fewer fibres than the TgG93A;Sod1ko mice resulting in fewer NMJs.

To address the question of whether differences in NMJ number are due to a degenerative or developmental difference, neural cell adhesion molecule (NCAM) staining of muscle sections could be used for the detection of denervated muscle fibres (Gordon et al., 2009) to see if there is also a higher level of denervated muscle fibres in TgG93A;Sod1wt mice compared to the TgG93A;Sod1ko mice.

The pattern of decline apparent in the grip-strength measured in our TgG93A;Sod1wt mice is similar to that seen by other investigators (e.g. (Kong et al., 1998)) and also mirrors a pattern of MU loss reported in the TA and medial gastrocnemius (MG. Part of the triceps sura (TS) hind limb muscles (Hegedus et al., 2007), that of an initial decline in function plateauing at around 70-days, before another decline later. Several lines of evidence suggest that the MN populations that are most vulnerable to degeneration at early disease stages are the large-fast fatigable MNs that innervate the fastest, type 2B muscle fibres; Pathological signs of degeneration are seen specifically within the large MNs of the SC of SOD1-fALS mice from 56-days of age (Bendotti et al., 2001) and the large calibre MN axons of the ventral roots are the first to degenerate, from 80-days of age (Fischer et al., 2004). At the distal axon, both Pun et al., (2006) and Frey et al., (2000) have identified those MNs that innervate the fastest muscle fibres as the earliest to degenerate, with Frey et al., (2000) mapping this to a similar time frame of 45-80-days of age.

The attenuation of the initial fast decline stage seen in our TgG93A;Sod1ko mice could therefore be due to improved maintenance of the neuromuscular connections between large fast firing MNs and fast type 2b muscle fibres. Alternatively, an increased capacity of reinnervation by slower firing MNs could be the cause. We sought to assess this by examining the fibre type composition of hind limb muscles. As previously described, the planned analysis of classifying and counting individual muscle fibres was not possible and so alternative analysis based on the ratio of areas of staining was used. Although this analysis did not yield significant differences between TgG93A;Sod1wt and TgG93A;Sod1ko in the muscles assessed, there was a consistent non-significant trend of lower ratios of slow:fast MHC staining for the TgG93A;Sod1ko compared to the TgG93A;Sod1wt mice for all measures. This is suggestive of improved maintenance of the fastest, type 2b fibres in the TgG93A;Sod1ko mice compared to the TgG93A;Sod1wt. A lower level of reinnervation and consequent fibre type conversion by slower MNs in the TgG93A;Sod1ko mice could also account for the difference in ratios of MHC expression, however this would most likely be accompanied by a decrease in innervated NMJs and lower muscle strength. In this context of increased relative muscle strength and a higher number of total NMJs, with no difference in the pattern of innervation, this is the less likely explanation. That the difference between genotypes lies within the more vulnerable, fast-fatigable MNs is also consistent with the absence of a difference at later ages in our mice; as this population is the first to be lost, at later ages they will not be present to affect a difference between the two genotypes.

It is important to keep in mind that this analysis was based on the *area* of staining, rather than the *number* of fibres. Cross sectional area of muscle fibres can change in response to fibre type

conversion produced by changes in innervation or activity (Gordon et al., 2009; Hegedus et al., 2008). This means that another explanation for the difference in ratios of slow:fast MHC types is that the TgG93A;Sod1ko mice maintain type 2b fibres with a larger cross sectional area whereas, in TgG93A;Sod1wt there is a relative reduction in the size/area of the type 2b muscle fibres, without a reduction in their number. However, either explanation – a difference in number or cross sectional area – indicates a lower level of degeneration of type 2b fibres in TgG93A;Sod1ko mice at 75-days of age. In order to overcome the problem of quantification, an alternative staining protocol has now been identified which uses anti-laminin antibodies to delineate the borders of the fibres (Li et al., 2007). This may aid in identification of individual fibres for counting and classification. Total quantification of muscle fibres may also aid in delineating whether the difference in the total number of NMJs is due to denervation or differences in the number of muscle fibres.

Hegedus et al., (2007) has questioned whether compensatory reinnervation of muscle fibres occurs in SOD1-fALS mice, particularly in muscles composed of fast fibres; they find a direct relationship between MU number and muscle force, precluding the possibility of surviving MUs increasing their force producing capacity as a result of sprouting. However, immunohistochemical evaluation of the neuromuscular network provides direct evidence for reinnervation, including increased MU size concomitant with decreasing numbers of MUs and *in vivo* longitudinal imaging of reinnervation of unoccupied end-plates, although, in agreement with Hegedus et al., (2007) reinnervation does appear to be limited to the longer surviving slower MNs (Frey et al., 2000; Schaefer et al., 2005; Pun et al., 2006). If the increased grip-strength at 75-days of age seen in our TgG93A;Sod1ko mice, relative to the TgG93A;Sod1wt mice, were due to increased capacity for reinnervation by surviving MNs, a concomitant increase in the proportion of slower muscle fibre types, signifying reinnervation by surviving slower-MNs, might be expected as a result. This is not the case, instead an increased proportion of the fastest fibre type is apparent, and there is also no difference in the proportion of innervated, intermediate or denervated NMJs. These results are more compatible with improved maintenance of existing fast MUs, a difference which is not sustained as degeneration progresses.

Discussion of how huSOD1 and moSOD1 may interact to produce these effects can be found in Section 6.2.

#### **4.4.2 Can Transgenic Human SOD1 Compensate for *Sod1* KO Phenotypes?**

Our NTg;Sod1ko mice had significantly lower body weight at 57-70-days of age compared to our NTg;Sod1wt mice. Our TgG93A;Sod1wt and TgG93A;Sod1ko weighed similar amounts at



the same age and the TgG93A;Sod1ko mice weighed significantly more than the NTg;Sod1ko mice. This suggests that expression of the mutant G93A huSOD1 protein is able to attenuate for the reduced body weight seen in the NTg;Sod1ko mice, at least increasing the weight to equal that of TgG93A;Sod1wt mice.

We sought to further evaluate whether transgenically expressed huSOD1 was able to rescue Sod1ko phenotypes by examining the subfertility reported in female Sod1ko mice (Matzuk et al., 1998; Noda et al., 2012). For this experiment we used TgWT dams because TgG93A females are reported as poor breeders by Jackson Laboratories (<http://jaxmice.jax.org/strain/004435.html> accessed March 2014) whereas no such issue is reported for TgWT mice (<http://jaxmice.jax.org/strain/002298.html> accessed March 2014). In fact, our results were that both TgWT;Sod1wt and TgWT;Sod1ko females are profoundly subfertile; over a 6 month mating period only 2 out of 12 females of each genotype produced any litters, the maximum litter size being 2 and none of the pups survived to weaning age. Due to the severe subfertility of TgWT;Sod1wt mice, it is apparent that transgenically expressed WT huSOD1 is not able to compensate for the reduced fertility of Sod1ko mice. The reduced fertility of Sod1ko mice may be due to increased oxidative stress either via effects on gonadotropin hormone in the pituitary or by direct effects in the tissue of the ovaries (Matzuk et al., 1998; Noda et al., 2012). Although somewhat counterintuitive, mice transgenically expressing high levels of G93A mutant huSOD1, which has increased SOD1 activity, actually display increased oxidative stress in multiple tissues (as reviewed by (Hensley et al., 2006)) and have oxidative damage to various cellular components (e.g. (Ferrante et al., 1997b; Andrus et al., 1998; Poon et al., 2005; Liu et al., 1998; Liu et al., 1999; Casoni et al., 2005; Liu et al., 2007; Cha et al., 2000; Lee et al., 2009)). However, transgenic overexpression of WT huSOD1 has been found to reduce sensitivity to chemically induced oxidative stress (Mele et al., 2006; Pérez et al., 2009) and oxidative lipid damage resulting from a high fat diet (Liu et al., 2013) suggesting that increased oxidative stress may not be a feature of TgWT mice and may not account for the subfertility seen in these mice.

Similar to previously published data, our NTg;Sod1ko mice displayed reduced fertility compared to NTg;Sod1wt mice when assessed over a 6-month mating period, although our mice appear to be more fertile than previous reports; Matzuk et al., (1998) reported 2.7 pups per litter and a figure equating to an average of 1.38 litters over 6-months, compared to our data of 3.99 and 3.71 respectively. One female in their cohort died at 2-months. It is not reported whether this female had a significantly different number of litters to the remaining 15 mice examined. The males used in the present experiments were initially placed in matings with WT C57BL/6J females to ensure that they were themselves fertile. It is possible that the

increased fertility apparent in our data is in part due to this precaution to exclude infertile stud males. A possible confound in our data is that the age of males when entering the matings was identified as a significant covariate with number of litters, number of pups and number of pups surviving to weaning (but not when pups/litter was analysed for NTg dams) and was lower in matings with NTg;Sod1wt females than any of the other genotypes and may therefore be partially responsible for the difference found between NTg;Sod1wt and NTg;Sod1ko females.

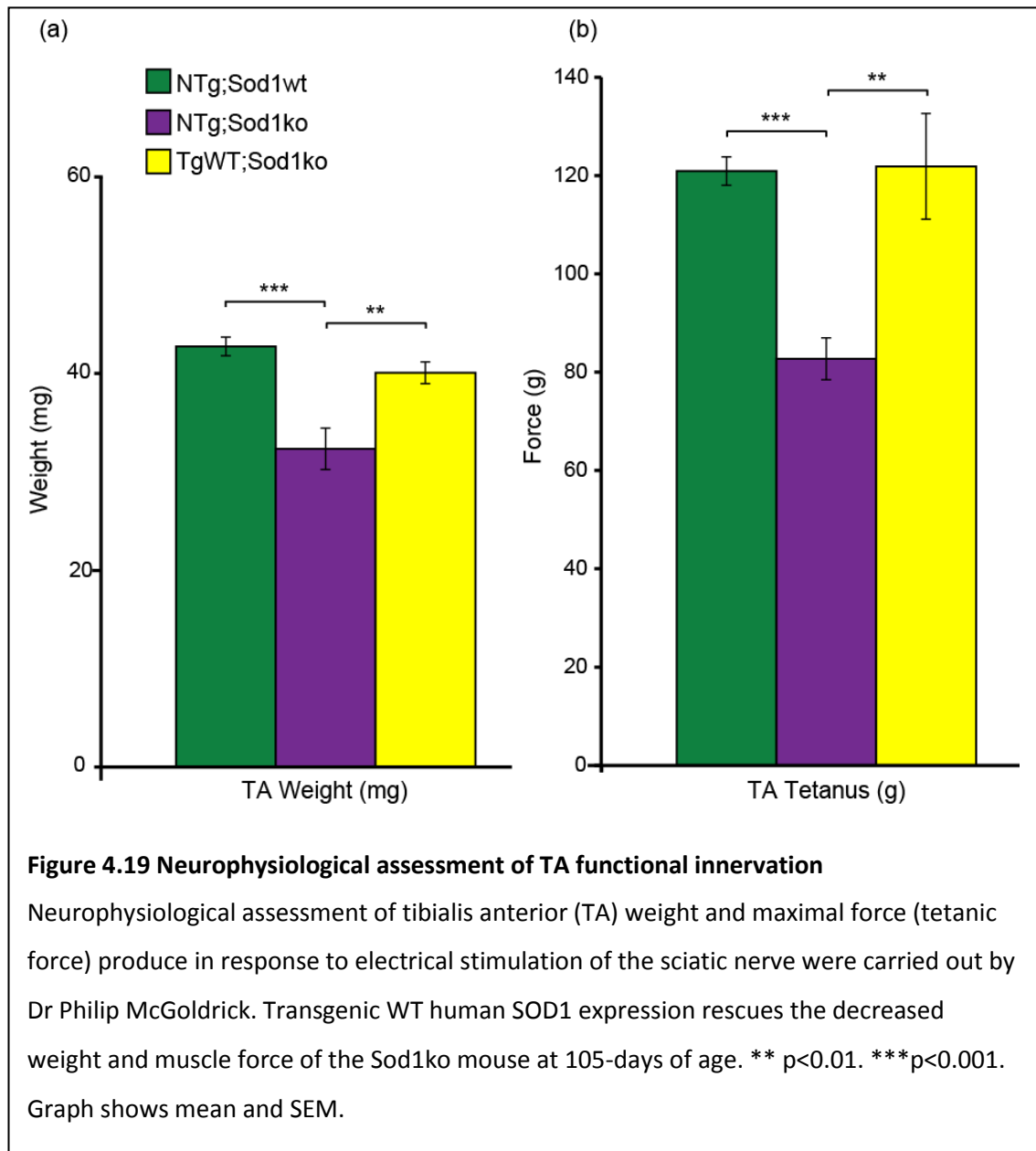
#### *4.4.2.1 TRANSGENICALLY EXPRESSED WT HUMAN SOD1 RESCUES MN AXONOPATHY IN SOD1 KO ANIMALS*

Another phenotype of the Sod1ko mice of more relevance to SOD1-fALS is the degenerative muscle denervation and associated reduction in skeletal muscle contractile force, as described in Section 1.4.2. In order to assess whether transgenic expression of WT huSOD1 can attenuate the functional denervation of skeletal muscles seen in Sod1ko mice, a neurophysiological assessment was carried out by Dr Philip McGoldrick (unpublished data). Female mice at 105-days of age and of 3 genotypes (5X NTg;Sod1wt; 5X NTg;Sod1ko and 4X TgWT;Sod1ko) were assessed by measuring the weight and maximum tetanic force produced by the TA in response to electrical stimulation of the sciatic nerve. As illustrated in Figure 4.19, both TA weight and tetanic force are reduced in the NTg;Sod1ko mice compared to both the NTg;Sod1wt mice and the TgWT;Sod1ko mice suggesting that transgenic WT huSOD1 expression can rescue at least some of the neuromuscular deficits of the Sod1ko mouse. This work complements an earlier publication by Fischer et al., (2011) who used immunohistochemistry to show that NMJ innervation of the TA muscles in Sod1ko mice at ~120-days of age was restored to WT like levels by transgenic expression of a SOD1-mitofilin fusion protein which is targeted specifically to the mitochondrial intermembrane space. NMJ integrity was maintained for up to 1 year and a measure of muscle strength at 1-year of age also showed that the mitochondrially targeted WT huSOD1 maintained the motor performance of Sod1ko mice at WT like levels.

Together these data suggest that transgenically expressed huSOD1 can compensate for some of the Sod1ko phenotypes, such as early reduced body weight and functional denervation of the TA. However this compensation is not universal, as reduced fertility of Sod1ko mice cannot be alleviated by transgenic WT huSOD1 expression as this causes a profound loss of fertility itself.

Of note, the MN specific toxic effects of ubiquitous WT huSOD1 expression, such as signs of MN axonal degeneration from as early as 30-weeks (210-days) of age and mild motor deficits from 58-weeks of age (Jaarsma et al., 2000; Dal Canto et al., 1995) mean that the early compensation for Sod1ko may not be sustained at later ages and, in conjunction with the data

from Fischer et al., (2011), suggest that such toxicity is affected in cellular compartments other than the mitochondria.



#### 4.4.3 Future Work

Work is underway to increase the number of animals in our onset and survival cohorts to make up for mice excluded due to reduced transgene array copy number and incomplete data.

Further examination of the muscle fibre type composition is required, including testing alternative staining protocols to include laminin to discern fibre borders, as described by Li et al., (2007). This would help us to delineate, 1) whether differences in NMJ number between TgG93A;Sod1wt and TgG93A;Sod1ko mice is due to denervation or differences in the number of muscle fibres and 2) whether an increase in type 2B MHC staining area in TgG93A;Sod1ko mice compared to TgG93A;Sod1wt mice is apparent when quantified using the more usual

technique of counting the number of fibres expressing different MHC isoforms. Similar histological staining of transverse muscle section for NCAM could also provide an alternative measure of fibre denervation which, if the laminin staining protocol proves successful, could be applied alongside fibre type staining of serial sections to allow discernment of which fibre types are denervated.

# Chapter 5. Towards Making a Humanised *SOD1* Mouse

## 5.1 AIMS

The aim of the work described in this chapter is to make a new mouse model of SOD1-fALS by genomically humanising the mouse *Sod1* locus with a conditional, Cre dependent, switch from expression of mutant to wild-type (WT) SOD1.

This chapter will describe the design and cloning of the targeting construct which will be used to make the new mouse line.

## 5.2 RESULTS

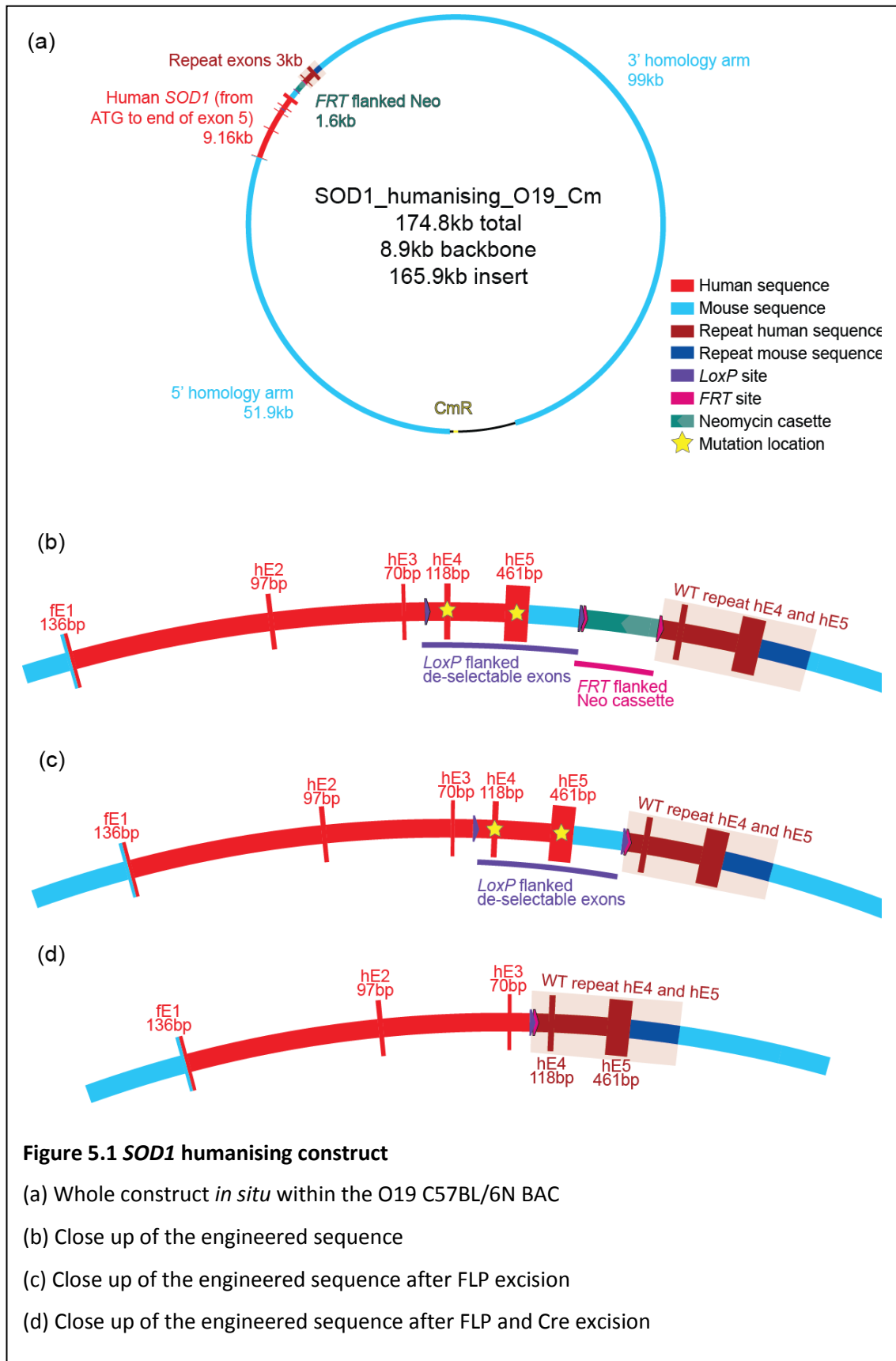
### 5.2.1 Construct Design

The targeting construct and primary cloning strategy were designed by Dr Anny Devoy. This project is part of a larger body of work being undertaken by Dr Devoy to produce a series of new models of fALS using similarly strategies to genomically humanise two ALS causative genes: *SOD1* and *FUS*.

#### Overview

The full targeting construct is shown in Figure 5.1a, with an expanded view of the engineered region in Figure 5.1b. The region of the mouse genome to be replaced is ~5.5 kb from the ATG start codon to the end of the 3' UTR of exon 5 (the final exon) of *Sod1*. This region will be replaced with ~14.9 kb of engineered sequence, including:

- the human *SOD1* genomic locus from start codon, to the end of the 3' UTR of exon 5 (~9 kb)
- one kb mouse genomic sequence 3' of the *Sod1* locus (1 kb terminator)
- a kanamycin/neomycin selection cassette (neo. Gene Bridges) (~1 kb)
- a repeat cassette which includes *SOD1* genomic sequence from intron 3 to the end of exon 5 (~2 kb)
- other engineered elements comprising the conditional Cre dependent mutant/WT “machinery”, described in more detail below
- large (> 10 kb) homology arms: regions of flanking sequence homologous to the region of mouse chromosome that the construct is targeted to



The large homology arms are designed to facilitate efficient targeting in mouse embryonic stem cells (mESCs). The neo cassette allows selection of targeted mESCs.

The conditional allele allows expression of an exon 4 or 5 mutant human SOD1 (huSOD1) to be switched to expression of WT huSOD1. The human *SOD1* sequence in the allele's starting configuration will include an ALS mutation in either exon 4-5 (Figure 5.1c). Upon expression of Cre, the *LoxP* flanked (floxed) region is excised and the WT repeat moves into frame, switching the transcript from mutant to WT (Figure 5.1c-d transition).

### **Neomycin/Kanamycin Selection Cassette**

The neo cassette is positioned 1 kb downstream from the end of the 3' UTR of *SOD1*. The cassette has 2 promoters; transcription of the *neo* gene from a prokaryotic *gb2* promoter confers kanamycin resistance in *E.coli* and transcription from the eukaryotic PGK promoter confers neomycin resistance in mammalian cells. It is included in the construct so that neomycin selection can be used in mESC targeting. The inclusion of this exogenous sequence has the potential to cause undesired/off-target effects on *SOD1* or surrounding genes. The retention of such cassettes in knock-out (KO) alleles can cause perturbation of the expression of the surrounding genes which can lead to phenotypes, including embryonic lethality, which are caused by the cassette and not the KO itself (e.g. (Hug et al., 1996; Pham et al., 1996; Olson et al., 1996; Fiering et al., 1995)). Novel fusion transcripts have also been reported (Scacheri et al., 2001).

To reduce the likelihood of this occurring, several precautions have been taken; firstly, the selection cassette has been positioned 1 kb downstream from the end of the 3' UTR of humanised *SOD1* to allow a run off for the transcription machinery without any exogenous sequence interfering with correct transcription termination. *Scaf4* is 2.6 kb downstream of *Sod1* and in the reverse orientation. The positioning of the selection cassette, 1 kb downstream of *Sod1*, also allows over 1.5 kb uninterrupted run off for transcription of *Scaf4*. The cassette is also flanked by Flippase Recognition Target (*FRT*) sites to allow excision of the cassette by expression of Flippase site-specific recombinase (FLP), leaving a single *FRT* "scar" (Figure 5.1, transition from b-c). This excision would usually be done once germ-line transmission of the modification has been achieved in mice, by crossing to a FLP transgenic mouse line.

The positioning of the neo cassette here also aids cloning of the targeting construct; a repeat cassette must be inserted downstream of the 1 kb terminator. Having the neo cassette in this location provides a unique region of sequence for targeting by recombineering.

### Conditional Mutant/WT Allele

The conditional allele allows a switch from expression of mutant to WT huSOD1 by Cre excision of the floxed mutant exon 4-5 cassette (Figure 5.1c-d). The floxed cassette contains a ~3 kb region spanning from within intron 3 to 1 kb downstream of the 3' UTR, with an ALS mutation in either exon 4 or exon 5. The downstream WT repeat cassette contains sequence almost identical but with the exception that there is no ALS mutation.

In its starting configuration (Figure 5.1c) the allele directs expression of huSOD1 with an ALS mutation in either exon 4 or 5. Expression of Cre excised the floxed cassette, moving the WT repeat cassette into frame, changing expression to WT huSOD1 (Figure 5.1d). Expression of Cre can be achieved by crossing to a Cre transgenic mouse line. Many conditional and inducible Cre transgenic mouse lines are now available (e.g. (Heffner et al., 2012)).

### Homology Arms

As is shown in Figure 5.1a, by engineering the construct into a BAC containing the mouse *Sod1* locus, large homology arms are provided to facilitate more efficient mESC targeting. Several BACs containing the required mouse genomic region with *Sod1* in a relatively central position are available (described later in Section 5.2.3) and the size of the homology arms is dependent on which BAC is used. In the example shown in Figure 5.1a, the construct is shown in a B6Ng01-068O19 BAC which provides homology arms of 51.9 kb and 99 kb.

### 5.2.2 Selection of Mutations

The design of the conditional allele allows the use of any mutation within the repeat region encompassing exons 4 and 5. The starting point for selection of a mutation was to identify all the disease causative mutations within these exons by searching the ALS online database (<http://alsod.iop.kcl.ac.uk/>) and PubMed (<http://www.ncbi.nlm.nih.gov/pubmed/>). These mutations are shown in graphical format in Figure 1.2. It was decided that in the first instance two mutant constructs would be made, one with a wild-type like enzymatically active mutation and one highly destabilised mutation. A literature search was carried out and two mutations were chosen based upon:

- **Causality**- many mutations have been reported in only single cases. The chosen mutation should have been reported in multiple probands and where familial pedigrees are available, segregation with disease should be apparent.
- **High penetrance**- based on the pedigrees available a high level of penetrance should be apparent.
- **Absence of evidence for unusually long disease course or late onset.**



In addition to these criteria, mutations for which biochemical or biophysical information was also available were viewed favourably. The 2 mutations chosen were the stable WT-like E100G mutation and the highly destabilising L126delTT mutation. Information presented below includes details of the patient literature available and a brief summary of the *in vitro* experimental and mouse data, where available.

#### 5.2.2.1 *SOD1*<sup>E100G</sup>

The first mutation chosen was an adenine to guanine (GAA to GGA) mutation in the 101<sup>st</sup> codon residing in exon 4 of *SOD1* causing a substitution from glutamic acid to glycine (E100G) (Figure 5.2). This is one of the mutations to have been reported in the paper that first identified *SOD1* mutation as causative of ALS (Rosen et al., 1993). Further details of this particular cohort are not detailed in this paper.

##### 5.2.2.1.1 Patient Literature for the *SOD1*<sup>E100G</sup> Mutation

The patient data described in this section are summarised in Table 5.1 where individual data are available and in Table 5.2, where averages are presented.

From a literature search, a possible 9 independent probands/pedigrees have been identified. Each will be briefly described.

#### **Pedigree 1**

The first case identified by Rosen et al., (1993) was also examined in Deng et al., (1993) who measured dismutase activity from RBCs from 2 patients from the same family. Dismutase activity was less than 50% that of WT control levels. A third paper (Yulug et al., 1995) identifies an individual with this mutation but gives no further information. The samples used for mutation identification were supplied by Professor Guy Rouleau, a co-author on the original Rosen paper. The samples are described as being of “unknown etiology”. It is not clear whether this is one of the cases identified by Rosen et al., (1993) and Deng et al., (1993), from the same pedigree, or an independent case.

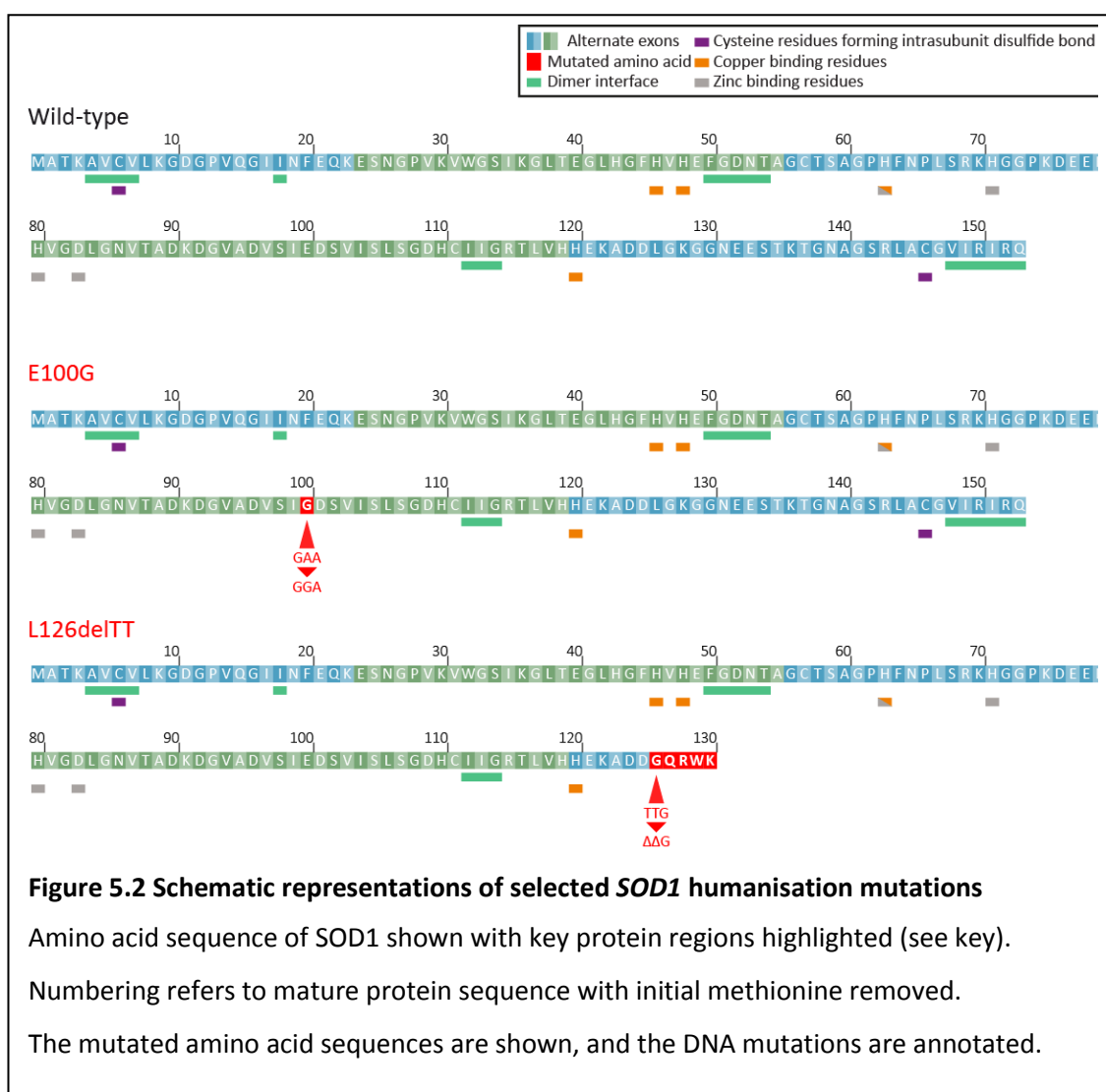


**Table 5.1 Summary of clinical data for E100G individuals**

Reference	ID	Onset age (years)	Site of onset	Duration (years)	Age at death (years)	Sex	Mutation confirmed	Comments
Calder et al., (1995)	III-2	46	legs	4.75	51	m		Mutation identified in a cousin and offspring. Appears as female in the pedigree chart
Calder et al., (1995)	III-3	49	legs	5.5	54	f		Mutation identified in a cousin and offspring. Appears as male in the pedigree chart
Ince et al., (1996)		36	legs	3.25		f	y	4 relatives died aged 46, 42, 52 and unknown
Aggarwal (2012)		48	legs	0.3		f	y	
Aggarwal (2012)		44	legs	0.17		m	y	Treated with Riluzole. Alive on ventilation with tube feeding
Vucic et al., (2008)		34				m	y	
Vucic et al., (2008)		49		1.17		f	y	
AVERAGE		43.71		2.5	52.5			

**Table 5.2 Summary of averaged clinical data for E100G cases**

Reference	Mean onset age (years)	Mean duration (years)	Mean age at death (years)	Comments
Juneja et al., (1997)	48.5	5.1		23 individuals
Orrell et al., (1999)	57-75	7		3 pedigrees
Orrell et al., (1997)	47-50	6-8		2 pedigrees including same patients as Rosen et al., (1993) and Yulug et al., (1995)
Aggarwal and Nicholson (2005)			54 .17	33 individuals from 1 pedigree
Cudkowicz et al., (1997)	46 3/4	4		26 individuals from 2 pedigrees

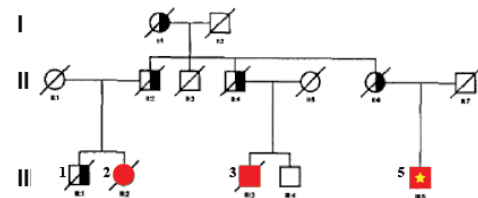
## Pedigree 2

A four generation pedigree with 8 affected individuals was identified in New Zealand in 1995 by Calder et al.,. An autosomal dominant pattern of inheritance was displayed, as shown in Figure 5.3a. One surviving affected case, III-5, was genotyped and found to have the E100G mutation. Seven individuals from generation four (not shown on the pedigree), who were offspring of the affected cousins of III-5 (III-1, 2 and 3), were also genotyped. Five out of the 7 offspring were found to have the mutation. None of these generation four individuals were clinically affected, however no information is given as to their ages. Dismutase activity measured from RBCs found that in family members with the mutation, activity was between 70-85% that of controls, higher than was reported in patients by Deng et al., (1993). The authors also note that when measured on multiple occasions, the dismutase activity of E100G cases was more variable than that of non-mutant family members or controls, and state that, from unpublished data, the E100G mutant is less heat stable than the wild-type. They suggest that the reduced activity may be due to decreased stability and that inconsistencies in measured activity between reports may be due to the more labile nature of the protein to differences in sample handling. Calder et al., (1995) also show that WT homodimers, mutant homodimers and WT:mutant heterodimers are present in the RBCs and that mutant homodimers and heterodimers have lower activity than the WT homodimers. However, what is not clear is whether this lower activity level is due to a lower number of including the mutant protein, or the reduced activity of the mutant protein.

Two case studies of deceased members of generation three are presented by Calder et.al., (1995). There is some discrepancy in the nomenclature, as III-2 is referred to as male in the text but female in the pedigree chart and vice versa for case III-3. Here I will use the reference given in the text. Case III-2 was a male, with onset at age 46 in the lower limbs later spreading to the upper limbs. He survived 4.75-years. Case III-3 was a female, with lower limb onset at 49-years of age. Symptoms spread to upper limbs and included, at later stages, bulbar symptoms in the jaw and neck. She survived 5.2-years. Cause of death is not described for either case. Although the mutation was not confirmed in either of these cases, it was identified in an affected cousin and offspring.

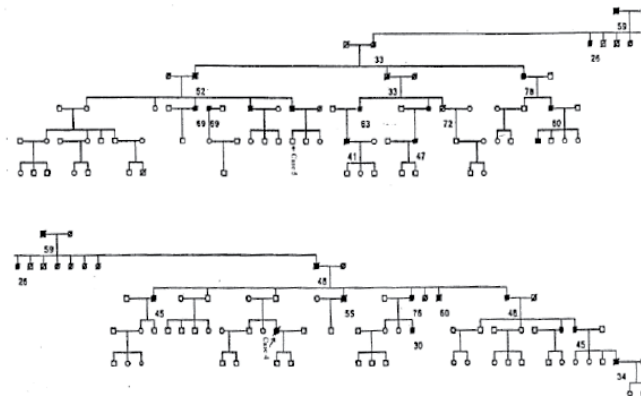
### E100G Pedigrees

(a)



Calder Family E100G Pedigree  
Modified from Calder et al., (1995)

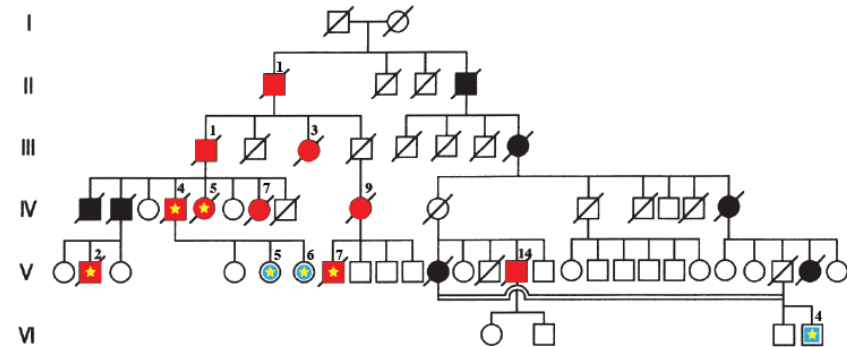
(b)



Aggarwal Family E100G Pedigree. No key is given in the paper  
Modified from Aggarwal et al., (2005)

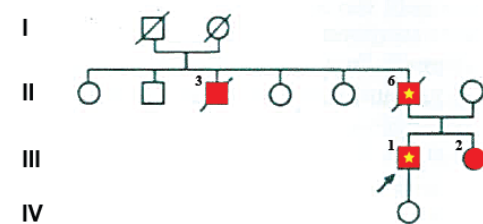
### L126delTT Pedigrees

(c)



Oki Family L126delTT Pedigree  
Modified from Watanabe et al., (2001)

(d)



Kawamata Family L126delTT Pedigree  
Modified from Kawamata et al., (1996)

### Figure 5.3 Humanisation mutation pedigrees

(a) and (b) show the two available E100G pedigrees. (c) and (d) show the available L126delTT pedigrees

Square= male, circle = female. Confirmed or suspected ALS cases are filled/half-filled in black. Deceased cases are struck through. Cases of ALS or suspected ALS for which details are reported in the literature are highlighted in red. Non-symptomatic carriers of the mutation are highlighted in blue. Cases in which the mutation has been confirmed are denoted by a yellow star.

### **Pedigree 3**

The next case was reported in 1996 by a UK based group (Ince et al., 1998) and is a single case report with autopsy. The proband was female with onset in the upper and lower limbs of the left-hand side, at age 36. At a late stage she became severely tetraplegic with only mild bulbar involvement. She survived 3.25-years from presentation due to respiratory failure.

Post mortem diagnosis was “ALS with posterior column involvement”. Briefly, examination of the spinal cord (SC) showed severe astrocytosis in the cord and roots, microglial infiltration and loss of lower motor neurons (LMNs) with some of the remaining LMNs appearing atrophic. In several motor nuclei in the brain a similar pattern was reported. Few ubiquitin inclusions were identified, and no SOD1 inclusions were identified, neither was neurofilament pathology. Demyelination was apparent in the white matter of the SC.

Four relatives of the same lineage suffered from “progressive motor disorders”, suggesting an autosomal dominant inheritance. They died at ages 46, 42, 52 and one at an unascertained age. None of her three siblings had signs of disease.

The same case was also examined by Shaw et al., (1997) for the presence of somatic mutations in *SOD1*, which were not found.

### **Pedigrees 4, 5 and 6**

Orrell et al., (1997) present data from two E100G families, both from the UK, with an autosomal dominant pattern of inheritance. Dismutase activity was assayed from RBCs as 63.5% that of controls. Graphs show survival of around 6-8-years, onset between ~47-50-years, and age at death between ~40-70-years of age. A later follow up in 1999 (Orrell et al., 1999) reports data including a 3<sup>rd</sup> family and graphs showing duration of ~7-years and age at death of ~57-75-years of age.

### **Pedigree 7 and 8**

Cudkowicz et al., (1997) examined a very large group of 366 families with fALS based in America and Europe. Two E100G families were identified, encompassing 26 patients. These may include the same patients reported by Deng et al., (1993) and Rosen et al., (1993). The mean age of onset for the E100G cases was 46.9-years of age (matching the average across all SOD1 families), with a range of 21-72-years. The mean duration was 4-years (3.9 averaged for all *SOD1* mutations), ranging from 1-10-years with a median of 4.

### **Pedigree 9**

Aggarwal et al., (2001; 2002; 2005; 2012) carried out a prospective study following an Australian family with the E100G mutation including 5 asymptomatic, E100G mutation carrying relatives of known ALS case. This first study examined whether the electrophysiological test of motor unit number estimation (MUNE) was able to detect pre-symptomatic loss of MUs. Eighteen asymptomatic carriers of 4 different mutations were followed, and specific data for the E100G cases are not given. No pre-symptomatic MU loss was detected, and neither was there in a 3-year follow up (Aggarwal et al., 2002; Aggarwal et al., 2001). In 2005 (Aggarwal, 2012) Aggarwal and Nicholson, presented a large, 6 generation, E100G family tree (Figure 5.3b, presumed to be the same family reported in 2001), which includes 33 ALS cases showing an autosomal dominant pattern of inheritance. Details of which individuals within the pedigree were confirmed to have the E100G mutation are not given. The average age of ALS related death was 54.2-years, ranging from 26-78.

In a 5 year follow up, 2 out of the 5 E100G carriers had gone on to develop ALS (Aggarwal, 2012). The first case, a woman diagnosed at 48-years of age, died only 4-months later due to respiratory failure. The second case, a male and second cousin once removed from the first, had a longer disease course. Onset was at around 44-years of age, and within 3-months the patient was unable to stand unaided. He was treated with Riluzole and was still alive 10-months later, but was dependent on ventilation at night and tube feeding.

### **Pedigree 10?**

Another paper examining both asymptomatic and symptomatic E100G carriers gives brief details of one male case with upper and lower limb onset at age 34, and a second female case with lower limb onset at age 49, with a disease duration of 14-months. An asymptomatic 45 year old female with the E100G mutation is also described (Vucic et al., 2008). Similar to the previous pedigree, this group was based in Australia, and a co-author (Garth Nicholson) is shared, so it is possible that the same individuals/pedigrees are presented. Later, Vucic et al., (2013) presented evidence of anticipation, which included at least one E100G family with a three generation, autosomal dominant, pedigree.

Finally, Juneja et al., (1997), an American group, present averaged data for twenty-three E100G cases. The mean age of onset was 48.6-years and disease duration was 5.1-years. The cases are described as showing autosomal dominant inheritance. Whether the cases were from a single or multiple pedigrees is not stated.

#### 5.2.2.1.2 *In Vitro* SOD1<sup>E100G</sup> Literature

A number of papers have been published examining the *in vitro* properties of E100G mutant human SOD1 and shall be briefly reviewed here.

Several papers use a “pseudo WT” protein in which cysteines 6 and 111 (the 2 free cysteines not involved in native disulphide bonding) are mutated to alanine and/or serine, respectively, to allow reversibility of unfolding. In this context and using holo proteins, the E100G mutant has been reported as the most stable of 4 mutants (G85R, G93R, E100G, I113T), in regards its thermal unfolding kinetics, in the presence of chemical denaturants (Rumfeldt et al., 2006; Rumfeldt et al., 2009). Contrary to this, in the context of a normal WT sequence, and using apo proteins, Rodriguez et al., (2005), identified E100G as having the lowest thermal stability of 20 SOD1 recombinant mutants examined.

A number of other papers examining a variety of properties have compared mutant to WT SOD1, and reported no particular distinguishing features of the E100G mutant protein. Such properties include: the aggregation propensity of holo and apo proteins *in vitro* in response to chemical denaturants or heat (Stathopoulos et al., 2003); aggregation propensity in mammalian cell expression assay (Prudencio et al., 2009b); the effect of mutation on the kinetics of dimer dissociation and monomer unfolding of the apo and holo protein in pseudo WT contexts (Vassall et al., 2006; Rumfeldt et al., 2009; Lindberg et al., 2005); post-translational folding and modifications (Bruns et al., 2007).

#### 5.2.2.2 SOD1<sup>L126DELTT</sup>

The second mutation selected, referred to here as L126delTT, is a deletion of two thymines in the 127<sup>th</sup> codon (TTG to ΔΔG) of the *SOD1* gene. This mutation results in a frame shift, as shown in Figure 5.2, deleting the last 28 amino acids (aa), introducing 5 alternative C-terminal aa and producing a truncated protein totalling 130 aa (including the initial methionine) and lacking a region important for dimer contact (Watanabe et al., 1997a).

##### 5.2.2.2.1 Patient Literature for the SOD1<sup>L126delTT</sup> Mutation

All the patient data described in this section are summarised in Table 5.3.

#### **Pedigree 1. The Oki family**

The earliest reference for this mutation is from Pramatarova et al., (1994) who, identified the mutation in all 3 of the living ALS sufferers from a large pedigree from Japan, referred to as the Oki family. This pedigree has been well documented with at least 7 papers published which include details of members of the family. The pedigree (Watanabe et al., 2001b) is shown in Figure 5.1c, where cases referred to here are highlighted. The first published account of a



member of the Oki family is from 1972 (Takahashi et al., ) and describes an autosomal dominant pattern of inheritance through 3 generations including 5 cases of ALS. A case report described a woman (referred to as III-5 in this paper and as IV-5 in later papers) with onset in the right arm at 45-years of age who was diagnosed with fALS with posterior column involvement. Her symptoms progress to include all 4 limbs and the pelvic girdle. The patient died of respiratory failure 1.5-years after onset. Post mortem examination of the cervical and thoracic cord reveal MN loss, astrocytosis, hyaline inclusions and some demyelination. This case was further examined at a later date by Kato et al., (1996) who highlighted the presence of Lewy body hyaline inclusions (LBHI) in the MNs which were positive for SOD1, ubiquitin and phosphorylated neurofilament, along with SOD1 and ubiquitin positive glial inclusions which were negative for phosphorylated neurofilament.

In 1995 (Nakashima et al., ) the mutation was identified in 2 affected and 3 unaffected family members from generations IV, V and VI of the Oki family. The 2 affected family members, V-2 and IV-4, were aged 26 and 53 and had been on ventilatory support for 2 and 10-years respectively. The unaffected carriers, cases V-5, V-6 and VI-4, were aged 26, 23 and 33, respectively, at the time. All mutation carriers had reduced dismutase activity as assayed from RBCs, with affected cases having a reduction of 65-70% and unaffected carriers a reduction of around 35%.

Case IV-4 was described in some detail after his death, at age 65, caused by "accidental intraperitoneal hemorrhage" (Kato et al., 1996). This male patient had onset initially affecting the pelvic girdle, at 54-years of age. Within 6-months he was unable to walk and was dependent upon respiratory support within 2-years of diagnosis. He had a long disease duration once utilising respiratory support, surviving 11-years from diagnosis. Unusually, he experienced eye movement disturbance after 5-years of the disease. Pathology was similar to case IV-5; there was a loss of SC MNs and LBHIs were positive for SOD1, ubiquitin and phosphorylated neurofilament, however unlike case IV-5, such inclusions were present not only in the MNs but also in neurons outside of the motor regions. SOD1 and ubiquitin positive, phosphorylated neurofilament negative inclusion were also present in SC astrocytes and some demyelination was reported. SOD1 inclusions were negative for Congo red and thioflavin S suggesting a non-amyloid form. As well as degeneration and loss of SC MNs, severe degeneration was also noted in the dorsal horns (Kato et al., 1996). When assessed by western blot and in gel activity assay, the truncated mutant SOD1 protein was not detected in post mortem tissue obtained from case IV-4. Instead, western blot revealed only the WT sized protein which was at 50% the intensity of control WT samples, although RT-PCR from mRNA

confirmed that the mutant allele was being transcribed at normal levels (Watanabe et al., 1997a).

Two review papers from Watanabe et al., (2000; 2001b), present some more information on case V-2 who had a slightly unusual disease progression. This male proband had onset in the lower legs predominating on the left side, at an early age of 22-years. Symptoms spread to include the upper limbs and 14-months after onset bulbar symptoms developed. 1.5-years after onset the patient received a tracheotomy and respiratory support. The patient died 3-years and 8-months after diagnosis at which time eye movement and urinary disturbance were also noted.

The average age of onset for the Oki family is 42, ranging from 22 to 54-years of age, with an average duration to death, or dependence on respiratory support, of 2-years from onset (Watanabe et al., 2001b).

SOD1 activity and expression levels were examined in 10 non-specified Oki family members. Activity was found to be reduced by ~40% in non-affected carriers of the L126delTT mutation and by ~70% in affected carriers, as compared to WT family members. A positive correlation between SOD1 activity and quantity in RBCs suggests that the reduced activity is due to a lack of protein (Watanabe et al., 1997a).

Also of note is a case briefly presented by Bruijn et al., (1998). The case is only described as being a 2 bp deletion in codon 126 leading to a truncated protein, however, one of the co-authors is also a co-author in many of the Oki family papers, and so it is likely that the case presented is an Oki family member. A figure shows marked SOD1 pathology detected using an antibody specific to a region of SOD1 which is absent in the truncated protein, and so presumably detecting WT SOD1 aggregation in the absence of the mutant protein.

## **Pedigree 2**

At least two other pedigrees of the L126delTT mutation, both from Japan, have been reported. The first, reported in 1996 (Kawamata et al., ) is a brief case report of a male with onset in the right arm at 44-years of age. He was still alive 2-years after onset, when symptoms had spread to all 4 limbs. His father was suspected of having died of ALS and was confirmed as carrying the mutation from analysis of a muscle biopsy sample. The father had onset in the left arm at 66-years of age. His symptoms spread to include both arms and the intercostal muscles causing shortness of breath. He died at 68 from pneumonia and was still able to walk at this time. The paternal uncle also died of ALS, predominating in the lower limbs, 2-3-years after

onset. The proband's younger sister was also suspected as suffering from ALS. The pedigree chart is shown in Figure 5.3d.

### **Pedigree 3**

Kadekawa et al., (1997) present an autopsy case of a female who was diagnosed with ALS at 42-years of age with onset in the lower left leg spreading into the right. Within 1.5-years of diagnosis, the patient had developed bulbar signs and was dependent on a respirator. She died of pneumonia after 2-years and had also suffered 2 heart attacks during the later stages due to asphyxiation. Her older brother, father and paternal uncle had also died following a similar clinical disease course. The proband's details are summarised in Table 5.3, but her relatives are not included as no details are available. SOD1 activity from RBCs was reduced by ~70% and the truncated mutant protein was not evident by western blot. Post mortem examination of the brain and SC revealed MN loss and astrogliosis, with no dorsal horn involvement. MN LBHs were also found and were positive for ubiquitin, phosphorylated neurofilament, but unlike those cases from the Oki family, were found to be negative for SOD1. Different tissue processing protocols and antibodies were used by the two groups and may explain this difference.

Three further papers have been published examining various aspects of this case. Ogawa et al., (1997) used immunoprecipitation followed by high performance liquid chromatography (HPLC) and /electrospray ionization mass spectrometry (ESIMS) to quantify levels of WT and mutant protein from patient erythrocytes, but failed to detect any L126delTT SOD1 in the case described by Kadekawa et al., (1997). Similar to previous findings in sALS patients, 14-3-3 proteins, which are involved in apoptotic and cell proliferation signalling pathways, were found to localise in the LBHs of this patient (Kawamoto et al., 2005). Markers of increased oxidative stress were also identified in MNs and glia in SC sections from this patient (Shibata et al., 2007).

**Table 5.3 Summary of clinical data for L126delTT individuals**

\* figure in brackets is years to dependence on respirator

Pedigree	ID	Onset (years)	Site of onset	Duration (years)*	Age at death (years)	Sex	Mutation confirmed	Cause of death (where cited)	Comments	Ref
Oki	II-1	?			50	m			Died of progressive muscular wasting disease (referred to as I-4 in Takashi et al., 1972)	1,6
Oki	III-1	36	legs	2	38	m			Died of progressive neuromuscular disease (referred to as II-4 in Takashi et al., 1972)	1,6
Oki	III-3	52	legs	3	55	f			Died of progressive neuromuscular disease (referred to as II-5 in Takashi et al., 1972)	1,6
Oki	IV-4	54	pelvic girdle	11 (1)	65	m	y	"accidental intraperitoneal haemorrhage"	Reduced dismutase activity in RBCs. Extraocular involvement (referred to as 839 in Pramatarova et al., 1994)	2,3,4, 5,6,7
Oki	IV-5	45	right arm	1.5	47	f	y	asphyxiation		1,4,6
Oki	IV-7	?	arms			f			Alive at 54 (referred to as III-8 in Takashi et al., 1972)	1,6
Oki	IV-9	54	right thigh	3	57	f				6
Oki	V-2	22	left leg	1.6 (1.5)	25	m	y		Reduced dismutase activity in RBCs. Extraocular and urinary involvement (referred to as 859 in Pramatarova et al., 1994)	2,3,6, 7
Oki	V-5	n/a				f	y		Non-symptomatic at age 26	3
Oki	V-6	n/a				f	y		Non-symptomatic at age 23	3
Oki	V-7	?				m	y		Clinically affected, but no details given (Referred to as 847 in Pramatarova et al., 1994)	2

Pedigree	ID	Onset (years)	Site of onset	Duration (years)*	Age at death (years)	Sex	Mutation confirmed	Cause of death (where cited)	Comments	Ref
Oki	V-14	42	right shoulder girdle	3 (1)	45	f			V-14 respirator at 2 years	6
Oki	VI-4	n/a					y		VI-4 non-symptomatic at age 33	3
2	III-1	44	Right arm	Still alive at 2 years		m	y			8
2	II-3			2-3		m	n		Gait disturbance	8
2	II-6	66	Left arm	2	68	m	y	Pneumonia	Main symptoms in upper body (arms and trunk) still able to walk before death	8
2	III-2	<46				f	n		Younger sister of proband "suspected clinically of having ALS"	8
3	n/a	42	right leg	2 (1.5)		f	y	Pneumonia	Brother, father and paternal uncle also died of ALS like disease	9

1- (Takahashi et al., 1972); 2- (Pramatarova et al., 1994); 3- (Nakashima et al., 1995); 4- (Kato et al., 1996); 5- (Watanabe et al., 1997a); 6- (Watanabe et al., 2000); 7- (Watanabe et al., 2001b); 8- (Kawamata et al., 1996); 9- (Kadekawa et al., 1997)

#### 5.2.2.2.2 *In Vitro SOD1<sup>L126delTT</sup>* Literature

At least 2 papers have been published in which the *in vitro* properties of recombinant L126delTT mutant SOD1 have been examined.

The lack of dismutase activity of L126delTT SOD1 was confirmed in recombinant SOD1 fused to an N-terminal maltose binding domain (MBD) produced in *E.coli* by Watanabe et al., (1997b). Protein yield was ~3 times lower for the L126delTT mutant as compared to the WT within this expression system. Both the MBD fusion and cleaved versions of the WT protein displayed dismutase activity whereas neither MBD fusion nor cleaved L126delTT SOD1 did. The mutant protein also showed a much lower resistance to proteolysis by proteinase K. When expressed in mammalian cells (COS1) without the MBD, the mutant protein was not detectable by either western blot, or activity assay despite confirmation of its mRNA species.

Koide et al., (1998) expressed a number of FLAG tagged mutants and WT SOD1 in COS7 cells to examine their aggregation propensity. At 24 hours after transfection, cells expressing L126delTT were the only in which aggregates were detected and at 48 hours post-transfection ~30% of cells expressing L126delTT had SOD1 positive aggregates as compared to 3-9% of cells expressing A4V, G85R and G93A mutant SOD1 and none in those expressing WT SOD1.

#### 5.2.2.2.3 *SOD1<sup>L126delTT</sup>* Transgenic Mouse Literature

Transgenic mice harbouring L126delTT mutant SOD1 were published in 2005 by the same group who originally identified the mutation in the Oki family (Watanabe et al., 2005). The mice were made using the same human genomic *SOD1* plasmid as was used for the Gurney et al., (1994) WT and G93A mice. Mice with transgenic WT and L126delTT mutant and FLAG tagged versions of both were produced and 2 founder lines for each were phenotyped.

Neither the WT nor WT-FLAG lines developed ALS like disease during their life span. Those mice with the L126delTT mutant SOD1 transgene (either with or without the FLAG tag) with the highest number of copies did develop ALS like symptoms with hind limb paralysis, muscle atrophy, weakness and weight loss. As summarised in Table 5.4, mice homozygous for the transgene developed symptoms earlier and died earlier than hemizygous mice. Mice with the L126delTT-FLAG transgene had an earlier onset and death despite having a lower transgene copy number, however, while western blots detected small quantities of the mutant SOD1 in the L126delTT-FLAG mouse, immunoprecipitation followed by western blot was needed to detect the very low quantities of mutant SOD1 present in the L126delTT line without the FLAG tag. SOD1 activity was no different to non-transgenic mice when assayed from the L126delTT or L126delTT-FLAG hemizygous lines which develop disease, but was increased 3-4 times in a WT line (summarised in Table 5.4). Northern blot of mRNA isolated from fibroblasts from the

mice confirmed that the transgenes were being transcribed at the levels expected by their copy number and so the low level of protein in the mutant lines was either due to reduced protein translation or increased degradation. Histological examination of the SC of the mutant lines revealed loss of MNs of the ventral horn and gliosis. Inclusions resembling LBHIs were also present in the remaining MNs and these were positive for SOD1 and for FLAG in the FLAG tagged lines. At least 4 subsequent papers have been published using the homozygous L126delTT-FLAG mice as models of ALS.

Fukada et al., (2007) found that the L126delTT-FLAG mice, as compared to WT-FLAG mice, displayed differential expression of a number of genes, including heat shock proteins and genes related to inflammation and autophagy and found some parallels with similar work carried out in the G93A mutant SOD1 transgenic mouse. Doi et al., (2008) found low level SOD1 deposits in vacuolated mitochondria of the SC neurons of pre-symptomatic L126delTT-FLAG mice, along with fibrillar inclusion in the ventral horns with high levels of SOD1. This was similar to observations in other mutant SOD1 transgenic mice, however the quantity of SOD1 deposited in vacuolated mitochondria was lower than in other models; this may not be surprising considering that the L126delTT-FLAG mice have been shown to have only a very low level of mutant SOD1 protein.

**Table 5.4 Summary of L126delTT mutant *SOD1* transgenic mice phenotypes**

Data from Watanabe et al., (2005) is summarised. The human end point was defined as being unable to right themselves within 30 seconds of being placed on their side.

SOD1 activity assayed from brain and liver

Hemi= hemizygous; Hom=homozygous; n.d.= not determined

Genotype	Transgene copy number	Hemi or hom?	Develops symptoms?	Onset (days)	Death (days)	SOD1 activity (relative to non-transgenic)
WT	1	Hemi	no			n.d.
WT	3	Hemi	no			3-4
WT-FLAG	2	Hemi	no			n.d.
WT-FLAG	3	Hemi	no			n.d.
L126delTT	1	Hemi	no			n.d.
L126delTT	5	Hemi	yes	445	480	1
L126delTT	10	Hom	yes	239	251	n.d.
L126delTT-FLAG	3	Hemi	no			n.d.
L126delTT-FLAG	4	Hemi	yes	341	372	1
L126delTT-FLAG	8	Hom	yes	121	127	n.d.

Finally, Watanabe et al., (2008) carried out a proteomic analysis comparing binding partners of mutant and WT SOD1 in the SC of L126delTT-FLAG and WT-FLAG mice. They found 34 proteins interacting with L126delTT-FLAG SOD1 and only 3 with WT-FLAG SOD1. Among the binding partners of L126delTT-FLAG were ATPases, ATP synthases and heat shock proteins which had been detected in their earlier work carried out with G93A mutant SOD1 mice.

## 5.2.3 BACs Sequence Confirmation

### 5.2.3.1 HUMAN SOD1 BAC

A *SOD1* containing human BAC clone, RP11-535E10 (E10), was selected as described in Section 2.3.1. This BAC was sequenced from PCR amplified sections of between 1,500-2,300 bp, using a proof reading polymerase, *Pfx*, in the touchdown PCR protocol (Section 2.1.2.1). Amplicons covered whole entire *SOD1* gene plus at least 200 bp upstream and downstream (~9.7 kb total).

Four mismatches were found between the sequence of the E10 BAC and the reference sequence (GRCh37.p6, Feb 2009), all in intronic regions, detailed in Table 5.5

**Table 5.5 Mismatches between E10 BAC and reference sequence (GRCh37.p6)**

Chromosomal location	Region description	bp down-stream from exon 1	bp up-stream from exon 2	Reference (GRCh37.p6)	E10 BAC base	Identified in GRCh37.p12
Ch21: 33,032,287	SOD1 intron 1	134bp	> 3.5 kb	C	T	SNP ID rs17881180
Ch21: 33,033,782-33,033,783	SOD1 intron 1	> 1.5 kb	> 2 kb	TT	TTT	no
Ch21: 33,033,786-33,033,787	SOD1 intron 1	> 1.5 kb	> 2 kb	CC	CCC	no
Ch21: 33,033,805-33,033,806	SOD1 intron 1	> 1.5 kb	> 2 kb	TA	TAA	no

Later re-checking of the mismatches using the latest genome reference build (GRCh37.p12) in the Ensembl genome browser ([www.ensembl.org](http://www.ensembl.org)) to identify known sequence variants (tracks checked: all dbSNP, HapMap, all 1000 Genomes, all phenotype and curated variants, all LSDB-associated variants, all phenotype annotations, all individual genomes, all failed variants, all external variant data) revealed that the C>T mismatch at ch21: 33,032,287 has an average frequency of 0.035 (ranging from 0.002 in East Asia to 0.107 in Iberian population in Spain) and



has been given the SNP ID rs17881180. This SNP has been found to be associated with the development of severe nephropathy in people with type 1 diabetes (Al Kateb et al., 2008).

The remaining 3 mismatches, which were not identified as known variants, were single bp expansions, increasing either a double to a triple, or a triple to a quadruple single bp repeat (see Table 5.5). The Ensembl genome browser was used to examine the 25 bp region in which these 3 mismatches were found and the flanking 500 bp upstream and downstream (Chr21: 33,033,282-33,034,306 in reference build GRCh37.p12) to check for the presence of known regulatory or binding regions or transcribed sequences etc. Features checked were: CpG islands, tRNAs, GENCODE genes, all mRNA alignments, ncRNAs, all structural variants, all external variation data, all regulatory features, all other regulatory regions. The only feature identified within this region, an exon from a putative alternative transcript of *SOD1*, is over 50 bp away. This transcript (Ensembl ID ENST00000476106), which lacks an open reading frame, is a manual annotation from the Havana Project based on *ab initio* examination of the genome sequence and is not based on experimental data of an actual transcript. Based on this evidence, these discrepancies were deemed acceptable.

#### 5.2.3.2 MOUSE *Sod1* BACs

Two *Sod1* containing C57BL/6J mouse BAC clones, RP24-363N21 (N21) and RP24-238L18 (L18), were selected as described in Section 2.3.1. These BACs were sequenced in the same manner as the E10 BAC. The initial cloning plan involved subcloning a large region from the mouse BAC to include ~13 kb 5' and ~15 kb 3' homology arms for targeting, and so these two regions were sequenced in entirety. As the region to be used from the mouse BAC is several times larger than that of the human BAC, the chances of finding mutations/mismatches between the BAC and the reference sequence is also higher and so two BACs were selected for sequencing with the best match to be used for construct synthesis.

The first region spanned 13,284 bp 5' of the *Sod1* gene and included the 5' UTR and the start of exon 1. The second region spanned 15,357 bp 3' of *Sod1* and included 106 bp of exon 5.

Two mismatches between the BAC sequences and the reference sequence (NCBIM37) were found. The first was in an intergenic region between *Sod1* and *Scaf4*, was present in both L18 and N21 and the second was within intron 19 of *Scaf4*, and was present on L18 only. These are detailed in Table 5.6.

**Table 5.6 Mismatches between L18 and N21 BACs and reference sequence (NCBIM37)**

BAC	Chromo- somal location (build NCBIM37)	Region	Reference base	BAC base	Chromo- somal location (build GRCm38)	Identified in GRCm38
L18 & N21	Ch16: 90,229,075- 90,229,083	Intergenic between <i>Sod1</i> and <i>Scaf4</i>	TTTTTTTTT (9)	TTTTTTTTT TT (10)	Ch16: 90,228,831- 90,228,838	rs262788338
L18	Ch16: 90,240,240- 90,240,251	Intron 19 <i>Scaf4</i>	AAAAAAA AAAAA (12)	AAAAAAA AAAAAAA AA (14)	Ch16: 90,239,996 -90,240,006	rs387178423 and rs214928959 are both <i>single</i> bp adenine insertions

The Ensembl genome browser ([www.ensembl.org](http://www.ensembl.org)) was used to check if these were known sequence variants in build GRCm38. Tracks checked were: all sequence variants, all variation sets, all structural variants, phenotype annotations. The first mismatch, a single additional T in a 9 bp T repeat was identified as a known deletion/insertion variation with no overlap to Ensembl regulatory or motif sequences. The second mismatch, a 2 bp increase of a stretch of 12 As, was not identified, although a single bp increase was recorded as a known variant (see Table 5.6) and again there was no overlap to Ensembl regulatory sequences. The region surrounding the second mutation, 500 bp up and downstream, was manually checked for the presence of known regulatory or binding regions or transcribed sequences, etc. using the Ensembl genome browser with the following features checked: all genes, all external gene and transcript data, prediction transcripts, all mRNA alignments, all regulatory features, all other regulatory regions. The only feature found within this region, other than the intronic *Scaf4* transcript, was a predicted exon, >250 bp downstream, identified by gene prediction software. Clone N21 was therefore selected for use as it most closely matched the reference sequence.

After starting this project, a new BAC library constructed from C57BL/6N (BL/6N) DNA was made available from Riken. Using this library rather than the C57BL/6J library was desirable as currently mESCs used for gene targeting are derived from BL/6N mice and to increase targeting efficiency the ESC and targeting construct should ideally be isogenic. A *Sod1* containing C57BL/6N BAC, B6Ng01-068O19 (O19), was selected as described in Section 2.3.1.

The O19 BAC was directly sequenced rather than being sequenced from amplified PCR sections. This was desirable for 2 reasons: first it reduced the possibility of PCR introduced mutations being detected, and second, it reduced the number of steps required, making the

protocol faster and without the potential need for optimising PCR amplification steps. The protocol was optimised for sequencing directly from BACS by increasing the annealing temperature thus making annealing more specific, and increasing the extensions time (see Section 2.1.6).

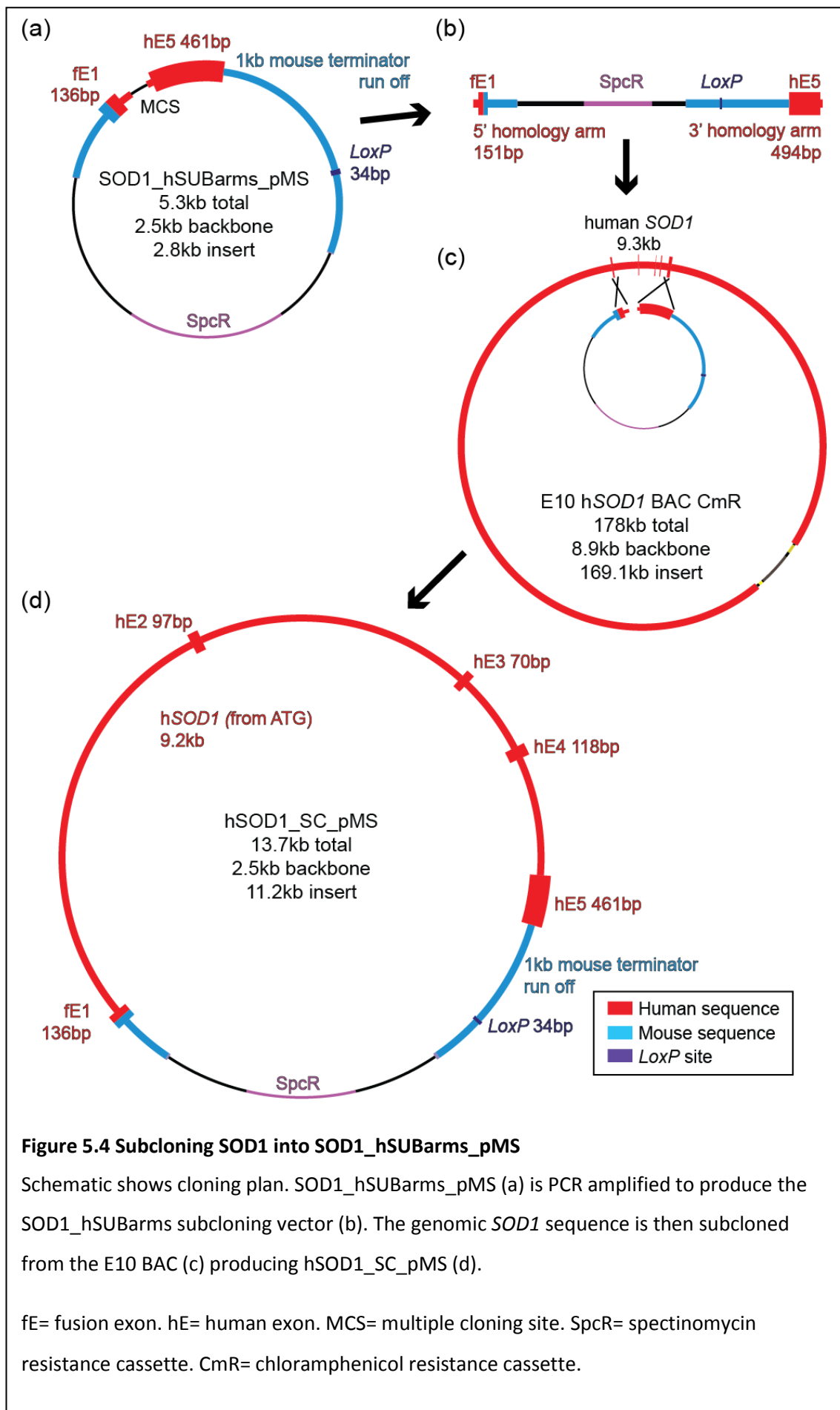
As a reference sequence is not currently available for the C57BL/6N mouse line, it was not possible to tell whether any discrepancies found between the BAC and the available reference sequence, for C57BL/6J, were due to mutation of the BAC clone or strain differences. Therefore, only those regions which would be targeted for homologous recombination during the cloning process were sequenced. No mismatches between the C57BL/6J reference sequence (GRCm38) and the O19 (C57BL/6N) BAC were found.

## 5.2.4 Cloning

Unless otherwise specified, screening PCRs were carried out using the General Plasmid Screening PCR protocol described in Section 2.1.2.2 using plasmid DNA prepared using the Fast protocol described in Section 2.1.1.4, and PCR amplified recombineering vectors were purified for use in recombineering experiments using the QIAprep Spin Miniprep Kit (Qiagen) (Section 2.1.1.2) and resuspended in ddH<sub>2</sub>O.

### 5.2.4.1 SUBCLONING *SOD1* INTO *SOD1\_hSUBARMS\_pMS*

The first step towards making the humanising construct was to subclone the genomic human *SOD1* sequence from the E10 BAC into the *SOD1\_hSUBArms\_pMS* plasmid (described in Section 2.3.3.1). The subcloning plan is summarised in Figure 5.4. The *SOD1\_hSUBArms\_pMS* plasmid was PCR amplified to produce a linear product to be used as a subcloning vector (Figure 5.4a-b). The vector includes a 151 bp, 5' homology arm, matching the human *SOD1* sequence spanning from the ATG in exon 1 into intron 1. A 3' homology arm, 494 bp in size maps to a region of *SOD1* starting within intron 4 and extending to the end of the 3' UTR of exon 5 (Figure 5.4b).



#### 5.2.4.1.1 Preparation of the Subcloning Vector

The SOD1\_hSUBarms vector was PCR amplified using the touchdown PCR protocol (Section 2.1.2.1), using SOD1\_hSUBarms\_pMS as the template with the primers listed in Table 5.7 to amplify the 5,200 bp product. The PCR product was purified using Qiagen PCR purification kit before digestion with *DpnI* (NEB). *DpnI* cuts at a common 4 bp motif (GA/TC) which appears 17 times in SOD1\_hSUBarms\_pMS. The enzyme cuts only methylated DNA so should digest only the parental plasmid template leaving the PCR product intact.

#### 5.2.4.1.2 Recombineering and Screening

The linear SOD1\_hSUBarms PCR product was used to subclone the *SOD1* sequence from the E10 BAC, to produce hSOD1\_SC\_pMS, using RedET recombineering as described in Section 2.4.1.

After selection on spectinomycin LB (LB-Spc) agar plates, an equal number of colonies formed on both the induced and un-induced plates. This suggested that plasmid template from the PCR was still present and able to confer resistance to spectinomycin without the need of recombination to circularise the plasmid.

To test this, 1 µL of the SOD1\_hSUBarms PCR product that was used in the recombineering experiment was transformed into electroMAX electro-competent DH10B *E.coli* (Invitrogen) and a control transformation was also carried out but with the omission of the PCR product. As suspected, transformation of the PCR product resulted in growth on LB-Spc plates, whereas control cells failed to grow. PCR screening of the clones obtained from the transformation experiment were carried out to further confirm the presence of the SOD1\_hSUBarms\_pMS using primers detailed in Table 5.8, SOD1\_SC screening PCR D. This screening PCR amplifies a 357 bp region spanning the multiple cloning site (MCS) of the SOD1\_hSUBarms\_pMS plasmid and, as shown in Figure 5.5, confirmed the presence of circular plasmid despite *DpnI* digestion of the PCR product.

An alternative *DpnI* enzyme (Roche) was also tested, but gave the same results.

**Table 5.7 Primers for amplification of SOD1\_hSUBarms subcloning vector**

	Sequence	Product size
SOD1_hSUB_R	ACCCGCTCCTAGCAAAGG	5,200bp amplified from SOD1_hSUBarms_pMS
SOD1_hSUB_L	GCCCAAAGTTATCTTCTTAAATTTTAC	

**Table 5.8 Primer pairs for *SOD1* subcloning screening PCRs**

<b>SOD1_SC screen A</b>	<b>Sequence</b>	<b>Binding site</b>	<b>Product size</b>
SOD1_mE1_FOR	GTCGGCTTCTCGT CTTGCTC	start mE1	314bp amplified from 5' side of correctly recombined hSOD1_SC_pMS
hSOD_SC_Scr1_R	CACTTGGGCACCG CACC	hI1 within subcloned BAC sequence	
<b>SOD1_SC screen B</b>	<b>Sequence</b>	<b>Binding site</b>	<b>Product size</b>
hSOD_SC_Scr1.2_F	GAAGCTGTTGTCC CAAGTTATCCTGG	hI4 within subcloned BAC sequence	1,194bp amplified from 3' side of correctly recombined hSOD1_SC_pMS
hSOD_SC_Scr1.3_R	CAGTCTCCATCAG CTGTCATTGC	downstream of mouse Sod1 within 1kb terminator	
<b>SOD1_SC screen C</b>	<b>Sequence</b>	<b>Binding site</b>	<b>Product size</b>
SOD1_hE1_FOR	GAGGTCTGGCCTA TAAAGTAGTCG	hE1 5' UTR	193bp amplified from human SOD1 exon1 within the E10 BAC
SOD1_hE1_REV	CTTCTGCTCGAAA TTGATGATG	hE1	
<b>SOD1_SC screen D</b>	<b>Sequence</b>	<b>Binding site</b>	<b>Product size</b>
hSOD_SC_Scr1_F	GCATCATCAATTT CGAGCAGAAGGC	end of hE1 in SOD1_hSUBarms_pMS	357bp amplified from SOD1_hSUBarms_pMS across the MCS OR 1,439bp amplified from SOD1_hSUBarms_pMS+ rpsL across the rpsL_Gen cassette
hSOD_SC_Scr1.2_R	CGATCCCAATTAC ACCACAAGCC	hE5 in SOD1_hSUBarms_pMS	
<b>SOD1_SC screen E</b>	<b>Sequence</b>	<b>Binding site</b>	<b>Product size</b>
SOD1_hSUBarms_L4	GCAGATATCCAGC ACAGTGGC	MCS of hSOD_hSUBarms_pMS	186bp amplified from SOD1_hSUBarms_pMS
hSOD_SC_Scr1.2_R	CGATCCCAATTAC ACCACAAGCC	hE5 in SOD1_hSUBarms_pMS	

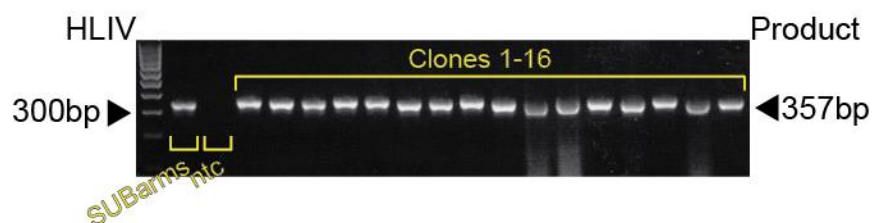


**Figure 5.5 PCR screen D of *E.coli* transformed with SOD1\_hSUBarms PCR**

Screening PCR to check for the presence of SOD1\_hSUBarms\_pMS. PCR D amplifies a 357bp product across the MCS in the presence of SOD1\_hSUBarms\_pMS PCR template.

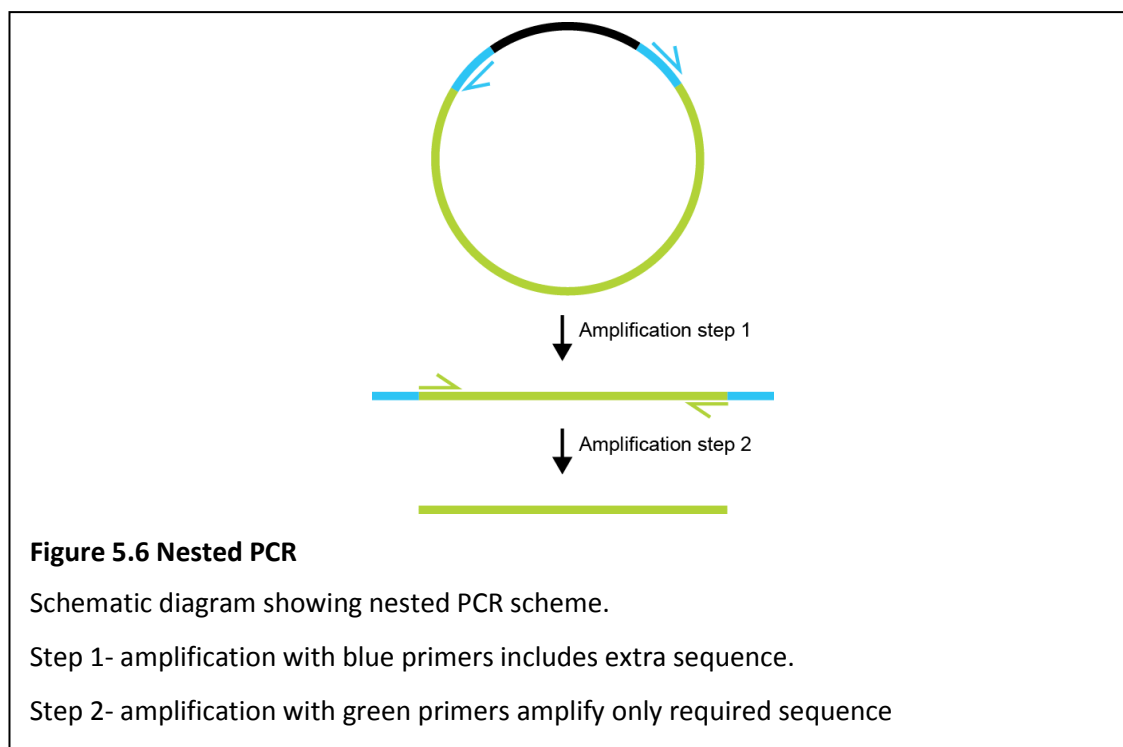
ntc= no template PCR control. SUBarms= SOD1\_hSUBarms\_pMS. HLIV= HyperLadder IV

#### 5.2.4.1.3 Using Nested PCR and Gel Extraction to Reduce SOD1\_hSUBarms\_pMS Background Contamination

As *DpnI* digestion did not appear to be efficiently removing the plasmid template from the SOD1\_hSUBarms vector PCR, a nested PCR strategy was employed. This reduces the amount of template DNA in the final PCR product as only a very small proportion of the first step PCR product is used as template for the second step. Size separation by agarose gel electrophoresis followed by gel extraction was also carried out in order to separate the PCR product from the template plasmid.

#### 5.2.4.1.4 Preparation of the Subcloning Vector

The nested PCR strategy is schematically depicted in Figure 5.6. The first amplification used new primers which bind within MCS of the SOD1\_hSUBarms\_pMS plasmid (depicted in blue in the Figure 5.6 and presented in Table 5.9) using the touchdown PCR protocol (Section 2.1.2.1). The primers amplify a 5,219 bp product which includes the linear vector needed for subcloning SOD1 from the E10 BAC (green in Figure 5.6) but with extra, unrequired sequence, which is not amplified in the second amplification step. The PCR product was gel purified to separate plasmid template from linear product (Section 2.1.1.5). Two  $\mu\text{L}$  of pre-gel purified and 2  $\mu\text{L}$  of post-gel purified PCR were electrophoresed to check that the product had been successfully purified. The second PCR step amplifies just the 5.2 kb SOD1\_hSUBarms vector using 10 ng of the first step PCR product as template and the original primers (Table 5.7. Shown in green in Figure 5.6).



### 5.2.4.1.5 Recombineering and Screening

SW102 recombineering (Section 2.4.2) was used to subclone *SOD1* from the E10 BAC using the nested PCR and gel purified SOD1\_hSUBarms subcloning vector.

After selection on LB-Spc plates, a similar number of colonies grew on both the induced and un-induced plates. Two screening PCRs to detect the presence of the SOD1\_hSUBarms\_pMS were carried out on 26 clones: SOD1\_SC screening PCR D, as above, amplifies a 357 bp product across the MCS of SOD1\_hSUBarms\_pMS. SOD1\_SC screening PCR E amplifies a 186 bp product from SOD1\_hSUBarms\_pMS with primers binding within the MCS and within human exon 5, in the 3' human homology arm of the plasmid. Primers are detailed in Table 5.8

Screening PCR results, examples of which are shown in Figure 5.7, show that all colonies screened contained background contamination from SOD1\_hSUBarms\_pMS.

**Table 5.9 Primers pair for amplification step 1 of SOD1\_hSUBarms nested PCR**

	Sequence
SOD1_hSUBarms_L4	GCAGATATCCAGCACAGTGGC
SOD1_hSUBarms_R4	GCTCGGTACCAAGCTTGGC

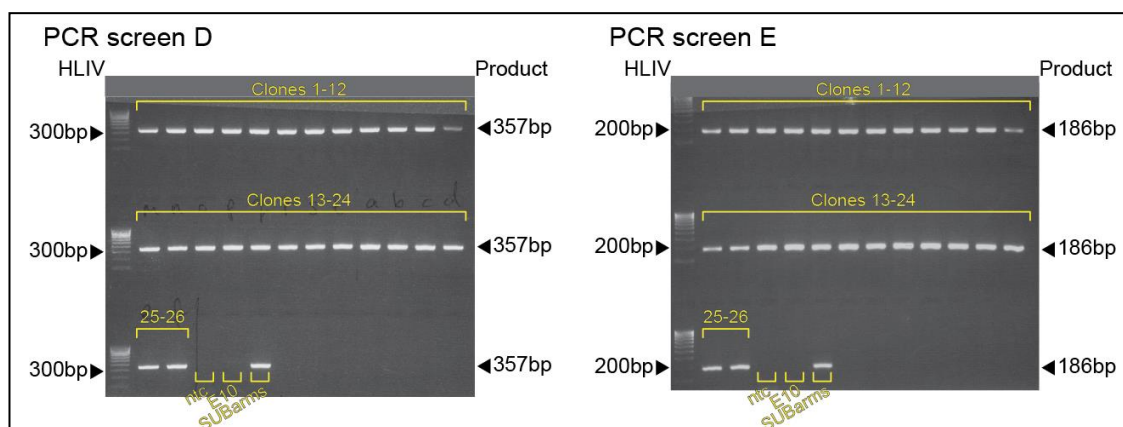


**Figure 5.7 Screening PCR D and E of hSOD1\_SC\_pMS with nested PCR strategy**

Example of screening PCR results to check for the presence of SOD1\_hSUBarms\_pMS after a recombineering experiment to subclone *SOD1* from the E10 BAC into SOD1\_hSUBarms vector, to produce hSOD1\_SC\_pMS, using a nested PCR strategy for vector amplification. PCR D amplifies a 357bp product and PCR E amplifies a 186bp product in the presence of SOD1\_hSUBarms\_pMS

ntc= no template PCR control. E10= human SOD1 containing BAC. SUBarms= SOD1\_hSUBarms\_pMS. HLIV= HyperLadder IV



#### 5.2.4.2 SUBCLONING SOD1 USING SOD1\_hSUBARMS\_pMS+rpsL AS VECTOR TEMPLATE

In a further attempt to overcome the problem of contamination from SOD1\_hSUBarms\_pMS during recombineering experiments, a new strategy was devised and is shown in Figure 5.8. The rpsL\_gen positive/negative selection cassette (see Section 2.3.2.2) was cloned into the MCS of the SOD1\_hSUBarms\_pMS plasmid using restriction endonuclease (RE) cloning with BamHI, and this modified plasmid, SOD1\_hSUBarms\_pMS+rpsL (Figure 5.8a) used as template to PCR amplify the subcloning vector. Inclusion of the rpsL\_gen cassette allows selection against the presence of template plasmid DNA after recombineering.

**5.2.4.2.1 Cloning the rpsL\_gen Cassette into SOD1\_hSUBarms\_pMS**  
*BamHI* sites were first added onto the 5' and 3' ends of the rpsL\_gen cassette by PCR amplification with modifying primers (Table 5.10) using the touchdown PCR protocol (Section 2.1.2.1). These primers amplified a 1,098 bp product using rpsL\_gen cassette PCR (Section 2.3.2.2) as template. The PCR product included the rpsL\_gen cassette (1,077 bp) plus *BamHI* sites (highlighted in red on the primer sequence in Table 5.10) and 5 extra additional bp (underlined in the primer sequence). These extra bp were added to ensure integrity of the RE site and because many REs require additional bases flanking the recognition site to allow efficient binding and cleavage.

**Table 5.10 Primer pair for amplification of rpsL\_gen+BamHI**

	Sequence	Product size
rpsL-ge_BamHI_F	<u>GATTAG</u> <b>GGATCC</b> GAGCATGTTTCTGCGTAGTGTCAGC	1,098bp
rpsL-ge_BamHI_R	<u>GTTAT</u> <b>GGATCC</b> ATCCTGTAGGTGTAGACGACGACG	

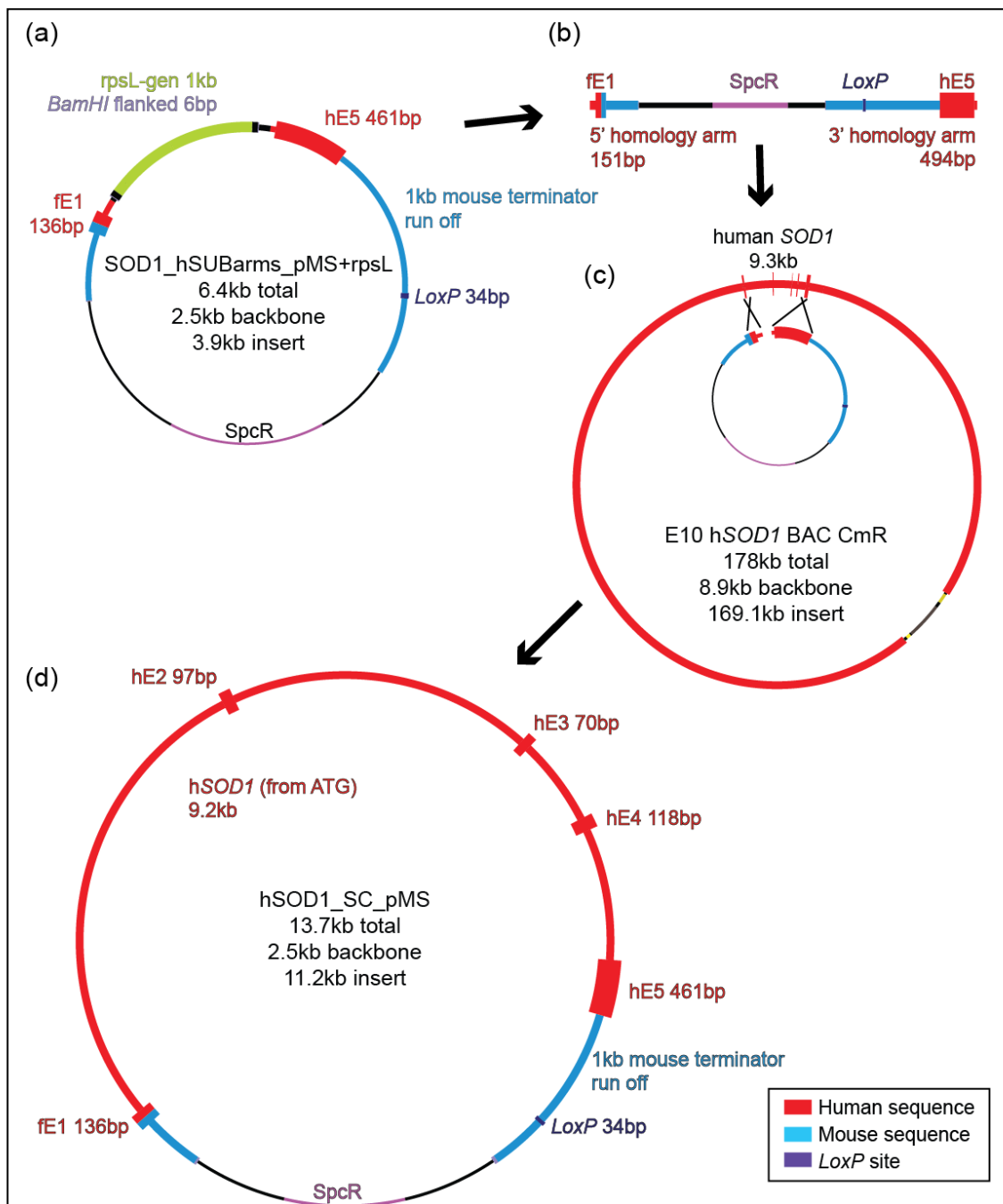


**Figure 5.8 Subcloning *SOD1* into *SOD1\_hSUBarms\_pMS+rpsL***

Schematic shows cloning plan. *SOD1\_hSUBarms\_pMS+rpsL* (a) is PCR amplified to produce *SOD1\_hSUBarms* linear vector (b). The genomic *SOD1* sequence is then subcloned from the E10 BAC into the vector (c) producing *hSOD1\_SC\_pMS* (d).

The presence of the *rpsL\_gen* cassette in the PCR template allows for counter selection against the presence of the PCR template.

fE= fusion exon. hE= human exon. MCS= multiple cloning site. SpcR= spectinomycin resistance cassette. CmR= chloramphenicol resistance cassette. hSOD1= human SOD1

The rpsL\_gen+BamHI cassette was introduced into SOD1\_hSUBarms\_pMS using the *Bam*HI site present in the MCS as described in Section 2.1.5. One µl of the ligation product, SOD1\_hSUBarms\_pMS+rpsL, was transformed into DH10B MAXefficiency chemically competent *E.coli* (Invitrogen) which were selected on gentamicin LB (LB-Gent) agar plates. Five colonies were screened by multiplex PCR using the primers detailed in Table 5.11. A 357 bp product is amplified with primers hSOD\_SC\_Scr1\_F and hSOD\_SC\_Scr1.2\_R in the presence of the original SOD1\_hSUBarms\_pMS plasmid. In the presence of SOD1\_hSUBarms\_pMS+rpsL a 1,445 bp product would be amplified. As the smaller PCR product would be preferentially amplified in the case of both modified and unmodified plasmid being present, a third primer, binding within the rpsL\_gen cassette (rpsL-gen\_IntScrn\_F) was also included. Primers rpsL-gen\_IntScrn\_F and hSOD\_SC\_Scr1.2\_R amplified a 555 bp or 486 bp product from SOD1\_hSUBarms+pMS+rpsL depending on the orientation of the insert. Screening PCR results (Figure 5.9) show that all 5 clones screened were positive for the modified plasmid and negative for the unmodified plasmid.

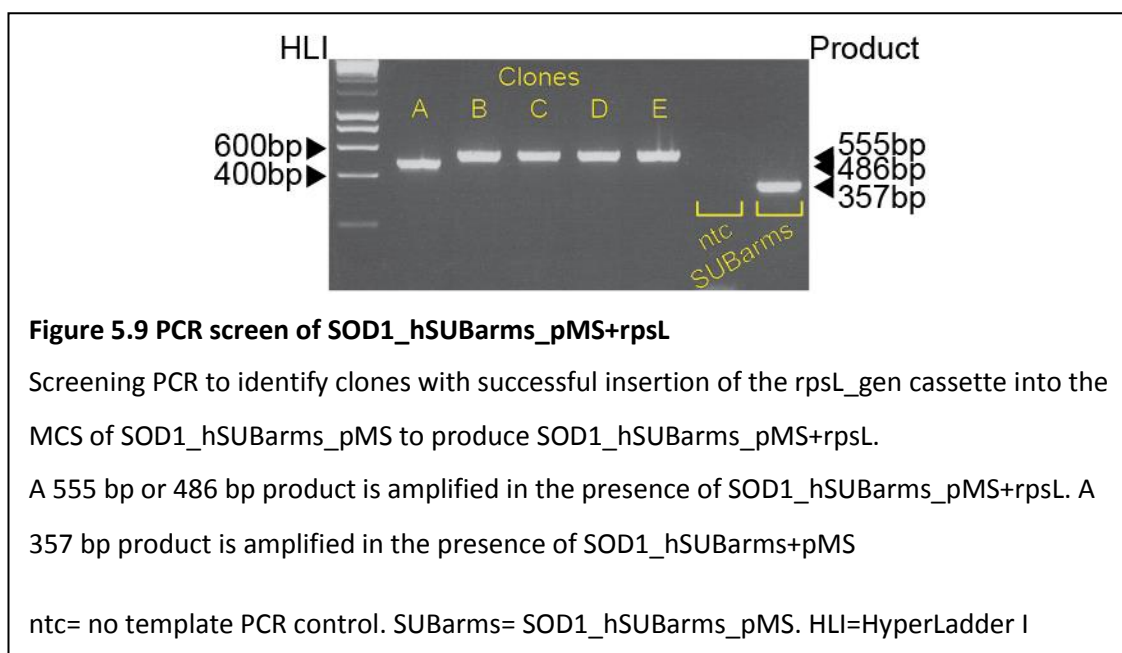
Plasmid DNA prepared from SOD1\_hSUBarms\_pMS+rpsL clone A was used as template for PCR amplification of the SOD1\_hSUBarms vector (primer details as above in Table 5.7).

#### 5.2.4.2.2 Recombineering and Screening

Both SW102 and pRed/ET recombineering (Sections 2.4.1 and 2.4.2) were used in parallel to subclone *SOD1* from the E10 BAC using subcloning vector amplified from SOD1\_hSUBarms\_pMS+rpsL.

**Table 5.11 Primers for SOD1\_hSUBarms\_pMS+rpsL screening PCR**

	Sequence	Binding site	Product size
hSOD_SC_Scr1_F	GCATCATCA ATTTCGAGC AGAAGGC	The end of hE1 in SOD1_hSUBarms_pMS	357bp amplified from SOD1_hSUBarms_pMS across the MCS OR 1,439bp amplified from SOD1_hSUBarms_pMS+rpsL across the rpsL_Gen cassette
rpsL-gen_IntScrn_F	CGCTTGCTG CCTTCGACC	Within rpsL_Gen cassette	486bp or 555 bp amplified from SOD1_hSUBarms_pMS+rpsL, depending on orientation of the insert
hSOD_SC_Scr1.2_R	CGATCCCAA TTACACCAC AAGCC	hE5 in SOD1_hSUBarms_pMS	



The recombineering experiments were plated out with both single (spectinomycin) and double (spectinomycin and streptomycin) selection. Spectinomycin selects for the recombined subclone, hSOD1\_SC\_pMS, and streptomycin selects against the parental template plasmid, SOD1\_hSUBarms\_pMS+rpsL.

With single selection, 32 colonies grew on the SW102 plate and 33 on the pRed/ET plate. With double selection 35 colonies grew on the SW102 plate and 70 on the pRed/ET plate. On the un-induced plates, 1 single colony formed on the SW102 single selection plate and on the double selection pRed/ET plate, suggesting that background contamination from the parental plasmid was not present.

Twenty-three colonies from each induced plate were picked and three PCR screens were carried out using the primers listed in Table 5.8 above. PCR A and PCR B amplify products of 314 bp and 1,194 bp at the 3' and 5' sides, respectively, from the correctly recombined SOD1 subclone (hSOD1\_SC\_pMS). PCR C amplifies a product of 193 bp, from exon 1 of the unmodified E10 BAC.

Results from PCR A and B (Figure 5.10, and summarised in Table 5.12) show that most clones were positive for correct recombination. PCR B also amplified a non-specific product of around 400 bp which was also amplified from SOD1\_hSUBarms\_pMS+rpsL. PCR C showed that the unmodified BAC was also present in all of the clones in which PCR amplification was successful.

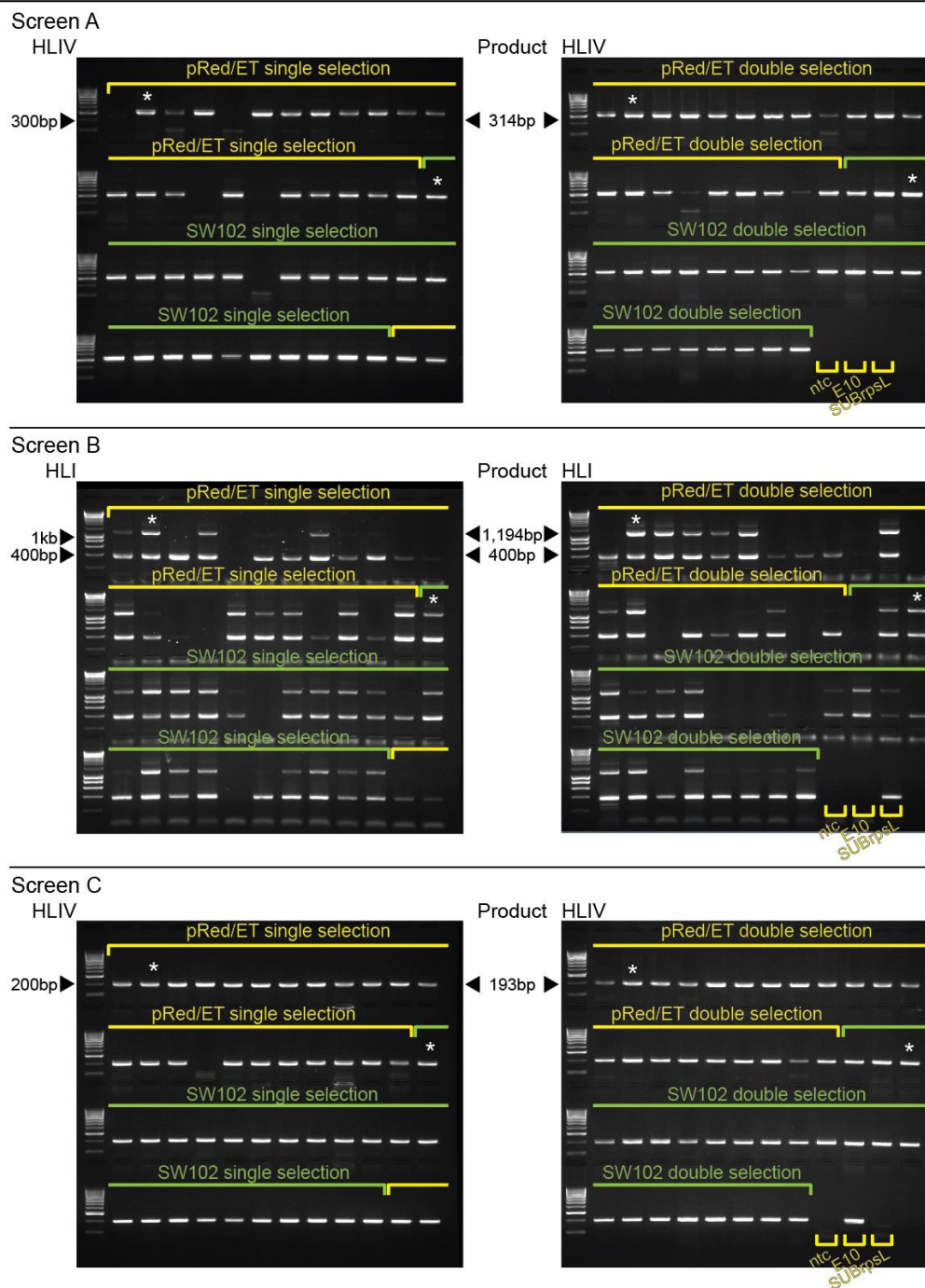


**Figure 5.10 Screening PCRs for *SOD1* subcloning recombineering experiment using *SOD1\_hSUBarms\_pMS+rpsL* as vector template**

**PCR A** amplifies a 314 bp product from 5' recombination of hSOD1\_SC\_pMS.

**PCR B** amplified a 1,194 bp product from 3' recombination of hSOD1\_SC\_pMS. A non-specific product of ~400bp is also amplified.

**PCR C** amplifies a 193 bp product from exon 1 of human *SOD1* in the E10 BAC

ntc= no template PCR control. E10= E10 BAC. SUBrpsL= *SOD1\_hSUBarms\_pMS+rpsL*. HLI= HyperLadder I. HLIV= HyperLadder IV

**Table 5.12 Results of SOD1 subcloning screening PCRs A, B and C**

Table summarises the results of three screening PCRs between the four conditions of the subcloning recombineering experiment. PCR results in brackets e.g. “(B)”, indicate faint a PCR product.

PCR A indicates correct 5’ recombination. PCR B indicates correct 3’ recombination. PCR C indicates presence of un-recombined E10 BAC.

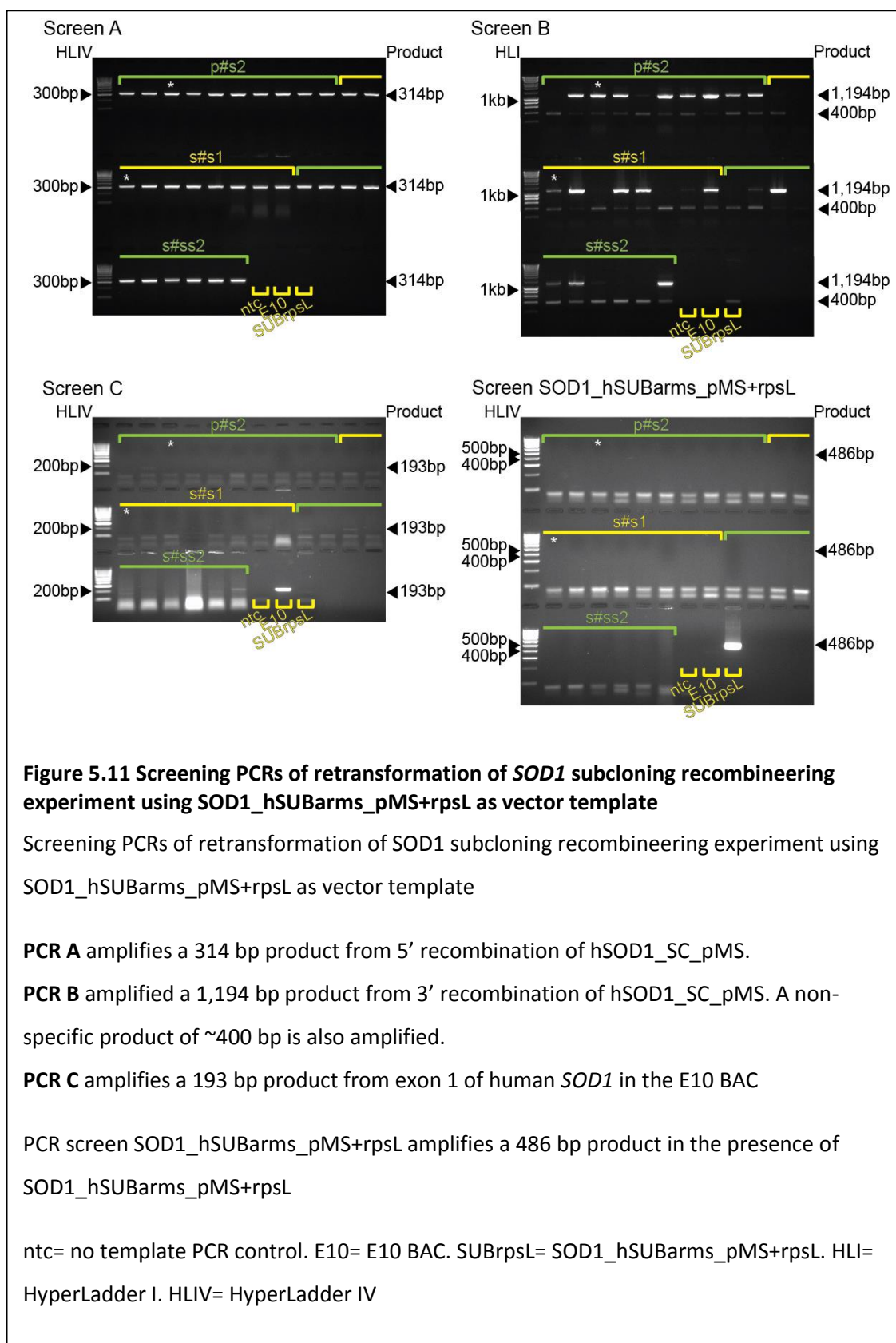
		Positive PCRs	pRed/ET Single selection	pRed/ET Double selection	SW102 Single selection	SW102 Double selection
5' and 3' recombination, plus E10 BAC contamination	ABC		8	6	13	8
	A(B)C			3	4	5
E10 BAC only	C		1		1	
E10 BAC and partial recombination	AC		10	11	5	10
	(A)C		1	3		
	(A)C		2			
All PCRs failed	none		1			

To separate the unmodified BAC from the subclone, plasmid DNA was prepared using the rapid protocol (Section 2.1.1.3) from 4 clones which were positive for both 5’ and 3’ recombination, one for each of the experimental conditions. The plasmid DNA was transformed into SW102 *E.coli* and spread onto spectinomycin and streptomycin LB (LB-Scp+Strep) agar plates.

Retransformed clone p#ss4 (pRed/ET double selection clone 4) did not form distinct colonies, but grew as a smear. Ten 10 colonies each were picked from the other 3 retransformations (p#s2 (pRed/ET single selection clone 2), s#s1 (SW102 single selection clone 1), s#ss2 (SW102 double selection clone 2). Colonies were re-screened using PCRs A, B and C and also the SOD1\_hSUBarms\_pMS+rpsL screening PCR, which amplifies a 486 bp product from SOD1\_hSUBarms\_pMS+rpsL or a 357 bp product from SOD1\_hSUBarms\_pMS (as above, Table 5.8 Table 5.11). PCR B was carried out with an increased annealing temperature of 60°C in order to increase specificity of the primer binding and reduce non-specific amplification.

Screening PCRs results are shown in Figure 5.11, and summarised in Table 5.13.

The 2 clones, highlighted with a star in Figure 5.11, were selected for sequence confirmation.



Plasmid DNA was prepared by Plasmid Maxi Kit (Qiagen) for sequencing, and sequenced directly from plasmid DNA as described in Section 2.1.6. One clone was found to have an 84 bp deletion within the spectinomycin selection cassette of the plasmid backbone. Visual inspection of this region revealed an 8 bp repeat (TGCGGTGG) which may have acted as a site for recombination, as shown in Figure 5.12. This clone was rejected because of the possibility of reduced spectinomycin resistance due to the deletion in the cassette. The second clone had no errors between the plasmid sequence and the reference sequence, other than the original C>T base change in intron 1 which was present in the E10 BAC.

**Table 5.13 Results of SOD1\_SC screening for retransformations PCRs A, B, C and SOD1\_hSUBarms\_pMS+rpsL**

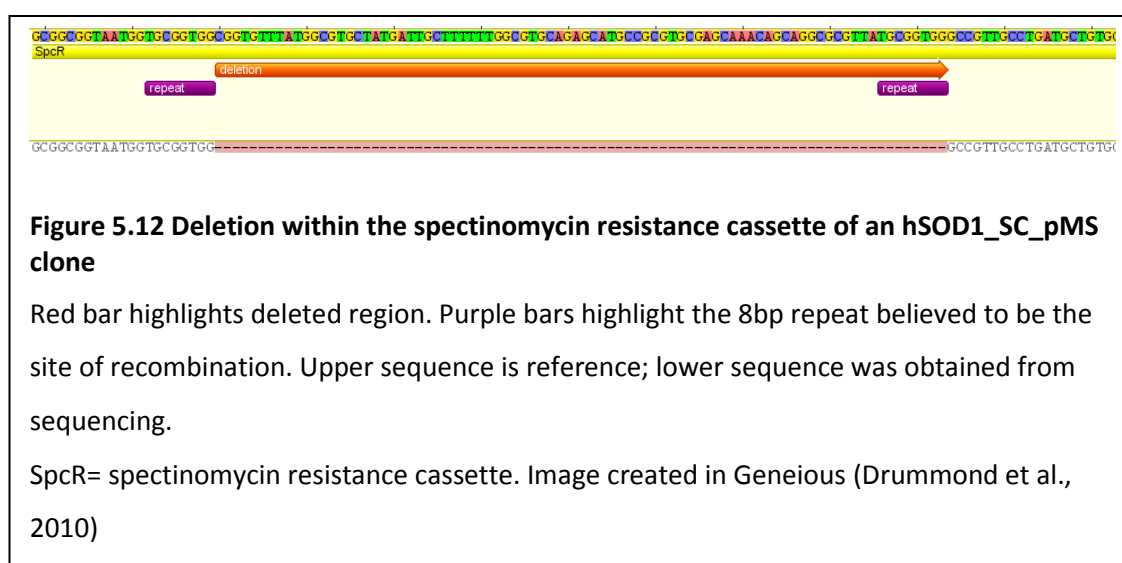
Table summarises the results of three screening PCRs on retransformed clones

PCR A indicates correct 5' recombination. PCR B indicates correct 3' recombination. PCR C

indicates presence of un-recombined E10 BAC. PCR screen SOD1\_hSUBarms\_pMS+rpsL

indicates the presence of SOD1\_hSUBarms\_pMS+rpsL

	Positive PCRs	pRed/ET	SW102	SW102
		Single selection	Single selection	Double selection
5' and 3' recombination	AB	7	5	2
5' and 3' recombination, plus E10 BAC contamination	AB(C)			3
5' recombination only	A	2	5	4
5' recombination and E10 BAC	A(C)			1





### 5.2.4.3 CLONING THE NEOMYCIN CASSETTE INTO *hSOD1\_SC\_pMS*

The next step in the cloning plan was to insert the neo selection cassette, in reverse orientation, into *hSOD1\_SC\_pMS* at the end of the 1 kb mouse terminator, as shown in Figure 5.13, to produce *hSOD1\_SC+neo\_pMS*.

#### 5.2.4.3.1 Preparation of the Targeting Vector

The *FRT* flanked neo cassette (*FRT*-PGK-gb2-neo-*FRT*, Gene Bridges. Section 2.3.2.1) was amplified by PCR as described in Section 2.3.2.1. The PCR product was then used as template in a second PCR using the modifying primers in Table 5.14 to add homology arms for targeting of the cassette to *hSOD1\_SC\_pMS* by recombineering. The 1,701 bp product, *FRT\_Neo\_SC\_Targ*, was amplified using the touchdown PCR protocol (Section 2.1.2.1) and included the cassette (1,601 bp) flanked by 50 bp homology arms on each end (highlighted in red on the primer sequences) targeting the cassette in reverse orientation.

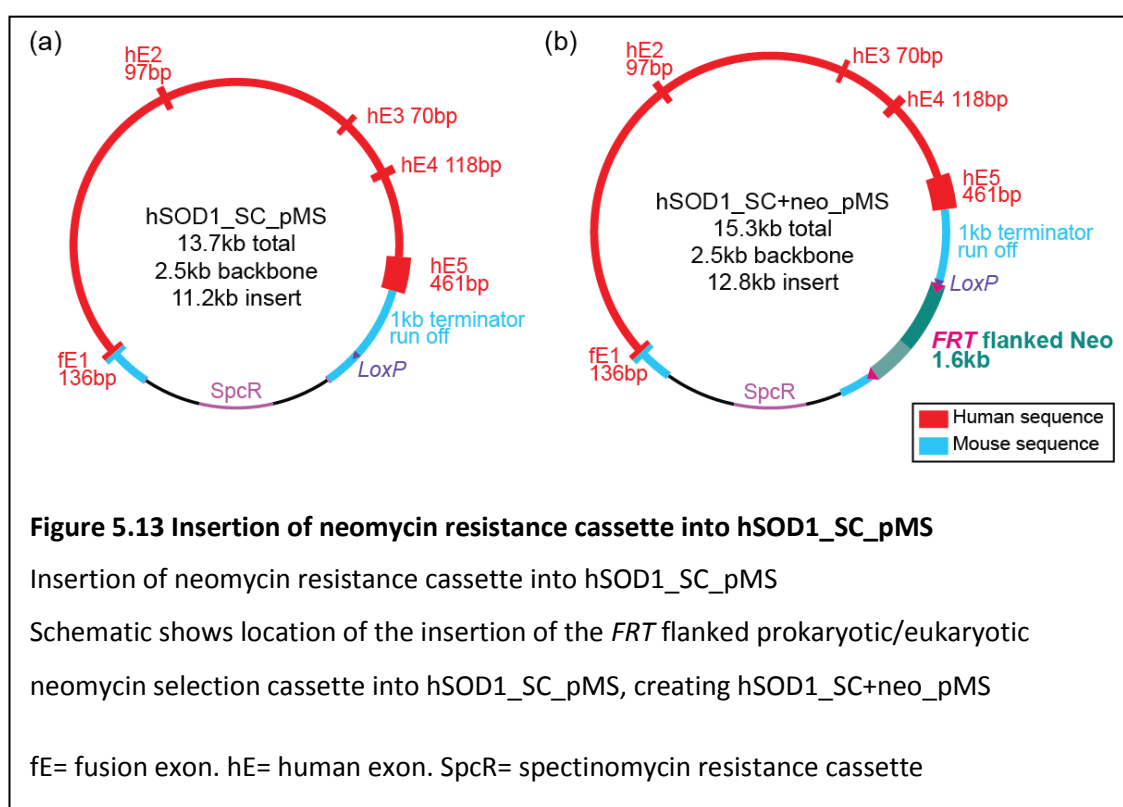


**Table 5.14 Primers for amplification of *FRT\_Neo\_SC\_targ***

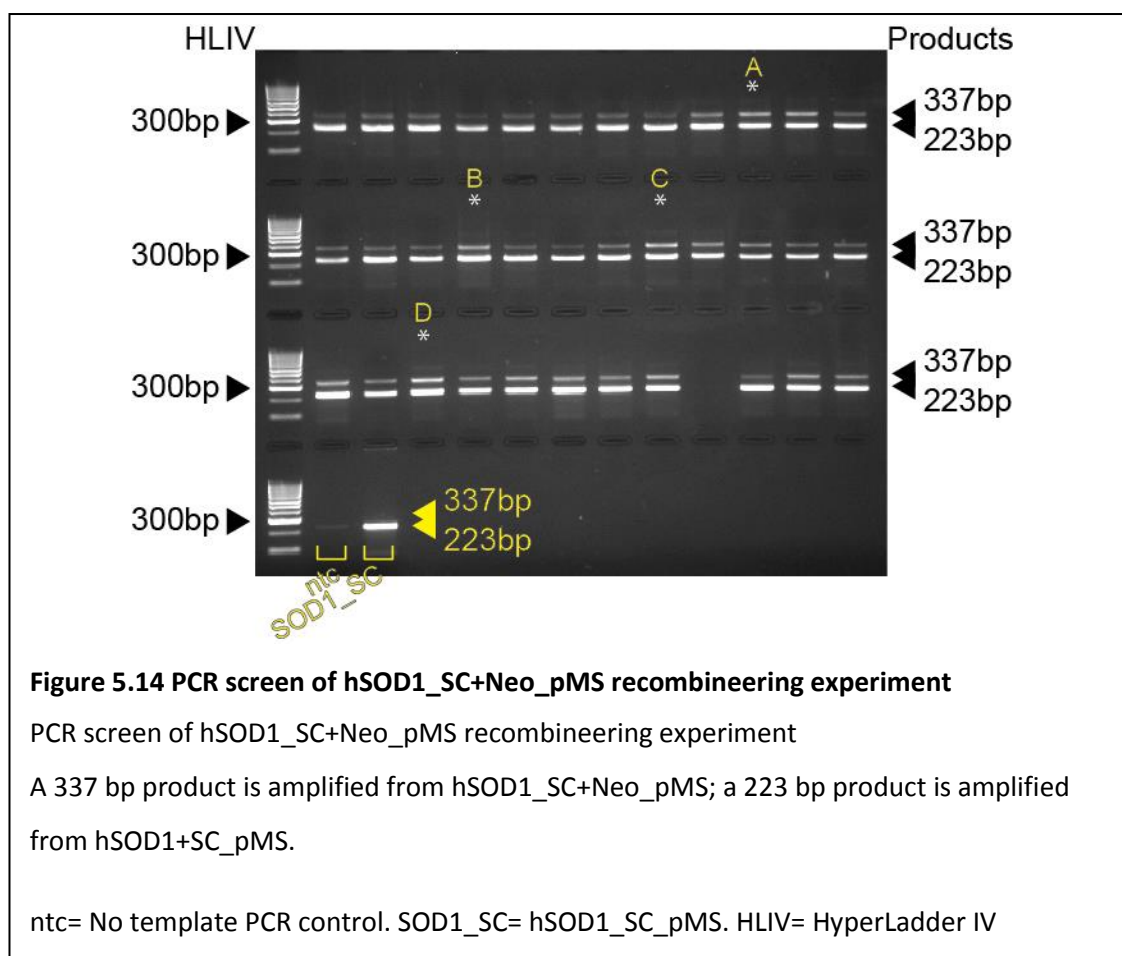
	Sequence	Product size
FRT_hSOD_Targ_F	CATTTAGTGGCTCACGATAACTTCGTATAATGTATGCTATACGAAGTTAT CTATAGGGCTCGAGGAAGTTC	1,107bp
FRT_hSOD_Targ_R	GATTCCAAGGACAGACTTGCAGCTTGTCTTTCCAACATAAAATACTGAG ACGCGAAGTTCCTATTCTCTAGAAAG	

### 5.2.4.3.2 Recombineering and Screening

SW102 recombineering (Section 2.4.2) was used to insert FRT\_Neo\_SC\_Targ into SOD1\_SC\_pMS and clones were selected on kanamycin LB (LB-Kana) agar plates. Over 200 colonies grew on the induced plate and none grew on the un-induced plate. Multiplex PCR screening was carried out using the primers in Table 5.15. The PCR screen was designed to amplify a 223 bp product from the unmodified hSOD1\_SC\_pMS (primers Neo\_Scrn\_F and Neo\_Scrn\_R2 which flank either side of the target site) and a 337 bp product following correct targeting (primers Neo\_Scrn\_R1, which binds within the cassette and Neo\_Scrn\_F). All clones screened positive for both the modified and unmodified target plasmid (Figure 5.14).

**Table 5.15 Primers for screening PCR for hSOD1\_SC+Neo\_pMS**

	Sequence	Binding site	Product size
Neo_Scrn_F	GATGACTCAATGC GGATTAACCTTGG	5' of target site	
Neo_Scrn_R1	CGCTTCCTCGTGCT TTACGG	Within Neo cassette	337bp amplified from hSOD1_SC+Neo_pMS
Neo_Scrn_R2	GGCTTCAGCTTTCT GGTGACC	3' of target site	223bp amplified from hSOD1_SC_pMS OR 1,824 amplified from hSOD1_SC+Neo_pMS



To separate hSOD1\_SC\_pMS from hSOD1\_SC+Neo\_pMS, 4 clones were selected (highlighted in Figure 5.14 with a star, and labelled A-D) and DNA was prepared using the rapid protocol (Section 2.1.1.3). The plasmid preparations were retransformed into SW102 *E.coli* and spread onto LB-Kana agar plates. Five clones from each of the 4 retransformations (A-D) were screened using the same screening PCR. As can be seen in Figure 5.15, 16 of these were pure positives with no background hSOD1\_SC\_pMS contamination. DNA was prepared from 4 of the pure clones (highlighted in Figure 5.15 with a star) using the rapid protocol (Section 2.1.1.3). The inserted neo cassette, homology arms, and at least 30 bp flanking was sequenced directly from the plasmids (Section 2.1.6) to confirm the absence of mutations and correct targeting.

#### 5.2.4.4 INTRON 3 *LoxP* INSERTION USING OLIGONUCLEOTIDE RECOMBINEERING

To allow the human *SOD1* gene to function as a conditional mutant allele, a *LoxP* site was introduced into intron 3 of hSOD1\_SC+neo\_pMS to produce hSOD1\_SC\_N\_L\_pMS.

This step used oligonucleotide recombineering, in which single stranded synthetic oligonucleotides (oligos) are used to mutate, insert or delete short stretches of DNA. As described in Section 1.3.2.2, ssDNA oligo recombineering is more efficient than recombineering using a dsDNA donor, particularly when the oligo is designed to act as an Okazaki fragment, annealing to the lagging strand of the replication fork. For this reason it is often possible to produce mutations in a single step, without antibiotic selection, by using sibling selection (see Section 2.4.5) to increase the number of clones screened.

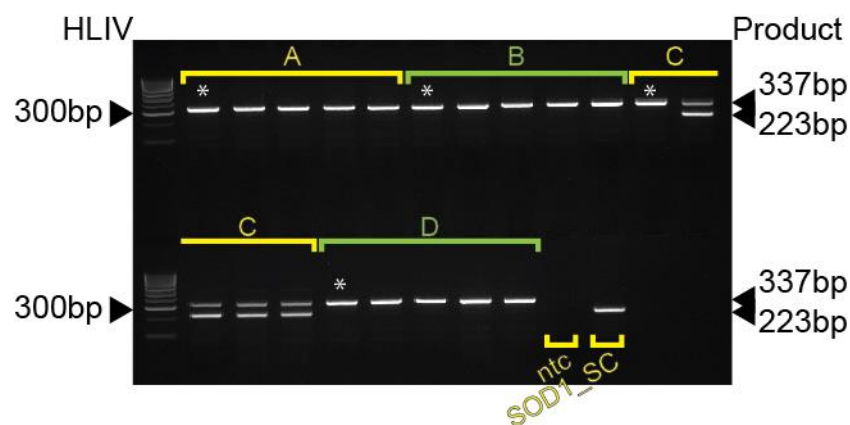


**Figure 5.15 PCR Screen of retransformation of hSOD1\_SC+Neo\_pMS recombineering experiment**

A 337 bp product is amplified from hSOD1\_SC+Neo\_pMS; a 223 bp product is amplified from hSOD1+SC\_pMS. Five colonies from each of 4 retransformed clones (A-D) were screened

ntc= no template PCR control. SOD1\_SC= hSOD1\_SC\_pMS. HLIV= HyperLadder IV

#### 5.2.4.4.1 Recombineering and Screening

The oligo, 3-4\_LoxP\_R (see Table 5.16) was used to target the hSOD1\_SC+neo\_pMS plasmid using SW102 recombineering (Section 2.4.2). The *LoxP* site is highlighted in red in the oligo sequence, and is flanked on either side by 40 bp homology arms.

After recovery, a 1/10,000 dilution of the recombineering experiment was made in LB-Kana and 10 µl aliquots were dispensed into 200 µL LB-Kana, in a 96-well cell culture plate. To estimate the number of cells dispensed into each well, 50 µl each of a 1/1,000 and 1/5,000 dilution were spread into LB-Kana agar plates. After overnight growth, 2 and 31 colonies grew on the 1/1,000 and 1/5,000 dilution plates, respectively, giving an estimate of 0.04-0.62 cells per well. This was much lower than intended; ideally this number would be close to 10, as this allows multiple clones to be screened at once while keeping the number low enough to allow clones to be separated at subsequent screening steps.

PCR screening of sibling pools was carried out using the primers in Table 5.17. The multiplex screening PCR amplifies a 361 bp product in the absence of the *LoxP* site, by primers binding on either side of the target location (primers LoxP\_scrn\_F and LoxP\_scrn\_R). In the presence of the *LoxP* site, a 395 bp product is amplified across the targeting site and a second product of 140 bp is amplified by binding of an additional forward primer (LoxP\_scrn\_F2) which binds within the inserted *LoxP* site.

A PCR product was amplified from almost all of the sibling pools suggesting that more cells were aliquoted into each well of the cell culture plate than had been estimated according to the numbers which grew on the LB-Kana agar plates.

**Table 5.16 *LoxP* targeting oligonucleotide**

	Sequence
3-4_LoxP_R	TTTTCTGAAAGGCTTTCAGAAAACATACACATATAAATGG <del>ATAACTTCGTATAGCA</del> <del>TACATTATACGAAGTTAT</del> AGTCTCGACTAGTTTTTCAGTATCAATTTTTTTTTTATCT

**Table 5.17 Screening primers for *LoxP* insertion**

	Sequence	Binding site	Product size
LoxP_scrn_F	CTTGCTGACTCATCTAAACC CCTGC	5' of target site	361bp amplified from SOD1_SC+neo_pMS
LoxP_scrn_F2	CTAGTCGAGACTATAACTTC G	5' into targeted <i>LoxP</i> site	395bp and 140bp amplified from hSOD1_N_L_pMS
LoxP_scrn_R	CAAAGCTATGTCCCAAGGC CTCTG	3' of target site	

Because the wells of some of the PCR gels were uneven (Figure 5.16) and the size difference between products being relatively small, differentiating a 361 bp and 395 bp band might not have been possible. Based on the migration of the negative control PCR, which used the unmodified hSOD1\_SC+neo\_pMS as template, none of the sibling pools showed an obviously larger product size. The internal primer (LoxP\_scrn\_F2), required for amplification of the 140 bp positive product, had a very low melting temperature (52.6°C), due to the low G/C content of the *LoxP* site and had moderate secondary structure. This was unavoidable as the primer needed to at least partially bind within the *LoxP* site in order to differentiate the targeted and untargeted plasmid. Due to the lack of an available positive control for the PCR, it was not clear whether all clones were, indeed negative, or if the PCR screen had failed to differentiate positive from negative clones.

To identify whether the screening PCR was able to detect a correctly targeted clone, plasmid DNA was extracted from the entire remaining volume of the recombineering experiment (~1 mL) to use as template DNA for an optimisation of the screening PCR protocol on the assumption that at least some correctly recombined plasmid would be present for amplification. PCR screening should be able to detect correct transformants if the frequency is above ~1/1,000-10,000 (Capecchi, 1989).

#### 5.2.4.4.2 Optimisation of the *LoxP* Insertion Screening PCR

A gradient PCR was set up to test a range of lower annealing temperatures, using the same screening primers. Plasmid DNA template was prepared from the entire remaining volume of the experiment using the rapid protocol (Section 2.1.1.3. Referred to as “full experiment”). A gradient PCR was used as described in Section 2.1.2.3. Annealing temperatures and results are shown in Figure 5.17. A clear 361 bp product was amplified, along with a fainter band at approximately ~140 bp. There is also a very faint third band of ~395 bp. With the gel run for longer (Figure 5.17b) the distinction between the 361 bp band and the 395 bp band is clearer, however, the band intensity is reduced (a section of the gel containing the strongest bands is shown). The optimisation showed all further screening PCRs should be carried out with a 55°C annealing temperature, as originally specified in the Screening PCR protocol (Section 2.1.2.2) with the 140 bp band being the primary amplicon for indicating correct recombination.

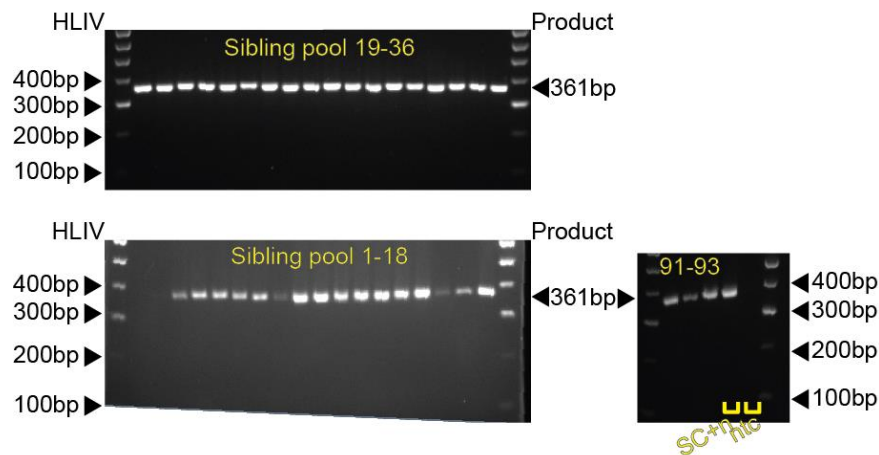


**Figure 5.16 Screening PCR sibling pools of LoxP site insertion into SOD1\_SC+neo\_pMS**

Examples of 3 gels. In the first gel, uneven wells produced by the el comb can be seen. In the second and third gel, uneven running due to a crooked electrode can be seen.

A 361bp product is amplified from hSOD1\_SC+neo\_pMS. When the LoxP site has been inserted, a 395bp and a 140bp product is amplified from hSOD1\_N\_L\_pMS

ntc= no template control. SC+n= hSOD1\_SC+neo\_pMS. HLIV= HyperLadder IV

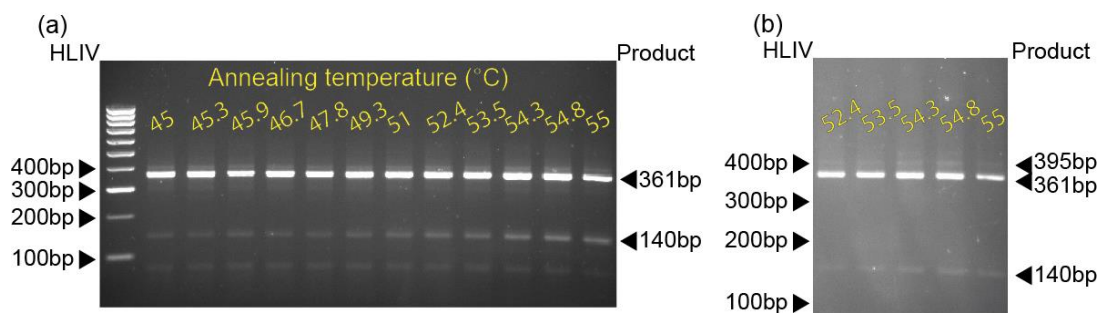


**Figure 5.17 Optimisation of LoxP insertion screening PCR**

Amplification of products across a range of annealing temperatures is shown. Template used was plasmid DNA extracted from the entire remaining volume (~1 mL) of the recombineering experiment to insert the LoxP site into hSOD1\_SC+neo\_pMS to make hSOD1\_SC\_N\_L\_pMS

A 361bp product is amplified from hSOD1\_SC+neo\_pMS. When the LoxP site has been inserted, a 395 bp and a 140bp product is amplified from hSOD1\_N\_L\_pMS

(b) shows gel (a) electrophoresed further to separate bands of 361bp and 395bp.

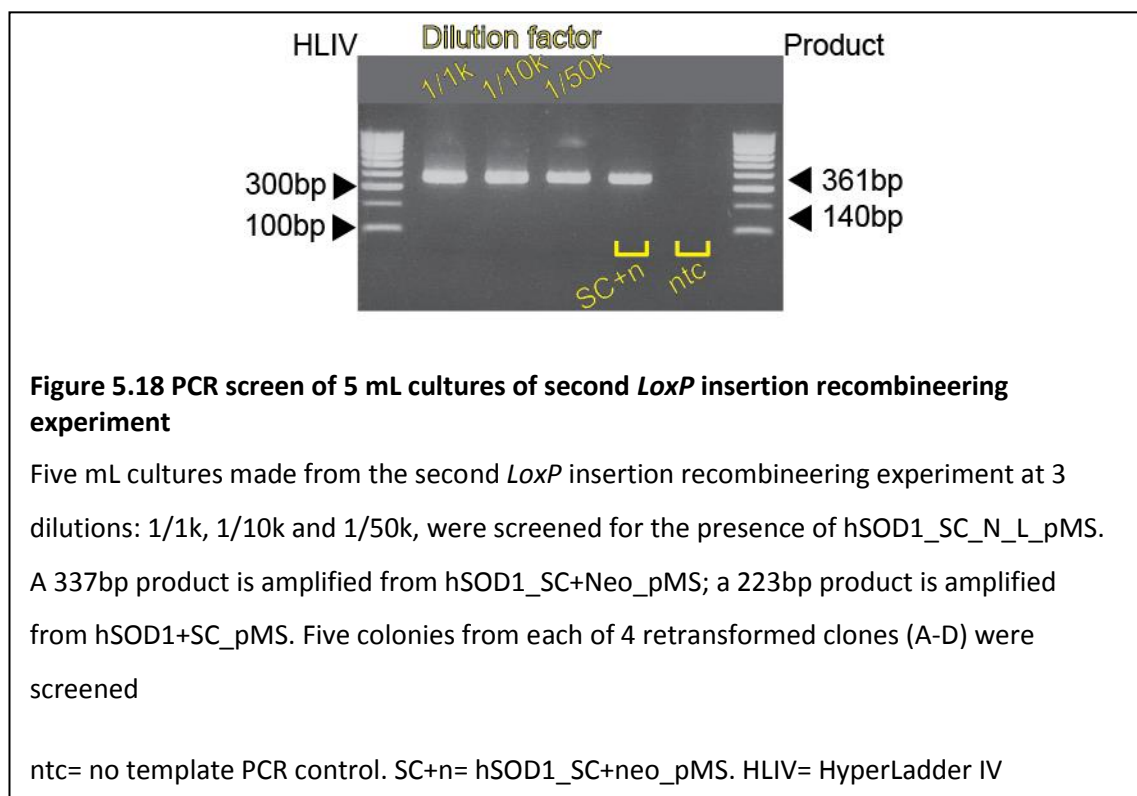
HLIV= HyperLadder IV

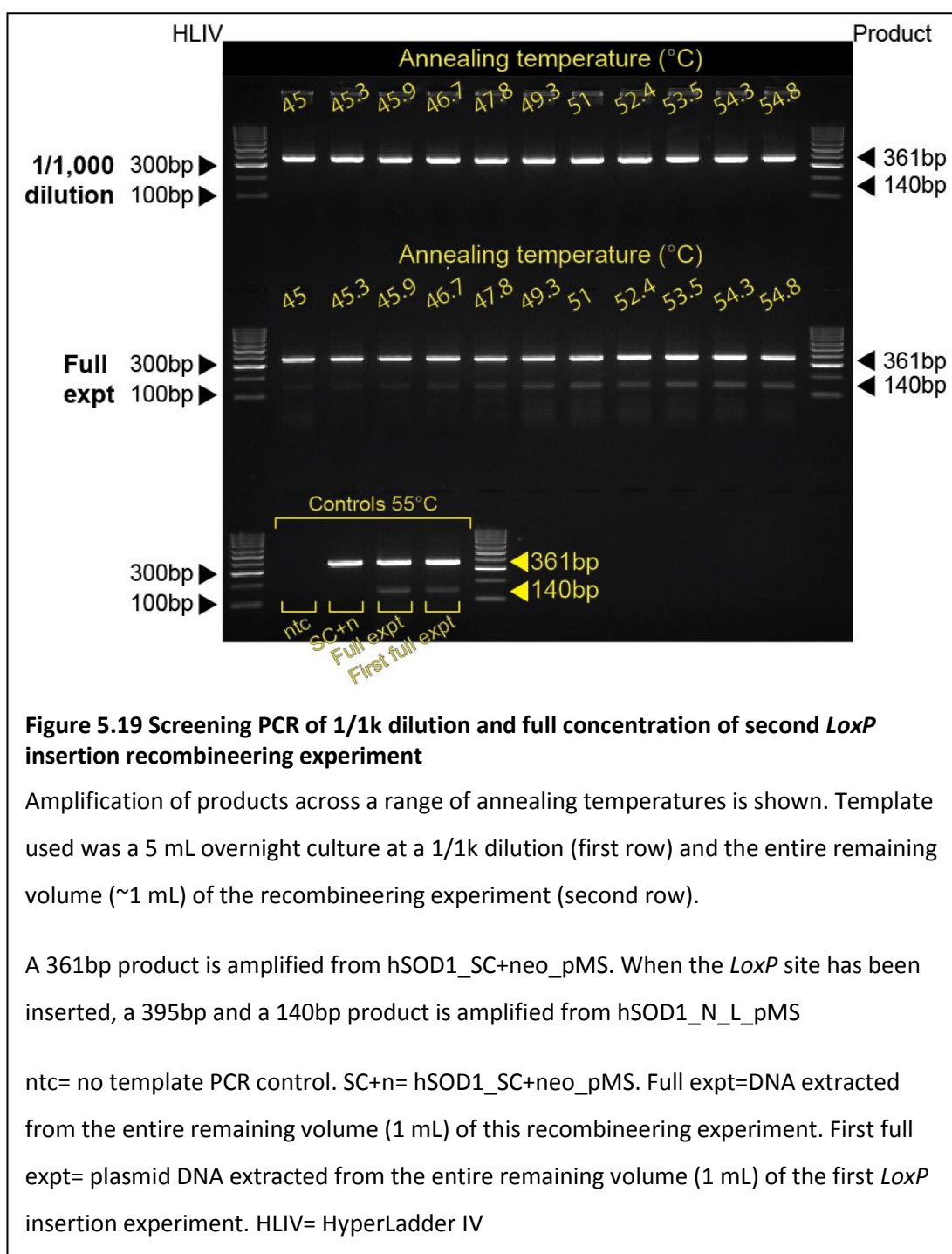
#### 5.2.4.4.3 Recombineering and Screening

The whole experiment was repeated, but this time, dilutions of 1/1,000, 1/10,000 and 1/50,000 were made in a 5 mL total volume LB-Kana. These dilutions were inoculated into 96-well plates and 50  $\mu$ L spread onto LB-Kana agar plates as above. Additionally, the dilutions themselves were also kept and cultured overnight. The number of colonies which grew on the LB-Kana agar plates were 17, 3 and 3 for the 1/1,000, 1/10,000 and 1/50,000 dilutions respectively.

This number was much lower than expected. Recombineering experiments were started when the OD<sub>600</sub> of the *E.coli* culture was between 0.5 and 0.6. An OD<sub>600</sub>=1 is equivalent of  $\sim 8 \times 10^8$  cells/mL, therefore a 1.5 mL aliquot of OD<sub>600</sub>=0.5 should contain  $\sim 4 \times 10^8$  (400,000,000) *E.coli*. A 1/1,000 dilution of would yield 400,000 cells/mL, 50  $\mu$ L of which should contain 20,000 cells. This means that less than 0.1% of the cells were surviving the recombineering experiment.

The 5 mL dilution cultures were screened and, as shown in Figure 5.18, all appeared to be negative for recombination. Another gradient PCR was set up to screen the 1/1,000 dilution and the remaining full concentration recombineering experiment. Results, shown in Figure 5.19, show that at least some correctly targeted clones were produced during the experiment, but at a frequency too low to detect within the sibling pools.





#### 5.2.4.4.4 Recombineering and Screening: Is the Oligo Toxic?

To check whether the oligo recombineering was having a toxic effect on the *E.coli*, beyond any effects of induction of the recombineering proteins and electroporation, the experiment was repeated again, this time including a “no-oligo” control in which the cells were treated identically except that no oligo was added before electroporation. The E10 BAC was also used as an additional target for the oligo, as a recombineering positive control. The BAC is at a lower copy number than the hSOD1\_SC+neo\_pMS plasmid within the *E.coli* and so if correct targeting occurs, it should be easier to identify as the signal to noise ratio would be reduced.



As a further check, two 5 mL cultures at a 1/50 dilution were prepared using LB-Kana and LB with no antibiotics, to see if the oligo recombineering was effecting the ability of the *E.coli* to survive antibiotic selection and if its removal would increase detection of correct recombinants.

The number of colonies that grew on each plate is given in Table 5.18. Nearly 20 times more cells survived the experiment when the oligo was omitted, suggesting that it had some toxic effect on the *E.coli* above the effect of the recombineering experiment itself.

Screening PCRs of DNA prepared from the full 5 mL volume of the liquid cultures, shown in Figure 5.20 , failed to reveal any correctly targeted clones, including in those in which antibiotic selection was omitted. PCR screening of the remaining full concentration experiments, shown in Figure 5.21 suggest that some correctly targeted clones were present. It appears that although recombination is occurring, the efficiency is too low for recovery in a non-selected experiment. An alternative targeting strategy using 2-step positive/negative selection cassette targeting followed by replacement with the *LoxP* site will be required to isolate correctly recombined clones.

**Table 5.18 Growth profiles**

Target	Oligo?	Dilution factor	Number of colonies	Surviving cells per ul (full concentration)	Average surviving cells
hSOD1_SC+neo_pMS	y	1/1,000	114	2,280	2,626.67
hSOD1_SC+neo_pMS	y	1/10,000	18	3,600	
hSOD1_SC+neo_pMS	y	1/50,000	2	2,000	
hSOD1_SC+neo_pMS	n	1/1,000	1,334	26,680	52,026.67
hSOD1_SC+neo_pMS	n	1/10,000	347	69,400	
hSOD1_SC+neo_pMS	n	1/50,000	60	60,000	
E10	y	1/1,000	480	9,600	28,666.67
E10	y	1/10,000	252	50,400	
E10	y	1/50,000	26	26,000	

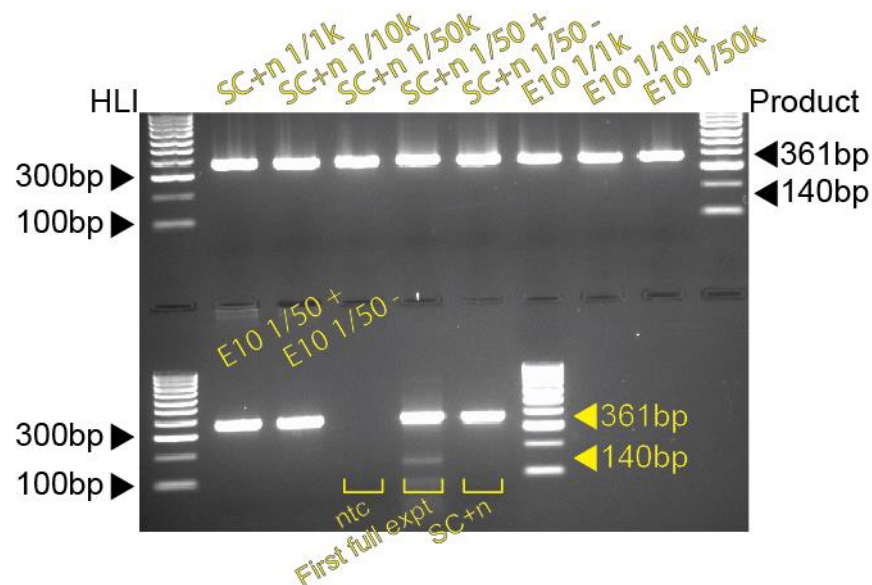


**Figure 5.20 PCR screen of 5 mL cultures of the third *LoxP* insertion recombineering experiment**

PCR screen of 5 mL cultures of the third *LoxP* insertion recombineering experiment

5 mL cultures at varying dilution factors, as shown, of the recombineering experiment to insert a *LoxP* site into hSOD1\_SC+neo\_pMS (SC+n) and the E10 BAC (E10) were screened. 1/50 dilutions were cultured overnight with (+) or without (-) kanamycin selection to see whether removing selection pressure increased the chance of seeing correct recombinants.

A 361bp product is amplified from hSOD1\_SC+neo\_pMS. When the *LoxP* site has been inserted, a 395bp and a 140bp product is amplified from hSOD1\_N\_L\_pMS

ntc= no template PCR control. First full expt= plasmid DNA extracted from the entire remaining volume (1 mL) of the first *LoxP* insertion experiment. SC+n= hSOD1\_SC+neo\_pMS. E10= E10 BAC. HLI= HyperLadder I

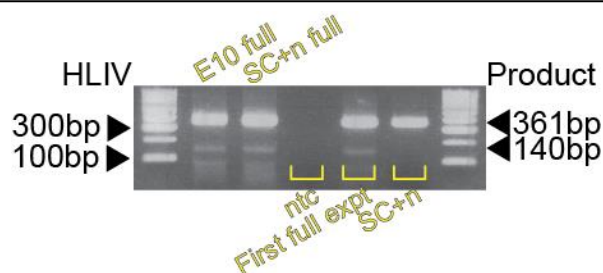


**Figure 5.21 PCR screen of ~1 mL full concentration of the third *LoxP* insertion recombineering experiment**

The remaining ~1 mL of the recombineering experiments to add insert a *LoxP* site into both the E10 BAC and hSOD1\_SC\_N\_pMS (SC+n) were screened for the presence of the correctly recombined hSOD1\_SC\_N\_L\_pMS.

A 361bp product is amplified from hSOD1\_SC+neo\_pMS. When the *LoxP* site has been inserted, a 395bp and a 140bp product is amplified from hSOD1\_N\_L\_pMS

ntc= no template PCR control. First full expt= plasmid DNA extracted from the entire remaining volume (1 mL) of the first *LoxP* insertion experiment. SC+n= hSOD1\_SC+neo\_pMS. E10= E10 BAC. HLI= HyperLadder I

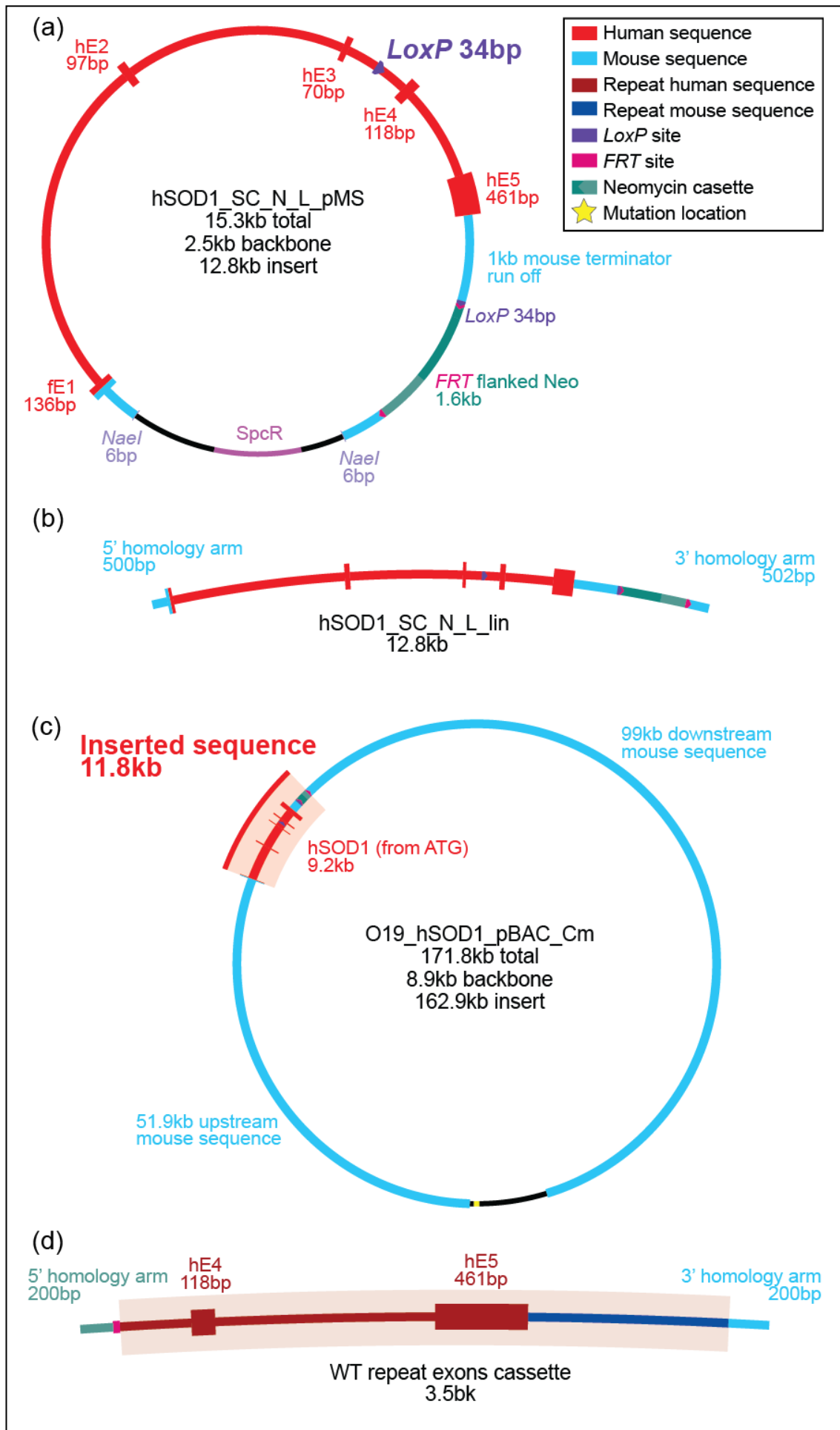
### 5.3 GENE BRIDGES CONSTRUCT COMPLETION

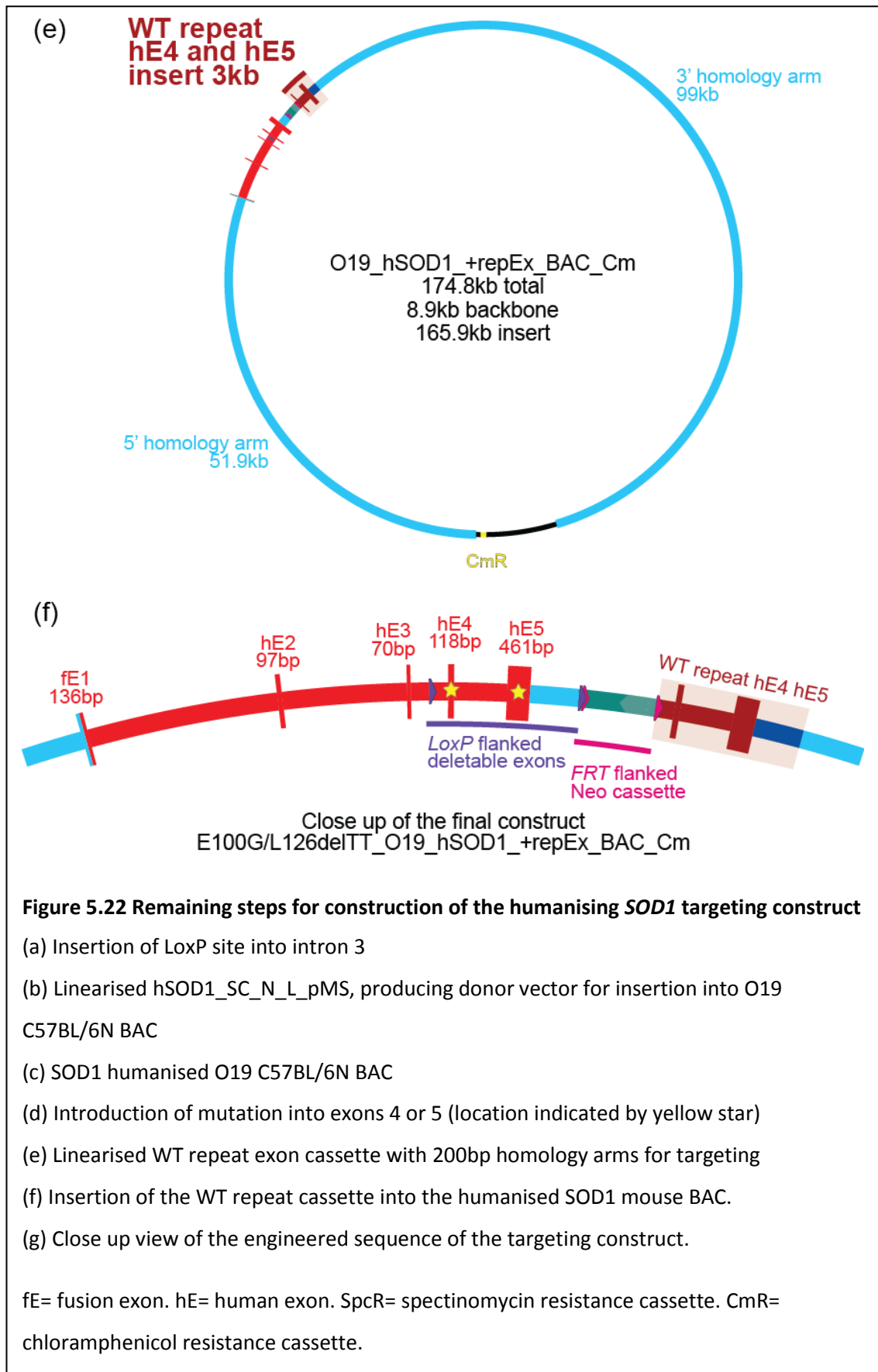
Due to increasing time constraints it was decided that the remainder of the cloning of the targeting construct would be outsourced to Gene Bridges. The custom made plasmid, SOD1\_Exon4-5\_pMA (see Section 2.3.3.2), along with hSOD1\_SC+neo\_pMS and the O19 mouse BAC were sent to Gene Bridges. The remaining steps to complete the construct, as carried out by Gene Bridges, are briefly described below and presented in Figure 5.22.

First, the *LoxP* site was introduced into intron 3 of hSOD1\_SC+neo\_pMS to produce hSOD1\_SC\_N\_L\_pMS (Figure 5.22a), using a 2-step strategy, as described above.

Next, the engineered insert from hSOD1\_SC\_N\_L\_pMS was subcloned into the O19 BAC, to produce O19\_hSOD1\_pBAC\_Cm. This was done by linearisation of the hSOD1\_SC\_N\_L\_pMS insert by digestion with *NaeI* (Figure 5.22b). The linearised product was then used as the donor vector to insert the sequence into the O19 mouse BAC with kanamycin selection (Figure 5.22c).

In our original cloning plan, the next step was adding the ALS mutations, creating 2 separate mutant humanised BACs, to which the repeat exon cassettes would be added subsequently. This was in order to avoid subsequent recombineering steps once the repeat cassette was in place, as the ~3 kb repeat that this would introduce would be liable to recombine during subsequent steps.





According to the information supplied to us by Gene Bridges, they first inserted the repeat cassette (Figure 5.22d-e). This would have been done using a 2 step process, inserting a positive/negative selection cassette and then replacing it with the SOD1\_Exon4-5 targeting vector, PCR amplified from the SOD1\_Exon4-5\_pMA plasmid. After this, the mutations would be targeted using oligo recombineering, resulting in the final targeting constructs Figure 5.22f E100G\_O19\_hSOD1\_+repEx\_BAC\_Cm and L126delTT\_O19\_hSOD1\_+repEx\_BAC\_Cm.

## 5.4 FUTURE WORK

### 5.4.1 Confirmation of Gene Bridges Finalised Construct

Gene Bridges supplied the finished constructs to us and PCR screening was carried out by Dr Anny Devoy. PCR screening revealed that the humanised BAC clones appeared to be a mixed population, containing BACs both with and without the repeat exon cassette. This suggests that the construct is unstable and possibly liable to unwanted recombination events between the initial and repeat exon regions.

In our original plan, the mutations were to be introduced into O19\_hSOD1\_pBAC\_Cm *before* carrying out 2 independent recombineering experiments to insert the repeat cassette into the 2 mutant humanised mouse BACs. The repeat cassette has 88% homology to the floxed exon 4-5 region of humanised mouse BACs, with 200 bp homology arms targeting it downstream of the *FRT* flanked neo cassette. This high level of off-target homology would likely result in a low efficiency of correct targeting of the repeat cassette, however it was deemed desirable due to the very high homology between the initial floxed exon 4-5 cassette, and repeat exon 4-5 cassette, differing by only 1 bp across a ~3 kb region. This high level of homology is likely to result in decreased stability of this region and a high chance of recombination events between the 2 regions. Once the repeat cassette has been inserted, it is therefore desirable to move the construct into a more stable *E.coli* host with reduced recombinase activities as repeat associated deletions can occur when propagating BAC clones in *E.coli* even without the induced expression of recombinases during recombineering experiments (Song et al., 2001; Westenberg et al., 2010). It is therefore highly undesirable to carry out further recombineering experiments once the repeat cassette has been inserted into the humanised BAC.

Further work is needed to obtain pure clonal populations from the material provided by Gene Bridges for further screening. The first step for this will be preparing BAC DNA and retransforming it into an *E.coli* line which has been modified to reduce recombination events to provide a more stable host for propagating unstable plasmid DNAs. Transformation should be done using a low concentration of DNA to increase the chance of obtaining single copy transformation and include kanamycin as well as chloramphenicol selection as deletions due to

recombination between the initial floxed and repeat exon 4-5 cassette may cause deletion of the neo cassette.

Although the final construct was confirmed by sequencing by Gene Bridges, once clonal populations of the humanised BAC have been achieved, re-sequencing will be required particularly for regions which are at risk of recombination. For example, the initial floxed and repeat exon 5-4 regions will need to be screened and re-sequenced to confirm that the WT and mutant exons have not undergone recombination, potentially swapping or replacing the WT/mutant alleles. Similarly, the region around the *LoxP* site of the initial intron 3 and the repeat intron 3, and the end of both the initial and repeat 1 kb terminator region are at risk of sequence swapping due to unwanted recombination events.

### **5.4.2 Using the Targeting Construct to Derive Humanised *SOD1* Mice**

As is described in Section 1.3.2.2, gene targeting will be achieved by electroporation of the linearised targeting construct into C57BL/6N mESCs followed by selection with neomycin to identify those cells which have incorporated the construct into their genome (in either in a targeted fashion or by random integration).

After neomycin selection qPCR will be used to quantify the copy number of the humanised *SOD1* and endogenous *Sod1* alleles. Two autosomal genes (*Tfrc* and *Tert* copy number control assays, Life Technologies) will be used as standards for gene copy number quantification (each should be present at 2 copies). Correctly targeted ESCs should have 1 copy each of the endogenous and humanised *SOD1* sequence, and if the conditional cassette has inserted correctly, the humanised allele should have an extra copy of the 3' region contained within the repeat cassette. Other genes both upstream and downstream of the targeting site will also be quantified to ensure they remain present in two copies only, as it has previously been reported that extensions of the targeting construct can take place within the targeted genomic region followed by ectopic insertion (Mangerich et al., 2009).

Once correctly targeted mESCs have been confirmed, the mESCs will be used in blastocyst injection followed by embryo implantation and coat colour selection. High coat colour pups will then be used for breeding and their offspring genotyped by PCR specific to the human *SOD1* sequence to identify germ-line transmission of the humanised allele. Once germ line transmission has been achieved, offspring can be mated to an appropriate C57BL/6 transgenic line with ubiquitous FLP expression in order to excise the *FRT* flanked neo cassette. Screening of offspring can be carried out using the screening PCR described in Section 5.2.4.3. Once the cassette is excised, breeding can be carried out by either backcrossing to the parental

C57BL/6N strain, or heterozygotes could be inter-crossed to produce homozygous humanised *SOD1* mice. Alternatively, the conditional/inducible allele can be utilised by crossing to an appropriate Cre transgenic mouse line.



## Chapter 6. Discussion

The work described in this Thesis has focussed on the roles of different types of SOD1 – WT, mutant, human (huSOD1) and mouse (moSOD1) – in SOD1-fALS mouse models. In particular, I have examined whether mutant or WT huSOD1 can be induced to aggregate via prion-like mechanisms *in vivo* and have found some limited evidence that this may occur, although further work is needed to confirm, or otherwise, this result. Next I looked at whether endogenous moSOD1 affects the degenerative phenotype of G93A mutant *SOD1* transgenic mouse. These data suggest that endogenous WT moSOD1 has an exacerbating effect on the disease phenotype in the earlier stages of degeneration, but that the difference is lost as degeneration progresses. Finally I have carried out molecular cloning towards the production of a targeting construct for use in the genomic humanisation of the endogenous mouse *Sod1* locus. The construct has been designed as a conditional allele with a Cre-dependent switch from mutant to WT huSOD1 expression, and will provide a tool suitable for further dissection of the interaction between WT and mutant SOD1, and huSOD1 and moSOD1.

### 6.1 MISFOLDING OF SOD1 WITHIN THE PRION PARADIGM

The concept of a prion-like spread of pathogenically misfolded protein within neurodegenerative disease is gaining increasing interest. Seeded aggregation and spread of pathology from the initial site of inoculation with recombinant aggregated proteins has been demonstrated *in vivo* in transgenic mice expressing proteins associated with neurodegenerative diseases, such as tau, A $\beta$ , and  $\alpha$ -synuclein (e.g. Iba et al., 2013; Masuda-Suzukake et al., 2013; Stöhr et al., 2012) see also Table 1.6). This work, along with experiments *in vitro* and in cell models demonstrating seeded-aggregation and cell-to-cell aggregate spread, and experiments *in vivo* using transgenic mouse models which are inoculated with “seeds” derived from patient or mouse model CNS tissue, strongly suggest that a prion-like spread of pathologically misfolded proteins may be at play in several neurodegenerative disease. The idea of prion-like spread is particularly compelling in ALS due to the stereotypical pattern of symptomatic spread often reported, whereby onset is focal and spreads through contiguous regions of the body along the axis of spinal cord innervation (Fujimura-Kiyono et al., 2011).

In the case of SOD1, it has been established that huSOD1 forms aggregates *in vitro* and that the process of aggregation can be hastened by both self-seeding and cross-seeding with pre-formed aggregates or with spinal cord homogenates from SOD1-fALS transgenic mice (Chia et al., 2010). Other experiments have also established that misfolded SOD1 is transferred between cultured cells and can act as a seed for misfolding and aggregation in naïve cells (Munch et al., 2011). Cross-culture experiments have also provided evidence that cell-to-cell

transmission may be involved in non-cell autonomous mechanisms of SOD1 toxicity, for example astrocytes of SOD1-fALS or sALS patients, or SOD1-fALS mice, are toxic to naïve MNs in co-culture, however SOD1 knock-down attenuates this toxicity, hinting that prion-like mechanisms may be at play here too (Haidet-Phillips et al., 2011; Kunze et al., 2013). Unlike several other neurodegenerative hallmark proteins however, an *in vivo* role for transmission of misfolded/aggregated protein has not previously been reported for SOD1.

Here we found no evidence that self-seeded-aggregation occurs *in vivo* in our experiments inoculating G93A mutant SOD1 transgenic mice with tissue homogenates derived from the same mouse line at a later, symptomatic age. There was no difference in the area of misfolded SOD1 pathology in any brain region between mice inoculated with SC homogenates from G93A mutant SOD1 mice, or those inoculated with homogenates prepared from *Sod1* null mouse SC.

The preliminary results of our cross-seeding experiment, in which mice expressing WT huSOD1 were inoculated with material containing mutant SOD1 species, have not provided conclusive evidence of a difference in misfolded SOD1 pathology between inocula groups. The area of misfolded SOD1 staining in the ventral roots only is larger in those mice inoculated with spinal cord homogenates derived from G93A mutant transgenic mouse as compared to *Sod1* null mouse, however, because the data set is incomplete at this time, a firm conclusion cannot yet be drawn.

### **6.1.1 SEDI/USOD Outcome Measures**

Our outcome measure for experiments examining prion-like properties of SOD1 and the potential for transmission of pathogenically misfolded species *in vivo*, was the extent of misfolded SOD1 burden measured histopathologically by conformation specific antibodies. The first antibody that we used, SEDI, has previously been reported to detect a progressive increase in histopathological staining, and later a decrease presumed to be due to loss of MNs, in the G93A SOD1-fALS mouse as degeneration proceeds (Rakhit et al., 2007). The USOD antibody has also been used to identify misfolded SOD1 pathology in a G93A SOD1-fALS mouse (Kerman et al., 2010). Although no time-course of pathology has been described so far with the USOD antibody, it was reported that similar structures were stained when the 2 antibodies were used on sequential sections of the same tissue samples (Kerman et al., 2010), and so one could infer that a similar pattern of staining may also occur through the course of degeneration. It should be noted, however, that the epitopes that the 2 antibodies detect are distinct (see Figure 3.1); SEDI recognises amino acids 143-153 and is expected to be exposed in natively folded but monomeric SOD1 (Rakhit et al., 2007). USOD, on the other hand, was raised against amino acids 42-48 and is expected to require unfolding of the monomer to expose the epitope (Kerman et al., 2010). We have not yet validated that we can use these antibodies to

differentiate stages of degeneration in SOD1 transgenic mice. This work needs to be completed before we can be confident in our interpretation of our results.

There are several alternative misfolded SOD1 antibodies which have been used to show changes in the level of misfolded SOD1 pathology over time, or in response to pharmacological treatment or genetic manipulation; a DSE2 antibody (disease specific epitope 2) detected reduced levels of misfolded SOD1 in 3 mutant SOD1-fALS mice (G37R, G85R and G93A) when crossed to a *CypD* KO line (Parone et al., 2013) and a progressive increase in motor neuronal and non-neuronal misfolded SOD1 in the spinal cords of SOD1-fALS transgenic rats as degeneration proceeded (Israelson et al., 2010). Three other antibodies, D3H5, B8H10 and A5C3, which recognise epitopes in exons 2, 3 and 4, respectively, were also used by Parone et al., (2013) and revealed similar patterns of a reduction in misfolded SOD1 pathology in G37R mutant SOD1 transgenic mice when crossed to a *CypD* (Cyclophilin D) KO. This same panel of 3 antibodies was also used by Gros-Louis et al., (2010) revealing a pattern of developing pathology in a G93A mutant SOD1 transgenic mice; immunofluorescence revealed an initially diffuse staining of MNs in the ventral horns that became more concentrated with time and eventually condensed into a punctate inclusion like pattern by 130-days of age. In WT SOD1 transgenic mice, on the other hand, an almost complete absence of staining was apparent, at least at 80-days of age. These antibodies represent potential alternatives for measuring differences in misfolded SOD1 pathology as they have been previously shown to differentiate different stages of degeneration in at least 2 different transgenic mouse lines. They also appear to have low reactivity to the spinal cords of WT SOD1 transgenic mice, although the specific WT transgenic line is not defined by Gros-Louis et al., (2010) so it is not possible to tell whether the expression level is comparable to the line used in the work described in this Thesis.

While both SEDI and USOD have been reported as histopathologically negative in cases of sALS and non-SOD1-fALS (Liu et al., 2009; Kerman et al., 2010) some other misfolded SOD1 antibodies have produced positive results in such cases; Pokrishevsky et al., (2012) found that the 10E11C11 antibody stained both the cytoplasm and axons of MNs in the cervical spinal cord of SOD1-fALS patients, and also the axons of some sALS and non-SOD1-fALS patients, but not in non-ALS control tissue. The C4F6 antibody is reported as staining MN of the ventral horn in 4 out of 9 sALS cases examined by Bosco et al., (2010) while no non-ALS control tissues were positive. Later, however, Brotherton et al., (2012) found that while the C4F6 antibody detected skein-like inclusions in the MNs of SOD1-fALS cases, in sALS and non-SOD1-fALS only a diffuse reactivity was present in MNs, which was also present in the majority of both neurological and non-neurological controls. This range of misfolded SOD1 antibodies represent potential

alternative neuropathological tools for detecting changes in the levels of misfolded SOD1 as a result of transmission of misfolded SOD1 species. As different misfolded SOD1 antibodies may detect different forms of SOD1 and it is not clear which of these are pathogenic (Prudencio et al., 2011) it may be appropriate to also test our tissue sample with a range of such antibodies, in particular those which have been described as reactive to non-SOD1-fALS and sALS tissues which may contain pathogenically misfolded WT SOD1 species.

### **6.1.2 SOD1 Aggregation and Pathogenicity**

Although the aggregation of WT SOD1 has been implicated in disease pathogenesis by experiments crossing WT and mutant *SOD1* transgenic mice (Deng et al., 2006; Prudencio et al., 2010; Wang et al., 2009b; Jaarsma et al., 2000; Fukada et al., 2001; Jaarsma et al., 2008), a direct correlation between aggregation and disease is not consistently reported and it is becoming increasingly recognised that a non-aggregated misfolded protein species is more likely responsible for disease pathogenesis; in WT:mutant double transgenic huSOD1 mice, aggregation of WT huSOD1 can occur with no effect on disease phenotype (Prudencio et al., 2010), while the disease phenotype can be exacerbated by the expression of WT huSOD1 without it becoming aggregated (Witan et al., 2009). A lack of correlation between aggregation of mutant huSOD1 and toxicity was also reported when a L126Z mutant *SOD1* transgenic mouse line was crossed to 2 different WT *SOD1* transgenics; one cross resulted in increased mutant aggregation with no change to the disease phenotype while the other produced a more aggressive disease phenotype with no increase in mutant aggregation (Prudencio et al., 2010).

A distinction between mutant SOD1 aggregation and disease have also been described as resulting from other genetic crosses. In one such example, genetic ablation of *CypD* in several SOD1-fALS mouse lines caused a reduction of SOD1 aggregation and improved other ALS related features such as gliosis, mitochondrial function and morphology and even MN death, however, axonal degeneration, onset and survival were left unchanged (Parone et al., 2013). In another example crossing a mutant *SOD1* transgenic to a *CCS* transgenic reduced the SOD1 aggregate burden while actually exacerbating the disease phenotype (Son et al., 2007). These studies strongly suggest that aggregation of SOD1 is a secondary effect of disease which may not be necessary for the initiation of muscle denervation or behavioural disease. Indeed it has been suggested that aggregation load may be related to disease duration rather than disease onset (Prudencio et al., 2009b).

Furthermore, we also show here, as has previously been reported (Rakhit et al., 2007), that WT *SOD1* transgenic mice have SEDI inclusion pathology in the spinal cord, particularly focused in the ventral horns and roots, despite having no overt motor phenotype at similar ages (Chiu et

al., 1995; Dal Canto et al., 1995; Tu et al., 1996; Jaarsma et al., 2000). Interestingly, a disconnect between aggregate pathology and disease phenotypes has also been described in infectious prion disease (Sandberg et al., 2011). Infectious prion diseases have been described as the prototypical protein misfolding disease due to the tight causal link between misfolded PrP and disease state (Goold et al., 2013). That such a differentiation between aggregate pathology and disease can be made in prion disease lends further weight to the notion that a non-aggregated, but misfolded form of SOD1 may be the primary cause of disease, while aggregates may be a secondary consequence of misfolding and also possibly responsible for secondary effects for example by causing deficits in proteostasis (Bence et al., 2001).

As previously discussed in Section 1.5.4, pre-aggregate species have been implicated as the toxic species using a number of different *in vitro* and *in vivo* models. If a pre-aggregate misfolded species is responsible for disease, an alternative outcome measure to misfolded aggregate pathology, could be to investigate whether pre-aggregate soluble misfolded SOD1 species are transmissible via prion-like template misfolding. Although SEDI has been reported as reactive to soluble SOD1 species, the assessment was qualitative and based on immunofluorescence intensity in transfected cells in culture (Prudencio et al., 2011). We have used SEDI to analyse animals with a high baseline level of immunoreactivity and our analysis was more suited to detecting changes in the area of inclusion type pathology, rather than diffuse staining or changes in intensity of misfolded SOD1 staining. The USOD antibody detects histopathological structures which are similar to those detected with SEDI (Kerman et al., 2010), although whether this would include both soluble and insoluble misfolded SOD1 has not been determined.

An alternative to histopathology for the detection of pre-aggregate misfolded SOD1 species would have been using biochemical methods, such as differential detergent extraction. Suitable samples were not collected during our experiments and so it has not been possible for us to carry out such analysis. These techniques have been used by other groups to quantify the levels of soluble, insoluble and aggregated SOD1 to differentiate mouse lines or stages of degeneration (e.g. (Karch et al., 2009; Prudencio et al., 2010; Wang et al., 2009b; Witan et al., 2009)). Such techniques can be used to differentiate and quantify multiple different species of SOD1 from the same sample based on their biochemical/biophysical behaviour. Unlike histopathology with misfolded SOD1 antibodies, they are not necessarily limited to the exposure of a particular epitope. However, just as with misfolded SOD1 antibody detection, it is not known which specific fraction or form of SOD1 is causal of disease (Koyama et al., 2006). Similarly, it would therefore not be possible to draw conclusions about potential pathogenic consequences of perturbations of a particular fraction measured using such techniques.

### 6.1.3 Alternative Outcome Measures

At present it is not clear which species of misfolded SOD1 is responsible for the pathogenic effects of mutant/misfolded SOD1. The mouse models that we have used have high baseline levels of total SOD1 and appreciable levels of misfolded SOD1 even without a potential further induction of misfolding by prion-like mechanisms, which may confound our ability to differentiate variation in misfolded SOD1 staining.

Rather than directly assaying misfolded forms of SOD1, an alternative could be to look at other histopathological markers of disease progression as evidence for toxicity resulting from misfolded SOD1 transmission caused by inoculation with pathogenic SOD1 inoculation. Histopathological markers of gliosis (Jaarsma et al., 2000; McGeer et al., 2002), ubiquitin and p62 (Mackenzie et al., 2007; Gal et al., 2007), or caspase activation (Pasinelli et al., 2000) are all potential markers of disease progression in SOD1-fALS mice with relevance to patient ALS pathology. Although this methodology would not provide a direct measurement of prion-like transmission of SOD1 misfolding, if the phenomenon does occur and is relevant to disease, then it may provide a measure of its effect, which is accessible to us using the tissues we have available.

### 6.1.4 Wild-type SOD1 Toxicity Outside the Prion Paradigm

Our data do not provide strong support for the hypothesis that misfolding of SOD1 can be induced by prion-like mechanisms and spread through the CNS by cell-to-cell transmission. Previous evidence however, in particular that from double transgenic mice with both WT and mutant *SOD1* transgenes, strongly indicates that WT SOD1 can contribute to the disease process, at least in SOD1-fALS mouse models (Deng et al., 2006; Prudencio et al., 2010; Wang et al., 2009b; Jaarsma et al., 2000; Jaarsma et al., 2008). If prion-like misfolding is not the cause of the synergistic relationship between WT and mutant SOD1, what alternative mechanisms could be responsible?

In double transgenic WT:mutant huSOD1 mice, cellular protein homeostasis may be antagonised purely due to the increase protein expression resulting from double, as compared to single, transgenic mice and this could have a detrimental effect on disease progression (Bence et al., 2001). However, the fact that double transgenic mice expressing mutant moSOD1 and WT huSOD1 do not display the disease exacerbation commonly reported in huSOD1 WT:mutant double transgenics (Audet et al., 2010) argues against this being a major cause of toxicity.

WT huSOD1 can become misfolded *in vivo* as a result of non-prion-like mechanisms, for example as a result of a lack or loss of structural metal ions or by oxidation (Ezzi et al., 2007;

Redler et al., 2011; Proctor et al., 2011; Rakhit et al., 2004; Lindberg et al., 2004; Urushitani et al., 2006; Estévez et al., 1999). Such forms of misfolded WT SOD1 have been detected in tissues and cultured cells derived from both SOD1-fALS and some sALS patients, and moreover, they share some toxic properties with mutant SOD1 (e.g. (Bosco et al., 2010; Guareschi et al., 2012)). As discussed in Section 1.5.3.1, although many SOD1 mutants retain full or partial dismutase activity, markers of increased oxidative stress are reported in both patient tissue and in SOD1-fALS mouse models, and SOD1 itself is highly oxidised in SOD1-fALS mice (Andrus et al., 1998). The misfolding of WT huSOD1, and the potentially toxic consequences of this, in double WT:mutant *SOD1* transgenic mice could therefore be the result of the highly oxidative environment caused by mutant huSOD1 expression.

Another way in which WT SOD1 has been proposed to exacerbate the toxicity of mutant SOD1 is via stabilisation of the mutant protein. Rather than increasing the level of aggregated SOD1, co-expression of both WT and mutant SOD1 has been shown to reduce aggregation relative to expression of mutant SOD1 alone in cellular models (Witan et al., 2008; Witan et al., 2009; Prudencio et al., 2009a; Prudencio et al., 2010; Brotherton et al., 2013). Compared to mutant homodimers, WT:mutant heterodimers not only have a lower propensity to aggregate but also higher cellular toxicity, while heterodimerisation appears to increase the stability of the mutant monomer, protecting it from degradation and/or aggregation (Witan et al., 2008; Witan et al., 2009; Weichert et al., 2014). However, heterodimerisation does not appear to be essential for stabilisation of pre-aggregate species; the L126Z SOD1 mutant is a truncation mutant incapable of dimerising which is highly labile with a short half-life *in vivo* and when expressed in a cell model it is primarily found in the insoluble fraction due to degradation of the soluble protein. When co-expressed with WT SOD1 its levels are reduced to below detectable levels in both soluble and insoluble fractions (Prudencio et al., 2010). Because of the short half-life of this mutant protein, this is likely explained by a shift from an insoluble to a soluble state, but that the soluble population is degraded too quickly to be measured. The fact that this reduction in aggregated protein occurs without heterodimerisation or an increase in the soluble levels suggests that the process may be better characterised as blocking the aggregation pathway rather than stabilising a pre-aggregate form.

WT SOD1 may exert toxicity due to a combination of these mechanisms; by heightening the toxicity of mutant SOD1 by increasing the availability of the toxic species, possibly through stabilisation and/or blocking its sequestration into aggregates; by becoming toxic itself via post-translational modification and misfolding, thereby taking on characteristic of mutant misfolded SOD1. From the data presented in this Thesis, it does not appear that seeded-aggregation of huSOD1 plays a significant role in the formation of misfolded SOD1 aggregate

pathology in TgG93A mice. Further analysis is needed for strong conclusions to be drawn in the case of TgWT mice. Future analysis is also planned to examine whether markers of neuronal degeneration are selectively increased in those mice inoculated with pathogenic mutant species to investigate potential functional consequences of templated misfolding.

## **6.2 HUMAN:MOUSE SOD1 INTERACTION IN SOD1-fALS MICE**

From the data presented in this Thesis the endogenous moSOD1 appears to have an exacerbating effect on the early degenerative process of the G93A mutant *SOD1* transgenic mouse. At a later stage this difference is lost. In TgG93A;*Sod1*ko mice, grip-strength and total number of NMJs are significantly higher than in TgG93A;*Sod1*wt mice at around 75-days of age and there is a non-significant trend suggesting increased preservation of the most vulnerable, fast firing, motor units innervating the hind limb muscles.

The effect of WT moSOD1 appears to be similar in quality to the effect of WT huSOD1 in that both have a negative impact on the degenerative process in the TgG93A mouse. Endogenous moSOD1 has previously been reported as having little or no effect on SOD1-fALS mouse models (Deng et al., 2006; Bruijn et al., 1998), although the small effect reported by Deng et al., (2006), is in agreement with the data presented here, in that the disease phenotype of a low copy G93A mutant *SOD1* transgenic mice was less severe on a *Sod1* null background. If the interaction between WT huSOD1 or moSOD1 and mutant huSOD1 are the same, or of a similar nature, then the effect size might be expected to be smaller here as compared to in double WT:mutant transgenic mice; although the ratio of transgenic to endogenous SOD1 is not known for either of the papers which have previously examined the effect of endogenous moSOD1 on SOD1-fALS transgenic mice, in the mouse line used in this Thesis the level of transgenic huSOD1 is several times higher than that of the endogenous (Chiu et al., 1995). In double transgenic mice in which an exacerbation of the phenotype is seen, the amount of WT huSOD1 tends to be at least equal, if not substantially higher than the mutant huSOD1 transgene expression (e.g. (Shibata et al., 1996b; Wang et al., 2009b; Jaarsma et al., 2000)) and the effect of WT huSOD1 in double transgenic mice appears to be dose dependent with higher levels of expression resulting in more profound exacerbation of the phenotype (Prudencio et al., 2010). It would therefore follow that the effect of endogenous WT moSOD1 would be smaller than that of transgenically expressed WT huSOD1. This would make it more difficult to detect, particularly with small sample sizes and high intra-group variability.

In addition to a simple dose effect, evidence suggests that there are differences between huSOD1 and moSOD1 limiting their interaction which could also impact the effect of endogenous moSOD1 in SOD1-fALS mouse models. Unlike transgenically expressed WT huSOD1, the endogenous WT moSOD1 is usually reported as absent from transgenic mutant



huSOD1 aggregates (Deng et al., 2006; Jonsson et al., 2004; Bruijn et al., 1998), although there is at least one case in which co-aggregation is reported and the lack of detected co-aggregation could be at least partially due to the relatively smaller amount of moSOD1 as compared to huSOD1 (Wang et al., 2002a). It is unlikely that the discrepancy in co-aggregation of WT huSOD1 or moSOD1 with mutant huSOD1 is due to a baseline difference in the propensity to form aggregates as cellular assay suggests that both WT huSOD1 and moSOD1 have similarly high resistance to aggregation (Karch et al., 2010).

The most obvious example of a functional consequence of the differences in the interactions of huSOD1 and moSOD1 was seen when a transgenic mouse expressing a G86R mutant moSOD1 was crossed to a WT *SOD1* transgenic line. Unlike crosses between mutant and WT *SOD1* transgenic mice where both transgenes are human, in which the disease tends to be exacerbated, co-expression of WT huSOD1 with G86R moSOD1 had no effect on the motor phenotype or survival of the G86R mouse line and co-aggregation of WT huSOD1 and mutant moSOD1 was not detected (Audet et al., 2010). This suggests that the disease exacerbating interaction between WT huSOD1 and mutant huSOD1 does not occur between WT huSOD1 and mutant moSOD1. However the data presented in this Thesis suggest a functional genetic interaction between WT moSOD1 and mutant huSOD1 does occur. Although behavioural phenotyping was carried out by Audet et al., (2010) the ages at which measures were taken are not described. It is therefore possible that early differences did occur, but that measures were taken at later ages when differences were no longer apparent. It should also be noted that in some cases of WT:mutant huSOD1 double transgenic mice, no disease exacerbation is reported, possibly due to differences in expression levels of WT *SOD1* transgenes (Bruijn et al., 1998; Prudencio et al., 2010).

A potential explanation for the apparent difference between the interaction of WT huSOD1:mutant moSOD1 and WT moSOD1:mutant huSOD1, described here and by Audet et al., (2010), could lie in the differential effect of mutation on huSOD1 and moSOD1. Although the WT proteins are similarly aggregate resistant, in the context of ALS mutation mutant huSOD1 has been reported as more aggregation prone than the corresponding mouse mutant (Karch et al., 2010).

Cellular assays of co-aggregation have revealed that when huSOD1 mutants are expressed in either human or mouse cell lines, WT endogenous huSOD1, but not endogenous moSOD1, co-aggregates with the human mutant protein. When the 32<sup>nd</sup> tryptophan (W32) residue of mutant huSOD1 was itself substituted for the mouse equivalent, serine, and expressed in human cells, a significant reduction in the co-aggregation of the endogenous huSOD1 resulted. This suggests that this residue is important for limiting co-aggregation between mutant and

WT huSOD1 (Grad et al., 2011). The effect of the W32S substitution on the co-aggregation of mutant huSOD1 and WT moSOD1 was not examined. It is possible that the W32 residue is necessary for the mutant protein to elicit co-aggregation of WT SOD1 generally, and could be linked to the increased aggregation propensity of mutant huSOD1 as compared to mutant moSOD1 described by Karch and Borchelt (2010). This would mean that WT moSOD1 would not have co-aggregated with the W32S substituted mutant huSOD1. Another explanation could be that this residue is important for limiting the interaction of human and mouse SOD1, and that the W32S substitution could increase the ability of mutant huSOD1 to recruit WT moSOD1 to co-aggregate. In other work using transfection driven expression of both WT and mutant SOD1, WT huSOD1, but not WT moSOD1, was found to co-aggregate with mutant huSOD1 (Prudencio et al., 2009a), while WT moSOD1, but not WT huSOD1, co-aggregates with mutant moSOD1 (Qualls et al., 2013). Together this suggests that the tryptophan/serine at residue 32 is important for limiting the co-aggregation of human and mouse SOD1 rather than causing a difference in the ability of the mutant protein to elicit co-aggregation more generally.

These assays specifically examine co-aggregation and, as discussed above, it is not clear that aggregation *per se* is primarily responsible for causing disease. I have presented evidence for a toxic interaction between transgenic mutant *SOD1* and the endogenous WT *Sod1*. This suggests that this interaction is not dependent on co-aggregation of these two proteins. There are several other possibilities; the interaction could be a physical interaction between the two proteins, but one that does not result in co-aggregation, such as a prion-like template misfolding interaction. A second possibility is an indirect interaction between the proteins. For example, the increased oxidative environment reported in SOD1-fALS mouse tissues (e.g. (Andrus et al., 1998; Liu et al., 1999)) may lead to the oxidation of WT moSOD1, which could potentially cause misfolding and toxicity as has been reported to result from the oxidation of WT huSOD1 (Bosco et al., 2010; Guareschi et al., 2012). A third possibility is that the interaction is genetic. As we have seen, transgenically expressed human SOD1 can rescue some, but not all phenotypes of *Sod1* null mice (see Section 4.4.2), suggesting that an interaction between genetic phenotypes could occur. This is considered a less likely explanation as the *Sod1* null phenotypes tend to be detrimental to neuronal health, rather than protective, as described in Section 1.4.2. If the interaction between mutant huSOD1 and WT moSOD1 involves the augmentation of the aggregation of the transgenically expressed G93A huSOD1, it may be possible to detect this by histological methods on our samples collected from 75 day old animals, either using pan-SOD1 or misfolded SOD1 antibodies. A biochemical technique to evaluate differentially fractions may be a more suitable technique as

it could allow the examination of a wider array of species, however, at this time, suitable samples are not available.

### **6.3 MECHANISMS OF WT SOD1 PATHOGENICITY**

WT SOD1 appears to have 3 main potential modes of toxicity in SOD1-fALS; the most obvious, is the aggregation of WT SOD1, often co-aggregated with mutant SOD1 (e.g. (Bruijn et al., 1998; Jaarsma et al., 2000; Fukada et al., 2001; Deng et al., 2006; Jaarsma et al., 2008; Wang et al., 2009b; Prudencio et al., 2010)). Although it is still not clear whether protein aggregates are a primary cause of disease, they are likely responsible for secondary cellular toxicity, thereby exacerbating the disease process (Pasinelli et al., 2004; Ligon et al., 2005; Zhang et al., 2007; Bergemalm et al., 2010; Sau et al., 2011; Weisberg et al., 2012; Mulligan et al., 2013). The evidence presented in this Thesis suggests that in transgenic mouse models the prion-like process of seeded-aggregation is not likely to be a primary cause of aggregation of either mutant or WT transgenically expressed huSOD1. Prion-like seeded aggregation is also unlikely to be involved in the effect of the endogenous moSOD1 on mutant huSOD1 in SOD1-fALS mice, as evidence from other groups described above suggests that human and mouse SOD1 do not easily co-aggregate.

The second route by which WT SOD1 may exert toxicity is to become misfolded itself, thereby taking on properties which mimic the toxic mutant species (Bosco et al., 2010; Sundaramoorthy et al., 2013; Pasinelli et al., 2004; Guareschi et al., 2012). Misfolding of WT SOD1 could be caused by prion-like templated misfolding as has been demonstrated *in vitro* and in cellular models (Chia et al., 2010; Hwang et al., 2010; Grad et al., 2011; Grad et al., 2014). Our current method may not be able to assess whether the level of pre-aggregated soluble misfolded SOD1 species is affected by intracerebral inoculation with mutant SOD1 species and thus whether prion-like templated misfolded is at play. Behavioural assessment was not carried out and so we cannot determine whether the disease phenotype of TgG93A mice was affected, or whether any disease phenotype was elicited in TgWT mice by our inoculation protocol. However, from analysis of the premature deaths occurring in our TgWT mice in our longest time-point group, it does not appear that inoculation with mutant SOD1 species had any specific effect on survival, as survival times of animals inoculated with such material did not differ from control inoculated mice. Rather than being due to prion-like mechanisms, the misfolding of WT huSOD1, as is reported in double transgenic mouse models and in some ALS cases, could be caused by other factors, such as oxidation or demetalation, which can destabilise this typically highly stable protein (e.g. (Estévez et al., 1999; Urushitani et al., 2006; Lindberg et al., 2004; Rakhit et al., 2004; Ezzi et al., 2007; Rumfeldt et al., 2009; Proctor et al., 2011; Redler et al., 2011)).

The third mechanism by which WT SOD1 may exert toxicity is by augmenting the aggregation/misfolding of mutant SOD1. The reduced or slowed aggregation of mutant huSOD1 that results from co-expression with WT SOD1 (human or mouse) could lead to increased toxicity by maintaining the levels of a toxic pre-aggregate species, blocking its sequestration into aggregates (Brotherton et al., 2012; Prudencio et al., 2009a; Prudencio et al., 2010; Witan et al., 2008; Witan et al., 2009). This mode of toxicity is not dependent on a prion-like mechanism. It is not clear at this time whether misfolded WT moSOD1 is capable of taking on toxic conformers and contributing directly to the disease process of SOD1-fALS mice. Until there is a consensus as to the identity of the ALS pathogenic SOD1 species (singular or plural) or epitope, answering this question will be challenging. In cellular models the aggregation of mutant huSOD1 is augmented by both WT huSOD1 and WT moSOD1 (Brotherton et al., 2012; Prudencio et al., 2009a; Prudencio et al., 2010); whether this augmentation is relevant to the ALS like disease seen in SOD1-fALS mouse models is also not yet clear. Further investigation of the time course of aggregation in such models will be required to answer this question.

## **6.4 THE *SOD1* HUMANISED MOUSE**

I have presented the initial stages of the production of a new type of mouse model of SOD1-fALS in which the endogenous *Sod1* locus will be genomically humanised with a conditional switch of expression from ALS mutant huSOD1 to WT huSOD1. By genomically humanising the endogenous *Sod1* locus, physiological levels of protein expression should be achieved under the control of the endogenous *cis* and *trans* acting transcriptional regulators. By developing such a model, using targeted genomic humanisation rather than the more traditional insertional transgenic techniques, we aim to produce a model of the disease process and mechanisms which more closely mimic that seen in humans with SOD1-fALS. For example, by removing the very common feature of over-expression of the transgenic SOD1, a more accurate picture of the role of protein homeostasis systems, such as the ER and UPR, should be presented.

One major risk of producing a mouse model of SOD1-fALS with only endogenous expression levels is that expression may not be high enough to produce an overt disease phenotype within the lifespan of a mouse; the disease phenotype of SOD1-fALS mice is known to be tightly correlated to the expression level of the transgene. Of note on this matter, an ENU induced mutation in the endogenous *Sod1* locus, equivalent to a mutation seen in SOD1-fALS cases, has been reported as displaying some features in common with transgenic SOD1-fALS mice (McGoldrick et al., 2012). However, even if no overt motor phenotype does occur, this may still be a useful model by allowing a more detailed examination of the very early stages of

disease and the interactions of SOD1. As degeneration progresses, more secondary and tertiary processes and pathways become activated as a response to the primary degeneration. Opening the window on the earliest stages of degeneration may facilitate the identification of the root causes of disease, something which has remained elusive despite 20 years of research on transgenic SOD1-fALS mouse models.

By crossing the humanised *SOD1* mouse to a suitable Cre expressing line, more questions can be explored using the conditional mutant-WT switch; for example, by using an inducible Cre expresser, this model could be used to further investigate whether prion-like mechanisms are involved in the pathogenesis of SOD1-fALS; switching from expression of mutant huSOD1 to WT huSOD1 either before the initial signs of, or at time-points during, degeneration would allow investigation of whether continued expression of mutant huSOD1 is necessary for the disease progression. Such investigation could have important implications for potential therapeutic interventions which aim to reduce the level of mutant SOD1 expression using technologies such as antisense oligonucleotides or RNA interference (e.g. (Miller et al., 2005; Raoul et al., 2005; Smith et al., 2006; Miller et al., 2013)).

## 6.5 CONCLUSIONS

In this Thesis preliminary evidence is presented suggesting that prion-like seeded aggregation does not play a role in the aggregate pathology of transgenic *SOD1* mice, although further analysis is required to confirm these results. A high copy G93A mutant *SOD1* transgenic line was used in the first set of experiments to investigate whether SOD1 displays the prion-like property of self-seeded aggregation *in vivo*. This mouse line may not have been ideal as the disease progression is aggressive, leaving only a limited time window between inoculation and harvesting of tissues. This also means that it has a high baseline level of aggregate pathology which may hamper the detection of potentially subtle changes in pathology. In the second set of experiments we investigated cross-seeded aggregation in WT *SOD1* transgenic mice. Although a significant difference in misfolded SOD1 aggregate pathology was detected for one of the spinal cord regions analysed, because of a low sample size of analysed animals in the control group, we cannot draw any strong conclusions based on this result until the remaining cases have been processed and analysed. Alternative outcome measures could still provide evidence for prion-like mechanisms *in vivo* in SOD1 pathogenicity. For example histopathological markers of degeneration could act as a surrogate, indicating changes in the levels of the pathogenic form of SOD1.

I also present evidence that the endogenous moSOD1 plays an augmenting role in the disease phenotype of the G93A mutant *SOD1* transgenic mouse at an early stage of the degenerative process. A functional advantage is found in mice null for the endogenous *Sod1* allele at 75-days

of age. I also present data that at the same age, compared to TgG93A;Sod1wt mice, TgG93A;Sod1ko mice have more neuromuscular junctions in hind limb muscles and a non-significant trend towards better maintenance of innervation by the most vulnerable, fast-firing MNs. It is well established, from double transgenic mice, that WT huSOD1 interacts with mutant huSOD1 to exacerbate the disease phenotype, however previous examination of whether WT endogenous moSOD1 effects the phenotype produced by mutant huSOD1 have not been fully conclusive (Bruijn et al., 1998; Fukada et al., 2001; Jaarsma et al., 2000; Deng et al., 2006; Jaarsma et al., 2008; Wang et al., 2009b; Prudencio et al., 2010). Here I provide evidence that the degenerative process in the TgG93A mouse is indeed affected by the endogenous WT moSOD1 however, just as is the case with WT and mutant huSOD1, further research will be required to delineate the mechanism of this interaction.

Finally I have presented the construction of a targeting vector for the production of a new type of mouse model of SOD1-fALS; a genomically humanised *SOD1* mouse with a conditional switch from mutant expression to WT. Further work is needed to ready the construct for genome targeting in mESCs but it is hoped that the resultant mouse model will be a valuable new tool to help elucidate the early and primary disease processes relevant to the instigation of disease in SOD1-fALS.

As has been discussed, it is becoming increasingly apparent that WT SOD1 is involved in SOD1-fALS and also possibly non SOD1-fALS and sALS. Here I have tried to answer some questions related to this phenomenon, such as whether prion-like seeded aggregation may be involved in the development of WT SOD1 aggregation, and whether an interaction between WT and mutant SOD1 might be augmenting the phenotype of the most commonly used SOD1-fALS mouse model. I have also presented preliminary work in developing a new type of SOD1-fALS mouse model that has been designed to allow further exploration of this topic and to act as a new and complementary model of this disease. Ultimately, it is our hope that by improving our understanding of this ALS and improving on our ability to accurately model it, we will help towards the development of effective treatments for this devastating disease, something that despite decades of research has so far eluded us.

## Chapter 7. Appendices

### 7.1 APPENDIX 1 - FULL TABLE OF MUTANT *SOD1* TRANSGENIC MICE

Rows are arranged by the location of the mutation used. Lines used in the work presented in this Thesis are highlighted in yellow. Lines which failed to develop disease are highlighted in pink.

All figures are for hemizygous mice unless specified. Protein expression and dismutase activity were assayed from spinal cord, unless specified.

(\*1)- Protein expression is expressed as fold increase relative to endogenous Sod1 level

(\*2) SOD1 activity is expressed as fold difference compared to NTg

Tg= Transgene; Hom= homozygous; nr= not reported; nq= measured but not quantified; (\$) = symptoms and survival shown for homozygotes; (#)= introduces a stop codon at position 133; ¥= promoter region 483 bp 3' of exon 1; ¤= EcoRI-BamHI human gDNA fragment is 11.58 kb and included SOD1 gene plus 0.5 kb 5' & 1.8 kb 3'.

Mutation	Promoter	Tg fragment	Tg copy	Protein (*1)	Activity (*2)	Symptom onset (weeks)	Survival (weeks)	notes	MGI Symbol	Ref
WT	Human SOD1 (¥)	gDNA E-B (α)	7	50 (reported as 24 fold in 39)	8.6	36 (hom)	52 (hom)		Tg(SOD1) 2Gur (N1029)	1, 2, 38
A4V	Human SOD1 (¥)	gDNA E-B (α)	~5	nr	~1.4	none			Tg(SOD1* A4V) A1073Gur	2
G37R (line 106)	Human SOD1 (¥)	gDNA E-B (α)	nr	4.2/5.3 (brain/spinal cord)	7.2	22-30	25-29		Tg(SOD1* G37R) 106Dpr	3
G37R (line 29)	Human SOD1 (¥)	gDNA E-B (α)	nr	4.0/5.0 (brain/spinal cord)	7	24-32			Tg(SOD1* G37R)29Dpr	3
G37R (line 42)	Human SOD1 (¥)	gDNA E-B (α)	nr	8.0/10.5 (brain/spinal cord)	14.5	14-16			Tg(SOD1* G37R)42Dpr	3
G37R (line 9)	Human SOD1 (¥)	gDNA E-B (α)	nr	5.4/6.2 (brain/spinal cord)	9	20-24			Tg(SOD1* G37R)9Dpr	3
G37R	Neuro-filament light chain promoter	cDNA		4.3 (line 3156) and 2.8 (line 4012)	nr	none (up to 1.5 years)	none (up to 1.5 years)	Neuron specific expression. Two lines reported		4
G37R (see notes)	Mouse prion promoter	cDNA	nr	nq	nq	28-36 (hom)	onset +1-3 weeks	Co-integration of SOD1 transgene with construct encoding wild-type human presenilin 1 (hPS1)with PrP promoter)	Tg(Prnp-SOD1*G37R,-PSEN1) 110Dbo	5



Mutation	Promoter	Tg fragment	Tg copy	Protein (*1)	Activity (*2)	Symptom onset (weeks)	Survival (weeks)	notes	MGI Symbol	Ref
G37R (floxed)	nr (human SOD1?)	gDNA unspecified fragment	nr	nq	nr	26-30	37-48		Tg(SOD1* G37R)1Dwc	6
G37R and G93A (see notes)	Chicken skeletal muscle $\alpha_{sk}$ actin	cDNA	1-8			32-40		Two mutants (G37R and G93A, plus the WT) created, results do not specify which mutant. Muscle-specific expression. Neuromuscular phenotype seen in both WT and mutant (G37R and G93A) mice. Mutants had reduced NMJ innervation and axonal degeneration and 50% MN loss by 1-year		7
H46R	Human SOD1 (¥)	gDNA E-B (ㄅ)	nr	nr	nr	22-26	onset +4 weeks			8
H46R	Human SOD1 (¥)	gDNA E-B (ㄅ)	nr	nr	nr	20	24		Tg(SOD1* H46R)#Maw	9
H46R/H48Q (line 139)	Human SOD1 (¥)	gDNA E-B (ㄅ)	nr	nq	1	nr	17-26		Tg(SOD1* H46R*H48Q) 139Dbo	10
H46R/H48Q (line 58)	Human SOD1 (¥)	gDNA E-B (ㄅ)	nr	nq	nr	nr	12-14		Tg(SOD1* H46R*H48Q) 58Dbo	10, 11

Mutation	Promoter	Tg fragment	Tg copy	Protein (*1)	Activity (*2)	Symptom onset (weeks)	Survival (weeks)	notes	MGI Symbol	Ref
H46R/ H48Q/ H63G/ H120G (line 121)	Human SOD1 (¥)	gDNA E-B (α)	nr	nq	nr	nr	over 69 weeks	H46R/H48Q ALS mutations with H63G/H120G experimental mutations to disrupt copper binding		11
H46R/ H48Q/ H63G/ H120G (line 125)	Human SOD1 (¥)	gDNA E-B (α)	nr	nq	1	nr	39-52	H46R/H48Q ALS mutations with H63G/H120G experimental mutations to disrupt copper binding	Tg(SOD1*) 125Dbo	11
H46R/ H48Q/ H63G/ H120G (line 187)	Human SOD1 (¥)	gDNA E-B (α)	nr	nq	nr	nr	35-48	H46R/H48Q ALS mutations with H63G/H120G experimental mutations to disrupt copper binding		11
E77X (stop)	Human SOD1 (¥)	gDNA E-B (α)	nq	nr (RNA "barely detected")	nr	none	normal	Experimental (rather than ALS) mutation to examine whether truncated proteins are capable of causing disease		12
L84V	Human SOD1 (¥)	gDNA E-B (α)	nr	nr	nr	22-26	26			13, 14
G85R (line 148)	Human SOD1 (¥)	gDNA E-B (α)	nr	1	1	33	35		Tg(SOD1* G85R)148Dw c	15
G85R (line 74)	Human SOD1 (¥)	gDNA E-B (α)	nr	0.2	nr	51-61	onset +2 weeks		Tg(SOD1* G85R)74Dwc	15

Mutation	Promoter	Tg fragment	Tg copy	Protein (*1)	Activity (*2)	Symptom onset (weeks)	Survival (weeks)	notes	MGI Symbol	Ref
G85R	Thy1.2	cDNA		nq	nq	none (up to 87)		Bicistronic expression of SOD1 and EGFP in postnatal motor neurons		16
G85R (floxed)	nr	A G85R genomic clone	nr	1.5	1	44	50	LoxP flanked transgene	Tg(SOD1* G85R)#Roos	17
G85R (YFP fusion) (line 641)	nr (but presumed to be Human SOD1 (¥))	gDNA E-B (α)		nr	nr	39 (hom)				18
G86R (mouse)	nr (mouse Sod1?)	gDNA mouse SalI fragment (see notes)	nr	nr	1	13-17	13-17	Reported as a SalI fragment of mouse gDNA, but SalI cuts within intron 3	Tg(Sod1* G86R)M1Jwg	19, 4
G86R (mouse) (line 2)	Mouse GFAP	cDNA from mouse brain	nq	nq		none (up to 70)		Astrocyte specific expression		20
G86R (mouse) (line 29)	Mouse GFAP	cDNA from mouse brain	10	nq		none (up to 70)		Astrocyte specific expression		20
D90A (line 134)	nr (but presumed to be Human SOD1 (¥))	gDNA E-B (α)	nr	nr	~6-9	50 (hom)	58 (hom)			21

Mutation	Promoter	Tg fragment	Tg copy	Protein (*1)	Activity (*2)	Symptom onset (weeks)	Survival (weeks)	notes	MGI Symbol	Ref
K91X (stop)	Human SOD1 (¥)	gDNA E-B (α)	nq	nr (RNA "barely detected")	nr	none	normal	Experimental (rather than ALS) mutation to examine whether truncated proteins are capable of causing disease		12
G93A (line G1)	Human SOD1 (¥)	gDNA E-B (α)	18	nr	~4	12-16	20		Tg(SOD1*G93A)2Gur (G1)	2
G93A (line G20)	Human SOD1 (¥)	gDNA E-B (α)	1.7	nr	~1.6	nr	49		Tg(SOD1*G93A)G20Gur	2, 22
G93A (line G1H)	Human SOD1 (¥)	gDNA E-B (α)	25	17 (described as equal to the N1029 line in 24)	>4 (reported as 8.9 in 26)	13	19.4	High transgene copy number derived from G1 line	Tg(SOD1*G93A)1Gur (subline of G1 with expansion)	23, 24
G93A (line G1del)	Human SOD1 (¥)	gDNA E-B (α)	8	nr	nr	28	36	Low transgene copy number derived from G1 line	Tg(SOD1*G93A)dl1Gur	25, 26
G93A	Rat myosin light chain (MLC1)	cDNA	nr	nq	nq	muscle atrophy from 4 weeks	nr	Muscle specific expression, especially fast fibres	Tg(Myf1-SOD1*G93A) #Amu	27
G93A (T1xT3 see notes)	Thy1.2	cDNA	nr			77-104	84-104	Compound hemizygote T1 and T3 transgene. Postnatal motor neurons specific expression		28
G93A (line T1)	Thy1.2	cDNA	nr			none	normal	Postnatal motor neurons specific expression	Tg(Thy1-SOD1*G93A) T1Hgrd	28

Mutation	Promoter	Tg fragment	Tg copy	Protein (*1)	Activity (*2)	Symptom onset (weeks)	Survival (weeks)	notes	MGI Symbol	Ref
G93A (line T3)	Thy1.2	cDNA	nr	nq		none (54-104 for hom)	62-104 (hom)	Postnatal motor neurons specific expression	Tg(Thy1-SOD1*G93A) T3Hgrd	28
G93A (with luciferase reporter)	BiTetO (see notes)	cDNA				none	over 64 weeks	Conditional Cre expression in some subgroups of embryonic motor neurons and interneurons from transgene with Lhx3 promoter. Cre expression allows transgenic expression of a tetracycline-repressible transactivator gene which activates transcription from a BiTetO (bicistronic tetracycline-repressible transactivator) promoter expressing a SOD1-G93A and luciferase transgene. WT line also made	Tg(tetO-SOD1*G93A,-luc)1Roos	29
G93A	MLC1f/3f	cDNA				See notes		Skeletal muscle specific expression, especially in fast fibres. Increasing muscle atrophy from 4 weeks. Decreased force by 4 months. Lipid peroxidation and microglial activation in spinal cord. No MN loss or change in fibre composition of muscles		27

Mutation	Promoter	Tg fragment	Tg copy	Protein (*1)	Activity (*2)	Symptom onset (weeks)	Survival (weeks)	notes	MGI Symbol	Ref
G93A	TRE (See notes)	cDNA				none		Bidirectional tetracycline/doxycycline response (TRE) transgene, controlling expression of SOD1-G93A and EGFP with unexpected translation restricted to olfactory bulb		30
I113T	nr	nr	nr	nr	nr	52	nr			31, 32
T116X (stop)	Human SOD1 (¥)	Minigene (see notes)	nr	nr	nr	survival minus 2 weeks (hom)	43 (hom)	EcoRI-BamHI gDNA fragment of SOD1 locus with engineered fusion exon 4-5. Experimental (rather than ALS) mutation to examine whether truncated proteins are capable of causing disease		12
L126delTT (see notes)	nr	gDNA (11 kb fragment)	nr	nr	nr	none (ALS specific unto 52 weeks)		Mouse created to model ALS but resultant phenotype was due to insertional disruption of the Ssd1p1 (single stranded DNA binding protein 1) locus in homozygous transgenics	Ssb1p3Tg(SOD1)1Hssk	33
L126delTT (#) (line D1)	Human SOD1 (¥)	gDNA E-B (α)	1	nr	nr	none				34

Mutation	Promoter	Tg fragment	Tg copy	Protein (*1)	Activity (*2)	Symptom onset (weeks)	Survival (weeks)	notes	MGI Symbol	Ref
L126delTT (#) (line D2)	Human SOD1 (¥)	gDNA E-B (α)	5	“below western detection threshold”	1	63 (34 for hom)	68 (36 for hom)			34
L126delTT-FLAG (#) (line DF2)	Human SOD1 (¥)	gDNA E-B (α)	3	nr	nr	none		FLAG tagged SOD1		34
L126delTT-FLAG (#) (line DF7)	Human SOD1 (¥)	gDNA E-B (α)	4	nq	1	49 (17 for hom)	53 (18 for hom)	FLAG tagged SOD1		34
L126Z (stop)	Human SOD1 (¥)	Minigene (see notes)	nr	0–0.5	nr	30-39	nq	EcoRI-BamHI gDNA fragment of SOD1 locus with engineered fusion exon 3, 4 and 5		35
L126Z (stop)	nr (but presumed to be (¥))	gDNA E-B (α)	nr	0–1	nr	48	51		Tg(SOD1*L126Z)#Deng	36
SOD1G127 insTGGG (line 716)	nr (but presumed to be Human SOD1 (¥))	gDNA E-B (α)	19	0.45–0.97	1	onset minus 7-10 (hom)	64 (36 for hom)		Tg(SOD1*G127X)716Mrkl	37
SOD1G127 insTGGG (line 832)	nr (but presumed to be (¥))	gDNA E-B (α)	28	nr	nr	nr	30 (18 for hom)		Tg(SOD1*G127X)832Mrkl	37

1- (Graffmo et al., 2012); 2- (Gurney et al., 1994); 3- (Wong et al., 1995); 4- (Pramatarova et al., 2001); 5- (Wang et al., 2005b); 6- (Boillée et al., 2006); 7- (Wong et al., 2010); 8- (Nagai et al., 2000); 9- (Chang-Hong et al., 2005); 10- (Wang et al., 2002b); 11- (Wang et al., 2003); 12- (Deng et al., 2008); 13- (Kato et al., 2001a); 14-

(Tobisawa et al., 2003); 15- (Bruijn et al., 1997); 16- (Lino et al., 2002); 17- (Wang et al., 2009b); 18- (Wang et al., 2009a); 19- (Ripps et al., 1995); 20- (Gong et al., 2000); 21- (Jonsson et al., 2006a); 22- (Dal Canto et al., 1995); 23- (Chiu et al., 1995); 24- (Tu et al., 1996); 25- (Zhang et al., 1997); 26- (Gurney, 1997); 27- (Dobrowolny et al., 2008); 28- (Jaarsma et al., 2008); 29- (Wang et al., 2008); 30- (Bao-Cutrona et al., 2009); 31- (Ryoichi et al., 2001); 32- (Kikugawa et al., 2000); 33- (Nishioka et al., 2005); 34- (Watanabe et al., 2005); 35- (Wang et al., 2005a); 36- (Deng et al., 2006); 37- (Jonsson et al., 2004); 38- (Jaarsma et al., 2000); 39- (Jonsson et al., 2006b)



## 7.2 APPENDIX 2 - DETAILED MATERIALS AND EQUIPMENT

### 7.2.1 Molecular Biology

#### 7.2.1.1 REAGENTS

Betaine solution 5 M, PCR Reagent	Sigma	B0300
BetterBase	Microzone	3BBR-5
BetterBuffer	Microzone	3BB-5
Buffer P1	Qiagen	19051 NB: RNase A added as per manufacturer's instructions
Buffer P2	Qiagen	19052
Buffer P3	Qiagen	19053
Crystal 5x DNA Loading Buffer Blue	Bioline	
DPBS 1X Dulbecco's Phosphate Buffered Saline (Minus CaCl <sub>2</sub> and MgCl <sub>2</sub> )	Gibco	14190
EB	Qiagen	
Ethidium bromide 500µg/ml in H <sub>2</sub> O	Sigma Aldrich	E1385-5ML
Extraction Solution	Sigma	E7526
HyperLadder I	Bioline	BIO-33025
HyperLadder IV	Bioline	BIO-33029
MicroCLEAN	Microzone	
Neutralisation Solution B	Sigma	N3910
PBS (phosphate buffered saline) solution 10x DNase RNase and protease free	Fisher BioReagents	10214733
RNase A	Qiagen	19101
TaqMan Universal PCR Master Mix with passive internal reference, and AmpErase UNG	Applied Biosystems	
Tissue Preparation Solution	Sigma	T3073
Tris-EDTA buffer solution pH 8.0	Sigma	93283 FLUKA
UltraPure™ Agarose	Invitrogen	
Quick & Easy BAC Modification Kit	Gene Bridges	K001

#### 7.2.1.2 KITS

QIAEX II Gel Extraction Kit	Qiagen	20021
QIAGEN Large-Construct Kit	Qiagen	12462
QIAGEN Plasmid Maxi Kit	Qiagen	12162
QIAprep Spin Miniprep Kit	Qiagen	27104
QIAquick Gel Extraction Kit	Qiagen	28704
QIAquick PCR Purification Kit	Qiagen	28104

#### 7.2.1.3 ENZYMES

ABI PRISM® BigDye® Terminator v1.1 Ready Reaction mix	Applied Biosystems	4337450
AccuPrime™ Pfx SuperMix	Invitrogen	12344-040
Alkaline Phosphatase, Calf Intestinal (CIP)	New England BioLabs	M0290L
REDTaq® ReadyMix™ PCR Reaction Mix	Sigma-Aldrich	R2523
T4 DNA Ligase	New England BioLabs	M0202
TaqMan(R) Universal PCR Master Mix	Invitrogen	4304437

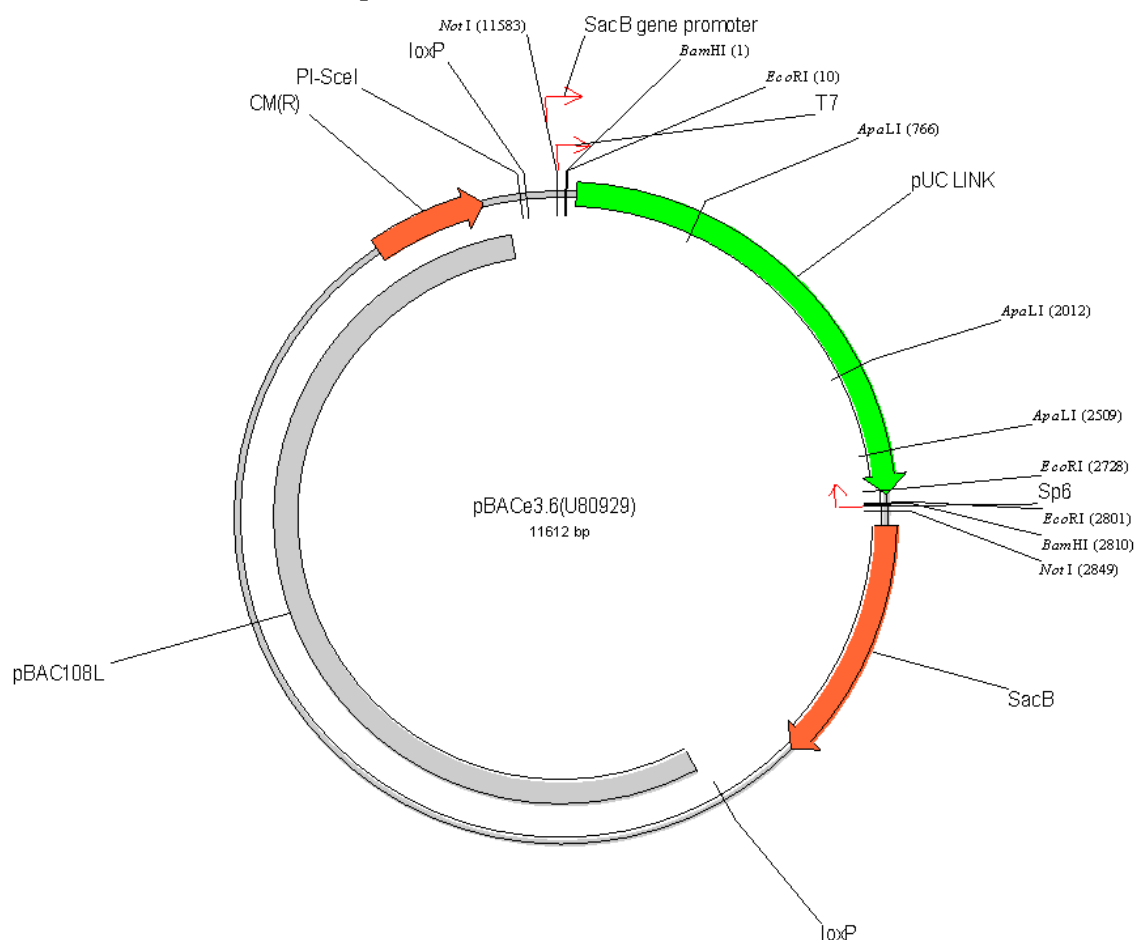
## 7.2.2 Bacterial Artificial Chromosomes

### 7.2.2.1 HUMAN SOD1 BAC

BACs were ordered from Children's Hospital Oakland Research Institute (CHORI) BACPAC Resource Center (<http://bacpac.chori.org/home.htm>).

Human SOD1 BAC (E10)	
Feature	RP11-535E10
Description	Library: RP11
Chromosome	21
Chromosome position	32,928,199 – 33,097,333
Contig	NT_011512.11
Contig position	18,590,070 - 18,759,204
Span	169135
Clone ends	AZ301041.3 span: 467
	AZ301042.2 span: 457
Backbone	pBACe3.6 at EcoRI sites
5' of SOD1	103,735bp
3' of SOD1	56,090bp

#### 7.2.2.1.1 Vector Map



### 7.2.2.2 C57BL/6J *MOUSE Sod1* BACs

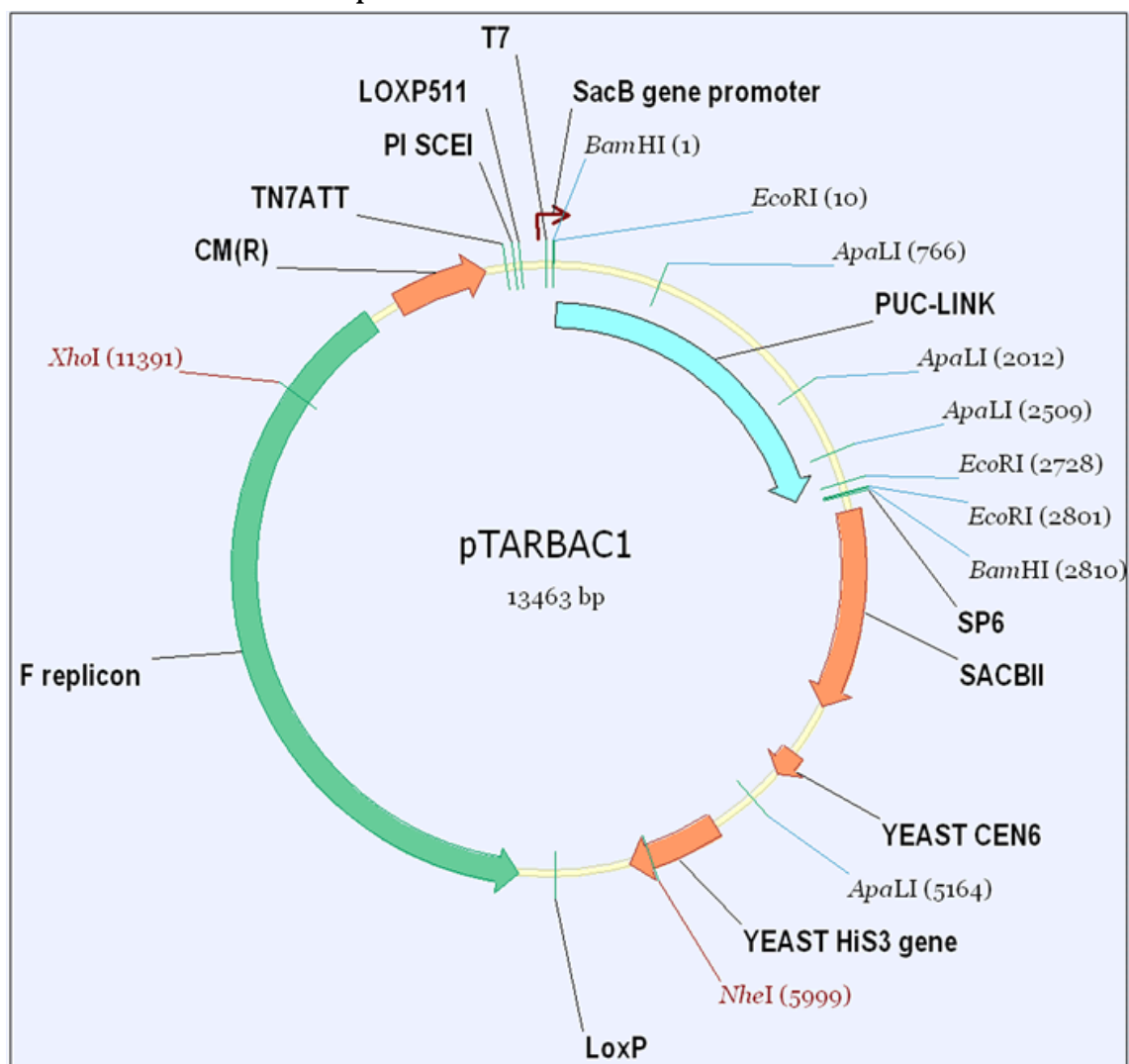
BACs were ordered from Children's Hospital Oakland Research Institute (CHORI) BACPAC

Resource Center (<http://bacpac.chori.org/home.htm>).

<b>C57BL/6J Sod1 BAC (N21)</b>	
Clone name	RP24-363N21
Library	RP24
Chromosome	16
Chromosome position	90,198,557 - 90,376,511
Strain name	C57BL/6J Male from Jackson Laboratory
Contig	NT_039625.7
Contig position	24,903,634 - 25,081,588
Span	177955
Clone ends	BH102801.1 span: 621
	BH102799.1 span: 600
Backbone	pTARBAC1 at BamHI sites
5' of Sod1	22,431bp
3' of Sod1	149,943bp

<b>C57BL/6J Sod1 BAC (L18)</b>	
Clone name	RP24-238L18
Library	RP24
Chromosome	16
Chromosome position	90,078,076 - 90,243,716
Strain name	C57BL/6J Male from Jackson Laboratory
Contig	NT_039625.7
Contig position	24,783,153 - 24,948,793
Span	165641
Clone ends	BH111706.1 span: 310
	BH111705.1 span: 511
Backbone	pTARBAC1 at BamHI sites

### 7.2.2.2.1 Vector Map



### 7.2.2.3 C57BL/6N MOUSE SOD1 BAC

Ordered from Riken Bioresource Center (<http://dna.brc.riken.jp/en/NBRPB6Nbacen.html>).

<b>C57BL/6N Sod1 BAC #1 (O19)</b>	
Clone name	B6Ng01-068O19
Library	B6Ng01
Chromosome	16
Strain name	C57BL/6NCrI CrIj
Chromosome position	90,169,050 - 90,326,628
Contig	
Contig position	
Span	157579
Clone ends	DH887377.1 span: 964
	DH887378.1 span: 1019
Backbone	pBACe3.6 at EcoRI sites
5' of Sod1	51,937bp
3' of Sod1	100,054bp

## 7.2.3 Bacterial Culture

### 7.2.3.1 REAGENTS

ElectroMAX DH10B Cells	Invitrogen	18290-015
Glycerol	Sigma	G5516
L-arabinose	Sigma	A3256
LB agar	Sigma	L3147
Luria Broth (Miller's Modification)	Sigma	L3397
MAX Efficiency DH10B Competent Cells	Invitrogen	18297.01

### 7.2.3.2 ANTIBIOTICS

<b>Ampicillin (Amp) Sigma A0166</b>	
Stock	100 mg/ml in 50% EtOH
Working	50 ug/ml for BACs (2000x dilution)
	100 ug/ml for high copy plasmid (1000 x dilution)
<b>Chloramphenicol (Cm) Sigma C7795</b>	
Stock	30 mg/ml in 100% EtOH
Working	15 ug/ml for BACs (2000x dilution)
	50 ug/ml for high copy plasmid (600x dilution)
<b>Gentamicin (Gent) Sigma G1914</b>	
Stock	10 mg/ml in H <sub>2</sub> O
Working	10 ug/ml (1000x dilution)
<b>Kanamycin (Kana) Sigma K0254</b>	
Stock	50 mg/ml in 0.9% NaCl (ready-made stock)
Working	15 ug/ml for BACs (3300x dilution)
	50 ug/ml for high copy plasmid (1000x dilution)
<b>Spectinomycin (Spc) Sigma S4014</b>	
Stock	50 mg/mL in H <sub>2</sub> O
Working	100 ug/mL for BACs and high copy plasmid (500x dilution)
<b>Streptomycin (Strep) Sigma S6501</b>	
Stock	10 mg/ml in H <sub>2</sub> O
Working	5 ug/ml (2000x dilution)
<b>Tetracycline (Tet) T7660</b>	
Stock	5 mg/ml in 75% EtOH
Working	3 ug/ml for pRedET (1650x dilution)
	10 ug/ml for BACs and high copy plasmid (500x dilution)

## 7.2.4 Histology

### 7.2.4.1 REAGENTS AND KITS

0.5% eosin aqueous solution	Prolab	
10% Buffered Formal Saline	Pioneer Research Chemicals	PRC/R/2
DPX mounting medium	VWR	360292F
Fluorescence mounting medium	Dako	S3023
Harris' haematoxylin for microscopy	Prolab	
Histo-clear	National Diagnostics	HS-200
Paraformaldehyde	Sigma-Aldrich	P6148-500g
PBS-DA Phosphate Buffered Saline (Dulbecco A) tablets (no calcium or magnesium) pH7.3	Oxoid	BR0014G
Pertex mounting medium	Leica	3808706E
Tissue-Tek® O.C.T. Compound	Sakura	4583
Vector M.O.M. Immunodetection Kit BASIC	Vector Labs	BMK-2202

### 7.2.4.2 ANTIBODIES

#### 7.2.4.2.1 Primary Antibodies

Anti-β-actin (mouse)	Sigma	A5441
Mouse monoclonal anti-myosin heavy chain 2A	Developmental Studies Hybridoma Bank	SC-71
Mouse monoclonal anti-myosin heavy chain 2B	Developmental Studies Hybridoma Bank	BF-F3
Mouse monoclonal anti-myosin heavy chain, all but 2X	Developmental Studies Hybridoma Bank	BF-35
Mouse monoclonal anti-myosin heavy chain, slow, alpha and beta-	Developmental Studies Hybridoma Bank	BA-D5
Mouse monoclonal anti-neurofilament (165kDa)	Developmental Studies Hybridoma Bank	2H3
Mouse monoclonal anti-synaptic vesicle	Developmental Studies Hybridoma Bank	SV2
SOD100. Rabbit, pan-anti-SOD1	Enzo	ADI-SOD-100-D

#### 7.2.4.2.2 Secondary Antibodies

Alexa Fluor 488 goat anti-mouse IgM (μ chain) 2mg/ml	Invitrogen	A21042
Alexa Fluor 568 goat anti-mouse IgG (H+L) 2mg/ml	Invitrogen	A11004
Alpha-bungarotoxin	Sigma	T0195
DAPI	Sigma	D8417
Goat anti-mouse IgG-AP (alkaline phosphatase)	Southern biotech	1070-04
Poly-clonal goat anti-rabbit IgG-HRP	Dako	
Streptavidin Alexafluor 488 conjugated 2mg/ml	Invitrogen	S32354

## 7.2.5 Protein Biochemistry Reagents

CDP-Star	Roche	11685627001
Pierce ECL Western Blotting Substrate	Pierce	32106

Protease inhibitor cocktail	Roache	05892791001
Protein A agarose beads	Sigma	P3476
RIPA Buffer	Sigma	R0278

## 7.2.6 Equipment

Bench top refrigerated microfuge. Heraeus Fresco 17	Thermo Fisher	
Bright™ cryostat		
Electroporation cuvettes. 1mm black cap	Eurogentec	CE-0001-50
Electroporator. <i>E.coli</i> Pulser	Biorad	Model 1652104
Grip-strength meter bio-GS3	Bioseb	
MaxQ Mini 4450 compact bench top incubated shaker, analogue	Barnstead	SHKA4450-1CE
PAP pen	VWR	72-0169
Poly-lysine coated slides	VWR	631-0107
polystyrene disposable cuvettes 1.6ml	VWR	634-2501
Standard bench top microfuge	Eppendorf Centrifuge 5424	
Thermomixer compact	Eppendorf	5350 000.013
Ventana automated immunohistochemical staining machine using a basic diaminobenzidine detection system according to the manufacturer's instructions (Ventana Medical Systems, Tucson, AZ)		

## 7.2.7 Prepared Solutions and Materials

### 7.2.7.1 LB MEDIA

For liquid bacterial cultures Luria Broth (LB) Miller's Modification was made according to manufacturer's instruction and autoclaved to sterilise. Once sterilised LB was stored indefinitely in sealed glass bottles as room temperature. Antibiotics were added only immediately before use and at concentrations give in table 7.1 above.

### 7.2.7.2 LB AGAR PLATES

LB agar was prepared according to manufacturer's instructions and autoclaved to sterilise. Once cooled to around 50°C antibiotics were added using concentrations given in table 7.1 above and agar was mixed thoroughly. 25ml was used per petri dish. Once set and dried at room temperature plates were stored at 4°C for up to 1 month.

### 7.2.7.3 BACTERIAL FREEZING MEDIA 2X

LB Miller's Modification was made according to manufacturer's instructions, but replacing ddH<sub>2</sub>O with 1:1 glycerol:ddH<sub>2</sub>O. Medium was autoclaved to sterilise and kept indefinitely in sealed glass bottles at room temperature.

#### *7.2.7.4 TRIS-EDTA-CITRATE BUFFER PH 7.8 10X*

For a 10X stock solution: 55g EDTA, 2.5g Trizma Base, 3.2g Tri-sodium citrate was dissolve in 1 litre ddH<sub>2</sub>O. pH to 7.8 using 2M hydrochloric acid to reduce pH and 2M sodium hydroxide to increase pH. Store at 4°C.

#### *7.2.7.5 TRIS (0.5M) BUFFERED SALINE (9%) 10X*

30.29g TRIS base, 45g Sodium chloride, 15ml ddH<sub>2</sub>O. pH to 7.8 using concentrated hydrochloric acid. Make upto 500ml with ddH<sub>2</sub>O

#### *7.2.7.6 4% PARAFORMALDEHYDE IN DULBECCO'S PHOSPHATE BUFFERED SALINE*

40g paraformaldehyde (PFA, Sigma-Aldrich) was dissolved in 1L ddH<sub>2</sub>O by heating to 60°C and stirring for 30mins. 5-15µl 5M NaHO was then added until PFA was completely dissolved. Ten PBS (Dulbecco A, pH 7.3) tablets (Oxoid) were then added and stirred until dissolved. The solution was then brought back down to room temperature and filter sterilised using a 0.45µM Stericup (Millipore). If not for use within 24 hours, sterilised PFA was aliquot and stored at -20°C. Aliquots were defrosted at 4°C overnight.

#### *7.2.7.7 GALLOCYANINE STAIN*

1.5g gallocyanine (C.I. 51030)

50g chromium potassium sulphate

500mL ddH<sub>2</sub>O

Dissolve chromium potassium sulphate in water by heating. Add gallocyanine and boil for 20-30 mins. Cool to room temperature before filtering and adding ddH<sub>2</sub>O to return the volume to 500mL.

#### *7.2.7.8 LAEMMLI SAMPLE BUFFER - 20 ML*

Final 1X concs:

60 mM Tris-Cl pH 6.8, 2% SDS, 10% glycerol, 5% β-mercaptoethanol, 0.01% bromophenol blue

#### **2X sample buffer:**

1.6 ml 1.5 M Tris-Cl pH 6.8

4 ml glycerol

2 ml β-mercaptoethanol

0.8 g SDS (sodium dodecyl sulfate / sodium lauryl sulfate)

0.4 ml 1% bromophenol blue (Sigma 3-8026)



**\*\* CAUTION \*\***  $\beta$ -mercaptoethanol and SDS powder are hazardous. Prepare solution in a ventilated fume hood.

- 1) Add 0.4 ml of 1% bromophenol blue to 1.6 ml of 1.5 M Tris-Cl pH 6.8.
- 2) Add 4ml of glycerol and mix.
- 3) Add 0.8 g of SDS and mix (the SDS will take a few minutes to dissolve).
- 4) top upto 18ml (11.2ml ddH<sub>2</sub>O)
- 5) Aliquot (450ul aliquots) and store at -20°C.

Add  $\beta$ -mercaptoethanol to 10% when thawed (50ul per aliquot)

#### *7.2.7.9 1.5 M TRIS-CL PH 6.8 – 50ML*

Reagents:

9.0825 g Tris base

35 ml ddH<sub>2</sub>O

6 ml Concentrated HCl (37.2% - 12.1M)

**\*\* NOTE:** Many electronic pH Meters are unable to accurately determine the pH of concentrated Tris solutions. Be sure to use an appropriate probe. **\*\***

Directions:

- 1) Mix 9.0825 g of Tris base with 35 ml of ddH<sub>2</sub>O by stirring.
- 2) Adjust the pH by adding the concentrated HCl. Begin by adding 5 ml and then fine adjust if needed.
- 3) Add ddH<sub>2</sub>O until final volume is 50ml.
- 4) Autoclave to sterilize.

### 7.3 APPENDIX 3 - PREMATURE DEATHS FOR THE CROSS-SEEDED SOD1 TRANSMISSION EXPERIMENT

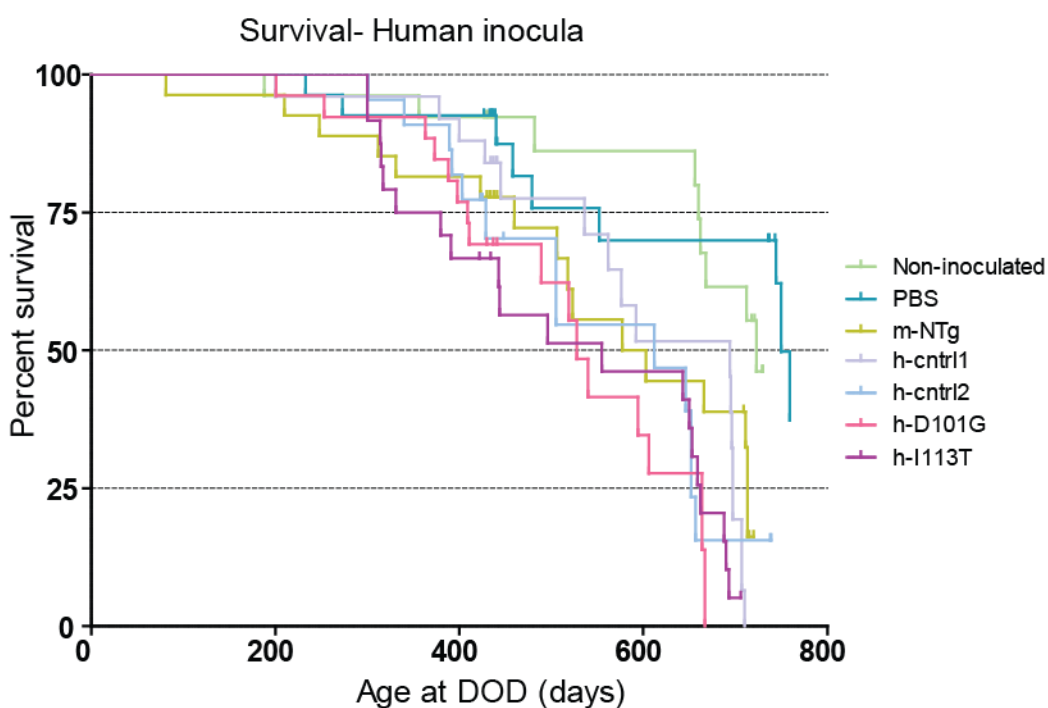
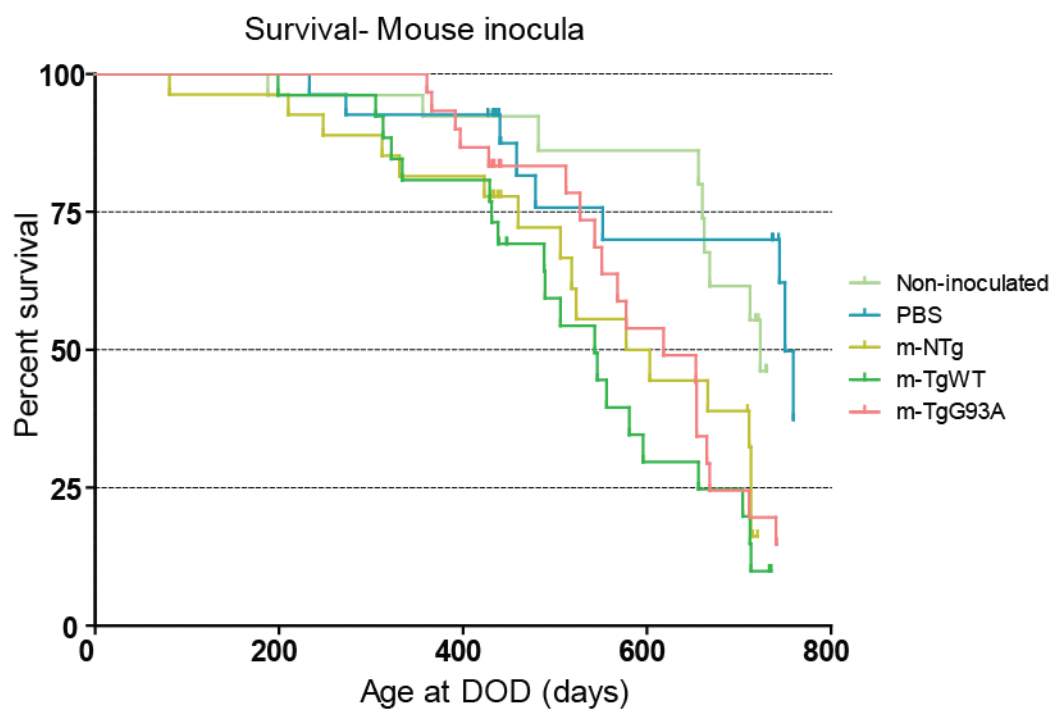
Full breakdown of premature deaths for the cross-seeded SOD1 transmission experiment split by inocula and time-point group

Inocula	Time-point (days post inoc')	Inoculation / anaesthetic	Scratching	weight loss	Found dead	Swollen abdomen	Abnormal breath- ing	Hind- limb paralysis	Impaired righting reflex	Missing presumed dead	Culled in error	Pro- lapsed rectum	Tumour	TOTAL premature deaths	Reached cull date
Non-inoculated	7									3				3	8
Non-inoculated	90													0	10
Non-inoculated	180													0	10
Non-inoculated	365										1			1	9
Non-inoculated	660		2	7	1								2	12	8
PBS	7													0	10
PBS	90		1											1	9
PBS	180	1												1	9
PBS	365	2	2			1					1			6	9
PBS	660	1	4	3	1					1		1		11	9
m-NTg	7													0	10
m-NTg	90													0	10
m-NTg	180	4												4	9
m-NTg	365		2	1										3	7
m-NTg	660	1	4	8		1		1			1			16	4
m-TgWT	7													0	10

Inocula	Time-point (days post inoc')	Inoculation / anaesthetic	Scratching	weight loss	Found dead	Swollen abdomen	Abnormal breath- ing	Hind- limb paralysis	Impaired righting reflex	Missing presumed dead	Culled in error	Pro- lapsed rectum	Tumour	TOTAL premature deaths	Reached cull date
m-TgWT	90													0	10
m-TgWT	180													0	10
m-TgWT	365		5	1										6	4
m-TgWT	660	2	6	7	2				1					18	2
m-TgG93A	7													0	10
m-TgG93A	90													0	10
m-TgG93A	180													0	10
m-TgG93A	365		2											2	8
m-TgG93A	660	1	7	10							1			19	3
h-cntrl1	7	1												1	9
h-cntrl1	90	3								1				4	9
h-cntrl1	180	1												1	9
h-cntrl1	365		1	1										2	8
h-cntrl1	660	3	2	13		1	1							20	
h-cntrl2	7	1												1	9
h-cntrl2	90	1												1	9
h-cntrl2	180	5												5	10
h-cntrl2	365	1		1	1									3	7
h-cntrl2	660	1	7	5										13	2
h-D101G	7	1												1	9
h-D101G	90													0	10
h-D101G	180	2												2	10

Inocula	Time-point (days post inoc')	Inoculation / anaesthetic	Scratching	weight loss	Found dead	Swollen abdomen	Abnormal breath- ing	Hind- limb paralysis	Impaired righting reflex	Missing presumed dead	Culled in error	Pro- lapsed rectum	Tumour	TOTAL premature deaths	Reached cull date
h-D101G	365		2											2	8
h-D101G	660	3	9	6	1				1					20	
h-I113T	7													0	10
h-I113T	90	1												1	9
h-I113T	180	1												1	9
h-I113T	365	2	5											7	3
h-I113T	660	5	4	10	2	1			1					23	1
TOTAL		44	65	73	8	4	1	1	3	5	4	1	2	211	349

## 7.4 APPENDIX 4 - KAPLAN-MEIER SURVIVAL GRAPHS OF TgWT;SOD1KO MICE SPLIT BETWEEN MOUSE AND HUMAN INOCULA



### Kaplan-Meier survival graph of TgWT;Sod1ko mice split between mouse and human inocula

Mice from the 2 longest time-points (365 and 660-days post-inoculation) that were culled before their scheduled cull date due to weight loss, self-inflicted scratching wounds, hind limb paralysis and impaired righting reflex were included in the analysis.

Data are split over 2 graphs to aid visualisation.

## 7.5 APPENDIX 5 - RELATIVE TRANSGENE COPY NUMBER AND OTHER EXCLUSION FOR INDIVIDUAL ANIMALS

animal ID	genotype	mean $\Delta\Delta CT$	std dev	Other exclusions
EF14/115.3d	TgG93A;Sod1wt	1.3574	0.0514	excluded from weights and survival as wasn't weighed daily
EF14/115.4b	TgG93A;Sod1wt	1.1010	0.0973	
EF14/143.1b	TgG93A;Sod1wt	1.1919	0.1031	
EF14/145.2g	TgG93A;Sod1wt	1.2268	0.0973	
EF14/147.1b	TgG93A;Sod1wt	1.2354	0.1276	
EF14/157.1b	TgG93A;Sod1wt	1.0086	0.1230	
EF14/157.1e	TgG93A;Sod1wt	1.4492	0.1083	excluded from weights and survival as wasn't weighed daily
EF14/157.2c	TgG93A;Sod1wt	1.0472	0.0850	
EF14/176.3b	TgG93A;Sod1wt	2.0437	0.1044	
EF14/185.4f	TgG93A;Sod1wt	1.5086	0.2259	
EF14/193.1b	TgG93A;Sod1wt	1.2661	0.1127	
EF14/193.1d	TgG93A;Sod1wt	0.9832	0.1325	
EF14/197.1a	TgG93A;Sod1wt	1.3250	0.1031	
EF14/200.1b	TgG93A;Sod1wt	1.3323	0.0417	
EF14/200.4g	TgG93A;Sod1wt	0.9412	0.0930	
EF14/205.3c	TgG93A;Sod1wt	0.9571	0.0604	
EF14/211.2a	TgG93A;Sod1wt	1.0634	0.1038	
EF14/213.2a	TgG93A;Sod1wt	0.9941	0.0743	
EF14/208.3c	TgG93A;Sod1wt	1.0225	0.0498	
EF14/214.1b	TgG93A;Sod1wt	0.8470	0.1604	
EF14/114.1a	TgG93A;Sod1ko	1.3005	0.1075	
EF14/114.1c	TgG93A;Sod1ko	1.0565	0.0572	excluded from weights and survival as wasn't weighed daily
EF14/114.2b	TgG93A;Sod1ko	1.2804	0.1829	
EF14/114.2c	TgG93A;Sod1ko	1.1921	0.2298	excluded from weights and survival as wasn't weighed daily
EF14/113.4c	TgG93A;Sod1ko	1.1287	0.0345	
EF14/121.1b	TgG93A;Sod1ko	1.0862	0.0598	
EF14/131.1e	TgG93A;Sod1ko	1.2263	0.0409	
EF14/131.1g	TgG93A;Sod1ko	1.2811	0.2507	
EF14/130.1a	TgG93A;Sod1ko	1.1084	0.0717	
EF14/132.1c	TgG93A;Sod1ko	1.3881	0.1810	
EF14/124.2a	TgG93A;Sod1ko	1.1574	0.0459	
EF14/125.2b	TgG93A;Sod1ko	1.0702	0.0939	
EF14/130.3d	TgG93A;Sod1ko	1.0635	0.0374	
EF14/136.1b	TgG93A;Sod1ko	1.0770	0.1205	
EF14/143.1a	TgG93A;Sod1ko	1.1568	0.0642	
EF14/145.1a	TgG93A;Sod1ko	1.2352	0.0757	
EF14/151.1c	TgG93A;Sod1ko	1.1880	0.0960	
EF14/145.2b	TgG93A;Sod1ko	1.1579	0.0818	
EF14/176.3a	TgG93A;Sod1ko	1.1937	0.0433	
EF14/186.2a	TgG93A;Sod1ko	1.2780	0.0813	excluded from weights- missing data
EF14/186.2b	TgG93A;Sod1ko	1.2890	0.0691	excluded from weights- missing data
EF14/185.3b	TgG93A;Sod1ko	1.4598	0.0604	
EF14/192.4d	TgG93A;Sod1ko	1.1827	0.1258	
EF14/197.1c	TgG93A;Sod1ko	1.2842	0.1079	
EF14/197.1d	TgG93A;Sod1ko	1.2642	0.1156	
EF14/202.2c	TgG93A;Sod1ko	1.0634	0.1251	
EF14/202.2d	TgG93A;Sod1ko	1.0335	0.0789	
EF14/200.4h	TgG93A;Sod1ko	1.0103	0.0310	
EF14/206.1a	TgG93A;Sod1ko	1.1998	0.0860	
EF14/206.1d	TgG93A;Sod1ko	1.3075	0.0862	
EF14/205.1a	TgG93A;Sod1ko	1.2728	0.0253	
EF14/205.3f	TgG93A;Sod1ko	0.9987	0.1361	
EF14/210.1a	TgG93A;Sod1ko	0.8438	0.0323	
EF14/213.1d	TgG93A;Sod1ko	1.1140	0.0834	
EF14/206.5b	TgG93A;Sod1ko	1.0848	0.1147	
EF14/211.2d	TgG93A;Sod1ko	1.0585	0.0796	

animal ID	genotype	mean $\Delta\Delta CT$	std dev	Other exclusions
EF14/210.3g	TgG93A;Sod1ko	0.9206	0.0300	
<b>Excluded</b>				
EF14/140.1a	TgG93A;Sod1wt	0.6162	0.0549	
EF14/140.1e	TgG93A;Sod1wt	0.6740	0.0176	
EF14/140.2a	TgG93A;Sod1wt	0.7329	0.0274	
EF14/140.3b	TgG93A;Sod1wt	0.6725	0.0470	
EF14/140.3e	TgG93A;Sod1wt	0.7021	0.0185	
EF14/141.1b	TgG93A;Sod1wt	0.6410	0.0850	
EF14/154.2a	TgG93A;Sod1wt	0.6413	0.0624	
EF14/155.1a	TgG93A;Sod1wt	0.5800	0.0383	
EF14/167.2d	TgG93A;Sod1wt	0.6383	0.0475	
EF14/167.2f	TgG93A;Sod1wt	0.6136	0.0243	
EF14/180.1a	TgG93A;Sod1wt	0.6338	0.0546	
EF14/198.1c	TgG93A;Sod1wt	0.7725	0.1376	
EF14/126.4d	TgG93A;Sod1ko	0.1121	0.0090	
EF14/140.1d	TgG93A;Sod1ko	0.6474	0.0815	
EF14/141.1e	TgG93A;Sod1ko	0.6472	0.0548	
EF14/154.3a	TgG93A;Sod1ko			Alive at 1 year. Not assayed for copy number
EF14/154.4c	TgG93A;Sod1ko			Alive at 1 year. Not assayed for copy number
EF14/155.2a	TgG93A;Sod1ko	0.6257	0.0088	
EF14/161.1d	TgG93A;Sod1ko	0.7445	0.0753	
EF14/169.2e	TgG93A;Sod1ko	0.6456	0.0290	
EF14/182.3c	TgG93A;Sod1ko	0.6034	0.0802	

## **7.6 APPENDIX 6 - FIBRE TYPING MONTAGES**

Transverse sections of hind limb muscles, extensor digitorum longus (EDL) and tibialis anterior (TA) were immunostained for myosin heavy chain isoforms as labelled. Antibodies are in brackets.

Scale bars of all images are 500  $\mu\text{m}$



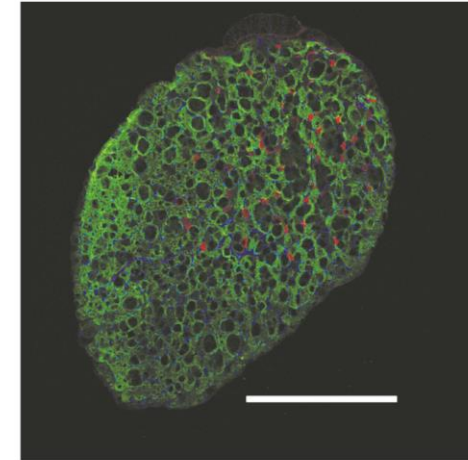
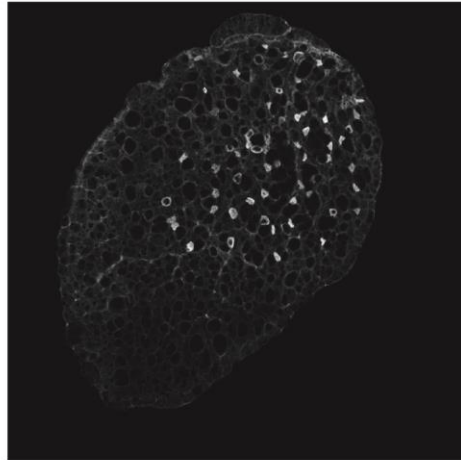
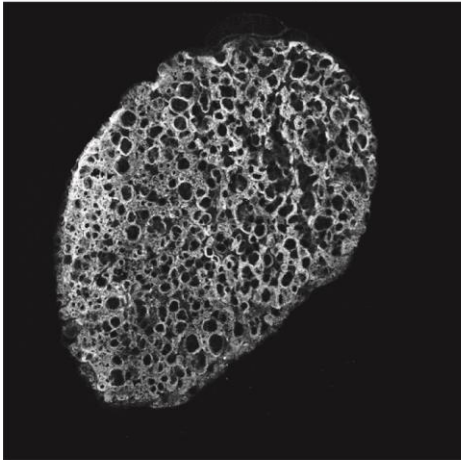
### 7.6.1 EDL Fibre Typing: Myosin Heavy Chain type 2A and 2B

Type 2B (BF-F3)

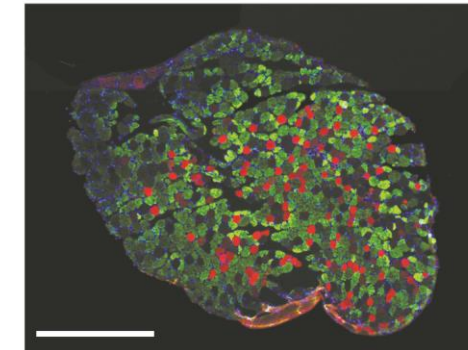
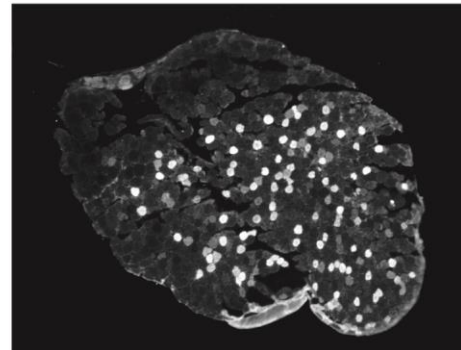
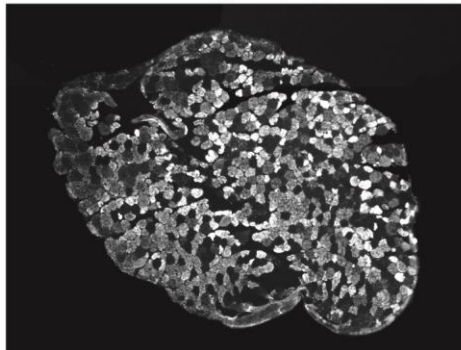
Type 2A (SC-71)

Merge

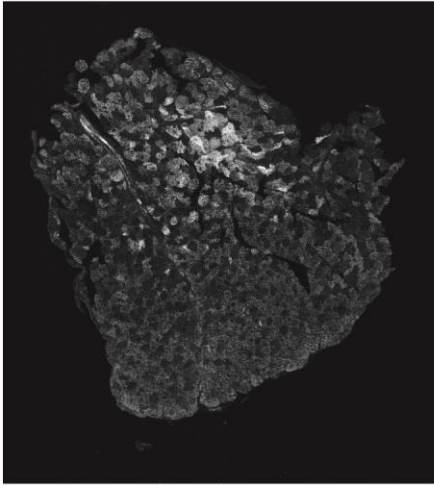
EF14 205 3c TgG93A;Sod1wt



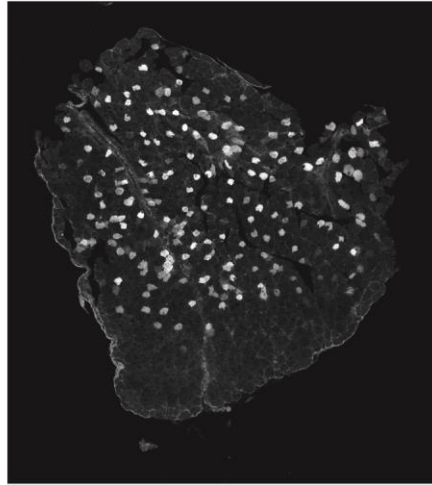
EF14 208 3c TgG93A;Sod1wt



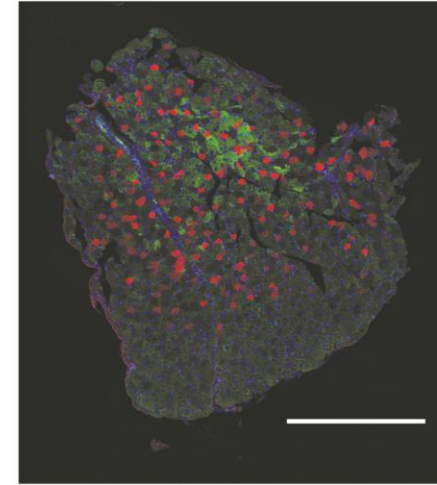
Type 2B (BF-F3)  
EF14 211 2a TgG93A;Sod1wt



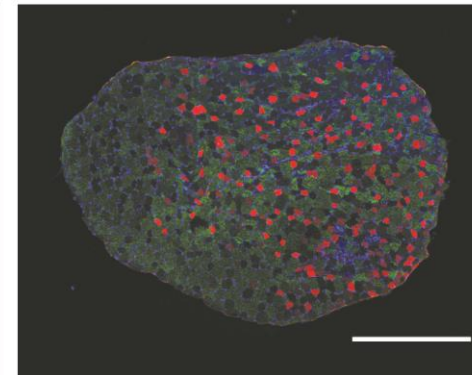
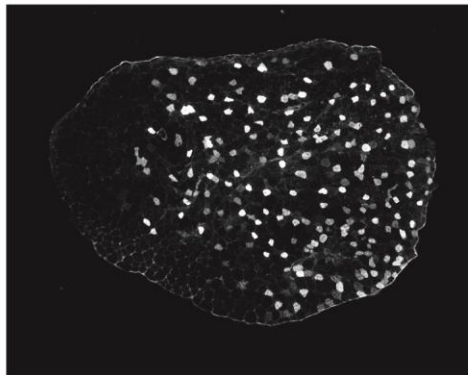
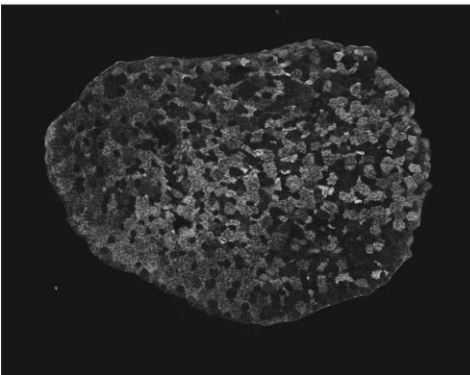
Type 2A (SC-71)



Merge



EF14 213 2a TgG93A;Sod1wt

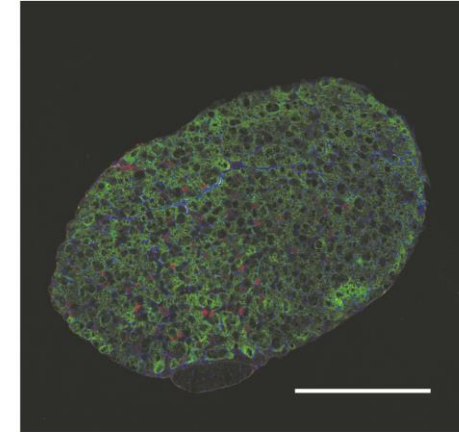
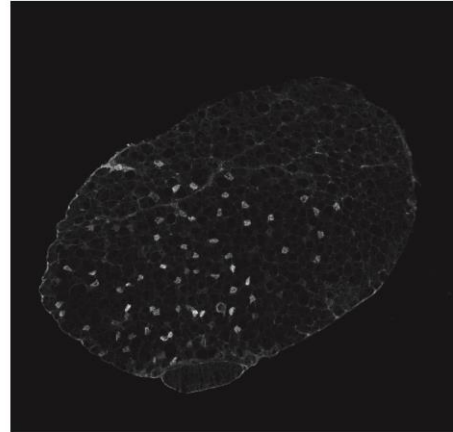
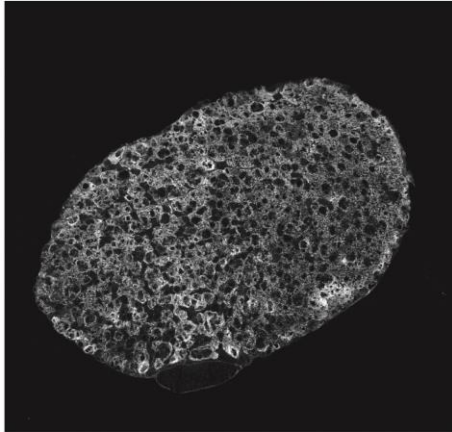


Type 2B (BF-F3)

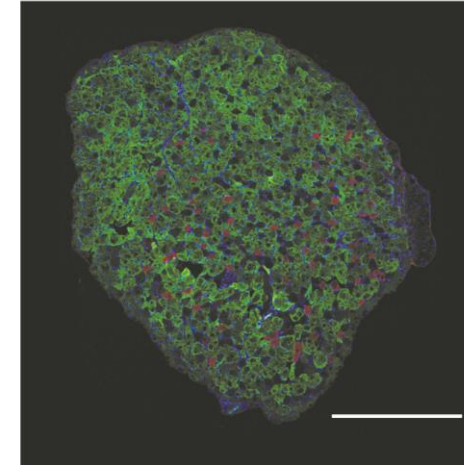
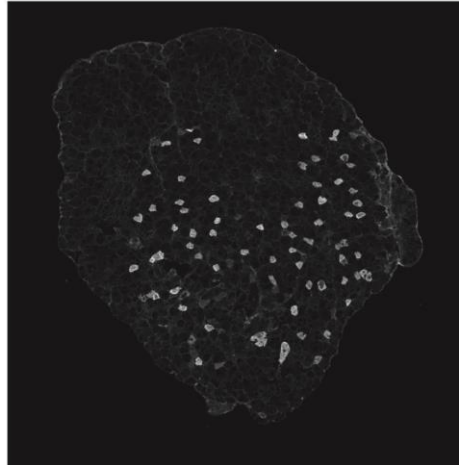
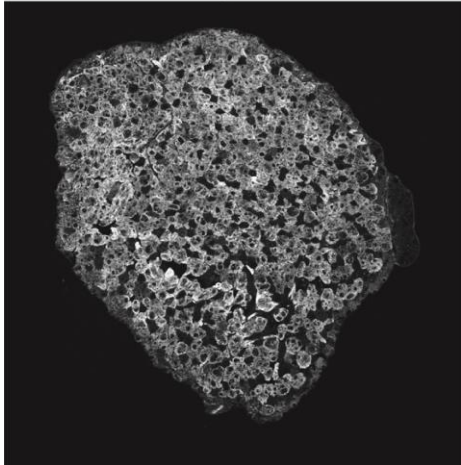
Type 2A (SC-71)

Merge

EF14 205 3f TgG93A;Sod1ko

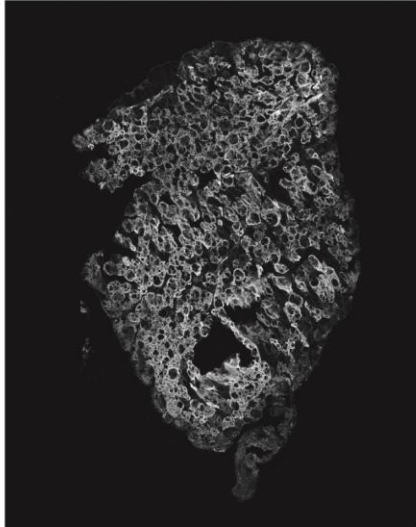


EF14 206 5b TgG93A;Sod1ko

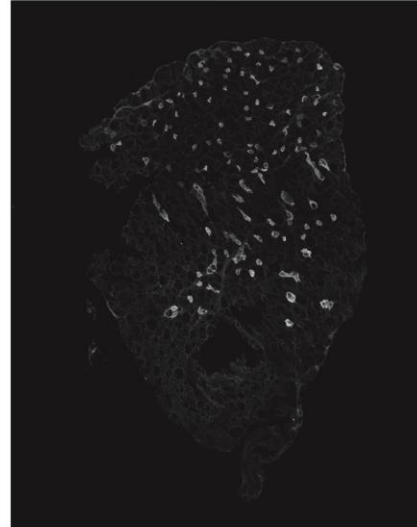




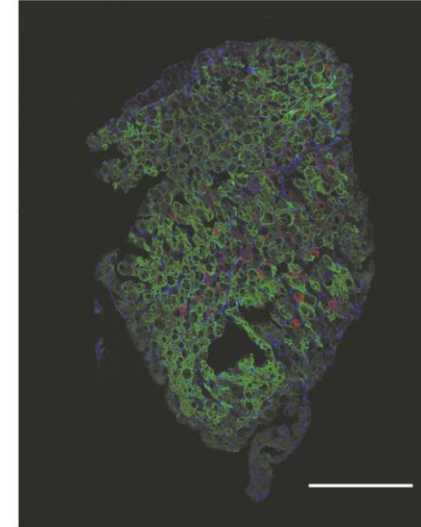
Type 2B (BF-F3)  
EF14 210 1a TgG93A;Sod1ko



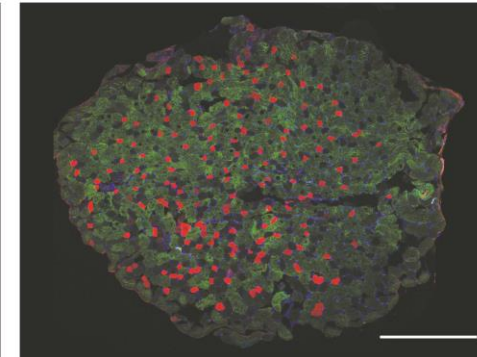
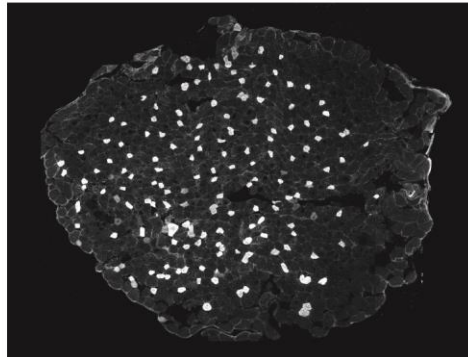
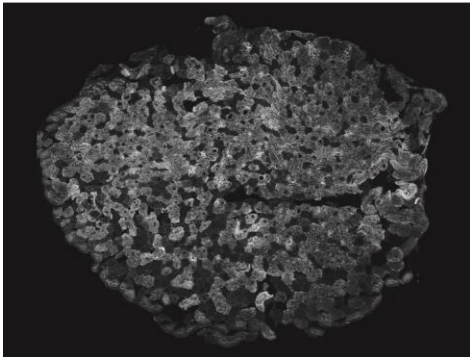
Type 2A (SC-71)



Merge



EF14 210 3g TgG93A;Sod1ko

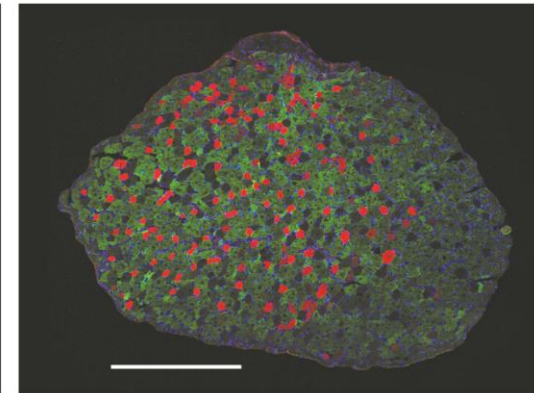
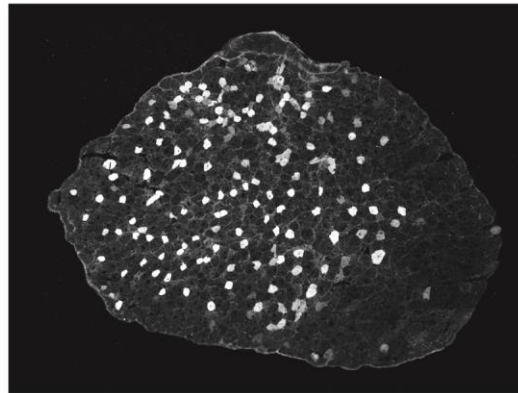
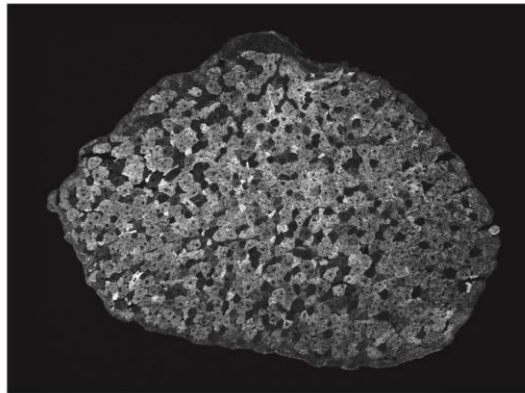


Type 2B (BF-F3)

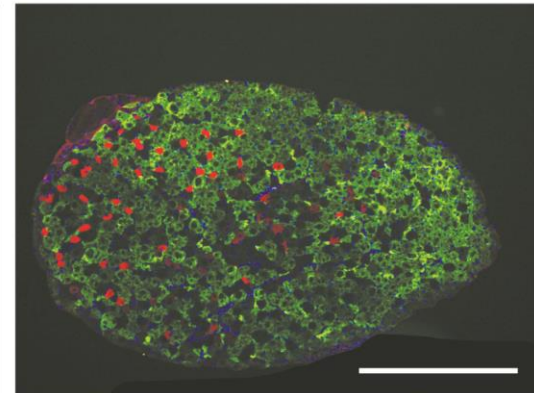
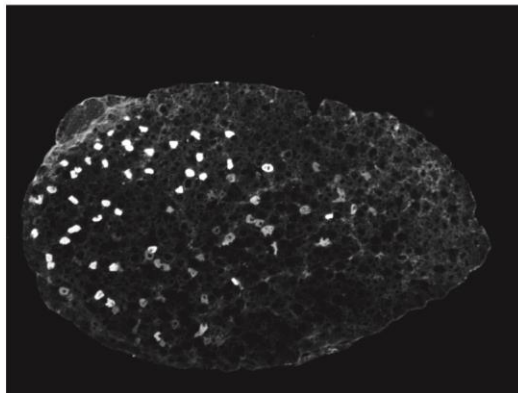
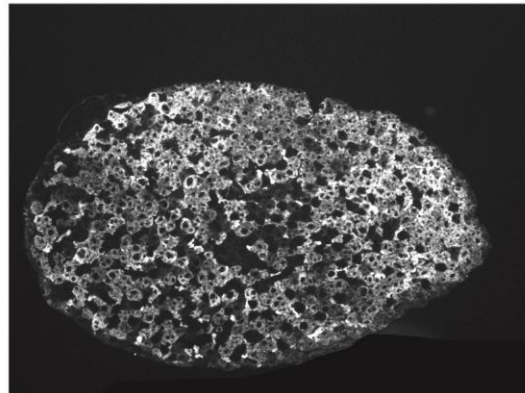
Type 2A (SC-71)

Merge

EF14 211 2d TgG93A;Sod1ko



EF14 213 1d TgG93A;Sod1ko



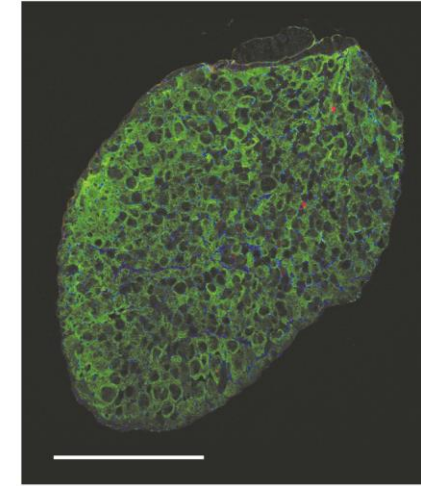
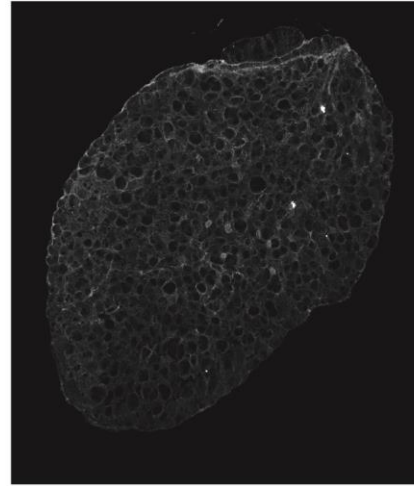
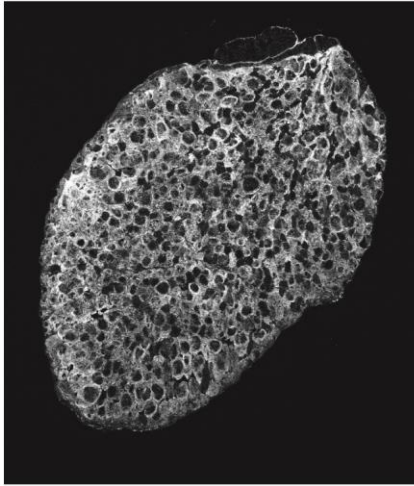
### 7.6.2 EDL Fibre Typing: Myosin Heavy Chain Type 1 and 2B

Type 2B (BF-F3)

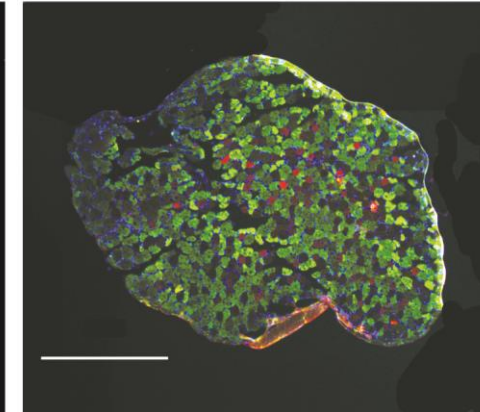
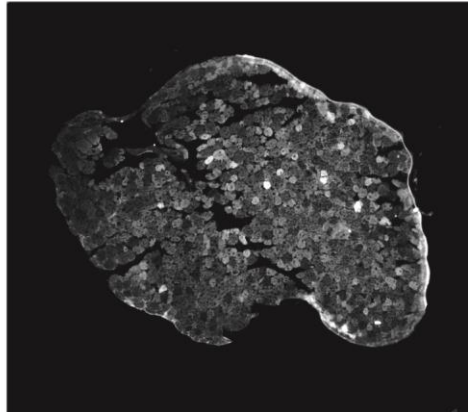
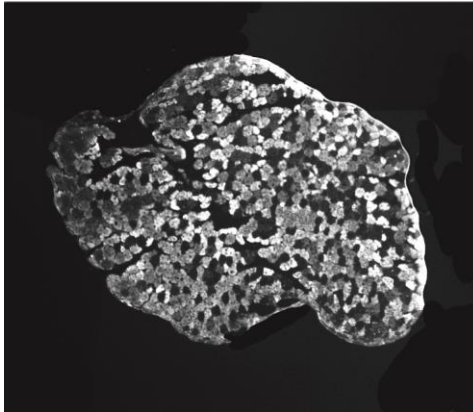
Type 1 (BA-D5)

Merge

EF14 205 3c TgG93A;Sod1wt



EF14 208 3c TgG93A;Sod1wt



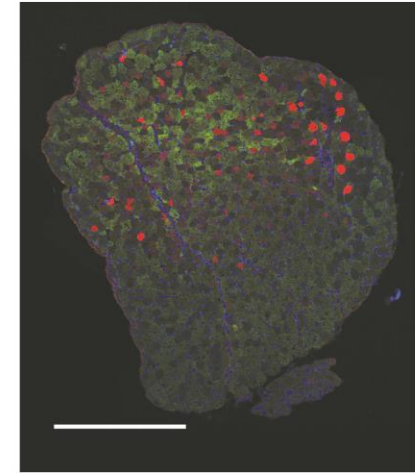
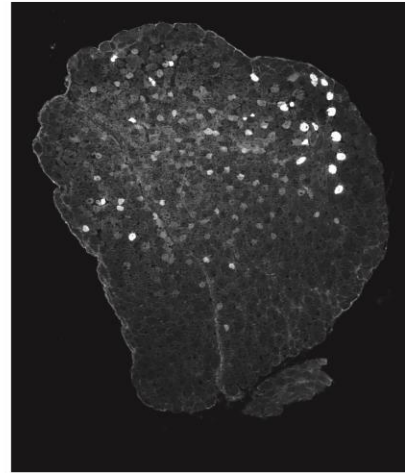
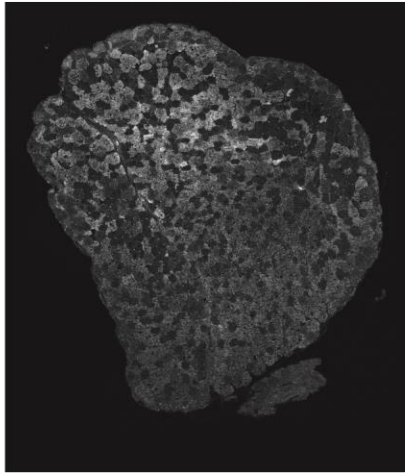


Type 2B (BF-F3)

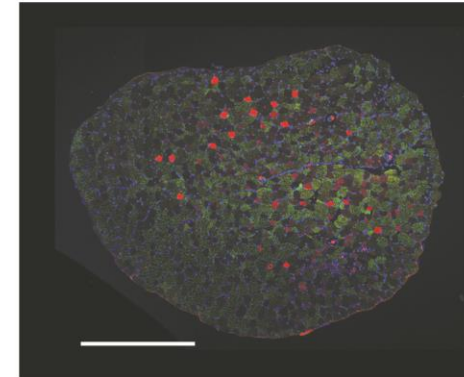
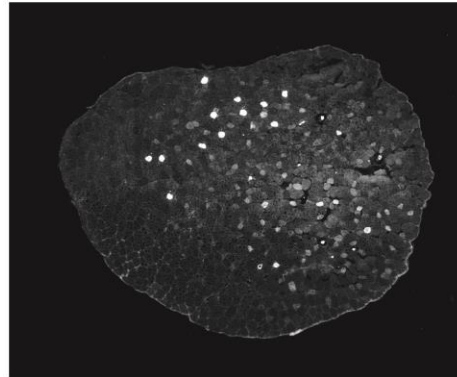
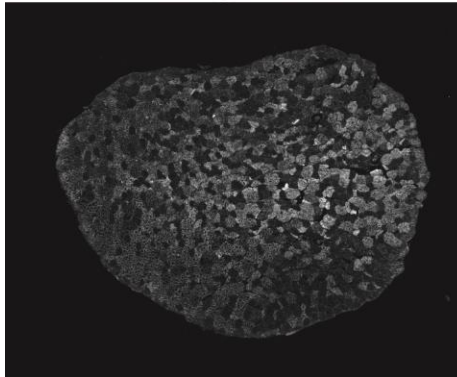
Type 1 (BA-D5)

Merge

EF14 211 2a TgG93A;Sod1wt



EF14 213 2a TgG93A;Sod1wt

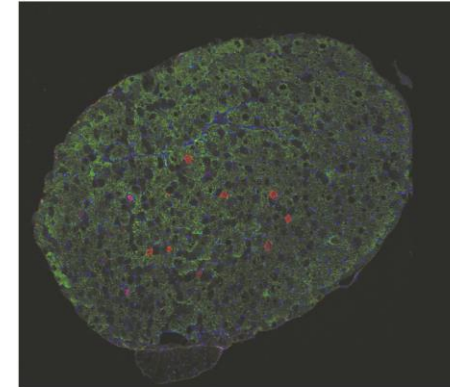
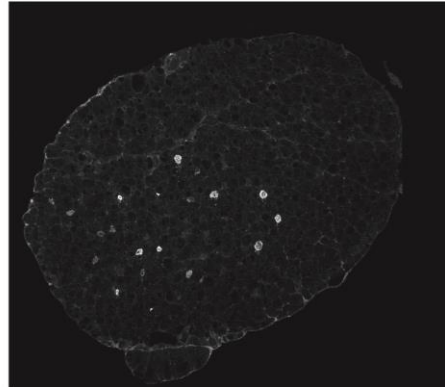
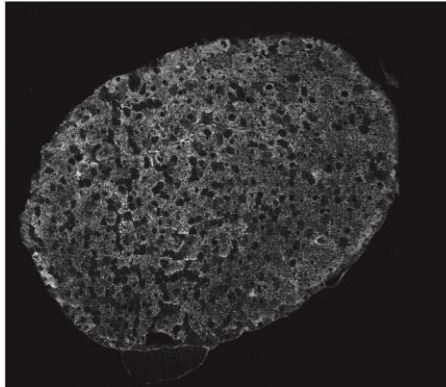


Type 2B (BF-F3)

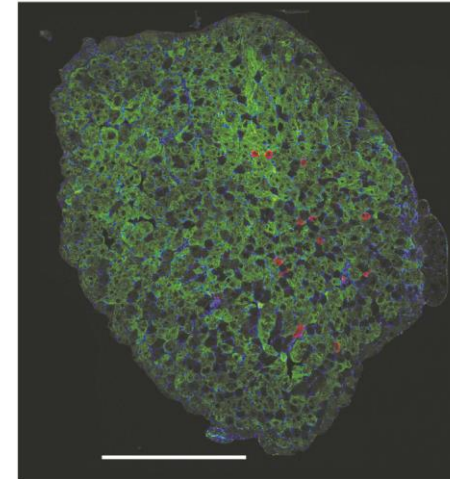
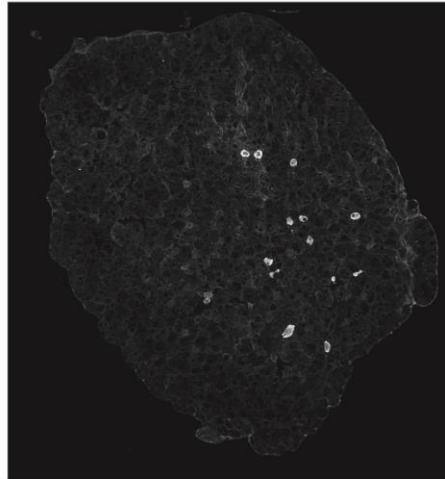
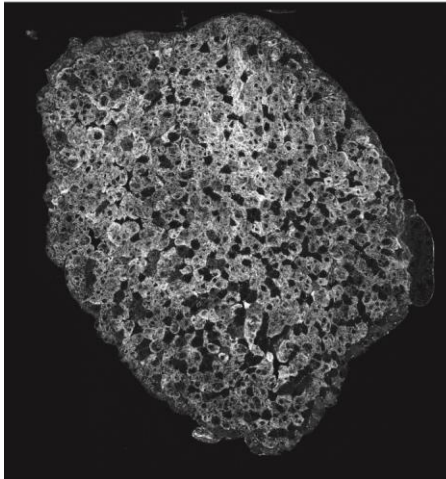
Type 1 (BA-D5)

Merge

EF14 205 3f TgG93A;Sod1ko



EF14 206 5b TgG93A;Sod1ko



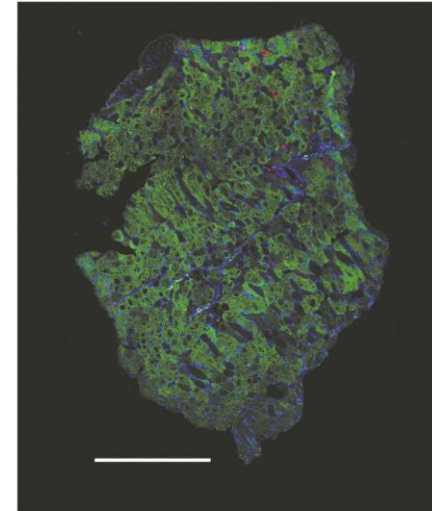
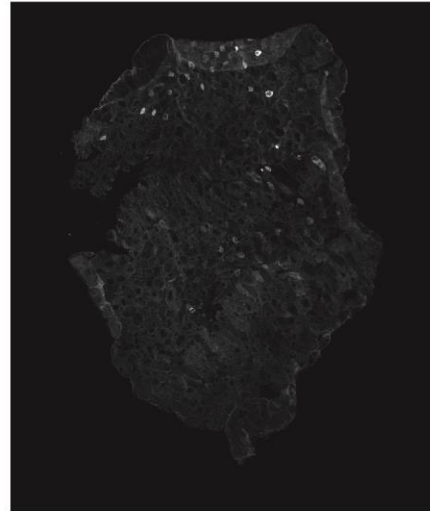
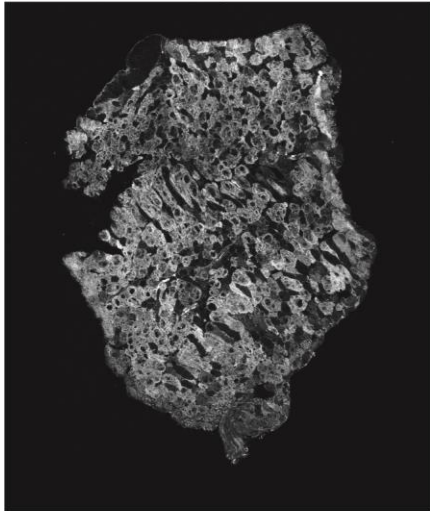


Type 2B (BF-F3)

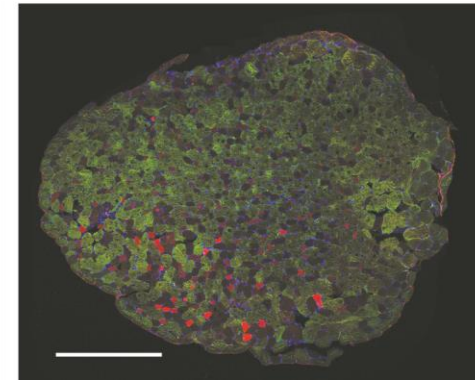
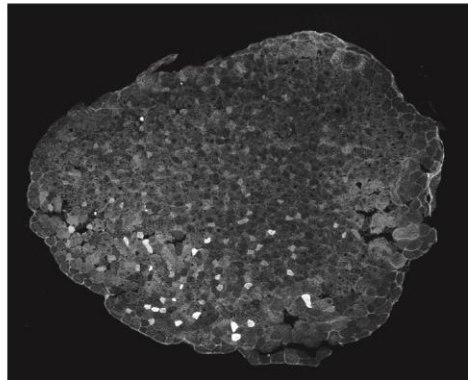
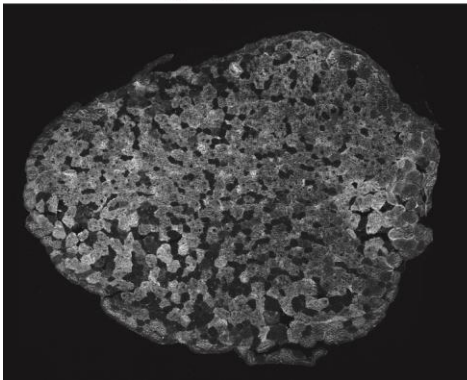
Type 1 (BA-D5)

Merge

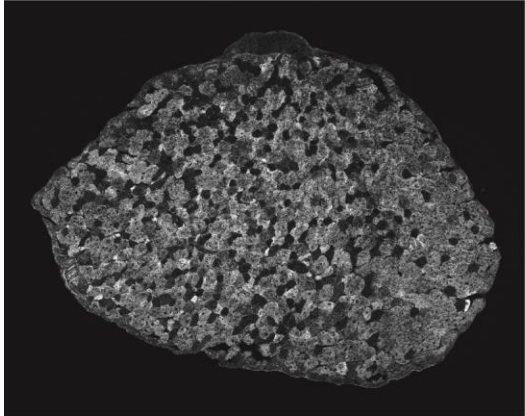
EF14 210 1a TgG93A;Sod1ko



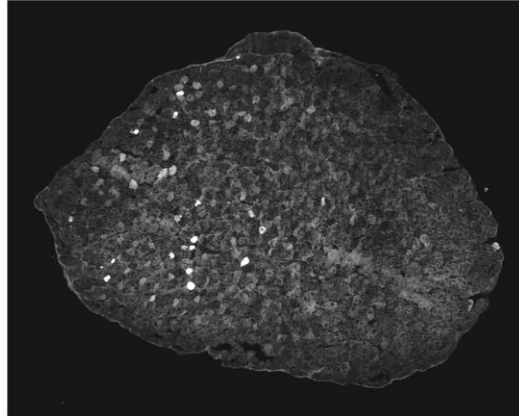
EF14 210 3g TgG93A;Sod1ko



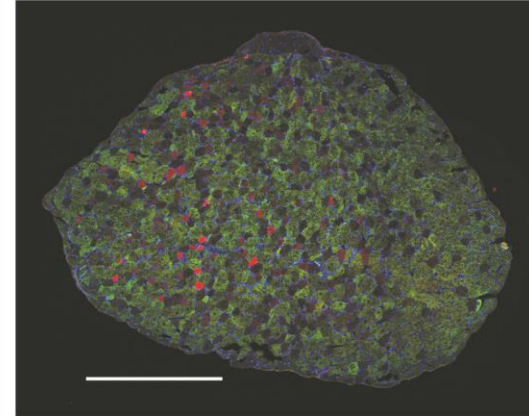
Type 2B (BF-F3)  
EF14 211 2d TgG93A;Sod1ko



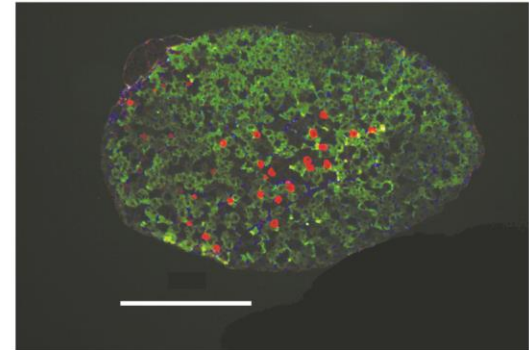
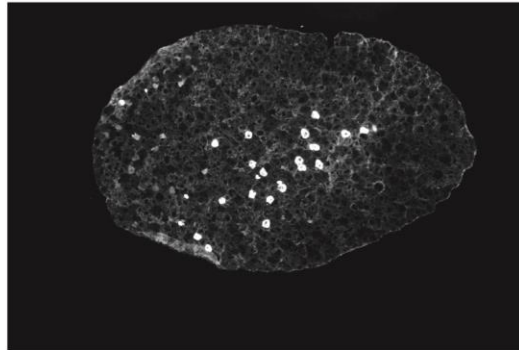
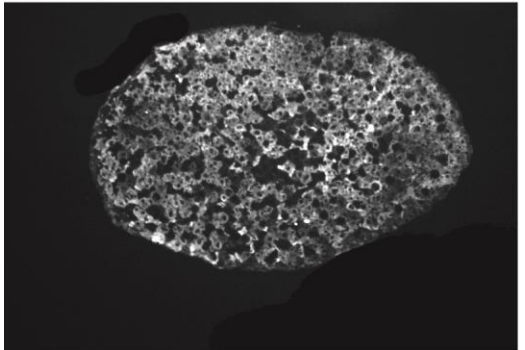
Type 1 (BA-D5)



Merge



EF14 213 1d TgG93A;Sod1ko



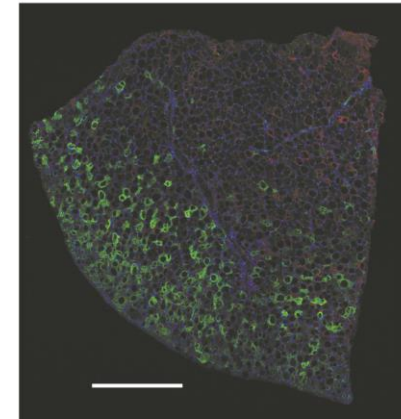
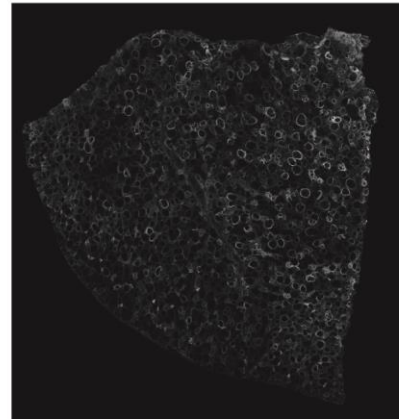
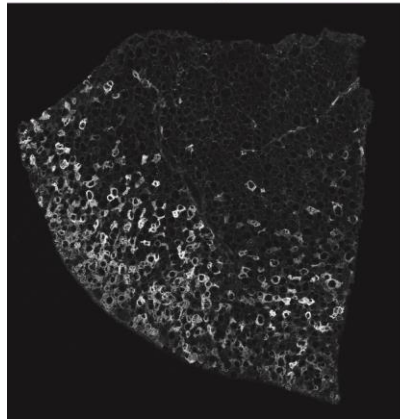
### 7.6.3 TA Fibre Typing: Myosin Heavy Chain Type 2A and 2B

Type 2B (BF-F3)

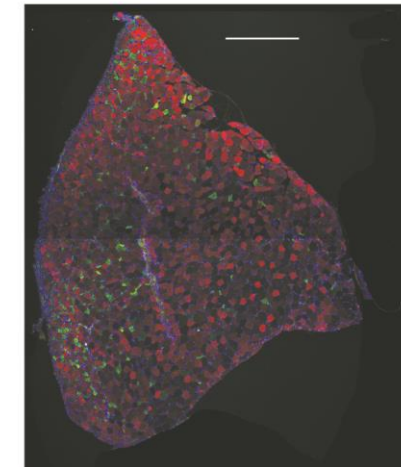
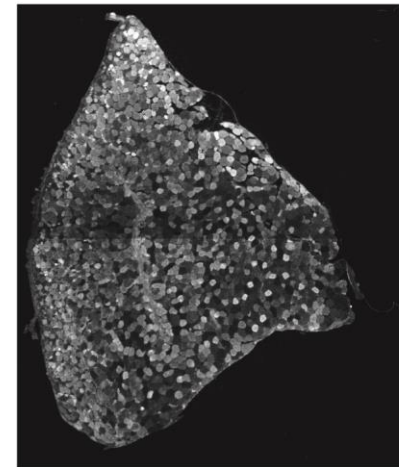
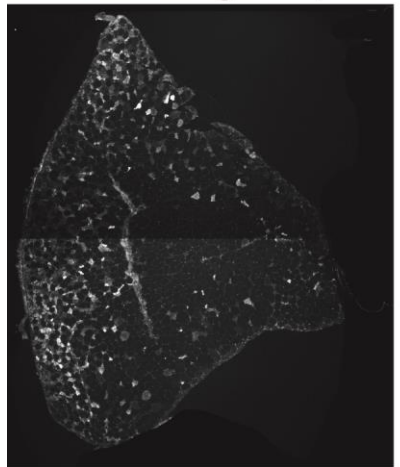
Type 2A (SC-71)

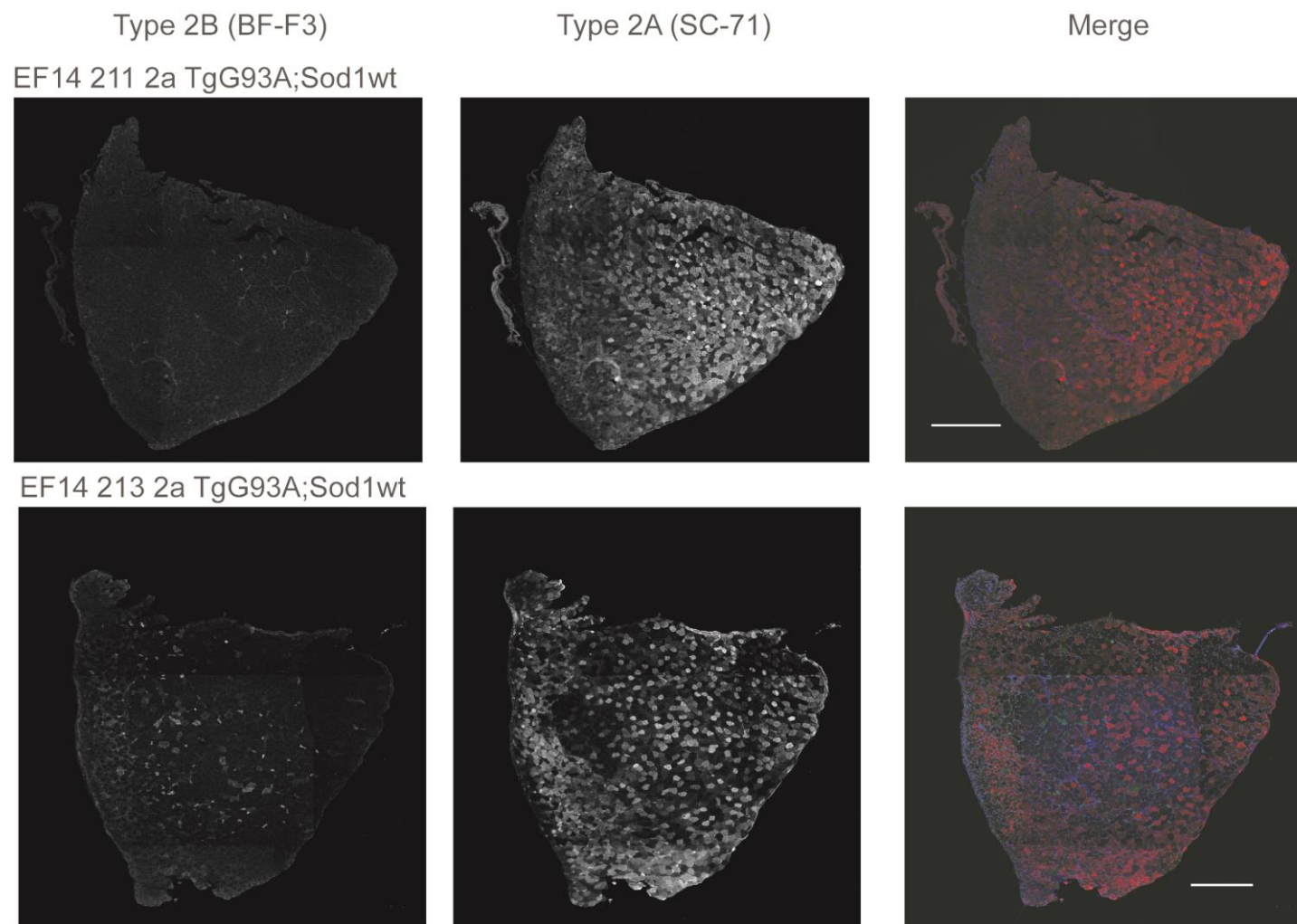
Merge

EF14 205 3c TgG93A;Sod1wt



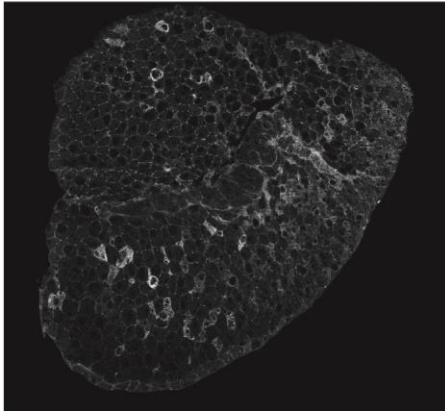
EF14 208 3c TgG93A;Sod1wt



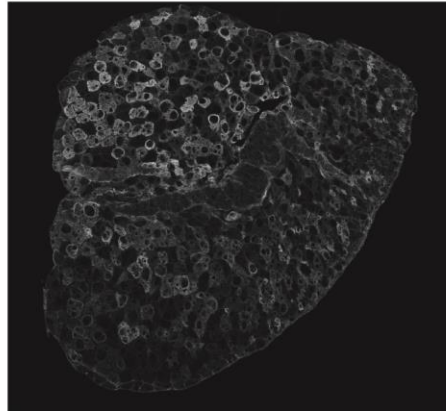




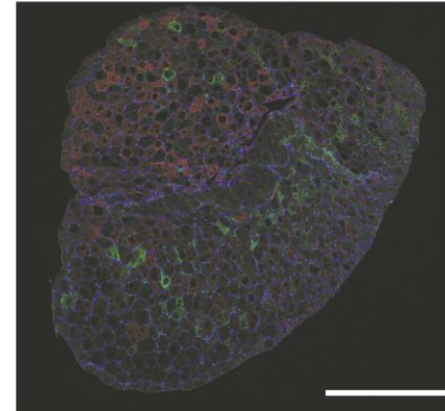
Type 2B (BF-F3)  
EF14 205 3f TgG93A;Sod1ko



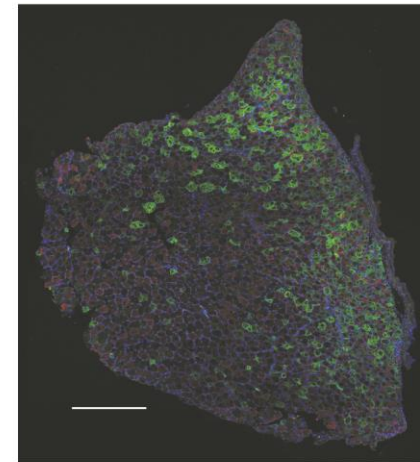
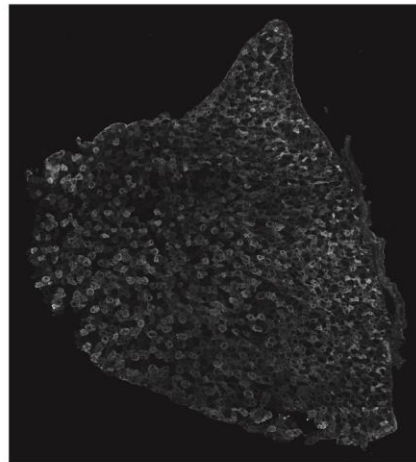
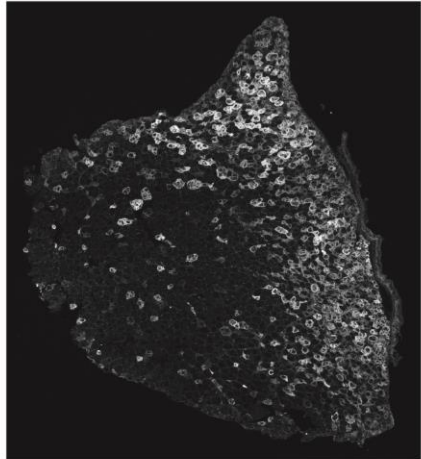
Type 2A (SC-71)



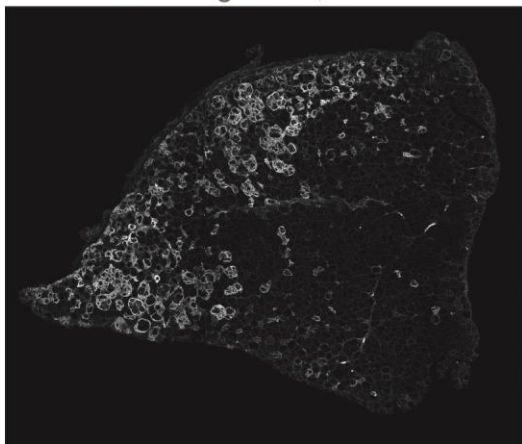
Merge



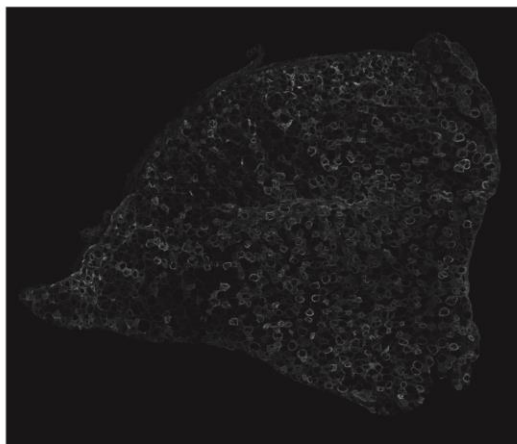
EF14 206 5b TgG93A;Sod1ko



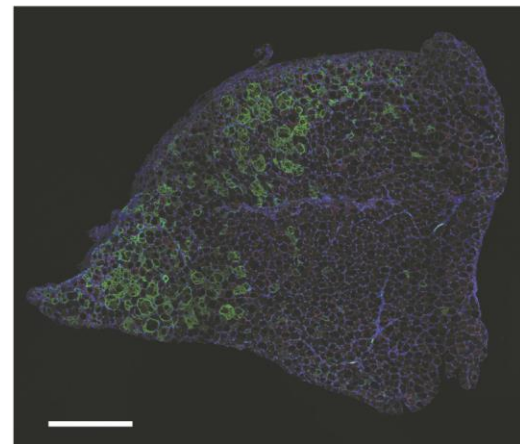
Type 2B (BF-F3)  
EF14 210 1a TgG93A;Sod1ko



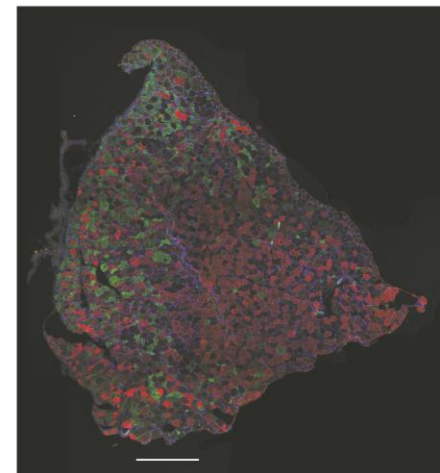
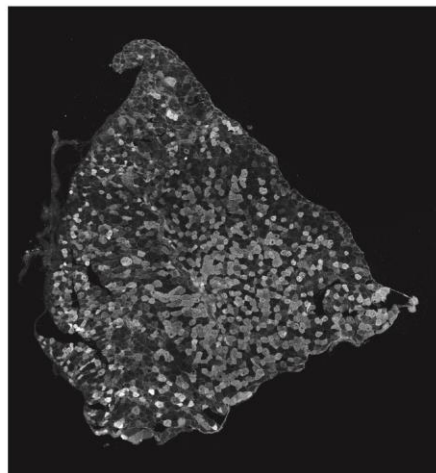
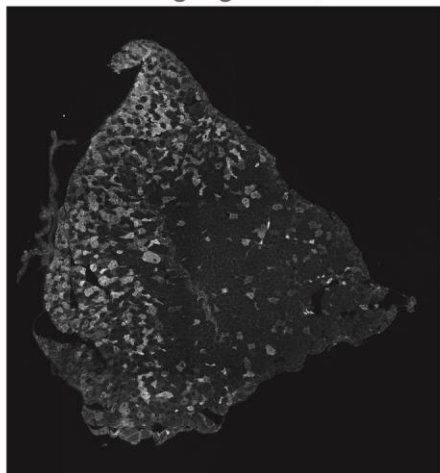
Type 2A (SC-71)



Merge



EF14 210 3g TgG93A;Sod1ko

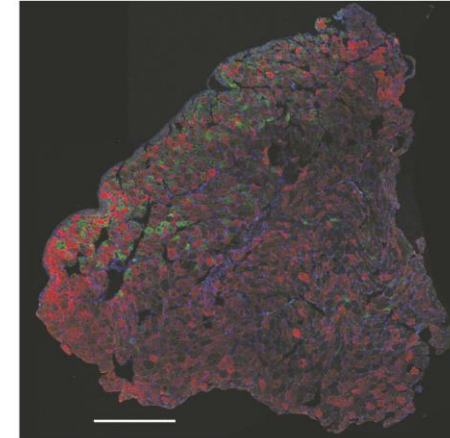
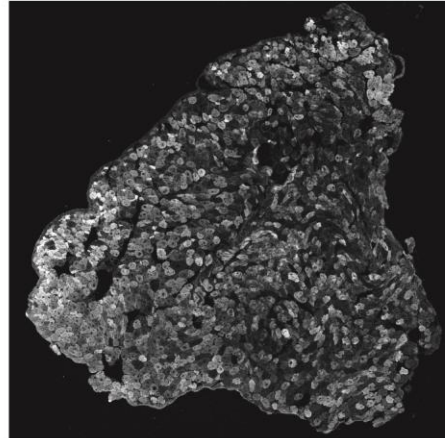
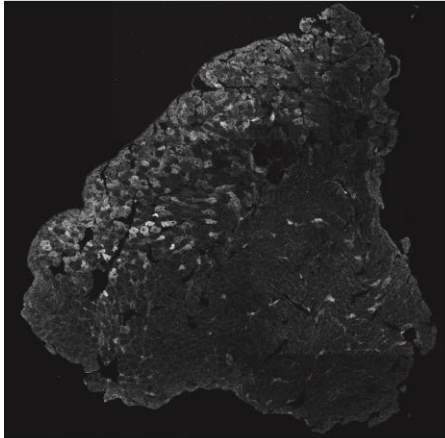


Type 2B (BF-F3)

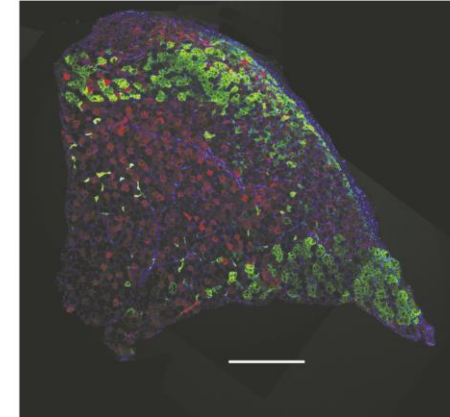
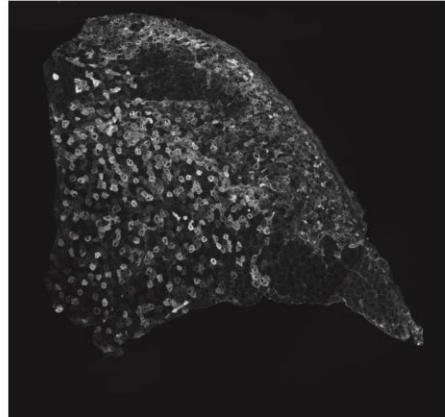
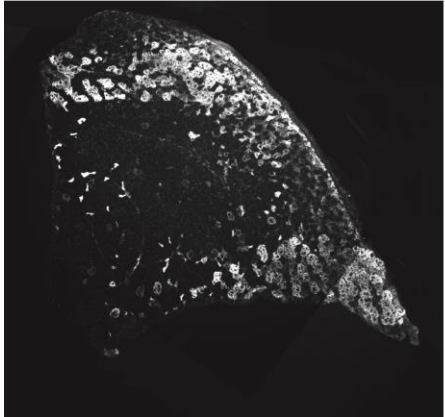
Type 2A (SC-71)

Merge

EF14 211 2d TgG93A;Sod1ko



EF14 213 1d TgG93A;Sod1ko





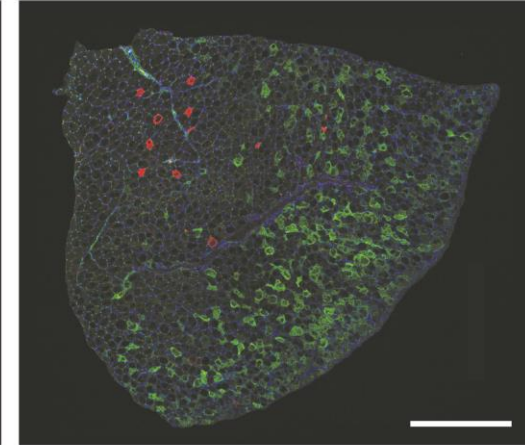
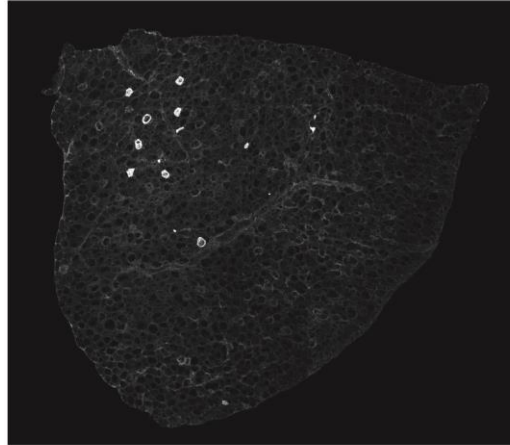
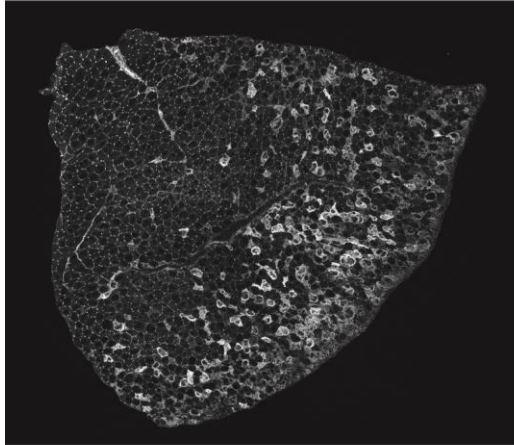
#### 7.6.4 TA Fibre Typing: Myosin Heavy Chain Type 1 and 2B

Type 2B (BF-F3)

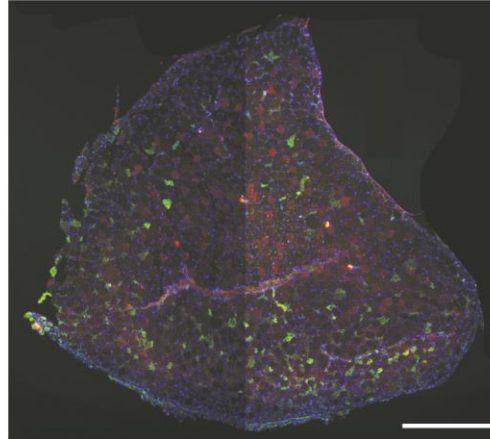
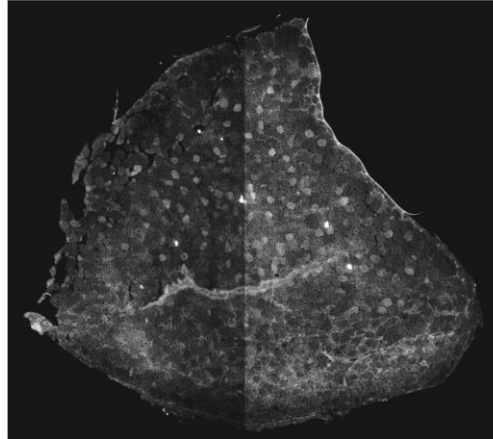
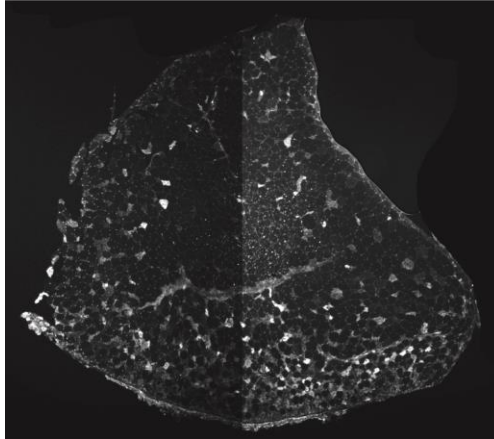
Type 1 (BA-D5)

Merge

EF14 205 3c TgG93A;Sod1wt

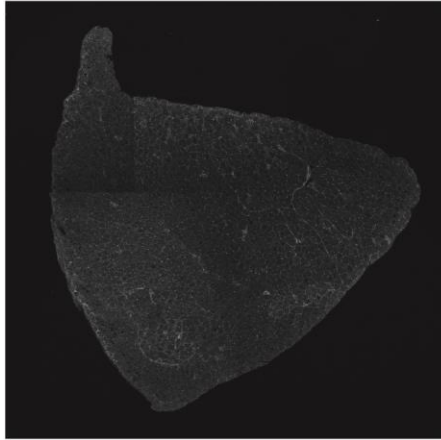


EF14 208 3c TgG93A;Sod1wt

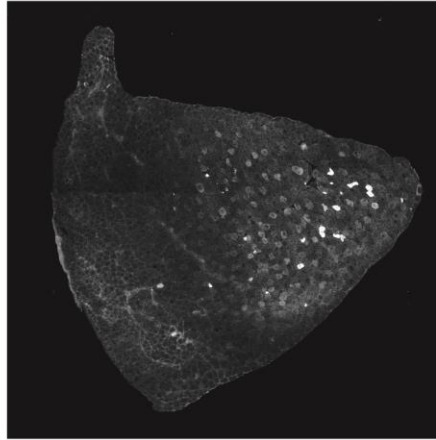




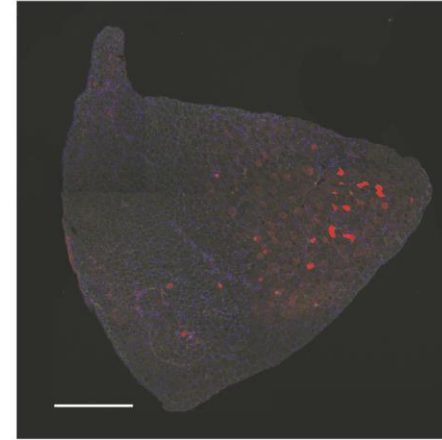
Type 2B (BF-F3)  
EF14 211 2a TgG93A;Sod1wt



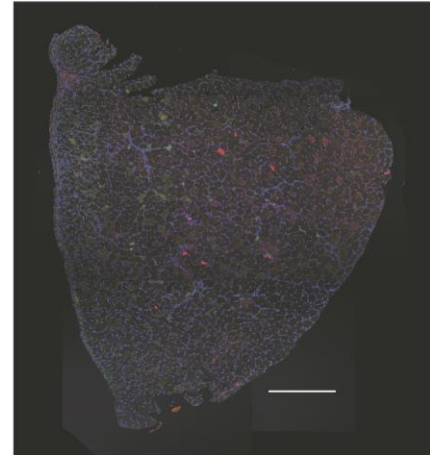
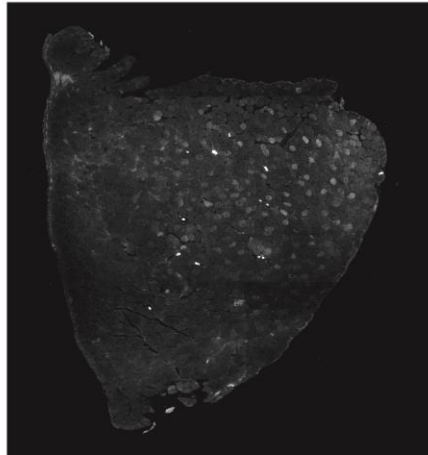
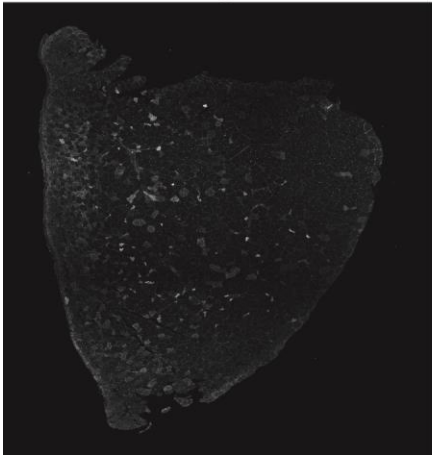
Type 1 (BA-D5)



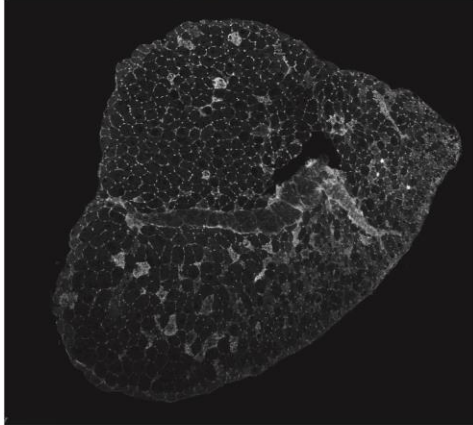
Merge



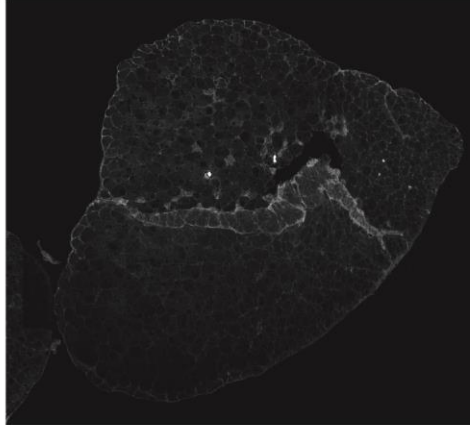
EF14 213 2a TgG93A;Sod1wt



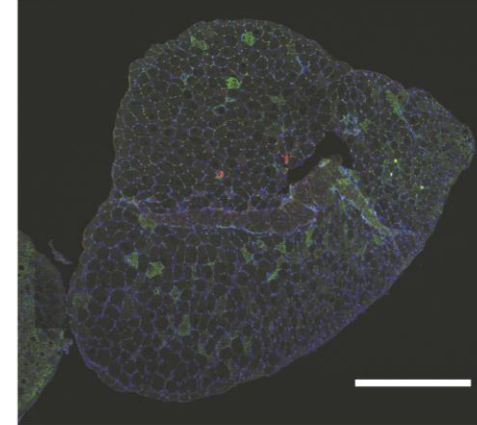
Type 2B (BF-F3)  
EF14 205 3f TgG93A;Sod1ko



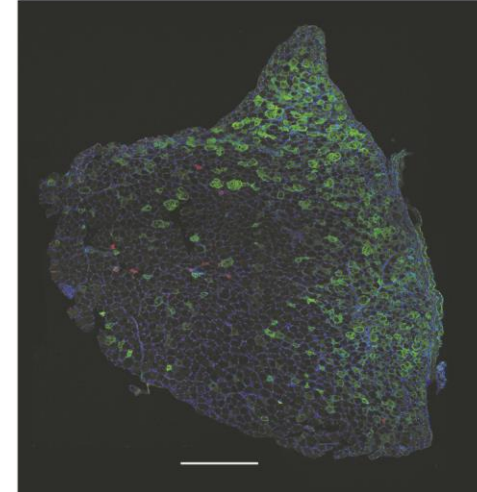
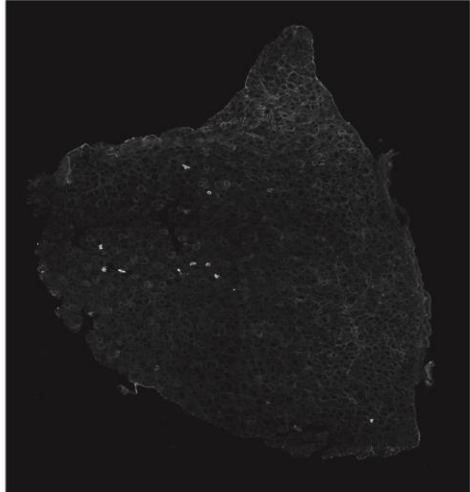
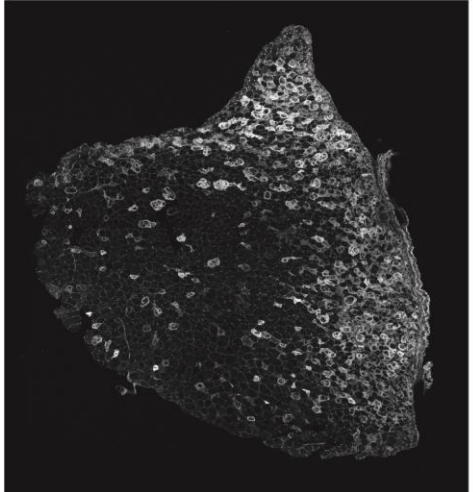
Type 1 (BA-D5)



Merge



EF14 206 5b TgG93A;Sod1ko

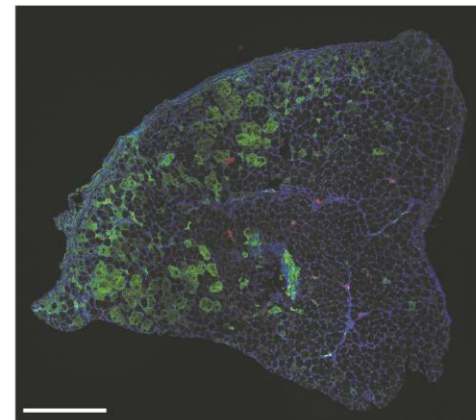
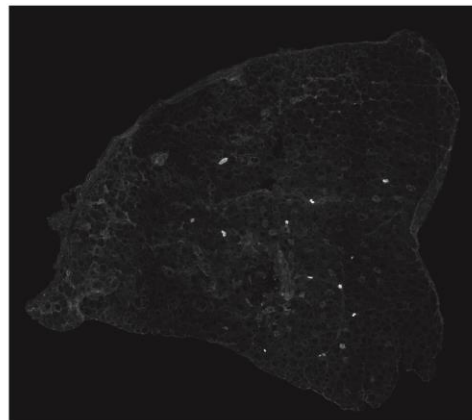
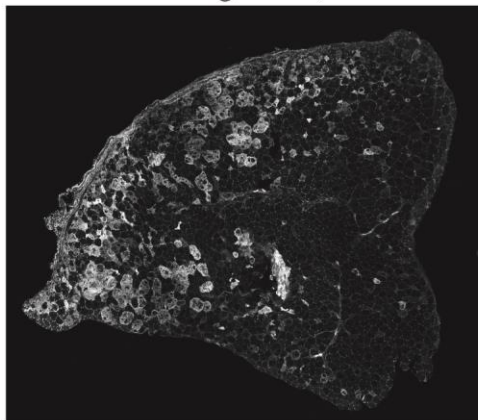


Type 2B (BF-F3)

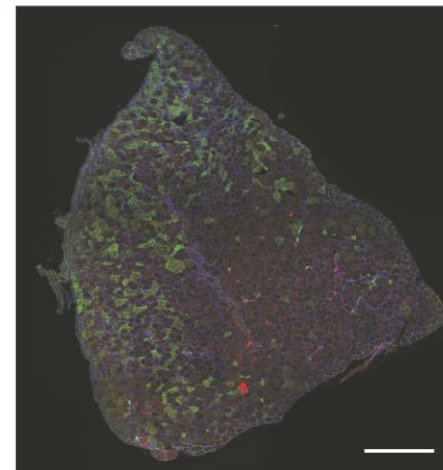
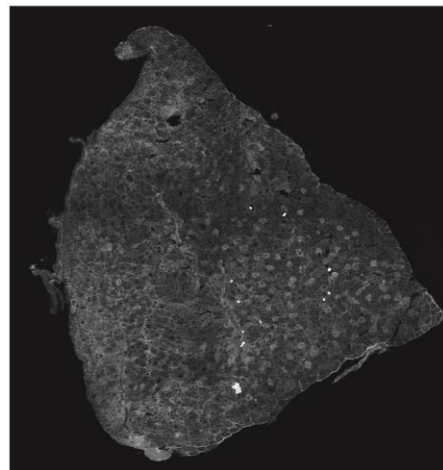
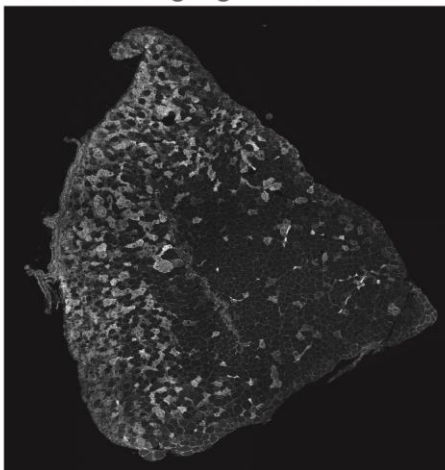
Type 1 (BA-D5)

Merge

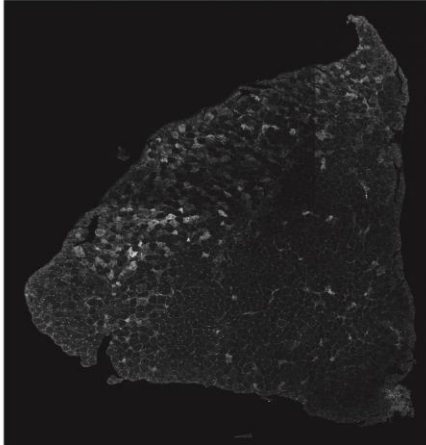
EF14 210 1a TgG93A;Sod1ko



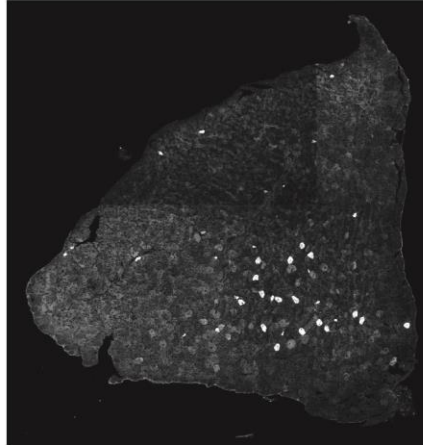
EF14 210 3g TgG93A;Sod1ko



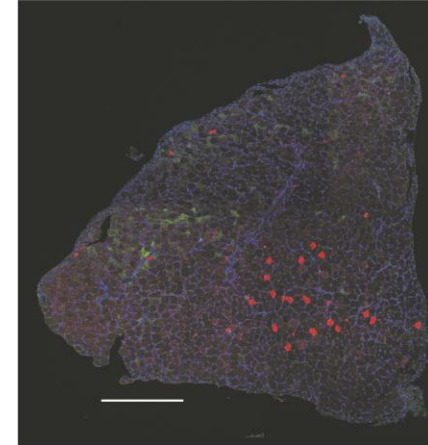
Type 2B (BF-F3)  
EF14 211 2d TgG93A;Sod1ko



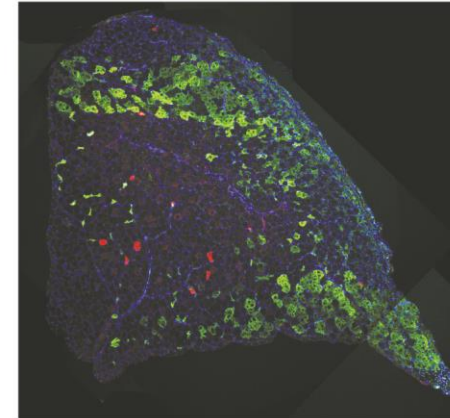
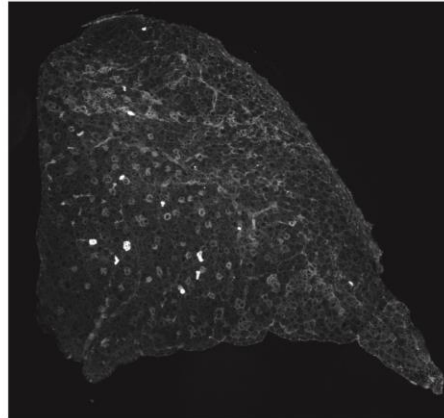
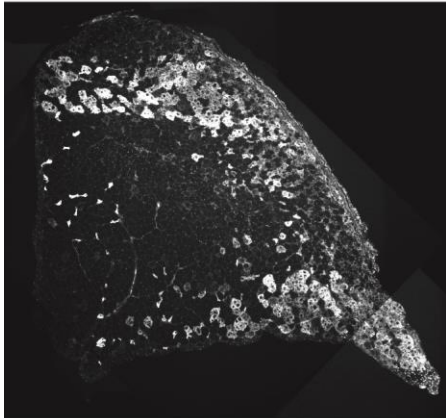
Type 1 (BA-D5)



Merge



EF14 213 1d TgG93A;Sod1ko





## References

- Abe,K., Pan,L.H., Watanabe,M., Kato,T., & Itoyama,Y. (1995). Induction of nitrotyrosine-like immunoreactivity in the lower motor neuron of amyotrophic lateral sclerosis. *Neuroscience Letters*, 199, 152-154.
- Acevedo-Arozena,A., Wells,S., Potter,P., Kelly,M., Cox,R.D., & Brown,S.D.M. (2008). ENU mutagenesis, a way forward to understand gene function. *Annual Review of Genomics and Human Genetics*, 9, 49-69.
- Acevedo-Arozena,A., Kalmar,B., Essa,S., Ricketts,T., Joyce,P., Kent,R., Rowe,C., Parker,A., Gray,A., Hafezparast,M., Thorpe,J.R., Greensmith,L., & Fisher,E.M.C. (2011). A comprehensive assessment of the SOD1G93A low-copy transgenic mouse, which models human amyotrophic lateral sclerosis. *Disease Models & Mechanisms*, 4, 686-700.
- Achilli,F., Boyle,S., Kieran,D., Chia,R., Hafezparast,M., Martin,J.E., Schiavo,G., Greensmith,L., Bickmore,W., & Fisher,E.M.C. (2005). The SOD1 transgene in the G93A mouse model of amyotrophic lateral sclerosis lies on distal mouse chromosome 12. *Amyotrophic Lateral Sclerosis*, 6, 111-114.
- Acquatella-Tran Van Ba,I., Imberdis,T., & Perrier,V. (2013). From Prion Diseases to Prion-Like Propagation Mechanisms of Neurodegenerative Diseases. *International Journal of Cell Biology*, 2013, 975832.
- Aggarwal,A. (2012). Protection of Motor Neurons in Pre-Symptomatic Individuals Carrying SOD1 Mutations: Results of Motor Unit Number Estimation (MUSE) Electrophysiology. In Maurer,M. (Ed.), *Amyotrophic Lateral Sclerosis*. ( In Tech.
- Aggarwal,A. & Nicholson,G. (2001). Normal complement of motor units in asymptomatic familial (SOD1 mutation) amyotrophic lateral sclerosis carriers. *Journal of Neurology Neurosurgery and Psychiatry*, 71, 478-481.
- Aggarwal,A. & Nicholson,G. (2002). Detection of preclinical motor neurone loss in SOD1 mutation carriers using motor unit number estimation. *Journal of Neurology Neurosurgery and Psychiatry*, 73, 199-201.
- Aggarwal,A. & Nicholson,G. (2005). Age dependent penetrance of three different superoxide dismutase 1 (SOD 1) mutations. *International Journal of Neuroscience*, 115, 1119-1130.
- Al Chalabi,A., Fang,F., Hanby,M.F., Leigh,P.N., Shaw,C.E., Ye,W., & Rijsdijk,F. (2010). An estimate of amyotrophic lateral sclerosis heritability using twin data. *Journal of Neurology, Neurosurgery and Psychiatry*, 81, 1324-1326.
- Al Chalabi,A. & Hardiman,O. (2013). The epidemiology of ALS: A conspiracy of genes, environment and time. *Nature Reviews Neurology*, 9, 617-628.
- Al Kateb,H., Boright,A.P., Mirea,L., Xie,X., Sutradhar,R., Mowjoodi,A., Bharaj,B., Liu,M., Bucksa,J.M., Arends,V.L., Steffes,M.W., Cleary,P.A., Sun,W., Lachin,J.M., Thorner,P.S., Ho,M., McKnight,A.J., Maxwell,A.P., Savage,D.A., Kidd,K.K., Kidd,J.R., Speed,W.C., Orchard,T.J., Miller,R.G., Sun,L., Bull,S.B., Paterson,A.D., & the Diabetes Control and Complications Trial/Epidemiology of Diabetes Interventions and Complications Research Group (2008). Multiple Superoxide Dismutase 1/Splicing Factor Serine Alanine 15 Variants Are Associated With the Development and Progression of Diabetic Nephropathy: The Diabetes Control and

- Complications Trial/Epidemiology of Diabetes Interventions and Complications Genetics Study. *Diabetes*, 57, 218-228.
- Al-Saif,A., Al Mohanna,F., & Bohlega,S. (2011). A mutation in sigma-1 receptor causes juvenile amyotrophic lateral sclerosis. *Annals of Neurology*, 70, 913-919.
- Alexander,G.M., Erwin,K.L., Byers,N., Deitch,J.S., Augelli,B.J., Blankenhorn,E.P., & Heiman-Patterson,T.D. (2004). Effect of transgene copy number on survival in the G93A SOD1 transgenic mouse model of ALS. *Molecular Brain Research*, 130, 7-15.
- Andersen,P.M., Forsgren,L., Binzer,M., Nilsson,P., Ala-Hurula,V., Keränen,M.L., Bergmark,L., Saarinen,A., Haltia,T., Tarvainen,I., Kinnunen,E., Udd,B., & Marklund,S.L. (1996). Autosomal recessive adult-onset amyotrophic lateral sclerosis associated with homozygosity for Asp90A1a CuZn-superoxide dismutase mutation A clinical and genealogical study of 36 patients. *Brain*, 119, 1153-1172.
- Andersen,P.M. & Al Chalabi,A. (2011). Clinical genetics of amyotrophic lateral sclerosis: what do we really know? *Nature Reviews Neurology*, 7, 603-615.
- Andorfer,C., Acker,C.M., Kress,Y., Hof,P.R., Duff,K., & Davies,P. (2005). Cell-cycle reentry and cell death in transgenic mice expressing nonmutant human tau isoforms. *Journal of Neuroscience*, 25, 5446-5454.
- Andorfer,C., Kress,Y., Espinoza,M., De Silva,R., Tucker,K.L., Barde,Y.A., Duff,K., & Davies,P. (2003). Hyperphosphorylation and aggregation of tau in mice expressing normal human tau isoforms. *Journal of Neurochemistry*, 86, 582-590.
- Andrus,P.K., Fleck,T.J., Gurney,M.E., & Hall,E.D. (1998). Protein Oxidative Damage in a Transgenic Mouse Model of Familial Amyotrophic Lateral Sclerosis. *Journal of Neurochemistry*, 71, 2041-2048.
- Atkin,J.D., Farg,M.A., Walker,A.K., McLean,C., Tomas,D., & Horne,M.K. (2008). Endoplasmic reticulum stress and induction of the unfolded protein response in human sporadic amyotrophic lateral sclerosis. *Neurobiology of Disease*, 30, 400-407.
- Audet,J.N., Gowing,G., & Julien,J.P. (2010). Wild-type human SOD1 overexpression does not accelerate motor neuron disease in mice expressing murine Sod1G86R. *Neurobiology of Disease*, 40, 245-250.
- Augusto,V., Padovani,C.R., & Campos,G.E.R. (2004). Skeletal muscle fibre types in C57BL6J mice. *Brazilian Journal of Morphological Science*, 21, 89-94.
- Austin,S., Ziese,M., & Sternberg,N. (1981). A novel role for site-specific recombination in maintenance of bacterial replicons. *Cell*, 25, 729-736.
- Babu,G.N., Kumar,A., Chandra,R., Puri,S.K., Singh,R.L., Kalita,J., & Misra,U.K. (2008). Oxidant/antioxidant imbalance in the erythrocytes of sporadic amyotrophic lateral sclerosis patients correlates with the progression of disease. *Neurochemistry International*, 52, 1284-1289.
- Banci,L., Bertini,I., Cantini,F., Kozyreva,T., Massagni,C., Palumaa,P., Rubino,J.T., & Zovo,K. (2012). Human superoxide dismutase 1 (hSOD1) maturation through interaction with human copper chaperone for SOD1 (hCCS). *Proceedings of the National Academy of Sciences*, 109, 13555-13560.

- Bao-Cutrona,M. & Moral,P. (2009). Unexpected Expression Pattern of Tetracycline-Regulated Transgenes in Mice. *Genetics*, 181, 1687-1691.
- Basso,M., Pozzi,S., Tortarolo,M., Fiordaliso,F., Bisighini,C., Pasetto,L., Spaltro,G., Lidonnici,D., Gensano,F., Battaglia,E., Bendotti,C., & Bonetto,V. (2013). Mutant Copper-Zinc Superoxide Dismutase (SOD1) Induces Protein Secretion Pathway Alterations and Exosome Release in Astrocytes: Implications for disease spreading and motor neuron pathology in amyotrophic lateral sclerosis. *Journal of Biological Chemistry*, 288, 15699-15711.
- Battistini,S., Giannini,F., Greco,G., Bibbò,G., Ferrera,L., Marini,V., Causarano,R., Casula,M., Lando,G., Patrosso,M.C., Caponnetto,C., Origone,P., Marocchi,A., Corona,A., Siciliano,G., Carrera,P., Mascia,V., Giagheddu,M., Carcassi,C., Orrù,S., Garrè,C., & Penco,S. (2005). SOD1 mutations in amyotrophic lateral sclerosis. *Journal of neurology*, 252, 782-788.
- Beal,M.F., Ferrante,R.J., Browne,S.E., Matthews,R.T., Kowall,N.W., & Brown,R.H. (1997). Increased 3-nitrotyrosine in both sporadic and familial amyotrophic lateral sclerosis. *Annals of Neurology*, 42, 644-654.
- Beers,D.R., Henkel,J.S., Xiao,Q., Zhao,W., Wang,J., Yen,A.A., Siklos,L., McKercher,S.R., & Appel,S.H. (2006). Wild-type microglia extend survival in PU.1 knockout mice with familial amyotrophic lateral sclerosis. *Proceedings of the National Academy of Sciences of the United States of America*, 103, 16021-16026.
- Bence,N.F., Sampat,R.M., & Kopito,R.R. (2001). Impairment of the Ubiquitin-Proteasome System by Protein Aggregation. *Science*, 292, 1552-1555.
- Bendotti,C., Calvaresi,N., Chiveri,L., Prella,A., Moggio,M., Braga,M., Silani,V., & De Biasi,S. (2001). Early vacuolization and mitochondrial damage in motor neurons of FALS mice are not associated with apoptosis or with changes in cytochrome oxidase histochemical reactivity. *Journal of the Neurological Sciences*, 191, 25-33.
- Bendotti,C., Marino,M., Cheroni,C., Fontana,E., Crippa,V., Poletti,A., & De Biasi,S. (2012). Dysfunction of constitutive and inducible ubiquitin-proteasome system in amyotrophic lateral sclerosis: Implication for protein aggregation and immune response. *Progress in Neurobiology*, 97, 101-126.
- Bergemalm,D., Forsberg,K., Srivastava,V., Graffmo,K.S., Andersen,P.M., Brännström,T., Wingsle,G., & Marklund,S.L. (2010). Superoxide dismutase-1 and other proteins in inclusions from transgenic amyotrophic lateral sclerosis model mice. *Journal of Neurochemistry*, 114, 408-418.
- Bilsland,L.G., Sahai,E., Kelly,G., Golding,M., Greensmith,L., & Schiavo,G. (2010). Deficits in axonal transport precede ALS symptoms in vivo. *Proceedings of the National Academy of Sciences*, 107, 20523-20528.
- Birve,A., Neuwirth,C., Weber,M., Marklund,S.L., Nilsson,A.C., Jonsson,P.A., & Andersen,P.M. (2010). A novel SOD1 splice site mutation associated with familial ALS revealed by SOD activity analysis. *Human Molecular Genetics*, 19, 4201-4206.
- Blokhuys,A., Groen,E., Koppers,M., Berg,L., & Pasterkamp,R.J. (2013). Protein aggregation in amyotrophic lateral sclerosis. *Acta Neuropathologica*, 125, 777-794.
- Bogdanov,M., Brown,J., Matson,W., Smart,R., Hayden,D., O'Donnell,H., Flint Beal,M., & Cudkowicz,M. (2000). Increased oxidative damage to DNA in ALS patients. *Free Radical Biology and Medicine*, 29, 652-658.

- Bogdanove,A.J. & Voytas,D.F. (2011). TAL effectors: customizable proteins for DNA targeting. *Science*, 333, 1843-1846.
- Boill  e,S., Yamanaka,K., Lobsiger,C.S., Copeland,N.G., Jenkins,N.A., Kassiotis,G., Kollias,G., & Cleveland,D.W. (2006). Onset and Progression in Inherited ALS Determined by Motor Neurons and Microglia. *Science*, 312, 1389-1392.
- Borchelt,D.R., Lee,M.K., Slunt,H.S., Guarnieri,M., Xu,Z.S., Wong,P.C., Brown,R.H., Price,D.L., Sisodia,S.S., & Cleveland,D.W. (1994). Superoxide dismutase 1 with mutations linked to familial amyotrophic lateral sclerosis possesses significant activity. *Proceedings of the National Academy of Sciences of the United States of America*, 91, 8292-8296.
- Bordo,D., Djino  ic,K., & Bolognesi,M. (1994). Conserved Patterns in the Cu,Zn Superoxide Dismutase Family. *Journal of Molecular Biology*, 238, 366-386.
- Bosco,D.A., Morfini,G., Karabacak,N.M., Song,Y., Gros-Louis,F., Pasinelli,P., Goolsby,H., Fontaine,B.A., Lemay,N., McKenna-Yasek,D., Frosch,M.P., Agar,J.N., Julien,J.P., Brady,S.T., & Brown,R.H. (2010). Wild-type and mutant SOD1 share an aberrant conformation and a common pathogenic pathway in ALS. *Nature Neuroscience*, 13, 1396-1403.
- Bouhassira,E.E., Westerman,K., & Leboulch,P. (1997). Transcriptional Behavior of LCR Enhancer Elements Integrated at the Same Chromosomal Locus by Recombinase-Mediated Cassette Exchange. *Blood*, 90, 3332-3344.
- Bowling,A.C., Schulz,J.B., Brown,R.H., & Beal,M.F. (1993). Superoxide Dismutase Activity, Oxidative Damage, and Mitochondrial Energy Metabolism in Familial and Sporadic Amyotrophic Lateral Sclerosis. *Journal of Neurochemistry*, 61, 2322-2325.
- Bradley,A., Evans,M., Kaufman,M.H., & Robertson,E. (1984). Formation of germ-line chimaeras from embryo-derived teratocarcinoma cell lines. *Nature*, 309, 255-256.
- Brady,M.L., Allan,A.M., & Caldwell,K.K. (2012). A Limited Access Mouse Model of Prenatal Alcohol Exposure that Produces Long-Lasting Deficits in Hippocampal-Dependent Learning and Memory. *Alcoholism: Clinical and Experimental Research*, 36, 457-466.
- Branco,L.M.T., De Albuquerque,M., De Andrade,H.M., Bergo,F.P.G., Nucci,A., & Fran  a,M.C. (2013). Spinal cord atrophy correlates with disease duration and severity in amyotrophic lateral sclerosis. *Amyotrophic Lateral Sclerosis and Frontotemporal Degeneration*, 15, 93-97.
- Brooks,B.R., Miller,R.G., Swash,M., & Munsat,T.L. (2000). El Escorial revisited: Revised criteria for the diagnosis of amyotrophic lateral sclerosis. *Amyotrophic Lateral Sclerosis*, 1, 293-299.
- Brotherton,T.E., Li,Y., Cooper,D., Gearing,M., Julien,J.P., Rothstein,J.D., Boylan,K., & Glass,J.D. (2012). Localization of a toxic form of superoxide dismutase 1 protein to pathologically affected tissues in familial ALS. *Proceedings of the National Academy of Sciences*, 109, 5505-5510.
- Brotherton,T.E., Li,Y., & Glass,J.D. (2013). Cellular toxicity of mutant SOD1 protein is linked to an easily soluble, non-aggregated form in vitro. *Neurobiology of Disease*, 49, 49-56.
- Bruijn,L.I., Becher,M.W., Lee,M.K., Anderson,K.L., Jenkins,N.A., Copeland,N.G., Sisodia,S.S., Rothstein,J.D., Borchelt,D.R., Price,D.L., & Cleveland,D.W. (1997). ALS-Linked SOD1 Mutant G85R Mediates Damage to Astrocytes and Promotes Rapidly Progressive Disease with SOD1-Containing Inclusions. *Neuron*, 18, 327-338.



- Bruijn, L.I., Houseweart, M.K., Kato, S., Anderson, K.L., Anderson, S.D., Ohama, E., Reaume, A.G., Scott, R.W., & Cleveland, D.W. (1998). Aggregation and Motor Neuron Toxicity of an ALS-Linked SOD1 Mutant Independent from Wild-Type SOD1. *Science*, 281, 1851-1854.
- Bruns, C.K. & Kopito, R.R. (2007). Impaired post-translational folding of familial ALS-linked Cu, Zn superoxide dismutase mutants. *EMBO Journal*, 26, 855-866.
- Buehr, M., Meek, S., Blair, K., Yang, J., Ure, J., Silva, J., McLay, R., Hall, J., Ying, Q.L., & Smith, A. (2008). Capture of Authentic Embryonic Stem Cells from Rat Blastocysts. *Cell*, 135, 1287-1298.
- Burrell, J.R., Vucic, S., & Kiernan, M.C. (2011). Isolated bulbar phenotype of amyotrophic lateral sclerosis. *Amyotrophic Lateral Sclerosis*, 12, 283-289.
- Cabin, D.E., Gispert-Sanchez, S., Murphy, D., Auburger, G., Myers, R.R., & Nussbaum, R.L. (2005). Exacerbated synucleinopathy in mice expressing A53T SNCA on a Snca null background. *Neurobiology of Aging*, 26, 25-35.
- Calder, V.L., Domigan, N.M., George, P.M., Donaldson, I.M., & Winterbourn, C.C. (1995). Superoxide dismutase (glu100 - gly) in a family with inherited motor neuron disease: detection of mutant superoxide dismutase activity and the presence of heterodimers. *Neuroscience Letters*, 189, 143-146.
- Capecchi, M.R. (1989). Altering the Genome by Homologous Recombination. *Science*, 244, 1288-1292.
- Casoni, F., Basso, M., Massignan, T., Gianazza, E., Cheroni, C., Salmona, M., Bendotti, C., & Bonetto, V. (2005). Protein Nitration in a Mouse Model of Familial Amyotrophic Lateral Sclerosis: Possible Multifunctional Role in the Pathogenesis. *Journal of Biological Chemistry*, 280, 16295-16304.
- Cha, C.I., Chung, Y.H., Shin, C.m., Shin, D.H., Kim, Y.S., Gurney, M.E., & Lee, K.W. (2000). Immunocytochemical study on the distribution of nitrotyrosine in the brain of the transgenic mice expressing a human Cu/Zn SOD mutation. *Brain Research*, 853, 156-161.
- Chandler, K., Chandler, R., Broeckelmann, E., Hou, Y., Southard-Smith, E., & Mortlock, D. (2007). Relevance of BAC transgene copy number in mice: transgene copy number variation across multiple transgenic lines and correlations with transgene integrity and expression. *Mammalian Genome*, 18, 693-708.
- Chang, Y., Kong, Q., Shan, X., Tian, G., Ilieva, H., Cleveland, D.W., Rothstein, J.D., Borchelt, D.R., Wong, P.C., & Lin, C.I.G. (2008). Messenger RNA Oxidation Occurs Early in Disease Pathogenesis and Promotes Motor Neuron Degeneration in ALS. *PLoS ONE*, 3, e2849.
- Chang-Hong, R., Wada, M., Koyama, S., Kimura, H., Arawaka, S., Kawanami, T., Kurita, K., Kadoya, T., Aoki, M., Itoyama, Y., & Kato, T. (2005). Neuroprotective effect of oxidized galectin-1 in a transgenic mouse model of amyotrophic lateral sclerosis. *Experimental Neurology*, 194, 203-211.
- Chen, H., Qian, K., Du, Z., Cao, J., Petersen, A., Liu, H., Blackburn IV, L.W., Huang, C.-L., Errigo, A., Yin, Y., Lu, J., Ayala, M., & Zhang, S.-C. (2014). Modeling ALS with iPSCs Reveals that Mutant SOD1 Misregulates Neurofilament Balance in Motor Neurons. *Cell Stem Cell*, doi.org/10.1016/j.stem.2014.02.004.
- Chen, Y.Z., Bennett, C.L., Huynh, H.M., Blair, I.P., Puls, I., Irobi, J., Dierick, I., Abel, A., Kennerson, M.L., Rabin, B.A., Nicholson, G.A., Auer-Grumbach, M., Wagner, K., De Jonghe, P.,

- Griffin,J.W., Fischbeck,K.H., Timmerman,V., Cornblath,D.R., & Chance,P.F. (2004). DNA/RNA Helicase Gene Mutations in a Form of Juvenile Amyotrophic Lateral Sclerosis (ALS4). *American Journal of Human Genetics*, 74, 1128-1135.
- Cheroni,C., Peviani,M., Cascio,P., DeBiasi,S., Monti,C., & Bendotti,C. (2005). Accumulation of human SOD1 and ubiquitinated deposits in the spinal cord of SOD1G93A mice during motor neuron disease progression correlates with a decrease of proteasome. *Neurobiology of Disease*, 18, 509-522.
- Cheroni,C., Marino,M., Tortarolo,M., Veglianesi,P., De Biasi,S., Fontana,E., Zuccarello,L.V., Maynard,C.J., Dantuma,N.P., & Bendotti,C. (2009). Functional alterations of the ubiquitin-proteasome system in motor neurons of a mouse model of familial amyotrophic lateral sclerosisGÇá. *Hum.Mol.Genet.*, 18, 82-96.
- Chevalier-Larsen,E. & Holzbaur,E.L.F. (2006). Axonal transport and neurodegenerative disease. *Biochimica et Biophysica Acta (BBA) - Molecular Basis of Disease*, 1762, 1094-1108.
- Chia,R., Tattum,M.H., Jones,S., Collinge,J., Fisher,E.M.C., & Jackson,G.S. (2010). Superoxide Dismutase 1 and tgSOD1<sup>G93A</sup> Mouse Spinal Cord Seed Fibrils, Suggesting a Propagative Cell Death Mechanism in Amyotrophic Lateral Sclerosis. *PLoS ONE*, 5, e10627.
- Chiò,A., Logroscino,G., Traynor,B.J., Collins,J., Simeone,J.C., Goldstein,L.A., & White,L.A. (2013). Global epidemiology of amyotrophic lateral sclerosis: A systematic review of the published literature. *Neuroepidemiology*, 41, 118-130.
- Chiò,A., Mora,G., Leone,M., Mazzini,L., Cocito,D., Giordana,M.T., Bottacchi,E., & Mutani,R. (2002). Early symptom progression rate is related to ALS outcome: A prospective population-based study. *Neurology*, 59, 99-103.
- Chiu,A.Y., Zhai,P., Dal Canto,M.C., Peters,T.M., Kwon,Y.W., Prattis,S.M., & Gurney,M.E. (1995). Age-Dependent Penetrance of Disease in a Transgenic Mouse Model of Familial Amyotrophic Lateral Sclerosis. *Molecular and Cellular Neuroscience*, 6, 349-362.
- Clavaguera,F., Bolmont,T., Crowther,R.A., Abramowski,D., Frank,S., Probst,A., Fraser,G., Stalder,A.K., Beibel,M., Staufenbiel,M., Jucker,M., Goedert,M., & Tolnay,M. (2009). Transmission and spreading of tauopathy in transgenic mouse brain. *Nature Cell Biology*, 11, 909-913.
- Clavaguera,F., Akatsu,H., Fraser,G., Crowther,R.A., Frank,S., Hench,J., Probst,A., Winkler,D.T., Reichwald,J., Staufenbiel,M., Ghetti,B., Goedert,M., & Tolnay,M. (2013). Brain homogenates from human tauopathies induce tau inclusions in mouse brain. *Proceedings of the National Academy of Sciences*, 110, 9535-9540.
- Cohen-Adad,J., Mendili,M.M.E., Morizot-Koutlidis,R., Lehericy,S., Meininger,V., Blanche,S., Rossignol,S., Benali,H., & Pradat,P.F. (2012). Involvement of spinal sensory pathway in ALS and specificity of cord atrophy to lower motor neuron degeneration. *Amyotrophic Lateral Sclerosis and Frontotemporal Degeneration*, 14, 30-38.
- Collinge,J., Palmer,M.S., Sidle,K.C.L., Hill,A.F., Gowland,I., Meads,J., Asante,E., Bradley,R., Doey,L.J., & Lantos,P.L. (1995). Unaltered susceptibility to BSE in transgenic mice expressing human prion protein. *Nature*, 378, 779-783.
- Cooke,C.L. & Davidge,S.T. (2003). Endothelial-dependent vasodilation is reduced in mesenteric arteries from superoxide dismutase knockout mice. *Cardiovascular Research*, 60, 635-642.

- Coolican, H. (1999). *Research Methods and Statistics* (3rd ed.). London: Hodder and Stoughton.
- Costantini, F. & Lacy, E. (1981). Introduction of a rabbit  $\beta$ -globin gene into the mouse germ line. *Nature*, 294, 92-94.
- Court, D.L., Sawitzke, J.A., & Thomas, L.C. (2002). Genetic engineering using homologous recombination. *Annual Review of Genetics*, 36, 361-388.
- Cova, E., Bongioanni, P., Cereda, C., Metelli, M.R., Salvaneschi, L., Bernuzzi, S., Guareschi, S., Rossi, B., & Ceroni, M. (2010). Time course of oxidant markers and antioxidant defenses in subgroups of amyotrophic lateral sclerosis patients. *Neurochemistry International*, 56, 687-693.
- Crapo, J.D., Oury, T., Rabouille, C., Slot, J.W., & Chang, L.Y. (1992). Copper, zinc superoxide dismutase is primarily a cytosolic protein in human cells. *Proceedings of the National Academy of Sciences of the United States of America*, 89, 10405-10409.
- Crugnola, V., Lamperti, C., & Lucchini, V. (2010). Mitochondrial respiratory chain dysfunction in muscle from patients with amyotrophic lateral sclerosis. *Arch Neurol*, 67, 849-854.
- Cudkovic, M.E., McKenna-Yasek, D., Sapp, P.E., Chin, W., Geller, B., Hayden, D.L., Schoenfeld, D.A., Hosler, B.A., Horvitz, H.R., & Brown, R.H. (1997). Epidemiology of mutations in superoxide dismutase in amyotrophic lateral sclerosis. *Annals of Neurology*, 41, 210-221.
- D'Acunzo, P., Badaloni, A., Ferro, M., Zimarino, V., Ripamonti, M., Malgaroli, A., & Consalez, G.G. (2014). A conditional transgenic reporter of presynaptic terminals reveals novel features of the mouse corticospinal tract. *Frontiers in Neuroanatomy*, 7.
- Dal Canto, M.C. & Gurney, M.E. (1994). Development of central nervous system pathology in a murine transgenic model of human amyotrophic lateral sclerosis. *American Journal of Pathology*, 145, 1271-1279.
- Dal Canto, M.C. & Gurney, M.E. (1995). Neuropathological changes in two lines of mice carrying a transgene for mutant human Cu,Zn SOD, and in mice overexpressing wild type human SOD: a model of familial amyotrophic lateral sclerosis (FALS). *Brain Research*, 676, 25-40.
- de Saint Vincent, B.R. & Wahl, G.M. (1983). Homologous recombination in mammalian cells mediates formation of a functional gene from two overlapping gene fragments. *Proceedings of the National Academy of Sciences of the United States of America*, 80, 2002-2006.
- De Vos, K.J., Chapman, A.L., Tennant, M.E., Manser, C., Tudor, E.L., Lau, K.F., Brownlee, J., Ackerley, S., Shaw, P.J., McLoughlin, D.M., Shaw, C.E., Leigh, P.N., Miller, C.C.J., & Grierson, A.J. (2007). Familial amyotrophic lateral sclerosis-linked SOD1 mutants perturb fast axonal transport to reduce axonal mitochondria content. *Human Molecular Genetics*, 16, 2720-2728.
- DeJesus-Hernandez, M., Mackenzie, I., Boeve, B., Boxer, A., Baker, M., Rutherford, N., Nicholson, A., Finch, N., Flynn, H., Adamson, J., Kouri, N., Wojtas, A., Sengdy, P., Hsiung, G.Y., Karydas, A., Seeley, W., Josephs, K., Coppola, G., Geschwind, D., Wszolek, Z., Feldman, H., Knopman, D., Petersen, R., Miller, B., Dickson, D., Boylan, K., Graff-Radford, N., & Rademakers, R. (2011). Expanded GGGGCC Hexanucleotide Repeat in Noncoding Region of C9ORF72 Causes Chromosome 9p-Linked FTD and ALS. *Neuron*, 72, 245-256.
- Deng, H.X., Hentati, A., Tainer, J.A., Iqbal, Z., Cayabyab, A., Hung, W.Y., Getzoff, E.D., Hu, P., Herzfeldt, B., Roos, R.P., & et al. (1993). Amyotrophic lateral sclerosis and structural defects in Cu,Zn superoxide dismutase. *Science*, 261, 1047-1051.

Deng,H.X., Chen,W., Hong,S.T., Boycott,K.M., Gorrie,G.H., Siddique,N., Yang,Y., Fecto,F., Shi,Y., Zhai,H., Jiang,H., Hirano,M., Rampersaud,E., Jansen,G.H., Donkervoort,S., Bigio,E.H., Brooks,B.R., Ajroud,K., Sufit,R.L., Haines,J.L., Mugnaini,E., Pericak-Vance,M.A., & Siddique,T. (2011). Mutations in UBQLN2 cause dominant X-linked juvenile and adult-onset ALS and ALS/dementia. *Nature*, 477, 211-215.

Deng,H.X., Jiang,H., Fu,R., Zhai,H., Shi,Y., Liu,E., Hiran,M., Dal Canto,M.C., & Siddique,T. (2008). Molecular dissection of ALS-associated toxicity of SOD1 in transgenic mice using an exon-fusion approach. *Human Molecular Genetics*, 17, 2310-2319.

Deng,H.X., Shi,Y., Furukawa,Y., Zhai,H., Fu,R., Liu,E., Gorrie,G.H., Khan,M.S., Hung,W.Y., Bigio,E.H., Lukas,T., Dal Canto,M.C., O'Halloran,T.V., & Siddique,T. (2006). Conversion to the amyotrophic lateral sclerosis phenotype is associated with intermolecular linked insoluble aggregates of SOD1 in mitochondria. *Proceedings of the National Academy of Sciences of the United States of America*, 103, 7142-7147.

Dengler,R., Konstanzer,A., Küther,G., Hesse,S., Wolf,W., & Strupplerdr,A. (1990). Amyotrophic lateral sclerosis: Macro-EMG and twitch forces of single motor units. *Muscle & Nerve*, 13, 545-550.

Desplats,P., Lee,H.J., Bae,E.J., Patrick,C., Rockenstein,E., Crews,L., Spencer,B., Masliah,E., & Lee,S.J. (2009). Inclusion formation and neuronal cell death through neuron-to-neuron transmission of a-synuclein. *Proceedings of the National Academy of Sciences*, 106, 13010-13015.

Di Giorgio,F.P., Boulting,G.L., Bobrowicz,S., & Eggan,K.C. (2008). Human Embryonic Stem Cell-Derived Motor Neurons Are Sensitive to the Toxic Effect of Glial Cells Carrying an ALS-Causing Mutation. *Cell Stem Cell*, 3, 637-648.

Didion,S.P., Ryan,M.J., Didion,L.A., Fegan,P.E., Sigmund,C.D., & Faraci,F.M. (2002). Increased Superoxide and Vascular Dysfunction in CuZnSOD-Deficient Mice. *Circulation Research*, 91, 938-944.

Dobrowolny,G., Aucello,M., Rizzuto,E., Beccafico,S., Mammucari,C., Boncompagni,S., Belia,S., Wannenes,F., Nicoletti,C., Del Prete,Z., Rosenthal,N., Molinaro,M., Protasi,F., Fanò,G., Sandri,M., & Musarò,A. (2008). Skeletal Muscle Is a Primary Target of SOD1G93A-Mediated Toxicity. *Cell metabolism*, 8, 425-436.

Doi,K., Nakano,T., Kitayama,M., Watanabe,Y., Yasui,K., Fukada,Y., Morino,S., Kaidoh,T., Nakashima,K., & Inoué,T. (2008). Mitochondrial changes in motor neurons of homozygotes of leucine 126 TT deletion SOD1 transgenic mice. *Neuropathology*, 28, 269-276.

Drummond,A.J., Ashton,B., Cheung,M., Cooper,A., Heled,J., Kearse,M., Moir,R., Stones-Havas,S., Sturrock,S., Thierer,T., & Wilson,A. (2010). Geneious v5.3. Available from <http://geneious.com>.

Duff,K., Knight,H., Refolo,L.M., Sanders,S., Yu,X., Picciano,M., Malester,B., Hutton,M., Adamson,J., Goedert,M., Burki,K., & Davies,P. (2000). Characterization of Pathology in Transgenic Mice Over-Expressing Human Genomic and cDNA Tau Transgenes. *Neurobiology of Disease*, 7, 87-98.

Economides,A.N., Friendewey,D., Yang,P., Dominguez,M.G., Dore,A.T., Lobov,I.B., Persaud,T., Rojas,J., McClain,J., Lengyel,P., Droguett,G., Chernomorsky,R., Stevens,S., Auerbach,W., DeChiara,T.M., Pouyemirou,W., Cruz,J.M., Feeley,K., Mellis,I.A., Yasenack,J., Hatsell,S.J., Xie,L., Latres,E., Huang,L., Zhang,Y., Pefanis,E., Skokos,D., Deckelbaum,R.A., Croll,S.D., Davis,S.,

- Valenzuela,D.M., Gale,N.W., Murphy,A.J., & Yancopoulos,G.D. (2013). Conditionals by inversion provide a universal method for the generation of conditional alleles. *Proceedings of the National Academy of Sciences*, 110, E3179-E3188.
- Elliott,J.L. (2001). Zinc and copper in the pathogenesis of amyotrophic lateral sclerosis. *Progress in Neuro-Psychopharmacology and Biological Psychiatry*, 25, 1169-1185.
- Ellis,H.M., Yu,D., DiTizio,T., & Court,D. (2001). High efficiency mutagenesis, repair, and engineering of chromosomal DNA using single-stranded oligonucleotides. *Proceedings of the National Academy of Sciences of the United States of America*, 98, 6742-6746.
- Epstein,C.J., Avraham,K.B., Lovett,M., Smith,S., Elroy-Stein,O., Rotman,G., Bry,C., & Groner,Y. (1987). Transgenic mice with increased Cu/Zn-superoxide dismutase activity: animal model of dosage effects in Down syndrome. *Proceedings of the National Academy of Sciences of the United States of America*, 84, 8044-8048.
- Estévez,A.G., Crow,J.P., Sampson,J.B., Reiter,C., Zhuang,Y., Richardson,G.J., Tarpey,M.M., Barbeito,L., & Beckman,J.S. (1999). Induction of Nitric Oxide -- Dependent Apoptosis in Motor Neurons by Zinc-Deficient Superoxide Dismutase. *Science*, 286, 2498-2500.
- Evans,M.J. & Kaufman,M.H. (1981). Establishment in culture of pluripotential cells from mouse embryos. *Nature*, 292, 154-156.
- Ezzi,S.A., Urushitani,M., & Julien,J.P. (2007). Wild-type superoxide dismutase acquires binding and toxic properties of ALS-linked mutant forms through oxidation. *Journal of Neurochemistry*, 102, 170-178.
- Fecto,F. & Siddique,T. (2011). Making Connections: Pathology and Genetics Link Amyotrophic Lateral Sclerosis with Frontotemporal Lobe Dementia. *Journal of Molecular Neuroscience*, 45, 663-675.
- Feng,Y., Zhang,S., & Huang,X. (2013). A robust TALENs system for highly efficient mammalian genome editing. *Scientific Reports*, 4.
- Ferrante,R.J., Browne,S.E., Shinobu,L.A., Bowling,A.C., Baik,M.J., MacGarvey,U., Kowall,N.W., Brown,R.H., & Beal,M.F. (1997a). Evidence of Increased Oxidative Damage in Both Sporadic and Familial Amyotrophic Lateral Sclerosis. *Journal of Neurochemistry*, 69, 2064-2074.
- Ferrante,R.J., Shinobu,L.A., Schulz,J.B., Matthews,R.T., Thomas,C.E., Kowall,N.W., Gurney,M.E., & Beal,M.F. (1997b). Increased 3-nitrotyrosine and oxidative damage in mice with a human copper/zinc superoxide dismutase mutation. *Annals of Neurology*, 42, 326-334.
- Ferrari,R., Kapogiannis,D., Huey,E.D., & Momeni,P. (2011). Ftd and als: A tale of two diseases. *Current Alzheimer Research*, 8, 273-294.
- Ferri,A., Cozzolino,M., Crosio,C., Nencini,M., Casciati,A., Gralla,E.B., Rotilio,G., Valentine,J.S., & Carri,M.T. (2006). Familial ALS-superoxide dismutases associate with mitochondria and shift their redox potentials. *Proceedings of the National Academy of Sciences of the United States of America*, 103, 13860-13865.
- Fiering,S., Epner,E., Robinson,K., Zhuang,Y., Telling,A., Hu,M., Martin,D.I., Enver,T., Ley,T.J., & Groudine,M. (1995). Targeted deletion of 5'HS2 of the murine beta-globin LCR reveals that it is not essential for proper regulation of the beta-globin locus. *Genes & Development*, 9, 2203-2213.

- Fischer, L.R., Culver, D.G., Tennant, P., Davis, A.A., Wang, M., Castellano-Sanchez, A., Khan, J., Polak, M.A., & Glass, J.D. (2004). Amyotrophic lateral sclerosis is a distal axonopathy: evidence in mice and man. *Experimental Neurology*, 185, 232-240.
- Fischer, L.R., Igoudjil, A., Magrané, J., Li, Y., Hansen, J.M., Manfredi, G., & Glass, J.D. (2011). SOD1 targeted to the mitochondrial intermembrane space prevents motor neuropathy in the Sod1 knockout mouse. *Brain*, 134, 196-209.
- Flood, D.G., Reaume, A.G., Gruner, J.A., Hoffman, E.K., Hirsch, J.D., Lin, Y.G., Dorfman, K.S., & Scott, R.W. (1999). Hindlimb Motor Neurons Require Cu/Zn Superoxide Dismutase for Maintenance of Neuromuscular Junctions. *The American journal of pathology*, 155, 663-672.
- Folger, K., Thomas, K., & Capecchi, M.R. (1984). Analysis of Homologous Recombination in Cultured Mammalian Cells. *Cold Spring Harbor Symposia on Quantitative Biology*, 49, 123-138.
- Folger, K.R., Wong, E.A., Wahl, G., & Capecchi, M.R. (1982). Patterns of integration of DNA microinjected into cultured mammalian cells: evidence for homologous recombination between injected plasmid DNA molecules. *Molecular and Cellular Biology*, 2, 1372-1387.
- Forsberg, K., Andersen, P.M., Marklund, S.L., & Brännström, T. (2011). Glial nuclear aggregates of superoxide dismutase-1 are regularly present in patients with amyotrophic lateral sclerosis. *Acta Neuropathologica*, 121, 623-634.
- Forsberg, K., Jonsson, P.A., Andersen, P.M., Bergemalm, D., Graffmo, K.S., Hultdin, M., Jacobsson, J., Rosquist, R., Marklund, S.L., & Brännström, T. (2010). Novel Antibodies Reveal Inclusions Containing Non-Native SOD1 in Sporadic ALS Patients. *PLoS ONE*, 5, e11552.
- Frengen, E., Weichenhan, D., Zhao, B., Osoegawa, K., van Geel, M., & de Jong, P.J. (1999). A Modular, Positive Selection Bacterial Artificial Chromosome Vector with Multiple Cloning Sites. *Genomics*, 58, 250-253.
- Frey, D., Schneider, C., Xu, L., Borg, J., Spooren, W., & Caroni, P. (2000). Early and Selective Loss of Neuromuscular Synapse Subtypes with Low Sprouting Competence in Motoneuron Diseases. *The Journal of Neuroscience*, 20, 2534-2542.
- Freyer, L., Nowotschin, S., Pirity, M., Baldini, A., & Morrow, B. (2013). Conditional and constitutive expression of a Tbx1-GFP fusion protein in mice. *BMC Developmental Biology*, 13, 33.
- Friedman, S.A. & Hays, J.B. (1986). Selective inhibition of Escherichia coli RecBC activities by plasmid-encoded GamS function of phage lambda. *Gene*, 43, 255-263.
- Fritz, E., Izaurieta, P., Weiss, A., Mir, F.R., Rojas, P., Gonzalez, D., Rojas, F., Brown, R.H., Madrid, R., & van Zundert, B. (2013). Mutant SOD1-expressing astrocytes release toxic factors that trigger motoneuron death by inducing hyperexcitability. *Journal of Neurophysiology*, 109, 2803-2814.
- Frost, B., Jacks, R.L., & Diamond, M.I. (2009). Propagation of Tau Misfolding from the Outside to the Inside of a Cell. *Journal of Biological Chemistry*, 284, 12845-12852.
- Fujimura-Kiyono, C., Kimura, F., Ishida, S., Nakajima, H., Hosokawa, T., Sugino, M., & Hanafusa, T. (2011). Onset and spreading patterns of lower motor neuron involvements predict survival in sporadic amyotrophic lateral sclerosis. *Journal of Neurology, Neurosurgery & Psychiatry*, 82, 1244-1249.
- Fujisawa, T., Homma, K., Yamaguchi, N., Kadowaki, H., Tsuburaya, N., Naguro, I., Matsuzawa, A., Takeda, K., Takahashi, Y., Goto, J., Tsuji, S., Nishitoh, H., & Ichijo, H. (2012). A novel monoclonal

antibody reveals a conformational alteration shared by amyotrophic lateral sclerosis-linked SOD1 mutants. *Annals of Neurology*, 72, 739-749.

Fujita,K., Yamauchi,M., Shibayama,K., Ando,M., Honda,M., & Nagata,Y. (1996). Decreased cytochrome c oxidase activity but unchanged superoxide dismutase and glutathione peroxidase activities in the spinal cords of patients with amyotrophic lateral sclerosis. *Journal of Neuroscience Research*, 45, 276-281.

Fukada,K., Nagano,S., Satoh,M., Tohyama,C., Nakanishi,T., Shimizu,A., Yanagihara,T., & Sakoda,S. (2001). Stabilization of mutant Cu/Zn superoxide dismutase (SOD1) protein by coexpressed wild SOD1 protein accelerates the disease progression in familial amyotrophic lateral sclerosis mice. *European Journal of Neuroscience*, 14, 2032-2036.

Fukada,Y., Yasui,K., Kitayama,M., Doi,K., Nakano,T., Watanabe,Y., & Nakashima,K. (2007). Gene expression analysis of the murine model of amyotrophic lateral sclerosis: Studies of the Leu126delTT mutation in SOD1. *Brain Research*, 1160, 1-10.

Furukawa,Y. (2012). Pathological roles of wild-type Cu, Zn-superoxide dismutase in amyotrophic lateral sclerosis. *Neurology Research International*, 2012, 323261.

Furukawa,Y., Kaneko,K., Watanabe,S., Yamanaka,K., & Nukina,N. (2011). A Seeding Reaction Recapitulates Intracellular Formation of Sarkosyl-insoluble Transactivation Response Element (TAR) DNA-binding Protein-43 Inclusions. *Journal of Biological Chemistry*, 286, 18664-18672.

Furukawa,Y., Kaneko,K., Watanabe,S., Yamanaka,K., & Nukina,N. (2013). Intracellular seeded aggregation of mutant Cu,Zn-superoxide dismutase associated with amyotrophic lateral sclerosis. *FEBS Letters*, 587, 2500-2505.

Furukawa,Y., Kaneko,K., Yamanaka,K., O'Halloran,T.V., & Nukina,N. (2008). Complete Loss of Post-translational Modifications Triggers Fibrillar Aggregation of SOD1 in the Familial Form of Amyotrophic Lateral Sclerosis. *Journal of Biological Chemistry*, 283, 24167-24176.

Gaj,T., Gersbach,C.A., & Barbas III,C.F. (2013). ZFN, TALEN, and CRISPR/Cas-based methods for genome engineering. *Trends in Biotechnology*, 31, 397-405.

Gajdusek,D.C. & Gibbs,C.J. (1964). Attempts to Demonstrate a Transmissible Agent in Kuru, Amyotrophic Lateral Sclerosis, and other Sub-Acute and Chronic Nervous System Degenerations of Man. *Nature*, 204, 257-259.

Gal,J., Ström,A.L., Kilty,R., Zhang,F., & Zhu,H. (2007). p62 Accumulates and Enhances Aggregate Formation in Model Systems of Familial Amyotrophic Lateral Sclerosis. *Journal of Biological Chemistry*, 282, 11068-11077.

Garratt,M., Bathgate,R., de Graaf,S.P., & Brooks,R.C. (2013). Copper-zinc superoxide dismutase deficiency impairs sperm motility and in vivo fertility. *Reproduction*, 146, 297-304.

Ge,W.-W., Wen,W., Strong,W., Leystra-Lantz,C., & Strong,M.J. (2005). Mutant Copper-Zinc Superoxide Dismutase Binds to and Destabilizes Human Low Molecular Weight Neurofilament mRNA. *Journal of Biological Chemistry*, 280, 118-124.

Gibbs,C.J. & Gajdusek,D.C. (1972). Amyotrophic lateral sclerosis, Parkinson's disease, and the amyotrophic lateral sclerosis-Parkinsonism-dementia complex on Guam: a review and summary of attempts to demonstrate infection as the aetiology. *Journal of Clinical Pathology*, 25, 132-140.

- Giordana,M., Ferrero,P., Grifoni,S., Pellerino,A., Naldi,A., & Montuschi,A. (2011). Dementia and cognitive impairment in amyotrophic lateral sclerosis: a review. *Neurological Sciences*, 32, 9-16.
- Gong,Y.H., Parsadanian,A.S., Andreeva,A., Snider,W.D., & Elliott,J.L. (2000). Restricted Expression of G86R Cu/Zn Superoxide Dismutase in Astrocytes Results in Astrocytosis But Does Not Cause Motoneuron Degeneration. *The Journal of Neuroscience*, 20, 660-665.
- Goold,R., McKinnon,C., Rabbanian,S., Collinge,J., Schiavo,G., & Tabrizi,S.J. (2013). Alternative fates of newly formed PrPSc upon prion conversion on the plasma membrane. *Journal of Cell Science*, 126, 3552-3562.
- Gordon,J.W. & Ruddle,F.H. (1981). Integration and stable germ line transmission of genes injected into mouse pronuclei. *Science*, 214, 1244-1246.
- Gordon,J.W., Scangos,G.A., Plotkin,D.J., Barbosa,J.A., & Ruddle,F.H. (1980). Genetic transformation of mouse embryos by microinjection of purified DNA. *Proceedings of the National Academy of Sciences of the United States of America*, 77, 7380-7384.
- Gordon,T., Ly,V., Hegedus,J., & Tyreman,N. (2009). Early detection of denervated muscle fibers in hindlimb muscles after sciatic nerve transection in wild type mice and in the G93A mouse model of amyotrophic lateral sclerosis. *Neurological Research*, 31, 28-42.
- Gordon,T., Thomas,C.K., Munson,J.B., & Stein,R.B. (2004). The resilience of the size principle in the organization of motor unit properties in normal and reinnervated adult skeletal muscles. *Canadian Journal of Physiology and Pharmacology*, 82, 645-661.
- Gossler,A., Doetschman,T., Korn,R., Serfling,E., & Kemler,R. (1986). Transgenesis by means of blastocyst-derived embryonic stem cell lines. *Proceedings of the National Academy of Sciences of the United States of America*, 83, 9065-9069.
- Gould,T.W., Buss,R.R., Vinsant,S., Prevette,D., Sun,W., Knudson,C.M., Milligan,C.E., & Oppenheim,R.W. (2006). Complete Dissociation of Motor Neuron Death from Motor Dysfunction by Bax Deletion in a Mouse Model of ALS. *The Journal of Neuroscience*, 26, 8774-8786.
- Gouveia,L.O. & de Carvalho,M. (2007). Young-onset sporadic amyotrophic lateral sclerosis: A distinct nosological entity? *Amyotrophic Lateral Sclerosis*, 8, 323-327.
- Grad,L.I., Guest,W.C., Yanai,A., Pokrishevsky,E., O'Neill,M.A., Gibbs,E., Semchenko,V., Yousefi,M., Wishart,D.S., Plotkin,S.S., & Cashman,N.R. (2011). Intermolecular transmission of superoxide dismutase 1 misfolding in living cells. *Proceedings of the National Academy of Sciences*, 108, 16398-16403.
- Grad,L.I., Yerbury,J.J., Turner,B.J., Guest,W.C., Pokrishevsky,E., O'Neill,M.A., Yanai,A., Silverman,J.M., Zeineddine,R., Corcoran,L., Kumita,J.R., Luheshi,L.M., Yousefi,M., Coleman,B.M., Hill,A.F., Plotkin,S.S., Mackenzie,I.R., & Cashman,N.R. (2014). Intercellular propagated misfolding of wild-type Cu/Zn superoxide dismutase occurs via exosome-dependent and -independent mechanisms. *Proceedings of the National Academy of Sciences*, doi: 10.1073/pnas.1312245111.
- Graffmo,K.S., Forsberg,K., Bergh,J., Birve,A., Zetterström,P., Andersen,P.M., Marklund,S.L., & Brännström,T. (2012). Expression of wild-type human superoxide dismutase-1 in mice causes amyotrophic lateral sclerosis. *Human Molecular Genetics*, 22, 51-60.



- Green,E.L. (1941). Genetic and non-genetic factors which influence the type of the skeleton in an inbred strain of mice. *Genetics*, 26, 192-222.
- Green,E.L. (1951). The Genetics of a Difference in Skeletal Type Between Two Inbred Strains of Mice (BalbC and C57blk). *Genetics*, 36, 391-409.
- Grohme,K., Maravic,M., Gasser,T., & Borasio,G.D. (2001). A case of amyotrophic lateral sclerosis with a very slow progression over 44 years. *Neuromuscular Disorders*, 11, 414-416.
- Groleau,J., Dussault,S., Turgeon,J., Haddad,P., & Rivard,A. (2011). Accelerated Vascular Aging in CuZnSOD-Deficient Mice: Impact on EPC Function and Reparative Neovascularization. *PLoS ONE*, 6, e23308.
- Gros-Louis,F., Soucy,G., Larivière,R., & Julien,J.P. (2010). Intracerebroventricular infusion of monoclonal antibody or its derived Fab fragment against misfolded forms of SOD1 mutant delays mortality in a mouse model of ALS. *Journal of Neurochemistry*, 113, 1188-1199.
- Gruzman,A., Wood,W.L., Alpert,E., Prasad,M.D., Miller,R.G., Rothstein,J.D., Bowser,R., Hamilton,R., Wood,T.D., Cleveland,D.W., Lingappa,V.R., & Liu,J. (2007). Common molecular signature in SOD1 for both sporadic and familial amyotrophic lateral sclerosis. *Proceedings of the National Academy of Sciences*, 104, 12524-12529.
- Guareschi,S., Cova,E., Cereda,C., Ceroni,M., Donetti,E., Bosco,D.A., Trotti,D., & Pasinelli,P. (2012). An over-oxidized form of superoxide dismutase found in sporadic amyotrophic lateral sclerosis with bulbar onset shares a toxic mechanism with mutant SOD1. *Proceedings of the National Academy of Sciences*, 109, 5074-5079.
- Guest,W.C., Silverman,J.M., Pokrishevsky,E., O'Neill,M.A., Grad,L.I., & Cashman,N.R. (2011). Generalization of the Prion Hypothesis to Other Neurodegenerative Diseases: An Imperfect Fit. *Journal of Toxicology and Environmental Health, Part A*, 74, 1433-1459.
- Gurney,M.E. (1997). The use of transgenic mouse models of amyotrophic lateral sclerosis in preclinical drug studies. *Journal of the Neurological Sciences*, 152, S67-S73.
- Gurney,M.E., Pu,H., Chiu,A.Y., Dal Canto,M.C., Polchow,C.Y., Alexander,D.D., Caliendo,J., Hentati,A., Kwon,Y.W., Deng,H.X., Chen,W., Zhai,P., Sufit,R.L., & Siddique,T. (1994). Motor neuron degeneration in mice that express a human Cu,Zn superoxide dismutase mutation. *Science*, 264, 1772-1775.
- Guzman,L.M., Belin,D., Carson,M.J., & Beckwith,J. (1995). Tight regulation, modulation, and high-level expression by vectors containing the arabinose PBAD promoter. *Journal of Bacteriology*, 177, 4121-4130.
- Hafezparast,M., Klocke,R., Ruhrberg,C., Marquardt,A., Ahmad-Annur,A., Bowen,S., Lalli,G., Witherden,A.S., Hummerich,H., Nicholson,S., Morgan,P.J., Oozageer,R., Priestley,J.V., Averill,S., King,V.R., Ball,S., Peters,J., Toda,T., Yamamoto,A., Hiraoka,Y., Augustin,M., Korthaus,D., Wattler,S., Wabnitz,P., Dickneite,C., Lampel,S., Boehme,F., Peraus,G., Popp,A., Rudelius,M., Schlegel,J., Fuchs,H., de Angelis,M.H., Schiavo,G., Shima,D.T., Russ,A.P., Stumm,G., Martin,J.E., & Fisher,E.M.C. (2003). Mutations in Dynein Link Motor Neuron Degeneration to Defects in Retrograde Transport. *Science*, 300, 808-812.
- Haidet-Phillips,A.M., Hester,M.E., Miranda,C.J., Meyer,K., Braun,L., Frakes,A., Song,S., Likhite,S., Murtha,M.J., Foust,K.D., Rao,M., Eagle,A., Kammesheidt,A., Christensen,A., Mendell,J.R., Burghes,A.H.M., & Kaspar,B.K. (2011). Astrocytes from familial and sporadic ALS patients are toxic to motor neurons. *Nature Biotechnology*, 29, 824-828.

- Hall, E.D., Oostveen, J.A., & Gurney, M.E. (1998). Relationship of microglial and astrocytic activation to disease onset and progression in a transgenic model of familial ALS. *Glia*, 23, 249-256.
- Hansen, C., Angot, E., Ann, L., Steiner, J.A., Pieri, L., Paul, G., Outeiro, T.F., Melki, R., Kallunki, P., Fog, K., Li, J.Y., & Brundin, P. (2011).  $\alpha$ -Synuclein propagates from mouse brain to grafted dopaminergic neurons and seeds aggregation in cultured human cells. *The Journal of clinical investigation*, 121, 715-725.
- Hashizume, K., Hirasawa, M., Imamura, Y., Noda, S., Shimizu, T., Shinoda, K., Kurihara, T., Noda, K., Ozawa, Y., Ishida, S., Miyake, Y., Shirasawa, T., & Tsubota, K. (2008). Retinal Dysfunction and Progressive Retinal Cell Death in SOD1-Deficient Mice. *The American journal of pathology*, 172, 1325-1331.
- Hauschild-Quintern, J., Petersen, B., Cost, G.J., & Niemann, H. (2013). Gene knockout and knockin by zinc-finger nucleases: current status and perspectives. *Cellular and Molecular Life Sciences*, 70, 2969-2983.
- Heaney, J.D., Rettew, A.N., & Bronson, S.K. (2004). Tissue-specific expression of a BAC transgene targeted to the Hprt locus in mouse embryonic stem cells. *Genomics*, 83, 1072-1082.
- Heffner, C.S., Herbert Pratt, C., Babiuk, R.P., Sharma, Y., Rockwood, S.F., Donahue, L.R., Eppig, J.T., & Murray, S.A. (2012). Supporting conditional mouse mutagenesis with a comprehensive cre characterization resource. *Nature Communications*, 3.
- Hegedus, J., Putman, C.T., & Gordon, T. (2007). Time course of preferential motor unit loss in the SOD1 G93A mouse model of amyotrophic lateral sclerosis. *Neurobiology of Disease*, 28, 154-164.
- Hegedus, J., Putman, C.T., Tyreman, N., & Gordon, T. (2008). Preferential motor unit loss in the SOD1G93A transgenic mouse model of amyotrophic lateral sclerosis. *The Journal of Physiology*, 586, 3337-3351.
- Heiman-Patterson, T.D., Deitch, J.S., Blankenhorn, E.P., Erwin, K.L., Perreault, M.J., Alexander, B.K., Byers, N., Toman, I., & Alexander, G.M. (2005). Background and gender effects on survival in the TgN(SOD1-G93A)1Gur mouse model of ALS. *Journal of the Neurological Sciences*, 236, 1-7.
- Heiman-Patterson, T.D., Sher, R.B., Blankenhorn, E.A., Alexander, G., Deitch, J.S., Kunst, C.B., Maragakis, N., & Cox, G. (2011). Effect of genetic background on phenotype variability in transgenic mouse models of amyotrophic lateral sclerosis: A window of opportunity in the search for genetic modifiers. *Amyotrophic Lateral Sclerosis*, 12, 79-86.
- Hensley, K., Mhatre, M., Mou, S., Pye, Q.N., Stewart, C., West, M., & Williamson, K.S. (2006). On the relation of oxidative stress to neuroinflammation: Lessons learned from the G93A-SOD1 mouse model of amyotrophic lateral sclerosis. *Antioxidants and Redox Signaling*, 8, 2075-2087.
- Hill, F., Benes, V., Thomasova, D., Stewart, A.F., Kafatos, F.C., & Ansorge, W. (2000). BAC Trimming: Minimizing Clone Overlaps. *Genomics*, 64, 111-113.
- Hill, S.A., Stahl, M.M., & Stahl, F.W. (1997). Single-strand DNA intermediates in phage I's Red recombination pathway. *Proceedings of the National Academy of Sciences of the United States of America*, 94, 2951-2956.

- Hineno,A., Nakamura,A., Shimojima,Y., Yoshida,K., Oyanagai,K., & Ikeda,S.i. (2012). Distinctive clinicopathological features of 2 large families with amyotrophic lateral sclerosis having L106V mutation in SOD1 gene. *Journal of the Neurological Sciences*, 319, 63-74.
- Hirano,N., Muroi,T., Takahashi,H., & Haruki,M. (2011). Site-specific recombinases as tools for heterologous gene integration. *Applied Microbiology and Biotechnology*, 92, 227-239.
- Homma,K., Fujisawa,T., Tsuburaya,N., Yamaguchi,N., Kadowaki,H., Takeda,K., Nishitoh,H., Matsuzawa,A., Naguro,I., & Ichijo,H. (2013). SOD1 as a Molecular Switch for Initiating the Homeostatic ER Stress Response under Zinc Deficiency. *Molecular cell*, 52, 75-86.
- Hu,J., Chen,K., Ni,B., Li,L., Chen,G., & Shi,S. (2011). A novel SOD1 mutation in amyotrophic lateral sclerosis with a distinct clinical phenotype. *Amyotrophic Lateral Sclerosis*, 13, 149-154.
- Huang,G., Ashton,C., Kumbhani,D.S., & Ying,Q.L. (2011). Genetic manipulations in the rat: Progress and prospects. *Current Opinion in Nephrology and Hypertension*, 20, 391-399.
- Huang,T.T., Yasunami,M., Carlson,E.J., Gillespie,A.M., Reaume,A.G., Hoffman,E.K., Chan,P.H., Scott,R.W., & Epstein,C.J. (1997). Superoxide-Mediated Cytotoxicity in Superoxide Dismutase-Deficient Fetal Fibroblasts. *Archives of Biochemistry and Biophysics*, 344, 424-432.
- Hug,B.A., Wesselschmidt,R.L., Fiering,S., Bender,M.A., Epner,E., Groudine,M., & Ley,T.J. (1996). Analysis of mice containing a targeted deletion of beta-globin locus control region 5' hypersensitive site 3. *Molecular and Cellular Biology*, 16, 2906-2912.
- Hwang,Y.M., Stathopoulos,P.B., Dimmick,K., Yang,H., Badiei,H.R., Tong,M.S., Rumfeldt,J.A.O., Chen,P., Karanassios,V., & Meiering,E.M. (2010). Nonamyloid Aggregates Arising from Mature Copper/Zinc Superoxide Dismutases Resemble Those Observed in Amyotrophic Lateral Sclerosis. *Journal of Biological Chemistry*, 285, 41701-41711.
- Iba,M., Guo,J.L., McBride,J.D., Zhang,B., Trojanowski,J.Q., & Lee,V.M.Y. (2013). Synthetic Tau Fibrils Mediate Transmission of Neurofibrillary Tangles in a Transgenic Mouse Model of Alzheimer's-Like Tauopathy. *The Journal of Neuroscience*, 33, 1024-1037.
- Igoudjil,A., Magrané,J., Fischer,L.R., Kim,H.J., Hervias,I., Dumont,M., Cortez,C., Glass,J.D., Starkov,A.A., & Manfredi,G. (2011). In Vivo Pathogenic Role of Mutant SOD1 Localized in the Mitochondrial Intermembrane Space. *The Journal of Neuroscience*, 31, 15826-15837.
- Imamura,Y., Noda,S., Hashizume,K., Shinoda,K., Yamaguchi,M., Uchiyama,S., Shimizu,T., Mizushima,Y., Shirasawa,T., & Tsubota,K. (2006). Drusen, choroidal neovascularization, and retinal pigment epithelium dysfunction in SOD1-deficient mice: A model of age-related macular degeneration. *Proceedings of the National Academy of Sciences of the United States of America*, 103, 11282-11287.
- Ince,P.G., Ince,P.G., Lowe,J., & Shaw,P.J. (1998). Amyotrophic lateral sclerosis: current issues in classification, pathogenesis and molecular pathology. *Neuropathology and Applied Neurobiology*, 24, 104-117.
- Ishii,T., Matsuki,S., Iuchi,Y., Okada,F., Toyosaki,S., Tomita,Y., Ikeda,Y., & Fujii,J. (2005). Accelerated impairment of spermatogenic cells in sod1-knockout mice under heat stress. *Free Radical Research*, 39, 697-705.
- Israelson,A., Arbel,N., Da Cruz,S., Ilieva,H., Yamanaka,K., Shoshan-Barmatz,V., & Cleveland,D.W. (2010). Misfolded Mutant SOD1 Directly Inhibits VDAC1 Conductance in a Mouse Model of Inherited ALS. *Neuron*, 67, 575-587.

- Ito,Y., Yamada,M., Tanaka,H., Aida,K., Tsuruma,K., Shimazawa,M., Hozumi,I., Inuzuka,T., Takahashi,H., & Hara,H. (2009). Involvement of CHOP, an ER-stress apoptotic mediator, in both human sporadic ALS and ALS model mice. *Neurobiology of Disease*, 36, 470-476.
- Jaarsma,D., Haasdijk,E.D., Grashorn,J.A.C., Hawkins,R., van Duijn,W., Verspaget,H.W., London,J., & Holstege,J.C. (2000). Human Cu/Zn Superoxide Dismutase (SOD1) Overexpression in Mice Causes Mitochondrial Vacuolization, Axonal Degeneration, and Premature Motoneuron Death and Accelerates Motoneuron Disease in Mice Expressing a Familial Amyotrophic Lateral Sclerosis Mutant SOD1. *Neurobiology of Disease*, 7, 623-643.
- Jaarsma,D., Teuling,E., Haasdijk,E.D., De Zeeuw,C.I., & Hoogenraad,C.C. (2008). Neuron-Specific Expression of Mutant Superoxide Dismutase Is Sufficient to Induce Amyotrophic Lateral Sclerosis in Transgenic Mice. *The Journal of Neuroscience*, 28, 2075-2088.
- Jaenisch,R. (1976). Germ line integration and Mendelian transmission of the exogenous Moloney leukemia virus. *Proceedings of the National Academy of Sciences of the United States of America*, 73, 1260-1264.
- Jaenisch,R. & Mintz,B. (1974). Simian virus 40 DNA sequences in DNA of healthy adult mice derived from preimplantation blastocysts injected with viral DNA. *Proceedings of the National Academy of Sciences of the United States of America*, 71, 1250-1254.
- Jang,Y.C., Lustgarten,M.S., Liu,Y., Muller,F.L., Bhattacharya,A., Liang,H., Salmon,A.B., Brooks,S.V., Larkin,L., Hayworth,C.R., Richardson,A., & Van Remmen,H. (2010). Increased superoxide in vivo accelerates age-associated muscle atrophy through mitochondrial dysfunction and neuromuscular junction degeneration. *The FASEB Journal*, 24, 1376-1390.
- Johansson,A., Engler,H., Blomquist,G., Scott,B., Wall,A., Aquilonius,S.M., Långström,B., & Askmark,H. (2007). Evidence for astrocytosis in ALS demonstrated by [<sup>11</sup>C](I)-deprenyl-D2 PET. *Journal of the Neurological Sciences*, 255, 17-22.
- Johnson,J.O., Mandrioli,J., Benatar,M., Abramzon,Y., Van Deerlin,V.M., Trojanowski,J.Q., Gibbs,J.R., Brunetti,M., Gronka,S., Wu,J., Ding,J., McCluskey,L., Martinez-Lage,M., Falcone,D., Hernandez,D.G., Arepalli,S., Chong,S., Schymick,J.C., Rothstein,J., Landi,F., Wang,Y.D., Calvo,A., Mora,G., Sabatelli,M., Monsurro,M.R., Battistini,S., Salvi,F., Spataro,R., Sola,P., Borghero,G., Galassi,G., Scholz,S.W., Taylor,J.P., Restagno,G., Chiò,A., & Traynor,B.J. (2010a). Exome Sequencing Reveals VCP Mutations as a Cause of Familial ALS. *Neuron*, 68, 857-864.
- Johnson,K.R., Yu,H., Ding,D., Jiang,H., Gagnon,L.H., & Salvi,R.J. (2010b). Separate and combined effects of Sod1 and Cdh23 mutations on age-related hearing loss and cochlear pathology in C57BL/6J mice. *Hearing Research*, 268, 85-92.
- Johnston,J.A., Dalton,M.J., Gurney,M.E., & Kopito,R.R. (2000). Formation of high molecular weight complexes of mutant Cu,Zn-superoxide dismutase in a mouse model for familial amyotrophic lateral sclerosis. *Proceedings of the National Academy of Sciences of the United States of America*, 97, 12571-12576.
- Jones,J.M. & Meisler,M.H. (2014). Modeling human epilepsy by TALEN targeting of mouse sodium channel Scn8a. *genesis*, 52, 141-148.
- Jonsson,P.A., Graffmo,K.S., Brännström,T., Nilsson,P., Andersen,P.M., & Marklund,S.L. (2006a). Motor neuron disease in mice expressing the wild type-like D90A mutant superoxide dismutase-1. *Journal of Neuropathology & Experimental Neurology*, 65, 1126-1136.

- Jonsson,P.A., Ernhill,K., Andersen,P.M., Bergemalm,D., Brännström,T., Gredal,O., Nilsson,P., & Marklund,S.L. (2004). Minute quantities of misfolded mutant superoxide dismutase-1 cause amyotrophic lateral sclerosis. *Brain*, 127, 73-88.
- Jonsson,P.A., Graffmo,K.S., Andersen,P.M., Brännström,T., Lindberg,M., Oliveberg,M., & Marklund,S.L. (2006b). Disulphide-reduced superoxide dismutase-1 in CNS of transgenic amyotrophic lateral sclerosis models. *Brain*, 129, 451-464.
- Julien,J.P. (1999). Neurofilament functions in health and disease. *Current Opinion in Neurobiology*, 9, 554-560.
- Juneja,T., Pericak-Vance,M.A., Laing,N.G., Dave,S., & Siddique,T. (1997). Prognosis in familial amyotrophic lateral sclerosis: Progression and survival in patients with glu100gly and ala4val mutations in Cu,Zn superoxide dismutase. *Neurology*, 48, 55-57.
- Jung,C., Higgins,C.M.J., & Xu,Z. (2002). Mitochondrial electron transport chain complex dysfunction in a transgenic mouse model for amyotrophic lateral sclerosis. *Journal of Neurochemistry*, 83, 535-545.
- Kadekawa,J., Fujimura,H., Ogawa,Y., Hattori,N., Kaido,M., Nishimura,T., Yoshikawa,H., Shirahata,N., Sakoda,S., & Yanagihara,T. (1997). A clinicopathological study of a patient with familial amyotrophic lateral sclerosis associated with a two base pair deletion in the copper/zinc superoxide dismutase (SOD1) gene. *Acta Neuropathologica*, 94, 617-622.
- Kalmar,B., Edet-Amana,E., & Greensmith,L. (2012). Treatment with a coinducer of the heat shock response delays muscle denervation in the SOD1-G93A mouse model of amyotrophic lateral sclerosis. *Amyotrophic Lateral Sclerosis*, 13, 378-392.
- Kalmar,B., Novoselov,S., Gray,A., Cheetham,M.E., Margulis,B., & Greensmith,L. (2008). Late stage treatment with arimoclomol delays disease progression and prevents protein aggregation in the SOD1G93A mouse model of ALS. *Journal of Neurochemistry*, 107, 339-350.
- Karakousis,G., Ye,N., Li,Z., Chiu,S.K., Reddy,G., & Radding,C.M. (1998). The beta protein of phage I binds preferentially to an intermediate in DNA renaturation. *Journal of Molecular Biology*, 276, 721-731.
- Karch,C.M. & Borchelt,D.R. (2010). Aggregation modulating elements in mutant human superoxide dismutase 1. *Archives of Biochemistry and Biophysics*, 503, 175-182.
- Karch,C.M., Prudencio,M., Winkler,D.D., Hart,P.J., & Borchelt,D.R. (2009). Role of mutant SOD1 disulfide oxidation and aggregation in the pathogenesis of familial ALS. *Proceedings of the National Academy of Sciences*, 106, 7774-7779.
- Kato,M., Aoki,M., Nagai,M., Miyoshi,I., Imanishi,T., Kasai,N., & Itoyama,Y. (2001a). Transgenic mice with ALS-linked SOD1 mutant L84V. *Neuroscience Meeting Planner.San Diego, CA: Society for Neuroscience, 2001.Online..*
- Kato,S. (1999). Recent advances in research on neuropathological aspects of familial amyotrophic lateral sclerosis with superoxide dismutase 1 gene mutations: Neuronal Lewy body-like hyaline inclusions and astrocytic hyaline inclusions. *Histology and Histopathology*, 14, 973-989.
- Kato,S., Hayashi,H., Nakashima,K., Nanba,E., Kato,M., Hirano,A., Nakano,I., Asayama,K., & Ohama,E. (1997). Pathological characterization of astrocytic hyaline inclusions in familial amyotrophic lateral sclerosis. *American Journal of Pathology*, 151, 611-620.

- Kato,S., Shimoda,M., Watanabe,Y., Nakashima,K., Takahashi,K., & Ohama,E. (1996). Familial amyotrophic lateral sclerosis with a two base pair deletion in superoxide dismutase 1: gene multisystem degeneration with intracytoplasmic hyaline inclusions in astrocytes. *Journal of Neuropathology & Experimental Neurology*, 55, 1089-1101.
- Kato,S. (2008). Amyotrophic lateral sclerosis models and human neuropathology: similarities and differences. *Acta Neuropathologica*, 115, 97-114.
- Kato,S., Nakashima,K., Horiuchi,S., Nagai,R., Cleveland,D.W., Liu,J., Hirano,A., Takikawa,M., Kato,M., Nakano,I., Sakoda,S., Asayama,K., & Ohama,E. (2001b). Formation of advanced glycation end-product-modified superoxide dismutase-1 (SOD1) is one of the mechanisms responsible for inclusions common to familial amyotrophic lateral sclerosis patients with SOD1 gene mutation, and transgenic mice expressing human SOD1 gene mutation. *Neuropathology*, 21, 67-81.
- Kato,S., Takikawa,M., Nakashima,K., Hirano,A., Cleveland,D.W., Kusaka,H., Shibata,N., Kato,M., Nakano,I., & Ohama,E. (2000). New consensus research on neuropathological aspects of familial amyotrophic lateral sclerosis with superoxide dismutase 1 (SOD1) gene mutations: Inclusions containing SOD1 in neurons and astrocytes. *Amyotrophic Lateral Sclerosis*, 1, 163-184.
- Katz,J.S., Katzberg,H.D., Woolley,S.C., Marklund,S.L., & Andersen,P.M. (2012). Combined fulminant frontotemporal dementia and amyotrophic lateral sclerosis associated with an I113T SOD1 mutation. *Amyotrophic Lateral Sclerosis*, 13, 567-569.
- Kawamata,H. & Manfredi,G. (2010). Import, maturation, and function of SOD1 and its copper chaperone CCS in the mitochondrial intermembrane space. *Antioxidants and Redox Signaling*, 13, 1375-1384.
- Kawamata,J., Shimahama,S., Hasegawa,H., Imura,T., Kimura,J., & Ueda,K. (1996). Deletion and point mutations in superoxide dismutase-1 gene in amyotrophic lateral sclerosis. In Nakano,I. & A.Hirano (Eds.), *Amyotrophic Lateral Sclerosis: Progress and perspectives in basic research and clinical application* (pp. 276-280). Elsevier.
- Kawamoto,Y., Akiguchi,I., Fujimura,H., Shirakashi,Y., Honjo,Y., & Sakoda,S. (2005). 14-3-3 proteins in Lewy body-like hyaline inclusions in a patient with familial amyotrophic lateral sclerosis with a two-base pair deletion in the Cu/Zn superoxide dismutase (SOD1) gene. *Acta Neuropathologica*, 110, 203-204.
- Keifer,J., O'Connor,D.M., & Boulis,N.M. (2014). Gene and protein therapies utilizing VEGF for ALS. *Pharmacology & Therapeutics*, 141, 261-271.
- Keithley,E.M., Canto,C., Zheng,Q.Y., Wang,X., Fischel-Ghodsian,N., & Johnson,K.R. (2005). Cu/Zn superoxide dismutase and age-related hearing loss. *Hearing Research*, 209, 76-85.
- Kerman,A., Liu,H.N., Croul,S., Bilbao,J., Rogaeva,E., Zinman,L., Robertson,J., & Chakrabartty,A. (2010). Amyotrophic lateral sclerosis is a non-amyloid disease in which extensive misfolding of SOD1 is unique to the familial form. *Acta Neuropathologica*, 119, 335-344.
- Kfoury,N., Holmes,B.B., Jiang,H., Holtzman,D.M., & Diamond,M.I. (2012). Trans-cellular Propagation of Tau Aggregation by Fibrillar Species. *Journal of Biological Chemistry*, 287, 19440-19451.
- Khare,S.D., Caplow,M., & Dokholyan,N.V. (2004). The rate and equilibrium constants for a multistep reaction sequence for the aggregation of superoxide dismutase in amyotrophic

lateral sclerosis. *Proceedings of the National Academy of Sciences of the United States of America*, 101, 15094-15099.

Khare,S.D., Caplow,M., & Dokholyan,N.V. (2006). FALS mutations in Cu, Zn superoxide dismutase destabilize the dimer and increase dimer dissociation propensity: A large-scale thermodynamic analysis. *Amyloid*, 13, 226-235.

Kiernan,D., Kalmar,B., Dick,J.R., Riddoch-Contreras,J., Burnstock,G., & Greensmith,L. (2004). Treatment with arimoclomol, a coinducer of heat shock proteins, delays disease progression in ALS mice. *Nature Medicine*, 10, 402-405.

Kiernan,M.C., Vucic,S., Cheah,B.C., Turner,M.R., Eisen,A., Hardiman,O., Burrell,J.R., & Zoing,M.C. (2011). Amyotrophic lateral sclerosis. *The Lancet*, 377, 942-955.

Kikuchi,H., Almer,G., Yamashita,S., Guégan,C., Nagai,M., Xu,Z., Sosunov,A.A., McKhann,G.M., & Przedborski,S. (2006). Spinal cord endoplasmic reticulum stress associated with a microsomal accumulation of mutant superoxide dismutase-1 in an ALS model. *Proceedings of the National Academy of Sciences of the United States of America*, 103, 6025-6030.

Kikugawa,K., Nankano,R., Otaki,R., & Takashi,I. (2000). Generation of mutant SOD1-expressing mice. *Program of 41st Annual meeting of Societas Neurologica Japonica.Tokyo: Societas Neurologica Japonica* 220..

Kilk,A., Laan,M., & Torp,A. (1995). Human CuZn superoxide dismutase enzymatic activity in cells is regulated by the length of the mRNA. *FEBS Letters*, 362, 323-327.

Kim,H.J., Kim,N.C., Wang,Y.D., Scarborough,E.A., Moore,J., Diaz,Z., MacLea,K.S., Freibaum,B., Li,S., Molliex,A., Kanagaraj,A.P., Carter,R., Boylan,K.B., Wojtas,A.M., Rademakers,R., Pinkus,J.L., Greenberg,S.A., Trojanowski,J.Q., Traynor,B.J., Smith,B.N., Topp,S., Gkazi,A.S., Miller,J., Shaw,C.E., Kottlors,M., Kirschner,J., Pestronk,A., Li,Y.R., Ford,A.F., Gitler,A.D., Benatar,M., King,O.D., Kimonis,V.E., Ross,E.D., Weihl,C.C., Shorter,J., & Taylor,J.P. (2013). Mutations in prion-like domains in hnRNPA2B1 and hnRNPA1 cause multisystem proteinopathy and ALS. *Nature*, 495, 467-473.

Kishigami,H., Nagano,S., Bush,A.I., & Sakoda,S. (2010). Monomerized Cu,Zn-superoxide dismutase induces oxidative stress through aberrant Cu binding. *Free Radical Biology and Medicine*, 48, 945-952.

Kitamura,F., Fujimaki,N., Okita,W., Hiramatsu,H., & Takeuchi,H. (2011). Structural Instability and Cu-Dependent Pro-Oxidant Activity Acquired by the Apo Form of Mutant SOD1 Associated with Amyotrophic Lateral Sclerosis. *Biochemistry*, 50, 4242-4250.

Kobayashi,J., Kuroda,M., Kawata,A., Mochizuki,Y., Mizutani,T., Komori,T., Ikeuchi,T., & Koide,R. (2012). Novel G37V mutation of SOD1 gene in autopsied patient with familial amyotrophic lateral sclerosis. *Amyotrophic Lateral Sclerosis*, 13, 570-572.

Koide,T., Igarashi,S., Kikugawa,K., Nakano,R., Inuzuka,T., Yamada,M., Takahashi,H., & Tsuji,S. (1998). Formation of granular cytoplasmic aggregates in COS7 cells expressing mutant Cu/Zn superoxide dismutase associated with familial amyotrophic lateral sclerosis. *Neuroscience Letters*, 257, 29-32.

Kong,J. & Xu,Z. (1998). Massive Mitochondrial Degeneration in Motor Neurons Triggers the Onset of Amyotrophic Lateral Sclerosis in Mice Expressing a Mutant SOD1. *The Journal of Neuroscience*, 18, 3241-3250.

- Kostrominova,T.Y. (2009). Comparison of advanced age-related denervation and fiber type grouping in two different strains of homozygous Sod1 knockout mice. *FEBS Journal*, April 2009 23 (Meeting Abstract Supplement) 954.6.
- Kostrominova,T.Y. (2010). Advanced age-related denervation and fiber-type grouping in skeletal muscle of SOD1 knockout mice. *Free Radical Biology and Medicine*, 49, 1582-1593.
- Kostrominova,T.Y., Pasyk,K.A., Remmen,H., Richardson,A.G., & Faulkner,J.A. (2007). Adaptive changes in structure of skeletal muscles from adult *Sod1* homozygous knockout mice. *Cell Tissue Research*, 327, 595-605.
- Koyama,S., Arawaka,S., Chang-Hong,R., Wada,M., Kawanami,T., Kurita,K., Kato,M., Nagai,M., Aoki,M., Itoyama,Y., Sobue,G., Chan,P.H., & Kato,T. (2006). Alteration of familial ALS-linked mutant SOD1 solubility with disease progression: Its modulation by the proteasome and Hsp70. *Biochemical and Biophysical Research Communications*, 343, 719-730.
- Krasnianski,A., Deschauer,M., Neudecker,S., Gellerich,F.N., Müller,T., Schoser,B.G., Krasnianski,M., & Zierz,S. (2005). Mitochondrial changes in skeletal muscle in amyotrophic lateral sclerosis and other neurogenic atrophies. *Brain*, 128, 1870-1876.
- Kucherlapati,R.S., Eves,E.M., Song,K.Y., Morse,B.S., & Smithies,O. (1984). Homologous recombination between plasmids in mammalian cells can be enhanced by treatment of input DNA. *Proceedings of the National Academy of Sciences of the United States of America*, 81, 3153-3157.
- Kunst,C.B., Messer,L., Gordon,J., Haines,J., & Patterson,D. (2000). Genetic Mapping of a Mouse Modifier Gene That Can Prevent ALS Onset. *Genomics*, 70, 181-189.
- Kunze,A., Lengacher,S., Dirren,E., Aebischer,P., Magistretti,P.J., & Renaud,P. (2013). Astrocyte–neuron co-culture on microchips based on the model of SOD mutation to mimic ALS. *Integrative Biology*, 5, 964-975.
- Kushner,P.D., Stephenson,D.T., & Wright,S. (1991). Reactive astrogliosis is widespread in the subcortical white matter of amyotrophic lateral sclerosis brain. *Journal of Neuropathology & Experimental Neurology*, 50, 263-277.
- Kwiatkowski,T.J., Bosco,D.A., LeClerc,A.L., Tamrazian,E., Vanderburg,C.R., Russ,C., Davis,A., Gilchrist,J., Kasarskis,E.J., Munsat,T., Valdmanis,P., Rouleau,G.A., Hosler,B.A., Cortelli,P., de Jong,P.J., Yoshinaga,Y., Haines,J.L., Pericak-Vance,M.A., Yan,J., Ticozzi,N., Siddique,T., McKenna-Yasek,D., Sapp,P.C., Horvitz,H.R., Landers,J.E., & Brown,R.H. (2009). Mutations in the FUS/TLS Gene on Chromosome 16 Cause Familial Amyotrophic Lateral Sclerosis. *Science*, 323, 1205-1208.
- Larkin,L.M., Davis,C.S., Sims-Robinson,C., Kostrominova,T.Y., Van Remmen,H., Richardson,A., Feldman,E.L., & Brooks,S.V. (2011). Skeletal muscle weakness due to deficiency of Cu,Zn superoxide dismutase is associated with loss of functional innervation. *American Journal of Physiology - Regulatory, Integrative and Comparative Physiology*, DOI: 10.1152/ajpregu.00093.2011.
- Larkin,L.M., Hanes,M.C., Kayupov,E., Clafin,D.R., Faulkner,J.A., & Brooks,S.V. (2013). Weakness of whole muscles in mice deficient in Cu, Zn superoxide dismutase is not explained by defects at the level of the contractile apparatus. *AGE*, 35, 1173-1181.



- Lattante,S., Conte,A., Zollino,M., Luigetti,M., Del Grande,A., Marangi,G., Romano,A., Marcaccio,A., Meleo,E., Bisogni,G., Rossini,P.M., & Sabatelli,M. (2012). Contribution of major amyotrophic lateral sclerosis genes to the etiology of sporadic disease. *Neurology*, 79, 66-72.
- Lattante,S., Rouleau,G.A., & Kabashi,E. (2013). TARDBP and FUS Mutations Associated with Amyotrophic Lateral Sclerosis: Summary and Update. *Human Mutation*, 34, 812-826.
- Lee,J.P., Gerin,C., Bindokas,V.P., Miller,R., Ghadge,G., & Roos,R.P. (2002). No correlation between aggregates of Cu/Zn superoxide dismutase and cell death in familial amyotrophic lateral sclerosis. *Journal of Neurochemistry*, 82, 1229-1238.
- Lee,J., Ryu,H., & Kowall,N.W. (2009). Differential regulation of neuronal and inducible nitric oxide synthase (NOS) in the spinal cord of mutant SOD1 (G93A) ALS mice. *Biochemical and Biophysical Research Communications*, 387, 202-206.
- Leigh,P.N., Whitwell,H., Garofalo,O., Buller,J., Swash,M., Martin,J.E., Gallo,J.M., Weller,R.O., & Anderton,B.H. (1991). Ubiquitin-immunoreactive intraneuronal inclusions in amyotrophic lateral sclerosis: Morphology, distribution, and specificity. *Brain*, 114, 775-788.
- Leitch,J.M., Yick,P.J., & Culotta,V.C. (2009). The Right to Choose: Multiple Pathways for Activating Copper,Zinc Superoxide Dismutase. *Journal of Biological Chemistry*, 284, 24679-24683.
- Li,P., Waters,R.E., Redfern,S.I., Zhang,M., Mao,L., Annex,B.H., & Yan,Z. (2007). Oxidative phenotype protects myofibers from pathological insults induced by chronic heart failure in mice. *American Journal of Pathology*, 170, 599-608.
- Li,P., Tong,C., Mehrian-Shai,R., Jia,L., Wu,N., Yan,Y., Maxson,R.E., Schulze,E.N., Song,H., Hsieh,C.L., Pera,M.F., & Ying,Q.L. (2008). Germline Competent Embryonic Stem Cells Derived from Rat Blastocysts. *Cell*, 135, 1299-1310.
- Li,X., Costantino,N., Lu,L., Liu,D., Watt,R.M., Cheah,K.S.E., Court,D., & Huang,J.-D. (2003). Identification of factors influencing strand bias in oligonucleotideG $\ddot{C}$ Émediated recombination in Escherichia coli. *Nucleic Acids Research*, 31, 6674-6687.
- Li,X., Lu,L., Bush,D.J., Zhang,X., Zheng,L., Suswam,E.A., & King,P.H. (2009). Mutant copper-zinc superoxide dismutase associated with amyotrophic lateral sclerosis binds to adenine/uridine-rich stability elements in the vascular endothelial growth factor 3'-untranslated region. *Journal of Neurochemistry*, 108, 1032-1044.
- Ligon,L.A., LaMonte,B.H., Wallace,K.E., Weber,N., Kalb,R.G., & Holzbaur,E.L.F. (2005). Mutant superoxide dismutase disrupts cytoplasmic dynein in motor neurons. *Neuroreport*, 16, 533-536.
- Lin,F.L., Sperle,K., & Sternberg,N. (1984). Model for homologous recombination during transfer of DNA into mouse L cells: role for DNA ends in the recombination process. *Molecular and Cellular Biology*, 4, 1020-1034.
- Lin,F.L., Sperle,K., & Sternberg,N. (1985). Recombination in mouse L cells between DNA introduced into cells and homologous chromosomal sequences. *Proceedings of the National Academy of Sciences of the United States of America*, 82, 1391-1395.
- Linares,E., Seixas,L.V., dos Prazeres,J.N., Ladd,F.V.L., Ladd,A.A.B.L., Coppi,A.A., & Augusto,O. (2013). Tempol Moderately Extends Survival in a hSOD1<sup>G93A</sup> ALS Rat Model by Inhibiting

Neuronal Cell Loss, Oxidative Damage and Levels of Non-Native hSOD1<sup>G93A</sup> Forms. *PLoS ONE*, 8, e55868.

Lindberg,M.J., Byström,R., Boknäs,N., Andersen,P.M., & Oliveberg,M. (2005). Systematically perturbed folding patterns of amyotrophic lateral sclerosis (ALS)-associated SOD1 mutants. *Proceedings of the National Academy of Sciences of the United States of America*, 102, 9754-9759.

Lindberg,M.J., Normark,J., Holmgren,A., & Oliveberg,M. (2004). Folding of human superoxide dismutase: Disulfide reduction prevents dimerization and produces marginally stable monomers. *Proceedings of the National Academy of Sciences of the United States of America*, 101, 15893-15898.

Lindberg,M.J., Tibell,L., & Oliveberg,M. (2002). Common denominator of Cu/Zn superoxide dismutase mutants associated with amyotrophic lateral sclerosis: Decreased stability of the apo state. *Proceedings of the National Academy of Sciences of the United States of America*, 99, 16607-16612.

Lindenau,J., Noack,H., Possel,H., Asayama,K., & Wolf,G. (2000). Cellular distribution of superoxide dismutases in the rat CNS. *Glia*, 29, 25-34.

Ling,S.C., Polymenidou,M., & Cleveland,D. (2013). Converging Mechanisms in ALS and FTD: Disrupted RNA and Protein Homeostasis. *Neuron*, 79, 416-438.

Lino,M.M. & Caroni,P. (2002). Accumulation of SOD1 Mutants in Postnatal Motoneurons Does Not Cause Motoneuron Pathology or Motoneuron Disease. *Journal of Neuroscience*, 22, 4825-4832.

Liu,D., Bao,F., Wen,J., & Liu,J. (2007). Mutation of superoxide dismutase elevates reactive species: Comparison of nitration and oxidation of proteins in different brain regions of transgenic mice with amyotrophic lateral sclerosis. *Neuroscience*, 146, 255-264.

Liu,D., Wen,J., Liu,J., & Li,L. (1999). The roles of free radicals in amyotrophic lateral sclerosis: reactive oxygen species and elevated oxidation of protein, DNA, and membrane phospholipids. *The FASEB Journal*, 13, 2318-2328.

Liu,H.N., Sanelli,T., Horne,P., Pioro,E.P., Strong,M.J., Rogaeva,E., Bilbao,J., Zinman,L., & Robertson,J. (2009). Lack of evidence of monomer/misfolded superoxide dismutase-1 in sporadic amyotrophic lateral sclerosis. *Annals of Neurology*, 66, 75-80.

Liu,H.N., Tjostheim,S., DaSilva,K., Taylor,D., Zhao,B., Rakhit,R., Brown,M., Chakrabartty,A., McLaurin,J., & Robertson,J. (2012). Targeting of Monomer/Misfolded SOD1 as a Therapeutic Strategy for Amyotrophic Lateral Sclerosis. *The Journal of Neuroscience*, 32, 8791-8799.

Liu,R., Althaus,J.S., Ellerbrock,B.R., Becker,D.A., & Gurney,M.E. (1998). Enhanced oxygen radical production in a transgenic mouse model of familial amyotrophic lateral sclerosis. *Annals of Neurology*, 44, 763-770.

Liu,Y., Qi,W., Richardson,A., Van Remmen,H., Ikeno,Y., & Salmon,A.B. (2013). Oxidative damage associated with obesity is prevented by overexpression of CuZn- or Mn-superoxide dismutase. *Biochemical and Biophysical Research Communications*, 438, 78-83.

Lo,C.W. (1986). Localization of low abundance DNA sequences in tissue sections by in situ hybridization. *Journal of Cell Science*, 81, 143-162.

- Lu, L., Wang, S., Zheng, L., Li, X., Suswam, E.A., Zhang, X., Wheeler, C.G., Nabors, L.B., Filippova, N., & King, P.H. (2009). Amyotrophic Lateral Sclerosis-linked Mutant SOD1 Sequesters Hu Antigen R (HuR) and TIA-1-related Protein (TIAR): Implications for impaired post-transcriptional regulation of vascular endothelial growth factor. *Journal of Biological Chemistry*, 284, 33989-33998.
- Lu, L., Zheng, L., Viera, L., Suswam, E., Li, Y., Li, X., Estévez, A.G., & King, P.H. (2007). Mutant Cu/Zn-Superoxide Dismutase Associated with Amyotrophic Lateral Sclerosis Destabilizes Vascular Endothelial Growth Factor mRNA and Downregulates Its Expression. *The Journal of Neuroscience*, 27, 7929-7938.
- Luk, K.C., Kehm, V.M., Zhang, B., O'Brien, P., Trojanowski, J.Q., & Lee, V.M.Y. (2012). Intracerebral inoculation of pathological  $\alpha$ -synuclein initiates a rapidly progressive neurodegenerative  $\alpha$ -synucleinopathy in mice. *The Journal of Experimental Medicine*, 209, 975-986.
- Luty, A.A., Kwok, J.B.J., Dobson-Stone, C., Loy, C.T., Coupland, K.G., Karlström, H., Sobow, T., Tchorzewska, J., Maruszak, A., Barcikowska, M., Panegyres, P.K., Zekanowski, C., Brooks, W.S., Williams, K.L., Blair, I.P., Mather, K.A., Sachdev, P.S., Halliday, G.M., & Schofield, P.R. (2010). Sigma nonopioid intracellular receptor 1 mutations cause frontotemporal lobar degeneration G $\beta$  motor neuron disease. *Ann Neurol.*, 68, 639-649.
- Mackenzie, I.R.A., Bigio, E.H., Ince, P.G., Geser, F., Neumann, M., Cairns, N.J., Kwong, L.K., Forman, M.S., Ravits, J., Stewart, H., Eisen, A., McClusky, L., Kretschmar, H.A., Monoranu, C.M., Highley, J.R., Kirby, J., Siddique, T., Shaw, P.J., Lee, V.M.Y., & Trojanowski, J.Q. (2007). Pathological TDP-43 distinguishes sporadic amyotrophic lateral sclerosis from amyotrophic lateral sclerosis with SOD1 mutations. *Annals of Neurology*, 61, 427-434.
- Mackenzie, I., Frick, P., & Neumann, M. (2014). The neuropathology associated with repeat expansions in the C9ORF72 gene. *Acta Neuropathologica*, 127, 347-357.
- Maekawa, S., Leigh, P.N., King, A., Jones, E., Steele, J.C., Bodi, I., Shaw, C.E., Hortobagyi, T., & Sarraj, S. (2009). TDP-43 is consistently co-localized with ubiquitinated inclusions in sporadic and Guam amyotrophic lateral sclerosis but not in familial amyotrophic lateral sclerosis with and without SOD1 mutations. *Neuropathology*, 29, 672-683.
- Magnus, T., Beck, M., Giess, R., Puls, I., Naumann, M., & Toyka, K.V. (2002). Disease progression in amyotrophic lateral sclerosis: Predictors of survival. *Muscle & Nerve*, 25, 709-714.
- Mancuso, R., Oliván, S., Mancera, P., Pastén-Zamorano, A., Manzano, R., Casas, C., Osta, R., & Navarro, X. (2012). Effect of genetic background on onset and disease progression in the SOD1-G93A model of amyotrophic lateral sclerosis. *Amyotrophic Lateral Sclerosis*, 13, 302-310.
- Mangerich, A., Scherthan, H., Diefenbach, J., Klotz, U., van der Hoeven, F., Beneke, S., & Burkle, A. (2009). A caveat in mouse genetic engineering: ectopic gene targeting in ES cells by bidirectional extension of the homology arms of a gene replacement vector carrying human PARP-1. *Transgenic Research*, 18, 261-279.
- Manjaly, Z.R., Scott, K.M., Abhinav, K., Wijesekera, L., Ganesalingam, J., Goldstein, L.H., Janssen, A., Dougherty, A., Willey, E., Stanton, B.R., Turner, M.R., Ampong, M.A., Sakel, M., Orrell, R.W., Howard, R., Shaw, C.E., Leigh, P.N., & Al Chalabi, A. (2010). The sex ratio in amyotrophic lateral sclerosis: A population based study. *Amyotrophic Lateral Sclerosis*, 11, 439-442.
- Marchetto, M.C.N., Muotri, A.R., Mu, Y., Smith, A.M., Cezar, G.G., & Gage, F.H. (2008). Non-Cell-Autonomous Effect of Human SOD1G37R Astrocytes on Motor Neurons Derived from Human Embryonic Stem Cells. *Cell Stem Cell*, 3, 649-657.

- Maresca, M., Erler, A., Fu, J., Friedrich, A., Zhang, Y., & Stewart, A.F. (2010). Single-stranded heteroduplex intermediates in lambda Red homologous recombination. *BMC Molecular Biology*, 11, 54.
- Marinkovic, P., Reuter, M.S., Brill, M.S., Godinho, L., Kerschensteiner, M., & Misgeld, T. (2012). Axonal transport deficits and degeneration can evolve independently in mouse models of amyotrophic lateral sclerosis. *Proceedings of the National Academy of Sciences*, 109, 4296-4301.
- Martin, G.R. (1981). Isolation of a pluripotent cell line from early mouse embryos cultured in medium conditioned by teratocarcinoma stem cells. *Proceedings of the National Academy of Sciences of the United States of America*, 78, 7634-7638.
- Martin, L.J., Liu, Z., Chen, K., Price, A.C., Pan, Y., Swaby, J.A., & Golden, W.C. (2007). Motor neuron degeneration in amyotrophic lateral sclerosis mutant superoxide dismutase-1 transgenic mice: Mechanisms of mitochondriopathy and cell death. *Journal of Comparative Neurology*, 500, 20-46.
- Maruyama, H., Morino, H., Ito, H., Izumi, Y., Kato, H., Watanabe, Y., Kinoshita, Y., Kamada, M., Nodera, H., Suzuki, H., Komure, O., Matsuura, S., Kobatake, K., Morimoto, N., Abe, K., Suzuki, N., Aoki, M., Kawata, A., Hirai, T., Kato, T., Ogasawara, K., Hirano, A., Takumi, T., Kusaka, H., Hagiwara, K., Kaji, R., & Kawakami, H. (2010). Mutations of optineurin in amyotrophic lateral sclerosis. *Nature*, 465, 223-226.
- Masè, G., Ros, S., Gemma, A., Bonfigli, L., Carraro, N., Cazzato, G., Rolfo, M., Zanconati, F., Sepcic, J., Jurjevic, A., Pirulli, D., Boniotto, M., Zezlina, S., Crovella, S., & Amoroso, A. (2001). ALS with variable phenotypes in a six-generation family caused by leu144phe mutation in the SOD1 gene. *Journal of the Neurological Sciences*, 191, 11-18.
- Masuda-Suzukake, M., Nonaka, T., Hosokawa, M., Oikawa, T., Arai, T., Akiyama, H., Mann, D.M.A., & Hasegawa, M. (2013). Prion-like spreading of pathological  $\alpha$ -synuclein in brain. *Brain*, 136, 1128-1138.
- Matsumoto, S., Kusaka, H., Ito, H., Shibata, N., Asayama, T., & Imai, T. (1996). Sporadic amyotrophic lateral sclerosis with dementia and Cu/Zn superoxide dismutase-positive Lewy body-like inclusions. *Clinical Neuropathology*, 15, 41-46.
- Mattiazzi, M., D'Aurelio, M., Gajewski, C.D., Martushova, K., Kiaei, M., Beal, M.F., & Manfredi, G. (2002). Mutated Human SOD1 Causes Dysfunction of Oxidative Phosphorylation in Mitochondria of Transgenic Mice. *Journal of Biological Chemistry*, 277, 29626-29633.
- Matzuk, M.M., Dionne, L., Guo, Q., Kumar, T.R., & Lebovitz, R.M. (1998). Ovarian Function in Superoxide Dismutase 1 and 2 Knockout Mice. *Endocrinology*, 139, 4008-4011.
- McAlary, L., Yerbury, J.J., & Aquilina, A. (2013). Glutathionylation potentiates benign superoxide dismutase 1 variants to the toxic forms associated with amyotrophic lateral sclerosis. *Scientific Reports*, 3, 3275.
- McGeer, P.L. & McGeer, E.G. (2002). Inflammatory processes in amyotrophic lateral sclerosis. *Muscle & Nerve*, 26, 459-470.
- McGoldrick, Philip., Joyce, P., Acevedo-Arozena, A., Fisher, Elizabeth M. C., and Greensmith, L. An ENU-induced point mutation in mouse Sod1 causes aberrant mitochondrial function and axonal maintenance in primary motor neurons. Neuroscience Meeting Planner. New Orleans, LA: Society for Neuroscience, 2012. Online. Program No. 155.15/H10.2012. 2012.

Ref Type: Abstract

McLaren,A. & Michie,D. (1955). Factors Affecting Vertebral Variation in Mice. *Journal of Embryology and Experimental Morphology*, 3, 366-375.

McLeod,M., Craft,S., & Broach,J.R. (1986). Identification of the crossover site during FLP-mediated recombination in the *Saccharomyces cerevisiae* plasmid 2 microns circle. *Molecular and Cellular Biology*, 6, 3357-3367.

Mead,R.J., Bennett,E.J., Kennerley,A.J., Sharp,P., Sunyach,C., Kasher,P., Berwick,J., Pettmann,B., Battaglia,G., Azzouz,M., Grierson,A., & Shaw,P.J. (2011). Optimised and Rapid Pre-clinical Screening in the SOD1<sup>G93A</sup> Transgenic Mouse Model of Amyotrophic Lateral Sclerosis (ALS). *PLoS ONE*, 6, e23244.

Mele,J., Van Remmen,H., Vijg,J., & Richardson,A. (2006). Characterization of transgenic mice that overexpress both copper zinc superoxide dismutase and catalase. *Antioxidants and Redox Signaling*, 8, 628-638.

Mendonça,D.M., Chimelli,L., & Martinez,A.M. (2005). Quantitative evidence for neurofilament heavy subunit aggregation in motor neurons of spinal cords of patients with amyotrophic lateral sclerosis. *Brazilian Journal of Medical and Biological Research*, 38, 925-933.

Menzies,F.M., Grierson,A.J., Cookson,M.R., Heath,P.R., Tomkins,J., Figlewicz,D.A., Ince,P.G., & Shaw,P.J. (2002). Selective loss of neurofilament expression in Cu/Zn superoxide dismutase (SOD1) linked amyotrophic lateral sclerosis. *Journal of Neurochemistry*, 82, 1118-1128.

Meyer-Luehmann,M., Coomaraswamy,J., Bolmont,T., Kaeser,S., Schaefer,C., Kilger,E., Neuenschwander,A., Abramowski,D., Frey,P., Jaton,A.L., Vigouret,J.M., Paganetti,P., Walsh,D.M., Mathews,P.M., Ghiso,J., Staufenbiel,M., Walker,L.C., & Jucker,M. (2006). Exogenous induction of cerebral b-Amyloidogenesis is governed by agent and host. *Science*, 313, 1781-1784.

Miao,L. & St.Clair,D.K. (2009). Regulation of superoxide dismutase genes: Implications in disease. *Free Radical Biology and Medicine*, 47, 344-356.

Miki,Y., Mori,F., Nunomura,J., Ookawa,K., Yajima,N., Yagihashi,S., & Wakabayashi,K. (2010). Sporadic amyotrophic lateral sclerosis with pallido-nigro-luysian degeneration: A TDP-43 immunohistochemical study. *Neuropathology*, 30, 149-153.

Miller,C.A., Ingmer,H., & Cohen,S.N. (1995). Boundaries of the pSC101 minimal replicon are conditional. *Journal of Bacteriology*, 177, 4865-4871.

Miller,C.L. & Termin,H.M. (1983). High-efficiency ligation and recombination of DNA fragments by vertebrate cells. *Science*, 220, 606-609.

Miller,R.G., Jackson,C.E., Kasarskis,E.J., England,J.D., Forshew,D., Johnston,W., Kalra,S., Katz,J.S., Mitsumoto,H., Rosenfeld,J., Shoesmith,C., Strong,M.J., & Woolley,S.C. (2009a). Practice parameter update: The care of the patient with amyotrophic lateral sclerosis: Drug, nutritional, and respiratory therapies (an evidence-based review): Report of the quality standards subcommittee of the American academy of neurology. *Neurology*, 73, 1218-1226.

Miller,R.G., Jackson,C.E., Kasarskis,E.J., England,J.D., Forshew,D., Johnston,W., Kalra,S., Katz,J.S., Mitsumoto,H., Rosenfeld,J., Shoesmith,C., Strong,M.J., & Woolley,S.C. (2009b). Practice Parameter update: The care of the patient with amyotrophic lateral sclerosis: Multidisciplinary care, symptom management, and cognitive/behavioral impairment (an

evidence-based review): Report of the Quality Standards Subcommittee of the American Academy of Neurology. *Neurology*, 73, 1227-1233.

Miller,R.G., Mitchell,J.D., & Moore,D.H. (2012). Riluzole for amyotrophic lateral sclerosis (ALS)/motor neuron disease (MND). *Cochrane database of systematic reviews (Online)*, 3.

Miller,T.M., Kaspar,B.K., Kops,G.J., Yamanaka,K., Christian,L.J., Gage,F.H., & Cleveland,D.W. (2005). Virus-delivered small RNA silencing sustains strength in amyotrophic lateral sclerosis. *Annals of Neurology*, 57, 773-776.

Miller,T.M., Pestronk,A., David,W., Rothstein,J., Simpson,E., Appel,S.H., Andres,P.L., Mahoney,K., Allred,P., Alexander,K., Ostrow,L.W., Schoenfeld,D., Macklin,E.A., Norris,D.A., Manousakis,G., Crisp,M., Smith,R., Bennett,C.F., Bishop,K.M., & Cudkowicz,M.E. (2013). An antisense oligonucleotide against SOD1 delivered intrathecally for patients with SOD1 familial amyotrophic lateral sclerosis: a phase 1, randomised, first-in-man study. *The Lancet Neurology*, 12, 435-442.

Mitchell,J., Paul,P., Chen,H.J., Morris,A., Payling,M., Falchi,M., Habgood,J., Panoutsou,S., Winkler,S., Tisato,V., Hajitou,A., Smith,B., Vance,C., Shaw,C., Mazarakis,N.D., & de Bellerocche,J. (2010). Familial amyotrophic lateral sclerosis is associated with a mutation in D-amino acid oxidase. *Proceedings of the National Academy of Sciences*, 107, 7556-7561.

Mizuno,Y., Amari,M., Takatama,M., Aizawa,H., Mihara,B., & Okamoto,K. (2006). Immunoreactivities of p62, an ubiquitin-binding protein, in the spinal anterior horn cells of patients with amyotrophic lateral sclerosis. *Journal of the Neurological Sciences*, 249, 13-18.

Mori,F., Tanji,K., Miki,Y., Kakita,A., Takahashi,H., & Wakabayashi,K. (2010). Relationship between Bunina bodies and TDP-43 inclusions in spinal anterior horn in amyotrophic lateral sclerosis. *Neuropathology and Applied Neurobiology*, 36, 345-352.

Morikawa,K., Shimokawa,H., Matoba,T., Kubota,H., Akaike,T., Talukder,M.A.H., Hatanaka,M., Fujiki,T., Maeda,H., Takahashi,S., & Takeshita,A. (2003). Pivotal role of Cu,Zn-superoxide dismutase in endothelium-dependent hyperpolarization. *Journal of Clinical Investigation*, 112, 1871-1879.

Mosberg,J.A., Lajoie,M.J., & Church,G.M. (2010). Lambda Red Recombineering in Escherichia coli Occurs Through a Fully Single-Stranded Intermediate. *Genetics*, 186, 791-799.

Mougenot,A.L., Nicot,S., Bencsik,A., Morignat,E., Verchère,J., Lakhdar,L., Legastelois,S., & Baron,T. (2012). Prion-like acceleration of a synucleinopathy in a transgenic mouse model. *Neurobiology of Aging*, 33, 2225-2228.

Muller,F.L., Song,W., Liu,Y., Chaudhuri,A., Pieke-Dahl,S., Strong,R., Huang,T.T., Epstein,C.J., Roberts II,L.J., Csete,M., Faulkner,J.A., & Van Remmen,H. (2006). Absence of CuZn superoxide dismutase leads to elevated oxidative stress and acceleration of age-dependent skeletal muscle atrophy. *Free Radical Biology and Medicine*, 40, 1993-2004.

Mulligan,V.K. & Chakrabartty,A. (2013). Protein misfolding in the late-onset neurodegenerative diseases: Common themes and the unique case of amyotrophic lateral sclerosis. *Proteins: Structure, Function, and Bioinformatics*, 81, 1285-1303.

Munch,C., OBrien,J., & Bertolotti,A. (2011). Prion-like propagation of mutant superoxide dismutase-1 misfolding in neuronal cells. *Proceedings of the National Academy of Sciences*, 108, 3548-3553.

- Muniyappa,K. & Radding,C.M. (1986). The homologous recombination system of phage lambda. Pairing activities of beta protein. *Journal of Biological Chemistry*, 261, 7472-7478.
- Murakami,K., Inagaki,J., Saito,M., Ikeda,Y., Tsuda,C., Noda,Y., Kawakami,S., Shirasawa,T., & Shimizu,T. (2009). Skin atrophy in cytoplasmic SOD-deficient mice and its complete recovery using a vitamin C derivative  
7. *Biochemical and Biophysical Research Communications*, 382, 457-461.
- Murata,T., Ohtsuka,C., & Terayama,Y. (2008). Increased mitochondrial oxidative damage in patients with sporadic amyotrophic lateral sclerosis. *Journal of the Neurological Sciences*, 267, 66-69.
- Nagai,M., Aoki,M., Miyoshi,I., Okamura,T., Kato,M., Kasai,N., & Itoyaa,Y. (2000). Transgenic mice with ALS-linked SOD1 mutant H46R. *Neuroscience Meeting Planner*.New Orleans, LA: Society for Neuroscience, 2000.Online..
- Nagai,M., Re,D.B., Nagata,T., Chalazonitis,A., Jessell,T.M., Wichterle,H., & Przedborski,S. (2007). Astrocytes expressing ALS-linked mutated SOD1 release factors selectively toxic to motor neurons. *Nature Neuroscience*, 10, 615-622.
- Nagy,D., Kato,T., & Kushner,P.D. (1994). Reactive astrocytes are widespread in the cortical gray matter of amyotrophic lateral sclerosis. *Journal of Neuroscience Research*, 38, 336-347.
- Nakamura,S., Wate,R., Kaneko,S., Ito,H., Oki,M., Tsuge,A., Nagashima,M., Asayama,S., Fujita,K., Nakamura,M., Maruyama,H., Kawakami,H., & Kusaka,H. (2014). An autopsy case of sporadic amyotrophic lateral sclerosis associated with the I113T SOD1 mutation. *Neuropathology*, 34, 58-63.
- Nakashima,K., Watanabe,Y., Kuno,N., Nanba,E., & Takahashi,K.F. (1995). Abnormality of Cu/Zn superoxide dismutase (SOD1) activity in Japanese familial amyotrophic lateral sclerosis with two base pair deletion in the SOD1 gene. *Neurology*, 45, 1019-1020.
- Nardo,G., Iennaco,R., Fusi,N., Heath,P.R., Marino,M., Trolese,M.C., Ferraiuolo,L., Lawrence,N., Shaw,P.J., & Bendotti,C. (2013). Transcriptomic indices of fast and slow disease progression in two mouse models of amyotrophic lateral sclerosis. *Brain*, 136, 3305-3332.
- Nishihira,Y., Tan,C.F., Onodera,O., Toyoshima,Y., Yamada,M., Morita,T., Nishizawa,M., Kakita,A., & Takahashi,H. (2008). Sporadic amyotrophic lateral sclerosis: two pathological patterns shown by analysis of distribution of TDP-43-immunoreactive neuronal and glial cytoplasmic inclusions. *Acta Neuropathologica*, 116, 169-182.
- Nishimura,A.L., Mitne-Neto,M., Silva,H.C.A., Richieri-Costa,A., Middleton,S., Cascio,D., Kok,F., Oliveira,J.R.M., Gillingwater,T., Webb,J., Skehel,P., & Zatz,M. (2004). A Mutation in the Vesicle-Trafficking Protein VAPB Causes Late-Onset Spinal Muscular Atrophy and Amyotrophic Lateral Sclerosis. *The American Journal of Human Genetics*, 75, 822-831.
- Nishioka,N., Nagano,S., Nakayama,R., Kiyonari,H., Ijiri,T., Taniguchi,K., Shawlot,W., Hayashizaki,Y., Westphal,H., Behringer,R.R., Matsuda,Y., Sakoda,S., Kondoh,H., & Sasaki,H. (2005). Ssd1 regulates head morphogenesis of mouse embryos by activating the Lim1-Ldb1 complex. *Development*, 132, 2535-2546.
- Nishitoh,H., Kadowaki,H., Nagai,A., Maruyama,T., Yokota,T., Fukutomi,H., Noguchi,T., Matsuzawa,A., Takeda,K., & Ichijo,H. (2008). ALS-linked mutant SOD1 induces ER stress- and ASK1-dependent motor neuron death by targeting Derlin-1. *Genes & Development*, 22, 1451-1464.

- Niu,Y., Shen,B., Cui,Y., Chen,Y., Wang,J., Wang,L., Kang,Y., Zhao,X., Si,W., Li,W., Xiang,A.P., Zhou,J., Guo,X., Bi,Y., Si,C., Hu,B., Dong,G., Wang,H., Zhou,Z., Li,T., Tan,T., Pu,X., Wang,F., Ji,S., Zhou,Q., Huang,X., Ji,W., & Sha,J. (2014). Generation of Gene-Modified Cynomolgus Monkey via Cas9/RNA-Mediated Gene Targeting in One-Cell Embryos. *Cell*, 156, 836-843.
- Noda,Y., Ota,K., Shirasawa,T., & Shimizu,T. (2012). Copper/Zinc Superoxide Dismutase Insufficiency Impairs Progesterone Secretion and Fertility in Female Mice. *Biology of Reproduction*, 86, 1-8.
- Nonaka,T., Masuda-Suzukake,M., Arai,T., Hasegawa,Y., Akatsu,H., Obi,T., Yoshida,M., Murayama,S., Mann,D., Akiyama,H., & Hasegawa,M. (2013). Prion-like Properties of Pathological TDP-43 Aggregates from Diseased Brains. *Cell Reports*, 4, 124-134.
- O'Reilly,S.A., Roedica,J., Nagy,D., Hallewell,R.A., Alderson,K., Marklund,S.L., Kuby,J., & Kushner,P.D. (1995). Motor neuron-astrocyte interactions and levels of Cu,Zn superoxide dismutase in sporadic amyotrophic lateral sclerosis. *Experimental Neurology*, 131, 203-210.
- Oberdoerffer,P., Otipoby,K.L., Maruyama,M., & Rajewsky,K. (2003). Unidirectional Cre-mediated genetic inversion in mice using the mutant loxP pair lox66/lox71. *Nucleic Acids Research*, 31, e140.
- Ogawa,Y., Kosaka,H., Nakanishi,T., Shimizu,A., Ohoi,N., Shouji,H., Yanagihara,T., & Sakoda,S. (1997). Stability of Mutant Superoxide Dismutase-1 Associated with Familial Amyotrophic Lateral Sclerosis Determines the Manner of Copper Release and Induction of Thioredoxin in Erythrocytes. *Biochemical and Biophysical Research Communications*, 241, 251-257.
- Okamoto,K., Hirai,S., Yamazaki,T., Sun,X., & Nakazato,Y. (1991). New ubiquitin-positive intraneuronal inclusions in the extra-motor cortices in patients with amyotrophic lateral sclerosis. *Neuroscience Letters*, 129, 233-236.
- Okamoto,Y., Ihara,M., Urushitani,M., Yamashita,H., Kondo,T., Tanigaki,A., Oono,M., Kawamata,J., Ikemoto,A., Kawamoto,Y., Takahashi,R., & Ito,H. (2011). An autopsy case of SOD1-related ALS with TDP-43 positive inclusions. *Neurology*, 77, 1993-1995.
- Olson,E.N., Arnold,H.H., Rigby,P.W.J., & Wold,B.J. (1996). Know Your Neighbors: Three Phenotypes in Null Mutants of the Myogenic bHLH Gene MRF4. *Cell*, 85, 1-4.
- Oosthuyse,B., Moons,L., Storkebaum,E., Beck,H., Nuyens,D., Brusselmans,K., Dorpe,J.V., Hellings,P., Gorselink,M., Heymans,S., Theilmeier,G., Dewerchin,M., Laudénbach,V., Vermylen,P., Raat,H., Acker,T., Vleminckx,V., Bosch,L.V.D., Cashman,N., Fujisawa,H., Drost,M.R., Sciot,R., Bruyninckx,F., Hicklin,D.J., Ince,C., Gressens,P., Lupu,F., Plate,K.H., Robberecht,W., Herbert,J.M., Collen,D., & Carmeliet,P. (2001). Deletion of the hypoxia-response element in the vascular endothelial growth factor promoter causes motor neuron degeneration. *Nature Genetics*, 28, 131-138.
- Orlacchio,A., Babalini,C., Borreca,A., Patrono,C., Massa,R., Basaran,S., Munhoz,R.P., Rogaeva,E.A., George-Hyslop,P.H., Bernardi,G., & Kawai,T. (2010). SPATACIN mutations cause autosomal recessive juvenile amyotrophic lateral sclerosis. *Brain*, 133, 591-598.
- Orr,H.T. (2011). FTD and ALS: Genetic Ties that Bind. *Neuron*, 72, 189-190.
- Orrell,R.W., Habgood,J.J., Gardiner,I., King,A.W., Bowe,F.A., Hallewell,R.A., Marklund,S.L., Greenwood,J., Lane,R.J.M., & DeBelleroche,J. (1997). Clinical and functional investigation of 10 missense mutations and a novel frameshift insertion mutation of the gene for copper-zinc



superoxide dismutase in UK families with amyotrophic lateral sclerosis. *Neurology*, 48, 746-751.

Orrell, Richard W., Habgood, James J., Malaspina, Andrea, Mitchell, John, Greenwood, Juliet, Lane, Russell J. M., and deBellerocche, Jackie S. Clinical characteristics of SOD1 gene mutations in UK families with ALS. *Journal of the Neurological Sciences* 169(1), 56-60. 31-10-1999.

Ref Type: Abstract

Ota,S., Tsuchiya,K., & Akiyama,H. (2005). Forme fruste of amyotrophic lateral sclerosis with dementia: A report of five autopsy cases without dementia and with ubiquitinated intraneuronal inclusions. *Neuropathology*, 25, 326-335.

Pan,L., Yoshii,Y., Otomo,A., Ogawa,H., Iwasaki,Y., Shang,H.F., & Hadano,S. (2012). Different Human Copper-Zinc Superoxide Dismutase Mutants, SOD1G93A and SOD1H46R, Exert Distinct Harmful Effects on Gross Phenotype in Mice. *PLoS ONE*, 7, e33409.

Park,E. & Rho,H. (2002). The transcriptional activation of the human copper/zinc superoxide dismutase gene by 2,3,7,8-tetrachlorodibenzo-p-dioxin through two different regulator sites, the antioxidant responsive element and xenobiotic responsive element. *Mol Cell Biochem*, 240, 47-55.

Parone,P.A., Da Cruz,S., Han,J.S., McAlonis-Downes,M., Vetto,A.P., Lee,S.K., Tseng,E., & Cleveland,D.W. (2013). Enhancing Mitochondrial Calcium Buffering Capacity Reduces Aggregation of Misfolded SOD1 and Motor Neuron Cell Death without Extending Survival in Mouse Models of Inherited Amyotrophic Lateral Sclerosis. *The Journal of Neuroscience*, 33, 4657-4671.

Pasinelli,P., Belford,M.E., Lennon,N., Bacskai,B.J., Hyman,B.T., Trotti,D., & Brown,R.H. (2004). Amyotrophic Lateral Sclerosis-Associated SOD1 Mutant Proteins Bind and Aggregate with Bcl-2 in Spinal Cord Mitochondria. *Neuron*, 43, 19-30.

Pasinelli,P. & Brown,R.H. (2006). Molecular biology of amyotrophic lateral sclerosis: insights from genetics. *Nature Reviews Neuroscience*, 7, 710-723.

Pasinelli,P., Houseweart,M.K., Brown,R.H., & Cleveland,D.W. (2000). Caspase-1 and -3 are sequentially activated in motor neuron death in Cu,Zn superoxide dismutase-mediated familial amyotrophic lateral sclerosis. *Proceedings of the National Academy of Sciences of the United States of America*, 97, 13901-13906.

Pérez,V.I., Bokov,A., Remmen,H.V., Mele,J., Ran,Q., Ikeno,Y., & Richardson,A. (2009). Is the oxidative stress theory of aging dead? *Biochimica et Biophysica Acta*, 1790, 1005-1014.

Petkova,A.T., Leapman,R.D., Guo,Z., Yau,W.M., Mattson,M.P., & Tycko,R. (2005). Self-Propagating, Molecular-Level Polymorphism in Alzheimer's  $\beta$ -Amyloid Fibrils. *Science*, 307, 262-265.

Pham,C.T.N., MacIvor,D.M., Hug,B.A., Heusel,J.W., & Ley,T.J. (1996). Long-range disruption of gene expression by a selectable marker cassette. *Proceedings of the National Academy of Sciences of the United States of America*, 93, 13090-13095.

Pizzasegola,C., Caron,I., Daleno,C., Ronchi,A., Minoia,C., Carri,M.T., & Bendotti,C. (2009). Treatment with lithium carbonate does not improve disease progression in two different strains of SOD1 mutant mice. *Amyotrophic Lateral Sclerosis*, 10, 221-228.

- Pokrishevsky,E., Grad,L.I., Yousefi,M., Wang,J., Mackenzie,I.R., & Cashman,N.R. (2012). Aberrant Localization of FUS and TDP43 Is Associated with Misfolding of SOD1 in Amyotrophic Lateral Sclerosis. *PLoS ONE*, 7, e35050.
- Pollock,R. & Clackson,T. (2002). Dimerizer-regulated gene expression. *Current Opinion in Biotechnology*, 13, 459-467.
- Poon,H.F., Hensley,K., Thongboonkerd,V., Merchant,M.L., Lynn,B.C., Pierce,W.M., Klein,J.B., Calabrese,V., & Butterfield,D.A. (2005). Redox proteomics analysis of oxidatively modified proteins in G93A-SOD1 transgenic mice-a model of familial amyotrophic lateral sclerosis. *Free Radical Biology and Medicine*, 39, 453-462.
- Pramatarova,A., Goto,J., Nanba,E., Nakashima,K., Takahashi,K., Takagi,A., Kanazawa,I., Giglewicz,D.A., & Rouleau,G.A. (1994). A two basepair deletion in the SOD 1 gene causes familial amyotrophic lateral sclerosis. *Human Molecular Genetics*, 3, 2061-2062.
- Pramatarova,A., Laganière,J., Roussel,J., Brisebois,K., & Rouleau,G.A. (2001). Neuron-Specific Expression of Mutant Superoxide Dismutase 1 in Transgenic Mice Does Not Lead to Motor Impairment. *The Journal of Neuroscience*, 21, 3369-3374.
- Prather,R.S., Shen,M., & Dai,Y. (2008). Genetically Modified Pigs for Medicine and Agriculture. *Biotechnology and Genetic Engineering Reviews*, 25, 245-266.
- Proctor,E.A., Ding,F., & Dokholyan,N.V. (2011). Structural and Thermodynamic Effects of Post-translational Modifications in Mutant and Wild Type Cu, Zn Superoxide Dismutase. *Journal of Molecular Biology*, 408, 555-567.
- Prudencio,M. & Borchelt,D. (2011). Superoxide dismutase 1 encoding mutations linked to ALS adopts a spectrum of misfolded states. *Molecular Neurodegeneration*, 6, 77.
- Prudencio,M., Durazo,A., Whitelegge,J.P., & Borchelt,D.R. (2009a). Modulation of mutant superoxide dismutase 1 aggregation by co-expression of wild-type enzyme. *Journal of Neurochemistry*, 108, 1009-1018.
- Prudencio,M., Durazo,A., Whitelegge,J.P., & Borchelt,D.R. (2010). An examination of wild-type SOD1 in modulating the toxicity and aggregation of ALS-associated mutant SOD1. *Human Molecular Genetics*, 19, 4774-4789.
- Prudencio,M., Hart,P.J., Borchelt,D.R., & Andersen,P.M. (2009b). Variation in aggregation propensities among ALS-associated variants of SOD1: Correlation to human disease. *Human Molecular Genetics*, 18, 3217-3226.
- Pun,S., Santos,A.F., Saxena,S., Xu,L., & Caroni,P. (2006). Selective vulnerability and pruning of phasic motoneuron axons in motoneuron disease alleviated by CNTF. *Nature Neuroscience*, 9, 408-419.
- Qualls,D., Prudencio,M., Roberts,B., Crosby,K., Brown,H., & Borchelt,D. (2013). Features of wild-type human SOD1 limit interactions with misfolded aggregates of mouse G86R Sod1. *Molecular Neurodegeneration*, 8, 46.
- Radyuk,S.N., Klichko,V.I., & Orr,W.C. (2004). Profiling Cu,Zn-superoxide dismutase expression in *Drosophila melanogaster* GÇöa critical regulatory role for intron/exon sequence within the coding domain. *Gene*, 328, 37-48.

- Rakhit,R., Crow,J.P., Lepock,J.R., Kondejewski,L.H., Cashman,N.R., & Chakrabartty,A. (2004). Monomeric Cu,Zn-superoxide Dismutase Is a Common Misfolding Intermediate in the Oxidation Models of Sporadic and Familial Amyotrophic Lateral Sclerosis. *Journal of Biological Chemistry*, 279, 15499-15504.
- Rakhit,R., Cunningham,P., Furtos-Matei,A., Dahan,S., Qi,X.F., Crow,J.P., Cashman,N.R., Kondejewski,L.H., & Chakrabartty,A. (2002). Oxidation-induced Misfolding and Aggregation of Superoxide Dismutase and Its Implications for Amyotrophic Lateral Sclerosis. *Journal of Biological Chemistry*, 277, 47551-47556.
- Rakhit,R., Robertson,J., Velde,C.V., Horne,P., Ruth,D.M., Griffin,J., Cleveland,D.W., Cashman,N.R., & Chakrabartty,A. (2007). An immunological epitope selective for pathological monomer-misfolded SOD1 in ALS. *Nature Medicine*, 13, 754-759.
- Ran,F.A., Hsu,P.D., Wright,J., Agarwala,V., Scott,D.A., & Zhang,F. (2013). Genome engineering using the CRISPR-Cas9 system. *Nature Protocols*, 8, 2281-2308.
- Raoul,C., Abbas-Terki,T., Bensadoun,J.C., Guillot,S., Haase,G., Szulc,J., Henderson,C.E., & Aebischer,P. (2005). Lentiviral-mediated silencing of SOD1 through RNA interference retards disease onset and progression in a mouse model of ALS. *Nature Medicine*, 11, 423-428.
- Rathinam,C., Poueymirou,W.T., Rojas,J., Murphy,A.J., Valenzuela,D.M., Yancopoulos,G.D., Rongvaux,A., Eynon,E.E., Manz,M.G., & Flavell,R.A. (2011). Efficient differentiation and function of human macrophages in humanized CSF-1 mice. *Blood*, 118, 3119-3128.
- Ratovitski,T., Corson,L.B., Strain,J., Wong,P., Cleveland,D.W., Culotta,V.C., & Borchelt,D.R. (1999). Variation in the Biochemical/Biophysical Properties of Mutant Superoxide Dismutase 1 Enzymes and the Rate of Disease Progression in Familial Amyotrophic Lateral Sclerosis Kindreds. *Human Molecular Genetics*, 8, 1451-1460.
- Ravits,J., Laurie,P., Fan,Y., & Moore,D.H. (2007a). Implications of ALS focality: Rostral-caudal distribution of lower motor neuron loss postmortem. *Neurology*, 68, 1576-1582.
- Ravits,J., Paul,P., & Jorg,C. (2007b). Focality of upper and lower motor neuron degeneration at the clinical onset of ALS. *Neurology*, 68, 1571-1575.
- Ray,S.S., Nowak,R.J., Strokovich,K., Robert,H., Walz,T., & Lansbury,P.T. (2004). An Intersubunit Disulfide Bond Prevents in Vitro Aggregation of a Superoxide Dismutase-1 Mutant Linked to Familial Amyotrophic Lateral Sclerosis. *Biochemistry*, 43, 4899-4905.
- Reaume,A.G., Elliott,J.L., Hoffman,E.K., Kowall,N.W., Ferrante,R.J., Siwek,D.F., Wilcox,H.M., Flood,D.G., Beal,M.F., Brown,R.H., Scott,R.W., & Snider,W.D. (1996). Motor neurons in Cu/Zn superoxide dismutase-deficient mice develop normally but exhibit enhanced cell death after axonal injury. *Nature Genetics*, 13, 43-47.
- Reddi,A.R. & Culotta,V.C. (2013). SOD1 Integrates Signals from Oxygen and Glucose to Repress Respiration. *Cell*, 152, 224-235.
- Redler,R.L., Wilcox,K.C., Proctor,E.A., Fee,L., Caplow,M., & Dokholyan,N.V. (2011). Glutathionylation at Cys-111 induces dissociation of wild type and FALS mutant SOD1 dimers. *Biochemistry*, 50, 7057-7066.
- Renton,A.E., Majounie,E., Waite,A., Simón-Sánchez,J., Rollinson,S., Gibbs,J.R., Schymick,J.C., Laaksovirta,H., van Swieten,J.C., Myllykangas,L., Kalimo,H., Paetau,A., Abramzon,Y., Remes,A.M., Kaganovich,A., Scholz,S.W., Duckworth,J., Ding,J., Harmer,D.W., Hernandez,D.G.,

- Johnson, J.O., Mok, K., Ryten, M., Trabzuni, D., Guerreiro, R.J., Orrell, R.W., Neal, J., Murray, A., Pearson, J., Jansen, I.E., Sondervan, D., Seelaar, H., Blake, D., Young, K., Halliwell, N., Callister, J.B., Toulson, G., Richardson, A., Gerhard, A., Snowden, J., Mann, D., Neary, D., Nalls, M.A., Peuralinna, T., Jansson, L., Isoviiita, V.-M., Kaivorinne, A.-L., Hölttä-Vuori, M., Ikonen, E., Sulkava, R., Benatar, M., Wu, J., Chiò, A., Restagno, G., Borghero, G., Sabatelli, M., Heckerman, D., Rogaeve, E., Zinman, L., Rothstein, J.D., Sendtner, M., Drepper, C., Eichler, E.E., Alkan, C., Abdullaev, Z., Pack, S.D., Dutra, A., Pak, E., Hardy, J., Singleton, A., Williams, N.M., Heutink, P., Pickering-Brown, S., Morris, H.R., Tienari, P.J., & Traynor, B.J. (2011). A Hexanucleotide Repeat Expansion in C9ORF72 Is the Cause of Chromosome 9p21-Linked ALS-FTD. *Neuron*, 72, 257-268.
- Rich, M.M. & Lichtman, J.W. (1989). In vivo visualization of pre- and postsynaptic changes during synapse elimination in reinnervated mouse muscle. *The Journal of Neuroscience*, 9, 1781-1805.
- Rigaud, M., Gemes, G., Barabas, M.E., Chernoff, D.I., Abram, S.E., Stucky, C.L., & Hogan, Q.H. (2008). Species and strain differences in rodent sciatic nerve anatomy: Implications for studies of neuropathic pain. *Pain*, 136, 188-201.
- Ringholz, G.M., Appel, S.H., Bradshaw, M., Cooke, N.A., Mosnik, D.M., & Schulz, P.E. (2005). Prevalence and patterns of cognitive impairment in sporadic ALS. *Neurology*, 65, 586-590.
- Ripps, M.E., Huntley, G.W., Hof, P.R., Morrison, J.H., & Gordon, J.W. (1995). Transgenic mice expressing an altered murine superoxide dismutase gene provide an animal model of amyotrophic lateral sclerosis. *Proceedings of the National Academy of Sciences of the United States of America*, 92, 689-693.
- Rivera, V.M. (1998). Controlling Gene Expression Using Synthetic Ligands. *Methods*, 14, 421-429.
- Robberecht, W., Sapp, P., Viaene, M.K., Rosen, D., McKenna-Yasek, D., Haines, J., Horvitz, R., Theys, P., & Brown, R. (1994). Rapid Communication: Cu/Zn Superoxide Dismutase Activity in Familial and Sporadic Amyotrophic Lateral Sclerosis. *Journal of Neurochemistry*, 62, 384-387.
- Robertson, E., Bradley, A., Kuehn, M., & Evans, M. (1986). Germ-line transmission of genes introduced into cultured pluripotent cells by retroviral vector. *Nature*, 323, 445-448.
- Robertson, J., Sanelli, T., Xiao, S., Yang, W., Horne, P., Hammond, R., Piro, E.P., & Strong, M.J. (2007). Lack of TDP-43 abnormalities in mutant SOD1 transgenic mice shows disparity with ALS. *Neuroscience Letters*, 420, 128-132.
- Rodriguez, J.A., Shaw, B.F., Durazo, A., Sohn, S.H., Doucette, P.A., Nersissian, A.M., Faull, K.F., Eggers, D.K., Tiwari, A., Hayward, L.J., & Valentine, J.S. (2005). Destabilization of apoprotein is insufficient to explain Cu,Zn-superoxide dismutase-linked ALS pathogenesis. *Proceedings of the National Academy of Sciences of the United States of America*, 102, 10516-10521.
- Rodriguez, J.A., Valentine, J.S., Eggers, D.K., Roe, J.A., Tiwari, A., Brown, R.H., & Hayward, L.J. (2002). Familial Amyotrophic Lateral Sclerosis-associated Mutations Decrease the Thermal Stability of Distinctly Metallated Species of Human Copper/Zinc Superoxide Dismutase. *Journal of Biological Chemistry*, 277, 15932-15937.
- Roe, J.A., Wiedau-Pazos, M., Moy, V.N., Goto, J.J., Butler Gralla, E., & Selverstone Valentine, J. (2002). In vivo peroxidative activity of FALS-mutant human CuZnSODs expressed in yeast. *Free Radical Biology and Medicine*, 32, 169-174.

- Romanuik,T., Wang,G., Holt,R., Jones,S., Marra,M., & Sadar,M. (2009). Identification of novel androgen-responsive genes by sequencing of LongSAGE libraries. *BMC Genomics*, 10, 476.
- Rosen,D.R., Siddique,T., Patterson,D., Figlewicz,D.A., Sapp,P., Hentati,A., Donaldson,D., Goto,J., O'Regan,J.P., Deng,H.X., Rahmani,Z., Krizus,A., McKenna-Yasek,D., Cayabyab,A., Gaston,S.M., Berger,R., Tanzi,R.E., Halperin,J.J., Herzfeldt,B., Van den Bergh,R., Hung,W.Y., Bird,T., Deng,G., Mulder,D.W., Smyth,C., Laing,N.G., Soriano,E., Pericak-Vance,M.A., Haines,J., Rouleau,G.A., Gusella,J.S., Horvitz,H.R., & Brown,R.H. (1993). Mutations in Cu/Zn superoxide dismutase gene are associated with familial amyotrophic lateral sclerosis. *Nature*, 362, 59-62.
- Rumfeldt,J.A.O., Lepock,J.R., & Meiering,E.M. (2009). Unfolding and Folding Kinetics of Amyotrophic Lateral Sclerosis-Associated Mutant Cu,Zn Superoxide Dismutases. *Journal of Molecular Biology*, 385, 278-298.
- Rumfeldt,J.A.O., Stathopoulos,P.B., Chakrabarty,A., Lepock,J.R., & Meiering,E.M. (2006). Mechanism and Thermodynamics of Guanidinium Chloride-induced Denaturation of ALS-associated Mutant Cu,Zn Superoxide Dismutases. *Journal of Molecular Biology*, 355, 106-123.
- Ryoichi,N., Kiminori,K., Takao,F., Keiko,T., Mitsunori,Y., Hitoshi,T., Takashi,K., Takashi,I., & Shoji,T. (2001). Preparation and analysis of the I113T mutation SOD1 transgenic mouse (Ministry of Health,Labour,Welfare S ). *Annual Report of the Group Research in the Pathogenesis and Pathomechanism of Amyotrophic Lateral Sclerosis.2000*, 19-20.
- Saccon,R.A., Bunton-Stasyshyn,R.K.A., Fisher,E.M.C., & Fratta,P. (2013). Is SOD1 loss of function involved in amyotrophic lateral sclerosis? *Brain*, 136, 2342-2358.
- Sahawneh,M.A., Ricart,K.C., Roberts,B.R., Bomben,V.C., Basso,M., Ye,Y., Sahawneh,J., Franco,M.C., Beckman,J.S., & Estévez,A.G. (2010). Cu,Zn-Superoxide Dismutase Increases Toxicity of Mutant and Zinc-deficient Superoxide Dismutase by Enhancing Protein Stability. *Journal of Biological Chemistry*, 285, 33885-33897.
- Sandberg,M.K., Al-Doujaily,H., Sharps,B., Clarke,A.R., & Collinge,J. (2011). Prion propagation and toxicity in vivo occur in two distinct mechanistic phases. *Nature*, 470, 540-542.
- Sandhu,U., Cebula,M., Behme,S., Riemer,P., Wodarczyk,C., Metzger,D., Reimann,J., Schirmbeck,R., Hauser,H., & Wirth,D. (2011). Strict control of transgene expression in a mouse model for sensitive biological applications based on RMCE compatible ES cells. *Nucleic Acids Research*, 39, e1.
- Santa-Maria,I., Varghese,M., Ksiezak-Reding,H., Dzhun,A., Wang,J., & Pasinetti,G.M. (2012). Paired Helical Filaments from Alzheimer Disease Brain Induce Intracellular Accumulation of Tau Protein in Aggresomes. *Journal of Biological Chemistry*, 287, 20522-20533.
- Sapp,P.C., Hosler,B.A., McKenna-Yasek,D., Chin,W., Gann,A., Genise,H., Gorenstein,J., Huang,M., Sailer,W., Scheffler,M., Valesky,M., Haines,J.L., Pericak-Vance,M., Siddique,T., Horvitz,H.R., & Brown,R.H. (2003). Identification of Two Novel Loci for Dominantly Inherited Familial Amyotrophic Lateral Sclerosis. *The American Journal of Human Genetics*, 73, 397-403.
- Sasaki,S. & Iwata,M. (1996a). Impairment of fast axonal transport in the proximal axons of anterior horn neurons in amyotrophic lateral sclerosis. *Neurology*, 47, 535-540.
- Sasaki,S. & Iwata,M. (1996b). Ultrastructural study of synapses in the anterior horn neurons of patients with amyotrophic lateral sclerosis. *Neuroscience Letters*, 204, 53-56.

- Sasaki,S., Komori,T., & Iwata,M. (2010). Neuronal inclusions in sporadic motor neuron disease are negative for alpha-synuclein. *Neuroscience Letters*, 397, 15-19.
- Sasaki,S., Shibata,N., Komori,T., & Iwata,M. (2000). iNOS and nitrotyrosine immunoreactivity in amyotrophic lateral sclerosis. *Neuroscience Letters*, 291, 44-48.
- Sau,D., Rusmini,P., Crippa,V., Onesto,E., Bolzoni,E., Ratti,A., & Poletti,A. (2011). Dysregulation of axonal transport and motoneuron diseases. *Biology of the Cell*, 103, 87-107.
- Saxena,S., Cabuy,E., & Caroni,P. (2009). A role for motoneuron subtype-selective ER stress in disease manifestations of FALS mice. *Nature Neuroscience*, 12, 627-636.
- Scacheri,P.C., Crabtree,J.S., Novotny,E.A., Garrett-Beal,L., Chen,A., Edgemon,K.A., Marx,S.J., Spiegel,A.M., Chandrasekharappa,S.C., & Collins,F.S. (2001). Bidirectional transcriptional activity of PGK-neomycin and unexpected embryonic lethality in heterozygote chimeric knockout mice. *genesis*, 30, 259-263.
- Schaefer,A.M., Sanes,J.R., & Lichtman,J.W. (2005). A compensatory subpopulation of motor neurons in a mouse model of amyotrophic lateral sclerosis. *The Journal of Comparative Neurology*, 490, 209-219.
- Schiffer,D., Cordera,S., Cavalla,P., & Migheli,A. (1996). Reactive astrogliosis of the spinal cord in amyotrophic lateral sclerosis. *Journal of the Neurological Sciences*, 139, 27-33.
- Schmied,A., Pouget,J., & Vedel,J.P. (1999). Electromechanical coupling and synchronous firing of single wrist extensor motor units in sporadic amyotrophic lateral sclerosis. *Clinical Neurophysiology*, 110, 960-974.
- Schröder,M. (2008). Endoplasmic reticulum stress responses. *Cell and Molecular Life Sciences*, 65, 862-894.
- Schuster,C., Kasper,E., Machts,J., Bittner,D., Kaufmann,J., Benecke,R., Teipel,S., Vielhaber,S., & Prudlo,J. (2013). Focal thinning of the motor cortex mirrors clinical features of amyotrophic lateral sclerosis and their phenotypes: a neuroimaging study. *Journal of neurology*, 260, 2856-2864.
- Schwartzberg,P.L., Goff,S.P., & Robertson,E.J. (1989). Germ-line transmission of a c-abl mutation produced by targeted gene disruption in ES cells. *Science*, 246, 799-803.
- Seibler,J. & Bode,J. (1997). Double-Reciprocal Crossover Mediated by FLP-Recombinase: A Concept and an Assay. *Biochemistry*, 36, 1740-1747.
- Seijffers,R., Zhang,J., Matthews,J.C., Chen,A., Tamrazian,E., Babaniyi,O., Selig,M., Hynynen,M., Woolf,C.J., & Brown,R.H. (2014). ATF3 expression improves motor function in the ALS mouse model by promoting motor neuron survival and retaining muscle innervation. *Proceedings of the National Academy of Sciences*, 111, 1622-1627.
- Sekiguchi,T., Kanouchi,T., Shibuya,K., Noto,Y.i., Yagi,Y., Inaba,A., Abe,K., Misawa,S., Orimo,S., Kobayashi,T., Kamata,T., Nakagawa,M., Kuwabara,S., Mizusawa,H., & Yokota,T. (2014). Spreading of amyotrophic lateral sclerosis lesions-multifocal hits and local propagation? *Journal of Neurology, Neurosurgery & Psychiatry*, 85, 85-91.
- Shan,X., Voadlo,D., & Krieger,C. (2009). Mislocalization of TDP-43 in the G93A mutant SOD1 transgenic mouse model of ALS. *Neuroscience Letters*, 458, 70-74.

- Shaw,P.J., Tomkins,J., Slade,J.Y., Usher,P., Curtis,A., Bushby,K., & Ince,P.G. (1997). CNS tissue Cu/Zn superoxide dismutase (SOD1) mutations in motor neurone disease (MND). *Neuroreport*, 8, 3923-3927.
- Shaw,P.J., Ince,P.G., Falkous,G., & Mantle,D. (1995). Oxidative damage to protein in sporadic motor neuron disease spinal cord. *Annals of Neurology*, 38, 691-695.
- Shefner,J.M., Reaume,A.G., Flood,D.G., Scott,R.W., Kowall,N.W., Ferrante,R.J., Siwek,D.F., Upton-Rice,M., & Brown,R.H. (1999). Mice lacking cytosolic copper/zinc superoxide dismutase display a distinctive motor axonopathy. *Neurology*, 53, 1239.
- Sherman,L., Dafni,N., Lieman-Hurwitz,J., & Groner,Y. (1983). Nucleotide sequence and expression of human chromosome 21-encoded superoxide dismutase mRNA. *Proceedings of the National Academy of Sciences of the United States of America*, 80, 5465-5469.
- Shibata,N., Asayama,K., Hirano,A., & Kobayashi,M. (1996a). Immunohistochemical Study on Superoxide Dismutases in Spinal Cords from Autopsied Patients with Amyotrophic Lateral Sclerosis. *Developmental Neuroscience*, 18, 492-498.
- Shibata,N., Hirano,A., Kobayashi,M., Siddique,T., Deng,H.-X., Hung,W.-Y., Kato,T., & Asayama,K. (1996b). Intense Superoxide Dismutase-1 immunoreactivity in intracytoplasmic hyaline inclusions of familial amyotrophic lateral sclerosis with posterior column involvement. *Journal of Neuropathology & Experimental Neurology*, 55, 481-490.
- Shibata,N., Hirano,A., Kobayashi,M., Sasaki,S., Takeo,K., Matsumoto,S., Shiozawa,Z., Komori,T., Ikemoto,A., Umahara,T., & Asayama,K. (1994). CuZn superoxide dismutase-like immunoreactivity in Lewy body-like inclusions of sporadic amyotrophic lateral sclerosis. *Neuroscience Letters*, 179, 149-152.
- Shibata,N., Kawaguchi,M., Uchida,K., Kakita,A., Takahashi,H., Nakano,R., Fujimura,H., Sakoda,S., Ihara,Y., Nobukuni,K., Takehisa,Y., Kuroda,S., Kokubo,Y., Kuzuhara,S., Honma,T., Mochizuki,Y., Mizutani,T., Yamada,S., Toi,S., Sasaki,S., Iwata,M., Hirano,A., Yamamoto,T., Kato,Y., Sawada,T., & Kobayashi,M. (2007). Protein-bound crotonaldehyde accumulates in the spinal cord of superoxide dismutase-1 mutation-associated familial amyotrophic lateral sclerosis and its transgenic mouse model. *Neuropathology*, 27, 49-61.
- Shibata,N., Nagai,R., Uchida,K., Horiuchi,S., Yamada,S., Hirano,A., Kawaguchi,M., Yamamoto,T., Sasaki,S., & Kobayashi,M. (2001). Morphological evidence for lipid peroxidation and protein glycoxidation in spinal cords from sporadic amyotrophic lateral sclerosis patients. *Brain Research*, 917, 97-104.
- Shibata,N., Yamada,S., Uchida,K., Hirano,A., Sakoda,S., Fujimura,H., Sasaki,S., Iwata,M., Toi,S., Kawaguchi,M., Yamamoto,T., & Kobayashi,M. (2004). Accumulation of protein-bound 4-hydroxy-2-hexenal in spinal cords from patients with sporadic amyotrophic lateral sclerosis. *Brain Research*, 1019, 170-177.
- Siklós,L., Engelhardt,J., Harati,Y., Smith,R.G., Joó,F., & Appel,S.H. (1996). Ultrastructural evidence for altered calcium in motor nerve terminals in amyotrophic lateral sclerosis. *Annals of Neurology*, 39, 203-216.
- Silver,L.M. (1995). *Mouse Genetics. Concepts and Applications* Oxford, United Kingdom: Oxford University Press.
- Simpson,E.P., Henry,Y.K., Henkel,J.S., Smith,R.G., & Appel,S.H. (2004). Increased lipid peroxidation in sera of ALS patients. *Neurology*, 62, 1758-1765.

- Smith,A.J.H. & Berg,P. (1984). Homologous Recombination between Defective neo Genes in Mouse 3T6 Cells. *Cold Spring Harbor Symposia on Quantitative Biology*, 49, 171-181.
- Smith,R.G., Henry,Y.K., Mattson,M.P., & Appel,S.H. (1998). Presence of 4-hydroxynonenal in cerebrospinal fluid of patients with sporadic amyotrophic lateral sclerosis. *Annals of Neurology*, 44, 696-699.
- Smith,R.A., Miller,T.M., Yamanaka,K., Monia,B.P., Condon,T.P., Hung,G., Lobsiger,C.S., Ward,C.M., McAlonis-Downes,M., Wei,H., Wancewicz,E.V., Bennett,C.F., & Cleveland,D.W. (2006). Antisense oligonucleotide therapy for neurodegenerative disease. *The Journal of clinical investigation*, 116, 2290-2296.
- Smithies,O., Koralewski,M.A., Song,K.Y., & Kucherlapati,R.S. (1984). Homologous Recombination with DNA Introduced into Mammalian Cells. *Cold Spring Harbor Symposia on Quantitative Biology*, 49, 161-170.
- Smittkamp,S.E., Brown,J.W., & Stanford,J.A. (2008). Time-course and characterization of orolingual motor deficits in B6SJL-Tg(SOD1-G93A)1Gur/J mice. *Neuroscience*, 151, 613-621.
- Son,M., Puttaparthi,K., Kawamata,H., Rajendran,B., Boyer,P.J., Manfredi,G., & Elliott,J.L. (2007). Overexpression of CCS in G93A-SOD1 mice leads to accelerated neurological deficits with severe mitochondrial pathology. *Proceedings of the National Academy of Sciences*, 104, 6072-6077.
- Song,J., Dong,F., Lilly,J.W., Stupar,R.M., & Jiang,J. (2001). Instability of bacterial artificial chromosome (BAC) clones containing tandemly repeated DNA sequences. *Genome*, 44, 463-469.
- Sreedharan,J., Blair,I.P., Tripathi,V.B., Hu,X., Vance,C., Rogelj,B., Ackerley,S., Durnall,J.C., Williams,K.L., Buratti,E., Baralle,F., de Bellerocche,J., Mitchell,J.D., Leigh,P.N., Al Chalabi,A., Miller,C.C., Nicholson,G., & Shaw,C.E. (2008). TDP-43 Mutations in Familial and Sporadic Amyotrophic Lateral Sclerosis. *Science*, 319, 1668-1672.
- Stathopoulos,P.B., Rumfeldt,J.A.O., Scholz,G.A., Irani,R.A., Frey,H.E., Hallewell,R.A., Lepock,J.R., & Meiering,E.M. (2003). Cu/Zn superoxide dismutase mutants associated with amyotrophic lateral sclerosis show enhanced formation of aggregates in vitro. *Proceedings of the National Academy of Sciences of the United States of America*, 100, 7021-7026.
- Sternberg,N. & Hamilton,D. (1981). Bacteriophage P1 site-specific recombination: I. Recombination between loxP sites. *Journal of Molecular Biology*, 150, 467-486.
- Stöhr,J., Watts,J.C., Mensinger,Z.L., Oehler,A., Grillo,S.K., DeArmond,S.J., Prusiner,S.B., & Giles,K. (2012). Purified and synthetic Alzheimer's amyloid beta (Ab) prions. *Proceedings of the National Academy of Sciences*, 109, 11025-11030.
- Ström,A.L., Shi,P., Zhang,F., Gal,J., Kilty,R., Hayward,L.J., & Zhu,H. (2008). Interaction of Amyotrophic Lateral Sclerosis (ALS)-related Mutant Copper-Zinc Superoxide Dismutase with the Dynein-Dynactin Complex Contributes to Inclusion Formation. *Journal of Biological Chemistry*, 283, 22795-22805.
- Strong,M.J., Grace,G.M., Orange,J.B., & Leeper,H.A. (1996). Cognition, language, and speech in amyotrophic lateral sclerosis: A review. *Journal of Clinical and Experimental Neuropsychology*, 18, 291-303.



Sturtz,L.A., Diekert,K., Jensen,L.T., Lill,R., & Culotta,V.C. (2001). A Fraction of Yeast Cu,Zn-Superoxide Dismutase and Its Metallochaperone, CCS, Localize to the Intermembrane Space of Mitochondria: A physiological role for SOD1 in guarding against mitochondrial oxidative damage. *Journal of Biological Chemistry*, 276, 38084-38089.

Su,X.W., Broach,J.R., Connor,J.R., Gerhard,G.S., & Simmons,Z. (2014). Genetic heterogeneity of ALS: implications for clinical practice and research. *Muscle & Nerve*, doi: 10.1002/mus.24198.

Subramani,S. & Berg,P. (1983). Homologous and nonhomologous recombination in monkey cells. *Molecular and Cellular Biology*, 3, 1040-1052.

Subramaniam,J.R., Lyons,W.E., Liu,J., Bartnikas,T.B., Rothstein,J., Price,D.L., Cleveland,D.W., Gitlin,J.D., & Wong,P.C. (2002). Mutant SOD1 causes motor neuron disease independent of copper chaperone-mediated copper loading. *Nature Neuroscience*, 5, 301-307.

Sugiyama,M., Takao,M., Hatsuta,H., Funabe,S., Ito,S., Obi,T., Tanaka,F., Kuroiwa,Y., & Murayama,S. (2013). Increased number of astrocytes and macrophages/microglial cells in the corpus callosum in amyotrophic lateral sclerosis. *Neuropathology*, 33, 591-599.

Sumi,H., Kato,S., Mochimaru,Y., Fujimura,H., Etoh,M., & Sakoda,S. (2009). Nuclear TAR DNA binding protein 43 expression in spinal cord neurons correlates with the clinical course in amyotrophic lateral sclerosis. *Journal of Neuropathology & Experimental Neurology*, 68, 37-47.

Sundaramoorthy,V., Walker,A., Yerbury,J., Soo,K., Farg,M., Hoang,V., Zeineddine,R., Spencer,D., & Atkin,J. (2013). Extracellular wildtype and mutant SOD1 induces ER-Golgi pathology characteristic of amyotrophic lateral sclerosis in neuronal cells. *Cellular and Molecular Life Sciences*, 70, 4181-4195.

Swaminathan,S., Ellis,H.M., Waters,L.S., Yu,D., Lee,E.-C., Court,D., & Sharan,S.K. (2001). Rapid engineering of bacterial artificial chromosomes using oligonucleotides. *genesis*, 29, 14-21.

Swerdlow,R.H., Parks,J.K., Cassarino,D.S., Trimmer,P.A., Miller,S.W., Maguire,D.J., Sheehan,J.P., Maguire,R.S., Pattee,G., Juel,V.C., Phillips,L.H., Tuttle,J.B., Bennett,J., Davis,R.E., & Parker,J. (1998). Mitochondria in Sporadic Amyotrophic Lateral Sclerosis. *Experimental Neurology*, 153, 135-142.

Synofzik,M., Fernández-Santiago,R., Maetzler,W., Schöls,L., & Andersen,P.M. (2010). The human G93A SOD1 phenotype closely resembles sporadic amyotrophic lateral sclerosis. *Journal of Neurology, Neurosurgery & Psychiatry*, 81, 764-767.

Takahashi,K., Nakamura,H., & Okada,E. (1972). Hereditary amyotrophic lateral sclerosis: Histochemical and electron microscopic study of hyaline inclusions in motor neurons. *Archives of Neurology*, 27, 292-299.

Takahashi,T., Yagishita,S., Amano,N., Yamaoka,K., & Kamei,T. (1997). Amyotrophic lateral sclerosis with numerous axonal spheroids in the corticospinal tract and massive degeneration of the cortex. *Acta Neuropathologica*, 94, 294-299.

Talbot,K. (2009). Another gene for ALS. *Neurology*, 73, 1172-1173.

Talbot,K. & Ansorge,O. (2006). Recent advances in the genetics of amyotrophic lateral sclerosis and frontotemporal dementia: common pathways in neurodegenerative disease. *Human Molecular Genetics*, 15, R182-R187.

- Tan,C.F., Eguchi,H., Tagawa,A., Onodera,O., Iwasaki,T., Tsujino,A., Nishizawa,M., Kakita,A., & Takahashi,H. (2007). TDP-43 immunoreactivity in neuronal inclusions in familial amyotrophic lateral sclerosis with or without SOD1 gene mutation. *Acta Neuropathologica*, 113, 535-542.
- Tchorz,J.S., Suply,T., Ksiazek,I., Giachino,C., Cloëtta,D., Danzer,C.P., Doll,T., Isken,A., Lemaistre,M., Taylor,V., Bettler,B., Kinzel,B., & Mueller,M. (2012). A Modified RMCE-Compatible Rosa26 Locus for the Expression of Transgenes from Exogenous Promoters. *PLoS ONE*, 7, e30011.
- Telling,G.C., Scott,M., Mastrianni,J., Gabizon,R., Torchia,M., Cohen,F.E., DeArmond,S.J., & Prusiner,S.B. (1995). Prion propagation in mice expressing human and chimeric PrP transgenes implicates the interaction of cellular PrP with another protein. *Cell*, 83, 79-90.
- Teuchert,M., Fischer,D., Schwalenstoecker,B., Habisch,H.J., Böckers,T.M., & Ludolph,A.C. (2006). A dynein mutation attenuates motor neuron degeneration in SOD1G93A mice. *Experimental Neurology*, 198, 271-274.
- Thomas,K.R., Folger,K.R., & Capecchi,M.R. (1986). High frequency targeting of genes to specific sites in the mammalian genome. *Cell*, 44, 419-428.
- Thompson,S., Clarke,A.R., Pow,A.M., Hooper,M.L., & Melton,D.W. (1989). Germ line transmission and expression of a corrected HPRT gene produced by gene targeting in embryonic stem cells. *Cell*, 56, 313-321.
- Thonhoff,J.R., Gao,J., Dunn,T.J., Ojeda,L., & Wu,P. (2012). Mutant SOD1 microglia-generated nitroxidative stress promotes toxicity to human fetal neural stem cell-derived motor neurons through direct damage and noxious interactions with astrocytes. *American Journal of Stem Cells*, 1, 2-21.
- Thorns,J., Jansma,H., Peschel,T., Grosskreutz,J., Mohammadi,B., Dengler,R., & Munte,T. (2013). Extent of cortical involvement in amyotrophic lateral sclerosis - an analysis based on cortical thickness. *BMC Neurology*, 13, 148.
- Tobisawa,S., Hozumi,Y., Arawaka,S., Koyama,S., Wada,M., Nagai,M., Aoki,M., Itoyama,Y., Goto,K., & Kato,T. (2003). Mutant SOD1 linked to familial amyotrophic lateral sclerosis, but not wild-type SOD1, induces ER stress in COS7 cells and transgenic mice. *Biochemical and Biophysical Research Communications*, 303, 496-503.
- Tohgi,H., Abe,T., Yamazaki,K., Murata,T., Ishizaki,E., & Isobe,C. (1999). Remarkable increase in cerebrospinal fluid 3-nitrotyrosine in patients with sporadic amyotrophic lateral sclerosis. *Annals of Neurology*, 46, 129-131.
- Traxinger,K., Kelly,C., Johnson,B.A., Lyles,R.H., & Glass,J.D. (2013). Prognosis and epidemiology of amyotrophic lateral sclerosis Analysis of a clinic population, 1997-2011. *Neurology: Clinical Practice*, 3, 313-320.
- Troost,D., Sillevs Smitt,P.A.E., De Jong,J.M.B.V., & Swaab,D.F. (1992). Neurofilament and glial alterations in the cerebral cortex in amyotrophic lateral sclerosis. *Acta Neuropathologica*, 84, 664-673.
- Tsunoda,S., Kawano,N., Miyado,K., Kimura,N., & Fujii,J. (2012). Impaired Fertilizing Ability of Superoxide Dismutase 1-Deficient Mouse Sperm During In Vitro Fertilization. *Biology of Reproduction*, 87, 121.

- Tu, P.H., Raju, P., Robinson, K.A., Gurney, M.E., Trojanowski, J.Q., & Lee, V.M. (1996). Transgenic mice carrying a human mutant superoxide dismutase transgene develop neuronal cytoskeletal pathology resembling human amyotrophic lateral sclerosis lesions. *Proceedings of the National Academy of Sciences of the United States of America*, 93, 3155-3160.
- Tuntufye, H.N. & Goddeeris, B.M. (2011). Use of lambda Red-mediated recombineering and Cre/lox for generation of markerless chromosomal deletions in avian pathogenic *Escherichia coli*. *FEMS Microbiology Letters*, 325, 140-147.
- Turan, S., Galla, M., Ernst, E., Qiao, J., Voelkel, C., Schiedlmeier, B., Zehe, C., & Bode, J. (2011). Recombinase-Mediated Cassette Exchange (RMCE): Traditional Concepts and Current Challenges. *Journal of Molecular Biology*, 407, 193-221.
- Turner, B.J., Lopes, E.C., & Cheema, S.S. (2003). Neuromuscular accumulation of mutant superoxide dismutase 1 aggregates in a transgenic mouse model of familial amyotrophic lateral sclerosis. *Neuroscience Letters*, 350, 132-136.
- Turner, B.J. & Talbot, K. (2008). Transgenics, toxicity and therapeutics in rodent models of mutant SOD1-mediated familial ALS. *Progress in Neurobiology*, 85, 94-134.
- Turner, M.R., Parton, M.J., & Leigh, P.N. (2001). Clinical trials in ALS: an overview. *Seminars in neurology*, 21, 167-175.
- Urushitani, M., Sik, A., Sakurai, T., Nukina, N., Takahashi, R., & Julien, J.P. (2006). Chromogranin-mediated secretion of mutant superoxide dismutase proteins linked to amyotrophic lateral sclerosis. *Nature Neuroscience*, 9, 108-118.
- Urushitani, M., Kurisu, J., Tsukita, K., & Takahashi, R. (2002). Proteasomal inhibition by misfolded mutant superoxide dismutase 1 induces selective motor neuron death in familial amyotrophic lateral sclerosis. *Journal of Neurochemistry*, 83, 1030-1042.
- Valdmanis, P.N., Belzil, V.V., Lee, J., Dion, P.A., St Onge, J., Hince, P., Funalot, B., Couratier, P., Clavelou, P., Camu, W., & Rouleau, G.A. (2009). A Mutation that Creates a Pseudoexon in SOD1 Causes Familial ALS. *Annals of Human Genetics*, 73, 652-657.
- Valdmanis, P.N. & Rouleau, G.A. (2008). Genetics of familial amyotrophic lateral sclerosis. *Neurology*, 70, 144-152.
- Valsasina, P., Agosta, F., Benedetti, B., Caputo, D., Perini, M., Salvi, F., Prella, A., & Filippi, M. (2007). Diffusion anisotropy of the cervical cord is strictly associated with disability in amyotrophic lateral sclerosis. *Journal of Neurology, Neurosurgery & Psychiatry*, 78, 480-484.
- Vance, C., Rogelj, B., Hortobágyi, T., De Vos, K.J., Nishimura, A.L., Sreedharan, J., Hu, X., Smith, B., Ruddy, D., Wright, P., Ganesalingam, J., Williams, K.L., Tripathi, V., Al Saraj, S., Al Chalabi, A., Leigh, P.N., Blair, I.P., Nicholson, G., de Belleruche, J., Gallo, J.M., Miller, C.C., & Shaw, C.E. (2009). Mutations in FUS, an RNA Processing Protein, Cause Familial Amyotrophic Lateral Sclerosis Type 6. *Science*, 323, 1208-1211.
- Vassall, K.A., Stathopoulos, P.B., Rumfeldt, J.A.O., Lepock, J.R., & Meiering, E.M. (2006). Equilibrium Thermodynamic Analysis of Amyotrophic Lateral Sclerosis-Associated Mutant Apo Cu,Zn Superoxide Dismutases. *Biochemistry*, 45, 7366-7379.
- Vassall, K.A., Stubbs, H.R., Primmer, H.A., Tong, M.S., Sullivan, S.M., Sobering, R., Srinivasan, S., Briere, L.A., Dunn, S.D., Colón, W., & Meiering, E.M. (2011). Decreased stability and increased

- formation of soluble aggregates by immature superoxide dismutase do not account for disease severity in ALS. *Proceedings of the National Academy of Sciences*.
- Vielhaber,S., Winkler,K., Kirches,E., Kunz,D., Büchner,M., Feistner,H., Elger,C.E., Ludolph,A.C., Riepe,M.W., & Kunz,W.S. (1999). Visualization of defective mitochondrial function in skeletal muscle fibers of patients with sporadic amyotrophic lateral sclerosis. *Journal of the Neurological Sciences*, 169, 133-139.
- Volkening,K., Leystra-Lantz,C., Yang,W., Jaffee,H., & Strong,M.J. (2009). Tar DNA binding protein of 43 kDa (TDP-43), 14-3-3 proteins and copper/zinc superoxide dismutase (SOD1) interact to modulate NFL mRNA stability. Implications for altered RNA processing in amyotrophic lateral sclerosis (ALS). *Brain Research*, 1305, 168-182.
- Vucic,S., Nicholson,G.A., Chio,A., & Kiernan,M.C. (2013). Apparent anticipation in SOD1 familial amyotrophic lateral sclerosis. *Amyotrophic Lateral Sclerosis and Frontotemporal Degeneration*, 14, 452-456.
- Vucic,S., Nicholson,G.A., & Kiernan,M.C. (2008). Cortical hyperexcitability may precede the onset of familial amyotrophic lateral sclerosis. *Brain*, 131, 1540-1550.
- Wagner,E.F., Stewart,T.A., & Mintz,B. (1981a). The human b-globin gene and a functional viral thymidine kinase gene in developing mice. *Proceedings of the National Academy of Sciences of the United States of America*, 78, 5016-5020.
- Wagner,T.E., Hoppe,P.C., Jollick,J.D., Scholl,D.R., Hodinka,R.L., & Gault,J.B. (1981b). Microinjection of a rabbit b-globin gene into zygotes and its subsequent expression in adult mice and their offspring. *Proceedings of the National Academy of Sciences of the United States of America*, 78, 6376-6380.
- Wallace,H.A.C., Marques-Kranc,F., Richardson,M., Luna-Crespo,F., Sharpe,J.A., Hughes,J., Wood,W.G., Higgs,D.R., & Smith,A.J.H. (2007). Manipulating the Mouse Genome to Engineer Precise Functional Syntenic Replacements with Human Sequence. *Cell*, 128, 197-209.
- Wang,J., Farr,G.W., Zeiss,C.J., Rodriguez-Gil,D.J., Wilson,J.H., Furtak,K., Rutkowski,D.T., Kaufman,R.J., Ruse,C.I., Yates,J.R., Perrin,S., Feany,M.B., & Horwich,A.L. (2009a). Progressive aggregation despite chaperone associations of a mutant SOD1-YFP in transgenic mice that develop ALS. *Proceedings of the National Academy of Sciences*, 106, 1392-1397.
- Wang,J., Slunt,H., Gonzales,V., Fromholt,D., Coonfield,M., Copeland,N.G., Jenkins,N.A., & Borchelt,D.R. (2003). Copper-binding-site-null SOD1 causes ALS in transgenic mice: aggregates of non-native SOD1 delineate a common feature. *Human Molecular Genetics*, 12, 2753-2764.
- Wang,J., Xu,G., & Borchelt,D.R. (2002a). High Molecular Weight Complexes of Mutant Superoxide Dismutase 1: Age-Dependent and Tissue-Specific Accumulation. *Neurobiology of Disease*, 9, 139-148.
- Wang,J., Xu,G., & Borchelt,D.R. (2006a). Mapping superoxide dismutase 1 domains of non-native interaction: roles of intra- and intermolecular disulfide bonding in aggregation. *Journal of Neurochemistry*, 96, 1277-1288.
- Wang,J., Xu,G., Gonzales,V., Coonfield,M., Fromholt,D., Copeland,N.G., Jenkins,N.A., & Borchelt,D.R. (2002b). Fibrillar Inclusions and Motor Neuron Degeneration in Transgenic Mice Expressing Superoxide Dismutase 1 with a Disrupted Copper-Binding Site. *Neurobiology of Disease*, 10, 128-138.

- Wang,J., Xu,G., Li,H., Gonzales,V., Fromholt,D., Karch,C., Copeland,N.G., Jenkins,N.A., & Borchelt,D.R. (2005a). Somatodendritic accumulation of misfolded SOD1-L126Z in motor neurons mediates degeneration: aB-crystallin modulates aggregation. *Human Molecular Genetics*, 14, 2335-2347.
- Wang,J., Xu,G., Slunt,H.H., Gonzales,V., Coonfield,M., Fromholt,D., Copeland,N.G., Jenkins,N.A., & Borchelt,D.R. (2005b). Coincident thresholds of mutant protein for paralytic disease and protein aggregation caused by restrictively expressed superoxide dismutase cDNA. *Neurobiology of Disease*, 20, 943-952.
- Wang,J., Sarov,M., Rientjes,J., Hu,J., Hollak,H., Kranz,H., Xie,Y., Stewart,A.F., & Zhang,Y. (2006b). An improved recombineering approach by adding RecA to  $\lambda$  Red recombination. *Molecular Biotechnology*, 32, 43-53.
- Wang,L., Deng,H.X., Grisotti,G., Zhai,H., Siddique,T., & Roos,R.P. (2009b). Wild-type SOD1 overexpression accelerates disease onset of a G85R SOD1 mouse. *Human Molecular Genetics*, 18, 1642-1651.
- Wang,L., Gutmann,D.H., & Roos,R.P. (2011a). Astrocyte loss of mutant SOD1 delays ALS disease onset and progression in G85R transgenic mice. *Human Molecular Genetics*, 20, 286-293.
- Wang,L., Popko,B., & Roos,R.P. (2011b). The unfolded protein response in familial amyotrophic lateral sclerosis. *Human Molecular Genetics*, 20, 1008-1015.
- Wang,L., Sharma,K., Deng,H.X., Siddique,T., Grisotti,G., Liu,E., & Roos,R.P. (2008). Restricted expression of mutant SOD1 in spinal motor neurons and interneurons induces motor neuron pathology. *Neurobiology of Disease*, 29, 400-408.
- Wang,L., Sharma,K., Grisotti,G., & Roos,R.P. (2009c). The effect of mutant SOD1 dismutase activity on non-cell autonomous degeneration in familial amyotrophic lateral sclerosis. *Neurobiology of Disease*, 35, 234-240.
- Wang,S., Zhao,Y., Leiby,M., & Zhu,J. (2009d). A New Positive/Negative Selection Scheme for Precise BAC Recombineering. *Molecular Biotechnology*, 42, 110-116.
- Warita,H., Itoyama,Y., & Abe,K. (1999). Selective impairment of fast anterograde axonal transport in the peripheral nerves of asymptomatic transgenic mice with a G93A mutant SOD1 gene. *Brain Research*, 819, 120-131.
- Warming,S., Costantino,N., Court,D., Jenkins,N.A., & Copeland,N.G. (2005). Simple and highly efficient BAC recombineering using galK selection. *Nucleic Acids Research*, 33, e36.
- Watanabe,M., Dykes-Hoberg,M., Cizewski Culotta,V., Price,D.L., Wong,P.C., & Rothstein,J.D. (2001a). Histological Evidence of Protein Aggregation in Mutant SOD1 Transgenic Mice and in Amyotrophic Lateral Sclerosis Neural Tissues. *Neurobiology of Disease*, 8, 933-941.
- Watanabe,Y., Kato,S., Adachi,Y., & Nakashima,K. (2000). Frameshift, nonsense and non amino acid altering mutations in SOD1 in familial ALS: report of a Japanese pedigree and literature review. *Amyotroph Lateral Scler Other Motor Neuron Disord*, 1, 251-258.
- Watanabe,Y., Kuno,N., Kuno,Y., Nanba,E., Ohama,E., Nakashima,K., & Takahashi,K. (1997a). Absence of the mutant SOD1 in familial amyotrophic lateral sclerosis (FALS) with two base pair deletion in the SOD1 gene. *Acta Neurologica Scandinavica*, 95, 167-172.

- Watanabe,Y., Adachi,Y., & Nakashima,K. (2001b). Japanese familial amyotrophic lateral sclerosis family with a two-base deletion in the superoxide dismutase-1 gene. *Neuropathology*, 21, 61-66.
- Watanabe,Y., Kono,Y., Nanba,E., Ohama,E., & Nakashima,K. (1997b). Instability of expressed Cu/Zn superoxide dismutase with 2 bp deletion found in familial amyotrophic lateral sclerosis. *FEBS Letters*, 400, 108-112.
- Watanabe,Y., Morita,E., Fukada,Y., Doi,K., Yasui,K., Kitayama,M., Nakano,T., & Nakashima,K. (2008). Adherent Monomer-Misfolded SOD1. *PLoS ONE*, 3, e3497.
- Watanabe,Y., Yasui,K., Nakano,T., Doi,K., Fukada,Y., Kitayama,M., Ishimoto,M., Kurihara,S., Kawashima,M., Fukuda,H., Adachi,Y., Inoue,T., & Nakashima,K. (2005). Mouse motor neuron disease caused by truncated SOD1 with or without C-terminal modification. *Molecular Brain Research*, 135, 12-20.
- Watts,J.C., Giles,K., Oehler,A., Middleton,L., Dexter,D.T., Gentleman,S.M., DeArmond,S.J., & Prusiner,S.B. (2013). Transmission of multiple system atrophy prions to transgenic mice. *Proceedings of the National Academy of Sciences*, 110, 19555-19560.
- Weichert,A., Besemer,A.S., Liebl,M., Hellmann,N., Koziollek-Drechsler,I., Ip,P., Decker,H., Robertson,J., Chakrabartty,A., Behl,C., & Clement,A.M. (2014). Wild-type Cu/Zn superoxide dismutase stabilizes mutant variants by heterodimerization. *Neurobiology of Disease*, 62, 479-488.
- Weisberg,S.J., Lyakhovetsky,R., Werdiger,A.c., Gitler,A.D., Soen,Y., & Kaganovich,D. (2012). Compartmentalization of superoxide dismutase 1 (SOD1G93A) aggregates determines their toxicity. *Proceedings of the National Academy of Sciences*, 109, 15811-15816.
- Westenberg,M., Soedling,H.M., Mann,D.A., Nicholson,L.J., & Dolphin,C.T. (2010). Counter-selection recombineering of the baculovirus genome: a strategy for seamless modification of repeat-containing BACs. *Nucleic Acids Research*, 38, e166.
- Wicks,P., Abrahams,S., Papps,B., Al Chalabi,A., Shaw,C., Leigh,P., & Goldstein,L. (2009). SOD1 and cognitive dysfunction in familial amyotrophic lateral sclerosis. *Journal of neurology*, 256, 234-241.
- Wiedau-Pazos,M., Goto,J.J., Rabizadeh,S., Gralla,E.B., Roe,J.A., Lee,M.K., Valentine,J.S., & Bredesen,D.E. (1996). Altered Reactivity of Superoxide Dismutase in Familial Amyotrophic Lateral Sclerosis. *Science*, 271, 515-518.
- Wiedemann,F.R., Winkler,K., Kuznetsov,A.V., Bartels,C., Vielhaber,S., Feistner,H., & Kunz,W.S. (1998). Impairment of mitochondrial function in skeletal muscle of patients with amyotrophic lateral sclerosis. *Journal of the Neurological Sciences*, 156, 65-72.
- Wijesekera,L. & Leigh,P.N. (2009). Amyotrophic lateral sclerosis. *Orphanet Journal of Rare Diseases*, 4.
- Wilcox,K.C., Zhou,L., Jordon,J.K., Huang,Y., Yu,Y., Redler,R.L., Chen,X., Caplow,M., & Dokholyan,N.V. (2009). Modifications of Superoxide Dismutase (SOD1) in Human Erythrocytes. *Journal of Biological Chemistry*, 284, 13940-13947.
- Williamson,T.L., Bruijn,L.I., Zhu,Q., Anderson,K.L., Anderson,S.D., Julien,J.P., & Cleveland,D.W. (1998). Absence of neurofilaments reduces the selective vulnerability of motor neurons and slows disease caused by a familial amyotrophic lateral sclerosis-linked superoxide dismutase 1

- mutant. *Proceedings of the National Academy of Sciences of the United States of America*, 95, 9631-9636.
- Williamson, T.L. & Cleveland, D.W. (1999). Slowing of axonal transport is a very early event in the toxicity of ALS-linked SOD1 mutants to motor neurons. *Nature Neuroscience*, 2, 50-56.
- Witan, H., Gorlovoy, P., Kaya, A.M., Koziollek-Drechsler, I., Neumann, H., Behl, C., & Clement, A.M. (2009). Wild-type Cu/Zn superoxide dismutase (SOD1) does not facilitate, but impedes the formation of protein aggregates of amyotrophic lateral sclerosis causing mutant SOD1. *Neurobiology of Disease*, 36, 331-342.
- Witan, H., Kern, A., Koziollek-Drechsler, I., Wade, R., Behl, C., & Clement, A.M. (2008). Heterodimer formation of wild-type and amyotrophic lateral sclerosis-causing mutant Cu/Zn-superoxide dismutase induces toxicity independent of protein aggregation. *Human Molecular Genetics*, 17, 1373-1385.
- Wong, M. & Martin, L.J. (2010). Skeletal muscle-restricted expression of human SOD1 causes motor neuron degeneration in transgenic mice. *Human Molecular Genetics*, 19, 2284-2302.
- Wong, P.C., Pardo, C.A., Borchelt, D.R., Lee, M.K., Copeland, N.G., Jenkins, N.A., Sisodia, S.S., Cleveland, D.W., & Price, D.L. (1995). An adverse property of a familial ALS-linked SOD1 mutation causes motor neuron disease characterized by vacuolar degeneration of mitochondria. *Neuron*, 14, 1105-1116.
- Wooley, C.M., Sher, R.B., Kale, A., Frankel, W.N., Cox, G.A., & Seburn, K.L. (2005). Gait analysis detects early changes in transgenic SOD1(G93A) mice. *Muscle & Nerve*, 32, 43-50.
- Wu, C.H., Fallini, C., Ticozzi, N., Keagle, P.J., Sapp, P.C., Piotrowska, K., Lowe, P., Koppers, M., McKenna-Yasek, D., Baron, D.M., Kost, J.E., Gonzalez-Perez, P., Fox, A.D., Adams, J., Taroni, F., Tiloca, C., LeClerc, A.L., Chafe, S.C., Mangroo, D., Moore, M.J., Zitzewitz, J.A., Xu, Z.S., Van Den Berg, L.H., Glass, J.D., Siciliano, G., Cirulli, E.T., Goldstein, D.B., Salachas, F., Meininger, V., Rossoll, W., Ratti, A., Gellera, C., Bosco, D.A., Bassell, G.J., Silani, V., Drory, V.E., Brown, J., & Landers, J.E. (2012). Mutations in the profilin 1 gene cause familial amyotrophic lateral sclerosis. *Nature*, 488, 499-503.
- Yamanaka, K., Chun, S.J., Boillee, S., Fujimori-Tonou, N., Yamashita, H., Gutmann, D.H., Takahashi, R., Misawa, H., & Cleveland, D.W. (2008a). Astrocytes as determinants of disease progression in inherited amyotrophic lateral sclerosis. *Nature Neuroscience*, 11, 251-253.
- Yamanaka, K., Boillee, S., Roberts, E.A., Garcia, M.L., McAlonis-Downes, M., Mikse, O.R., Cleveland, D.W., & Goldstein, L.S.B. (2008b). Mutant SOD1 in cell types other than motor neurons and oligodendrocytes accelerates onset of disease in ALS mice. *Proceedings of the National Academy of Sciences*, 105, 7594-7599.
- Yang, Y., Hentati, A., Deng, H.X., Dabbagh, O., Sasaki, T., Hirano, M., Hung, W.Y., Ouahchi, K., Yan, J., Azim, A.C., Cole, N., Gascon, G., Yagmour, A., Ben Hamida, M., Pericak-Vance, M., Hentati, F., & Siddique, T. (2001). The gene encoding alsin, a protein with three guanine-nucleotide exchange factor domains, is mutated in a form of recessive amyotrophic lateral sclerosis. *Nature Genetics*, 29, 160-165.
- Yim, H.S., Kang, J.H., Chock, P.B., Stadtman, E.R., & Yim, M.B. (1997). A Familial Amyotrophic Lateral Sclerosis-associated A4V Cu,Zn-Superoxide Dismutase Mutant Has a Lower Km for Hydrogen Peroxide: Correlation between clinical severity and the Km value. *Journal of Biological Chemistry*, 272, 8861-8863.

- Yim,M.B., Kang,J.H., Yim,H.S., Kwak,H.S., Chock,P.B., & Stadtman,E.R. (1996). A gain-of-function of an amyotrophic lateral sclerosis-associated Cu,Zn-superoxide dismutase mutant: An enhancement of free radical formation due to a decrease in Km for hydrogen peroxide. *Proceedings of the National Academy of Sciences of the United States of America*, 93, 5709-5714.
- Yonetani,M., Nonaka,T., Masuda,M., Inukai,Y., Oikawa,T., Hisanaga,S.i., & Hasegawa,M. (2009). Conversion of Wild-type  $\alpha$ -Synuclein into Mutant-type Fibrils and Its Propagation in the Presence of A30P Mutant. *Journal of Biological Chemistry*, 284, 7940-7950.
- Yoo,H.Y., Chang,M.S., & Rho,H.M. (1999a). Heavy metal-mediated activation of the rat Cu/Zn superoxide dismutase gene via a metal-responsive element. *Molecular and General Genetics MGG*, 262, 310-313.
- Yoo,H.Y., Chang,M.S., & Rho,H.M. (1999b). The Activation of the Rat Copper/Zinc Superoxide Dismutase Gene by Hydrogen Peroxide through the Hydrogen Peroxide-responsive Element and by Paraquat and Heat Shock through the Same Heat Shock Element. *Journal of Biological Chemistry*, 274, 23887-23892.
- Yulug,I.G., Katsanis,N., de Bellerocche,J., Collinge,J., & Fisher,E.M.C. (1995). An improved protocol for the analysis of SOD1 gene mutations, and a new mutation in exon 4. *Human Molecular Genetics*, 4, 1101-1104.
- Zelko,I.N., Mariani,T.J., & Folz,R.J. (2002). Superoxide dismutase multigene family: a comparison of the CuZn-SOD (SOD1), Mn-SOD (SOD2), and EC-SOD (SOD3) gene structures, evolution, and expression. *Free Radical Biology and Medicine*, 33, 337-349.
- Zeng,C., Kouprina,N., Zhu,B., Cairo,A., Hoek,M., Cross,G., Osoegawa,K., Larionov,V., & de Jong,P. (2001). Large-Insert BAC/YAC Libraries for Selective Re-isolation of Genomic Regions by Homologous Recombination in Yeast. *Genomics*, 77, 27-34.
- Zetterström,P., Graffmo,K.S., Andersen,P.M., Brännström,T., & Marklund,S.L. (2011). Proteins That Bind to Misfolded Mutant Superoxide Dismutase-1 in Spinal Cords from Transgenic Amyotrophic Lateral Sclerosis (ALS) Model Mice. *Journal of Biological Chemistry*, 286, 20130-20136.
- Zetterström,P., Graffmo,K.S., Andersen,P.M., Brännström,T., & Marklund,S.L. (2013). Composition of Soluble Misfolded Superoxide Dismutase-1 in Murine Models of Amyotrophic Lateral Sclerosis. *NeuroMolecular Medicine*, 1-12.
- Zetterström,P., Stewart,H.G., Bergemalm,D., Jonsson,P.A., Graffmo,K.S., Andersen,P.M., Brännström,T., Oliveberg,M., & Marklund,S.L. (2007). Soluble misfolded subfractions of mutant superoxide dismutase-1s are enriched in spinal cords throughout life in murine ALS models. *Proceedings of the National Academy of Sciences*, 104, 14157-14162.
- Zhang,B., Tu,P.h., Abtahian,F., Trojanowski,J.Q., & Lee,V.M.Y. (1997). Neurofilaments and Orthograde Transport Are Reduced in Ventral Root Axons of Transgenic Mice that Express Human SOD1 with a G93A Mutation. *The Journal of Cell Biology*, 139, 1307-1315.
- Zhang,F., Ström,A.L., Fukada,K., Lee,S., Hayward,L.J., & Zhu,H. (2007). Interaction between Familial Amyotrophic Lateral Sclerosis (ALS)-linked SOD1 Mutants and the Dynein Complex. *Journal of Biological Chemistry*, 282, 16691-16699.
- Zhao,W., Beers,D.R., Henkel,J.S., Zhang,W., Urushitani,M., Julien,J.P., & Appel,S.H. (2010). Extracellular mutant SOD1 induces microglial-mediated motoneuron injury. *Glia*, 58, 231-243.



- Zhu,J.-H., Zhang,X., Roneker,C.A., McClung,J.P., Zhang,S., Thannhauser,T.W., Ripoll,D.R., Sun,Q., & Lei,X.G. (2008). Role of copper,zinc-superoxide dismutase in catalyzing nitrotyrosine formation in murine liver. *Free Radical Biology and Medicine*, 45, 611-618.
- Zijlstra,M., Li,E., Sajjadi,F., Subramani,S., & Jaenisch,R. (1989). Germ-line transmission of a disrupted beta 2-microglobulin gene produced by homologous recombination in embryonic stem cells. *Nature*, 342, 435-438.
- Zil'ber,L.A., Bajdakova,Z.L., Gardas'jan,A.N., Konovalov,N.V., Bunina,T.L., & Barabadze,E.M. (1963). Study of the etiology of amyotrophic lateral sclerosis. *Bulletin of the World Health Organization*, 29, 449-456.
- Zinman,L., Liu,H.N., Sato,C., Wakutani,Y., Marvelle,A.F., Moreno,D., Morrison,K.E., Mohlke,K.L., Bilbao,J., Robertson,J., & Rogaeva,E. (2009). A mechanism for low penetrance in an ALS family with a novel SOD1 deletion. *Neurology*, 72, 1153-1159.
- Zu,J.S., Deng,H.X., Lo,T.P., Mitsumoto,H., Ahmed,M.S., Hung,W.Y., Cai,Z.J., Tainer,J.A., & Siddique,T. (1997). Exon 5 encoded domain is not required for the toxic function of mutant SOD1 but essential for the dismutase activity: identification and characterization of two new SOD1 mutations associated with familial amyotrophic lateral sclerosis. *Neurogenetics*, 1, 65-71.